British Journal of Pharmacology (1999) 126, 391–398
http://www.stockton-press.co.uk/bjp

REVIEW ARTICLE

Secretory pathways in endothelin synthesis

[1]Fraser D. Russell & *,[1]Anthony P. Davenport

[1]Clinical Pharmacology Unit, University of Cambridge, Level 6, Centre for Clinical Investigation, Box 110, Addenbrooke's Hospital, Cambridge CB2 2QQ, England, U.K.

Keywords: Endothelin; endothelin converting enzyme; secretory pathways

Abbreviations: ECE, endothelin converting enzyme; ET, endothelin; HUVEC, human umbilical vein endothelial cell; NEP, neutral endopeptidase

Introduction

Endothelin (ET) is a potent vasoconstrictor peptide that is generated *via* unique processing of a low activity precursor, big ET-1 by endothelin converting enzymes (ECEs). ET has a physiological role in the maintenance of basal tone in humans (Haynes & Webb, 1994; Haynes, 1995; Haynes *et al*., 1995), but may also have a role in the pathophysiology of cardiovascular diseases, including atherosclerosis, coronary vasospasm and congestive heart disease (Kurihara *et al*., 1989; Bacon *et al*., 1996; Cohn, 1996). The ET system is therefore a potential therapeutic target in the effective management of these diseases. There are two current strategies being pursued to attenuate adverse haemodynamic effects and the migration and proliferation of vascular smooth muscle cells by ET. These include the use of antagonists to receptors that mediate responses to ET and the use of selective inhibitors to ECE. The pathways involved in big ET-1 processing and ET transport are only now being elucidated and these findings will be useful in predicting the characteristics of inhibitors that best suit inhibition of ECE. It will be important to determine whether ECE is expressed on the cell surface and/or intracellularly to decide whether inhibitors are required to penetrate the plasma membrane. This article reviews the secretory pathways involved in ET transport and the subcellular processing of big ET-1 by ECE.

ECEs are membrane-bound proteases with structural homology to neutral endopeptidase 24.11 (NEP) and Kell blood group protein (for review, see Opgenorth *et al*., 1992; Turner, 1993; Turner & Murphy, 1996). The cDNA sequences of two converting enzymes, ECE-1 and ECE-2 have been reported (Schmidt *et al*., 1994; Emoto & Yanagisawa, 1995; Shimada *et al*., 1995; Valdenaire *et al*., 1995; Yorimitsu *et al*., 1995). The enzymes, which have 59% overall homology, are membrane bound phosphoramidon-sensitive metalloproteases with specificity for big ET-1. ECE-1 appears to be the predominant endothelin converting enzyme in humans (Emoto & Yanagisawa, 1995). Two isoforms of ECE-1 (ECE-1α and ECE-1β) are encoded by a single gene and differ only in their cytoplasmic N-terminal domains. Studies on a soluble construct of ECE-1 (Korth *et al*., 1997), and molecular modelling experiments (Sansom *et al*., 1995) reveal that the putative extracellular domain contains the catalytic site for ECE activity. A third converting enzyme, ECE-3 has recently been purified from bovine iris microsomes (Hasegawa *et al*., 1998) and this enzyme has specificity for big ET-3. With the exception of studies exploiting selective antisera, the precise identity of the enzyme catalyzing conversion of big ET in tissues in functional studies is not yet known and therefore is referred to as ECE activity.

* Author for correspondence.

ECE expression in the human vasculature

ECE is widely expressed in human blood vessel endothelium, including the cerebral, pulmonary, coronary, splanchnic, renal, forearm and adrenal vasculature (Ahlborg *et al*., 1994; Haynes, 1995; Hemsén *et al*., 1995; Plumpton *et al*., 1995; Saleh *et al*., 1997; Davenport *et al*., 1998a; Herman *et al*., 1998; Russell *et al*., 1998a,b). ECE has also been identified in endocardial cells lining the ventricles of the heart and in endothelial cells of foetal vasculature including umbilical veins and arteries (Moldovan *et al*., 1996; Davenport *et al*., 1998a; Russell *et al*., 1998c). The pattern of ECE-like immunoreactive staining in human blood vessels corresponds to the distribution of ET and big ET (Bacon *et al*., 1996; Saleh *et al*., 1997; Davenport *et al*., 1998a; Russell *et al*., 1998d). Interestingly, infusion of ET-1 into the dorsal hand vein produced marked vasoconstriction whereas infusion of big ET-1 had no effect (Haynes *et al*., 1995), thus raising the possibility that endogenous big ET-1 is only processed by an intracellular enzyme in this vessel.

In contrast to the high level of ECE that is expressed in human endothelial cells, only low to moderate levels of expression have been detected in adjacent intimal and medial vascular smooth muscle cells (Davenport *et al*., 1998a). Human umbilical vein smooth muscle cells synthesize and secrete immunoreactive ET-1 and ET-3 (Yu & Davenport, 1995), indicating a possible physiological relevance of the smooth muscle converting enzyme.

Evidence for expression of an intracellular ECE

ECE expression is high in endothelial cells and processing of big ET-1 to ET-1 has been attributed to activity of a converting enzyme that is located on the plasma membrane and within intracellular compartments (Harrison *et al*., 1993; Xu *et al*., 1994; Corder *et al*., 1995). Some studies indicate that ECE is predominantly expressed or has main activity as an ectoenzyme (Harrison *et al*., 1993; Waxman *et al*., 1994; Corder *et al*., 1995; Takahashi *et al*., 1995; Barnes *et al*., 1996), and therefore acts mainly in a post-secretory processing role. When a homogenate prepared from a human endothelial hybrid cell line, EAHY 926, was sub-fractionated on a sucrose gradient the majority of ECE activity (60%) was associated

with a plasma membrane enriched fraction (Waxman *et al*., 1994). In contrast, other studies have suggested that ECE is either primarily expressed or has predominant activity within intracellular compartments (Gui *et al*., 1993; Xu *et al*., 1994; Davenport *et al*., 1998b; Russell *et al*., 1998c). Immunocytochemical studies revealed only a low level of ECE-like immunoreactivity on the plasma membrane of cultured HUVECs and intense immunoreactive staining within intracellular organelles, determined by scanning electron microscopy, confocal laser scanning microscopy and immuno-electron microscopy (Russell *et al*., 1998c). Biochemical studies showed predominant ECE activity in intracellular compartments by comparing big ET-1 processing in permeabilized and non-permeabilized HUVECs (Davenport *et al*., 1998b).

Pathways involved in peptide transport

Proteins are transported from the endoplasmic reticulum to the plasma membrane in human endothelial cells *via* two distinct secretory pathways; the constitutive pathway involving continuous release and the regulated pathway involving stimulated release. The constitutive secretory pathway is modulated at the level of mRNA transcription and has been proposed as the mechanism for ET release from porcine endothelial cells (Yanagisawa *et al*., 1988). Although involvement of the regulated pathway in ET secretion was dismissed, based in part on a perceived lack of storage granules in endothelial cells (Yanagisawa *et al*., 1988), early morphological studies had successfully identified endothelial specific storage granules called Weibel-Palade bodies (Weibel & Palade, 1964).

Basal ET release from endothelial cells is via *the constitutive secretory pathway*

Secretory and plasmalemmal proteins, proteoglycans and lysosomal enzymes follow a common pathway through the endoplasmic reticulum and Golgi complex (Farquhar, 1985). The proteins are continuously shuttled from the *trans*-Golgi network to the cell surface in secretory vesicles *via* the constitutive secretory pathway. ET-like immunoreactivity has been detected in bovine aortic and human coronary artery endothelial cell secretory vesicles, indicating involvement of the constitutive pathway in peptide transport (Harrison *et al*., 1993; 1995; Russell *et al*., 1998d). Indeed, the constitutive pathway may be involved in peptide processing since ECE and big ET-like immunoreactive staining was found to be co-localized in endothelial secretory vesicles (Barnes *et al*., 1998). *In vivo* evidence suggest that endogenous synthesis, transport and release of ET contribute to maintenance of vascular tone in humans. Forearm vasodilatation, measured by increased blood flow, was observed when either phosphoramidon or the ET_A selective antagonist BQ123 was infused into the brachial artery of healthy subjects (Haynes & Webb, 1994).

Evidence for a role of the regulated secretory pathway in ET transport

Weibel-Palade bodies store vasoactive compounds including histamine, von Willebrand factor, P-selectin and calcitonin gene-related peptide (Fujimoto *et al*., 1982; Wagner *et al*., 1982; McEver *et al*., 1989; Doi *et al*., 1995; Ozaka *et al*., 1997). These granules are also a repository for ET in rat (Doi *et al*., 1996; Ozaka *et al*., 1997), rabbit (Sakamoto *et al*., 1993), and human endothelial cells (Hamasaki *et al*., 1995; Russell *et al*., 1998d). Endothelial storage granules that are distinct from Weibel-Palade bodies were identified as storage sites for tissue-type plasminogen activator (Emeis *et al*., 1997). However, these granules are unlikely to be involved in storage of ET since, unlike ET, tissue-type plasminogen activator does not co-localize with von Willebrand factor. Similarly, the soluble protein multimerin which was identified in round to rod-shaped, dense core granules resembling Weibel-Palade bodies did not co-localize with the Weibel-Palade body proteins von Willebrand factor or P-selectin (Hayward *et al*., 1998).

Peptides and proteins may contain signalling motifs that serve as important determinants for differential packaging at the *trans*-Golgi network. For example, the cytoplasmic and transmembrane domains of the integral membrane glycoprotein, P-selectin enhance the efficiency of endothelial storage graunule targeting (Fleming *et al*., 1998). Factor VIII is a coagulation protein that does not appear to possess signalling motifs for mobilization to the regulated pathway. However, when Factor VIII was co-transfected with von Willebrand factor in AtT-20 cells it displayed altered intracellular trafficking from a constitutive to a regulated secretory pathway (Rosenberg *et al*., 1998). This suggests that proteins containing signalling motifs, such as von Willebrand factor, may chaperone other proteins that lack such structural determinants. It is not known whether big ET-1 contains signalling motifs that confer granular targeting. The localization of big ET-1 like immunoreactivity in Weibel-Palade bodies (Russell *et al*., 1998c) and secretory vesicles (Harrison *et al*., 1995) suggest that the peptide has no sorting domain. Mobilization of big ET-1 into secretory vesicles and granules may involve passive bulk flow in which the amount of peptide entering each pathway is determined by internal volume of the vesicle or granule and the number of the compartments formed per unit time (Kelly, 1985).

We have recently proposed that endothelial cell storage granules are an important site in the processing of big ET-1 to the mature peptide (Russell *et al*., 1998c,d). Antisera raised against big ET-1 and the isoforms of ECE-1 (ECE-1α and ECE-1β) were found to co-localize with von Willebrand factor in round to rod-shaped structures located beneath the plasma membrane (Figure 1). ECE activity that was sensitive to phosphoramidon and the ECE-1 selective inhibitor, PD159790 (Ahn *et al*., 1998) but insensitive to thiorphan was identified in subcellular sucrose fractions of HUVECs prepared by gradient centrifugation (unpublished findings). 5′-Nucleotidase activity, a marker for the plasma membrane, was identified in several fractions containing ECE activity, consistent with expression of ECE on the cell surface. However, high density fractions that contained only low levels of 5′-nucleotidase activity contained ECE activity and the storage granule glycoprotein, von Willebrand factor thus presenting the possibility that an active converting enzyme is expressed in the endothelial granules.

Several *in vivo* findings indicate that physiological or pathophysiological stimuli can lead to release of ET *via* the regulated secretory pathway. For example, high plasma ET levels were measured in a patient during the early phase of treatment for accidental hypothermia induced by cold water immersion (Yoshitomi *et al*., 1998). This type of stimulus has been proposed to mediate release of ET from endothelial cell storage granules. When healthy volunteers were subjected to a cold pressor test in which the forearm was immersed in ice water, an increase in venous plasma ET concentration was detected within 2 min (Fyhrquist *et al*., 1990). The detection of ET was too rapid to indicate *de novo* synthesis of the peptide and suggests release from intracellular stores.

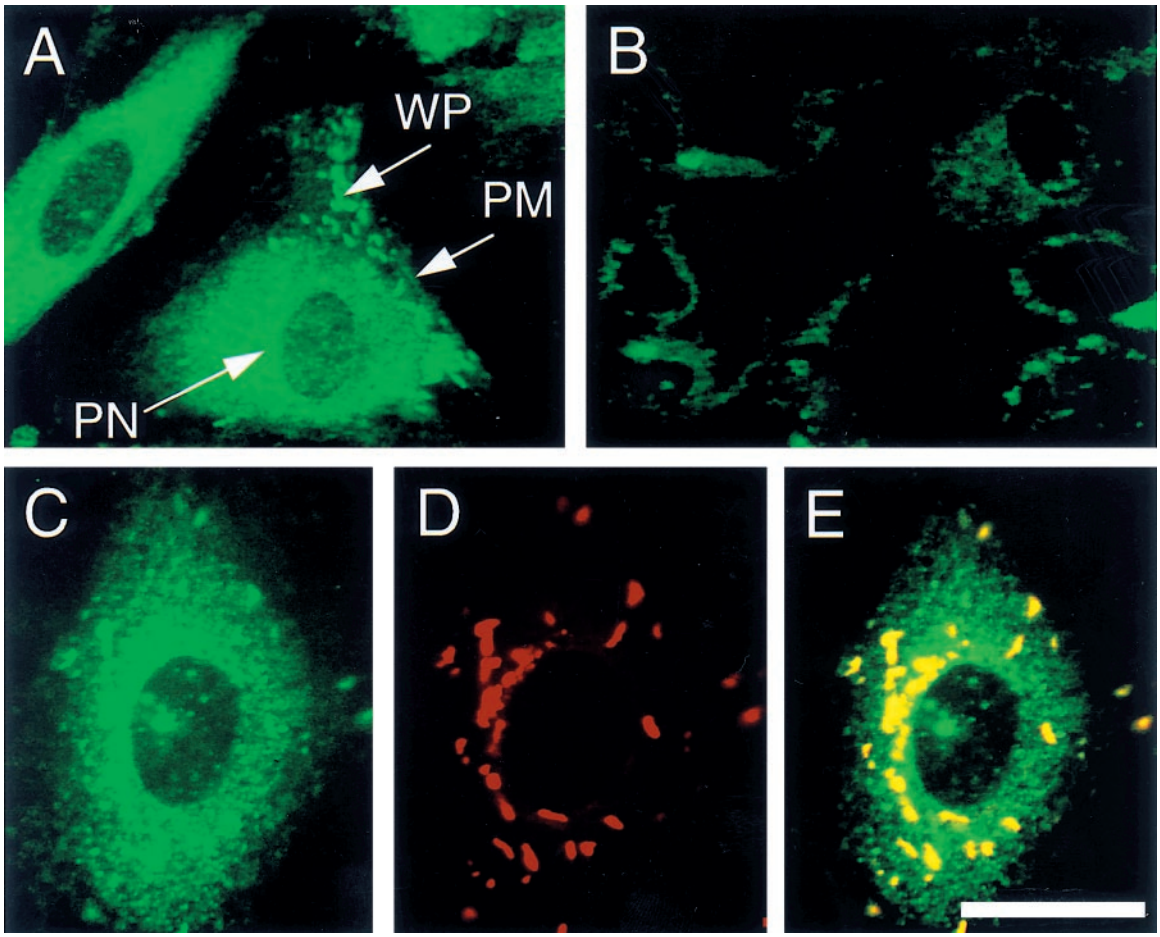

Figure 1 Microscopy of permeabilized human umbilical vein endothelial cells immunolabelled with antisera raised against ECE-1. Cells labelled with the ECE-1 antibody and a secondary fluoresceinated goat anti-rabbit antibody showed positive immunofluorescence staining over the perinuclear region (PN) and Weibel-Palade bodies (WP) (A). Only a moderate level of immunoreactive staining was detected over the plasma membrane (PM). Cells incubated with preimmune serum showed negligible staining (B). Cells were double labelled with antisera to ECE-1 (C) and von Willebrand factor (D). Electronic overlay of images to ECE-1 and von Willebrand factor (E) revealed co-localization in Weibel-Palade bodies (yellow). Scale bar = 70 μm (A, B) and 40 μm (C–E).

Other mechanical and chemical stimuli mediate degranulation of Weibel-Palade bodies. Mechanical stretch applied to cultured bovine aortic endothelial cells produced rapid release of ET into the culture medium ($\leqslant$20 min) (Macarthur *et al*., 1994). The calcium ionophore A23187, which elevates $[Ca^{2+}]_i$, also mediated release of von Willebrand factor (Loesberg *et al*., 1983; Sporn *et al*., 1989) and ET (Russell *et al*., 1998c) from cultured HUVECs. Phorbol 12-myristate 13-acetate mediates degranulation by activation of protein kinase C and it is speculated that other as yet uncharacterized signal-transduction mechanisms may be important for full induction of the regulated secretory pathway by agonists such as histamine and thrombin (Carew *et al*., 1992).

Physiological and pathophysiological implications of dual transport pathways for ET

Identification of a dual secretory pathway for release of ET-1 is a recent and novel finding, not previously reported for a vasoactive peptide (Figure 2). Dual transport pathways have been described for other proteins, including von Willebrand factor and tissue-type plasminogen activator in endothelial cells and adrenocorticotropic hormone (ACTH) in pituitary tumor cells (Gumbiner & Kelly, 1982; Sporn *et al*., 1986; Mayadas *et al*., 1989; Emeis *et al*., 1997). ACTH precursor and all multimeric forms of von Willebrand factor are released constitutively whilst only mature ACTH and von Willebrand factor are released following an appropriate stimulus (Gumbiner & Kelly, 1982; Sporn *et al*., 1986; Mayadas *et al*., 1989).

Several studies have examined the polarity of secretion of proteins from endothelial cells. Whereas constitutive release of von Willebrand factor from HUVECs is reportedly nonpolarized, 90% of the glycoprotein secreted by the regulated pathway is toward the basolateral membrane (Sporn *et al*., 1989). Other studies show that the constitutive pathway may be polarized with the majority of ET-1 produced in HUVECs and porcine cerebral microvessel endothelia released from the basolateral membrane (Yoshimoto *et al*., 1991; Wagner *et al*., 1992). Directional secretion of ET-1 to the smooth muscle layer is consistent with the hypothesis that the peptide modulates vasomotor tone through local paracrine rather than humoral systemic effects. An additional autocrine effect is involved in ET-1 mediated vasodilatation. Activation of endothelial ET_B receptors by ET-1 mediates synthesis of nitric oxide which in turn stimulates guanylate cyclase in the smooth muscle leading to relaxation.

Under normal physiological conditions endothelin and nitric oxide are constitutively released by the endothelium and provide a balance between vasoconstrictor and vasodilator activity. However, vascular injury can compromise endothelial cell integrity and cause reduced nitric oxide synthesis and over production of ET-1. Release of ET and von Willebrand factor (Ewenstein *et al*., 1987) *via* the regulated secretory pathway may provide an initial haemostatic response to vascular endothelial cell damage.

Novel ECE inhibitors

Intracellular ECE activity amounts to 85% of total activity in endothelial cells (Davenport *et al*., 1998b) which leads us to propose that an effective therapeutic inhibitor of the enzyme must first penetrate the plasma membrane. Although phosphoramidon is a valuable tool that enables examination of ECE activity, the compound is non-selective, efficiently blocking NEP activity. ECE and NEP activity can be

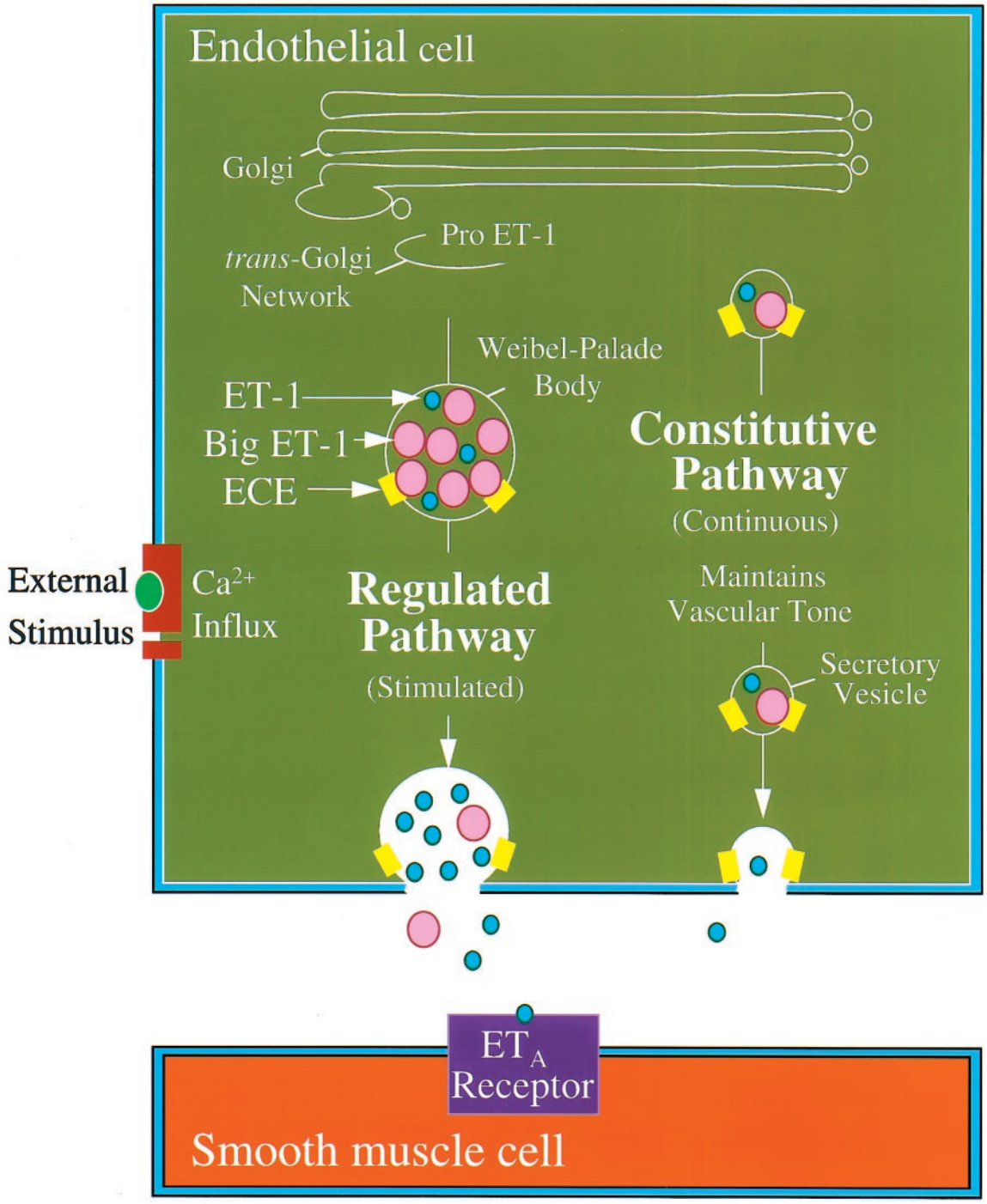

Figure 2 Schematic model of ET-1 transport in the human coronary artery. In this model, it is proposed that two distinct exocytic pathways are involved in the transport of ET-1 to the cell surface. ET-1 is stored in Weibel-Palade bodies with other vasoactive compounds and is released at the cell surface following an appropriate stimulus. ET-1 is also sorted into secretory vesicles and continuously released by a cyclic AMP independent constitutive pathway. It is proposed that a small amount of ET-1 is released luminally from this pathway, binding to ET_B receptors on the endothelial cells to indirectly release vasodilators. However, most ET-1 is released (>80%) from the abluminal surface where it can activate the vasoconstrictor ET_A receptors that predominate on human vascular smooth muscle cells. It is hypothesized that this continuous release *via* the constitutive pathway contributes to the maintenance of normal physiological tone.

differentiated by comparing the effects of phosphoramidon with the NEP selective inhibitor, thiorphan.

CGS 26303 and CGS 31447 are non-peptide ECE inhibitors that have IC_{50} values of 1.1 μM and 17 nM, respectively for ECE-1 inhibition (De Lombaert *et al*., 1994; 1997). However, neither compound is selective for ECE-1 with IC_{50} values of 0.9 and 4.8 nM, respectively, for inhibition of NEP. In a rabbit model of subarachnoid haemorrhage, administration of CGS 26303 both prevented and reversed cerebral vasospasm (Kwan *et al*., 1997), thus indicating the therapeutic potential of ECE inhibitors. SCH 54470 is an orally active triple inhibitor of ECE, NEP and the angiotensin converting enzyme, with IC_{50} values of 80, 90 and 2.5 nM, respectively (Vemulapalli *et al*., 1997). This inhibitor reduced ischaemia induced ET release in isolated perfused guinea-pig lungs, indicating inhibition of endogenous converting enzyme activity. The therapeutic benefit of non-selective inhibitors of ECE and NEP awaits further investigation. Whilst inhibition of NEP may be beneficial in reducing degradation of atrial natriuretic peptide, an endogenous vasodilator, its inhibition has been shown to cause vasoconstriction of human resistance vessels *in vivo* (Ferro *et al*., 1998). This latter effect is presumably a result of decreased ET degradation since NEP is highly efficient at cleaving the mature peptide at Asp^{18}-Ile^{19} to produce inactive fragments (Sokolovsky *et al*., 1990).

A number of ECE inhibitors that are derived from natural products have been reported with varying degrees of selectivity for ECE (Table 1). WS75624A and WS75624B are ECE inhibitors isolated from the fermentation broth of *Saccharothrix sp*. (Tsurumi *et al*., 1995a). The compounds have similar inhibitory characteristics against selected metalloproteases with 30–40 fold selectivity for ECE ($IC_{50} = 0.03$ $\mu g\ ml^{-1}$) over collagenase ($IC_{50} = 1.0$ $\mu g\ ml^{-1}$) and NEP ($IC_{50} = 1.25$ $\mu g\ ml^{-1}$). WS79089B, isolated from the culture broth of *Streptosporangium roseum* (Tsurumi *et al*., 1995b), has a higher reported selectivity for ECE ($IC_{50} = 0.14$ μM) over collagenase and NEP (no inhibition at 50 μM). The sodium salt of this compound, FR901533 was effective in inhibiting the pressor effect of big ET-1 when administered intravenously in rats (Tsurumi *et al*., 1995b). This compound was also protective against the development of right ventricular overload and medial thickening of pulmonary arteries in rats with monocrotaline-induced pulmonary hypertension (Takahashi *et al*., 1998).

A series of arylacetylene-containing compounds also display selectivity for the inhibition of ECE over NEP (Wallace *et al*., 1998). An arylacetylene amino phosphonate dipeptide was found to inhibit ECE and NEP with IC_{50} values of 28 nM and 6.3 μM, respectively (225 fold selectivity for ECE over NEP). Greater selectivity (725 fold) was obtained with a tripeptide derivative, with IC_{50} values of 8 nM and 5.8 μM for the inhibition of ECE and NEP, respectively. Pretreatment of rats with these compounds inhibited increased mean arterial pressure produced by intravenous bolus injection of big ET-1. PD069185, a trisubstituted quinazoline, is the first ECE-1 selective inhibitor to be reported ($IC_{50} = 0.9$ μM). This compound has no effect on ECE-2 at a concentration of 100 μM and only marginal effects on NEP, stromelysin, gelatinase A, collegenase, interleukin-1β converting enzyme and thrombin at 100–300 μM (Ahn *et al*., 1998). Replacement of the $-CCl_3$ group of PD069185 with $-CF_3$ (PD159790) increased solubility without affecting selectivity. In biochemical experiments, 100 μM PD159790 effectively abolished conversion of big ET-1 to ET-1 in HUVEC cultures (Russell *et al*., 1998e). Although PD069185 was slightly more potent than PD159790 in inhibiting ET-1 production by cocultures of CHO/ECE-1 and CHO/prepro-ET-1 cells ($EC_{50} = 3.8$ and 11.5 μM, respectively), the latter compound was less toxic (Ahn *et al*., 1998). The cellular toxicity concentration for PD069185 was $TC_{50} = 56$ μM whereas no toxicity was observed at concentrations up to 100 μM for PD159790.

Do other ECEs exist?

Although ECE-1 appears to be the predominant endothelin converting enzyme in mammalian tissues, recent studies indicate that other ECEs may also have a physiological role in big ET processing. Future studies will need to identify converting enzymes involved in processing of the big ET isoforms and to determine their cell surface or intracellular localization.

Recently, Schweizer *et al*. (1997) proposed three isoforms of ECE-1 encoded by the same gene. The isoform designated as ECE-1a has an identical sequence to ECE-1β (Valdenaire *et al*., 1995; Schweizer *et al*., 1997). The isoforms designated ECE-1b and ECE-1c have an identical sequence to ECE-1α except that the N-terminus is predicted to be extended by an additional 17 and 1 amino acids, respectively in each isoform. The functional importance of the different isoforms is presently unclear since all three enzymes expressed in CHO cells have similar kinetic rate constants for processing of big ET precursors to the corresponding mature peptides. However, ELISAs using antisera directed to the N-terminus of ECE-1α/ECE-c indicate that this isoform predominates in human tissue compared with ECE-1β/ECE-1a (Mockridge *et al*., 1998).

Targeted null mutation in the mouse ECE-1 gene produces embryos that exhibit marked craniofacial and cardiac defects as well as an absence of epidermal melanocytes and enteric neurons of the distal gut (Yanagisawa *et al*., 1998). Surprisingly, high levels of mature ET peptide were detectable in the homozygous ECE-1 knockout embryos, leading the authors to speculate that a further non-ECE-1 protease is expressed, for example ECE-2 (Yanagisawa *et al*., 1998). It has

Table 1 Selected endothelin converting enzyme inhibitors

Type of inhibitor	*Compound*	*IC_{50}*	*Reference*
Natural products	WS75624A WS75624B	0.03 $\mu g\ ml^{-1}$	(Tsurumi *et al*., 1995a)
	WS79089B (FR901533)	0.14 μM	(Tsurumi *et al*., 1995b)
Trisubstituted quinazolines	PD069185	0.9 μM	(Ahn *et al*., 1998)
	PD159790	–	
Arylacetylene aminophosphates	–	8–28 nM	(Wallace *et al*., 1998)

–, value not reported.

been postulated that ECE-2, which has optimal activity at pH = 5.5, may have a role in processing big ET-1 in the *trans*-Golgi network where the vesicular fluid is acidified (Emoto & Yanagisawa, 1995). It remains to be determined whether converting enzymes with acidic pH optimum, such as ECE-2 have a pathogenic role in diseases in which cellular pH is reduced, for example ischaemic heart disease. Hearts subjected to global ischaemia show lactate accumulation with concomitant intracellular acidosis (intracellular pH = 5.8; Docherty *et al*., 1997), and a correlation between myocardial ischaemia and increased plasma levels of ET is now well established (Tonnessen *et al*., 1993; Cohn, 1996).

ET-3 has been detected in human plasma but the efficiency of cloned ECE-1 to convert big ET-3 to the mature peptide is usually low or not detectable. Several findings have indicated the possible existence of another converting enzyme in neuronal cells. These cells lack detectable levels of ECE-1 mRNA (Xu *et al*., 1994), but produce ET-3 (Shinmi *et al*., 1989; Fuxe *et al*., 1991) suggesting the existence of a big ET-3 specific converting enzyme. Interestingly, a novel endothelin converting enzyme (ECE-3) was purified by SDS–PAGE from bovine iris microsomes that has specificity for big ET-3 (Hasegawa *et al*., 1998). This enzyme contrasts to ECE-1 and ECE-2, both of which have specificity for big ET-1 and big ET-2, and may potentially modulate ET-3 production in the nerve terminals.

ECE expressed on endothelial cells may also differ to ECE expressed on vascular smooth muscle cells. Whilst endothelial ECE has been found to have specificity for big ET-1 (Plumpton *et al*., 1996; Davenport *et al*., 1998b), smooth muscle ECE is capable of processing big ET-1, big ET-2 and big ET-3 (Tsukahara *et al*., 1993; Maguire *et al*., 1997; Davenport *et al*., 1998b). The physiological role of this and other novel putative converting enzymes on regulation of ET production remains to be determined.

In conclusion, evidence is emerging within endothelial cells for the continuous release of ET *via* the constitutive pathway for maintenance of normal vascular tone. In addition, further release of ET, possibly in high concentrations *via* the regulated pathway, may be involved in responses to vascular injury. Intracellular ECEs present within the secretory pathways are therefore potential therapeutic targets for diseases in which ET has been implicated.

This work was supported by grants from the British Heart Foundation, Isaac Newton Trust, and the Royal Society.

References

AHLBORG, G., OTTOSSON-SEEBERGER, A., HEMSÉN, A. & LUNDBERG, J.M. (1994). Big ET-1 infusion in man causes renal ET-1 release, renal and splanchnic vasoconstriction, and increased mean arterial blood pressure. *Cardiovasc. Res.,* **28,** 1559–1563.

AHN, K., SISNEROS, A.M., HERMAN, S.B., PAN, S.M., HUPE, D., LEE, C., NIKAM, S., CHENG, X.-M., DOHERTY, A.M., SCHROEDER, R.L., HALEEN, S.J., KAW, S., EMOTO, N. & YANAGISAWA, M. (1998). Novel selective quinazoline inhibitors of endothelin converting enzyme-1. *Biochem. Biophys. Res. Commun.,* **243,** 184–190.

BACON, C.R., CARY, N.R.B. & DAVENPORT, A.P. (1996). Endothelin peptide and receptors in human atherosclerotic coronary artery and aorta. *Circ. Res.,* **79,** 794–801.

BARNES, K., BROWN, C. & TURNER, A.J. (1998). Endothelin-converting enzyme. Ultrstructural localization and its recycling from the cell surface. *Hypertension,* **31,** 3–9.

BARNES, K., SHIMADA, K., TAKAHASHI, M., TANZAWA, K. & TURNER, A.J. (1996). Metallopeptidase inhibitors induce an up-regulation of endothelin-converting enzyme levels and its redistribution from the plasma membrane to an intracellular compartment. *J. Cell. Sci.,* **109,** 919–928.

CAREW, M.A., PALEOLOG, E.M. & PEARSON, J.D. (1992). The roles of protein kinase C and intracellular Ca^{2+} in the secretion of von Willebrand factor from human vascular endothelial cells. *Biochem. J.,* **286,** 631–635.

COHN, J.N. (1996). Is there a role for endothelin in the natural history of heart failure? *Circulation,* **94,** 604–606.

CORDER, R., KHAN, N. & HARRISON, V.J. (1995). A simple method for isolating human endothelin converting enzyme free from contamination by neutral endopeptidase 24.11. *Biochem. Biophys. Res. Commun.,* **207,** 355–362.

DAVENPORT, A.P., KUC, R.E. & MOCKRIDGE, J.W. (1998b). Endothelin-converting enzyme in the human vasculature: evidence for differential conversion of big endothelin-3 by endothelial and smooth-muscle cells. *J. Card. Pharmacol.,* **31,** S1–S3.

DAVENPORT, A.P., KUC, R.E., PLUMPTON, C., MOCKRIDGE, J.W., BARKER, P.J. & HUSKISSON, N.S. (1998a). Endothelin-converting enzyme in human tissues. *Histochem. J.,* **30,** 359–374.

DE LOMBAERT, S., GHAI, R.D., JENG, A.Y., TRAPANI, A.J. & WEBB, R.L. (1994). Pharmacological profile of a non-peptidic dual inhibitor of neutral endopeptidase 24.11 and endothelin-converting enzyme. *Biochem. Biophys. Res. Commun.,* **204,** 407–412.

DE LOMBAERT, S., STAMFORD, L.B., BLANCHARD, L., TAN, J., HOYER, D., DIEFENBACHER, C.G., WEI, D.C., WALLACE, E.M., MOSKAL, M.A., SAVAGE, P. & JENG, A.Y. (1997). Potent non-peptidic dual inhibitors of endothelin-converting enzyme and neutral endopeptidase 24.11. *Bioorg. Med. Chem. Lett.,* **7,** 1059–1064.

DOCHERTY, J.C., GUNTER, H.E., KUZIO, B., SHOEMAKER, L., YANG, L.J. & DESLAURIERS, R. (1997). Effects of cromakalim and glibenclamide on myocardial high energy phosphates and intracellular pH during ischemia-reperfusion: P-31 NMR studies. *J. Mol. Cell. Cardiol.,* **29,** 1665–1673.

DOI, Y., OZAKA, T., FUKUSHIGE, H., FURUKAWA, H., YOSHIZUKA, M. & FUJIMOTO, S. (1996). Increase in number of Weibel-Palade bodies and endothelin-1 release from endothelial cells in the cadmium-treated rat thoracic aorta. *Virchows Arch.,* **428,** 367–373.

DOI, Y., OZAKA, T., KATSUKI, M., FUKUSHIGE, H., TOYAMA, E., KANAZAWA, Y., ARASHIDANI, K. & FUJIMOTO, S. (1995). Histamine release from Weibel-Palade bodies of toad aortas induced by endothlin-1 and sarafotoxin-S6b. *Anat. Rec.,* **242,** 374–382.

EMEIS, J.J., VAN DEN EIJNDEN-SCHRAUWEN, Y., VAN DEN HOOGEN, C.M., DE PRIESTER, W., WESTMUCKETT, A. & LUPU, F. (1997). An endothelial storage granule for tissue-type plasminogen activator. *J. Cell. Biol.,* **139,** 245–256.

EMOTO, N. & YANAGISAWA, M. (1995). Endothelin-converting enzyme-2 is a membrane-bound, phosphoramidon-sensitive metalloprotease with acidic pH optimum. *J. Biol. Chem.,* **270,** 15262–15268.

EWENSTEIN, B.M., WARHOL, M.J., HANDIN, R.I. & POBER, J.S. (1987). Comparison of the von Willebrand factor storage organelle (Weibel-Palade body) isolated from cultured human umbilical vein endothelial cells. *J. Cell. Biol.,* **104,** 1423–1433.

FARQUHAR, M.G. (1985). Progress in unraveling pathways of Golgi traffic. *Annu. Rev. Cell. Biol.,* **1,** 447–488.

FERRO, C.J., SPRATT, J.C., HAYNES, W.G. & WEBB, D.J. (1998). Inhibition of neutral endopeptidase causes vasoconstriction of human resistance vessels in vivo. *Circulation,* **97,** 2323–2330.

FLEMING, J.C., BERGER, G., GUICHARD, J., CRAMER, E.M. & WAGNER, D.D. (1998). The transmembrane domain enhances granular targeting of P-selectin. *Eur. J. Cell. Biol.,* **75,** 331–343.

FUJIMOTO, S., YAMAMOTO, K., ARASHIDANI, K., HAYABUCHUCHI, I., YOSHIZUKA, M. & NOMIYAMA, T. (1982). Endothelial specific granules in the umbilical veins of the postnatal rabbit. *Cell. Tissue Res.,* **227,** 509–518.

FUXE, K., TINNER, B., STAINES, W., HEMSEN, A., HERSH, L. & LUNDBERG, J.M. (1991). Demonstration and nature of endothelin-3-like immunoreactivity in somatostatin and choline acetyltransferase-immunoreactive nerve-cells of the neostratum of the rat. *Neurosc. Lett.,* **123,** 107–111.

FYHRQUIST, F., SAIJONMAA, O., METSÄRINNE, K., TIKKANEN, I., ROSENLÖF, K. & TIKKANEN, T. (1990). Raised plasma endothelin-1 concentration following cold pressor test. *Biochem. Biophys. Res. Commun.,* **169,** 217–221.

GUI, G., XU, D., EMOTO, N. & YANAGISAWA, M. (1993). Intracellular localization of membrane-bound endothelin-converting enzyme from rat lung. *J. Cardiovasc. Pharmacol.,* **22,** S53–S56.

GUMBINER, B. & KELLY, R.B. (1982). Two distinct intracellular pathways transport secretory and membrane glycoproteins to the surface of pituitary tumor cells. *Cell,* **28,** 51–59.

HAMASAKI, K., DOI, Y., SAKAMOTO, Y., KASHIMURA, M. & FUJIMOTO, S. (1995). The contraction of small arteries in the perimetrium by presurgical medication with the luteinizing hormone-releasing hormone agonist to patients with leiomyomas: an electron and immunoelectron microscopy. *Fukuoka Acta Med.,* **86,** 389–397.

HARRISON, V.J., BARNES, K., TURNER, A.J., WOOD, E., CORDER, R. & VANE, J.R. (1995). Identification of endothelin 1 and big endothelin 1 in secretory vesicles isolated from bovine aortic endothelial cells. *Proc. Natl. Acad. Sci. U.S.A.,* **92,** 6344–6348.

HARRISON, V.J., CORDER, R., ÄNGGÅRD, E.E. & VANE, J.R. (1993). Evidence for vesicles that transport endothelin-1 in bovine aortic endothelial cells. *J. Cardiovasc. Pharmacol.,* **22,** S57–S60.

HASEGAWA, H., HIKI, K., SAWAMURA, T., AOYAMA, T., OKAMOTO, Y., MIWA, S., SHIMOHAMA, S., KIMURA, J. & MASAKI, T. (1998). Purification of a novel endothelin-converting enzyme specific for big endothelin-3. *FEBS. Lett.,* **428,** 304–308.

HAYNES, W.G. (1995). Endothelins as regulators of vascular tone in man. *Clin. Sci.,* **88,** 509–517.

HAYNES, W.G., FERRO, C.E. & WEBB, D.J. (1995). Physiologic role of endothelin in maintenance of vascular tone in humans. *J. Cardiovasc. Pharmacol.,* **26,** S183–S185.

HAYNES, W.G. & WEBB, D.J. (1994). Contribution of endogenous generation of endothelin-1 to basal vascular tone. *Lancet,* **344,** 852–854.

HAYWARD, C.P.M., CRAMER, E.M., SONG, Z., ZHENG, S., FUNG, R., MASSÉ, J.-M., STEAD, R.H. & PODOR, T.J. (1998). Studies of multimerin in human endothelial cells. *Blood,* **91,** 1304–1317.

HEMSÉN, A., AHLBORG, G., OTTOSSON-SEEBERGER, A. & LUNDBERG, J.M. (1995). Metabolism of big endothelin-1 (1-38) and (22-38) in the human circulation in relation to production of endothelin-1 (1-21). *Reg. Peptides,* **55,** 287–297.

HERMAN, W.H., EMANCIPATOR, S.N., RHOTEN, R.L.P. & SIMONSON, M.S. (1998). Vascular and glomerular expression of endothelin-1 in normal human kidney. *Am. J. Physiol.,* **44,** F8–F17.

KELLY, R.B. (1985). Pathways of protein secretion in eukaryotes. *Science,* **230,** 25–32.

KORTH, P., EGIDY, G., PARNOT, C., LEMOULLEC, J.-M., CORVOL, P. & PINET, F. (1997). Construction, expression and characterization of a soluble form of human endothelin-converting-enzyme-1. *FEBS. Lett.,* **417,** 365–370.

KURIHARA, H., YOSHIZUMI, M., SUGIYAMA, T., YAMAOKI, K., NAGAI, R., TAKAKU, F., SATOH, H., INUI, J., YANAGISAWA, M., MASAKI, T. & YAZAKI, Y. (1989). The possible role of endothelin-1 in the pathogenesis of coronary vasospasm. *J. Cardiovasc. Pharmacol.,* **13,** S132–S137.

KWAN, A.L., BAVBEK, M., JENG, A.Y., MANIARA, W., TOYODA, T., LAPPE, R.W., KASSELL, N.F. & LEE, K.S. (1997). Prevention and reversal of cerebral vasospasm by an endothelin-converting enzyme inhibitor, CGS 26303, in an experimental model of subarachnoid hemorrhage. *J. Neurosurg.,* **87,** 281–286.

LOESBERG, C., GONSALVES, M.D., ZANDBERGEN, J., WILLEMS, C., VAN AKEN, W.G., STEL, H.V., VAN MOURIK, J.A. & DE GROOT, P.G. (1983). The effect of calcium on the secretion of factor VIII-related antigen by cultured human endothelial cells. *Biochim. Biophys. Acta.,* **763,** 160–168.

MACARTHUR, H., WARNER, T.D., WOOD, E.G., CORDER, R. & VANE, J.R. (1994). Endothelin-1 release from endothelial cells in culture is elevated both acutely and chronically by short periods of mechanical stretch. *Biochem. Biophys. Res. Commun.* **200,** 395–400.

MAGUIRE, J.J., JOHNSON, C.M., MOCKRIDGE, J.W. & DAVENPORT, A.P. (1997). Endothelin converting enzyme (ECE) activity in human vascular smooth muscle. *Br. J. Pharmacol.,* **122,** 1647–1654.

MAYADAS, T., WAGNER, D.D. & SIMPSON, P.J. (1989). von Willebrand factor biosynthesis and partitioning between constitutive and regulated pathways of secretion after thrombin stimulation. *Blood,* **73,** 706–711.

MCEVER, R.P., BECKSTEAD, J.H., MOORE, K.L., MARSHALL-CARLSON, L. & BAINTON, D.F. (1989). GMP-140, a platelet α-granule membrane protein, is also synthesized by vascular endothelial cells and is localized in Weibel-Palade bodies. *J. Clin. Invest.,* **84,** 92–99.

MOCKRIDGE, J.W., KUC, R.E., HUSKISSON, N.S., BARKER, P.J. & DAVENPORT, A.P. (1998). Characterization of site-directed antisera against endothelin-converting enzymes (ECE-1α and ECE-1β). *J. Cardiovasc. Pharmacol.,* **31,** S35–S37.

MOLDOVAN, F., BENANNI, H., FIET, J., CUSSENOT, O., DUMAS, J., DARBORD, C. & SOLIMAN, H.R. (1996). Establishment of permanent human endothelial-cells achieved by transfection with SV40 large T-antigen that retain typical phenotypical and functional-characteristics. *In Vitro Cell. Dev. Biol.,* **32,** 16–23.

OPGENORTH, T.J., WU-WONG, J.R. & SHIOSAKI, K. (1992). Endothelin-converting enzymes. *FASEB. J.,* **6,** 2653–2659.

OZAKA, T., DOI, Y., KAYASHIMA, K. & FUJIMOTO, S. (1997). Weibel-Palade bodies as a storage site of calcitonin gene-related peptide and endothelin-1 in blood vessels of the rat carotid body. *Anat. Rec.,* **247,** 388–394.

PLUMPTON, C., ASHBY, M.J., KUC, R.E., O'REILLY, G. & DAVENPORT, A.P. (1996). Expression of endothelin peptides and mRNA in the human heart. *Clin. Sci.,* **90,** 37–46.

PLUMPTON, C., HAYNES, W.G., WEBB, D.J. & DAVENPORT, A.P. (1995). Phosphoramidon inhibition of the *in vivo* conversion of big endothelin-1 to endothelin-1 in the human forearm. *Br. J. Pharmacol.,* **116,** 1821–1828.

ROSENBERG, J.B., FOSTER, P.A., KAUFMAN, R.J., VOKAC, E.A., MOUSSALLI, M., KRONER, P.A. & MONTGOMERY, R.R. (1998). Intracellular trafficking of factor VIII to von Willebrand factor storage grranules. *J. Clin. Invest.,* **101,** 613–624.

RUSSELL, F.D., COPPELL, A.L. & DAVENPORT, A.P. (1998a). In vitro enzymatic processing of radiolabelled big ET-1 in human kidney. *Biochem. Pharmacol.,* **55,** 697–701.

RUSSELL, F.D., SKEPPER, J.N. & DAVENPORT, A.P. (1998b). Endothelin peptide and converting enzymes in human endothelium. *J. Cardiovasc. Pharmacol.,* **31,** S19–S21.

RUSSELL, F.D., SKEPPER, J.N. & DAVENPORT, A.P. (1998c). Human endothelial cell storage granules. A novel intracellular site for isoforms of the endothelin-converting enzyme. *Circ. Res.,* **83,** 314–321.

RUSSELL, F.D., SKEPPER, J.N. & DAVENPORT, A.P. (1998d). Evidence using immunoelectron microscopy for regulated and constitutive pathways in the transport and release of endothelin. *J. Cardiovasc. Pharmacol.,* **31,** 424–430.

RUSSELL, F.D., SKEPPER, J.N., CHENG, X.M., AHN, K. & DAVENPORT, A.P. (1998e). Evidence for an intracellular endothelin converting enzyme in human endothelial cells. *Nuanyn Schmiedebergs Arch. Pharmacol.,* **358,** R710.

SAKAMOTO, Y., DOI, Y., OHSATO, K. & FUJIMOTO, S. (1993). Immunoelectron microscopy on the localization of endothelin in the umbilical vein of perinatal rabbits. *Anat. Rec.,* **237,** 482–488.

SALEH, D., FURUKAWA, K., TSAO, M.S., MAGHAZACHI, A., CORRIN, B., YANAGISAWA, M., BARNES, P.J. & GIAID, A. (1997). Elevated expression of endothelin-1 and endothelin-converting enzyme-1 in idiopathic pulmonary fibrosis: possible involvement of proinflammatory cytokines. *Am. J. Resp. Cell. Mol. Biol.,* **16,** 187–193.

SANSOM, C.E., HOANG, V.M. & TURNER, A.J. (1995). Molecular modeling of the active site of endotehlin-converting enzyme. *J. Card. Pharmacol.,* **26,** S75–S77.

SCHMIDT, M., KRÖGER, B., JACOB, E., SEULBERGER, H., SUBKOWSKI, T., OTTER, R., MEYER, T., SCHMALZING, G. & HILLEN, H. (1994). Molecular characterization of human and bovine endothelin converting enzyme (ECE-1). *FEBS. Lett.,* **356,** 238 – 243.

SCHWEIZER, A., VALDENAIRE, O., NELBÖCK, P., DEUSCHLE, U., DUMAS MILNE EDWARDS, J.-B., STUMPF, J.G. & LÖFFLER, B.-M. (1997). Human endothelin-converting enzyme (ECE-1): three isoforms with distinct subcellular localizations. *Biochem. J.,* **328,** 871 – 877.

SHIMADA, K., MATSUSHITA, Y., WAKABAYASHI, K., TAKAHASHI, M., MATSUBARA, A., IIJIMA, Y. & TANZAWA, K. (1995). Cloning and functional expression of human endothelin-converting enzyme cDNA. *Biochem. Biophys. Res. Commun.,* **207,** 807 – 812.

SHINMI, O., KIMURA, S., SAWAMURA, T., SUGITA, Y., YOSHIZAWA, T., UCHIYAMA, Y., YANAGISAWA, M., GOTO, K., MASAKI, T. & KANAZAWA, I. (1989). Endothelin-3 is a novel neuropeptide: isolation and sequence determination of endothelin-1 and endothelin-3 in porcine brain. *Biochem. Biophys. Res. Commun.,* **164,** 587 – 593.

SOKOLOVSKY, M., GALRON, R., KLOOG, Y., BDOLAH, A., INDIG, F.E., BLUMBERG, S. & FLEMINGER, G. (1990). Endothelins are more sensitive than sarafotoxins to neutral endopeptidase: possible physiological significance. *Proc. Natl. Acad. Sci. U.S.A.,* **87,** 4702 – 4706.

SPORN, L.A., MARDER, V.J. & WAGNER, D.D. (1986). Inducible secretion of large, biologically potent von Willebrand factor multimers. *Cell,* **46,** 185 – 190.

SPORN, L.A., MARDER, V.J. & WAGNER, D.D. (1989). Differing polarity of the constitutive and regulated pathways for von Willebrand factor in endothelial cells. *J. Cell. Biol.,* **108,** 1283 – 1289.

TAKAHASHI, M., FUKUDA, K., SHIMADA, K., BARNES, K., TURNER, A.J., IKEDA, M., KOIKE, H., YAMAMOTO, Y. & TANZAWA, K. (1995). Localization of rat endothelin-converting enzyme to vascular endothelial cells and some secretory cells. *Biochem. J.,* **311,** 657 – 665.

TAKAHASHI, T., KANDA, T., INOUE, M., SUMINO, H., KOBAYASHI, I., IWAMOTO, A. & NAGAI, R. (1998). Endothelin converting enzyme inhibitor protects development of right ventricular overload and medial thickening of pulmonary arteries in rats with monocrotaline-induced pulmonary hypertension. *Life Sci.,* **63,** PL137 – PL143.

TONNESSEN, T., NAESS, P.A., KIRKEBOEN, K.A., OFFSTAD, J., ILEBEKK, A. & CHRISTENSEN, G. (1993). Release of endothelin from the porcine heart after short-term coronary-artery occlusion. *Cardiovasc. Res.,* **27,** 1482 – 1485.

TSUKAHARA, Y., MATSUMURA, Y., KUNINOBU, K., KOJIMA, T., TAKAOKA, M. & MORIMOTO, S. (1993). Phosphoramidon-sensitive endothelin converting enzyme in cultured vascular smooth muscle cells converts big endothelin-3 to endothelin-3. *Life Sci.,* **53,** 465 – 471.

TSURUMI, Y., FUJIE, K., NISHIKAWA, M., KIYOTO, S. & OKUHARA, M. (1995b). Biological and pharmacological properties of highly selective new endothelin converting enzyme inhibitor WS79089B isolated from *Streptosporangium roseum* No. 79089. *J. Antibiotics,* **48,** 169 – 174.

TSURUMI, Y., UEDA, H., HAYASHI, K., TAKASE, S., NISHIKAWA, M., KIYOTO, S. & OKUHARA, M. (1995a). WS75624 A and B, new endothelin converting enzyme inhibitors isolated from *Saccharothrix sp.* No. 75624. *J. Antibiotics.,* **48,** 1066 – 1072.

TURNER, A.J. (1993). Endothelin-converting enzymes and other families of metallo-endopeptidases. *Biochem. Soc. Transactions,* **21,** 697 – 701.

TURNER, A.J. & MURPHY, L.J. (1996). Molecular Pharmacology of endothelin converting enzymes. *Biochem. Pharmacol.,* **51,** 91 – 102.

VALDENAIRE, O., ROHRBACHER, E. & MATTEI, M.-G. (1995). Organization of the gene encoding the human endothelin-converting enzyme (ECE-1). *J. Biol. Chem.,* **270,** 29794 – 29798.

VEMULAPALLI, S., CHINTALA, M., STAMFORD, A., WATKINS, R., CHIU, P., SYBERTZ, E. & FAWZI, A.B. (1997). Renal effects of SCH 54470: a triple inhibitor of ECE, ACE, and NEP. *Cardiovasc. Drug Rev.,* **15,** 260 – 272.

WAGNER, D.D., OLMSTED, J.B. & MARDER, V.J. (1982). Immunolocalization of von Willebrand protein in Weibel-Palade bodies of human endothelial cells. *J. Cell. Biol.,* **95,** 355 – 360.

WAGNER, O.F., CHRIST, G., WOJTA, J., VIERHAPPER, H., PARZER, S., NOWOTNY, P.J., SCHNEIDER, B., WALDHÄUSL, W. & BINDER, B.R. (1992). Polar secretion of endothelin-1 by cultured endothelial cells. *J. Biol. Chem.,* **267,** 16066 – 16068.

WALLACE, E.M., MOLITERNI, J.A., MOSKAL, M.A., NEUBERT, A.D., MARCOPULOS, N., STAMFORD, L.B., TRAPANI, A.J., SAVAGE, P., CHOU, M. & JENG, A.Y. (1998). Design and synthesis of potent, selective inhibitors of endothelin-converting enzyme. *J. Med. Chem.,* **41,** 1513 – 1523.

WAXMAN, L., DOSHI, K.P., GAUL, S.L., WANG, S., BEDNAR, R.A. & STERN, A.M. (1994). Identification and characterization of endothelin converting activity from EAHY 926 cells: evidence for the physiologically relevant human enzyme. *Arch. Biochem. Biophys.,* **308,** 240 – 253.

WEIBEL, E.R. & PALADE, G.E. (1964). New cytoplasmic components in arterial endothelia. *J. Cell. Biol.,* **23,** 101 – 112.

XU, D., EMOTO, N., GIAID, A., SLAUGHTER, C., KAW, S., DEWIT, D. & YANAGISAWA, M. (1994). ECE-1: A membrane-bound metalloprotease that catalyzes the proteolytic activation of big endothelin-1. *Cell,* **78,** 473 – 485.

YANAGISAWA, H., YANAGISAWA, M., KAPUR, R.P., RICHARDSON, J.A., WILLIAMS, S.C., CLOUTHIER, D.E., DE WIT, D., EMOTO, N. & HAMMER, R.E. (1998). Dual genetic pathways of endothelin-mediated intercellular signaling revealed by targeted disruption of endothelin converting enzyme-1 gene. *Development,* **125,** 825 – 836.

YANAGISAWA, M., KURIHARA, H., KIMURA, S., TOMOBE, Y., KOBAYASHI, M., MITSUI, Y., YAZAKI, Y., GOTO, K. & MASAKI, T. (1988). A novel potent vasoconstrictor peptide produced by vascular endothelial cells. *Nature,* **332,** 411 – 415.

YORIMITSU, K., MOROI, K., INAGAKI, N., SAITO, T., MASUDA, Y., MASAKI, T., SEINO, S. & KIMURA, S. (1995). Cloning and sequencing of a human endothelin converting enzyme in renal adenocarcinoma (ACHN) cells producing endothelin-2. *Biochem. Biophys. Res. Commun.,* **208,** 721 – 727.

YOSHIMOTO, S., ISHIZAKI, Y., SASAKI, T. & MUROTA, S. (1991). Effect of carbon dioxide and oxygen on endothelin production by cultured porcine cerebral endothelial cells. *Stroke,* **22,** 378 – 383.

YOSHITOMI, Y., KOJIMA, S., OGI, M. & KURAMOCHI, M. (1998). Acute renal failure in accidental hypothermia of cold water immersion. *Am. J. Kid. Diseases,* **31,** 856 – 859.

YU, J.C.M. & DAVENPORT, A.P. (1995). Secretion of endothelin-1 and endothelin-3 by human cultured vascular smooth muscle cells. *Br. J. Pharmacol.,* **114,** 551 – 557.

(Received September 7, 1998
Revised October 6, 1998
Accepted October 22, 1998)

British Journal of Pharmacology (1999) 126, 399–406
http://www.stockton-press.co.uk/bjp

Pharmacological characterization of β_2-adrenoceptor in PGT-β mouse pineal gland tumour cells

[1]Byung-Chang Suh, [1]Hee-Don Chae, [2]Joo-Ho Chung & [*,1]Kyong-Tai Kim

[1]Department of Life Science and Basic Science Research Institute, Pohang University of Science and Technology, Pohang, 790-784, and [2]Department of Pharmacology, College of Medicine, Kyung Hee University, Seoul, 130-710, Republic of Korea

1 The adrenoceptor in a mouse pineal gland tumour cell line (PGT-β) was identified and characterized using pharmacological and physiological approaches.

2 Adrenaline and noradrenaline, adrenoceptor agonists, stimulated cyclic AMP generation in a concentration-dependent manner, but had no effect on inositol 1,4,5-trisphosphate production. Adrenaline was a more potent activator of cyclic AMP generation than noradrenaline, with half maximal-effective concentrations (EC_{50}) seen at 175 ± 22 nM and 18 ± 2 μM for adrenaline and noradrenaline, respectively.

3 The addition of forskolin synergistically stimulated the adrenaline-mediated cyclic AMP generation in a concentration-dependent manner.

4 The pA_2 value for the specific β_2-adrenoceptor antagonist ICI-118,551 (8.7 ± 0.4) as an antagonist of the adrenaline-stimulated cyclic AMP generation were ~ 3 units higher than the value for the β_1-adrenoceptor antagonist atenolol (5.6 ± 0.3).

5 Treatment of the cells with adrenaline and forskolin evoked a ~ 3 fold increase in the activity of serotonin N-acetyltransferase with the peak occurring 6 h after stimulation.

6 These results suggest the presence of β_2-adrenoceptors in mouse pineal cells and a functional relationship between the adenylyl cyclase system and the regulation of N-acetyltransferase expression.

Keywords: Mouse pineal gland cell; β_2-adrenoceptor; adrenaline; noradrenaline; serotonin N-acetyltransferase; adenylyl cyclase

Introduction

The pineal gland mediates the environmental and circadian regulation of the neuroendocrine system by producing the hormone melatonin (Aronson *et al*., 1993; Brezezinski, 1997). Melatonin synthesis is controlled by a complex system that includes the circadian oscillator in the suprachiasmatic nucleus (Klein & Moore, 1979). Rhythmic noradrenergic input occurs from the sympathetic fibres originating in the superior cervical ganglia to the pineal gland activating the pineal adrenoceptors which are coupled to adenylyl cyclase and thus cause an increase of the intracellular level of cyclic AMP (Ebadi & Govitrapong, 1986; Takahashi, 1993). The cyclic AMP-mediated signalling then governs the circadian fluctuation of serotonin N-acetyltransferase gene expression which controls melatonin synthesis (Coon *et al*., 1995; Roseboom *et al*., 1996; Baler *et al*., 1997)

Many recent studies have addressed the regulation of adrenoceptors in pineal gland, as it has become evident that the daily rhythm of melatonin production is linked to the obligate action of α- and β-adrenoceptors. Studies in the rat pineal have described that nocturnally released noradrenaline stimulates melatonin synthesis by acting through β_1-adrenoceptors linked to the generation of cyclic AMP (Brownstein, 1973; Machida *et al*., 1990). In addition, α_1-adrenoceptors which triggers the phosphoinositide pathway and increases intracellular Ca^{2+} are also present and known to be involved in the potentiation of the stimulatory effects of the β-adrenoceptors (Sugden *et al*., 1985; Yu *et al*., 1993). However, the small size of pure pinealocytes in primary culture makes difficulties in studying mouse pineal gland. Previously, therefore, a clonal neuroendocrine pineal cell line (PGT-β) was developed from pineal tumour which was established by targeted expression of the tissue-specific regulatory region of tryptophan hydroxylase gene fused to the SV40 early region encoding the large T-antigen in transgenic mice (Son *et al*., 1996). Several lines of evidence demonstrated that PGT-β cells are immortalized pinealocytes. They express functionally active forms of two characteristic marker enzymes of the pinealocyte, tryptophan hydroxylase and N-acetyltransferase, and the activity of the enzymes was enhanced by pharmacological stimulation of the cells with the cyclic AMP analogue dibutyryl cyclic AMP or the β-adrenergic receptor agonist isoprenaline. Here, utilizing the pineal tumour cell line, we characterized the adrenergic regulation of mouse pineal function. The present study demonstrates the existence of β_2-adrenoceptors on the cells and the evidence indicating that the β_2-adrenoceptor-mediated signalling is involved in the pineal regulation of expression of N-acetyltransferase.

Methods

Cell culture method

The cells were cultured in Dulbecco's modified Eagle's medium (DMEM) (GIBCO, Gaithersburg, MD, U.S.A.) supplemented

*Author for correspondence at: Department of Life Science, POSTECH, San 31, Hyoja dong, Pohang, 790-784, Republic of Korea.

with 10% (v/v) heat-inactivated bovine calf serum (Hyclone, Logan, UT, U.S.A.) and 1% (v/v) antibiotics containing 5,000 units ml^{-1} penicillin G (sodium) and 5,000 $\mu g\ ml^{-1}$ streptomycin sulphate in 0.85% saline buffer (GIBCO), pH 7.4. Cell cultures were maintained in a humidified atmosphere of 5% CO_2 at 37°C. Cells grown to confluence were removed from the dishes after a 5 min incubation with 0.25% (w/v) trypsin containing 1 mM EDTA (GIBCO). They were subcultured about twice a week.

Cyclic AMP accumulation in whole cells

Intracellular cyclic AMP was determined by measuring the formation of cyclic [^{3}H]AMP from [^{3}H]adenine nucleotide pools as we previously described (Suh & Kim, 1995). The cells were grown in 6-well dishes to confluency and loaded with [^{3}H]adenine (2 $\mu Ci\ ml^{-1}$) in complete medium for 24 h. After the loading, the cells were washed three times with Locke's solution (NaCl, 154 mM; KCl, 5.6 mM; $MgCl_2$, 1.2 mM; $CaCl_2$, 2.2 mM; HEPES, 5.0 mM; glucose, 10 mM, pH 7.4) and preincubated with 1 mM isobutylmethylxanthine (IBMX) for 15 min in Locke's solution to inhibit phosphodiesterase. IBMX was also added to the stimulating solution. The reaction was stopped by aspirating the medium off and adding 1 ml of ice-cold 5% (w/v) trichloroacetic acid containing 1 μM unlabelled cyclic AMP. The plates were left on ice for 30 min to extract the water-soluble cyclic AMP. Then, the extracts were transferred to Eppendorf tubes and centrifuged at $5000 \times g$ for 5 min to remove cell debris. [^{3}H]cyclic AMP and [^{3}H]ATP were separated by sequential chromatography on Dowex AG50W-X4 (200–400 mesh) cation exchanger and neutral alumina columns. The [^{3}H]ATP fraction was obtained by elution with 2 ml distilled water from the Dowex column, and the sequential elution with 3.5 ml distilled water was loaded onto an alumina column. The alumina column was washed with 4 ml imidazole solution (0.1 M, pH 7.2), and eluant fractions were collected into scintillation vials containing 15 ml scintillation fluid prior to counting radioactive decay of the cyclic [^{3}H]AMP. The increase in intracellular cyclic AMP concentration was calculated as [^{3}H]cyclic AMP $([^3H]ATP + [^3H]\text{cyclic AMP})^{-1} \times 10^3$.

Quantification of inositol 1,4,5-trisphosphate in whole cells

The inositol 1,4,5-trisphosphate concentration in the cells was determined by [^{3}H]-inositol 1,4,5-trisphophate competition assay in binding to inositiol 1,4,5-trisphosphate binding protein (Suh *et al*., 1997). To determine the inositol 1,4,5-trisphosphate production induced by catecholamine or α_1-selective agonist, the pineal tumour cells were grown in 6-well culture plates to 95% confluency. The cells were stimulated with agonist for specific intervals, and the reaction was terminated by aspirating the medium off the cells followed by addition of 0.3 ml of ice-cold 15% (w/v) trichloroacetic acid containing 10 mM EGTA. The plates were left on ice for 30 min to extract the water-soluble inositol phosphate. The extract was then transferred to an Eppendorf tube, and the trichloroacetic acid was removed with four extractions with diethyl ether. Finally the extract was neutralized with 200 mM Trizma base, and its pH was adjusted to 7.4. Twenty microlitres of the cell extract was added to 20 μl of the assay buffer (0.1 M tris(hydroxymethyl)aminomethane buffer containing 4 mM EDTA and 4 $mg\ ml^{-1}$ bovine serum albumin) and 20 μl of [^{3}H]inositol 1,4,5-trisphosphate (0.1 $\mu Ci\ ml^{-1}$). Then 20 μl of a solution containing the binding protein was added, and the mixture was incubated for 15 min on ice and centrifuged at $2000 \times g$ for 5 min. The pellet was resuspended in 100 μl of water, and 1 ml of scintillation cocktail were added to the pellet to measure radioactivity. The inositol 1,4,5-trisphosphate concentration in the sample was determined based on a standard curve and expressed as picomols per milligram protein in cell extract with trichloroacetic acid. The inositol 1,4,5-trisphosphate binding protein was prepared from bovine adrenal cortex according to the method of Challiss *et al*. (1990).

N-acetyltransferase activity assay

PGT-β cells were grown in 60 mm culture dishes to ~90% confluence and stimulated with adrenaline and forskolin for various periods of time. Then the cells were rapidly detached and transferred to an Eppendorf tube and pelleted. The cells in the pellet were disrupted with ultrasound in 80 μl ice-cold phosphate buffer (50 mM, pH 6.8). Debris was removed by centrifugation ($15{,}000 \times g$, 5 min, 4°C), and the supernatants were transferred to a new tube. The extract of the PGT-β cells was then incubated in the presence of 5 μl tryptamine-HCl (10 mM), 1 μl acetyl CoA (0.5 mM), and 1 μl [^{3}H]acetyl CoA (3.6 Ci $mmol^{-1}$, 250 $\mu Ci\ ml^{-1}$). 50 mM phosphate buffer (pH 6.8) was then added to make a final volume of 20 μl. Incubation at 37°C for 40 min was stopped by diluting the reaction mixture with an additional 180 μl of 50 mM phosphate buffer (pH 6.8). The whole reaction mixture was transferred into a vial containing 3 ml of Econofluor, a water-immiscible scintillation fluid. After an incubation of 15 min without mixing the amount of radiolabelled acetyltryptamine was determined in a liquid scintillation counter.

Materials

(±)-adrenaline, (±)-noradrenaline, ionomycin, alumina, imidazole, dowex AG50W-X4 (200–400 mesh), trichloroacetic acid, Triton X-100, glucose, HEPES, cyclic AMP, forskolin, acetyl CoA, and tryptamine were obtained from Sigma Chemical Co. (St. Louis, MO, U.S.A.). Isobutylmethylxanthine (IBMX), (±)-atenolol, ICI-118,551 (erythro-(±)-1-(7-methyllindane-4-yloxy)-3-isopropylaminobutane-2-olhydrochloride), BRL 37344 (4-[2-[[2-(3-chlorophenyl)-2-hydroxyethyl] amino] propyl] phenoxy)-acetic acid), prazosine, yohimbine, phenylephrine, clonidine, and (±)-propranolol were purchased from Research Biochemicals Inc. (Natick, MA, U.S.A.). [^{3}H]Acetyl CoA was obtained from Amersham (Arlington Heights, IL, U.S.A.) and [^{3}H]adenine from DuPont NEN Research Products (Boston, MA, U.S.A.).

Analysis of data

All quantitative data are expressed as means ± s.e.mean. Comparison between two groups was analysed using Student's unpaired *t*-test, and comparison among more than two groups was carried out using one-way analysis of variance (ANOVA). Differences were considered to be significant when the degree of confidence in the significance was 95% or better ($P < 0.05$). Antagonist potencies were evaluated by calculating their pA_2 values. Concentration-response curves for agonist were made in the presence of 3–4 different concentrations of antagonists. Allfit program was used to obtain the EC_{50} from the individual experiments (De Lean *et al*., 1978) and the pA_2 values ($-\log mol\ l^{-1}$) were calculated.

Results

Effect of adrenaline and noradrenaline on cyclic AMP generation

The coupling between adrenoceptors and adenylyl cyclase was investigated in a mouse PGT-β cell line. Stimulation of the PGT-β cells with adrenaline and noradrenaline evoked cyclic AMP generation. The maximal and half maximal responses were obtained by treatments with 1.2 ± 0.5 μM and 175 ± 22 nM adrenaline, respectively, and 300 ± 46 μM and 18 ± 2 μM noradrenaline, respectively (Figure 1A). Figure 1B shows the time course of cyclic AMP generation induced by 1 μM adrenaline and 300 μM noradrenaline, the maximal effective concentrations used for each agonist. The peak level of cyclic AMP was obtained 3 min after stimulation with either agonists and was followed by a rapid decline to the basal level within 30 min. The accumulation of cyclic AMP induced by adrenaline was clearly detectable within 1 min and was saturated after 20 min in the presence of the phosphodiesterase inhibitor IBMX (Figure 1B, inset). The results thus indicate that β-adrenoceptor-mediated cyclic AMP generation is present on the cells.

To investigate whether α-adrenoceptors are also expressed in the cells, we treated the cells with subtype selective agonists. Figure 2A shows that treatment with adrenaline and the specific α_1-adrenoceptor agonist phenylephrine had no stimulatory effect on inositol 1,4,5-trisphosphate generation, whereas extracellular ATP significantly increased the inositol 1,4,5-trisphosphate levels through P_2 purinoceptor as previously described (Suh *et al*., 1997). Figure 2B shows that treatment with the α_2-adrenoceptor agonist clonidine and the α_2-adrenoceptor antagonist yohimbine did not affect the adrenaline-induced cyclic AMP accumulation, while a general β-adrenoceptor antagonist propranolol completely inhibited

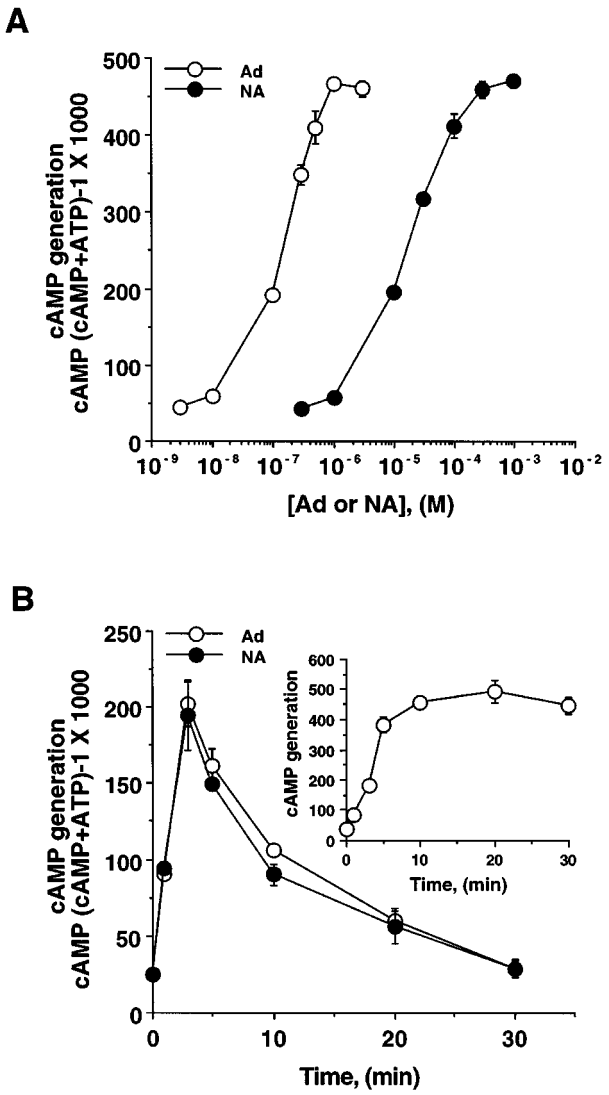

Figure 1 Adrenaline- and noradrenaline-induced cyclic AMP production in PGT-β cells. (A) [^{3}H]adenine-loaded cells were preincubated with IBMX (1 mM) for 20 min and then stimulated with variable concentrations of adrenaline (Ad) and noradrenaline (NA) for 20 min. (B) The cells were stimulated with 1 μM adrenaline (Ad) or 300 μM noradrenaline (NA) for the indicated times (0, 1, 3, 5, 10, 20, 30 min) and cyclic AMP generation was measured as described in Methods. The inset shows the time-dependent changes in cyclic AMP accumulation induced by 1 μM adrenaline in the presence of 1 mM IBMX. The experiments were done three times and each point is the mean $\pm$ s.e.mean.

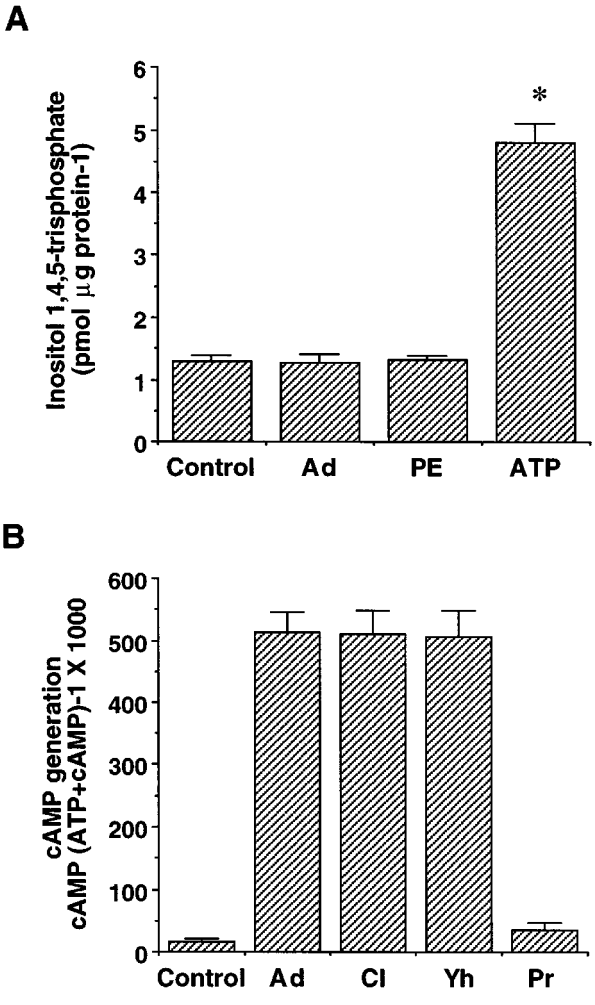

Figure 2 Effect of α-adrenoceptor agonist and antagonist in PGT-β cells. (A) Cells were stimulated with 1 μM adrenaline, 10 μM phenylephrine, or 300 μM ATP for 30 s, and the reactions were stopped by addition of 15% (w/v) trichloroacetic acid containing 10 mM EGTA. The inositol 1,4,5-trisphosphate generation was measured as described in Methods. (B) [^{3}H]adenine-loaded cells were preincubated with IBMX (1 mM) for 20 min and then stimulated with 1 μM adrenaline (Ad) in the absence or presence of 10 μM clonidine (Cl), 30 μM yohimbine (Yh), and 1 μM propranolol (Pr) for 20 min. The cyclic AMP generation was measured as described in Methods. The experiments were done three times and each point is the mean $\pm$ s.e.mean. $^*P < 0.05$, compared to control.

the adrenaline-induced cyclic AMP generation. The results, therefore, indicate that α_1-adrenoceptor which is coupled to phospholipase C and α_2-adrenoceptor which is negatively linked to adenylyl cyclase are not expressed in the PGT-β cells.

Synergistic activation of adenylyl cyclase by forskolin

To determine the susceptibility of the adenylyl cyclase coupled to the β-adrenoceptor to other activating signalling, the effect of a co-treatment with adrenaline and forskolin was examined. Forskolin by itself induced a concentration-dependent cyclic AMP accumulation (Figure 3A, inset), but addition of 1 μM adrenaline to each concentration of forskolin synergistically enhanced the forskolin-activated cyclic AMP generation. Co-treatment with 10 μM forskolin plus 1 μM adrenaline produced a $\sim$20 fold increase over the 10 μM forskolin-generated cyclic AMP level (Figure 3A). Time course of cyclic AMP generation demonstrates that the peak cyclic AMP level was obtained 3 min after stimulation with 10 μM forskolin as shown in that of adrenaline or noradrenaline (Figure 3B, inset). However, co-treatment with forskolin and adrenaline resulted in synergistic enhancement of the response with the peak level of cyclic AMP seen at 20 min after stimulation (Figure 3B). The high level of cyclic AMP induced by simultaneous treatment was persistent up to 1 h even in the absence of IBMX (data not shown). The results thus indicate that the adenylyl cyclase after being maximally stimulated via β-adrenoceptors could be further stimulated by other G_s-protein-mediated signalling.

Cytosolic Ca^{2+}-mediated inhibition of adrenaline- and forskolin-stimulated adenylyl cyclase activity

To examine the regulatory role of intracellular Ca^{2+} on adenylyl cyclase, the cells were treated with ionomycin, a Ca^{2+} ionophore. Figure 4A shows the time course of cyclic AMP generation induced by adrenaline treatment in the presence or absence of 1 μM ionomycin. Addition of ionomycin significantly decreased the adrenaline-induced cyclic AMP generation. The inhibition by ionomycin was concentration-dependent and significant in micromolar concentrations (Figure 4B). Forskolin-stimulated cyclic AMP generation was also inhibited by $\sim$30% in the presence of 1 μM ionomycin (Figure 4C), indicating that intracellular Ca^{2+} has a direct effect on the adenylyl cyclase rather than the adrenoceptor or other components of the receptor-mediated signalling pathways.

Pharmacological characterization with β-adrenoceptor antagonists and agonists

To investigate which subtype of β-adrenoceptor mediates the effect of adrenaline on cyclic AMP generation, we determined the pA_2 values for specific β_1- and β_2-adrenoceptor blockers in adrenaline concentration-response experiments performed at several concentrations of antagonist in each individual experiment. Figure 5A and B show that the pA_2 value of the selective β_2-adrenoceptor antagonist ICI 118,551 versus adrenaline was 8.7 ± 0.4. In a corresponding way the pA_2 value for the selective β_1-adrenoceptor antagonist atenolol versus adrenaline was 5.6 ± 0.3 (Figure 5C and D). On the other hand, the presence of β_3-adrenoceptor was tested with the specific β_3-adrenoceptor agonist BRL 37344. Figure 6 shows that the addition of isoprenaline, a general β-adrenoceptor agonist, stimulated cyclic AMP generation with EC_{50} seen at 120 ± 15 nM. In contrast, BRL 37344 exhibited an

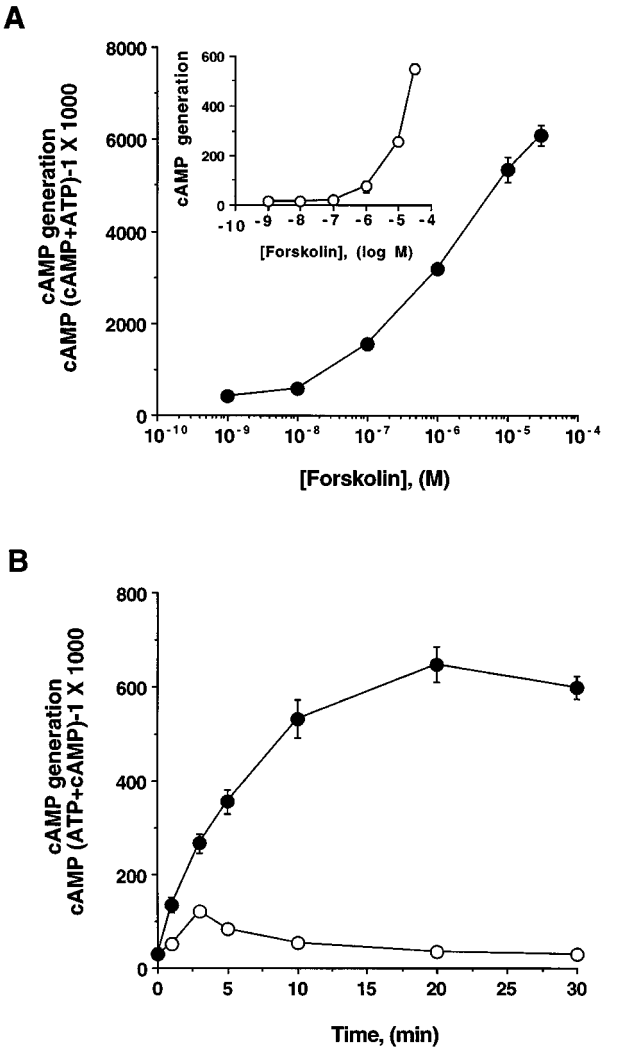

Figure 3 Enhancement of forskolin-stimulated cyclic AMP generation by adrenaline. (A) [^{3}H]adenine-loaded PGT-β cells were preincubated with IBMX (1 mM) for 20 min and then stimulated with various concentrations of forskolin plus 1 μM adrenaline (●) for 20 min. The inset shows the concentration-dependent changes in forskolin-stimulated (○) cyclic AMP generation. (B) The time-dependent changes in cyclic AMP accumulation induced by 10 μM forskolin plus 1 μM adrenaline (●) or forskolin alone (○) for the indicated times (0, 1, 3, 5, 10, 20, 30 min) in the absence of IBMX. The cyclic AMP levels were measured as described in Methods. The experiments were done three times and each point is the mean $\pm$s.e.mean.

EC_{50} of 184 ± 28 μM, which is approximately 10^3 fold higher concentration than that of isoprenaline. The data, therefore, indicate that the effects of adrenaline or noradrenaline on cyclic AMP generation occur primarily through the β_2-adrenoceptors on the cells.

Elevation of the N-acetyltransferase activity upon β_2-adrenoceptor stimulation

Because it has been known that β-adrenoceptor-induced cyclic AMP generation is responsible for N-acetyltransferase gene expression in the pineal gland by involvement of the cyclic AMP response element (Baler *et al*., 1997), we measured the N-acetyltransferase activity after stimulating the adrenoceptors. Figure 7 shows that treatment with 1 μM adrenaline and 10 μM forskolin elevated the N-acetyltransferase activity according to

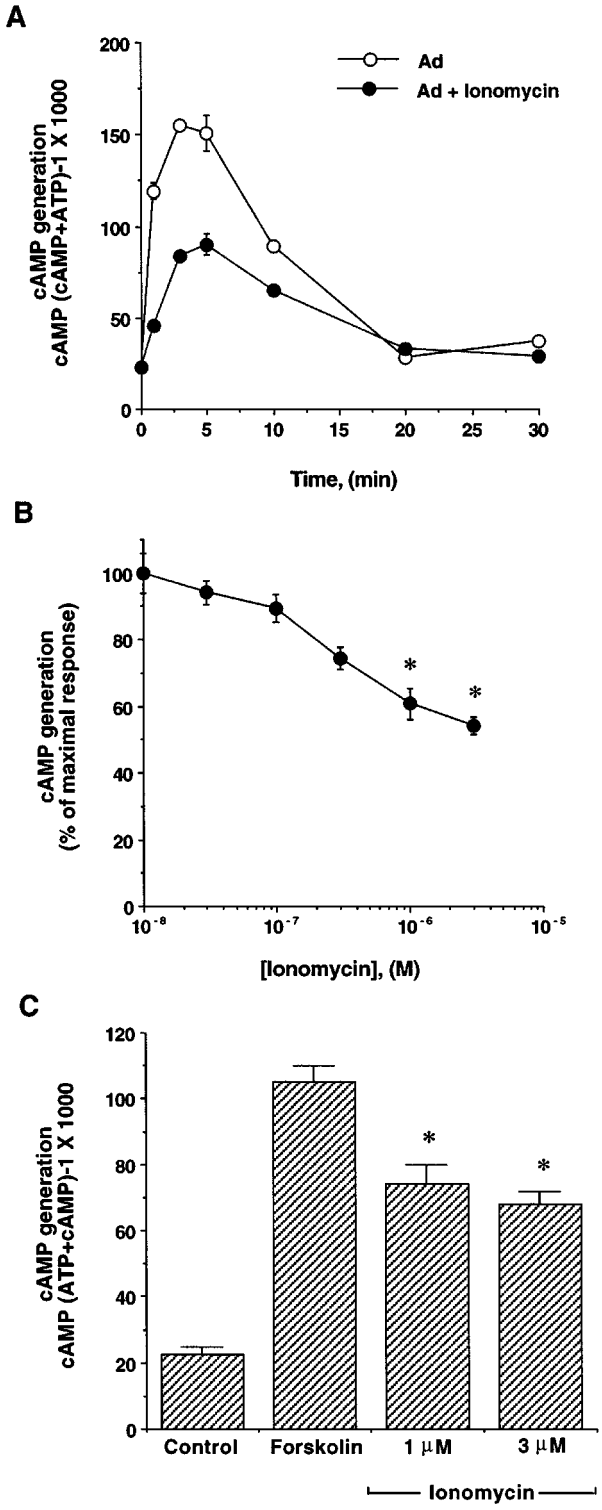

Figure 4 Effects of ionomycin on cyclic AMP generation. (A) Time-dependent changes in intracellular cyclic AMP levels stimulated by 1 μM adrenaline in the presence or absence of 1 μM ionomycin. (B) Concentration-dependent inhibition of adrenaline-stimulated cyclic AMP generation by ionomycin. [^{3}H]adenine-loaded cells were treated with 1 μM adrenaline and variable concentrations of ionomycin for 3 min. The cyclic AMP generation was presented as percentage of the maximal response induced by treatment with 1 μM adrenaline. (C) Inhibition of forskolin-stimulated cyclic AMP generation by ionomycin. [^{3}H]adenine-loaded cells were treated with 10 μM forskolin and ionomycin for 3 min. The cyclic AMP levels were measured as described in Methods. The experiments were done three times and the results were reproducible. Data are the means $\pm$ s.e.mean. $^*P<0.05$, compared to control.

incubation time. The peak level of N-acetyltransferase activity was achieved 6 h after agonist stimulation and was followed by a slow decrease to the basal level within 24 h. However, simultaneous addition of ICI-118,551 blocked the increase of enzyme activity. The results imply that the β_2-adrenoceptor-mediated cyclic AMP production is involved in the regulation of induction of the N-acetyltransferase gene expression.

Discussion

Adrenoceptors are found in nearly all peripheral tissues and on many neuronal populations within the central nervous system (Bond & Clarke, 1988). They mediate the central and peripheral action of the primary sympathetic neurotransmitter noradrenaline, and the primary adrenal medullary hormone and central neurotransmitter adrenaline. The adrenoceptors have been divided into three major types, α_1-, α_2- and β-adrenoceptors receptors based on several lines of evidence: differences in affinity of selective drugs, second-messenger responses, and differences in the predicted amino acid sequences of the adrenergic receptor proteins. However, as new pharmacological tools and new techniques for studying drug-receptor interactions have become available, each adrenoceptor type has been subdivided into an increasing number of distinct subtypes (Bylund *et al.*, 1994). Mammalian tissues contain three types of β-adrenoceptor, β_1, β_2, and β_3, based on their pharmacological properties (Emorine *et al.*, 1994). The β_1-adrenoceptor is equally sensitive to noradrenaline and adrenaline, whereas the β_2-adrenoceptor has a higher affinity for adrenaline than for noradrenaline (Blin *et al.*, 1993; Nantel *et al.*, 1993). In contrast, the β_3-adrenoceptor has a higher affinity for noradrenaline (Strosberg & Pietri-Rouxel, 1996). It has been suggested that the β_1- and β_2-adrenoceptors mediate the effects of circulating catecholamines and that the β_3-adrenoceptor subtype plays a major role in regulating lipolysis and thermogenesis in adipose tissue (Zilberfarb *et al.*, 1997) and sympathetic nerve stimulation in the large intestine (Luckensmeyer & Keast, 1998).

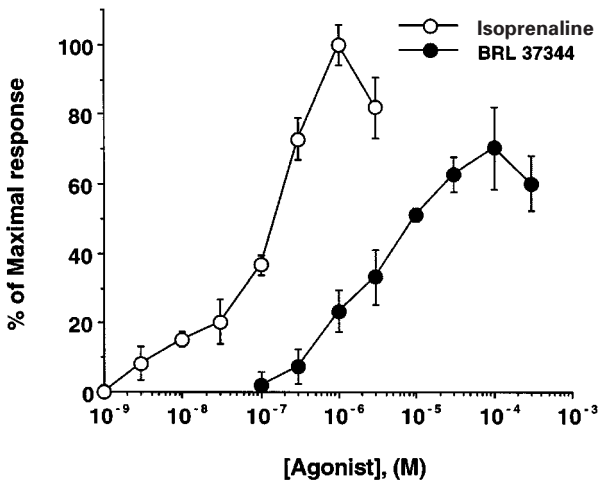

Figure 5 Effect of isoprenaline and BRL 37344 on cyclic AMP production in PGT-β cells. [^{3}H]adenine-loaded cells were preincubated with IBMX (1 mM) for 20 min and then stimulated with variable concentrations of isoproterenol and BRL 37344 for 20 min. The cyclic AMP generation was measured as described in Methods and presented as percentage of the maximal response induced by treatment with 1 μM isoproterenol. The experiments were done three times and each point is the mean $\pm$ s.e.mean.

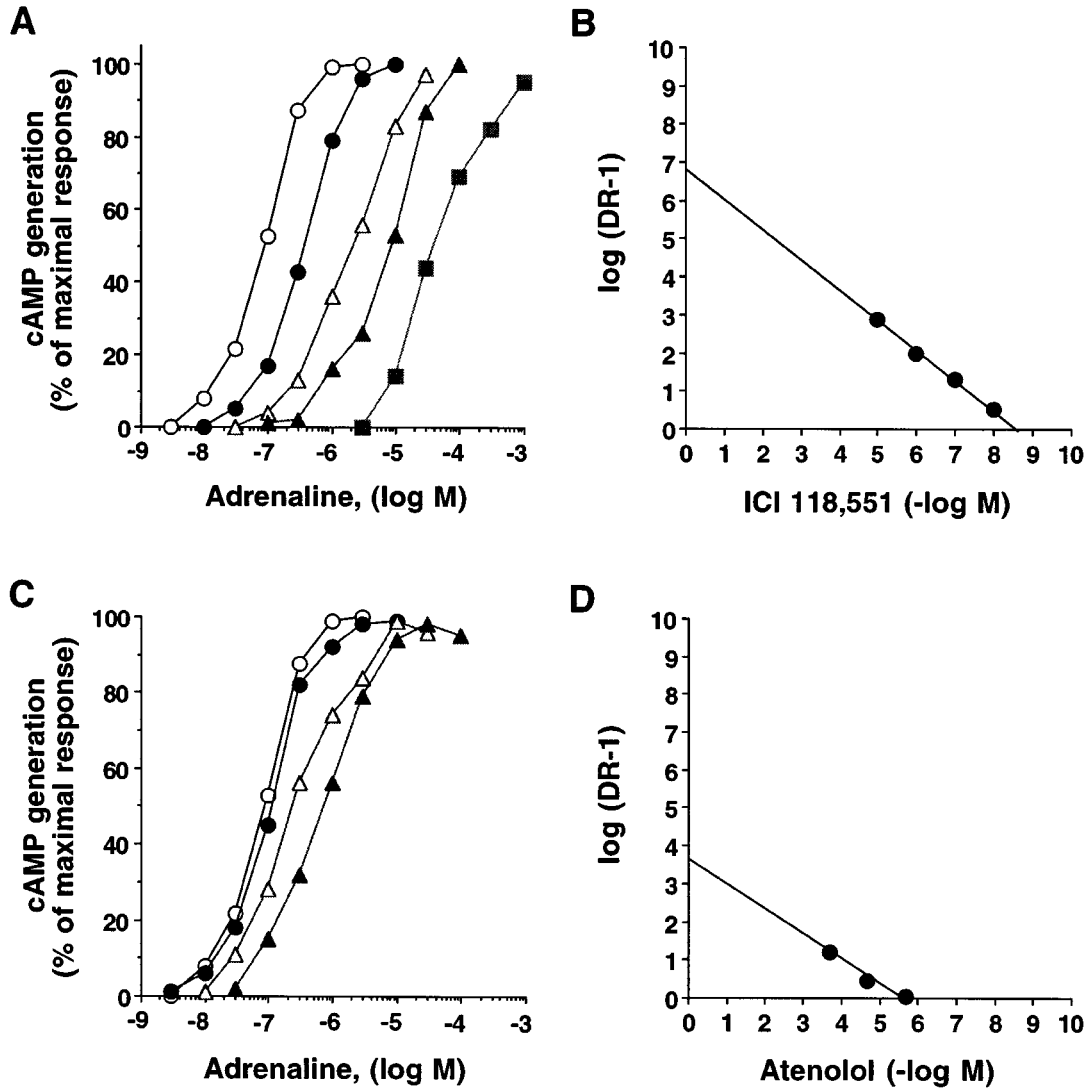

Figure 6 The antagonism by β-adrenoceptor antagonists of adrenaline-stimulated cyclic AMP generation. Concentration-response curves for the antagonistic effect of increasing concentrations of ICI 118,551 (A) and atenolol (C) on adrenaline-stimulated cyclic AMP generation are shown. The pA_2 values of ICI 118,551 (B) and atenolol (D) were calculated for each antagonist by plotting: log (dose ration^{-1}) vs $-$log(antagonist) concentration. The concentrations of ICI 118,551 used to counteract the effects of adrenaline were 0 (○), 10 nM (●), 100 nM (Δ), 1 μM (▲), and 10 μM (■). The concentrations of atenolol were 0 (○), 3 μM (●), 30 μM (Δ), and 300 μM (▲). The concentration of adrenaline ranged from 10^{-9}–10^{-3} M. The cyclic AMP generation was presented as percentage of the maximal response induced by treatment with adrenaline. One typical experiment out of three independent experiments in duplicate is shown.

The present study clearly demonstrates the existence of β_2-adrenoceptors on the PGT-β cell line which is established from the targeted pineal tumours in transgenic mice. In our experiments with subtype selective adrenergic receptor antagonists, the sensitivity to the inhibiting effect of the selective β_2-adrenoceptor antagonist ICI-118,551 was much more pronounced for the antagonistic effect of the selective β_1-adrenoceptor antagonist atenolol. The pA_2 value for the ICI-118,551 was $\sim$3 units higher than that for atenolol. In addition, the β_3-adrenoceptor agonist BRL 37344 was 100 fold less potent in stimulating adenylyl cyclase than that of the general β-adrenoceptor agonist isoproterenol, which is consistent with the property of β_2-adrenoceptor (Dolan *et al.*, 1994). Moreover, adrenaline was more effective in stimulating cyclic AMP generation than noradrenaline with a difference of $\sim$2 orders of magnitude. Previous studies have shown that the distribution of adrenoceptor subtypes in mammalian pineal gland presents a species dependent difference. For example, Machida *et al.* (1990) showed that the β_1-adrenoceptor is prominently distributed and functionally responsive to noradrenaline in the rat pineal gland. However, autoradiographic analysis in human post-mortem specimens demonstrate that β_2-adrenoceptors are present in an overlapping anatomical distribution with β_1-adrenoceptor throughout the gland (Little *et al.*, 1996). Therefore, although the anatomical pattern of adrenergic receptor subtypes present on mouse pinealocytes was not elucidated, β_2-adrenoceptors might be primarily situated on mouse pineal gland. However, a possibility that the prominence of β_2-adrenoceptor in PGT-β cells is due to the immature stage of the cells could not be excluded, since functional adrenergic stimulation required the developmental maturation of pinealocytes (Stehle *et al.*, 1995). Duman *et al.* (1989) also reported that the mRNA levels of β_1-adrenoceptor is low on postnatal day 1 but increases several fold in parallel with an increase in β_1-adrenoceptor binding sites to adult levels, although the level of G protein mRNA

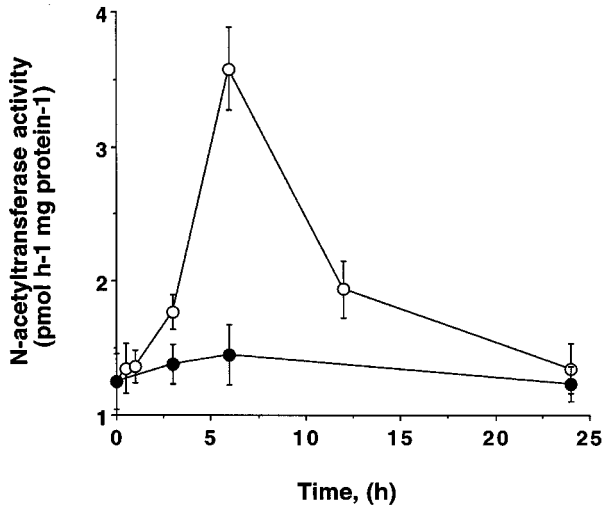

Figure 77 Time-dependent effect of β-adrenoceptor activation on N-acetyltransferase activity in PGT-β cells. The cells were treated with 1 μM adrenaline and 10 μM forskolin in the absence (○) or presence (●) of ICI-118,551 (10 μM) for the indicated times (0, 1, 3, 6, 12, 24 h) and N-acetyltransferase activity was assayed as described in Methods. Results were confirmed by two independent experiments and expressed as the means ± s.e.mean.

transcript on day 1 is equal to that of the adult. These reports, therefore, suggest that effective signalling of β_1-adrenoceptor in PGT-β cells might require the developmental switch to β_1-adrenergic innervation on the differentiating processes of the cells.

Noradrenaline plays an important role in controlling pineal function through its effect on N-acetyltransferase regulation in mammalian pineal glands (Roseboom & Klein, 1995). Recently, *in vitro* studies with isolated rat pineal glands showed that noradrenaline elevated N-acetyltransferase gene expression and enzyme activity more than 100 fold (Coon *et al*., 1995). The magnitude of the N-acetyltransferase activity rhythm occurred over a ~10 fold difference in sheep (Namboodiri *et al*., 1985) and a ~20 fold difference in chicken (Binkley *et al*., 1973). However, in our PGT-β cells, the N-acetyltransferase activity increased ~3 fold upon simultaneous stimulation with 1 μM adrenaline and 10 μM forskolin. This weak N-acetyltransferase response may be due to the origin of the cells, since these pineal tumour PGT-β cells were originated from transgenic mice which were hybrids of a circadian clock-expressing mouse (CBA/J) and a circadian clock-deficient mouse (C57BL/6J) (Son *et al*., 1996). Goto *et al*. (1989) demonstrates that most of the laboratory mice do not have pineal melatonin because of a genetic defect in the activity of N-acetyltransferase. For example, C57BL/6J mice do not have N-acetyltransferase activity because of a mutation in an autosomal gene required for the normal activity of N-acetyltransferase (Goto *et al*., 1994). However, our experiment with PGT-β cells shows that the noradrenaline's effect on cyclic AMP generation was only significant at above 100 micromolar concentrations. Accordingly, it seems likely that the coupling between noradrenaline released from superior cervical ganglion and adrenergic receptor could not function efficiently in the mouse pineal gland, which might be one of the causes for loss of pineal function in the circadian rhythm of the mouse.

Our finding that the elevation of N-acetyltransferase activity occurred 6 h after agonists stimulation was consistent with previous studies in which the pineal N-acetyltransferase activity peaked 6–9 h after adrenergic stimulation and then slowly declined to the basal level within 24 h (Roseboom & Klein, 1995). The time interval between receptor stimulation and the subsequent elevation of N-acetyltransferase activity indicates that the increase in N-acetyltransferase activity was the result of gene expression and subsequent enzyme protein synthesis.

The present results are particularly significant insofar as they show that the distribution of adrenoceptors and the adrenoceptor-adenylyl cyclase system differ according to the species. They also support the conclusion that the β-adrenoceptors-mediated signals are responsible for the regulation of N-acetyltransferase activity. The pharmacological results also clearly indicate that β_2-adrenoceptors are expressed and coupled to the adenylyl cyclase system in the mouse pineal gland.

We are grateful to S. Han for helping with the assay of cyclic AMP measurement. We also thank Ms G. Hoschek for editing the manuscript. This work was supported by grants from POSTECH/BSRI Special fund, the Korea Science and Engineering Foundation (KOSEF 97-0401-02), the Basic Science Research Institute Program (Project BSRI-98-4435) from the Ministry of Education.

References

ARONSON, B.D., BELL-PEDERSEN, D., BLOCK, G.D., BOS, N.P., DUNLAP, J.C., ESKIN, A., GARCEAU, N.Y., GEUSZ, M.E., JOHNSON, K.A., KHALSA, S.B., HOFFEN, G.C.K., KOUMENIS, C., LEE, T.M., LESAUTER, J., LINDGREN, K.M., LIU, Q., LOROS, J.J., MICHEL, S.H., MIRMIRAN, M., MOORE, R.Y., RUBY, N.F., SILVER, R., TUREK, F.W., ZATZ, M., & ZUCKER, I. (1993). Circadian rhythms. *Brain Res. Rev.*, **18,** 315–333.

BALER, R., COVINGTON, S. & KLEIN, D.C. (1997). The rat arylalkylamine N-acetyltransferase gene promoter. cAMP activation via a cAMP-responsive element-CCAAT complex. *J. Biol. Chem.*, **272,** 6979–6985.

BINKLEY, S.A., MACBRIDE, S.E., KLEIN, D.C. & RALPH, C.L. (1973). Pineal enzymes: regulation of avian melatonin synthesis. *Science,* **181,** 273–275.

BLIN, N., CAMOIN, L., MAIGRET, B. & STROSBERG, A.D. (1993). Structural and conformational features determining selective signal transduction in the β_3-adrenergic receptor. *Mol. Pharmacol.*, **44,** 1094–1104.

BOND, R.A. & CLARKE, D.E. (1988). Agonist and antagonist characterization of a putative adrenoceptor with distinct pharmacological properties from the alpha- and beta-subtypes. *Br. J. Pharmacol.*, **95,** 723–734.

BREZEZINSKI, A. (1997). Melatonin in humans. *N. Engl. J. Med.,* **336,** 186–193.

BROWNSTEIN, M., SAAVEDRA, J.M. & AXELROD, J. (1973). Control of pineal N-acetylserotonin by a β-adrenergic receptor. *Mol. Pharmacol.,* **9,** 605–611.

BYLUND, D.B., EIKENBERG, D.C., HIEBLE, J.P., LANGER, S.Z., LEFKOWITZ, R.J., MINNEMAN, K.P., MOLINOFF, P.B., RUFFOLO JR, R.R. & TRENDELENBURG, U. (1994). International union of pharmacology nomenclature of adrenoceptors. *Pharmacol. Rev.*, **46,** 121–136.

CHALLISS, R.A., CHILVERS, E.R., WILLCOCKS, A.L. & NAHORSKI, S.R. (1990). Heterogeneity of [^{3}H]inositol 1,4,5-trisphosphate binding sites in adrenal-cortical membranes. *Biochem. J.,* **265,** 421–427.

COON, S.L., ROSEBOOM, P.H., BALER, R., WELLER, J.L., NAMBOODIRI, M.A.A., KOONIN, E.V. & KLEIN, D.C. (1995). Pineal serotonin N-acetyltransferase: expression cloning and molecular analysis. *Science,* **270,** 1681 – 1683.

DE LEAN, A., MUNSON, P.J. & RODLAND, D. (1978). Simultaneous analysis of families of sigmoidal curves: application to bioassay, and physiological dose-curves. *Am. J. Physiol.,* **235,** E97 – E102.

DOLAN, J.A., MUENKEL, H.A., BURNS, M.G., PELLEGRINO, S.M., FRASER, C.M., PIETRI, F., STROSBERG, A.D., LARGIS, E.E., DUTIA, M.D., BLOOM, J.D., BASS, A.S., TANIKELLA, T.K., COBUZZI, A., LAI, F.M. & CLAUS, T.H. (1994). Beta-3 adrenoceptor selectivity of the dioxolane dicarboxylate phenethanolamines. *J. Pharmacol. Exp. Ther.,* **269,** 1000 – 1006.

DUMAN, R.S., SAITO, N. & TALLMAN, J.F. (1989). Development of β-adrenergic receptor and G protein messenger RNA in rat brain. *Mol. Brain Res.,* **5,** 289 – 296.

EBADI, M. & GOVITRAPONG, P. (1986). Neural pathways and neurotransmitters affecting melatonin synthesis. *J. Neural Transm. Suppl.,* **21,** 125 – 155.

EMORINE, L.J., BLIN, N. & STROSBERG, A.D. (1994). The human β_3-adrenoceptor: the search for a physiological function. *Trends Pharmacol. Sci.,* **15,** 3 – 7.

GOTO, M., OSHIMA, I., HASEGAWA, M. & EBIHARA, S. (1994). The locus controlling pineal serotonin N-acetyltransferase activity (Nat-2) is located on mouse chromosome 11. *Mol. Brain Res.,* **21,** 349 – 354.

GOTO, M., OSHIMA, I., TOMITA, T. & EBIHARA, S. (1989). Melatonin content of the pineal gland in different mouse strains. *J. Pineal Res.,* **7,** 195 – 204.

KLEIN, D.C. & MOORE, R.Y. (1979). Pineal N-acetyltransferase and hydroxyindol-*O*-methyltransferase: control by the retinohypothalamic tract and the suprachiasmatic nucleus. *Brain Res.,* **174,** 245 – 262.

LITTLE, K.Y., KIRKMAN, J.A. & DUNCAN, G.E. (1996). β-adrenergic receptor subtypes in human pineal gland. *J. Pineal Res.,* **20,** 15 – 20.

LUCKENSMEYER, G.B. & KEAST, J.R. (1998). Activation of α- and β-adrenoceptors by sympathetic nerve stimulation in the large intestine of the rat. *J. Physiol.,* **510,** 549 – 561.

MACHIDA, C.A., BUNZOW, J.R., SEARLES, R.P., TOL, H.V., TESTER, B., NEVE, K.A., TEAL, P., NIPPER, V. & CIVELLI, O. (1990). Molecular cloning and expression of the β_1-adrenergic receptor gene. *J. Biol. Chem.,* **265,** 12960 – 12965.

NAMBOODIRI, M.A.A., SUGDEN, D., KLEIN, D.C., GRADY, JR R. & MEFFORD, I.N. (1985). Rapid nocturnal increase in ovine pineal N-acetyltransferase activity and melatonin synthesis: effects of cycloheximide. *J. Neurochem.,* **45,** 832 – 835.

NANTEL, F., BONIN, H., EMORINE, L.J., ZILBERFARB, V., STROSBERG, A.D., BOUVIER, M. & MARULLO, S. (1993). The human β_3-adrenergic receptor is resistant to short term agonist-promoted desensitization. *Mol. Pharmacol.,* **43,** 548 – 555.

ROSEBOOM, P.H., COON, S.L., BALER, R., MCCUNE, S.K., WELLER, J.L. & KLEIN, D.C. (1996). Melatonin synthesis: analysis of the more than 150-fold nocturnal increase in serotonin N-acetyltranferase messenger ribonucleic acid in the rat pineal gland. *Endocrinology,* **137,** 3033 – 3044.

ROSEBOOM, P.H. & KLEIN, D.C. (1995). Noradrenaline stimulation of pineal CREB phosphorylation: primary role of a β-adrenergic $\rightarrow$ cyclic AMP mechanism. *Mol. Pharmacol.,* **47,** 439 – 449.

SON, J.H., CHUNG, J.H., HUH, S.O., PARK, D.H., PENG, C., ROSENBLUM, M.G., CHUNG, Y.I. & JOH, T.H. (1996). Immortalization of neuroendocrine pinealocytes from transgenic mice by targeted tumorigenesis using the tryptophan hydroxylase promoter. *Mol. Brain. Res.,* **37,** 32 – 40.

STEHLE, J.H., FOULKES, N.S., PEVET, P. & SASSONE-CORSI, P. (1995). Developmental maturation of pineal gland function: synchronized CREM inducibility and adrenergic stimulation. *Mol. Endocrinol.,* **9,** 706 – 716.

STROSBERG, A.D. & PIETRI-ROUXEL, F. (1996). Function and regulation of the β_3-adrenoceptor. *Trends Pharmacol. Sci.,* **17,** 373 – 381.

SUGDEN, D., VANECEK, J., KLEIN, D.C., THOMAS, T.P. & ANDERSON, W.B. (1985). Activation of protein kinase C potentiates isoprenaline-induced cyclic AMP accumulation in rat pinealocytes. *Nature,* **314,** 359 – 361.

SUH, B.C. & KIM, K.T. (1995). Stimulation of adenylyl cyclase mediated by phospholipase C-linked M_3 muscarinic receptor in human neuroblastoma SK-N-BE(2)C cells. *J. Neurochem.,* **64,** 2500 – 2508.

SUH, B.C., SON, J.H., JOH, T.H. & KIM, K.T. (1997). Two distinct P_2-purinergic receptors, P_{2Y} and P_{2U}, are coupled to phospholipase C in mouse pineal gland tumor cells. *J. Neurochem.,* **68,** 1622 – 1632.

TAKAHASHI, J.S. (1993). Circadian clocks *a la* CREM. *Nature,* **365,** 299 – 300.

YU, L., SCHAAD, N.C. & KLEIN, D.C. (1993). Calcium potentiates cAMP stimulation of pineal arylalkylamine N-acetyltransferase. *J. Neurochem.,* **60,** 1436 – 1443.

ZILBERFARB, V., PIETRI-ROUXEL, F., JOCKERS, R., KRIEF, S., DELOUIS, C., ISSAD, T. & STROSBERG, A.D. (1997). Human immortalized brown adipocytes express functional β_3-adrenoceptor coupled to lipolysis. *J. Cell Sci.,* **110,** 801 – 807.

(Received May 22, 1998
Revised September 2, 1998
Accepted September 23, 1998)

British Journal of Pharmacology (1999) 126, 407–414
http://www.stockton-press.co.uk/bjp

Beneficial effects of raxofelast (IRFI 016), a new hydrophilic vitamin E-like antioxidant, in carrageenan-induced pleurisy

*,[1]Salvatore Cuzzocrea, [1]Giuseppina Costantino, [2]Emanuela Mazzon & [1]Achille P. Caputi

[1]Institute of Pharmacology, University of Messina, Piazza XX Settembre no 4, 98123 Messina, Italy and [2]Department of Biomorphology, School of Medicine, University of Messina, Italy

1 Peroxynitrite is a strong oxidant that results from reaction between NO and superoxide. It has been recently proposed that peroxynitrite plays a pathogenetic role in inflammatory processes. Here we have investigated the therapeutic efficacy of raxofelast, a new hydrophilic vitamin E-like antioxidant agent, in rats subjected to carrageenan-induced pleurisy.

2 *In vivo* treatment with raxofelast (5, 10, 20 mg kg^{-1} intraperitoneally 5 min before carrageenan) prevented in a dose dependent manner carrageenan-induced pleural exudation and polymorphonuclear migration in rats subjected to carrageenan-induced pleurisy. Lung myeloperoxidase (MPO) activity and malondialdehyde (MDA) levels, as well as histological organ injury were significantly reduced by raxofelast.

3 Immunohistochemical analysis for nitrotyrosine, a footprint of peroxynitrite, revealed a positive staining in lungs from carrageenan-treated rats. No positive nitrotyrosine staining was found in the lungs of the carrageenan-treated rats, which received raxofelast (20 mg kg^{-1}) treatment.

4 Furthermore, *in vivo* raxofelast (5, 10, 20 mg kg^{-1}) treatment significantly reduced peroxynitrite formation as measured by the oxidation of the fluorescent dihydrorhodamine 123, prevented the appearance of DNA damage, the decrease in mitochondrial respiration and partially restored the cellular level of NAD^+ in *ex vivo* macrophages harvested from the pleural cavity of rats subjected to carrageenan-induced pleurisy.

5 In conclusion, our study demonstrates that raxofelast, a new hydrophilic vitamin E-like antioxidant agent, exerts multiple protective effects in carrageenan-induced acute inflammation.

Keywords: Raxofelast; peroxynitrite; carrageenan; free radicals; inflammation

Abbreviations: ecNOS, constitutive endothelial nitric oxide synthase; iNOS, inducible nitric oxide synthase; MPO, myeloperoxidase; NO, nitric oxide; NOS, nitric oxide synthase; PARS, poly (ADP-ribose) synthetase; PMN, polymorphonuclear cells

Introduction

The role of oxyradical formation in various forms of inflammation is well established. Recent data demonstrate that the expression of the inducible isoform of nitric oxide (NO) synthase also plays important pathogenetic roles in various models of inflammation (Moncada *et al*., 1991; Nathan 1992; Cuzzocrea *et al*., 1998a). The systemic inflammatory response is also associated with the production of oxygen-derived free radicals (Youn *et al*., 1991; McCord, 1993), and there is now substantial evidence that much of the cytotoxicity is due to a concerted action of oxygen- and nitrogen-derived free radicals and oxidants. Peroxynitrite, a cytotoxic oxidant species formed from the reaction of NO and superoxide (Beckman *et al*., 1990) may mediate part of the oxidative injury associated with simultaneous production of NO and oxyradicals. The biological activity and decomposition of peroxynitrite is very much dependent on the cellular or chemical environment (presence of proteins, thiols, glucose, the ratio of NO and superoxide, carbon dioxide levels and other factors), and these factors influence its toxic potential (Beckman *et al*., 1990; Villa *et al*., 1994; Rubbo *et al*., 1994; Pryor & Squadrito, 1995). Peroxynitrite formation has been demonstrated in various inflammatory disorders (Halliwell, 1995; Salvemini *et al*., 1996a,b; Cuzzocrea *et al*., 1997b,c; 1998a) and in circulatory shock (Wiseman *et al*., 1994; Szabò, 1996).

Using the experimental model described here, previous work has demonstrated the anti-inflammatory potential of various therapeutic approaches aimed at the inhibition of NO synthesis and peroxynitrite formation (Tracey *et al*., 1995; Cuzzocrea *et al*., 1997c; 1998a). In our studies we utilized raxofelast (IRFI 016; 5-acetyloxy-2,3-dihydro-4,6,7-trimethyl-2-benzofuranacetic acid; Figure 1) a new hydrophilic vitamin E-like antioxidant agent (Campo *et al*., 1997). It was selected from a series of new compounds (Ceccarelli *et al*., 1993) designed with the aim of maximizing the antioxidant potency of phenols chemically related to α-tocopherol (vitamin E). The antioxidant activity of raxofelast has been convincingly demonstrated in several *in vitro* studies (Mattioli *et al*., 1991) and in various models of ischaemia-reperfusion injury (Campo *et al*., 1992; 1994). The purpose of the present study was to investigate the protective effect of raxofelast against the cellular energetic failure and the development of inflammation in rats treated with carrageenan.

Methods

Experimental groups

In the treated group of animals, raxofelast, was given intraperitoneally (i.p.) 5 min before carrageenan (5, 10, 20 mg kg^{-1}) (carrageenan + raxofelast group). In a vehicle-treated group of rats, vehicle (saline) was given instead of raxofelast (carageenan group). In separate groups of rats, surgery was performed in its every aspect identical to the one in

* Author for correspondence; E-mail: salvator@imeuniv.unime.it

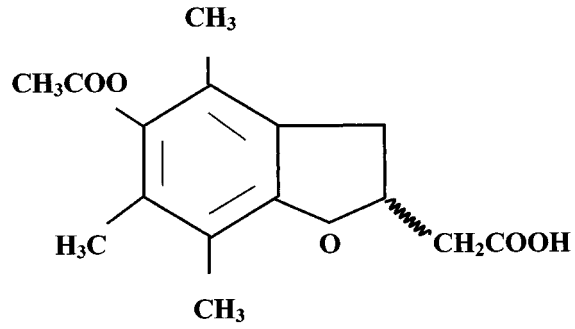

2,3-dihydro-5-acetyloxy-4,6,7-trimethyl-2-benzofuranacetic acid (IRFI-016)

Figure 1 Chemical structure of IRFI 016 (raxofelast).

the carrageenan group, except that carrageenan was not injected (control group). In an additional group of animals, control surgery was combined with the administration of raxofelast (dose as above) (control + raxofelast).

Carrageenan-induced pleurisy

Rats were lightly anaesthetized under isoflurane and submitted to a skin incision at the level of the left sixth intercostal space. The underlying muscles were dissected and 0.2 ml saline alone or containing 1% λ-carrageenan were injected into the pleural cavity. The skin incision was closed with a suture and the animals were allowed to recover. At 4 h after the injection of carrageenan, the animals were sacrificed under CO_2 vapour. The chest was carefully opened and the pleural cavity washed with 2 ml of saline solution with heparin (5 u ml^{-1}) and indomethacin (10 μg ml^{-1}). The exudate and washing were removed by aspiration and the total volume measured. Exudates contaminated with blood were discarded. The results were calculated by subtracting the volume injected (2 ml) from the total volume recovered. Leucocytes in the exudate were suspended in phosphate buffer saline and counted with an optical microscope using a Burker's chamber after vital Trypan Blue stain.

Cell culture

Resident pleural cells macrophages were collected 4 h after the carrageenan injection from rats treated with or without raxofelast (Cuzzocrea *et al*., 1998b). The cells (1×10^6 ml^{-1}), being mainly macrophages (approximately 70%) were cultured in DMEM medium, supplemented with M-glutamine (3.5 mM), penicillin (50 u ml^{-1}, streptomycin (50 μg ml^{-1}) and heparin sodium (10 u ml^{-1}) in 12-well 2 h and allowing cells to adhere at 37°C in a humidified 5% CO_2 incubator. Nonadherent cells were removed by rinsing the plates three times with 5% dextrose water. After removing nonadherent cells (approximately 10%), adherent macrophages were scraped from the measurement of DNA strand breaks and cellular NAD^+. Mitochondrial respiration and peroxynitrite formation were measured in the adherent cells in the subsequent 1 h period.

Measurement of peroxynitrite-induced oxidation of dihydrorhodamine 123

The formation of peroxynitrite was measured by the peroxynitrite-dependent oxidation of dihydrorhodamine 123 to rhodamine 123, as previously described (Cuzzocrea *et al*., 1998b). Cells were rinsed with phosphate-buffered saline and then medium was replaced with phosphate-buffered saline containing 5 μM dihydrorhodamine 123. After a 60 min incubation at 37°C, the fluorescence of rhodamine 123 was measured using a fluorimeter at an excitation wavelength of 500 nm, emission wavelength of 536 nm (slit widths 2.5 and 3.0 nm, respectively). Thus this method is an indirect measurement of peroxynitrite production because also other oxidant species can induce oxidation of dihydrorhodamine 123.

Measurement of mitochondrial respiration

Cell respiration was assessed by the mitochondrial-dependent reduction of MTT [3-(4,5-dimethylthiazol-2-yl)-2,5-diphenyl-tetrazolium bromide] to formazan (Zingarelli *et al*., 1996). Cells in 96-well plates were incubated at 37°C with MTT (0.2 mg ml^{-1}) for 1 h. Culture medium was removed by aspiration and the cells were solubilized in DMSO (100 μl). The extent of reduction of MTT to formazan within cells was quantitated by the measurement of OD_{550}. As previously discussed (Darley-Usmar & Halliwell, 1996), the measurement of reduction of MTT appears to be mainly by the mitochondrial complexes I and II, it also may involve NADH- and NADPH-dependent energetic processes that occur outside the mitochondrial inner membrane. Thus, this method cannot be used to separate the effect of free radicals, oxidants or other factors on the individual enzymes in the mitochondrial respiratory chain, but is useful to monitor changes in the general energetic status of the cells (Darley-Usmar & Halliwell, 1996).

Determination of DNA single-strand breaks

The formation of DNA strand breaks in double-stranded DNA was determined by the alkaline unwinding methods as previously described (Zingarelli *et al*., 1996; Schraufstatter *et al*., 1986). Cells in 12-well plates were scraped into 0.2 ml of solution A buffer (myoinositol 250 mM, NaH_2PO_3 10 mM, pH 7.2.). The cell lysate was then transferred into plastic tubes designated T (maximum fluorescence), P (fluorescence in sample used to estimate extent of DNA unwinding), or B (background fluorescence). To each tube, 0.2 ml of solution B (alkaline lysis solution: NaOH 10 mM, urea 9 M, ethylenediamineteraacetic acid 2.5 mM, sodium dodecyl sulphate 0.1%) was added and incubated at 4°C for 10 min to allow cell lysis and chromatin disruption. 0.1 ml each of solutions C (0.45 volume solution B in 0.2 N NaOH) and D (0.4 volume solution B in 0.2 N NaOH) were then added to the P and B tubes. 0.1 ml of solution E (neutralizing solution: glucose 1 M, mercaptoethanol 14 mM) was added to the T tubes before solutions C and D were added. From this point incubations were carried out in the dark. A 30 min incubation period at 0 °C was then allowed during which the alkali diffused into the viscous lysate. Since the neutralizing solution, solution E, was added to the T tubes before addition of the alkaline solutions C and D, the DNA in the T tubes was never exposed to a denaturing pH. At the end of the 30 min incubation, the contents of the B tubes were sonicated for 30 s to ensure rapid denaturation of DNA in the alkaline solution. All tubes were then incubated at 15°C for 10 min. Denaturation was stopped by chilling to 0°C and adding 0.4 ml of solution E to the P and B tubes. 1.5 ml of solution F (ethidium bromide 6.7 μg ml^{-1} in 13.3 mM NaOH) was added to all the tubes and fluorescence (excitation: 520 nm, emission: 590 nm) was measured by a fluorimeter. Under the conditions used, in which ethidium bromide binds preferentially to double stranded DNA, the

percentage of double stranded DNA (D) may be determined using the equation: % $D = 100 \times [F(P) - F(B)]/[F(T) - F(B)]$; where F(P) is the fluorescence of the sample, F(B) the background fluorescence, i.e. fluorescence due to all cell components other than double stranded DNA, and F(T) the maximum fluorescence.

Measurement of cellular NAD$^+$ levels

Cells in 12-well plates were extracted in 0.25 ml of 0.5 N $HC10_4$ scraped, neutralized with 3 M KOH, and centrifuged for 2 min at $10{,}000 \times g$. The supernatant was assayed for NAD^+ using a modification of the colorimetric method (Heller *et al*., 1995) in which NADH produced by enzymatic cycling with alcohol dehydrogenase, reduces MTT to formazan through the intermediation of phenazine methosulphate. The rate of MTT reduction is proportional to the concentration of the co-enzyme. The reaction mixture contained 10 μl of a solution of 2.5 mg ml^{-1} MTT, 20 μl of a solution of 4 mg ml^{-1} phenazine methosulphate, 10 μl of a solution of 0.6 mg ml^{-1} alcohol dehydrogenase (300 u mg^{-1}), and 190 μl of 0.065 M glycyl-glycine buffer, pH 7.4, that contained 0.1 M nicotinamide and 0.5 M ethanol. The mixture was warmed to 37°C for 10 min, and the reaction was started by the addition of 20 μl of the sample. The rate of increase in absorbance was read immediately after the addition of NAD^+ samples and after 10- and 20-min incubation at 37°C against blank at 560 nm in the ELISA microplate reader (SLT-Labinstruments Salzburg, Austria).

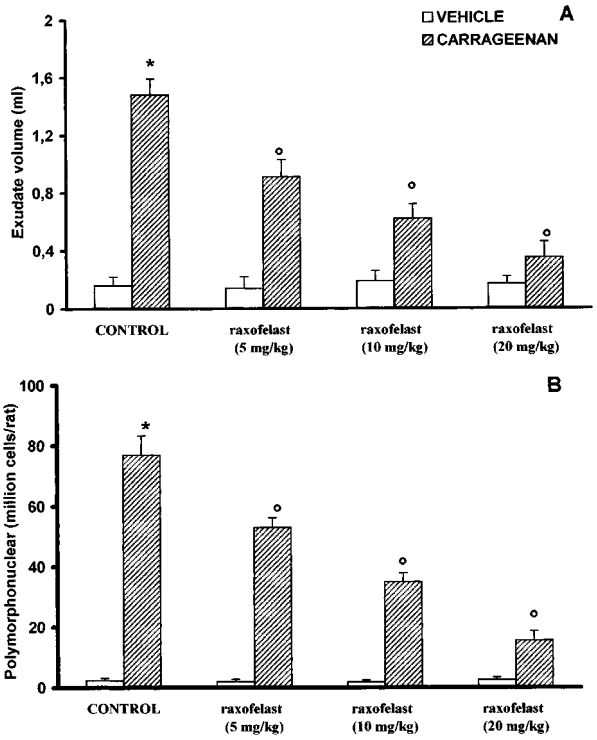

Figure 2 Volume exudate (A) and polymorphonuclear accumulation (B) in pleural cavity at 4 h after carrageenan injection. Raxofelast (5, 10, 20 mg kg^{-1}) treatment significantly reduced in a dose dependent manner pleural exudation and leukocyte migration. Data are means ± s.e.mean of ten rats for each group. *$P<0.01$ versus control; °$P<0.01$ versus carrageenan.

Light microscopy

Lung biopsies were taken 4 h after the induction of pleurisy by carrageenan injection. The tissue slices were fixed in Dietric solution (14.25% ethanol, 1.85% formaldehyde, 1% acetic acid) for 1 week at room temperature, dehydrated by graded ethanol and embedded in Paraplast (Sherwood Medical, Mahwah, NJ, U.S.A.). Section (thickness 7 μm) were deparaffinized with xylene, stained with trichromic Van Gieson and observed in Dialux 22 Leitz microscope.

Immunohistochemical localization of nitrotyrosine

Tyrosine nitration, a specific 'footprint' of peroxynitrite formation, was detected as previously described (Cuzzocrea *et al*., 1997b) in lung sections by immunohistochemistry. Tissues were fixed in 10% buffered formalin and 8 μm sections were prepared from paraffin embedded tissues. After deparaffinization, endogenous peroxidase was quenched with 0.3% H_2O_2 in 60% methanol for 30 min. The sections were permeabilized with 0.1% Triton X-100 in phosphate buffered saline for 20 min. Non-specific adsorption was minimized by incubating the section in 2% normal goat serum in phosphate

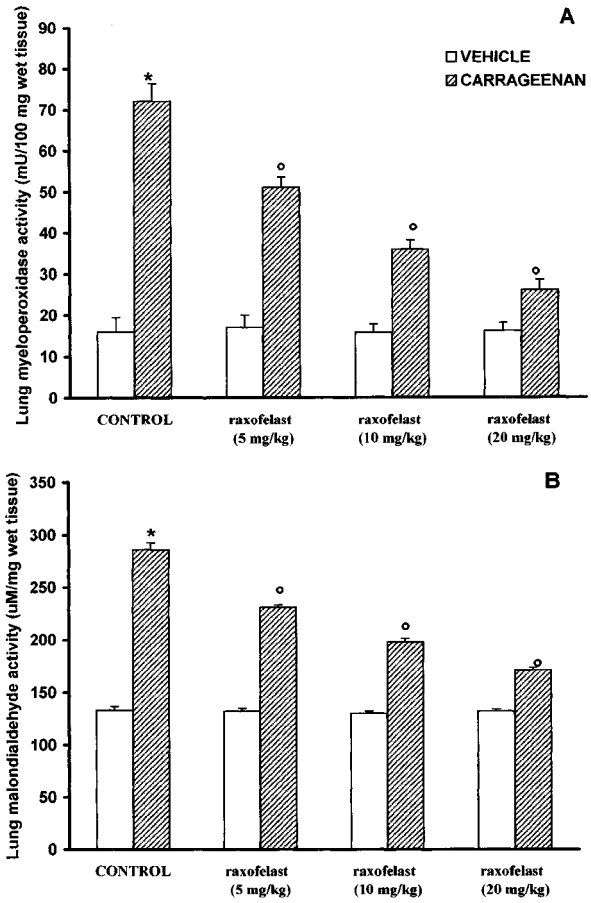

Figure 3 Myeloperoxidase (MPO) (A) and malondialdehyde (MDA) (B) in the lungs of carrageenan-treated rats. MPO activity and MDA levels were significantly increased in the lungs of the carrageenan-treated rats in comparison to control rats raxofelast (5, 10, 20 mg kg^{-1}) significantly reduced the carrageenan-induced increase in MPO activity and MDA levels. Values are means ± s.e.mean of ten rats for each group. *$P<0.01$ versus control; °$P<0.01$ versus carrageenan.

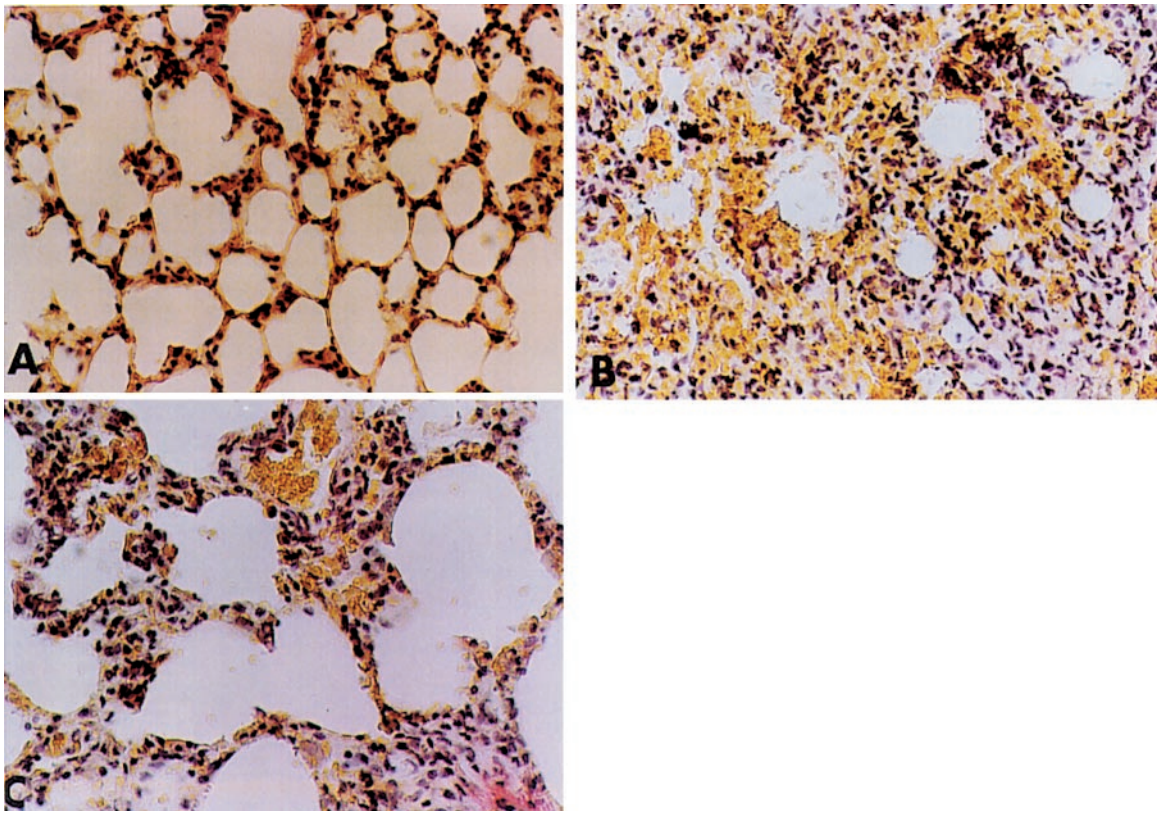

Figure 4 Representative lung sections from (A) control rats demonstrating the normal alveolar architecture. Lung sections from a carrageenan-treated rat (B) demonstrate inflammatory infiltration by neutrophil, lymphocytes and plasma. Lung sections from a carrageenan-treated rat that received raxofelast (20 mg kg^{-1}) (C) demonstrate reduced inflammatory infiltration. Original magnification: $\times 62.5$. Figure is representative of at least three experiments performed on different experimental days.

buffered saline for 20 min. Endogenous biotin or avidin binding sites were blocked by sequential incubation for 15 min with avidin and biotin (DBA, Milan, Italy). The sections were then incubated overnight with 1 : 1000 dilution of primary anti-nitrotyrosine antibody (DBA, Milan, Italy) or with control solutions. Controls included buffer alone or non specific purified rabbit IgG. Specific labelling was detected with a biotin-conjugated goat anti-rabbit IgG and avidin-biotin peroxidase complex (DBA, Milan, Italy).

Myeloperoxidase activity

Myeloperoxidase (MPO) activity, an index of polymorphonuclear leukocyte (PMN) accumulation, was determined as previously described (Mullane *et al*., 1988). At the specified time following the intrapleural injection of carrageenan lung tissues, were obtained and weighed. Each piece of tissue was homogenized in a solution containing 0.5% hexa-decyltrimethyl-ammonium bromide dissolved in 10 mM potassium phosphate buffer (pH 7) and centrifuged for 30 min at $20{,}000 \times g$ at 4°C. An aliquot of the supernatant was then allowed to react with a solution of tetra-methyl-benzidine (1.6 mM) and 0.1 mM H_2O_2. The rate of change in absorbance was measured spectrophotometrically at 650 nm. Myeloperoxidase activity was defined as the quantity of enzyme degrading 1 μmol of peroxide min^{-1} at 37°C and was expressed in milliunits per gram weight of wet tissue.

Malondialdehyde (MDA) measurement

Malondialdehyde (MDA) levels in the lung tissue were determined as an index of lipid peroxidation, as described by Okhawa *et al*. (1979). Lung tissue, collected at the specified time, were homogenized in 1.15% KCl solution. An aliquot (100 μl) of the homogenate was added to a reaction mixture containing 200 μl of 8.1% SDS, 1500 μl of 20% acetic acid (pH 3.5), 1500 μl of 0.8% thiobarbituric acid and 700 μl distilled water. Samples were then boiled for 1 h at 95°C and centrifuged at $3000 \times g$ for 10 min. The absorbance of the supernatant was measured by spectrophotometry at 650 nm.

Materials

Raxofelast was supplied by Biomedica Foscama, Ferentino (FR), Italy. Cell culture medium, heparin and foetal calf serum were obtained from Sigma (Milan, Italy). Biotin blocking kit, biotin-conjugated goat anti-rabbit IgG, primary anti-nitrotyrosine antibody and avidin-biotin peroxidase complex were obtained from DBA (Milan, Italy). All other reagents and compounds used were obtained from Sigma Chemical Company (Sigma, Milan, Italy).

Data analysis

All values in the figures and text are expressed as mean $\pm$ standard error (s.e.m.) of the mean of n observations. For the *in vitro* studies, data represent the number of wells studied (6–9 wells from 2–3 independent experiments). For the *in vivo* studies n represents the number of animals studied. In the experiments involving histology or immunohistochemistry, the figures shown are representative of at least three experiments performed on different experimental days. The results were analysed by one-way ANOVA followed by a *post-hoc*

Bonferroni test. A P-value less than 0.05 was considered significant.

Results

Effects of raxofelast in carrageenan-induced pleurisy

All carrageenan-injected rats developed an acute pleurisy, producing 1.8 ± 0.15 ml of turbid exudate (Figure 2A). Trypan blue stain revealed $77 \pm 6.4 \times 10^6$ rat^{-1} PMNs in comparison to control rat ($2.4 \pm 0.8 \times 10^6$ rat^{-1}) (Figure 2B). Control animals demonstrated no abnormalities in the pleural cavity or fluid. The degree of peritoneal exudation and polymorphonuclear migration were significantly reduced in rats with raxofelast (Figure 2A,B). Raxofelast treatment did not cause significant changes in these parameters in control rats (Figure 2A,B).

Lungs obtained from carrageenan-treated rats were examined for the measurement of MPO activity, the latter being indicative of neutrophil infiltration, and for MDA levels, in order to estimate lipid peroxidation. As shown in Figure 3A, B, MPO activity and MDA levels (7.2 ± 6.4 mu 100 mg^{-1} wet tissue and 286 ± 4.4 μM mg^{-1} wet tissue, respectively) were significantly ($P < 0.01$) increased in the lung from carrageenan-treated rats when compared to control rats (16 ± 3.5 mu 100 mg^{-1} wet tissue; 133 ± 6.8 μM mg^{-1} wet tissue respectively.) MPO activity and MDA levels were significantly ($P < 0.01$) reduced in a dose dependent manner by raxofelast treatment (Figure 3A,B).

Histological examination of lung section showed inflammatory infiltration by neutrophil, lymphocytes and plasma cells extravasation (Figure 4B). Raxofelast treatment reduced histological organ injury (Figure 4C).

Lung sections were also analysed for the presence of nitrotyrosine, a footprint of peroxynitrite. Immunohistochemical analysis, using a specific anti-nitrotyrosine antibody, revealed a positive staining in lungs from carrageenan-treated

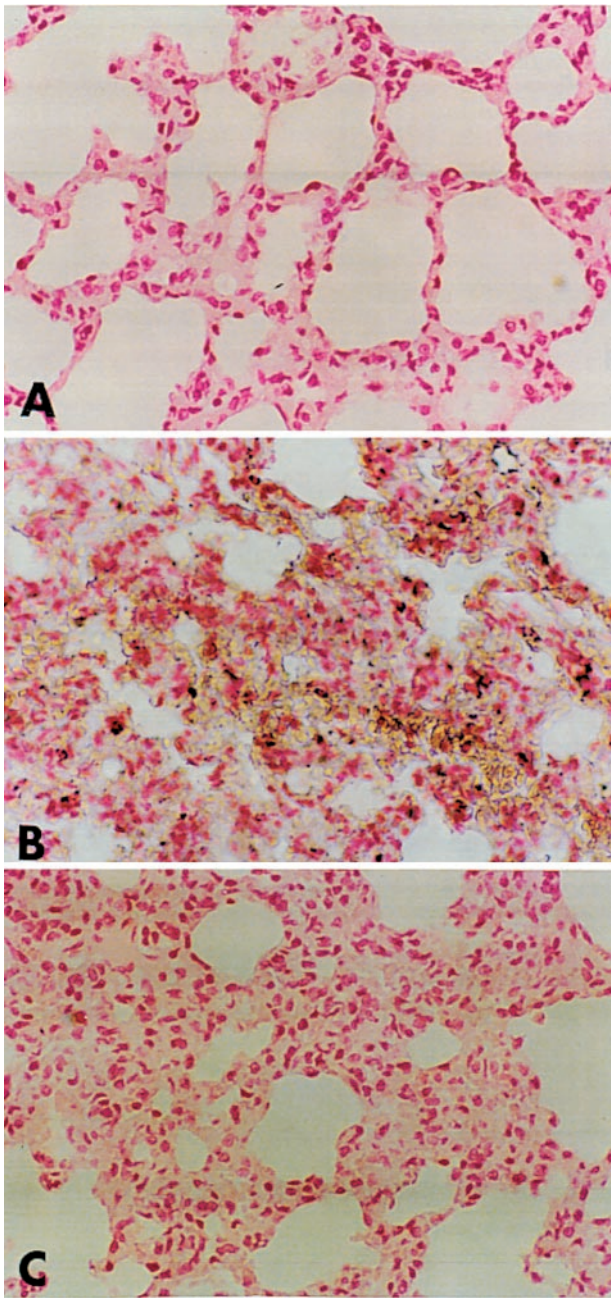

Figure 5 Immunohistochemical localization of nitrotyrosine in the rat lung. Staining was absent in control tissue (A). Four hours following carrageenan injection, nitrotyrosine immunoreactivity was localized mainly to macrophages and some epithelial cells (B). There is a marked reduction in the immunostaining in the lungs of carrageenan-treated rats when rats were pretreated with raxofelast (20 mg kg^{-1}) (C). Original magnification: $\times 125$. Figure is representative of at least three experiments performed on different experimental days.

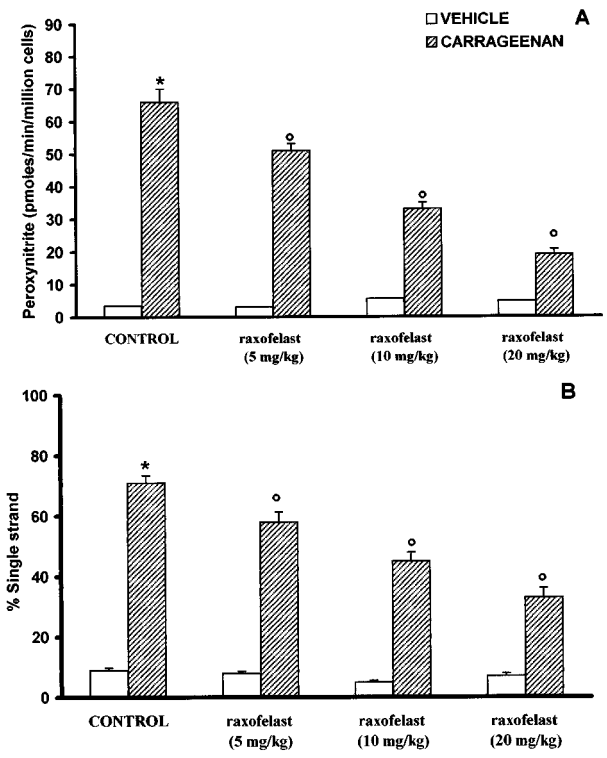

Figure 6 Peroxynitrite formation (A) and DNA single strand breakage development in pleural macrophages harvested from control and carrageenan-treated rats. Four hours after carrageenan injection a significant peroxynitrite production and a marked increase in DNA strand breakage was observed. Raxofelast significantly (5, 10, 20 mg kg^{-1}) inhibited in a dose dependent manner dihydrorhodamine 123 oxidation and prevented the carrageenan-induced DNA single strand breakage. Data represent the number of wells studied (6–9 wells from 2–3 independent experiments). *$P < 0.01$ versus macrophages from control rats; °$P < 0.01$ represents a significant inhibitory effect of raxofelast.

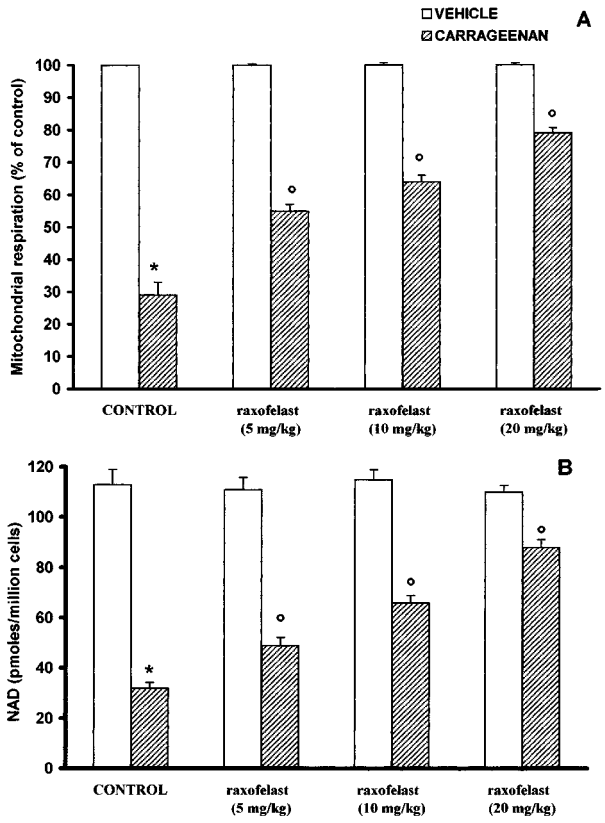

Figure 7 Reduction of mitochondrial respiration (A) and cellular levels of NAD^+ (B) in macrophages from control and carrageenan-treated rats. Four hours after carregeenan administration the disruption of cellular energetic pool was evidenced by a significant decrease in mitochondrial respiration and intracellular concentration of NAD^+. Raxofelast (5, 10, 20 mg kg^{-1}) significantly inhibited in a dose dependent manner the decrease in cellular respiration and partially restored the depletion of intracellular levels of NAD^+. Data represent the number of wells studied (6–9 wells from 2–3 independent experiments). $^*P<0.01$ versus macrophages from control rats; $^\circ P<0.01$ represents protective effects of raxofelast.

rats, which was primarily localized in alveolar macrophages and in airway epithelial cells (Figure 5B). No positive nitrotyrosine staining was found in the lungs of the carrageenan-treated rats when they were treated with raxofelast (Figure 5C).

Raxofelast protects against the cellular energetic failure

In pleural macrophages obtained from carrageenan-treated rats, a significant peroxynitrite production was detectable (66 ± 4 pmoles min^{-1} cells; Figure 6A). A marked increase in DNA strand breakage was also observed after carrageenan-induced pleurisy (Figure 6B). Carregeenan-mediated disruption of cellular energetic pool was evidenced by a significant decrease in mitochondrial respiration and intracellular concentration of NAD^+ (Figure 7A,B). The *in vivo* treatment of the animals with raxofelast significantly inhibited in a dose dependent manner dihydrorhodamine 123 oxidation, prevented the carrageenan-induced DNA single strand breakage (Figure 6A,B), significantly inhibited the decrease in cellular respiration and partially restored the depletion of intracellular levels of NAD^+ (Figure 7A,B).

Discussion

Inflammatory process is invariably characterized by a production of prostaglandins, leukotrienes, histamine, bradykinin, platelet-activing factor (PAF) and interleukin I (IL-1), by a release of chemicals from tissues and migrating cells (Vane & Botting, 1987; Tomlinson *et al*., 1994). Furthermore, one possibility that has been frequently discussed is that production of reactive oxidants such as hydrogen peroxide, superoxide and hydroxyl radical at site of inflammation contributes to tissue damage (Oh-Ishi *et al*., 1989; Dawson *et al*., 1991; Peskar *et al*., 1991; Da Motta *et al*., 1994; Salvemini *et al*., 1996a,b; Cuzzocrea *et al*., 1997c; 1998a). Pharmacological inhibitors of NOS have been shown to reduce the development of carrageenan-induced inflammation and support a role of NO in this model of inflammation (Tracey *et al*., 1995; Wei *et al*., 1995; Salvemini *et al*., 1996a,b; Cuzzocrea *et al*., 1997c; 1998a). More recent studies have shown the formation of peroxynitrite in carrageenan-induced inflammation (Salvemini *et al*., 1996a,b; Cuzzocrea *et al*., 1997c; 1998a,b). Using nitrotyrosine immunohistochemistry, this study has confirmed the production of peroxynitrite in the lung of rats subjected to carrageenan-induced pleurisy.

The biological activity and decomposition of peroxynitrite is very much dependent on the cellular or chemical environment (presence of proteins, thiols, glucose, the ratio of NO and superoxide, carbon dioxide levels and other factors), and these factors influence its toxic potential (Beckman *et al*., 1990; Villa *et al*., 1994; Rubbo *et al*., 1994; Pryor & Squadrito, 1996).

In the present study we found that (1) raxofelast reduces the development of carrageenan-induced pleurisy (2) raxofelast reduces morphological injury and neutrophil infiltration in carrageenan-induced inflammation; and (3) raxofelast reduces nitrotyrosine immunostaining, an indicator of peroxynitrite formation in inflammation.

It could be speculated that the pharmacological effects of raxofelast may be dependent upon a combination of: (1) a scavenging action toward oxygen radicals, which results in the prevention of peroxynitrite formation with consequent protection against the development of peroxynitrite-induced cellular energetic failure, (2) a reduced neutrophil recruitment into the inflammatory site, which may represent an important additional mechanism for the observed anti-inflammatory action. The reduced neutrophil infiltration into the inflamed tissue may be related to a prevention of endothelial oxidant injury by raxofelast and to a preservation of endothelial barrier function. Therefore, the relative contribution of the raxofelast's multiple modes of action observed in the current study to be determined in further studies.

Recent studies have proposed that a novel pathway, involving the nuclear enzyme poly (ADP-ribose) synthetase (PARS) play an important role in inflammation (Szabò *et al*., 1997a; 1998; Cuzzocrea *et al*., 1998b,c). It is well known that this pathway plays an important role in various forms of shock (Szabò *et al*., 1997b) and reperfusion injury (Thiemermann *et al*., 1997; Zingarelli *et al*., 1997; Cuzzocrea *et al*., 1997b). Raxofelast has been shown to display potent protective effects against oxidative damage in *in vitro* studies (Mattioli *et al*., 1991) and in various models of oxyradical-mediated ischaemia-reperfusion injury (Campo *et al*., 1992; 1994). The protection by raxofelast against the development of DNA single strand breakage and the partially restoration of intracellular NAD^+ depletion (as shown in Figures 6A and 7B), may thus be related to a decreased peroxynitrite formation, which may thus lead to a prevention of the activation of PARS in inflammation.

Taken together, the results of the present study coupled with recent data by several groups support the view that raxofelast can exert protective effects on cellular injury. In conclusion raxofelast, an α-tocopherol analogue with free radical scavenging properties, reduces the inflammatory response in rats subjected to carrageenan-induced pleurisy. It may therefore have potential therapeutic effects.

We gratefully acknowledge Biomedica Foscama Research Centre, Ferentino, (FR), Italy for the generous supply of raxofelast. We also thank Fabio Giuffrè and Carmelo La Spada for their excellent technical assistance during this study, Mrs Caterina Cutrona for secretarial assistance and Miss Valentina Malvagni for editorial assistance with the manuscript.

References

BECKMAN, J.S., BECKMAN, T.W., CHEN, J., MARSHALL, P.A. & FREEMAN, B.A. (1990). Apparent hydroxyl radical production by peroxynitrite: implication for endothelial injury from nitric oxide and superoxide. *Proc. Natl. Acad. Sci. U.S.A.,* **87,** 1620–1624.

CAMPO, G.M., SQUADRITO, F., IOCULANO, M., AVENOSO, A., ZINGARELLI, B., CALANDRA, S., SCURI, R., SAITTA, A. & CAPUTI, A.P. (1992). IRFI 016 a new radical scavenger limits ischemic damage following coronary artery occlusion in rats. *Res. Commun. Chem. Pathol. Pharmacol.,* **76,** 287–303.

CAMPO, G.M., SQUADRITO, F., IOCULANO, M., POLLICINO, A.M., RIZZO, A., CALAPAI, G., CALANDRA, S., SCURI, R. & CAPUTI, A.P. (1994). Protective effect of IRFI 016, a new antioxidant agent, in myocardial damage following coronary artery occlusion and reperfusion in rats. *Pharmacol.,* **48,** 157–166.

CAMPO, G.M., GECCARELLI, S., SQUADRITO, F., ALTAVILLA, D., DORIGOTTI, L. & CAPUTI, A.P. (1997). Raxofelast (IRFI 016): a new hydrophilic vitamin E-like antioxidant agent. *Cardiovasc. Drug Rev.,* **15,** 157–1173.

CECCARELLI, S., DE VELLIS, P., SCURI, R. & ZANARELLA S. (1993). Synthesis of novel 2-substituted-5-oxycoumarans via a direct route to 2,3-dihydro-5-hydroxy-2-benzofuranacetic acids. *J. Heterocycl. Chem.,* **30,** 679–690.

CUZZOCREA, S., ZINGARELLI, B., CALAPAI, G., NAVA, F. & CAPUTI, A.P. (1997a). Zymosan-activated plasma induces paw oedema by nitric oxide and prostaglandin production. *Life Sci.,* **60,** 215–220.

CUZZOCREA, S., ZINGARELLI, B., COSTANTINO, G., SZABÓ, A., SALZMAN, A.L., CAPUTI, A.P. & SZABÓ, C. (1997b). Beneficial effects of 3-aminobenzamide, an inhibitor of poly (ADP-ribose) synthetase in a rat model of splanchnic artery occlusion and reperfusion. *Br. J. Pharmacol.,* **121,** 1065–1074.

CUZZOCREA, S., ZINGARELLI, B., GILARD, E., HAKE, P., SALZMAN, A.L. & SZABÓ, C. (1997c). Protective effect of melatonin in carrageenan-induced models of local inflammation. *J. Pineal Res.,* **23,** 106–116.

CUZZOCREA, S., ZINGARELLI, B., GILARD, E., HAKE, P., SALZMAN, A.L. & SZABÓ, C. (1998a). Anti-inflammatory effects of mercaptoethylguanidine, a combined inhibitor of nitric oxide synthase and peroxynitrite scavenger, in carrageenan-induced models of inflammation. *Free Rad. Biol. Med.,* **24,** 450–459.

CUZZOCREA, S., CAPUTI, A.P. & ZINGARELLI, B. (1998b). Peroxynitrite-mediated DNA strand breakage activates poly (ADP-ribose) synthetase and causes cellular energy depletion in carrageenan-induced pleurisy. *Immunology,* **93,** 96–101.

CUZZOCREA, S., ZINGARELLI, B., GILARD, E., HAKE, P., SALZMAN, A.L. & SZABÓ, C. (1998c). Protective effects of 3-aminobenzamide, an inhibitor of poly (ADP-ribose) synthase in carrageenan-induced models of local inflammation. *Eur. J. Pharmacol.,* **342,** 67–76.

DA MOTTA, J.I., CUNHA, F.Q., VARGAFTIG, B.B. & FERREIRA, S.H. (1994). Drug modulation of antigen-induced paw oedema in guinea-pigs: effects of lipopolysaccharide, tumour necrosis factor and leucocyte depletion. *Br. J. Pharmacol.,* **112,** 111–116.

DARLEY-USMAR, V. & HALLIWELL, B. (1996). Blood radicals. Reactive nitrogen species, reactive oxygen species, transition metal ions, and the vascular system. *Pharmaceut. Res.,* **13,** 649–655.

DAWSON, J., SEDGWICK, A.D., EDWARDS, J.C. & LEES, P. (1991). A comparative study of the cellular, exudative and histological responses to carrageenan, dextran and zymosan in the mouse. *Int. J. Tissue React.,* **13,** 171–185.

HALLIWELL, B. (1995). Oxygen radicals, nitric oxide and human inflammatory joint disease. *Ann. Rheumat. Dis.,* **54,** 505–510.

HELLER, B., WANG, Z.Q., WAGNER, E.F., RADONS, J., BURKLE, A., FEHSEL, K., BURKART, V. & KOLB, H. (1995). Inactivation of the poly(ADP-ribose) polymerase gene affects oxygen radical and nitric oxide toxicity in islet cells. *J. Biol. Chem.,* **270,** 11176.

MATTOLI, S., MEZZETTI, M., ALLEGRA, L. & BRAGA, P.C. (1991). Dihydro-hydroxy-trimethyl-benzofuranyl acetic acid inhibits lipid peroxydation and lysosomal enzyme release in bronchial epithelial cells and macrophages. *Ital. J. Chest Dis.,* **45,** 78–80.

MCCORD, J. (1993). Oxygen-derived free radicals. *New Horizons,* **1,** 70–76.

MONCADA, S., PALMER, R.M.J. & HIGGS, E.A. (1991). Nitric oxide: Physiology, Pathophysiology and Pharmacology. *Pharmacol. Rev.,* **43,** 109–142.

MULLANE, K.M., WESTLIN, W. & KRAEMER, R. (1988). Activated neutrophils release mediators that may contribute to myocardial injury and dysfunction associated with ischemia and reperfusion. *Ann. N.Y. Acad. Sci. U.S.A.,* **524,** 103–121.

NATHAN, C. (1992). Nitric oxide as a secretory product of mammalian cells. *FASEB J.,* **6,** 3051–3064.

OHKAWA, H., OHISHI, N. & YAGI, K. (1979). Assay for lipid peroxides in animal tissues by thiobarbituric acid reaction. *Anal. Biochem.,* **95,** 351–358.

OH-ISHI, S., HAYASHI, I., HAYASHI, M., YAMAKI, K. & UTSUNOMIYA, I. (1989). Pharmacological demonstration of inflammatory mediators using experimental inflammatory models: rat pleurisy induced by carrageenin and phorbol myristate acetate. *Dermatologica,* **179** (suppl 1), 68–71.

PESKAR, B.M., TRAUTMANN, M., NOWAK, P. & PESKAR, B.A. (1991). Release of 15-hydroxy-5,8,11,13-eicosatetraenoic acid and cysteinyl-leukotrienes in carrageenin-induced inflammation: effect of non-steroidal anti-inflammatory drugs. *Agents Actions,* **33,** 240–246.

PRYOR, W. & SQUADRITO, G. (1995). The chemistry of peroxynitrite: a product from the reaction of nitric oxide with superoxide. *Am. J. Physiol.,* **268,** L699–L772.

RUBBO, H., RADI, R., TRUJILLO, M., TELLERI, R., KALYANARAMAN, B., BARNES, S., KIRK, M. & FREEMAN, B.A. (1994). Nitric oxide regulation of superoxide and peroxynitrite-dependent lipid peroxidation. Formation of novel nitrogen-containing oxidised lipid derivatives. *J. Biol. Chem.,* **269,** 26066–26075.

SALVEMINI, D., WANG, Z.Q., WYATT, P., BOURDON, D.M., MARINO, M.H., MANNING, P.T. & CURRIE, M.G. (1996a). Nitric oxide: a key mediator in the early and late phase of carrageenan-induced rat paw inflammation. *Br. J. Pharmacol.,* **118,** 829–838.

SALVEMINI, D., WANG, Z.Q., BOURDON, D.M., STERN, M.K., CURRIE, M.G. & MANNING, P.T. (1996b). Evidence of peroxynitrite involvement in the carrageenan-induced rat paw edema. *Eur. J. Pharmacol.,* **303,** 217–220.

SCHRAUFSTATTER, I.U., HINSHAW, D.B., HYSLOP, P.A., SPRAGG, R.G. & COCHRANE, C.G. (1986). Oxidant injury of cells: DNA strand-breaks activate polyadenosine diphosphate-ribose polymerase and lead to depletion of nicotinamide adenine dinucleotide. *J. Clin. Invest.,* **77,** 1312–1320.

SZABÓ, C. (1996). The role of peroxynitrite in the pathophysiology of shock, inflammation and ischemia-reperfusion injury. *Shock,* **6,** 79–87.

SZABÓ, C., LIM, L.H.K., CUZZOCREA, S., GETTING, S.J., ZINGARELLI, B., FLOWER, R.J., SALZMAN, A.L. & PERRETTI, M. (1997a). Inhibition of poly (ADP-ribose) synthetase exerts anti-inflammatory effects and inhibits neutrophil recruitment. *J. Exp. Med.,* **186,** 1041–1049.

SZABÓ, C., CUZZOCREA, S., ZINGARELLI, B., O'CONNOR, M. & SALZMAN, A.L. (1997b). Endothelial dysfunction in endotoxic shock: importance of the activation of poly (ADP ribose synthetase (PARS) by peroxynitrite. *J. Clin. Invest.,* **100,** 723–735.

SZABÓ, C., VIRÀG, L., CUZZOCREA, S., SCOTT, G.S., HAKE, P., O'CONNOR, M., ZINGARELI, B., MA, Y., HIRSCH, R., BOIOVIN, G.P., SALZMAN, A.L. & KUN, E. (1998). Protection against peroxynitrite-induced fibroblast injury and arthritis development by inhibition of poly (ADP-Ribose) synthetase. *Proc. Natl. Acad. Sci. U.S.A.,* **95,** 3867–3872.

THIEMERMANN, C., BOWES, J., MYNNY, F.P. & VANE, J.R. (1997). Inhibition of the activity of poly(ADP ribose) synthase reduces ischaemia-reperfusion injury in the heart and skeletal muscle. *Proc. Natl. Acad. Sci. U.S.A.,* **94,** 679–683.

TOMLINSON, A., APPLETON, I., MOORE, A.R., GILROY, D.W., WILLIS, D., MITCHELL, J.A. & WILLOUGHBY. (1994). Cyclo-oxygenase and nitric oxide isoforms in rat carrageenin-induced pleurisy. *Br. J. Pharmacol.,* **113,** 693–698.

TRACEY, W.R., NAKANE, M., KUK, J., BUDZIK, G., KLINGHOFER, V., HARRIS, R. & CARTER, G. (1995). The nitric oxide synthase inhibitor, L-NG-monomethylarginine, reduces carrageenan-induced pleurisy in the rat. *J. Pharmacol. Exp. Ther.,* **273,** 1295–1299.

VANE, J. & BLOTTING, R. (1987). Inflammation and the mechanism of action of antiinflammatory drugs. *FASEB J.,* **1,** 89–96.

VILLA, L.M., SALAS, E., DARLEY-USMAR, M., RADOMSKI, M.W. & MONCADA, S. (1994). Peroxynitrite induces both vasodilatation and impaired vascular relaxation in the isolated perfused rat heart. *Proc. Natl. Acad. Sci. U.S.A.,* **91,** 12383–12387.

WEI, X.Q., CHARLES, I.G., SMITH, A., URE, J., FENG, G.J., HUANG, F.P., XU, D., MULLER, W., MONCADA, S. & LIEW, F.Y. (1995). Altered immune responses in mice lacking inducible nitric oxide synthase. *Nature,* **375,** 408–411.

WIZEMANN, T., GARDNER, C., LASKIN, J., QUINONES, S., DURHAM, S., GOLLER, N., OHNISHI, T. & LASKIN, D. (1994). Production of nitric oxide and peroxynitrite in the lung during acute endotoxemia. *J. Leukoc. Biol.,* **56,** 759–768.

YOUN, Y.K., LALONDE, C. & DEMLING, R. (1991). Use of antioxidant therapy in shock and trauma. *Circ. Shock,* **35,** 245–249.

ZINGARELLI, B., CUZZOCREA, S., ZSENGELLER, Z., SALZMAN, A.L. & SZABÓ, C. (1997). Protection against myocardial ischemia and reperfusion injury by 3-aminobenzamide, an inhibitor of Poly (ADP-Ribose) synthetase. *Cardiovasc. Res.,* **36,** 205–215.

ZINGARELLI, B., O'CONNOR, M., WONG, H., SALZMAN, A.L. & SZABÓ, C. (1996). Peroxynitrite-mediated DNA strand breakage activates poly-adenosine diphosphate ribosyl synthetase and causes cellular energy depletion in macrophages stimulated with bacterial lipolysaccharide. *J. Immunol.,* **156,** 350–358.

(Received April 15, 1998
Revised September 25, 1998
Accepted October 6, 1998).

British Journal of Pharmacology (1999) 126, 415–420
http://www.stockton-press.co.uk/bjp

Specific inhibition of ADP-induced platelet aggregation by clopidogrel *in vitro*

[1]Artur-Aron Weber, [1]Stephanie Reimann & *,[1] Karsten Schrör

[1]Institut für Pharmakologie, Heinrich-Heine-Universität Düsseldorf, Germany

1 The thienopyridine clopidogrel is a specific inhibitor of ADP-induced platelet aggregation *ex vivo*. No direct effects of clopidogrel ($\leqslant 100$ μM) on platelet aggregation *in vitro* have been described so far.

2 Possible *in vitro* antiaggregatory effects (turbidimetry) of clopidogrel were studied in human platelet-rich plasma and in washed platelets.

3 Incubation of platelet-rich plasma with clopidogrel ($\leqslant 100$ μM) for up to 8 h did not result in any inhibition of ADP (6 μM)-induced platelet aggregation.

4 Incubation of washed platelets with clopidogrel resulted in a time- (maximum effects after 30 min) and concentration-dependent (IC_{50} 1.9 ± 0.3 μM) inhibition of ADP (6 μM)-induced platelet aggregation. Clopidogrel (30 μM) did not inhibit collagen (2.5 μg ml^{-1})-, U46619 (1 μM)- or thrombin (0.1 u ml^{-1})-induced platelet aggregation. The inhibition of ADP-induced aggregation by clopidogrel (30 μM) was insurmountable indicating a non-equilibrium antagonism of ADP actions. The R enantiomer SR 25989 C (30 μM) was significantly less active than clopidogrel (30 μM) in inhibiting platelet aggregation (32 ± 5 % vs 70 ± 1 % inhibition, $P < 0.05$, $n = 5$).

5 In washed platelets, clopidogrel ($\leqslant 30$ μM) did not significantly reverse the inhibition of prostaglandin E_1 (1 μM)-induced platelet cyclic AMP formation by ADP (6 μM).

6 The antiaggregatory effects of clopidogrel were unchanged when the compound was removed from the platelet suspension. However, platelet inhibition by clopidogrel was completely abolished when albumin (350 mg ml^{-1}) was present in the test buffer.

7 It is concluded that clopidogrel specifically inhibits ADP-induced aggregation of washed platelets *in vitro* without hepatic bioactivation. Inhibition of ADP-induced platelet aggregation by clopidogrel *in vitro* occurs in the absence of measurable effects on the reversal of PGE_1-stimulated cyclic AMP by ADP.

Keywords: Clopidogrel; SR 25989 C; platelets; aggregation; shape change; ADP

Abbreviations: ADP, adenosine 5′-diphosphate; cyclic AMP, adenosine 3′:5′- cyclic monophosphate; PGE_1, prostaglandin E_1

Introduction

Clopidogrel is an antiplatelet compound that has recently been shown to be effective in the secondary prevention of cardiovascular complications of atherosclerosis (CAPRIE Steering Committee, 1996). The thienopyridines clopidogrel and ticlopidine are specific inhibitors of ADP-induced platelet aggregation but not of ADP-induced shape change or Ca^{2+} transients (for reviews see Coukell & Markham, 1997; Schrör, 1998). Although the exact mechanisms are not known, treatment with clopidogrel reduces the binding of ADP or stable ADP analogues to high-affinity binding sites on platelets (Mills *et al*., 1992; Savi *et al*., 1994b; 1997; Gachet *et al*., 1995). The ADP receptors that are modified by clopidogrel are also believed to mediate the inhibition of prostaglandin I_2- or E_1-induced cyclic AMP formation by ADP (Defreyn *et al*., 1991; Mills *et al*., 1992).

In platelet-rich plasma, clopidogrel ($\leqslant 100$ μM) does not inhibit platelet aggregation *in vitro* (Herbert, 1994). In rats, the *in vivo* activity of clopidogrel has been proposed to be dependent on hepatic biotransformation to an active metabolite (Savi *et al*., 1992). In these studies, clopidogrel (40 mg kg^{-1}) was less effective in hepatectomized rats as compared to normal control rats. In addition, clopidogrel did inhibit platelet aggregation in isolated, blood-perfused rat livers. The bioactivation of clopidogrel has been suggested to be mediated by the hepatic cytochrome P450 system (Savi *et al*., 1994a).

However, an active metabolite of clopidogrel has not been published so far and the need for hepatic activation of clopidogrel has not been demonstrated in humans. In this context, it is noteworthy that in animal studies much higher doses of clopidogrel were used as compared to the standard dosage for humans (75 mg d^{-1}). Thus, different mechanisms may account for platelet inhibition in humans as compared to animal studies.

This study demonstrates that clopidogrel specifically inhibits ADP-induced aggregation of washed human platelets *in vitro* without the need of hepatic bioactivation. Inhibition of ADP-induced platelet aggregation by clopidogrel *in vitro* occurs in the absence of measurable effects on the reversal of PGE_1-stimulated cyclic AMP by ADP.

Methods

Preparation of washed human platelets

Washed human platelets were prepared as previously described (Weber *et al*., 1993). Fresh citrated blood was obtained from a local blood-bank. Platelet-rich plasma was prepared by

*Author for correspondence at: Institut für Pharmakologie, Heinrich-Heine-Universität Düsseldorf, Moorenstr. 5, D-40225 Düsseldorf, Germany; E-mail: schroer@pharma.uni-duesseldorf.de

centrifugation at $250 \times g$ for 10 min at room temperature. The pH was adjusted to 6.5 with acidic citrate dextrose (Biotest, Frankfurt, Germany). The platelets were washed twice in a buffer (pH 6.5) containing [mM]: NaCl 113, Na_2HPO_4 4, NaH_2PO_4 24, KH_2PO_4 4, supplemented with 0.05 u ml^{-1} apyrase (Grade V, Sigma, Deisenhofen, Germany), 5 mM glucose and 50 nM prostaglandin E_1. Washed platelets were resuspended in HEPES-buffered Tyrode solution (pH 7.4) of the following composition [mM]: NaCl 134, $NaHCO_3$ 12, KCl 2.9, NaH_2PO_4 0.36, $MgCl_2$ 1, $CaCl_2$ 2, HEPES 5, supplemented with 5 mM glucose. When indicated, clopidogrel (0.3–30 μM) or vehicle was incubated with the platelets for 2.5–120 min at 37°C prior to stimulation. In some experiments, platelet-rich plasma was pre-incubated with acetylsalicylic acid (10 μM) for 15 min.

Platelet aggregation and shape change

Platelet function was measured as previously described (Weber *et al*., 1993). Briefly, 400 μl of washed platelet suspension or 400 μl of platelet-rich plasma were incubated with 90 μl of test buffer (HEPES-buffered Tyrode, see above) supplemented with 1.5 mg ml^{-1} fibrinogen (final concentration 0.3 mg ml^{-1}) in a 2-channel aggregometer (Labor, Hamburg, Germany) for 2 min at 37°C. Platelets were stimulated by adding 10 μl of the respective stimulus (0.2–600 μM ADP, 2.5 μg ml^{-1} collagen, 1 μM U46619, or 0.1 u ml^{-1} thrombin, respectively). Changes in light transmission were recorded during constant stirring of the samples (1,200 r.p.m., 37°C). Aggregation responses were assessed by measuring the maximum change of light transmission (% of control) and the change of light transmission (% of control) 4 min after addition of the stimulus. For shape change measurements, washed platelets were resuspended in Ca^{2+}-free test buffer. 400 μl of washed platelet suspension were incubated with 90 μl of test buffer supplemented with 10 mM EGTA (final concentration 2 mM) in a 2-channel aggregometer (Labor, Hamburg, Germany) for 2 min at 37°C. Platelets were stimulated by adding 10 μl of the stimulus (0.2–20 μM ADP). Shape change responses were assessed by measuring the decrease in light transmission.

Determination of cyclic AMP in washed platelets

Washed platelets (480 μl) were incubated in an aggregometer for 1 min at constant stirring (1,200 r.p.m., 37°C). Then, 1 μM prostaglandin E_1 (10 μl) or buffer (10 μl) were added for 1 min. Subsequently, the platelets were stimulated with 6 μM ADP (10 μl). After 1 min, the reaction was terminated by adding 100 μl 25% $HClO_4$. The samples were neutralized with 125 μl 2 M K_2CO_3 and centrifuged at $10{,}000 \times g$ for 5 min. Cyclic AMP was determined in the supernatants by radioimmunoassay as previously described (Schröder & Schrör, 1993).

Materials

Acidic citrate-dextrose (Biostabil®, Biotest, Frankfurt, Germany); ADP (Boehringer, Mannheim, Germany); clopidogrel, SR 25989 C (Sanofi Recherche, Toulouse, France); collagen (Collagenreagent Horm®, Nycomed, München, Germany); [^{3}H]-cyclic AMP (New England Nuclear, Dreieich, Germany), U46619 (Upjohn Diagnostics, Heppenheim, Germany). α-Thrombin was a gift from Dr J. Stürzebecher, Erfurt, Germany. All other reagents were obtained from Sigma (Deisenhofen, Germany).

Statistics

Data are means ± s.e.mean from n experiments. Statistical analysis was performed using two-tailed Student's t-test for paired or unpaired data, as applicable. $P < 0.05$ was considered significant.

Results

Clopidogrel does not inhibit platelet aggregation in platelet-rich plasma

When clopidogrel ($\leqslant 100$ μM) was incubated with platelet-rich plasma, no inhibition of ADP (6 μM)-induced platelet aggregation was observed. Even an incubation of clopidogrel with platelet-rich plasma for up to 8 h did not result in any antiaggregatory activity of the compound (not shown).

Clopidogrel selectively inhibits ADP-induced aggregation in washed platelets

In contrast, when clopidogrel (0.3–30 μM) was incubated with washed platelets for 1 h, a concentration-dependent inhibition of ADP (6 μM)-induced platelet aggregation was seen (Figure 1). Incubation of washed platelets with clopidogrel resulted in a reduction of the maximum aggregation amplitude. In addition, there was a marked effect on the reversibility of ADP-induced aggregation in clopidogrel-treated platelets. Thus, both, maximum aggregation amplitudes as well as aggregation amplitudes 4 min after addition of the stimulus, were used for quantification of clopidogrel effects (Figure 2). Data analysis revealed a significant ($P < 0.05$) inhibition of ADP-induced platelet aggregation by $\geqslant 0.3$ μM clopidogrel. From the data presented in Figure 2B, an IC_{50} value of 1.9 ± 0.3 μM was calculated. Importantly, the inhibitory effects of clopidogrel on aggregation of washed platelets were selective for ADP. Platelet aggregation, induced by collagen (2.5 μg ml^{-1}), the thromboxane A_2 mimetic U46619 (1 μM) or thrombin (0.1 u ml^{-1}), was not significantly inhibited by clopidogrel (30 μM) (Figure 2). Interestingly, in the aggregation experiments, ADP (6 μM)-induced platelet shape change did not seem to be affected by clopidogrel. However, because platelet aggregation interferes with the measurement of platelet

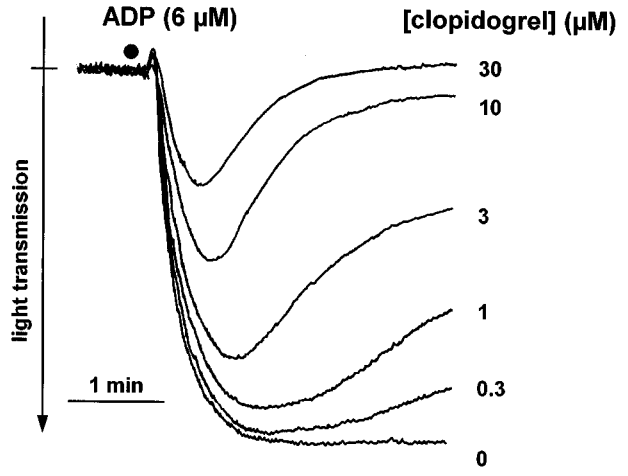

Figure 1 Representative original tracings demonstrating the effects of clopidogrel (0.3–30 μM) on ADP (6 μM)-induced aggregation and shape change of washed human platelets.

shape change, possible effects of clopidogrel on platelet shape change were studied in a separate series of experiments, performed in the presence of EGTA. In these studies, a complete inhibition of platelet shape change by clopidogrel was observed at low concentations of ADP (0.2 μM) (Figure 3). At higher ADP concentrations (2 μM, 20 μM), the inhibitory effects of clopidogrel on ADP-induced platelet shape change were less obvious (Figure 3).

The inhibitory effects on platelet aggregation are restricted to apyrase-sensitive mechanisms

In order to further characterize if the *in vitro* actions of clopidogrel are specific for ADP-mediated processes, the antiaggregatory effects of clopidogrel were compared with apyrase, an ADP/ATP-degrading enzyme. In control experiments, apyrase (1 u ml^{-1}) has been shown to completely inhibit ADP-induced platelet aggregation. The effects of apyrase on collagen (2.5 μg ml^{-1})- and U46619 (1 μM)-induced platelet aggregation were studied. Similar to clopidogrel, (see Figure 2), apyrase (1 u ml^{-1}) did not inhibit collagen (2.5 μg ml^{-1})- or U46619 (1 μM)-induced aggregation of washed platelets (not shown). Therefore, we have repeated the experiments with acetylsalicylic acid (10 μM) pre-treated platelets. In this system, apyrase significantly ($P<0.05$) inhibited collagen-induced platelet aggregation, indicating that ADP is an essential amplification mechanism for collagen-induced aggregation of acetylsalicylic acid-treated platelets (Figure 4). Interestingly, clopidogrel (30 μM) also significantly reduced the aggregation of acetylsalicylic acid-treated platelets to an extent similar to the effects of apyrase (Figure 4). In contrast, when the effects of apyrase and clopidogrel, respectively, on U46619-induced aggregation of acetylsalicylic acid-treated platelets were studied, apyrase did not inhibit U46619-induced platelet aggregation, indicating that the thromboxane A_2 mimetic is capable of stimulating platelet aggregation independently of ADP-mediated amplification mechanisms even after cyclooxygenase inhibition. Consistently, there was no inhibition of U46619-induced aggregation of acetylsalicylic acid-treated platelets by clopidogrel (30 μM). Thus, antiaggregatory actions of clopidogrel can only be observed in apyrase-sensitive systems. These data provide further evidence for the ADP selectivity of clopidogrel actions *in vitro*.

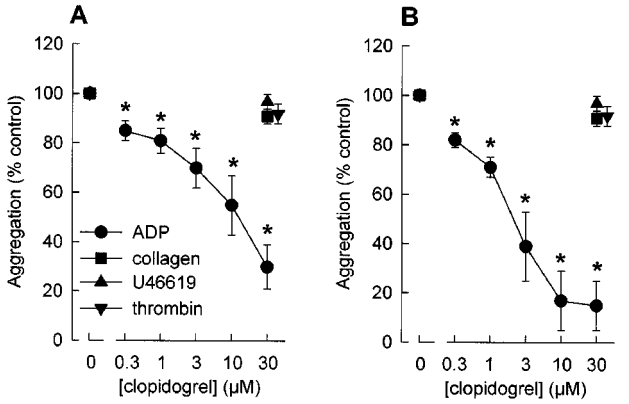

Figure 2 Effects of clopidogrel (0.3–30 μM) on ADP (6 μM)-, collagen (2.5 μg ml^{-1}), U46619 (1 μM) or thrombin (0.1 u ml^{-1})-induced aggregation of washed human platelets. The aggregation was assessed by measuring the maximum change of light transmission (A) and the change of light transmission 4 min after addition of the stimulus (B). Data are given as % of aggregation response induced by the respective agonists without clopidogrel (control = 100%). (means ± s.e.mean of $n=5-6$ independent experiments, $^*P<0.05$ vs control, Student's *t*-test for paired data).

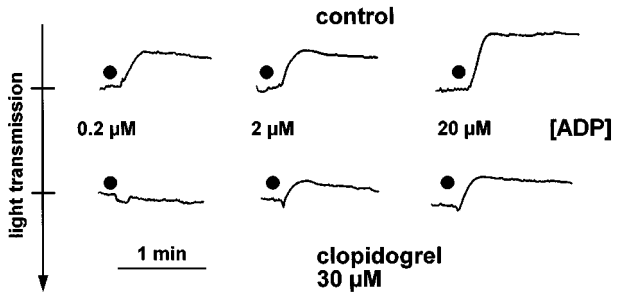

Figure 3 Original tracings demonstrating the effects clopidogrel (30 μM) on ADP (0.2–20 μM)-induced platelet shape change. The experiments were carried out in a Ca^{2+}- and fibrinogen-free medium supplemented with 2 mM EGTA. Shown is one representative experiment of $n=3$ with similar results.

The inhibition of ADP-induced aggregation by clopidogrel is insurmountable

In order to further characterize the effects of clopidogrel (30 μM, 60 min) on ADP-induced platelet aggregation *in vitro*, ADP concentration-effect curves had been constructed (Figure 5). In these experiments, the maximum response to ADP was reduced by clopidogrel indicating a non-equilibrium antagonism of ADP actions.

The antiaggregatory effects of clopidogrel are dependent on the incubation time but not on the presence of the compound in the test medium

The inhibition of ADP-induced platelet aggregation was time-dependent (Figure 6). Measurable effects could be detected after 2.5 min. However, there was an increase in the inhibitory effects of clopidogrel upon further incubation. Maximum and stable inhibition was observed after 30 min (Figure 6). In order to study if the presence of clopidogrel is required for the antiaggregatory effects of the compound, clopidogrel (30 μM, 60 min) pre-incubated washed platelets

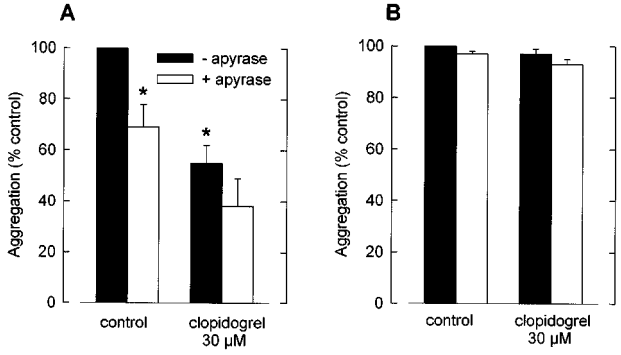

Figure 4 Effects of clopidogrel (30 μM) on collagen (2.5 μg ml^{-1}) (A) and U46619 (1 μM) (B)-induced aggregation of acetylsalicylic acid (10 μM)-treated washed human platelets. Experiments were carried out in the absence and presence of apyrase (1 u ml^{-1}). The aggregation was assessed by measuring the maximum change of light transmission. Data are given as % of aggregation response induced by the respective agonists without clopidogrel (control = 100%). (means ± s.e.mean of $n=4$ independent experiments, $^*P<0.05$ vs control, Student's *t*-test for paired data).

were washed again and resuspended in clopidogrel-free buffer. Untreated control platelets were processed in the same way and served as controls. In these experiments, the inhibitory effects of clopidogrel were not changed (not shown).

The antiaggregatory effects of clopidogrel are stereoselective

The *in vitro* antiaggregatory effects of clopidogrel were also compared with the R enantiomer SR 25989 C. In these experiments, SR 25989 C (30 μM) was significantly less active as compared to clopidogrel (30 μM) with respect to the inhibition of ADP (6 μM)-induced platelet aggregation ($32\pm5\%$ vs $70\pm1\%$ inhibition, $P<0.05$, Student's t-test for paired data, $n=5$), indicating a relative stereoselectivity of clopidogrel effects.

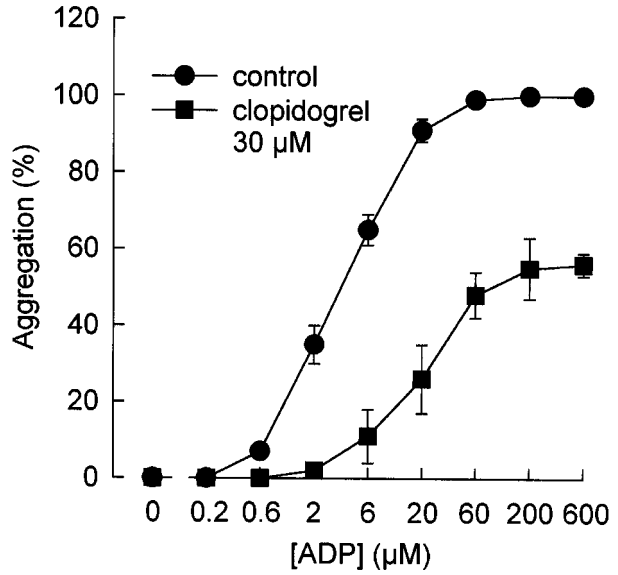

Figure 5 ADP (0.2–600 μM)-induced platelet aggregation in control and in clopidogrel (30 μM)-treated washed platelets. Data are given as % of maximum aggregation response (control = 100%). (means $\pm$s.e.mean of $n=3$ independent experiments).

Clopidogrel does not reverse the inhibitory effects of ADP on prostaglandin E_1-induced cyclic AMP formation

Stimulation of washed platelets with prostaglandin E_1 (1 μM) resulted in a significant ($P<0.05$) increase in cyclic AMP levels (Figure 5). When ADP (6 μM) was added to prostaglandin E_1-stimulated platelets, the stimulatory effects on cyclic AMP formation were completely abolished. Pretreatment of the platelets with clopidogrel (3–30 μM) for 1 h did not significantly reverse the ADP-mediated inhibition of platelet adenylate cyclase. The data are summarized in Figure 7.

Protein prevents in vitro *antiaggregatory actions of clopidogrel in platelet-rich plasma*

Finally, we have tested the hypothesis that proteins, present in platelet-rich plasma, might prevent the *in vitro* antiaggregatory actions of clopidogrel. Therefore, experiments were carried out, using washed human platelets in test buffer supplemented with albumin (350 mg ml^{-1}). When protein was present in the buffer, the antiaggregatory effects of clopidogrel (30 μM) were completely abolished (not shown). Interestingly, when washed platelets were preincubated with clopidogrel for 1 h, subsequent addition of albumin was not able to reverse the inhibition of platelet aggregation by clopidogrel (not shown).

Discussion

The thienopyridine clopidogrel is believed to be inactive *in vitro* and it has been suggested that its activity is dependent on hepatic biotransformation (for review see Coukell & Markham, 1997). The present study is the first to demonstrate direct inhibition of platelet aggregation by clopidogrel *in vitro*. The *in vitro* inhibition of platelet aggregation by clopidogrel is selective for ADP and does not require hepatic bioactivation.

In line with previous reports (for review see Herbert, 1994), we were not able to detect any direct antiaggregatory effects of clopidogrel ($\leqslant100$ μM) in platelet-rich plasma. However, when washed human platelets were studied, a concentration-dependent inhibition of ADP-induced platelet aggregation by clopidogrel was observed. Several lines of evidence indicate that the observed *in vitro* antiaggregatory effects of clopidogrel

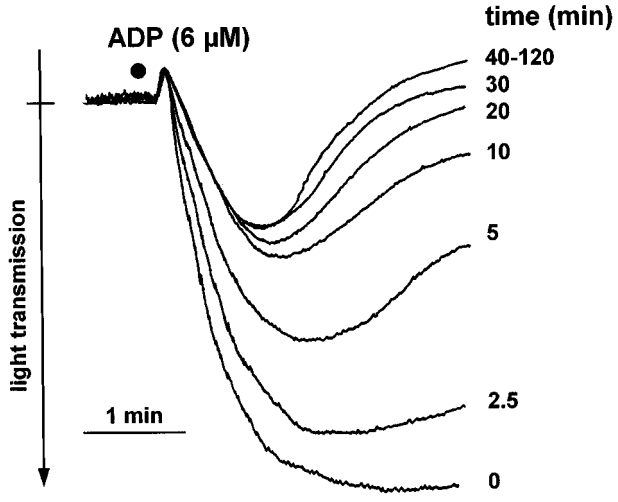

Figure 6 Original tracings demonstrating the time course of the inhibitory actions of clopidogrel (30 μM) on ADP (6 μM)-induced platelet aggregation. Shown is one representative experiment of $n=4$ with similar results.

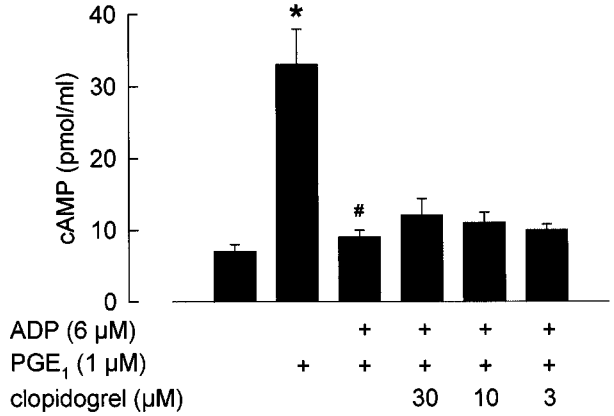

Figure 7 Effects of clopidogrel (3–30 μM) on the inhibitory effects of ADP (6 μM) on prostaglandin E_1 (PGE_1, 1 μM)-stimulated platelet adenylate cyclase. (means $\pm$ s.e.mean of $n=4$ independent experiments, $*P<0.05$ vs control, $\#P<0.05$ vs PGE_1, Student's t-test for unpaired data).

are due to a specific mechanism that is similar to the *ex vivo* inhibition of platelet aggregation by the compound.

The inhibitory effects of clopidogrel were selective for ADP, because no inhibition of platelet aggregation was seen when collagen, thrombin, or the thromboxane A_2 agonist U46619 were used as proaggregatory stimuli. In addition, the selectivity of clopidogrel for ADP-induced platelet activation was confirmed using apyrase, an ADP-degrading enzyme (Cattaneo *et al*., 1991). In these experiments, acetylsalicylic acid-treated platelets were sensitive to apyrase, when aggregation was stimulated with collagen. In contrast, U46619-induced aggregation of acetylsalicylic acid-treated platelets was not affected by apyrase. These data indicate that, when acetylsalicylic acid-treated platelets are used, collagen- but not U46619-induced platelet aggregation partially depends on endogenous ADP. Interestingly, in the presence of acetylsalicylic acid, clopidogrel inhibited collagen-induced platelet aggregation to an extent similar to apyrase. In contrast, there was no inhibition of U46619-induced aggregation of acetylsalicylic acid-treated platelets by clopidogrel. Thus, *in vitro* antiaggregatory actions of clopidogrel are restricted to apyrase-sensitive systems and involve the suppression of the effects of released ADP. This is in line with previous reports on the *ex vivo* inhibition of platelet aggregation by the compound (Feliste *et al*., 1987). The demonstration of synergistic effects of clopidogrel and acetylsalicylic acid is interesting and corresponds to experimental and clinical data with ticlopidine (De Caterina *et al*., 1991; Neumann *et al*., 1997). In addition, in accordance to *ex vivo* data that demonstrate antiaggregatory effects of clopidogrel in washed platelets (Gachet *et al*., 1990), *in vitro* platelet inhibition persisted even when clopidogrel-treated platelets were washed again in order to remove any free compound from the platelet suspension. Thus, the antiaggregatory activity of clopidogrel was associated with the platelets and was not dependent on the presence of the compound in the test buffer. Since the time periods to study inhibition of washed human platelets are limited (washed platelet preparations are stable only for several hours), no statement about possible irreversibility of platelet inhibition by clopidogrel *in vitro* can be made. In line with previous *ex vivo* studies (Defreyn *et al*., 1991; Savi *et al*., 1992), clopidogrel (SR 25990 C) was significantly less effective in inhibiting ADP-induced platelet aggregation as compared to its levorotatory enantiomer (SR 25989 C). Finally, the inhibitory effects of clopidogrel on ADP-induced platelet aggregation were insurmountable. Thus, the *in vitro* actions of clopidogrel on human platelets involve a non-equilibrium antagonism, similar to the effects observed *ex vivo* (Mills *et al*., 1992). In line with the *ex vivo* data (Gachet *et al*., 1990; 1992; Mills *et al*., 1992), incubation of clopidogrel with washed platelets did not appear to inhibit ADP (6 μM)-induced platelet shape change. However, when shape change was measured separately, i.e. under conditions precluding aggregation, a marked inhibition of ADP (0.2 μM)-induced platelet shape change was seen. With higher ADP concentrations (2 μM, 20 μM), the inhibition of platelet shape change by clopidogrel was less obvious.

Taken together, several lines of evidence indicate that clopidogrel specifically and selectively inhibits ADP-induced platelet aggregation *in vitro*. These data are in contrast to the general assumption that hepatic biotransformation is required for antiaggregatory activity of clopidogrel (Savi *et al*., 1992; 1994a). However, this assumption is based on animal studies only, and the requirement of hepatic biotransformation in humans has not yet been demonstrated. Although several metabolites are known, a biologically active metabolite has not been published so far. Our data indicate that hepatic biotransformation is not required for platelet inhibition by clopidogrel. It is well possible that clopidogrel itself and not an unknown metabolite accounts for the antiaggregatory activity of the compound. This view is supported by early pharmacokinetic studies with ticlopidine, a sister-compound of clopidogrel. In these studies (Di Perri *et al*., 1991), a single dose (500 mg) was given to healthy volunteers and the time course of platelet inhibition was correlated with the plasma concentrations of ticlopidine as well as with the amount of cell-associated (unchanged) compound. The maximum concentration of erythrocyte- and neutrophil-associated ticlopidine clearly paralleled the peak plasma concentration of the compound. In contrast, maximum inhibition of platelet aggregation occurred several hours later and paralleled the concentration of platelet-associated (unchanged) compound. Thus, it has been speculated that a redistribution into a platelet-compartment, possibly *via* a specific uptake mechanism, can explain the delayed platelet inhibition by ticlopidine (Di Perri *et al*., 1991). Alternatively, it is also possible that platelets are capable to generate the putative active metabolite of clopidogrel. This possibility is supported by the time-dependence of platelet inhibitory actions of clopidogrel, as demonstrated in the present study. Clearly, further studies are needed to address this issue.

The second interesting point of our study is the finding that the *in vitro* inhibition of ADP-induced platelet aggregation by clopidogrel can be observed without a significant reversal of the inhibitory effects of ADP on platelet adenylate cyclase. It is well known that clopidogrel treatment selectively reduces the number of functional ADP receptors mediating the inhibition of stimulated adenylate cyclase (Defreyn *et al*., 1991; Mills *et al*., 1992; for review see Coukell & Markham, 1997). However, in a recent study, Savi *et al*. (1996) have proposed that cyclic AMP is not an essential messenger for ADP-induced platelet aggregation. Although clopidogrel reversed the inhibitory effects of ADP on platelet adenylate cyclase, this mechanism was not responsible for the *ex vivo* antiaggregatory actions of the compound (Savi *et al*., 1996). Our data support this conclusion and demonstrate that inhibition of ADP-induced platelet aggregation by clopidogrel can occur without a measurable alteration of cyclic AMP metabolism. However, it is well possible that the measurement of cyclic AMP by radioimmunoassay is not sensitive enough to detect small, though functionally relevant changes in platelet cyclic AMP concentrations. Furthermore, additional studies examining the effects of clopidogrel using a wider range of ADP concentrations are also required.

Finally, the discrepancy between the antiaggregatory effects of clopidogrel in washed platelets as compared to platelet-rich plasma needs to be addressed. Using platelet-rich plasma, we were not able to detect any *in vitro* inhibition of platelet aggregation by clopidogrel. This is in line with previous studies (for review see Coukell & Markham, 1997). In contrast, when washed human platelets were used, clopidogrel concentration-dependently inhibited platelet aggregation. There is an early study with ticlopidine, demonstrating no *in vitro* antiaggregatory effects in washed platelets (Di Minno *et al*., 1985). However, in this study, albumin was present in the test medium. We have, therefore, hypothesized that the presence of protein might explain the lack of platelet inhibition of clopidogrel in platelet-rich plasma. In fact, the addition of albumin to the test medium completely prevented the antiaggregatory actions of clopidogrel. Although these data can explain why *in vitro* antiaggregatory effects of clopidogrel have not yet been described, the question why clopidogrel is active *in vivo*, i.e. in the presence of high protein concentrations, remains open. However, it is known that several days of

treatment with clopidogrel are needed to achieve maximum platelet inhibitory effects (Coukell & Markham, 1997). Thus, one might speculate that saturation of protein binding sites for clopidogrel might occur during this time. Alternatively, specific uptake or intercellular redistribution mechanisms (Di Perri *et al*., 1991) might explain the delayed onset of platelet inhibition *in vivo*.

In summary, we demonstrate that clopidogrel specifically and selectively inhibits ADP-induced aggregation of washed platelets *in vitro* without hepatic bioactivation. It is difficult to speculate about the ADP receptor(s) involved in the antiaggregatory actions of clopidogrel *in vitro*. At least three different ADP receptors are expressed in platelets (Hechler *et al*., 1998; Geiger *et al*., 1998): (i) the Gq-coupled $P2Y_1$ receptor which is thought to be involved in ADP-induced platelet shape change and aggregation; (ii) the Gi-coupled P2Y receptor, which has been termed 'P2Ycyc' and which is thought to complete and to potentiate the initial $P2Y_1$-mediated platelet activation; and (iii) $P2X_1$, a receptor-operated Ca^{2+} channel the role of which is unknown. Hechler *et al*. (1998) speculate that the Gi-coupled P2Y receptor is involved in the antithrombotic actions of clopidogrel. A significant reversal of the inhibitory effects of ADP on platelet adenylate cyclase was not involved in the inhibition of ADP-induced platelet aggregation by clopidogrel *in vitro*. Thus, our data do not support the concept of a Gi-coupled P2Y receptor-mediated inhibition of platelet function by clopidogrel. On the other hand, the marked inhibition of ADP (0.2 μM)-induced platelet shape change by clopidogrel is also compatible with the concept that the $P2Y_1$ receptor is the target of the compound. However, the present data do not allow definitive statements about the receptor(s) clopidogrel is acting on and further studies are needed to resolve this issue. The demonstration of an inhibition of platelet aggregation by clopidogrel *in vitro* should facilitate the investigation of many open questions regarding the mode of action of this exciting antiplatelet compound.

The authors gratefully acknowledge the competent secretarial help of Erika Lohmann.

References

CAPRIE STEERING COMMITTEE. (1996). A randomised, blinded, trial of clopidogrel versus aspirin in patients at risk of ischaemic events (CAPRIE). *Lancet,* **348,** 1329–1339.

CATTANEO, M., AKKAWAT, B., LECCHI, A., CIMMINIELLO, C., CAPITANIO A.M. & MANUCCI, P.M. (1991). Ticlopidine selectively inhibits human platelet responses to adenosine diphosphate. *Thromb. Haemost.,* **66,** 694–699.

COUKELL, A.J. & MARKHAM, A. (1997). Clopidogrel. *Drugs,* **54,** 745–750.

DE CATERINA, R., SICARI, R., BERNINI, W., LAZZERINI, G., BUTISTRATA, G. & GIANNESSI, D. (1991). Benefit/risk profile of combined antiplatelet therapy with ticlopidine and aspirin. *Thromb. Haemost.,* **65,** 504–510.

DEFREYN, G., GACHET, C., SAVI, P., DRIOT, F., CAZENAVE, J.P. & MAFFRAND, J.P. (1991). Ticlopidine and clopidogrel (SR 45990 C) selectively neutralize ADP inhibition of PGE_1-activated platelet cAMP formation in rats and rabbits. *Thromb. Haemost.,* **65,** 186–190.

DI MINNO, G., CERBONE, A.M., MATTIOLI, P.L., TURCO, S., IOVINE, C. & MANCINI, S. (1985). Functionally thrombasthenic state in normal patients following the administration of ticlopidine. *J. Clin. Invest.,* **75,** 328–338.

DI PERRI, T., PASINI, F.L., FRIGERIO, C., BLARDI, P., CENTINI, F., MESSA, G.L., GHEZZI, A. & VOLPI, L. (1991). Pharmacodynamics of ticlopidine in man in relation to plasma and blood cell concentration. *Eur. J. Clin. Pharmacol.,* **41,** 429–434.

FELISTE, R., DELEBASSEE, D., SIMON, M.F., CHAP, H., DEFREYN, G., VALLEE, E., DOUSTE-BLAZY, L. & MAFFRAND, J.P. (1987). Broad spectrum anti-platelet activity of ticlopidine and PCR 4099 involves the suppression of the effects of released ADP. *Thromb. Res.,* **48,** 403–415.

GACHET, C., CATTANEO, M., OHLMANN, P., HECHLER, B., LECCHI, A., CHEVALIER, J., CASSEL, D., MANNUCCI, P.M. & CAZENAVE, J.P. (1995). Purinoceptors on blood platelets: further pharmacological and clinical evidence to suggest the presence of two ADP receptors. *Br. J. Haematol.,* **91,** 434–444.

GACHET, C., SAVI, P., OHLMANN, P., MAFFRAND, J.-P., JAKOBS, K.H. & CAZENAVE, J.-P. (1992). ADP receptor induced activation of guanine nucleotide binding proteins in rat platelet membranes–an effect selectively blocked by the thienopyridine clopidogrel. *Thromb. Haemost.,* **6,** 79–83.

GACHET, C., STIERLE, A., CAZENAVE, J.P., OHLMANN, P., LANZA, F., BOULOUX, C. & MAFFRAND, J.P. (1990). The thienopyridine PCR 4099 selectively inhibits ADP-induced platelet aggregation and fibrinogen binding without modifying the membrane glycoprotein IIb-IIIa complex in rat and man. *Biochem. Pharmacol.,* **40,** 229–238.

GEIGER, J., HÖNIG-LIEDL, P., SCHANZENBÄCHER, P. & WALTER, U. (1998). Ligand specifity and ticlopidine effects distinguish three human platelet ADP receptors. *Eur. J. Pharmacol.,* **351,** 235–246.

HECHLER, B., LEON, C., VIAL, C., VIGNE, P., FRELIN, C., CAZENAVE, J.-P. GACHET, C. (1998). The $P2Y_1$ receptor is necessary for adenosine 5′-diphosphate-induced platelet aggregation. *Blood,* **92,** 152–159.

HERBERT, J-M. (1994). Clopidogrel and antiplatelet therapy. *Expert Opin. Invest. Drug,* **3,** 449–455.

MILLS, D.C.B., PURI, R., HU, C.-J., MINNITI, C., GRANA, G., FREEDMAN, M.D., COLMAN, R.F. & COLMAN, R.W. (1992). Clopidogrel inhibits the binding of ADP analogues to the receptor mediating inhibition of platelet adenylate cyclase. *Arterioscl. Thromb.,* **12,** 430–436.

NEUMANN, F.J., GAWAZ, M., DICKFELD, T., WEHNINGER, A., WALTER, H., BLASINI, R. & SCHÖMIG, A. (1997). Antiplatelet effects of ticlopidine after coronary stenting. *J. Am. Coll. Cardiol.,* **29,** 1515–1519.

SAVI, P., BORNIA, J., SALEL, V., DELFAUD, M. & HERBERT J.-M. (1997). Characterization of P2x1 purinoceptors on rat platelets: effect of clopidogrel. *Br. J. Haematol.,* **98,** 880–886.

SAVI, P., HERBERT, J.-M., PFLIEGER, A.M., DOL, F., DELABASSEE, D., COMBALBERT, J., DEFREYN, G. & MAFFRAND, J.P. (1992). Importance of hepatic metabolism in the antiaggregating activity of the thienopyridine clopidogrel. *Biochem. Pharmacol.,* **44,** 527–532.

SAVI, P., COMBALBERT, J., GAICH, C., ROUCHON, M.C., MAFFRAND, J.P., BERGER, Y. & HERBERT, J.-M. (1994a). The antiaggregating activity of clopidogrel is due to metabolic activation by the hepatic cytochrome P450-1A. *Thromb. Haemost.,* **72,** 313–317.

SAVI, P., LAPLACE, M.C., MAFFRAND, J.P. & HERBERT, J.-M. (1994b). Binding of [^{3}H]-2-methylthio ADP to rat platelets–effect of clopidogrel and ticlopidine. *J. Pharmacol. Exp. Ther.,* **269,** 772–777.

SAVI, P., PFLIEGER, A.M. & HERBERT, J.-M. (1996). cAMP is not an important messenger for ADP-induced platelet aggregation. *Blood Coagul. Fibrinol.,* **7,** 249–252.

SCHRÖDER, H. & SCHRÖR, K. (1993). Prostacyclin-dependent cyclic AMP formation in endothelial cells. *Naunyn-Schmiedeberg's Arch. Pharmacol.,* **347,** 101–104.

SCHRÖR, K. (1998). Clinical pharmacology of the adenosine diphosphate (ADP) receptor antagonist, clopidogrel. *Vasc. Med.,* **3,** (in press).

WEBER, A.-A., STROBACH, H. & SCHRÖR, K. (1993). Direct inhibition of platelet function by organic nitrates via nitric oxide formation. *Eur. J. Pharmacol.,* **247,** 29–37.

(Received June 23, 1998
Revised September 10, 1998
Accepted October 6, 1998)

British Journal of Pharmacology (1999) 126, 421–428
http://www.stockton-press.co.uk/bjp

Endothelium-dependent hyperpolarization in resting and depolarized mammary and coronary arteries of guinea-pigs

[1,2]Anna K.M. Hammarström, *,[1]Helena C. Parkington, [1]Marianne Tare & [1]H.A. Coleman

[1]Department of Physiology, Monash University, Clayton, Victoria 3168, Australia

1 The membrane potential responses in guinea-pig coronary and mammary arteries attributable to endothelium-derived nitric oxide (NO), prostaglandin (PG) and hyperpolarizing factor (EDHF), and to exogenous NO and the prostacyclin analogue, iloprost, were compared at rest and when depolarized with the thromboxane analogue, U46619.

2 In the coronary artery, stimulation of the endothelium with acetylcholine (ACh) evoked hyperpolarization attributable to NO and a PG with similar pD_2s at rest and in the presence of U46619. However, in depolarized tissues, the pD_2 of the response attributed to EDHF required a 10 fold lower concentration of ACh compared with at rest.

3 In the mammary artery, lower concentrations of ACh were required to evoke NO- and EDHF-dependent hyperpolarizations in depolarized mammary artery compared with at rest, while PG-dependent hyperpolarization did not occur until the concentration of ACh was increased some 10 fold both at rest and in U46619.

4 The smooth muscle of the coronary artery of guinea-pigs was some 4 fold more sensitive to exogenous NO and iloprost than was the mammary artery.

5 In conclusion, the membrane potential response in arteries at rest, that is, in the absence of constrictor, may be extrapolated to events in the presence of constrictor when NO and PG are under study. However, the sensitivity to ACh and the magnitude of the hyperpolarization attributed to EDHF obtained in tissues at rest may underestimate these parameters in depolarized tissues.

Keywords: Nitric oxide; prostacyclin; EDHF; iloprost; U46619; hyperpolarization; coronary artery; mammary artery

Abbreviations: ACh, acetylcholine; EDHF, endothelium-derived hyperpolarizing factor; Ilo, iloprost; Indo, indomethacin; L-NAME, N^{ω}-nitro L-arginine methylester; NO, nitric oxide; PG, prostaglandin; V_{max}, peak hyperpolarization amplitude

Introduction

The vascular endothelium is capable of releasing nitric oxide (NO), prostacyclin (PGI) and endothelium-derived hyperpolarizing factor (EDHF) which evoke hyperpolarization of the smooth muscle in a variety of vascular beds: NO, (Tare *et al*., 1990; Garland & McPherson, 1992; Parkington *et al*., 1993), PGI (Siegel *et al*., 1987; Parkington *et al*., 1993) and EDHF (Chen *et al*., 1988; Feletou & Vanhoutte, 1988). Attempts to understand the role of hyperpolarization in relaxation of vascular smooth muscle has received considerable attention. However, in many studies hyperpolarization is not recorded simultaneously with relaxation. While relaxation is studied in preconstricted arterial tissue, hyperpolarization is most commonly recorded in tissues at rest, in the absence of constrictors. Potassium channels are likely to be an important mechanism of endothelium-dependent hyperpolarization in many arterial beds (Nelson & Quayle, 1995). The open probability of some K^+ channels is influenced by membrane potential, while others are sensitive to cytoplasmic Ca^{2+}. Both membrane potential and cytoplasmic Ca^{2+} are commonly altered by constrictors.

It is well established that not all of the agents used to preconstrict arteries have the same effect on ionic conductances in vascular smooth muscle, an important consideration in view of the role of competing conductances in determining the ability to hyperpolarize. For example, α-adrenoceptor agonists provide a substantial increase in calcium-activated chloride conductance in arterial smooth muscle (Amédée *et al*., 1990), while the thromboxane A_2 analogue U46619 has been shown to inhibit Ca^{2+}-activated K^+ channels (Scornik & Toro, 1992). In rat mesenteric arteries that are depolarized and contracted with noradrenaline, stimulation of the endothelium causes relaxation and hyperpolarization that are resistant to blockade of NO synthesis, whereas in arteries that are depolarized and contracted with U46619 no hyperpolarization is observed (Plane & Garland, 1996).

The effectiveness of the agents released from the endothelium to relax an artery is pivotally dependent upon the ability of the smooth muscle to respond. This issue has been largely neglected, with few exceptions (Christie & Lewis, 1988). This omission may complicate interpretation of comparison between endothelium responsiveness in different arterial beds.

In the present study we compared the ability of endothelium-derived NO, PG and EDHF to hyperpolarize guinea-pig coronary and mammary arteries. The coronary artery has been studied in some detail in this laboratory and the mammary artery was included to broaden interpretation. The responsiveness of the smooth muscle of the two arteries to exogenous vasorelaxants was compared. Finally, the responses to endogenous and exogenous vasodilators were compared at rest and, in view of the focus on membrane hyperpolarization, under conditions where underlying membrane conductances were altered with U46619.

Some of these results have been presented previously (Hammarström *et al*., 1991).

*Author for correspondence.
[2]Current address: Division of Neuroscience, John Curtin School of Medical Research, Australian National University, Canberra, ACT 2601, Australia.

Methods

Preparations

Guinea-pigs of either gender (300–700 g) were killed by decapitation. The mammary artery, just proximal to its major branch point within the mammary fat, and the main descending coronary artery, just prior to its entry into the myocardium, were removed. Ring segments, 1–2 mm in length, were mounted on a myograph (bath capacity 1 ml) (Mulvany & Halpern, 1977) using a pair of stainless steel wires (40 μm in diameter) and continuously superfused with physiological solution (at 35°C) containing (mM): NaCl, 120; KCl, 5; $CaCl_2$, 2.5; $MgSO_4$, 1.2; KH_2PO_4, 1; $NaHCO_3$, 25; glucose, 11, bubbled with O_2, 95% and CO_2, 5%, at a rate of 3.6 ml min^{-1}. The preparations were stretched to a tension equivalent to approximately 60 mmHg, the mean blood pressure of guinea-pigs. Conventional intracellular glass microelectrodes, filled with 1 M KCl and having resistances of around 100 MΩ, were used to impale the smooth muscle cells and record membrane potential (Parkington *et al*., 1993). Isometric tension was recorded simultaneously *via* a force transducer (Kistler-Morse, DSC-6BE4-110) attached to one arm of the myograph. The data were recorded on chart (Linearcorder) and stored on video cassette using a digital data recorder for analysis.

Experiments

The endothelium was stimulated by injecting acetylcholine (ACh) straight into the perfusion line close to the tissue (1 s delay) for a period of 10 s. This method of stimulation allows the component of membrane hyperpolarization attributable to each of the vasorelaxants to be distinguished unambiguously, in contrast with the responses to more prolonged (1–2 min) applications (Parkington *et al*., 1993; 1995). The exogenous vasorelaxants NO and iloprost, a stable analogue of prostacyclin, were also applied for 10 s. Injection of 5–100 μl of saline (the range of volumes used when injecting agonists) had no effect on membrane potential or tension. The concentration of these agonists reached equilibrium within 3–5 s (see Parkington *et al*., 1993). Concentration-response relationships using this method of applying ACh have been shown not to differ from the relationship obtained when ACh is added to the superfusate for 1 min (Hammarström *et al*., 1995). NO synthesis was blocked using 5×10^{-5} M N^{ω}-nitro-L-arginine methyl ester (L-NAME) and prostaglandin synthesis was blocked using 10^{-6}M indomethacin, both applied for 30–40 min prior to and during testing. In a pilot study of five coronary and five mammary arteries, increasing the concentration of L-NAME to 10^{-4}M and then to 10^{-3}M had no additional inhibitory effect compared with that of 5×10^{-5}M on the concentration-hyperpolarization curve in response to ACh. Similarly, increasing indomethacin to 10^{-5}M failed to produce an effect additional to 10^{-6}M. NO solution was made by transferring the appropriate volume of NO gas, using a gas tight micro-syringe, to a sealed vial containing 0.9% saline that had been de-oxygenated by bubbling with argon for 60 min.

Analysis of data

The amplitude (mV) of the hyperpolarization was measured from the level of the membrane potential prior to the application of vasorelaxant to the peak of the response. The maximum amplitude of the response to each agonist has been designated as V_{max} according to convention. The sensitivity of the endothelium and smooth muscle was determined by converting the hyperpolarization to a percentage of the maximum hyperpolarization obtained in that particular preparation, whether the latter was due to an endogenously released relaxing factor or to exogenously applied vasorelaxant. A sigmoid curve was fitted to the data for each preparation, using the least-squares method, using the computer software package Prism (GraphPad Software, Inc.). The concentration of agonist which was effective in producing a response that was 50% of maximum (EC_{50}) and the Hill slope of the curve were determined for each tissue. The mean values of EC_{50} and the mean slope for 4–8 preparations were then used to generate a curve that was representative of all preparations in the group. pD_2 values ($-\log EC_{50}$) have been quoted throughout.

The statistic quoted with each mean is the standard error based on the number of animals tested (n). A Student's t-test was used to test for significance which was accepted at $P<0.05$.

Drugs

The following drugs were used: ACh (Merck), L-NAME and indomethacin (Sigma, U.S.A.), U46619 and PGE_2 (Cayman Chemical Co.), Iloprost (a gift from Schering, Germany), NO (Matheson Gas Products Inc., U.S.A.).

Results

When stretched to the equivalent of approximately 60 mmHg, the effective diameter of preparations of mammary artery was 476 ± 16 μm ($n=12$), which was not significantly different from the value of 519 ± 26 μm ($n=13$) for coronary artery. The resting membrane potential of the smooth muscle cells of the mammary artery was -57 ± 1 mV ($n=20$), which was not significantly different from the -55 ± 1 mV ($n=12$) recorded in the coronary artery.

Hyperpolarization evoked by acetylcholine at rest

At rest, ACh evoked hyperpolarization in the mammary artery that consisted of an initial transient component, followed by a slow component, similar to that reported previously for the coronary artery in this laboratory (Parkington *et al*., 1993). The amplitudes of both components were concentration dependent. Either L-NAME (5×10^{-5}M) or indomethacin (10^{-6}M) alone reduced the amplitude of the slow component in both arteries. In the presence of both blockers the slow component was completely abolished, and hence can be attributed to the combined actions of NO and PG in both arteries. The transient component remaining in the presence of both L-NAME and indomethacin has been attributed to the actions of EDHF (Komori & Suzuki, 1987; Taylor & Weston, 1988; Parkington *et al*., 1993).

L-NAME and indomethacin together caused significant depolarization, from -55 ± 1 to -45 ± 1 mV ($n=6$), in the coronary artery. In contrast, these blockers did not significantly change the resting membrane potential in the mammary artery (from -54 ± 1 to -51 ± 2 mV, $n=6$). Furthermore, the membrane potential of the smooth muscle cells of the mammary artery were unchanged following removal of the endothelium (-54 ± 1 mV, $n=6$), and this is in contrast with previous observations in coronary artery (Parkington *et al*., 1993).

Endogenous prostaglandin

ACh was applied at rest in the presence of L-NAME to abolish a contribution by NO to the slow component, allowing examination of the component of the hyperpolarization evoked by endothelium-derived PG (Figure 1A, and B). In the presence of L-NAME, the resting membrane potential in the coronary artery (-51 ± 2 mV, $n=6$) was less negative than that of the mammary artery (-58 ± 2 mV, $n=8$). The slow component of the hyperpolarization increased in amplitude as the concentration of ACh was increased, reaching a maximum of 15 ± 2 mV ($n=6$) in the coronary artery and a significantly smaller value of 10 ± 1 mV ($n=8$) in the mammary artery. However, the maximum absolute level of membrane potential reached during the slow component of hyperpolarization attributable to a PG was not different in the two arteries (to -68 ± 1 mV, $n=6$, in the coronary and to -71 ± 3 mV, $n=8$, in the mammary arteries). The ACh-induced hyperpolarization attributable to a PG in the coronary artery had a pD_2 of 6.66 ± 0.12 ($n=6$) and this was significantly larger than the pD_2 of 5.25 ± 0.14 ($n=7$) for the mammary artery (Figure 1C, Table 1).

Exogenous prostaglandin

Prostacyclin is the main PG released from the guinea-pig coronary artery by ACh (Parkington *et al*., 1993) and is also likely to be the principal vasodilator PG in the mammary artery since PGE_2 evoked only a small (0–2 mV) hyperpolarization in the latter ($n=3$, data not shown). The effects of the stable analogue of prostacyclin, iloprost, on membrane potential was tested, also in the presence of L-NAME. Iloprost evoked concentration-dependent hyperpolarization (Figure 2) with a pD_2 of 7.95 ± 0.09 ($n=5$) in the coronary artery and a significantly smaller pD_2 of 7.31 ± 0.14 ($n=7$) in the mammary artery (Figure 2, Table 1). V_{max} for the hyperpolarization was significantly greater in the coronary (17 ± 1 mV, $n=6$) than in the mammary (12 ± 1 mV, $n=8$) artery. However, the maximum level of the membrane potential reached during the response to iloprost was not different in the two arteries (to

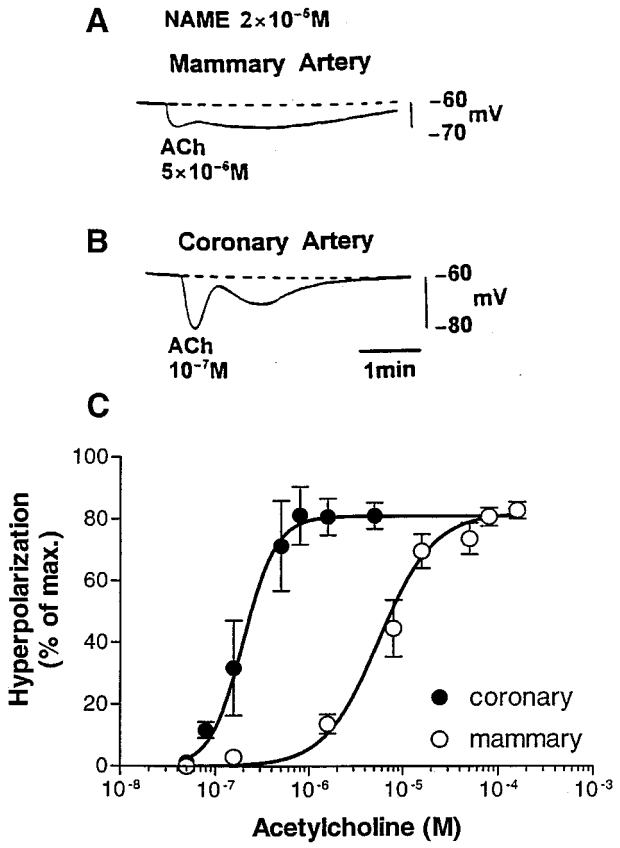

Figure 1 In the presence of L-NAME, ACh evoked hyperpolarization in the mammary (A) and coronary (B) arteries that consisted of an initial transient component followed by a slow, more sustained component. The amplitude of the slow component was expressed as a percentage of the maximum hyperpolarization in each respective tissue. C shows the mean±s.e.mean and the curves generated from the mean EC_{50} and mean Hill slope for responses from six coronary and seven mammary arteries.

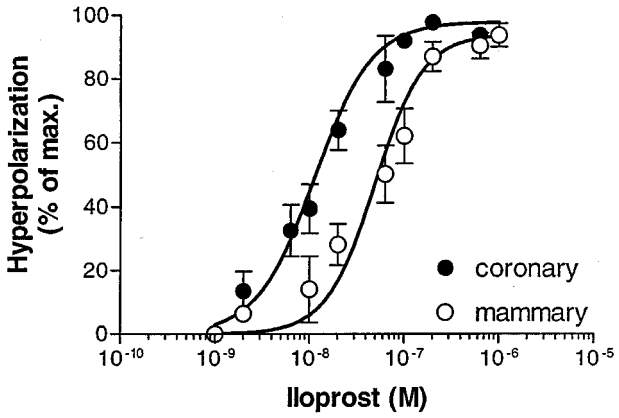

Figure 2 The hyperpolarizations evoked by iloprost, in the presence of L-NAME, were expressed as a percentage of the maximum hyperpolarization in each tissue (mean±s.e.mean). Curves were generated from the mean EC_{50} and mean Hill slope for responses from five coronary and seven mammary arteries.

Table 1 Sensitivity to vasorelaxants at rest

Source of factor	*Artery*	*L-NAME (PG)* ($pD_2\pm$s.e.)	*Indomethacin (NO)* ($pD_2\pm$s.e.)	*L-NAME+Indo (EDHF)* ($pD_2\pm$s.e.)
Endogenous	Coronary	6.66 ± 0.12	6.83 ± 0.15	6.5 ± 0.2
	(*n*)	(6)	(5)	(6)
	Mammary	5.25 ± 0.14	6.27 ± 0.18	6.4 ± 0.1
	(*n*)	(7)	(5)	(5)
Exogenous	Coronary	7.95 ± 0.09	5.56 ± 0.11	
	(*n*)	(5)	(4)	
	Mammary	7.31 ± 0.14	5.14 ± 0.08	
	(*n*)	(7)	(5)	

ACh evoked hyperpolarization that could be attributed to the release of endogenous PG, NO and EDHF in arteries at rest. Iloprost was used as the exogenous PG. The number of animals in each group is represented by *n*.

-68 ± 3 mV, $n=6$ in the coronary and to -72 ± 4 mV, $n=7$ in the mammary).

Endogenous NO

Indomethacin was used to block the release of PGs from the endothelium, and hence isolate the slow component of the hyperpolarization attributable to the actions of endogenous NO alone. In the presence of this blocker the resting membrane potential in the two arteries was not different (-53 ± 3 mV, $n=5$ in the coronary and -55 ± 1 mV, $n=5$ in the mammary). In these experiments L-NAME was applied at the end of the experiment and a range of concentrations of ACh applied again in order to unequivocally confirm the response to NO.

The slow component of hyperpolarization elicited by ACh in the presence of indomethacin had a pD_2 of 6.83 ± 0.15 ($n=5$) in the coronary artery and a pD_2 of 6.27 ± 0.18 ($n=5$) in the mammary artery (Figure 3 and Table 1), values that were significantly different. The V_{max} of the response attributable to NO had similar values in both preparations (13 ± 3 mV, $n=6$, in coronary and 10 ± 1 mV, $n=5$, in mammary artery).

Exogenous NO

Since the responses to endogenous NO were obtained in the presence of indomethacin, that blocker was also present when examining the effects of exogenous NO (Figure 4). The hyperpolarizations evoked by exogenous NO had similar maximum amplitudes in the coronary (11 ± 1 mV, $n=7$) and the mammary (9 ± 1 mV, $n=5$) arteries. The pD_2 of 5.56 ± 0.11 ($n=4$) in the coronary artery was significantly different from the value of 5.14 ± 0.08 ($n=5$) in the mammary artery (Figure 4, Table 1). However, the level of membrane potential reached was the same for both arteries (-64 ± 3 mV, $n=5$ for coronary; -63 ± 2 mV, $n=4$ for mammary).

Endothelium-derived hyperpolarizing factor (EDHF)

The initial transient component of the hyperpolarization in response to ACh, which was resistant to both L-NAME and indomethacin, was attributed to EDHF. In the presence of both blockers, to avoid contamination with endogenous NO and PG, the peak amplitude of the transient component increased progressively in both arteries as the concentration of ACh was increased, reaching a maximum of 24 ± 2 mV ($n=5$) in the coronary artery. This was significantly larger than the 8 ± 1 mV ($n=5$) evoked in the mammary artery (Figure 5). Furthermore, the absolute maximum level of membrane potential reached at the peak of the transient component was significantly more hyperpolarized in the coronary artery (to -72 ± 5 mV, $n=5$) than in the mammary artery (to -57 ± 3 mV, $n=6$) (Figure 5). The pD_2 for the transient component was 6.5 ± 0.2 ($n=6$) in the coronary artery and 6.4 ± 0.1 ($n=5$) in the mammary artery (Figure 5, Table 1). These values were not significantly different.

Hyperpolarization in the presence of U46619

The concentration of U46619 was varied (10^{-8}–10^{-7}M) in order to achieve a submaximal depolarization that was similar in both arteries (to -38 ± 1 mV). The depolarization was often accompanied by the firing of action potentials, as shown previously for coronary artery (Parkington *et al*., 1995) and an example in mammary artery is shown in Figure 6. ACh evoked concentration-dependent, biphasic hyperpolarizations, similar in form to those observed in tissues at rest (Figure 6). Application of L-NAME or indomethacin in the presence of U46619 evoked an additional depolarization of approximately

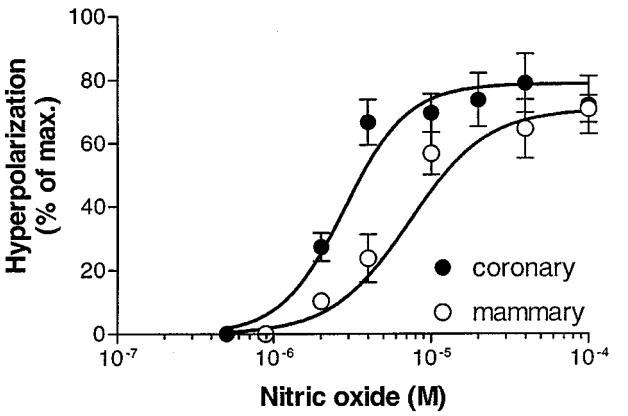

Figure 4 The hyperpolarizations evoked by NO, in the presence of indomethacin, were expressed as a percentage of the maximum hyperpolarization in each tissue (mean$\pm$s.e.mean). Curves were generated from the mean EC_{50} and the mean slope from four coronary and five mammary arteries.

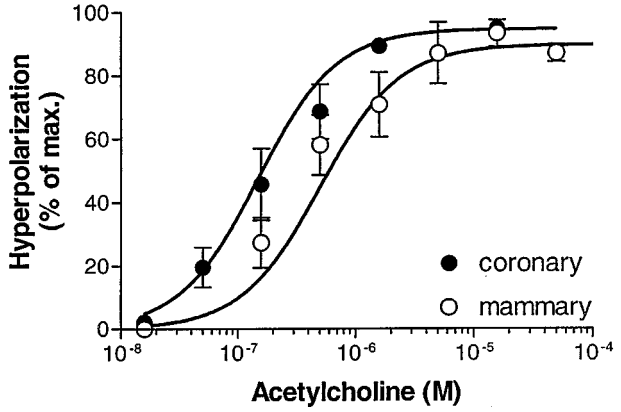

Figure 3 The slow component of the hyperpolarization evoked by ACh, in the presence of indomethacin, was expressed as a percentage of the maximum hyperpolarization in each tissue (mean$\pm$s.e.mean). Curves were generated from the mean EC_{50} and the mean Hill slope for responses from five coronary and five mammary arteries.

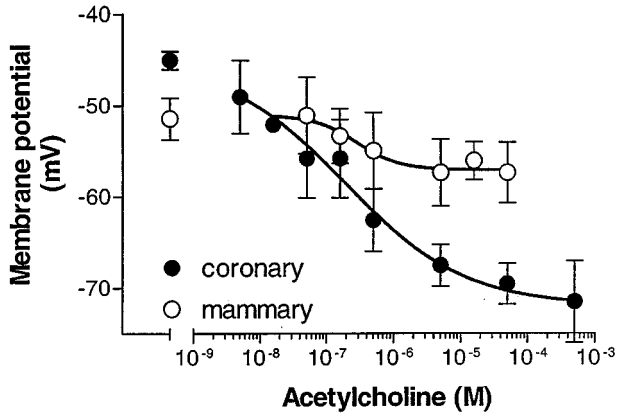

Figure 5 The level of membrane potential attained during the transient hyperpolarization evoked by ACh, in the presence of L-NAME and indomethacin, was plotted for six coronary and five mammary arteries.

5 mV in both arteries. In order to avoid a change in membrane potential the concentration of U46619 was reduced, for example, from 3×10^{-8}M to 2×10^{-8}M or from 7×10^{-8}M to 5×10^{-8}M, which maintained the starting level of membrane potential constant for all treatments.

Endogenous prostaglandin and NO in the presence of U46619

In the presence of L-NAME to block NO production, the slow component of hyperpolarization in response to ACh had a pD_2 of 6.54 ± 0.16 ($n=5$) in the coronary which was significantly different from the pD_2 of 5.59 ± 0.07 ($n=5$) in the mammary artery (Figure 7, Table 2). In the presence of indomethacin to block PG production, the pD_2s for the slow component evoked by ACh were similar in the coronary (6.80 ± 0.10, $n=5$) compared with the mammary (6.74 ± 0.29, $n=5$) (Figure 7, Table 2). The combined application of L-NAME and indomethacin abolished the slow component completely (solid squares in Figure 7).

V_{max} for the hyperpolarization attributable to NO and PG was similar in the coronary (18 ± 4 and 20 ± 4 mV, respectively, $n=5$ for each) and in the mammary (17 ± 3 and 15 ± 4 mV, respectively, $n=5$ for each tissue) artery. Since the starting membrane potential was the same, the maximum level of the

Table 2 Sensitivity to vasorelaxants in U46619

Artery	*L-NAME (PG)* ($pD_2\pm$s.e.)	*Indomethacin (NO)* ($pD_2\pm$s.e.)	*L-NAME+Indo (EDHF)* ($pD_2\pm$s.e.)
Coronary	6.54 ± 0.16	6.80 ± 0.10	7.77 ± 0.09
(*n*)	(5)	(5)	(10)
Mammary	5.59 ± 0.07	6.74 ± 0.29	6.93 ± 0.05
(*n*)	(5)	(5)	(10)

ACh evoked hyperpolarization that could be attributed to the release of endogenous PG, NO and EDHF in arteries depolarized using U46619. The number of animals in each group is represented by *n*.

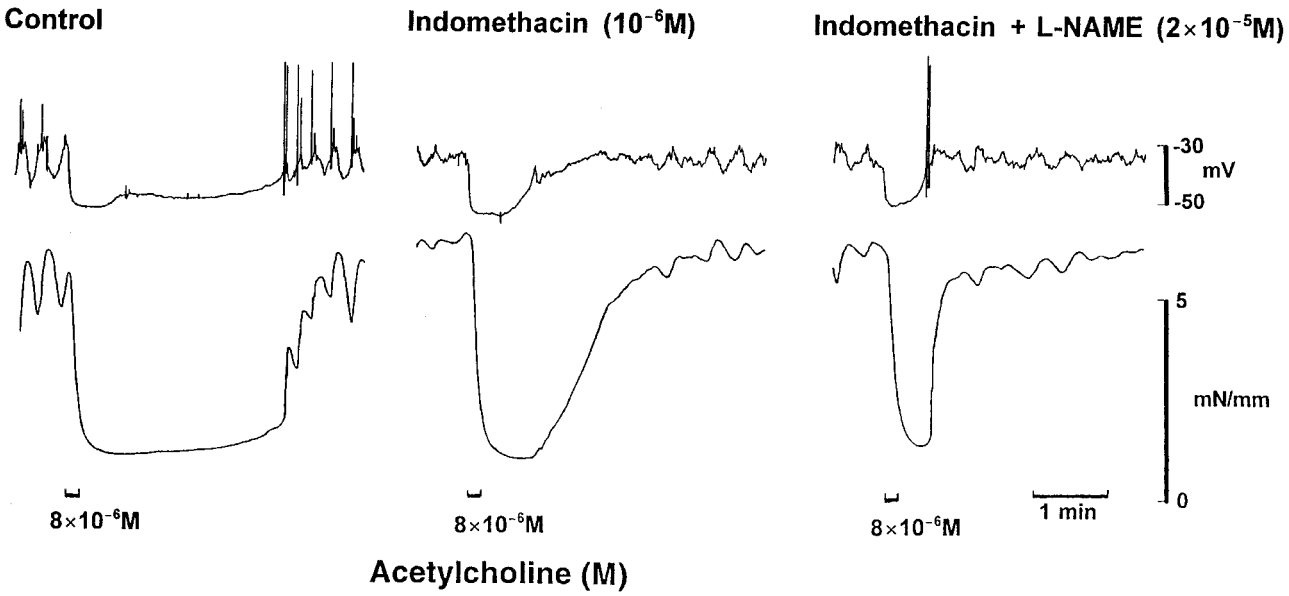

Figure 6 In the mammary artery ACh evoked hyperpolarization (upper panel) and relaxation (lower panel) in control solution. Indomethacin reduced the duration of the response. In the presence of indomethacin plus L-NAME the responses were brief: the slow component was abolished leaving the transient component that has been attributed to EDHF. U46619 was present throughout. All responses are from a continuous impalement in the same cell.

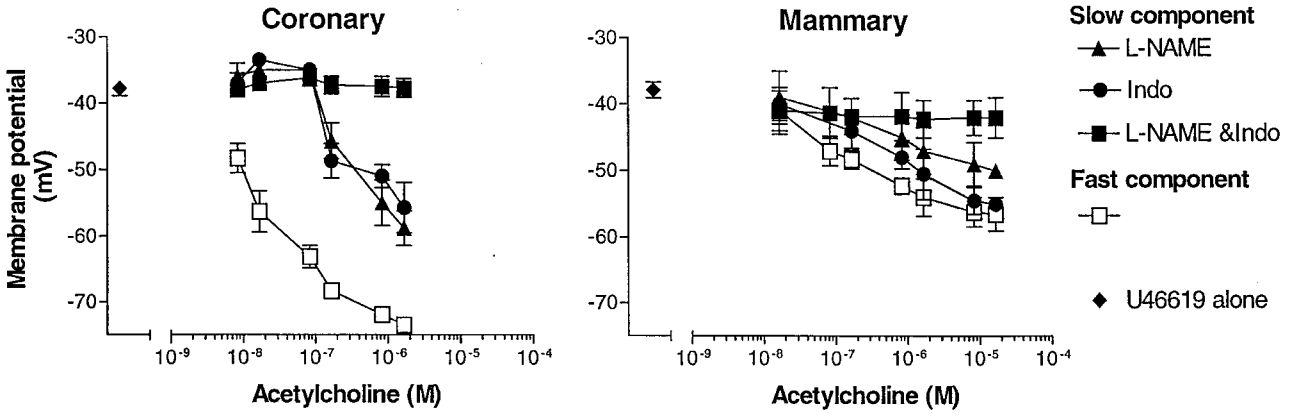

Figure 7 Effect of L-NAME, indomethacin and L-NAME plus indomethacin on the peak levels of the slow ($n=5$ in each group) and fast ($n=10$) components of hyperpolarization in response to ACh in coronary and mammary arteries in the presence of U46619.

membrane potential reached during the hyperpolarizations were not different (−51 to −59 mV).

EDHF in the presence of U46619

The initial fast component (in the presence of L-NAME and indomethacin) of the hyperpolarization in response to ACh, and attributable to EDHF, had a pD_2 of 7.77±0.09 ($n=10$) in the coronary artery and this was significantly different from the pD_2 for the mammary artery (6.93±0.05, $n=10$) (Figure 7, Table 2).

V_{max} for the hyperpolarization was significantly greater in the coronary (37±1 mV, $n=5$) than in the mammary artery (20±4 mV, $n=5$). Hence, the maximum level of the membrane potential reached during the initial hyperpolarization was greater in the coronary (−74±1 mV, $n=5$) compared with in the mammary artery (to −57±3 mV, $n=5$).

Direct effects of ACh on the smooth muscle

We have previously shown that high concentrations of ACh evoke only a small direct depolarization (1–3 mV) of the smooth muscle in preparations of coronary artery denuded of endothelium (Parkington *et al*., 1993). Following removal of the endothelium from preparations of mammary artery, ACh failed to evoke hyperpolarization. ACh, $>10^{-6}$M applied to the superfusate for 1 min, had only a weak direct depolarizing effect (1.5±0.4 mV) on the smooth muscle in 5 of 6 preparations, with no change in membrane potential in the remaining tissue. The depolarization was accompanied by a small (less than 3% of maximal) transient contraction (data not shown). The integrity of the smooth muscle was confirmed by the ability of nitroprusside or iloprost to hyperpolarize denuded preparations (data not shown).

Since L-NAME and indomethacin were used extensively in this study, their possible effects on the responses to exogenous NO and iloprost were tested. In five preparations of coronary artery L-NAME had no effect on the hyperpolarization evoked by iloprost or exogenous NO (data not shown). Likewise, indomethacin had no effect on the response to iloprost or exogenous NO in five other tissues (data not shown). The hyperpolarization evoked by either iloprost or exogenous NO was unaltered by removal of the endothelium.

Discussion

The results of the present study demonstrate that the ability of ACh to evoke L-NAME and indomethacin sensitive hyperpolarization is similar in coronary artery at rest as it is when depolarized with U46619. This contrasts with observations in the presence of both these blockers, in which the coronary is more than an order of magnitude more sensitive to ACh when depolarized compared with at rest. The mammary artery appears to be half an order of magnitude more sensitive to ACh when depolarized with U46619, irrespective of the presence of L-NAME, indomethacin or both blockers. The results presented here complement the study of Plane & Garland (1996) which demonstrated a difference in endothelium-dependent hyperpolarization according to the nature of the constrictor.

The peak levels of membrane potential attained during the hyperpolarization attributable to NO and PG were more negative at rest in both arteries. This presumably results from the inability of the conductance underlying the hyperpolarization to fully compete against the additional conductances associated with the U46619-induced depolarization. In contrast, the hyperpolarization attributed to EDHF attained the same absolute level at rest and in depolarized tissues and this is consistent with a more robust conductance underlying the response to EDHF. The nature of the conductance involved has not been resolved definitively. However, a channel that may be similar to the large conductance, Ca^{2+}-activated K^+ channel has been implicated (Hashitani & Suzuki, 1997; Zygmunt *et al*., 1997).

The pD_2s for hyperpolarization recorded here are of similar order of magnitude for relaxation reported previously by us (Parkington *et al*., 1995) and by others (Keef & Bowen, 1989; Bruch *et al*., 1997). The coronary artery was 4 fold more sensitive to the ACh-evoked hyperpolarization attributable to NO than was the mammary artery. This could be accounted for entirely by the similar lower sensitivity of the mammary smooth muscle to exogenous NO. Christie & Lewis (1988) have also reported a greater sensitivity to nitroprusside of pig coronary artery compared with aorta.

Stimulation of the coronary endothelium induced considerable indomethacin sensitive hyperpolarization, and the smooth muscle hyperpolarized in response to the prostacyclin mimetic, iloprost. This confirms previous observations on this vessel in which relaxation was recorded (Lee *et al*., 1990, Parkington *et al*., 1995). The present study revealed that the mammary artery does not behave similarly. While the smooth muscle was some 4 fold less sensitive to exogenous prostacyclin in the mammary compared with the coronary artery, the mammary appeared to be some 26 fold less sensitive to ACh-induced hyperpolarization attributable to PG than the coronary artery. Thus, there remained a 6 fold lower sensitivity of the mammary endothelium with respect to prostacyclin release compared with that of the coronary artery. Lee *et al*. (1990) also found that the guinea-pig aorta was not relaxed by endothelium-derived PG. It is interesting that the hyperpolarization attributable to endogenous PG is reduced to around one third of normal in human coronary artery with atherosclerosis (Siegel *et al*., 1993), while the literature abounds with reports of other arterial beds in which endothelium-dependent relaxation is resistant to indomethacin. Thus, it may be that prostacyclin is especially important in the physiology of the coronary circulation.

In the coronary artery, the concentration of ACh required to evoke the release of all three endogenous vasorelaxants, NO, PG and EDHF was similar in arteries at rest. Using different arteries and species, several studies have indicated that the muscarinic receptor responsible for the production of NO (Adeagbo & Triggle, 1993), PG (Jaiswal & Malik, 1990) and EDHF (Adeagbo & Triggle, 1993; Hammarström *et al*., 1995) is likely to be the M_3 sub-type. Hence, the lesser ability of the mammary endothelium to produce PG is unlikely to be a consequence of a lower density of muscarinic receptors. Possible factors contributing to the reduced response of the mammary endothelium include the availability of arachidonic acid or prostacyclin, or the shunting of the pathway towards the production of thromboxanes, or *via* the lipoxygenase or cytochrome P450-like enzyme pathways.

The responses of the two arteries to exogenous NO and prostacyclin were remarkably similar. The extent to which the smooth muscle of the coronary artery was more sensitive than that of the mammary was similar for both vasodilators, 3–4 fold. The maximum amplitudes of the hyperpolarizations were similar in both arteries.

The maximum amplitude of the hyperpolarization attributable to EDHF and the level of membrane potential reached was much larger in the coronary compared with the mammary

artery. This result was complicated by the different levels of the membrane potential in these tissues at rest, a problem that was overcome in the presence of U46619, which induced depolarization to the same value in both arteries. The result may reflect a greater number of receptors for EDHF in the coronary artery, enhanced post-receptor mechanisms or the nature and/or density of K^+ channels on the smooth muscle cells. Vascular smooth muscle cells possess a variety of different K^+ channels and considerable heterogeneity exists between different vascular beds (Nelson & Quayle, 1995; Garland *et al*., 1995).

When depolarized and constricted with U46619, the mammary artery was more sensitive to all three dilators, NO, PG and EDHF. This could reflect an increase in the driving force for K^+. The situation is more complicated in the coronary artery. The sensitivity of the latter to NO and PG was unchanged when depolarized and constricted with U46619 compared with at rest. This could reflect a significant conductance in response to NO and PG at rest, which is capable of withstanding the additional conductances evoked by U46619 in the coronary. The enhanced sensitivity to EDHF in the presence of U46619 could reflect an enhancement by U46619 of EDHF release. Another possibility is that U46619, or perhaps the associated increase in cytoplasmic Ca^{2+}, enhances the availability of the channel involved in the EDHF hyperpolarization. The differences in the effect of depolarization in the EDHF responses in the coronary and mammary arteries raises the possibility that the identity of EDHF may not be the same in the two arteries.

Removal of the endothelium was without effect on either the resting membrane potential or on resting tone in the mammary artery, in contrast with observations in coronary artery. Likewise, blockers of NO and PG synthesis were also without effect on these parameters in the mammary, in contrast with the coronary artery. The reasons for this are unclear but it suggests that at least some of the conflicting reports in the literature may be due to inherent differences between arteries.

In conclusion, the relatively clear-cut nature of the observations supports a role for measurement of membrane potential in the assessment of the role of hyperpolarization in mediating vasorelaxation. The recording of membrane potential at rest may be a reliable indicator of events over a wider range of conditions when dealing with the response to NO and PG. However, the arteries are likely to reveal the EDHF component of hyperpolarization more readily in depolarized tissues than at rest. The study of membrane potential alone to probe endothelial function can provide an alternative perspective on the possibilities of differential responsiveness to vasorelaxants uncomplicated by constrictor agents and elevated extracellular K^+, which can introduce variability in their own right according to agent, concentration and arterial bed. The study provides the basis from which to introduce some of these variables, one at a time and in a controlled manner and in this way facilitate interpretation of the observed differences between blood vessels.

The authors thank Dr Neela Kotecha for discussion of the manuscript. This work was supported by the National Heart Foundation of Australia and the National Health and Medical Research Council of Australia.

References

ADEAGBO, A.S.O. & TRIGGLE, C.R. (1993). Varying extracellular $[K^+]$: A functional approach to separating EDHF- and EDNO-related mechanisms in perfused rat mesenteric arterial bed. *J. Cardiovasc. Pharmacol.,* **21,** 423–429.

AMÈDÈE, T., BENHAM, C.D., BOLTON, T.B., BYRNE, N.G. & LARGE, W.A. (1990). Potassium, chloride and non-selective cation conductances opened by noradrenaline in rabbit ear artery cells. *J. Physiol.,* **423,** 551–568.

BRUCH, L., BYCHKOV, R., KÄSTNER, A., BÜLOW, T., REID, C., GOLLASCH, M., BAUMANN, G., LUFT, F.C. & HALLER, H. (1997). Pituitary adenylate-cyclase-activating peptides relax human coronary arteries by activating K_{ATP} and K_{Ca} channels in smooth muscle cells. *J. Vasc. Res.,* **34,** 11–18.

CHEN, G., SUZUKI, H. & WESTON, A.H. (1988). Acetylcholine releases endothelium-derived hyperpolarizing factor and EDRF from rat blood vessels. *Br. J. Pharmacol.,* **95,** 1165–1174.

CHRISTIE, M.I. & LEWIS, M.J. (1988). Vascular smooth muscle sensitivity to endothelium-derived relaxing factors is different in different arteries. *Br. J. Pharmacol.,* **95,** 630–636.

FELETOU, M. & VANHOUTTE, P.M. (1988). Endothelium-dependent hyperpolarization of canine coronary smooth muscle. *Br. J. Pharmacol.,* **93,** 515–524.

GARLAND, C.J. & MCPHERSON, G.A. (1992). Evidence that nitric oxide does not mediate the hyperpolarization and relaxation to acetylcholine in the rat small mesenteric artery. *Br. J. Pharmacol.,* **105,** 429–435.

GARLAND, C.J., PLANE, F., KEMP, B.K. & COCKS, T.M. (1995). Endothelium-dependent hyperpolarization: a role in the control of vascular tone. *Trends Pharmacol. Sci.,* **16,** 23–30.

HAMMARSTRÖM, A.K.M., PARKINGTON, H.C. & COLEMAN, H.A. (1995). Release of endothelium-derived hyperpolarizing factor (EDHF) by M_3 receptor stimulation in the guinea-pig coronary artery. *Br. J. Pharmacol.,* **115,** 717–722.

HAMMARSTRÖM, A.K., PARKINGTON, H.C., TONTA, M.A., TARE, M., & COLEMAN, H.A. (1991). The mammary artery of guinea-pigs is less sensitive to vasorelaxants than is the coronary artery. *Proc. Aust. Physiol. Pharmacol. Soc.,* **22,** 49P.

HASHITANI, H. & SUZUKI, H. (1997). K^+ channels which contribute to the acetylcholine-induced hyperpolarization in smooth muscle of the guinea-pig submucosal arteriole. *J. Physiol.,* **501,** 319–329.

JAISWAL, N. & MALIK, K.U. (1990). Prostacyclin synthesis elicited by cholinergic agonists is linked to activation of $M_{2\alpha}$ and $M_{2\beta}$ muscarinic receptors in the rabbit aorta. *Prostaglandins,* **39,** 267–280.

KEEF, K.D. & BOWEN, S.M. (1989). Effect of ACh on electrical and mechanical activity in guinea pig coronary arteries. *Am. J. Physiol.,* **257,** H1096–H1103.

KOMORI, K. & SUZUKI, H. (1987). Electrical responses of smooth muscle cells during cholinergic vasodilation in the rabbit saphenous artery. *Circ. Res.,* **61,** 586–593.

LEE, L., BRUNER, C.A. & WEBB, R.C. (1990). Prostanoids contribute to endothelium-dependent coronary vasodilation in guinea-pigs. *Blood Vessels,* **27,** 341–351.

MULVANY, M.J. & HALPERN, W. (1977). Contractile properties of small arterial resistance vessels in spontaneously hypertensive and normotensive rats. *Circ. Res.,* **41,** 19–26.

NELSON, M.T. & QUAYLE, J.M. (1995). Physiological roles and properties of potassium channels in arterial smooth muscle. *Am. J. Physiol.,* **268,** C799–C822.

PARKINGTON, H.C., TARE, M., TONTA, M.A. & COLEMAN, H.A. (1993). Stretch revealed three components in the hyperpolarization of guinea-pig coronary artery in response to acetylcholine. *J. Physiol.,* **465,** 459–476.

PARKINGTON, H.C., TONTA, M.A., COLEMAN, H.A. & TARE, M. (1995). Role of membrane potential in endothelium-dependent relaxation of guinea-pig coronary arterial smooth muscle. *J. Physiol.,* **484,** 469–480.

PLANE, F. & GARLAND, C.J. (1996). Influence of contractile agonist on the mechanism of endothelium-dependent relaxation in rat isolated mesenteric artery. *Br. J. Pharmacol.,* **119,** 191–193.

SCORNIK, F. & TORO, L. (1992). U46619, a thromboxane A_2 agonist, inhibits K_{Ca} channel activity from pig coronary artery. *Am. J. Physiol.,* **262,** C708–C713.

SIEGEL, G., RUCKBORN, K., SCHNALKE, F. & MULLER, J. (1993). Endothelial dysfunction in human atherosclerotic coronary arteries. *Eur. Heart J.,* **14,** S99–S103.

SIEGEL, G., STOCK, G., SCHNALKE, F. & LITZA, B. (1987). Electrical and mechanical effects of prostacyclin in canine carotid artery. In: *Prostacyclin and its stable analogue iloprost*. eds. Gryglewski, R.J. & Stock, G. pp. 143–149 Heidelberg: Springer-Verlag, 1987.

TARE, M., PARKINGTON, H.C., COLEMAN, H.A., NEILD, T.O. & DUSTING, G.J. (1990). Hyperpolarization and relaxation of arterial smooth muscle caused by nitric oxide derived from the endothelium. *Nature,* **346,** 69–71.

TAYLOR, S.G. & WESTON, A.H. (1988). Endothelium-derived hyperpolarising factor: a new endogenous inhibitor from the vascular endothelium. *Trends Pharmacol. Sci.,* **9,** 272–274.

ZYGMUNT, P.M., EDWARDS, G., WESTON, A.H., LARSSON, B. & HOGESTATT, E.D. (1997). Involvement of voltage-dependent potassium channels in the EDHF-mediated relaxation of rat hepatic artery. *Br. J. Pharmacol.,* **121,** 141–149.

(Received June 1, 1998
Revised October 19, 1998
Accepted October 22, 1998)

British Journal of Pharmacology (1999) 126, 429–436
http://www.stockton-press.co.uk/bjp

Cell type-specific ATP-activated responses in rat dorsal root ganglion neurons

[3]Shinya Ueno, [1]Makoto Tsuda, [2]Toshihiko Iwanaga & *,[1]Kazuhide Inoue

[1]Division of Pharmacology, National Institute of Health Sciences 1-18-1 Kamiyoga, Setagaya-ku, Tokyo Japan 158; [2]Department of Biomedical Science, Graduate School of Veterinary Medicine, Hokkaido University, Sapporo, Japan

1 The aim of our study is to clarify the relationship between expression pattern of P2X receptors and the cell type of male adult rat (Wistar) dorsal root ganglion (DRG) neurons. We identified the nociceptive cells of acutely dissociated DRG neurons from adult rats type using capsaicin sensitivity.

2 Two types of ATP-activated currents, one with fast, the other with slow desensitization, were found under voltage-clamp conditions. In addition, cells with fast but not slow desensitization responded to capsaicin, indicating that there was a relationship between current kinetics and capsaicin-sensitivity.

3 Both types of neurons were responsive to ATP and α, β methylene-ATP (α,βmeATP). The concentration of α,βmeATP producing half-maximal activation (EC_{50}) of neurons with fast desensitization was less (11 μM) than that of neurons with slow desensitization (63 μM), while the Hill coefficients were similar. Suramin and pyridoxal-phosphate-6-azophenyl-2′,4′-disulphonic acid tetrasodium (PPADS) antagonized α,βmeATP-induced currents in both types of neurons.

4 *In situ* hybridization revealed that small cells of the DRG predominantly expressed mRNAs of $P2X_3$ and medium-sized cells expressed mRNAs of $P2X_2$ and $P2X_3$. In contrast, both of mRNAs were not detected in large cells of the DRG.

5 These results suggest that capsaicin-sensitive, small-sized DRG neurons expressed mainly the homomeric $P2X_3$ subunit and that capsaicin-insensitive, medium-sized DRG neurons expressed the heteromultimeric receptor with $P2X_2$ and $P2X_3$.

Keywords: Dorsal root ganglia; P2X; ATP; capsaicin; patch-clamp; *in situ* hybridization; pain

Abbreviations: α,βmeATP, α,β-methylene ATP; DRG, dorsal root ganglia; HEK, human embryonic kidney; PPADS, pyridoxal-phosphate-6-azophenyl-2′,4′-disulphonic acid tetrasodium

Introduction

Extracellular ATP opens ligand-gated cation channels (P2X receptors) in neuronal preparations (Suprenant *et al*., 1995). In sensory neurons, the properties of ATP-gated cation channels have been extensively studied using electrophysiological approaches since the early 1980's (Jahr & Jessell, 1983; Krishtal *et al*., 1983; 1988; Bean, 1990). Recently, the P2X receptors have been cloned into seven subunits ($P2X_1-P2X_7$) (Soto *et al*., 1997). One of these, the $P2X_3$ receptor subunit, was cloned from a rat DRG cDNA library (Lewis *et al*., 1995; Chen *et al*., 1995) and expressed in capsaicin-sensitive, small-sized DRG neurons (Chen *et al*., 1995), suggesting that ATP might be involved in the transduction of pain *via* P2X receptors.

ATP-evoked currents in heterologously expressed $P2X_3$ receptor showed rapid desensitization, whereas $P2X_2$ receptor showed slow desensitization under voltage-clamp conditions. The sensitivity of P2X receptors to the ATP analogue, α,β-methylene ATP (α,βmeATP) is also different from homomeric P2X receptors. α,βmeATP can evoke a rapidly desensitizing current in homomeric $P2X_3$ receptors but evokes no response in homomeric $P2X_2$ receptors. Although two different P2X subtypes among the $P2X_1-P2X_4$ subunits were coexpressed in human embryonic kidney (HEK) 293 cells, only a combination of the $P2X_2$ and $P2X_3$ subtypes resulted in functional ligand-gated channels. This heteromer of $P2X_2$ and $P2X_3$ ($P2X_{2+3}$) showed distinct functional properties from homomeric $P2X_2$ or $P2X_3$ channels as regards agonist sensitivity, desensitization kinetics and Ca^{2+} influx (Lewis *et al*., 1995; Ueno *et al*., 1998; Virginio *et al*., 1998). These properties of $P2X_{2+3}$ were close to those observed in nodose ganglion neurons (Lewis *et al*., 1995). In fact, based on the early electrophysiological studies, ATP evoked non-desensitizing currents in sensory neurons (Krishtal *et al*., 1988; Bean *et al*., 1990; Khakh *et al*., 1995). Thus, the majority of native ATP-gated channels in sensory neurons were thought to be the $P2X_{2+3}$. However, controversial data were reported using cultured DRG neurons from neonatal rats and a part of the nociceptors in trigeminal ganglion neurons, indicating that ATP and α,βmeATP evoked rapidly desensitizing currents (Robertson *et al*., 1996; Cook *et al*., 1997a,b). These current properties were similar to those recorded in homomeric $P2X_3$ receptors. Additionally, nociceptors in trigeminal ganglion showed two types of currents with respect to the desensitizing kinetics (Cook *et al*., 1997a,b). These data suggest that there are several types of neurons with different expression of P2X subunits. However, there is no report which clearly demonstrate the relationship between current properties and cell characterization in DRG neurons.

In the present study using acutely dissociated DRG neurons from adult rats, capsaicin was used to discriminate between nociceptive and non-nociceptive DRG neurons under voltage-clamp conditions. We observed two types of the ATP-evoked responses in DRG neurons and clarified the relationship between the properties of ATP-evoked responses and the cell

*Author for correspondence; E-mail: inoue@nihs.go.jp
[3] Current address: Department of Pharmacology, School of Medicine Fukuoka University, 7-45-1 Nanakuma Jyonan-ku, Fukuoka, Japan 814-0180.

types according to cell size and responsiveness to capsaicin. Furthermore, the differential distribution of mRNAs for $P2X_2$ and $P2X_3$ in the DRG was confirmed using *in situ* hybridization histochemistry. These findings revealed that the character of ATP-activated responses in DRG neurons was dependent on the cell-type, and provided the first evidence that the $P2X_3$ and $P2X_{2+3}$ receptors can function in a subset of nociceptive and non-nociceptive cells, respectively, in the DRG.

Methods

DRG neuron isolation

Wistar rats (8-weeks-old) were decapitated under ether anaesthesia and the DRG were removed from the L4-6 segments. The DRG were treated first with 20 unit ml^{-1} papain (Worshington Biochemical Co. Freehold, NJ, U.S.A.) dissolved in Tyrode's solution for 10 min at 37°C. The tissue was then treated with 4 mg ml^{-1} collagenase typeII (CLS2; Worshington Biochemical Co.) and 2.5 unit ml^{-1} Dispase (Calbiochem, La Jolla, CA, U.S.A.) dissolved in Tyrode's solution for 60 min at 37°C. At the end of this treatment, the enzyme solution was removed and the cells were then mechanically dissociated by trituration through a pasteur pipette. Cells were plated on 35 mm polystyrene dishes for physiological experiments.

Electrical recording

Recordings were made using the conventional whole cell patch-clamp method (Hamill *et al*., 1981). All experiments were performed at room temperature (21–23°C). The pipette solution contained (in mM): CsCl 140, $MgCl_2$ 2, EGTA 5, HEPES 10, pH adjusted to 7.2 with CsOH. The pipette resistance was 2 to 5 MΩ. Series resistance (2–8 MΩ) and cell capacitance (12 to 80 pF) were compensated up to 80%. Currents were filtered at 300 Hz with a 8-pole Bessel filter (Frequency Devices, Haverhill, MA, U.S.A.) and measured with an Axopatch 200A amplifier (Axon Instruments, Foster City, CA, U.S.A.). Data were then sampled at 1 kHz and stored on-line with a 486 PC using pClamp (Axon Instruments). Drugs were dissolved in an external solution of the following composition (in mM): NaCl 150, KCl 5, $CaCl_2$ 2, $MgCl_2$ 1, D-glucose 10, HEPES 10, pH adjusted to 7.4 with NaOH. The solutions of drugs were applied with a polyethylene Y-tube (equilibration time <20 ms) (Ueno *et al*., 1997). The bath was continuously perfused with normal external solution from a separate perfusion line, and the solution was removed from the bath with a Leiden aspirator (Medical Systems, Greenvale, NY, U.S.A.). Concentration-effect curves were fitted with Hill equation:

$$I(\mathrm{X}) = I_{\max} \cdot (\mathrm{X}/\mathrm{EC}\ 50)^n / (1 + (\mathrm{X}/\mathrm{EC}\ 50)^n \qquad (1)$$

where I is the current elicited by the ATP concentration X, $I_{\max}$ is the fitted maximal current, EC_{50} is the concentration producing a half maximal response, and n is the Hill coefficient.

In situ *hybridization*

The following antisense oligonucleotides were used as probes for *in situ* hybridization, and these were complementary to nucleotide residues 2400–2444 of the rat $P2X_2$ cDNA (Y09910) and 1202–1246 of the rat $P2X_3$ cDNA (X91167); 5′-ttatggctgtagagcttgtttttgttcatgaacgttaacaaaatc-3′ for $P2X_2$ and 5′-caaacttcctggctttgtagtgatcagccccttgaggaaattga-3′ for $P2X_3$. These oligonucleotides were labelled with ^{35}S-dATP using terminal deoxyribonucleotidyl transferase (BRL, Gaithersburg, MD, U.S.A.) at a specific activity of 0.5×10^9 d.p.m. μg^{-1} DNA. Male Wistar rats, weighing approximately 200 g, were used. Under pentobarbitone anaesthesia at a lethal dose, the DRG were freshly removed and frozen in powdered dry ice. Cryostat sections, 20 μm in thickness, were prepared and mounted on glass slides precoated with 3-aminopropyltriethoxysilane. They were fixed with 4% paraformaldehyde for 10 min and acetylated for 10 min with 0.25% acetic anhydride in 0.1 M triethanolamine-HCl (pH 8.0). The sections were prehybridized for 1 h in a buffer containing 50% formamide 0.1 M Tris-HCl (pH 7.5), 4 × SSC (1 × SCC; 150 mM NaCl and 15 mM sodium citrate), 0.02% Ficoll, 0.02% polyvinylpyrrolidone, 0.02% bovine serum albumin, 0.6 M NaCl, 0.25% sodium dodecyl sulphate (SDS), 200 μg ml^{-1} tRNA, 1 mM EDTA, and 10% dextran sulphate. Hybridization was performed at 42°C for 10 h in the prehybridization buffer supplemented with 10,000 c.p.m. μl^{-1} of ^{33}P-labelled oligonucleotide probes. The slides were washed at room temperature for 20 min in 2 × SSC containing 0.1% sarkosyl and twice at 55°C for 40 min in 0.1 × SSC containing 0.1% sarkosyl. The sections were dipped in Kodak NTB2 nuclear track emulsion and exposed for 2 months.

Drugs

Drugs used were ATP (Sigma), α,βmeATP (Sigma), capsaicin, suramin (Wako Pure Chemistry, Osaka, Japan) and pyridoxal-phosphate-6-azophenyl-2′,4′-disulphonic acid tetrasodium (PPADS) (RBI, Natick, MA, U.S.A.). The pH of the solutions containing ATP or α,βmeATP was readjusted to 7.4 with NaOH.

Statistics

The reported probabilities for significant differences were obtained using the paired Student's *t*-test.

Results

There were two types of ATP-activated currents in dissociated DRG neurons and they showed rapid or slow desensitization kinetics. We found a mutual relevance between the properties of the desensitization kinetics and the capsaicin sensitivity. In Figure 1a and b, the typical current responses to ATP, α,βmeATP and capsaicin are shown in these two subpopulations of DRG neurons. DRG neurons with rapidly desensitizing currents were also responsive to capsaicin, while neurons with slow desensitizing ones were not. In our experiments, a cell was classified as capsaicin-sensitive neuron if there was an inward current in response to 3 μM capsaicin. Capsaicin (3 μM) evoked a rapid activation followed by a very slowly desensitizing inward current, and the value of the peak amplitude was −786 ± 148 pA (mean ± s.e.mean, $n = 12$). Capsaicin-sensitive neurons tested were small and medium size in diameter (21–37 μm). ATP produced the rapidly desensitizing currents in about 70% of the capsaicin-sensitive neurons tested (12/17). Capsaicin-insensitive neurons usually possessed medium and large size in diameter (29–63 μm). About 48% of capsaicin-insensitive neurons tested (10/21) responded to both ATP and α,βmeATP and these cells showed medium size in diameter (29–45 μm). Especially, all large-

sized cells (>48 μm) had no sensitivity to ATP and α,βmeATP (Figure 1c). The application of ATP in capsaicin-insensitive neurons evoked a rapid activation followed by a sustained inward current. With respect to desensitization kinetics, in capsaicin-sensitive neurons, the rapid desensitization of the α,βmeATP-induced current (100 μM) was well fitted to two exponential components, while in capsaicin-insensitive ones, it was well fitted to one exponential component. There were significant differences in the cell size and time constant for desensitization (τd) between the capsaicin-sensitive and

Table 1 Properties of agonists-induced responses in capsaicin-sensitive and -insensitive cells

	Capsaicin-sensitive cells average±s.e.mean	n[b]	*Capsaicin-insensitive cells average±s.e.mean*	n	P[a]
Cell size (μm)	29.0±1.3	12	36.0±1.7	10	$P<0.01$
Response to 100 μM ATP					
Peak current (pA)	−163±54	6	−422±101	8	N.S.
Response to 100 μM α,βmeATP					
Peak current (pA)	−152±50	5	−310±66	7	N.S.
Tau (τd) (ms)	τd1; 63±20	4			
	τd2; 884±227		5557±645	6	$P<0.01$

The maximum diameter of dissociated cells was measured using a light microscope before electrophysiological experiments were performed. [a]Probability that difference between capsaicin-sensitive and capsaicin-insensitive cells is fortuitous. N.S. indicates $P<0.05$. [b]Number of cells studied.

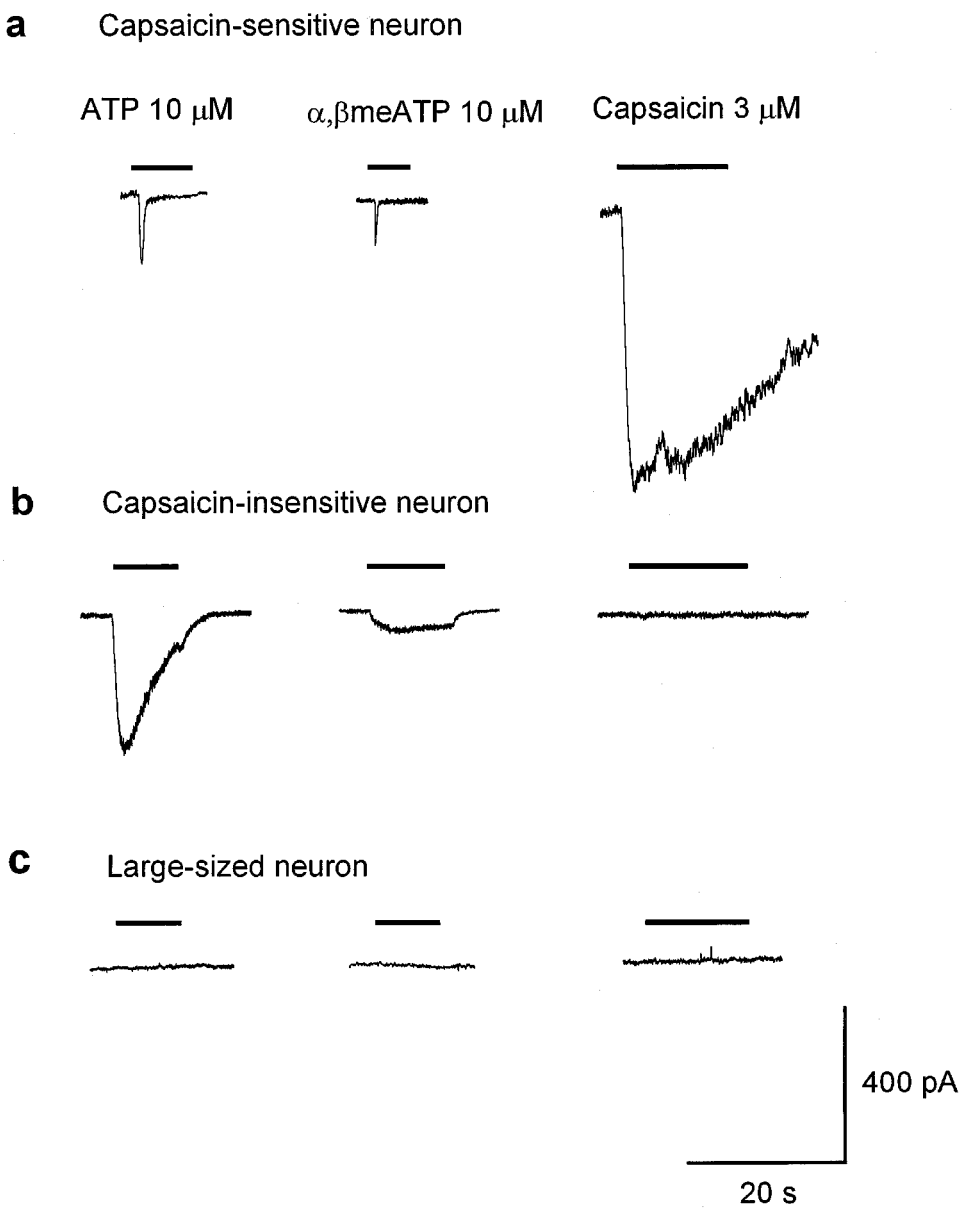

Figure 1 Responses of cells to ATP (10 μM), α,βmeATP (10 μM) and capsaicin (3 μM). (a) Representative current traces for capsaicin-sensitive neurons. (b) Representative current traces for capsaicin-insensitive neurons. (c) Representative current traces for large-sized (>50 μm) neurons. Data in a, b and c were obtained from a single cell, respectively. The application of agonists is indicated by bars above each record. Cells were voltage-clamped to −50 mV.

capsaicin-insensitive neurons, but not in the peak amplitude induced by each agonist (Table 1). Capsaicin-sensitive neurons were also small in diameter, suggesting that these cells were nociceptive neurons. α,βmeATP-induced currents (10 μM) in both types of neurons were completely inhibited by suramin (30 μM) ($n=3$ for each type of neurons) or PPADS (10 μM) ($n=3$ for each type of neurons).

When α,βmeATP (30 μM) was applied twice with an interval of 5 min, the current responses of capsaicin-sensitive and capsaicin-insensitive neurons reacted in a different manner. The α,βmeATP-evoked currents in capsaicin-sensitive neurons dramatically ran down at the second application of agonist (Figure 2a). In contrast, the α,βmeATP-evoked currents in capsaicin-insensitive neurons retained its responsiveness to repeated applications of α,βmeATP (Figure 2b).

We examined the concentration-response relationship for ATP activation in capsaicin-sensitive and capsaicin-insensitive DRG neurons (Figure 3). The capsaicin-sensitive neurons showed an EC_{50} value of 5.6 μM and a Hill coefficient of 1.0. For the capsaicin-insensitive neurons, the EC_{50} value and Hill coefficient were 23.7 and 1.0, respectively.

We also examined the concentration-response relationship for α,βmeATP activation for both types of DRG neurons since α,βmeATP is a relatively selective agonist for P2X receptors consisting of the $P2X_3$ subunit. The capsaicin-sensitive neurons showed an EC_{50} value of 10 μM and a Hill coefficient of 0.9. The capsaicin-insensitive neurons showed an EC_{50} value of 66 μM and a Hill coefficient of 1.0 (Figure 4).

In situ hybridization analysis using antisense oligonucleotide probes specific for either $P2X_2$ or $P2X_3$ mRNA exhibited consistent labellings in the neuronal somata of the DRG. The specificity of hybridization was confirmed by the disappearance of the signals when an excess dose of the corresponding cold probes was added into the hybridization fluid. DRG are composed of neurons showing various sizes, which are largely classified into small cells less than 25 μm, large cells greater than 35 μm, and medium-sized cells around 30 μm in diameter. Small cells were labelled only for $P2X_3$ mRNA and medium-sized cells were labelled both for $P2X_2$ and $P2X_3$ mRNAs. The intense labelling for $P2X_3$ mRNA was found in both small cells and medium-sized cells, but not in the large cells. On the other hand, signals for $P2X_2$ mRNA were localized exclusively in medium-sized cells.

Discussion

In the present study, we used acutely dissociated DRG neurons from adult rats and recorded the responses *via* P2X receptors under voltage-clamp conditions. Thus, functional receptors that are expressed on somata in DRG neurons were detected. About 70% of the capsaicin-sensitive neurons tested were responsive to both ATP and α,βmeATP. Furthermore, these agonists evoked rapidly desensitizing currents in this type of neuron. Capsaicin selectively activates nociceptors and causes burning pain and neurogenic inflammation *in vivo* (Simone *et al*., 1989). The effects of capsaicin are largely restricted to subpopulation of DRG neurons with small cell bodies *in vitro* (Holzer, 1991). These are presumably nociceptive neurons with unmyelinated (C) fibres or some thinly myelinated (Aδ) fibres. In addition, capsaicin-activated cation channels have been cloned recently and an *in situ* hybridization study has

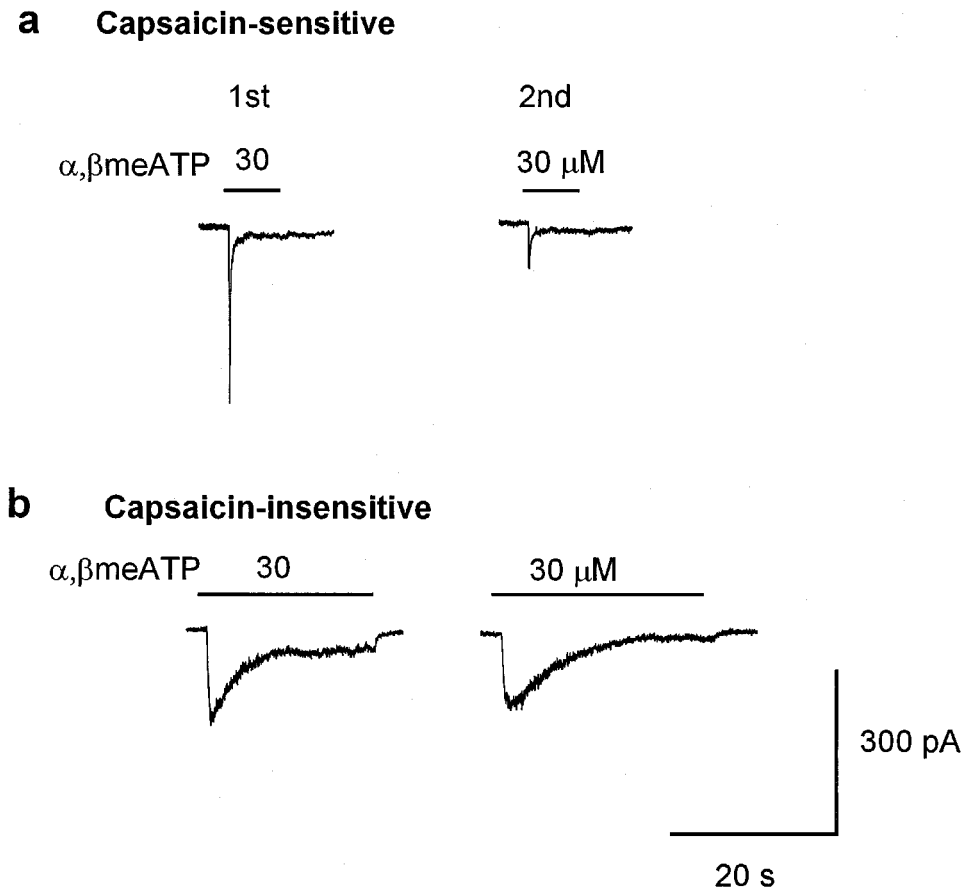

Figure 2 Effects of repeated applications of α,βmeATP. Typical current responses to α,βmeATP (30 μM) in capsaicin-sensitive (a) or -insensitive (b) neurons at every 5 min. Horizontal solid bars show the application of 30 μM α,\βmeATP.

demonstrated that these vanilloid receptors are located in small-sized DRG neurons (Caterina *et al*., 1997). The sizes of the capsaicin-sensitive neurons in our preparation were also consistent with these results. Therefore, in the present study, the ATP- or α,βmeATP-evoked responses in the capsaicin-sensitive neurons can be assumed to the expression pattern of P2X receptors in nociceptors.

The ATP-activated current in the capsaicin-sensitive neurons rapidly desensitized. Although the homomeric expression of $P2X_1$ subunit also showed rapidly desensitizing current, the desensitization of the $P2X_1$ subunit can be fitted to a single exponential decay (Collo *et al*., 1996). In contrast, the desensitization kinetics of the $P2X_3$ subunit were bi-exponential (Lewis *et al*., 1995). In the present study, the currents elicited by α,βmeATP in the capsaicin-sensitive neurons exhibited a bi-exponential decay. Additionally, the concentration-response curve for this type of neuron was similar to that showing $P2X_3$ expression alone (Lewis *et al*., 1995; Ueno *et al*., 1998), suggesting that homomeric $P2X_3$ receptors mainly express in capsaicin-sensitive neurons.

What do P2X subunits contribute to the ATP-activated response in capsaicin-insensitive DRG neurons? The ATP-activated currents in capsaicin-insensitive neurons were the slowly desensitizing type. Especially, the medium-sized cells of

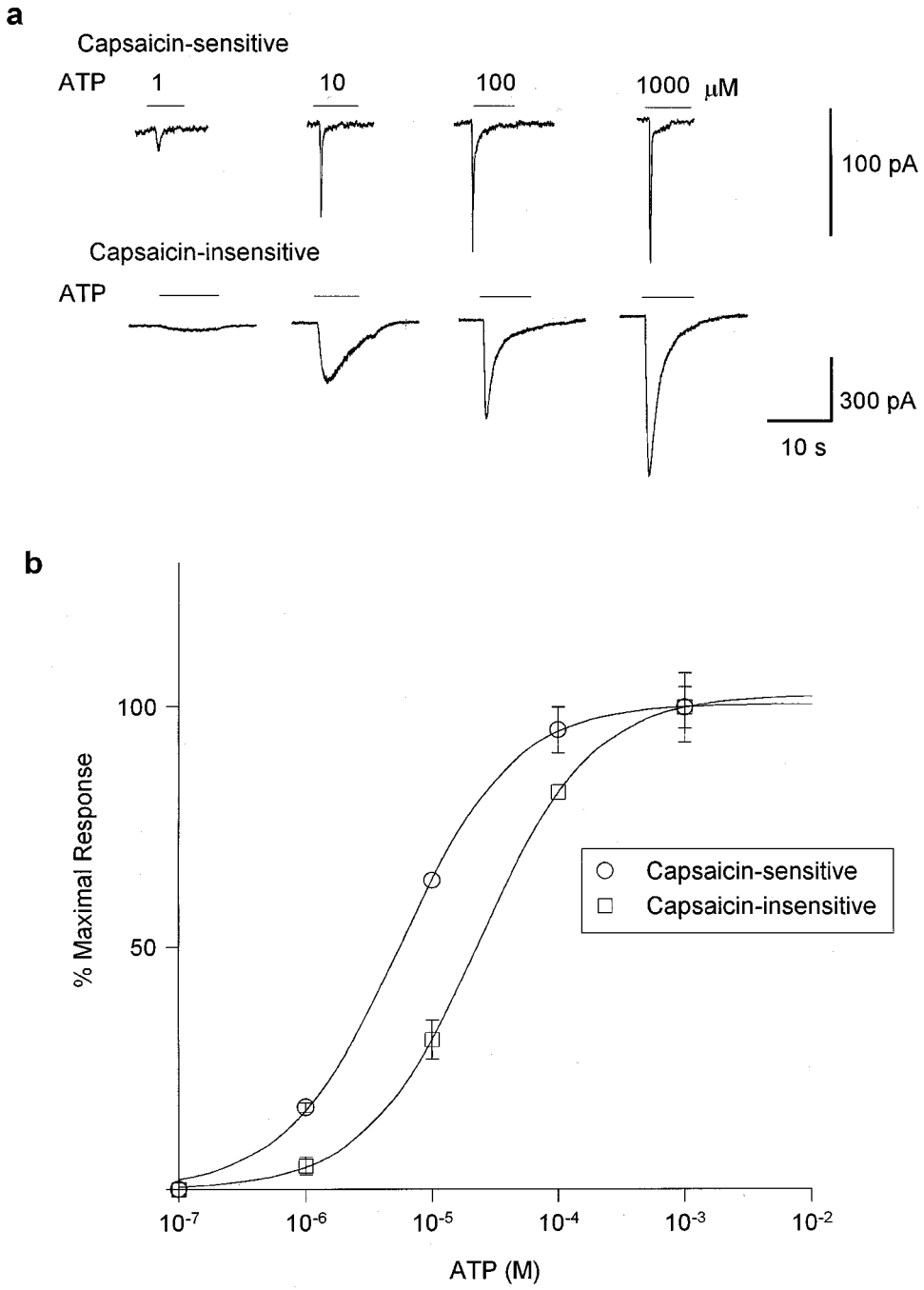

Figure 3 ATP concentration-response relationship for capsaicin-sensitive and -insensitive DRG neurons. (a) The currents in response to concentrations of ATP from 1 μM to 1 mM are shown for capsaicin-sensitive (upper panel) and capsaicin-insensitive (lower panel) neurons. (b) Concentration-response curves for ATP-elicited currents are plotted. The peak current elicited by ATP application was measured and this response was normalized to the response of the same cell to 10 μM α,βmeATP for capsaicin-sensitive neurons (○; mean ± s.e.mean for data from four to six cells) or to 100 μM ATP for capsaicin-insensitive neurons (□; mean ± s.e.mean for data from four to six cells). The mean normalized response was calculated for each concentration applied.

the capsaicin-insensitive neurons responded to applications of ATP and α,βmeATP, and the currents evoked by these agonists (10 μM) were completely blocked by suramin and PPADS at a concentration of 30 μM. The α,βmeATP-evoked currents (up to 30 μM) in the capsaicin-insensitive neurons showed sustained current kinetics in the continuous presence of the agonist. On the basis of the characterization of heterologously expressed P2X receptors, these current kinetics and pharmacological properties are in agreement with the coexpression of the $P2X_2$ and $P2X_3$ subunits (Ueno *et al.*, 1998). Although homomeric $P2X_2$ receptor is insensitive to α,βmeATP, $P2X_{2+3}$ showed slowly desensitizing current in response to both ATP and α,βmeATP (Lewis *et al.*, 1995; Ueno *et al.*, 1998). However, because *in situ* hybridization data

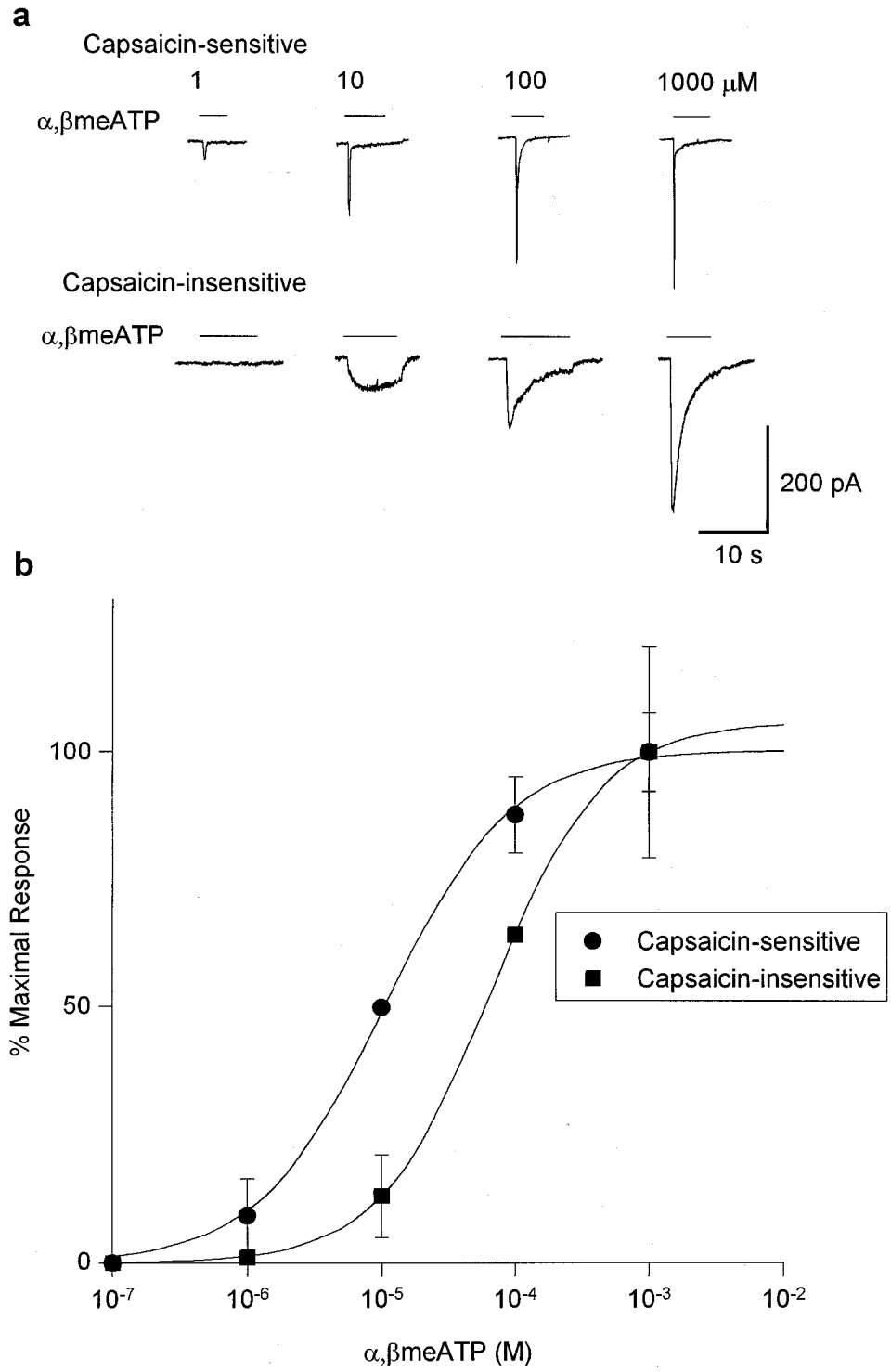

Figure 4 α,βmeATP concentration-response relationship for capsaicin-sensitive and -insensitive DRG neurons. (a) The currents in response to concentrations of α,βmeATP from 1 μM to 1 mM are shown for capsaicin-sensitive (upper panel) and capsaicin-insensitive (lower panel) neurons. (b) Concentration-response curves for α,βmeATP-elicited currents are plotted. The peak current elicited by the α,βmeATP applications was measured and this response was normalized to the response of the same cell to 10 μM α,βmeATP for capsaicin-sensitive neurons (●; mean ± s.e.mean for data from four to nine cells) or to 100 μM α,βmeATP for capsaicin-insensitive neurons (■; mean ± s.e.mean for data from four to seven cells). The mean normalized response was calculated for each concentration applied. The smooth lines show the values predicted by the Hill equation (1).

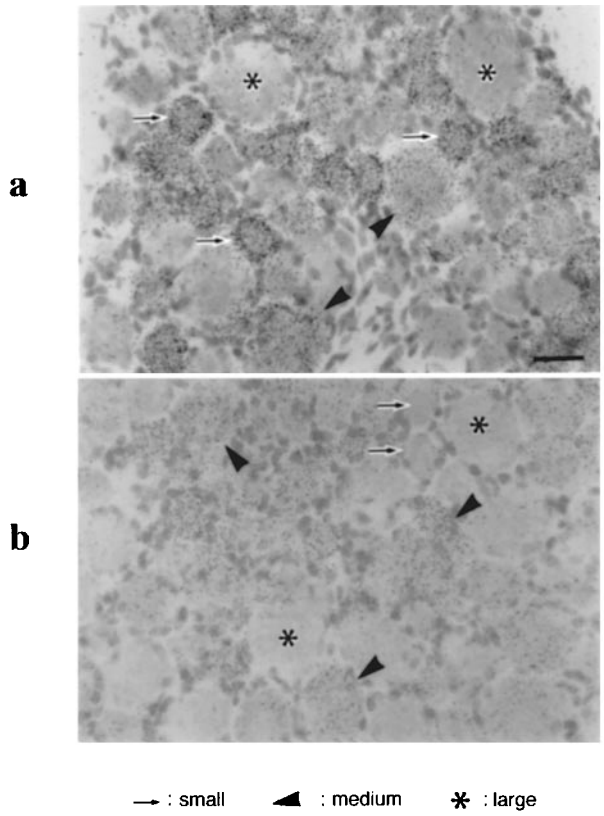

Figure 5 Bright-field micrographs showing signals for the $P2X_3$ (a) and $P2X_2$ (b) mRNA. In the dorsal root ganglion, intense signals of $P2X_3$ are seen in small (arrows) and medium-sized ganglion cells (arrowheads), but not in large cells (asterisks) which are more than 40 μm in diameter. Significant signals for $P2X_2$ were found in medium-sized cell bodies (arrowheads), but not in small (arrows) and large cell bodies (asterisks).

demonstrated the six mRNAs of the P2X receptors ($P2X_1$–$P2X_6$) in DRG (Collo *et al*., 1996), other subunits might be involved in the ATP- or α,βmeATP-evoked responses in capsaicin-insensitive neurons. The $P2X_4$ subunit was detected as one of the major subunits expressed in DRG (Lewis *et al*., 1995). The expression studies of the homomeric $P2X_4$ subunit revealed pharmacological properties distinctly different from the $P2X_2$ and $P2X_3$ subunits. The EC_{50} value for ATP activation was around 10 μM, and α,βmeATP produced less than 10% of the ATP-activated current in the $P2X_4$ subunit. The current evoked by ATP was almost insensitive to the P2X antagonists, suramin and PPADS. The inhibitory concentration of 50% (IC_{50}) values of these antagonists ranged from >100 μM to >500 μM (Bo *et al*., 1995; Buell *et al*., 1996; Seguela *et al*., 1996; Soto *et al*., 1996). In contrast, our results were not consistent with the homogenous expression of $P2X_4$. Therefore, the involvement of the $P2X_4$ subunit in the slowly desensitizing current of the capsaicin-insensitive neurons is less extensive than that of other subunits. Consequently, it is most likely the $P2X_{2+3}$ that is mainly expressed in the capsaicin-insensitive neurons. This type of DRG neuron showed a larger diameter than that of neurons with rapidly desensitizing current. The cell size ranged from 28–48 μm. DRG cells of this size largely consisted of neurons with myelinated A-fibre (Harper & Lawson, 1985). In the present experiments, diameter of dissociated cells seems to be a little larger than that of corresponding cell subpopulation observed in *in situ* hybridization. The difference is probably due to the fact that dissociated cells tends to enlarge the size by effects of dissociation damage and that diameter of cross-section does not always show the maximum value.

The current kinetics evoked by α,βmeATP and the sensitivity to the P2X antagonist in the capsaicin-insensitive neurons were consistent with the properties of $P2X_{2+3}$, whereas the concentration-response relationship for α,βmeATP was not identical with data observed in $P2X_{2+3}$ and nodose ganglion neurons (Lewis *et al*., 1995). The value of the EC_{50} for α,βmeATP in the capsaicin-insensitive neurons was about ten times larger. The coexpression of $P2X_2$ and $P2X_3$ subunits could make several subsets of heteromeric receptors with unknown stoichiometries. Indeed, the blocking effect of trinitrophenyl-ATP on nodose ganglion neurons and $P2X_{2+3}$ suggested the existence of heteromeric channels having various combinations of the $P2X_2$ and $P2X_3$ subunits (Thomas *et al*., 1998). In addition, our heterologous expression study using the C6BU-1 cell line provided a larger EC_{50} value for α,βmeATP than that observed when $P2X_2$ and $P2X_3$ subunits were coexpressed (Ueno *et al*., 1998). However, we can not exclude the possibility that other subunits such as $P2X_1$ and $P2X_4$ affect the concentration-response relationship for agonists.

Recently, specific antisera to $P2X_2$ and $P2X_3$ have been developed (Vulchanova *et al*., 1996; 1997). Using these antisera, immunohistochemical analysis has clarified the differential distribution of these immunoreactivities in the cell bodies of DRG neurons. The existence of these signals was restricted to a specific subpopulation of the DRG. The $P2X_3$ immunoreactivity was detected predominantly in small neurons (Vulchanova *et al*., 1997). As was the case with our *in situ* hybridization analysis, the $P2X_3$ signals were also extensively labelled in small-sized neurons. These results provide supporting evidence that the homomeric $P2X_3$ receptor is expressed in nociceptive neurons with unmyelinated fibres. As for the distribution of $P2X_2$, the overall intensity for $P2X_2$ immunoreactivity in the DRG was stronger than that of $P2X_3$ (Vulchanova *et al*., 1997). In our *in situ* hybridization analysis, the $P2X_2$ signal was not detected in small-sized neurons. Electrophysiological data also supported that the $P2X_2$ receptor functions in medium-sized neurons. Taken together the present results, $P2X_2$ is expressed in neurons with myelinated fibres, which are not related to nociception. The expression pattern of P2X receptors was different in each subpopulation of DRG neurons. However, the physiological significance of this differential expression of P2X receptors in the DRG was not clarified. It will be necessary to perform further investigations using behavioural approaches *in vivo*.

Two types of ATP-activated current were observed in acutely dissociated DRG neurons under the voltage clamp condition. The morphological differences and capsaicin sensitivity between two subpopulations provide an indication that capsaicin-sensitive DRG neurons expressed mainly homomeric $P2X_3$ subtype and capsaicin-insensitive neurons expressed heteromultimeric complex of $P2X_2$ and $P2X_3$ subtypes.

This work was supported by Grants-in-Aid for Scientific Research (No. 08457416) from the Ministry of Education, Science and Culture of Japan and Domestic research Fellowship from Japan Science and Technology Corporation.

References

BEAN, B.P. (1990). ATP-activated channels in rat and bullfrog sensory neurons: concentration dependence and kinetics. *J. Neurosci.,* **10,** 1–10.

BO, X., ZHANG, Y., NASSAR, M., BURNSTOCK, G. & SCHOEPFER, R. (1995). A P2X purinoceptor cDNA conferring a novel pharmacological profile. *FEBS Lett.,* **375,** 129–133.

BUELL, G., LEWIS, C., COLLO, G., NORTH, R.A. & SUPRENANT, A. (1996). An antagonist-insensitive P-2x receptor expressed in epithelial and brain. *EMBO J.,* **15,** 55–62.

CATERINA, M.J., SCHUMACHER, M.A., TOMINAGA, M., ROSEN, T.A., LEVINE, J.D. & JULIUS, D. (1997). The capsaicin receptor: a heat-activated ion channel in the pain pathway. *Nature,* **389,** 816–824.

CHEN, C.C., AKOPIAN, A.N., SIVILOTTI, L., COLQUHOUN, D., BURNSTOCK, G. & WOOD, J.N. (1995). A P2X purinoceptor expressed by a subset of sensory neurons. *Nature,* **377,** 428–431.

COLLO, G., NORTH, R.A., KAWASHIMA, E., MERLO-PICH, E., NEIDHART, S., SURPRENANT, A. & BUELL, G. (1996). Cloning of P2X5 and P2X6 receptors and the distribution and properties of an extended family of ATP-gated ion channels. *J. Neurosci.,* **16,** 2495–2507.

COOK, S.P. & MCCLESKEY, E.W. (1997a). Desensitization, recovery and Ca^{2+}-dependent modulation of ATP-gated P2X receptors in nociceptors. *Neuropharmacol.,* **36,** 1303–1308.

COOK, S.P., VULCHANOVA, L., HARGREAVES, K.M., ELDE, R. & MCCLESKEY, E.W. (1997b). Distinct ATP receptors on pain-sensing and stretch-sensing neurons. *Nature,* **387,** 505–508.

HAMILL, O.P., MARTY, A., NEHER, E., SAKMANN, B. & SIGWORTH, F.J. (1981). Improved patch-clamp techniques for high-resolution current recording from cells and cell-free membrane patches. *Pflugers Arch.,* **391,** 85–100.

HARPER, A.A. & LAWSON, S.N. (1985). Conduction velocity is related to morphological cell type in rat dorsal root ganglion neurones. *J. Physiol.,* **359,** 31–46.

HOLZER, P. (1991). Capsaicin: cellular targets, mechanisms of action, and selectivity for thin sensory neurons. *Pharmacol. Rev.,* **43,** 143–201.

JAHR, C.E. & JESSELL, T.M. (1983). ATP excites a subpopulation of rat dorsal horn neurones. *Nature,* **304,** 730–733.

KHAKH, B.S., HUMPHREY, P.P. & SUPRENANT, A. (1995). Electrophysiological properties of P2X-purinoceptors in rat superior cervical, nodose and guinea-pig coeliac neurones. *J. Physiol.,* **484,** 385–395.

KRISHTAL, O.A., MARCHENKO, S.M., OBUKHOV, A.G. & VOLKOVA, T.M. (1988). Receptors for ATP in rat sensory neurones: the structure-function relationship for ligands. *Br. J. Pharmacol.,* **95,** 1057–1062.

KRISHTAL, O.A., MARCHENKO, S.M. & PIDOPLICHKO, V.I. (1983). Receptor for ATP in the membrane of mammalian sensory neurones. *Neurosci. Lett.,* **35,** 41–45.

LEWIS, C., NEIDHART, S., HOLY, C., NORTH, R.A., BUELL, G. & SUPRENANT, A. (1995). Coexpression of P2X(2) and P2X(3) receptor subunits can account for ATP-gated currents in sensory neurons. *Nature,* **377,** 432–435.

ROBERTSON, S.J., RAE, M.G., ROWAN, E.G. & KENNEDY, C. (1996). Characterization of a P2X-purinoceptor in cultured neurons of the rat dorsal root ganglia. *Br. J. Pharmacol.,* **118,** 951–956.

SEGUELA, P., HAGHIGHI, A., SOGHOMONIAN, J.J. & COOPER, E. (1996). A novel neuronal P2x ATP receptor ion channel with widespread distribution in the brain. *J. Neurosci.,* **16,** 448–455.

SIMONE, D.A., BAUMANN, T.K. & LAMOTTE, R.H. (1989). Dose-dependent pain and mechanical hyperalgesia in humans after intradermal injection of capsaicin. *Pain,* **38,** 99–107.

SOTO, F., GARCIA-GUZMAN, M., GOMEZ-HERNANDEZ, J.M., HOLLMANN, M., KARSCHIN, C. & STUHMER, W. (1996). P2X4: an ATP-activated ionotropic receptor cloned from rat brain. *Proc. Natl. Acad. Sci. U.S.A.,* **93,** 3684–3688.

SOTO, F., GARCIA-GUZMAN, M. & STUHMER, W. (1997). Cloned ligand-gated channels activated by extracellular ATP (P2X receptors). *J. Memb. Biol.,* **160,** 91–100.

SURPRENANT, A., BUELL, G. & NORTH, R.A. (1995). P2X receptors bring new structure to ligand-gated ion channels. *Trends. Neurosci.,* **18,** 224–229.

THOMAS, S., VIRGINIO, C., NORTH, R.A. & SURPRENANT, A. (1998). The antagonist trinitrophenyl-ATP reveals co-existence of distinct P2X receptor channels in rat nodose neurons. *J. Physiol.,* **509,** 411–417.

UENO, S., BRACAMONTES, J., ZORUMSKI, C., WEISS, D.S. & STEINBACH, J.H. (1997). Bicuculline and gabazine are allosteric inhibitors of channel opening of the GABAA receptor. *J. Neurosci.,* **17,** 625–634.

UENO, S., KOIZUMI, S. & INOUE, E. (1998). Characterization of Ca^{2+} influx through recombinant P2X receptor in C6BU-1 cells. *Br. J. Pharmacol.,* **124,** 1484–1490.

VIRGINIO, C., NORTH, R.A. & SURPRENANT, A. (1998). Calcium permeability and block at homomeric and heteromeric P2X2 and P2X3 receptors, and P2X receptors in nodose neurones. *J. Physiol. (Lond.),* **510,** 27–35.

VULCHANOVA, L., ARVIDSSON, U., RIEDL, M., WANG, J., BUELL, G., SURPRENANT, A., NORTH, R.A. & ELDE, R. (1996). Differential distribution of two ATP-gated channels (P2X receptors) determined by immunocytochemistry. *Proc. Natl. Acad. Sci. U.S.A.,* **93,** 8063–8067.

VULCHANOVA, L., REIDL, M.S., SHUSTER, S.J., BUELL, G., SURPRENANT, A., NORTH, R.A. & ELDE, R. (1997). Immunohistochemical study of the P2X2 and P2X3 receptor subunits in rat and monkey sensory neurons and their central terminals. *Neuropharmacol.,* **36,** 1229–1242.

(Received September 1, 1998
Revised October 13, 1998
Accepted October 26, 1998)

British Journal of Pharmacology (1999) 126, 437–442
http://www.stockton-press.co.uk/bjp

Characterization of α_1-adrenoceptor subtypes mediating vasoconstriction in human umbilical vein

[1]Andrea Emilse Errasti, [1]María Pía Rogines Velo, [1]Rodrigo Martín Torres, [1]Sergio Pablo Sardi & *,[1]Rodolfo Pedro Rothlin

[1]Departamento de Farmacología, Facultad de Medicina, Universidad de Buenos Aires, Paraguay 2155, Piso 15, 1121, Buenos Aires, Argentina

1 The present study attempted to characterize pharmacologically the subtypes of α-adrenoceptors mediating contractions in human umbilical vein (HUV).

2 HUV rings were mounted in isolated organ baths and cumulative concentration-response curves were constructed for the α-adrenoceptor agonists phenylephrine and adrenaline. Adrenaline was more potent than phenylephrine ($pD_2 = 7.29$ and 6.04 respectively).

3 Isoproterenol exhibited no agonism on KCl pre-contracted HUV rings. Propranolol (1 μM) and rauwolscine (0.1 μM) did not affect the concentration-response curves to adrenaline. These results demonstrate the lack of involvement of functional β- or α_2-adrenoceptors in adrenaline-induced vasoconstriction.

4 The non subtype selective α_1-adrenoceptor antagonist prazosin was evaluated on phenylephrine and adrenaline concentration-response curves. The effects of the competitive α_{1A} and α_{1D}-adrenoceptor antagonists, 5-methyl urapidil and BMY 7378 and the irreversible α_{1B} selective compound chloroethylclonidine (CEC) were also evaluated on adrenaline concentration-response curves.

5 The potencies of prazosin against responses mediated by adrenaline ($pA_2 = 10.87$) and phenylephrine ($pA_2 = 10.70$) indicate the involvement of prazosin-sensitive functional α_1-adrenoceptor subtype in vasoconstriction of the HUV.

6 The potencies of 5-methyl urapidil ($pA_2 = 6.70$) and BMY 7378 ($pA_2 = 7.34$) were not consistent with the activation of an α_{1A}- or α_{1D}-adrenoceptor population.

7 Exposure to a relatively low CEC concentration (3 μM) abolished the maximum response to adrenaline suggesting that this response was mediated by an α_{1B}-adrenoceptor subtype.

8 We conclude that HUV express a prazosin-sensitive functional α_1-adrenoceptor resembling the α_{1B}-subtype according with the low pA_2 values for both 5-methyl urapidil and BMY 7378 and the high sensitivity to CEC.

Keywords: Human umbilical vein; α_1-adrenoceptors; adrenaline; isoproterenol; rauwolscine; propranolol; prazosin; BMY 7378; 5-methyl urapidil; chloroethylclonidine

Abbreviations: BK, bradykinin; CEC, chloroethylclonidine; HUV, human umbilical vein

Introduction

The umbilical vein transports the oxygenated blood from the placenta to the foetus, therefore, a normal blood flow is crucial for its growth. Umbilical and placental vessels lack autonomic innervation (Reilly & Russel, 1977; Fox & Khong, 1990). Furthermore, Kawano & Mori (1990) demonstrated that the human umbilical vein (HUV) has no adrenergic innervation and adrenergic nerve fibres are present only in umbilical arteries at the foetal end of the cord. Therefore, HUV is under no influence from the sympathetic nervous system and the regulation of its vascular tone must depend on the release of vasoactive substances which are locally produced or conveyed through the blood stream. Furthermore, it is known that the vasoconstrictor effects of adrenaline and noradrenaline depend on the stimulation of α-adrenoceptors in HUV (Altura *et al*., 1972).

α_1-Adrenoceptors are a heterogeneous group of receptors and have been subclassified into α_{1A}-, α_{1B}- and α_{1D}-adrenoceptor subtypes based on radioligand binding, molecular biology and isolated tissue experiments (Hieble *et al*., 1995). In addition, all three subtypes are expressed in vascular smooth muscle (Price *et al*., 1994; Vargas & Gorman, 1995; Piascik *et al*., 1996).

Although the functional affinity values span a broad range, all α_1-adrenoceptor mediated responses are sensitive to blockade by prazosin, and all show low affinity for the selective α_2-adrenoceptor antagonist rauwolscine (Bylund *et al*., 1994; Hieble *et al*., 1995).

The subdivision of α_1-adrenoceptors into α_{1A}- and α_{1B}-subtypes has been supported by the identification of several antagonists showing at least 100 fold selectivity for the α_{1A}-adrenoceptor, such as 5-methyl urapidil (Gross *et al*., 1988). Further evidence to support this subdivision was provided by studies which demonstrated that chloroethylclonidine selectively alkylated the α_{1B}-subtype (Han *et al*., 1987; Minneman *et al*., 1988).

*Author for correspondence; E-mail: farmaco3@fmed.uba.ar

On the other hand, a selective α_{1D}-antagonist, BMY 7378, has been described and was shown to have a high affinity in the rat aorta (Saussy *et al*., 1994). Furthermore, Kenny *et al*. (1995) have shown that in the rat aorta, BMY 7378 affinity, correlates well with binding affinities at cloned human α_{1D}-adrenoceptor but not with α_{1A}- or α_{1B}-subtypes.

The aim of the present work was to pharmacologically characterize the α-adrenoceptor subtypes mediating contractions in the human umbilical vein in light of current knowledge and the selective ligands available.

Methods

Preparation of the tissues for tension measurements

Approximately 15–35 cm segments were excised from human umbilical cords ($n=140$) midway between the placenta and infant. These cords were obtained from normal full-term deliveries and immediately placed in modified Krebs solution at 4°C (of the following mM composition: NaCl 119, KCl 4.7, $NaHCO_3$ 25, KH_2PO_4 1.2, $CaCl_2$ 2.5, $MgSO_4$ 1.0, EDTA 0.004, D-glucose 11 and ascorbic acid 0.11).

The veins (internal diameter approximately 5 mm) were dissected out of the cords and cut into rings of approximately 3 mm width. Typically, four rings were taken from each umbilical vein. The preparations were suspended in 10 ml organ baths and stretched with an initial tension of 3–5 g as described previously (Elgoyhen *et al*., 1993). The time from delivery until the tissue was set up in the organ baths was approximately 3 h. Changes in tension were measured with Grass isometric transducers (FT 03C, Grass Instrument, Quincy, MA, U.S.A.) and displayed on Grass polygraphs (Model 7D). The Krebs solution was maintained at 37°C and at pH 7.4 by constant bubbling with 95% O_2/5% CO_2. During the incubation period, the bath solution was replaced every 15 min with fresh Krebs. After 70 min of equilibration each preparation was contracted with 40 mM KCl and washed. This procedure was designed to test for the functional state of the tissue.

Adrenoceptor agonists studies

Cumulative concentration-response curves to either adrenaline or phenylephrine were obtained after a 120 min equilibration period. In all experiments, bradykinin (BK, 0.3 μM) was applied at the end of each experiment in order to determine the tissue maximum response (Sardi *et al*., 1997). In another series of experiments, human umbilical vein rings were contracted with 40 mM KCl after an equilibration period of 120 min. Then, in order to evaluate the possible relaxant effects of a β-adrenoceptor agonist, cumulative-concentration curves to isoproterenol were obtained.

Adrenoceptor antagonists studies

The procedure followed was essentially the same as in the α-adrenoceptor agonist protocol. Each antagonist was applied 30 min before the cumulative addition of agonists (adrenaline or phenylephrine), to ensure that equilibrium was obtained. Experiments were performed in parallel in rings from the same vein. The competitive adrenoceptor antagonists used were propranolol (1 μM), rauwolscine (0.1 μM), prazosin (0.03–1 nM), 5-methyl urapidil (1–10 μM) and BMY 7378 (0.1–1 μM).

Effects of chloroethylclonidine

The effect of the irreversible antagonist chloroethylclonidine (CEC) was also evaluated. Umbilical rings were exposed to CEC (1–3 μM) for a period of 30 min and then washed out (bathing fluid was changed twice every 5 min) for 30 min before cumulative concentration-response curves to adrenaline were obtained.

Drugs

Phenylephrine hydrochloride, adrenaline bitartrate, isoproterenol bitartrate, prazosin hydrochloride, BMY 7378 dihydrochloride, chloroethylclonidine dihydrochloride, 5-methyl urapidil and rauwolscine hydrochloride, were purchased from Research Biochemical Incorporated (Natick, MA, U.S.A.). (±)-Propranolol hydrochloride was purchased from the Sigma Chemical Company (St. Louis, MO, U.S.A.).

All concentrations of drugs are expressed as a final concentration in the organ bath. Preparation of all stock solutions and their subsequent dilution were made in distilled water, except for prazosin and adrenaline. Prazosin was initially dissolved in warmed HCl (0.1 N) then diluted in distilled water. Adrenaline was dissolved in HCl (0.01 N) then diluted in ascorbic acid Krebs solution to avoid oxidation. Stock solutions were stored frozen in aliquots and thawed and diluted daily.

Statistics

All data are presented as means ± s.e.mean. The number (n) of rings and veins is denoted: number rings / number veins. The responses were calculated as a percentage of the maximum in the cumulative concentration-response curves to adrenaline or phenylephrine. In CEC experiments, responses are expressed as g of developed contraction.

The pD_2 values, negative logarithm of the agonist concentration that produce 50% of the maximum effect, were determined using Graph Pad Prism Version 2.0 (Graph Pad Software Inc., San Diego, CA, U.S.A.). Antagonist pA_2 values and slopes of Schild regressions were calculated as described by Arunlakshana & Schild (1959). Statistical analysis was performed by means of unpaired Student's t-test. P values lower than 0.05 were taken to indicate significant differences between means.

Results

After a 120 min incubation period, phenylephrine as well as adrenaline produced a concentration-related contraction of human umbilical vein (HUV) rings. However, it should be noted that not every ring would always respond to adrenaline or phenylephrine. In this study 23 of 140 (16%) human umbilical veins did not show adrenergic responses. Adrenaline was more potent than the α_1-selective agonist phenylephrine. The pD_2 of adrenaline was 7.29 ± 0.06 ($n=13/13$) (n = rings/veins) and 6.04 ± 0.09 ($n=12/12$) for phenylephrine ($P<0.01$). The maximum response was 8.2 ± 1.3 g (72 ± 7% of BK_{max}) for phenylephrine and 11.8 ± 1.0 g (78 ± 3% of BK_{max}) for adrenaline.

Increasing concentrations of the α_1-adrenoceptor antagonist prazosin (0.1, 0.3, and 1 nM) produced a parallel rightward shift of the phenylephrine concentration-response curve without affecting the maximum response, indicative of competitive antagonism. Analysis of the data by Schild

regression gave a slope (0.97±0.19) which was not significantly different from unity and a pA_2 value of 10.70±0.17 (n=17/12, Figure 1a). The effect of prazosin on the contractile response to adrenaline was also evaluated. Increasing concentrations of the antagonist (0.03, 0.1, and 0.3 nM) produced a competitive shift of the adrenaline concentration-response curve. Analysis of the data by Schild regression gave a slope (1.28±0.29) not significantly different from unity and a pA_2 value of 10.87±0.13 (n=22/13, Figure 1b). On the other hand, neither the pD_2 nor maximum contraction of the umbilical vein to adrenaline were affected by the α_2-adrenoceptor antagonist rauwolscine (0.1 μM, n=6/6; data not shown) and the β-adrenoceptor antagonist propranolol (1 μM, n=4/4; data not shown). In addition, the β-adrenoceptor agonist isoproterenol (0.1 nM–100 μM) did not elicit any relaxant effect on KCl submaximum pre-contraction (8.4±1.1 g, n=5/5; data not shown).

The α_{1A}-adrenoceptor antagonist, 5-methyl urapidil (1, 3 and 10 μM) produced rightward shifts of the concentration-response curves to adrenaline, with no depression of the maximum response. Analysis of the data by Schild regression

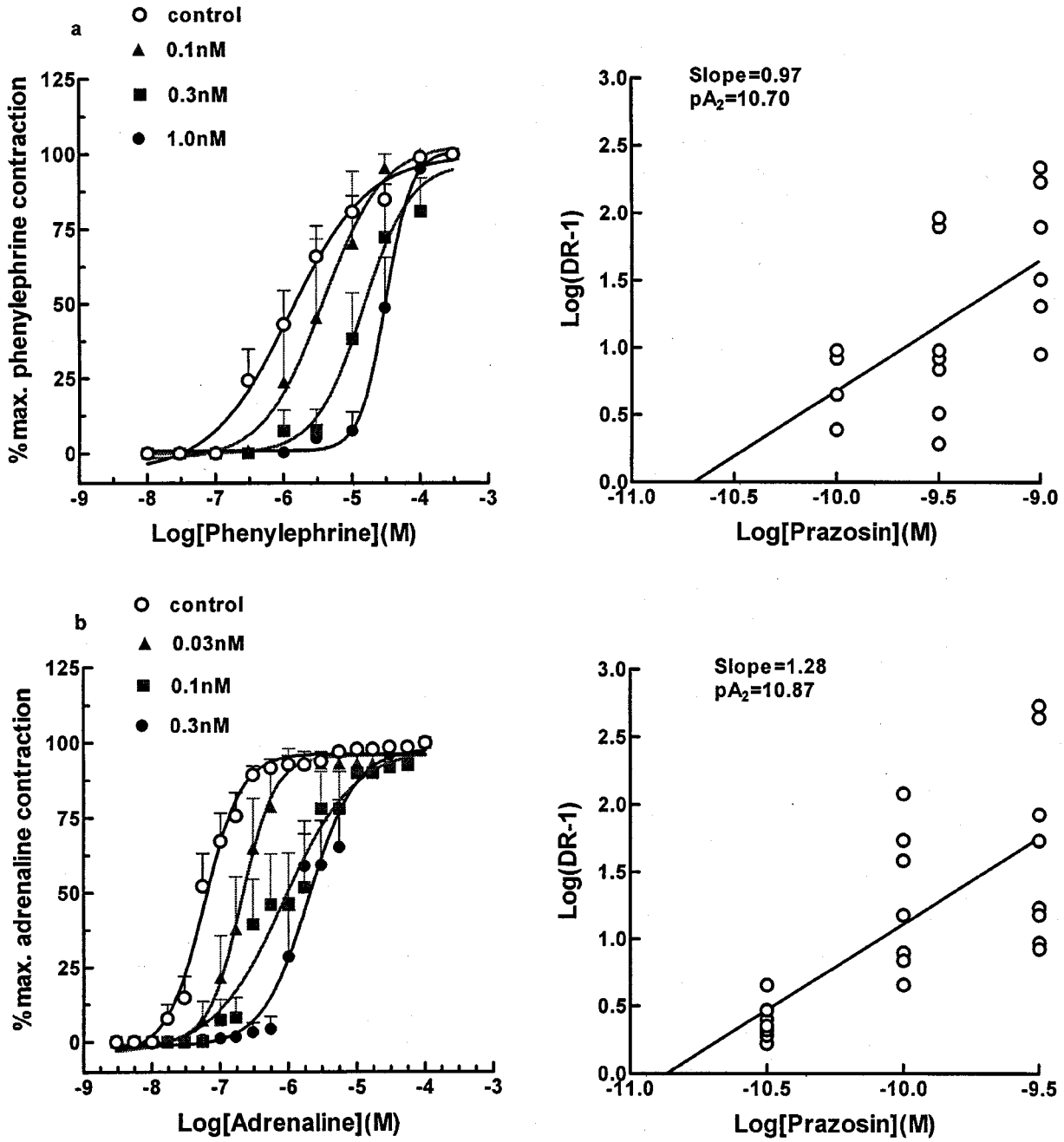

Figure 1 (a) Concentration-response curves and Schild plot for antagonism of phenylephrine induced contraction by prazosin (0.1, 0.3, and 1 nM). (b) Concentration-response curves and Schild plot for antagonism of adrenaline induced contraction by prazosin (0.03, 0.1, and 0.3 nM). Each symbol represents the mean and vertical lines show s.e.mean of at least four separate experiments. Schild plots were constructed with concentration-ratios from individual experiments. The estimates were: (a) pA_2=10.70±0.17, slope=0.97±0.19, r=0.98 (n=17/12); and (b) pA_2=10.87±0.13, slope=1.28±0.29, r=0.97 (n=22/13).

gave a slope which was not significantly different from unity (1.08 ± 0.26) and a pA_2 value of 6.70 ± 0.13 ($n = 25/17$, Figure 2).

The α_{1D}-adrenoceptor antagonist, BMY 7378 (0.1, 0.3 and 1 μM) produced rightward shifts of the concentration-response curves to adrenaline, without reducing the maximum responses over the ranges used for analysis. Analysis of the data by Schild regression gave a slope which was not significantly different from unity (1.14 ± 0.15) and a pA_2 value of 7.34 ± 0.14 ($n = 12/9$, Figure 3).

Exposure to the irreversible antagonist chloroethylclonidine (CEC, 1 μM) decreased the maximum response to adrenaline in seven of ten rings ($P < 0.05$). In the others, it caused a complete suppression of the response to adrenaline (data not shown). Furthermore, CEC (3 μM) completely abolished the response in all experiments ($n = 8/8$, Figure 4). On the other hand, CEC treatment neither exhibited agonism nor modified the maximum response to bradykinin (control, 17.3 ± 2 g; treated, 15.7 ± 2 g).

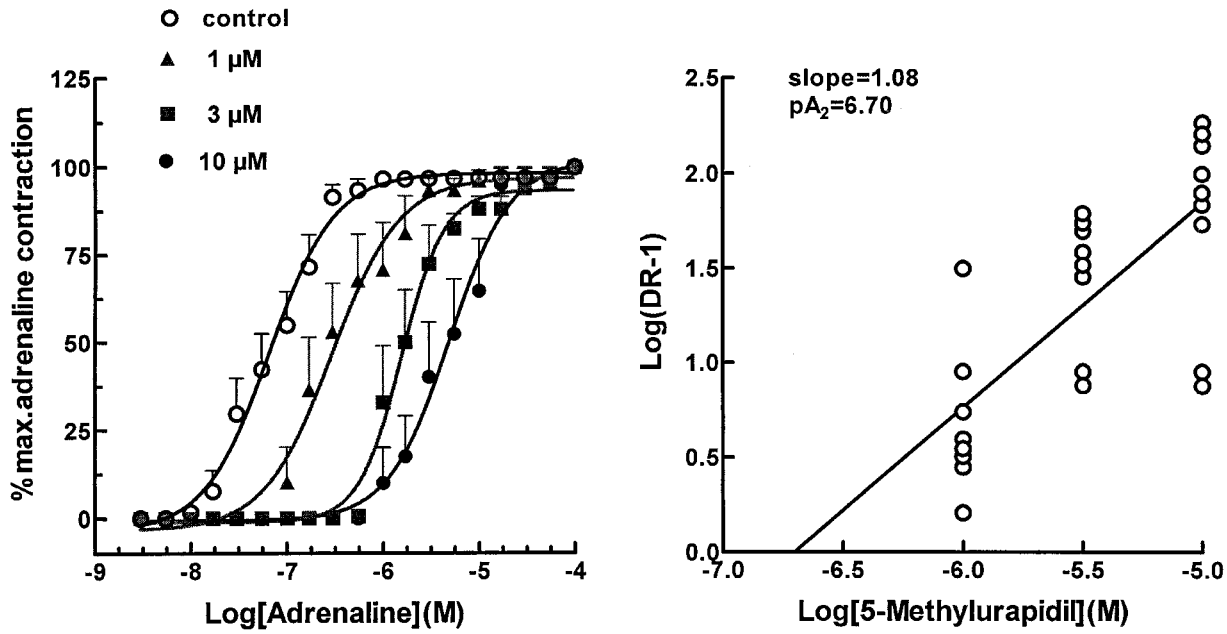

Figure 2 Concentration-response curves and Schild plot for antagonism of adrenaline induced contraction by 5-methyl urapidil (1, 3, and 10 μM). Each symbol represents the mean and vertical lines show s.e.mean of at least eight separate experiments. Schild plot was constructed with concentration-ratios from individual experiments. The estimates were: $pA_2 = 6.70 \pm 0.13$, slope $= 1.08 \pm 0.26$, and $r = 0.97$ ($n = 25/17$).

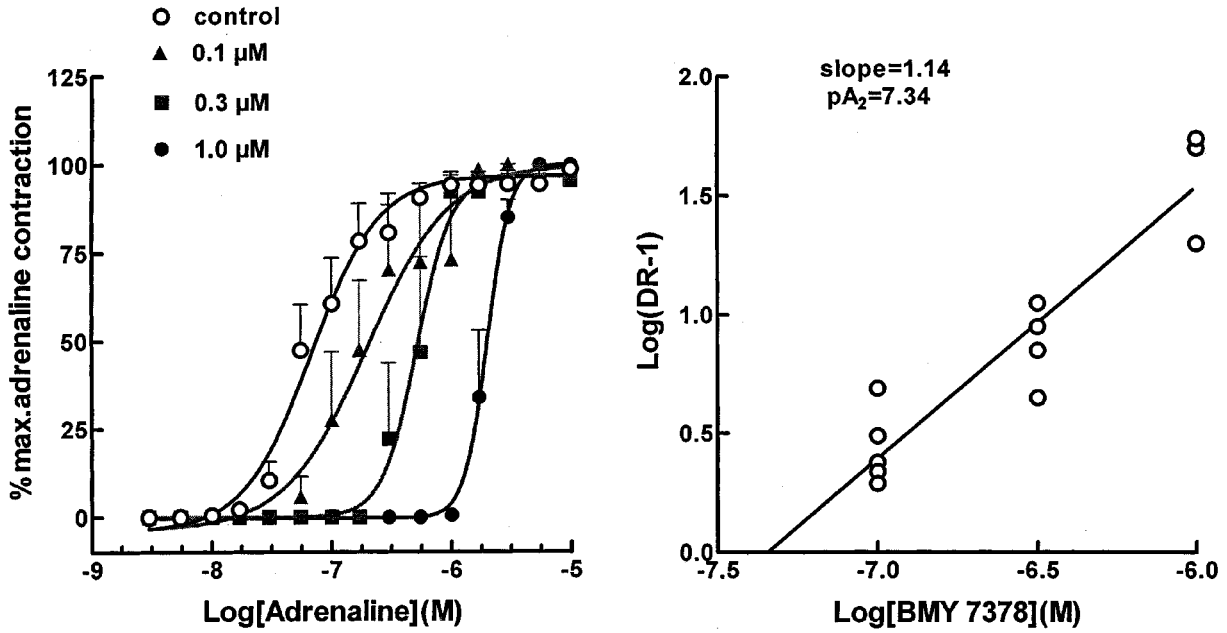

Figure 3 Concentration-response curves and Schild plot for antagonism of adrenaline induced contraction by BMY 7378 (0.1, 0.3, and 1 μM). Each symbol represents the mean and vertical lines show s.e.mean of at least three separate experiments. Schild plot was constructed with concentration-ratios from individual experiments. The estimates were: $pA_2 = 7.34 \pm 0.14$, slope $= 1.14 \pm 0.15$, and $r = 0.99$ ($n = 12/9$).

Table 1 Summary of published affinity data for α_1-adrenoceptors antagonists. Comparison with data obtained in this study

Competitive antagonists	*pK_i on cloned human α-adrenoceptors expressed in cells*			*pA_2 on contractile response in HUV*[d]
	α_{1A}	α_{1B}	α_{1D}	
Prazosin[a]	9.6±0.2	9.5±0.1	9.8±0.3	10.9±0.1
5-Methyl urapidil[b]	8.6±0.1	6.7±0.1	7.6±0.2	6.7±0.1
BMY 7378[c]	6.4±0.2	7.0±0.3	8.8±0.6	7.3±0.1
Irreversible antagonist		*% Inactivation*		*Sensitivity in HUV*
	α_{1A}	α_{1B}	α_{1D}	
CEC[e] 100 μM, 20 min, 37°C	+	+ + + +	+ + +	
CEC[f] 3 μM, 30 min, 37°C				+ + + +

[a,b]pK_i values represent means±s.e.mean of data taken from Forray *et al.* (1994); Goetz *et al.* (1995) and Kenny *et al.* (1995). [c]pK_i values taken from Kenny *et al.*, and Goetz *et al.*, 1995. [d]pA_2 values were obtained using Schild analysis between each antagonist versus adrenaline. [e]Sensitivity to CEC estimated as percentage of inactivation in ligand binding experiments: α_{1A}: 18%, α_{1B}: 91%, α_{1D}: 74% Forray *et al.* (1994); α_{1A}: 18%, α_{1B} 98%, α_{1D}: 75% Schwinn *et al.* (1995). [f]CEC completely abolished the response to adrenaline in HUV.

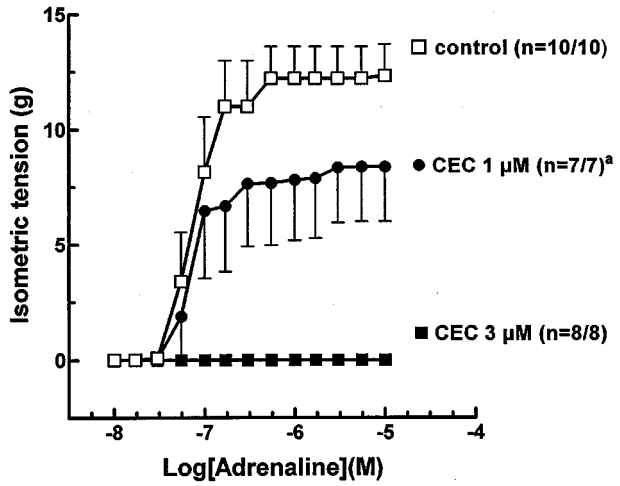

Figure 4 Effect of chloroethylclonidine (CEC) on adrenaline concentration-response curves. Each symbol represents the mean and vertical lines show s.e.mean of at least seven separate experiments. [a]CEC abolished the response to adrenaline in three of ten experiments. The maximum response to adrenaline in tissues exposed to CEC 1 μM was significantly different from control (Student's *t*-test, $P<0.05$).

Discussion

The objective of this study was to perform a pharmacological characterization of the α-adrenoceptor subtypes mediating contractions in the human umbilical vein (HUV) by use of both selective agonists and antagonists. Previous studies have demonstrated the existence of α-adrenoceptors in these vessels (Altura *et al.*, 1972).

Phenylephrine, the non-subtype selective α_1-agonist produced concentration-dependent contractions 23.8 fold less potent than adrenaline. Prazosin, a non-subtype selective α_1-adrenoceptor antagonist, competitively inhibited contractile responses induced by phenylephrine and adrenaline in HUV. The pA_2 values for prazosin versus both agonists are consistent with responses being mediated through α_1-adrenoceptors.

In this tissue, the lack of relaxant effect observed with isoproterenol shows the absence of functional β-adrenoceptors. Furthermore, the potency to adrenaline as well as the maximum response produced did not change with propranolol (1 μM) or rauwolscine (0.1 μM) confirming the absence of both functional β and α_2-adrenoceptors.

According to these results, adrenaline was considered better than phenylephrine as a pharmacological tool in order to characterize the α_1-adrenoceptor subtypes mediating contractions in HUV.

5-Methyl urapidil has been widely used for the classification of α_1-adrenoceptors (Forray *et al.*, 1994; Schwinn *et al.*, 1995; Testa *et al.*, 1995). Its affinity for the α_{1A}-subtype (pK_i approximately 8.6, Table 1) is approximately 10 fold greater than for the α_{1D}-subtype (pK_i approximately 7.6, Table 1) and some 100 fold greater than for the α_{1B}-subtype (pK_i approximately 6.7, Table 1). In this study, the estimated affinity of 5-methyl urapidil in the HUV ($pA_2=6.7$) was similar and close to the value expected for an interaction at the cloned α_{1B}-adrenoceptor.

Goetz *et al.* (1995) and Kenny *et al.* (1995) have demonstrated that BMY 7378 is a selective α_{1D}-adrenoceptor antagonist (pK_i approximately 8.8, Table 1) exhibiting about 100 fold selectivity over α_{1A} and α_{1B}-subtypes (pK_i approximately 6.4 and 7.0 respectively, Table 1). In the HUV the estimated affinity ($pA_2=7.3$, Table 1) of this antagonist was not consistent with its affinity for cloned α_{1D}-subtype, but is according with the value expected for an interaction with the α_{1B}-subtype.

The α_1-adrenoceptor subtypes exhibit different sensitivities to the alkylating effects of CEC (Perez *et al.*, 1991; Forray *et al.*, 1994; Schwinn *et al.*, 1995). Both α_{1B} and α_{1D}-adrenoceptor subtypes are effectively inactivated by CEC-treatment, the former subtype being relatively more sensitive (Forray *et al.*, 1994; Schwinn *et al.*, 1995). Although species-dependent variations in sensitivity have been obtained (García-Sainz *et al.*, 1992), α_{1A}-subtype is considerably more resistant to this alkylating agent. In HUV the effects of a 30 min exposure to 1 μM CEC caused a significant depression of the adrenaline concentration-response curves. Increasing the concentration of CEC (3 μM) resulted in complete abolition of the contractile response to adrenaline (Table 1). Membrane preparations from cells stably transfected with the cloned human α_{1B}-adrenoceptor gene showed approximately 100% inactivation in radioligand binding studies at a CEC concentration 30 fold greater than the one employed in HUV, where the α_1-adrenergic response was abolished (Table 1). CEC treatment had no effect on maximum responses to bradykinin at the end of each experiment demonstrating no effect on the tissue

functional state. On the other hand, it was reported that CEC functions as an irreversible α_2-adrenoceptor agonist (Bultmann & Starke, 1993). CEC treatment did not produce any contractions in HUV in the present study. The lack of contractions suggests the absence of functional α_2-adrenoceptors in this tissue.

In summary, the absence of both functional β- and α_2-adrenoceptors has been demonstrated in HUV based on the following observations. Firstly, isoproterenol failed to produce any relaxant effect on KCl pre-contraction. Secondly, propranolol as well as rauwolscine did not shift the concentration-response curve to adrenaline. Thirdly, CEC alone did not cause direct contractions. On the other hand, the high potency of prazosin, is consistent with a population of α_1-adrenoceptors mediating contractions in HUV. Furthermore, the very low affinity of 5-methyl urapidil, the low affinity of BMY 7378 and the high sensitivity to CEC, provide pharmacological evidence that α_1-adrenoceptor agonists-induced contractions in HUV are mediated by α_{1B}-subtypes.

This work was supported by the Fundación Alberto J. Roemmers and Universidad de Buenos Aires (UBA, Grant ME-041). We wish to thank the Instituto Médico de Obstetricia (Buenos Aires) for their efforts in providing umbilical tissues.

References

ALTURA, B.M., MALAVIYA, D., REICH, C.F. & ORKIN, L.R. (1972). Effects of vasoactive agents on isolated human umbilical veins. *Am. J. Physiol.,* **222,** 345 – 355.

ARUNLAKSHANA, O. & SCHILD, H.O. (1959). Some quantitative uses of drug antagonists. *Br. J. Pharmacol.,* **14,** 48 – 52.

BULTMANN, R. & STARKE, K. (1993). Chloroethylclonidine: an irreversible agonist at prejunctional alpha 2 adrenoceptors in rat vas deferens. *Br. J. Pharmacol.,* **108,** 336 – 341.

BYLUND, D.B., EIKENBERG, D.C., HIEBLE, J.P., LANGER, S.Z., LEFKOWITZ, R.J., MINNEMAN, K.P., MOLINOFF, P.B., RUFFOLO, R.R. & TRENDELENBURG, U. (1994). IV. International Union of Pharmacology Nomenclature of Adrenoceptors. *Pharmacol. Rev.,* **46,** 121 – 136.

ELGOYHEN, A.B., LORENZO, P.S., ROTHLIN, R.P., SPACCAVENTO, D. & ADLER-GRASCHINSKY, E. (1993). Relaxant effects of benzodiazepines on isolated human umbilical arteries and veins. *J. Auton. Pharmacol.,* **13,** 373 – 379.

FORRAY, C., BARD, J.A., WETZEL, J.M., CHIU, G., SHAPIRO, E., TANG, R., LEPOR, H., HARTIG, P.R., WEISSHANK, R.L., BRANCHEK, T.A. & GLUCHOWSKI, C. (1994). The α_1-adrenergic receptor that mediates smooth muscle contraction in human prostate has the pharmacological properties of the cloned human α_{1c}-subtype. *Mol. Pharmacol.,* **45,** 703 – 708.

FOX, S.B. & KHONG, T.Y. (1990). Lack of innervation of human umbilical cord. An immunohistological and histochemical study. *Placenta,* **11,** 59 – 62.

GARCIA-SAINZ, J.A., ROMERO-AVILA, M.T., ALCANTRA-HERNANDEZ, R., MACIAS-SILVA, M., OLIVARES-REYES, J.A. & GONZALES-ESPINOSA, C. (1992). Species heterogeneity of hepatic α_1-adrenoceptors: α_{1A}, α_{1B} and α_{1C}-subtypes. *Biochem. Biophys. Res. Commun.,* **186,** 760 – 767.

GOETZ, A.S., KING, H.K., WARD, S.D.C., TRUE, T.A., RIMELE, T.J. & SAUSSY, D.L. (1995). BMY 7378 is a selective antagonist of the D subtype of α_1-adrenoceptors. *Eur. J. Pharmacol.,* **272,** R5-R6.

GROSS, G., HANFT, G. & RUGEVICS, C. (1988). 5-Methyl-urapidil discriminates between subtypes of the α_1-adrenoceptor. *Eur. J. Pharmacol.,* **151,** 333 – 335.

HAN, C., ABEL, P.W. & MINNEMAN, K.P. (1987). Heterogeneity of α1-adrenoceptors revealed by chloroethylclonidine. *Mol. Pharmacol.,* **32,** 505 – 510.

HIEBLE, J.P., BYLUND, D.B., CLARKE, D.E., EIKENBURG, D.C., LANGER, S.Z., LEFKOWITZ, R.J., MINNEMAN, K.P. & RUFFOLO, R.R. (1995). International Union of Pharmacology X. Recommendation for nomenclature of α_1-adrenoceptor: consensus update. *Pharmacol. Rev.,* **47,** 267 – 270.

KAWANO, M. & MORI, N. (1990). Prostacyclin producing activity of human umbilical blood vessels in adrenergic innervated and non-innervated portions. *Prostagl. Leukotr. Essent. Fatty Acids,* **39,** 239 – 244.

KENNY, B.A., CHALMERS, D.H., PHILPOTT, P.C. & NAYLOR, A.M. (1995). Characterization of an α_{1D}-adrenoceptor mediating the contractile response of rat aorta to noradrenaline. *Br. J. Pharmacol.,* **115,** 981 – 986.

MINNEMAN, K.P., HAN, C. & ABEL, P.W. (1988). Comparison of α_1-adrenergic receptor subtypes distinguished by chloroethylclonidine and WB 4101. *Mol. Pharmacol.,* **33,** 509 – 514.

PEREZ, D.M., PIASCIK, M.T. & GRAHAM, R.M. (1991). Solution phase library screening for the identification of rare clones: isolation of an α_{1D} adrenergic receptor cDNA. *Mol. Pharmacol.,* **40,** 876 – 883.

PIASCIK, M.T., SOLTIS, E.E., PIASCIK, M.M. & MACMILLAN L.B. (1996). α-Adrenoceptors and vascular regulation: molecular, pharmacologic and clinical correlates. *Pharmacol. Ther.,* **72,** 215 – 241.

PRICE, D.T., LEFKOWITZ, R.J., CARON, M.G., BERKOWITZ, D. & SCHWINN, D.T. (1994). Localization of mRNA for three distinct α_1-adrenergic receptor subtypes in human tissues: implications for human α-adrenergic physiology. *Mol. Pharmacol.,* **45,** 171 – 175.

REILLY, F.D. & RUSSELL, P.T. (1977). Neurohistochemical evidence supporting an absence of adrenergic and cholinergic innervation in the human placenta and umbilical cord. *Anat. Rec.,* **188,** 277 – 286.

SARDI, S.P., PEREZ, H., ANTUNEZ, P. & ROTHLIN, R.P. (1997). Bradykinin B_1 receptors in human umbilical vein. *Eur. J. Pharmacol.,* **321,** 33 – 38.

SAUSSY, D.L., GOETZ, A.S., KING, H.K. & TRUE, T.A. (1994). BMY 7378 is a selective antagonist of α_{1D}-adrenoceptors: evidence that rat vascular α_1-adrenoceptors are of the α_{1D}-subtype. *Can. J. Physiol. Pharmacol.,* **72,** P31.1.008.

SCHWINN, D.A., JOHNSON, G.I., PAGE, S.O., MOSLEY, M.J., WILSON, K.A., WORMAN, N.P., CAMPBELL, B. & BAILRY, D.S. (1995). Cloning and pharmacological characterization of human α_1-adrenergic receptors: Sequence corrections and direct comparison with other species homologues. *J. Pharmacol. Exp. Ther.,* **272,** 134 – 142.

TESTA, R., GUARNERI, L., POGGESI, E., SIMONAZZI, I., TADDEI, C. & LEONARDI, A. (1995). Mediation of noradrenaline-induced contractions of rat aorta by the α_{1B}- adrenoceptor subtype. *Br. J. Pharmacol.,* **114,** 745 – 750.

VARGAS, H.M. & GORMAN, A.J. (1995). Vascular α_1-adrenergic receptors subtypes in regulation of arterial pressure. *Life Sci.,* **57,** 2291 – 2308.

(Received June, 29, 1998
Revised October 22, 1998
Accepted October, 26, 1998)

British Journal of Pharmacology (1999) 126, 443–450
http://www.stockton-press.co.uk/bjp

Endothelin receptor expression and pharmacology in human saphenous vein graft

*,[1]Janet J. Maguire & [1]Anthony P. Davenport

[1]Clinical Pharmacology Unit, University of Cambridge, Level 6, Centre for Clinical Investigation, Box 110, Addenbrooke's Hospital, Cambridge CB2 2QQ, England

1 We have investigated the expression and pharmacology of endothelin (ET) receptors in human aortocoronary saphenous vein grafts.

2 Subtype-selective ligands were used to autoradiographically identify ET_A ([^{125}I]-PD151242) and ET_B ([^{125}I]-BQ3020) receptors. In graft saphenous vein ET_A receptors predominated in the media, with few ET_B receptors identified. Neither subtype was detected in the thickened neointima.

3 The ratio of medial ET_A:ET_B receptors was 75% : 25% in both graft and control saphenous vein.

4 ET-1 contracted control (EC_{50} 2.9 nM) and graft (EC_{50} 4.5 nM) saphenous vein more potently than diseased coronary artery (EC_{50} 25.5 nM).

5 In all three blood vessels ET-1 was 100 times more potent than ET-3 and three times more potent than sarafotoxin 6b (S6b). Little or no response was obtained in any vessel with the ET_B agonist sarafotoxin 6c (S6c).

6 The ET_A antagonist PD156707 (100 nM) blocked ET-1 responses in all three vessels with pK_b values of approximately 8.0.

7 For individual graft veins the EC_{50} value for ET-1 and 'age' of graft in years showed a significant negative correlation.

8 In conclusion there is no alteration in ET receptor expression in the media of saphenous veins grafted into the coronary circulation compared to control veins. ET_A receptors predominantly mediate the vasoconstrictor response to ET-1 in graft vein, with no apparent up-regulation of ET_B receptors. The sensitivity of the graft vein to ET-1 increased with graft 'age', suggesting that these vessels may be particularly vulnerable to the increased plasma ET levels that are detected in patients with cardiovascular disease.

Keywords: Endothelin; endothelin receptors; ET_A; ET_B; human saphenous vein graft; intimal proliferation; vasospasm; vein graft disease

Abbreviations: BSA, bovine serum albumin; CABG, coronary artery bypass graft; ET, endothelin; 5-HT, 5-hydroxytryptamine; OD, optical density; S6b, sarafotoxin 6b; S6c, sarafotoxin 6c

Introduction

The saphenous vein is the most widely used graft vessel employed to bypass atherosclerotic blood vessels of the heart and thus relieve the symptoms of coronary artery disease. Perioperative aortocoronary vein graft spasm is a serious complication. It results in hypoperfusion of the vein and damage to the endothelium, thus contributing to graft failure (Roubos *et al*., 1995). Post-operative graft spasm is more rare, but can be fatal (Victor *et al*., 1981). In a small proportion of patients the vein grafts close completely following surgery. This occurs either within days of surgery, when the cause is frequently the development of occluding mural thrombi (Lie *et al*., 1977; Bourassa *et al*., 1982), or more usually, closure occurs over a period of 5–10 years (Lie *et al*., 1977; Atkinson *et al*., 1985). The fibrointimal proliferative nature of this late vein graft disease closely resembles that of atherosclerotic coronary artery disease (Bulkley & Hutchins, 1977; Campeau *et al*., 1983; Atkinson *et al*., 1985). Arterial grafts are less susceptible to long term failure (Rossiter *et al*., 1974; Ivert *et al*., 1988), however the requirement to bypass multiple vessels of the heart, in many patients, precludes the exclusive use of arterial preparations. Antiplatelet drugs can be of some benefit, particularly in preventing early vein graft stenosis (Chesebro *et al*., 1982; Fuster & Chesebro, 1986; Goldman *et al*., 1988). However, to improve the long term patency of the autogenous saphenous vein for coronary artery bypass surgery novel drug therapies must be developed.

Recent studies have shown that expression of the peptide endothelin-1 (ET-1) is increased in human failed vein grafts (Brody *et al*., 1996; Masood *et al*., 1996). ET-1 is a potent vasoconstrictor of human blood vessels (Maguire & Davenport, 1995) including saphenous vein (Costello *et al*., 1990; Lüscher *et al*., 1990; Bax *et al*., 1993; Akar *et al*., 1994; White *et al*., 1994) and is mitogenic or co-mitogenic for vascular smooth muscle cells (see Battistini *et al*., 1993). Endothelin (ET) may therefore be involved in the initiation and/or development of both vein graft spasm and stenosis following surgery. We have therefore determined which of the ET receptor subtypes are expressed in the blocked vein graft and which are responsible for the vasoconstrictor actions of the ET peptides in this diseased tissue and compared this to non-diseased saphenous vein harvested for grafting. We have previously shown that the media of human saphenous vein expresses mainly ET_A receptors but also has a small population of ET_B receptors that comprise less than 25% of total (Davenport *et al*., 1995). We were particularly interested to investigate whether or not the expression of ET_B receptors is augmented in late graft disease as it has been suggested that

* Author for correspondence; E-mail: JJM1003@medschl.cam.ac.uk

upregulation of this subtype may occur in coronary artery disease (Bacon *et al*., 1996).

Preliminary data were presented to the British Pharmacological Society (Maquire & Davenport, 1997) and the Fifth International Conference on Endothelin (Maguire & Davenport, 1998).

Methods

Tissue collection

Graft saphenous veins and atherosclerotic coronary arteries were obtained from eight male patients (41–61 years old) transplanted for ischaemic heart disease. All patients received coronary artery bypass grafts (CABG) 2–13 years prior to cardiac transplantation with a mean 'age' of saphenous vein grafts of 6.5 ± 3.4 years ($n=8$). Coronary arteries were additionally obtained from 12 patients (11 male, 1 female; 42–59 years) transplanted for ischaemic heart disease or cardiomyopathies. Drug therapies included diuretics, antiarrhythmics, angiotensin converting enzyme inhibitors, anticoagulants, nitrates, beta blockers, calcium channel blockers and aspirin. Non-diseased 'control' saphenous veins were obtained from 26 patients (25 male, 1 female; 35–75 years) undergoing CABG surgery. Veins were collected following surgical distension.

Receptor autoradiography

ET receptor subtypes were detected autoradiographically as previously described (Davenport *et al*., 1988). Briefly, 10 μm cryostat-cut sections of saphenous vein graft and saphenous vein were thaw mounted on gelatine coated slides and preincubated in HEPES buffer (HEPES 50 mM containing $MgCl_2$ 5 mM and 0.3% w/v BSA, pH 7.4) for 30 min at room temperature (23°C). To visualize the ET receptor subtypes present in these tissues the wash buffer was replaced with HEPES buffer containing 0.1 nM [^{125}I]-ET-1, to label both receptor subtypes, 0.1 nM [^{125}I]-PD151242 (Davenport *et al*., 1994) to label ET_A receptors or 0.3 nM [^{125}I]-BQ3020 (Molenaar *et al*., 1992) to identify ET_B receptors. The concentration of each ligand used was calculated to bind to approximately 30% of the respective receptor populations identified, according to the dissociation constant of each radioligand. Non-specific binding was defined by the inclusion of 1 μM of the corresponding unlabelled peptide. After a 2 h incubation period the sections were washed in ice-cold Tris buffer (50 mM, pH 7.4) and apposed to radiation sensitive film (Hyperfilm βmax, Amersham Pharmacia Biotech., Buckinghamshire, U.K.) for 5 days. Data were analysed by computer-assisted image analysis (Quantimet 920, Cambridge Instruments) to determine relative optical densities (OD) (mean ± s.e.mean) for each receptor subtype.

In vitro *pharmacology*

Ring preparations (4 mm) were cut from lengths of saphenous vein graft, saphenous vein or atherosclerotic coronary artery. We were primarily interested in the medial smooth muscle ET receptors that mediate vasoconstriction and whether, or not, these were altered in disease. The endothelium was therefore removed, by gently rubbing the luminal surface with a metal seeker (verified histologically).

Blood vessel rings were transferred to 5 ml organ baths (Linton Instrumentation, Diss, Norfolk, U.K.) containing oxygenated Krebs solution (37°C), set up for isometric force recordings (F30 isometric force transducers, Hugo Sachs Electronik, March-Hugstetten, Germany) and allowed to equilibrate for 1 h. Responses were obtained to KCl (50 mM) at increasing levels of basal tension until no further increase in KCl response was observed. The rings were then allowed to re-equilibrate for 30 min. Cumulative concentration-response curves were constructed to ET-1, ET-3, sarafotoxin 6b (S6b), sarafotoxin 6c (S6c) and 5-hydroxytryptamine (5-HT), one curve per preparation. Experiments were terminated by the addition of KCl (50 mM) to determine the maximum possible contractile response in each case. Agonist responses were expressed as a percentage of this KCl maximum (%KCl). For the antagonist experiments ET-1 curves were determined in the absence (control) and presence of the ET_A-selective, non-peptide PD156707 (100 nM) (Doherty *et al*., 1995) which was added to the bathing medium 30 min prior to the ET-1. Values of EC_{50} were determined for each experiment from the graphs of agonist concentration ($\log_{10}$) plotted against response (%KCl). Data for each agonist were pooled from all experiments and finally expressed as the geometric mean with 95% confidence intervals (CI). The potency (estimated pK_b) of PD156707 was determined from the Gaddum-Schild equation assuming a regression slope of unity.

Mean EC_{50} values were compared using the Mann-Whitney *U*-test, all other data (expressed as arithmetic mean ± s.e.mean) were compared using Student's two-tailed *t*-test. The significance level was set at 95% ($P<0.05$).

Materials

ET-1, ET-3, sarafotoxin 6b and sarafotoxin 6c were purchased from the Peptide Institute Inc. (Osaka, Japan), prepared as 10^{-4} M stock solutions in 0.1% acetic acid and kept at −20°C until required. BQ3020 ([Ala^{11,15}]-Ac-ET-1$_{(6-21)}$ (Molenaar *et al*., 1992) and PD151242 ((N-[(hexahydro-1-azepinyl)carbonyl])L-Leu(1-Me)-D-Trp-D-Tyr) (Davenport *et al*., 1994) were synthesized by solid phase t-Boc chemistry. PD156707 (Doherty *et al*., 1995) was a gift from Park-Davis Pharmaceutical Research, Annarbor, MI, U.S.A. PD156707 was prepared as a 10^{-2} M solution in DMSO and stored at −20°C. Radiolabelled chemicals (specific activity 2000 Ci mmol^{-1}) were from Amersham Pharmacia Biotech. (Buckinghamshire, U.K.). All other chemicals and reagents were from Sigma-Aldrich Co. Ltd. (Dorset, U.K.) and were of analar grade or better.

Krebs solution was of the following composition (mM): NaCl, 89; $NaHCO_3$, 45; KCl, 5; $MgSO_4$, 0.5; NaH_2PO_4, 1; D-glucose, 10; $CaCl_2$, 2.25; EDTA, 40 μM; glutamic acid, 5 mM; fumaric acid 5 mM; sodium pyruvate, 5 mM (pH 7.4).

Results

Distribution of ET receptor subtypes in saphenous vein grafts

[^{125}I]-PD151242 identified a high density of ET_A receptors localized to the medial layer of the saphenous vein graft sections. Binding was also observed to vasa vasorum in the surrounding adventitia. These same regions expressed much lower levels of ET_B receptors, which were detected with [^{125}I]-BQ3020 (Figure 1). Neither receptor subtype was detected over the thickened intimal smooth muscle layer. At this resolution it was not possible to detect binding of either ligand to the single layer of endothelial cells lining the vessel lumen.

Relative densities of ET receptor subtypes in diseased and control saphenous veins

Measurements of medial optical density (OD) were taken from the developed autoradiograms of sections of control saphenous vein and diseased saphenous vein grafts. In control saphenous vein the mean OD value for specific binding of [^{125}I]-PD151242 was 0.43 ± 0.06 ($n=7$) and for [^{125}I]-BQ3020 was 0.13 ± 0.02 ($n=7$) giving a relative density of ET_A receptors to ET_B receptors of 77 : 23%. In diseased saphenous vein grafts the OD values were respectively 0.14 ± 0.01 ($n=6$) and 0.05 ± 0.02 ($n=6$) giving a ratio of ET_A:ET_B of 74 : 26%.

Contractile responses in diseased saphenous vein graft and coronary artery compared with control saphenous vein

Immediately prior to construction of the agonist concentration response curves the basal resting tension for saphenous vein grafts (1.57 ± 0.26 g weight, $n=8$) was significantly greater than that for control saphenous vein (0.87 ± 0.17 g weight, $n=16$) (Student's two-tailed t-test, $P<0.05$), but not different than that for diseased coronary arteries obtained from the same explanted hearts (1.75 ± 0.44 g weight, $n=7$).

Maximum responses to KCl (50 mM) were comparable in saphenous vein graft (2.97 ± 0.54 g weight, $n=8$) and atherosclerotic coronary artery (2.76 ± 0.32 g weight, $n=7$). The response to KCl in control saphenous vein tended to be lower (1.96 ± 0.43 g weight, $n=16$), although this did not reach statistical significance.

ET-1 was a more potent constrictor than 5-HT in all three blood vessels (Figure 2). The sensitivity of the saphenous vein graft to ET-1 was not different to that of the control saphenous vein, however, ten times more ET-1 was required to contract the atherosclerotic coronary artery than either of the saphenous vein preparations (Table 1). There was no difference in the maximum response to ET-1 in the control and graft saphenous veins expressed as a percentage of the response to KCl (50 mM), but these two were significantly greater than that for ET-1 in diseased coronary artery (Student's two-tailed t-test, $P<0.05$). (Table 1, Figure 2). Similar data were obtained with 5-HT. EC_{50} values and maximum responses in saphenous vein graft and control were not different but higher concentrations of this agonist were required to contract the coronary artery and the maximum response in this artery was significantly depressed compared to the vein preparations (Student's two-tailed t-test, $P<0.05$) (Figure 2).

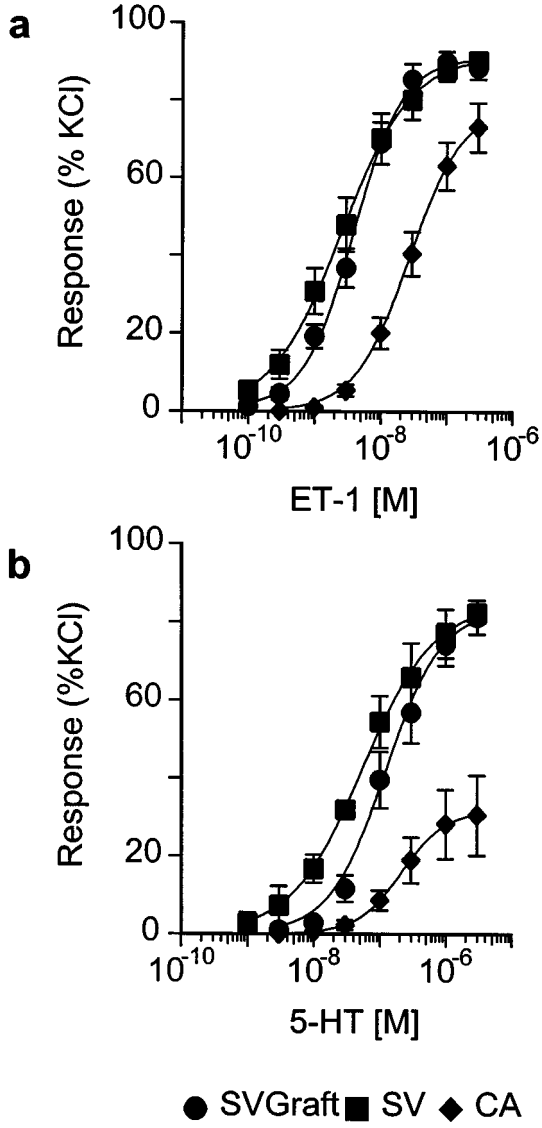

Figure 2 Cumulative concentration-response curves to (a) ET-1 and (b) 5-HT in saphenous vein graft (SVgraft), control saphenous vein (SV) and atherosclerotic coronary artery (CA). Agonist responses are expressed as a percentage of the maximal contraction to KCl (50 mM) and are the means ± s.e.mean ($n=3-15$).

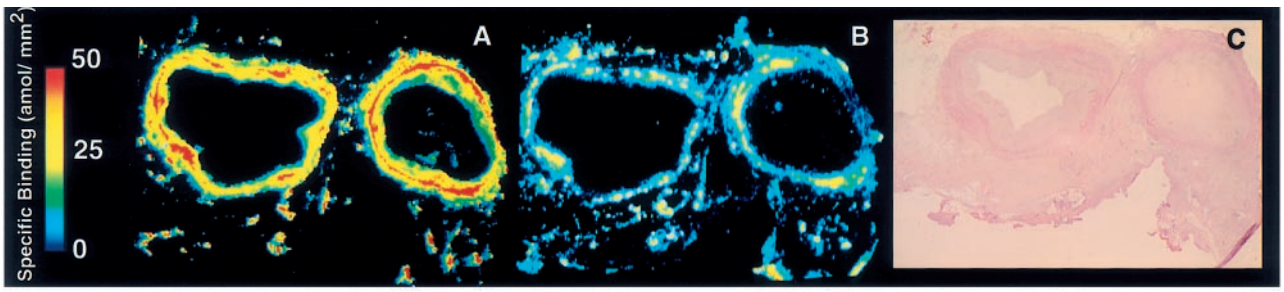

Figure 1 Colour-coded images of the distribution of ET receptors in transverse sections of two adjacent retrieved aortocoronary saphenous vein grafts. (A) Localization of specific ET_A binding with [^{125}I]-PD151242 (0.1 nM) and (B) specific ET_B binding with [^{125}I]-BQ3020 (0.3 nM). These images were computer generated by digitally subtracting the autoradiographic image of the non-specific binding, defined by inclusion of the respective unlabelled peptide (1 μM), from the total binding image for each radioligand. ^{125}I standards were co-exposed with the tissue sections and receptor density was colour-coded by interpolation from the resulting standards curve. (C) A section stained with haematoxylin and eosin. The graft on the left has a thickened intimal layer whilst the graft on the right is completely occluded.

Characterization of vasoconstrictor ET receptors

The relative potencies of the ET peptides and related compounds (Table 1) were used to determine the receptor subtypes responsible for vasoconstriction in atherosclerotic saphenous vein grafts and coronary arteries compared to non-diseased saphenous veins. In each of the three vessels ET-1 was more potent than ET-3. ET-1 was effective in the nanomolar range whilst the concentration-response curves to ET-3 were incomplete at 700 nM. Where tested, the non-selective endothelin agonist S6b was approximately four times less potent than ET-1 but elicited the same maximum response as ET-1. The responses obtained with the ET_B-selective agonist S6c were more variable. No response to S6c was obtained in any of the diseased coronary artery preparations investigated. In the saphenous vein graft and control saphenous vein responses to S6c were observed in 65 and 30% of vessels respectively. However where responses to S6c were elicited, although potent, the maximum response was less than 25% of that to ET-1 in the same vessel (Figure 3).

To further investigate the vasoconstrictor ET receptors in these blood vessels we determined the ability of an ET_A-selective antagonist, PD156707, to block the response to ET-1. In the presence of 100 nM PD156707 the concentration response curves to ET-1 were displaced to the right in saphenous vein graft, control saphenous vein and control coronary arteries which were obtained from patients other than those from whom the saphenous vein grafts were obtained and whom were diagnosed with either ischaemic heart disease or cardiomyopathy (Figure 4). The pK_b values for PD156707 were 8.05 ± 0.23 ($n=6$), 8.77 ± 0.29 ($n=5$) and 7.94 ± 0.13 ($n=7$) respectively, which are comparable to values reported for antagonism by this compound of ET_A receptors in animal vasculature (Reynolds *et al*., 1995). Importantly there was no evidence that any part of the ET-1 response was

Table 1. Potency of ET receptor agonists in *in vitro* preparations of saphenous vein (SV) graft, control saphenous vein and atherosclerotic coronary artery (CA)

	ET-1			*ET-3*		*S6b*			*S6c*		
	EC_{50} (nM)	R_{max} %KCl	n	EC_{50} (nM)	n	EC_{50} (nM)	R_{max} %KCl	n	EC_{50} (nM)	R_{max} %KCl	n
SV graft	4.5 (2.7–7.3)	90±2.8	8	>100	7	12.9 (5.7–29)	95±3.1	5	0.18 (0.002–14)	23±4.3	*4/6
SV control	2.9 (1.4–6.2)	88±2.9	15	>100	5	7.5 (5.1–11.2)	95±0.9	8	0.8 (0.6–1.0)	7.1±3.2	*2/7
CA	23.0 (12–46)	73±6.3	7	>100	3	N.D.			Inactive		4

EC_{50} (nM) values are expressed as the geometric mean (95% confidence intervals). R_{max} values are the maximum response to each agonist expressed as %KCl. R_{max} values are not given for ET-3 as concentration-response curves for this agonist were incomplete. *n* values are the number of patients from whom blood vessels were obtained. *Fraction of preparations which responded. N.D., Not determined.

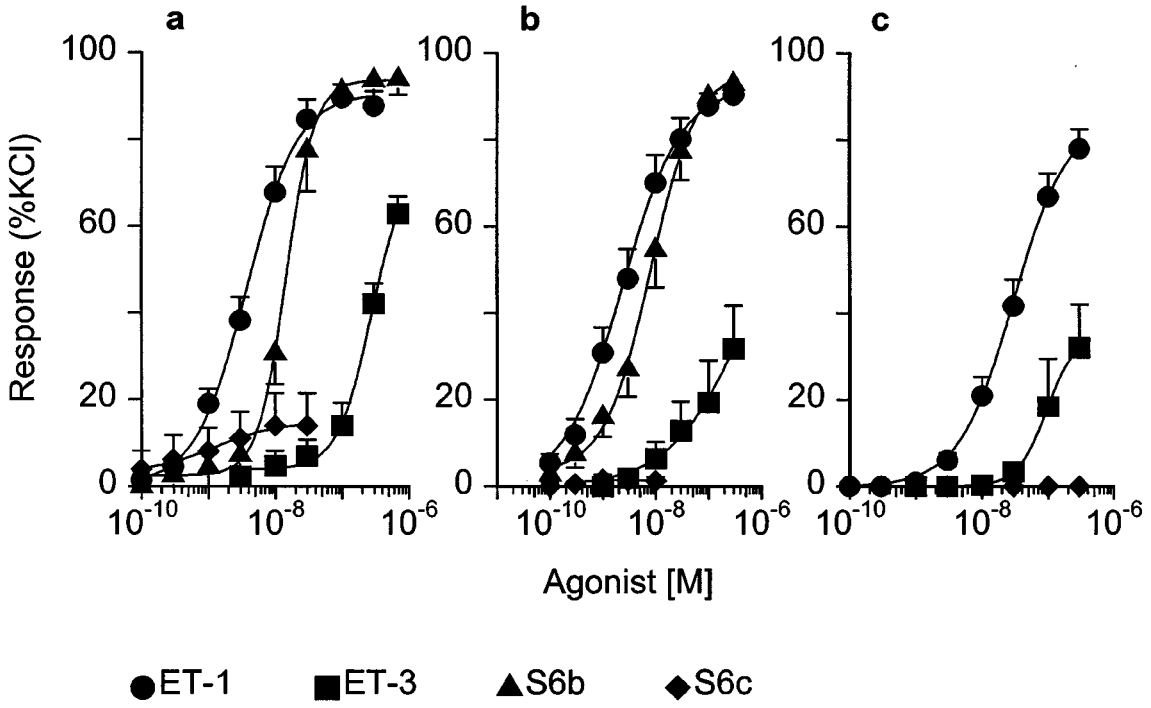

Figure 3 Cumulative concentration-response curves to ET receptor agonists in (a) saphenous vein graft, (b) control saphenous vein and (c) atherosclerotic coronary artery. Agonist responses are expressed as a percentage of the maximal contraction to KCl (50 mM) and are the means±s.e.mean ($n=3-15$).

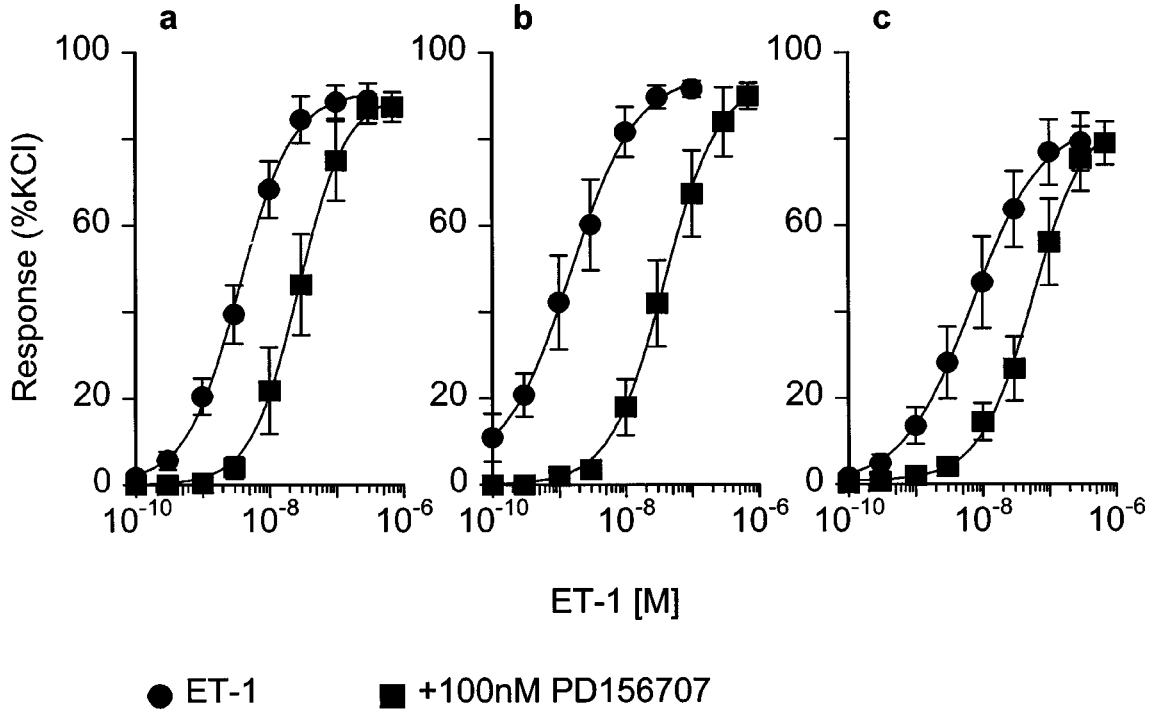

Figure 4 Antagonism of ET-1 by 100 nM PD156707 in (a) saphenous vein graft, (b) control saphenous vein and (c) control coronary artery. ET-1 responses are expressed as a percentage of the response to KCl (50 mM) and are the means ± s.e.mean ($n = 5–7$).

resistant to this antagonist in either the diseased or control tissues.

Potency of ET-1 with graft 'age'

The potency of ET-1 determined in each of the eight graft vein specimens was correlated (Pearson) against the number of years since bypass surgery (i.e. graft age). A negative correlation ($r = -0.82$, $P < 0.02$) was obtained with the sensitivity of saphenous vein graft increasing with the age of the graft (Figure 5).

Figure 5 Influence of graft age (years) on sensitivity of grafts from individual patients ($n = 8$) to ET-1 (EC_{50} nM). A significant correlation (Pearson; $r = -0.82$; $P < 0.02$) was obtained.

Discussion

Autoradiographical visualization of ET receptor subtypes in sections of human saphenous vein graft graphically demonstrated the presence of ET receptors over the medial smooth muscle layer and the absence (or very low expression) of receptors over the thickened intimal smooth muscle layer. In the media there was no change in the relative density of the two receptor subtypes in diseased graft saphenous vein compared to control vessels. This was consistent with findings in the atherosclerotic human coronary artery (Bacon *et al.*, 1996; Russell *et al.*, 1997) which showed no evidence for up-regulation of smooth muscle ET_B receptors in disease. In a rabbit model, both ET_B mRNA and S6c-mediated contractile responses were actually reduced in saphenous vein grafts compared to native veins (Eguchi *et al.*, 1997). Our data were from grafts that had failed after a number of years, however, alterations in receptor expression in the earlier stages of the disease process may have contributed to earlier graft failure. Such temporal receptor alterations have been noted in the arteries of rats in which proliferation has been initiated by balloon catheterization. An increase in receptor message and protein was observed over a few days and returned towards normal levels after a matter of weeks (Wang *et al.*, 1996; Viswanathan *et al.*, 1997).

Whilst we found no difference in the ratio of the two subtypes in control and graft saphenous vein this did not preclude functional alterations in agonist efficacy. However, characterization of the ET receptors responsible for vasoconstriction in saphenous vein graft clearly showed that the ET peptides mediate their effects through the ET_A receptor. There was, therefore, no change in agonist activity profile observed in graft saphenous vein compared to the control saphenous vein. Thus, as determined by the autoradiographical data, no up-regulation of the ET_B constrictor response was observed. The agonist data was confirmed using an ET_A receptor antagonist,

PD156707, which we had previously shown to exhibit high selectivity and affinity for human ET_A receptors (Maguire *et al*., 1997). PD156707 blocked the response to ET-1 in all three blood vessels with the estimated pK_b values in the range expected for the antagonism of the ET_A subtype.

We did not find ET receptors on proliferated smooth muscle cells of the intima of either saphenous vein graft or atherosclerotic coronary artery (Bacon *et al*., 1996). If migrating and proliferating medial smooth muscle cells, under the influence of locally derived factors, form the thickened intimal layer then apparently down regulation of ET receptor expression has occurred. In some investigations, ET_A receptor antagonists have been shown to reduce or prevent vascular smooth muscle cell proliferation both *in vitro* (Alberts *et al*., 1994; Kanse *et al*., 1995; Zamora *et al*., 1996) and *in vivo* (Ferrer *et al*., 1995; Chen *et al*., 1997). Thus proliferation is driven by activation of the ET_A receptor. Why smooth muscle cells, which are thought to have undergone this process, should then lose the receptors that are responsible is not clear. One possibility is that released ET-1, which is increased in proliferating smooth muscle cells both in culture (Haug *et al*., 1996) or in tissue from atherosclerotic human blood vessels (Zeiher *et al*., 1995; Bacon *et al*., 1996; Brody *et al*., 1996) may bind to adjacent receptors in the intima and effectively mask their presence. However this is unlikely as in the media of mammary arteries from hypertensives high, homogenous levels of ET_A receptor mRNA were identified, but in the thickened intima levels of mRNA were very low (Hasegawa *et al*., 1994). An alternative hypothesis is that as these cells change from the contractile phenotype to the synthetic phenotype (Campbell *et al*., 1988) receptors involved in vasoconstriction become redundant and are down-regulated. Indeed this has been demonstrated in rabbit aortic vascular smooth muscle cells that express ET_A receptors. Subcultures of these smooth muscle cells show an alteration in phenotype which changes from contractile to synthetic and this is associated with a 10 fold reduction in the density of [^{125}I]-ET-1 binding sites (Seradeil-Le Gal *et al*., 1991).

We found a tendency for the contractile response to a maximum concentration of KCl (50 mM) to be greater in the diseased saphenous vein and coronary artery than in the control saphenous vein. Adaptive changes would be expected in the wall structure and dynamics of saphenous vein that is grafted into the higher pressure arterial system. However it is clear from histological analyses that this does not represent true morphological arterialization, rather fibrotic thickening of the media combined with smooth muscle proliferation and extracellular connective tissue deposition of the intima (Bulkley & Hutchins, 1977; Lie *et al*., 1977; Atkinson *et al*., 1985). In contrast there did not appear to be any alteration in the maximum response to either ET-1 or 5-HT in diseased compared to non-diseased saphenous vein. This might be expected, at least for ET-1, as we have shown that the proliferated smooth muscle cells of the thickened intima in saphenous vein grafts do not have detectable ET receptors and therefore would not contribute to vasoconstriction. A similar observation has previously been made by O'Neil and colleagues (1994) who reported no significant difference between the maximum responses to ET-1 (as %KCl) in short (<1 year) and long (8–11 years) term saphenous vein grafts and control saphenous veins harvested following surgical distension. It was only when ET-1 responses were compared in control saphenous veins harvested before distension that a significant reduction in ET-1 maximum response was observed in graft vessels. In the present investigation distended veins were used as the control, as it is in this condition that they are grafted into the coronary circulation. The maximum for ET-1 and 5-HT were significantly lower in coronary artery compared to both of the saphenous vein groups. This may be due to differences in receptor density or coupling efficiency for transmitters in human arteries compared to veins.

We found that the control saphenous vein was more sensitive than the diseased coronary artery to both ET-1 and 5-HT and that this sensitivity was retained by the thickened saphenous vein graft. Thus saphenous veins grafted into the coronary vasculature are particularly vulnerable to the constricting effects of circulating and locally released vasoconstrictor mediators. Increased concentrations of ET have been measured not only in the plasma of patients with coronary artery disease (Yasuda *et al*., 1990; Lerman *et al*., 1991), but also within atheromatous plaques (Zeiher *et al*., 1995; Bacon *et al*., 1996). Additionally there are further transient increases of plasma ET-1 during cardiopulmonary bypass (Hynynen *et al*., 1992; Rammos *et al*., 1996). Increased ET-1 levels may result in direct constriction of the venous smooth muscle, or may potentiate the constricting effects of other mediators such as 5-HT (Chester *et al*., 1992). Interestingly we found that the sensitivity of the vein to ET-1 positively correlated with the time that had lapsed since grafting.

Our findings that the ET_A receptor is responsible for the profound vasoconstrictor responses of the aortocoronary saphenous vein graft to ET-1 both at the time of operation and in the late stages of disease has implications for the use of antagonists selective for this subtype in the management of patients. At present, during the harvesting and preparation of the saphenous vein, directly acting vasodilators such as papaverine, sodium nitroprusside and nifedipine are used to prevent or reduce spasm and thus maintain endothelial integrity (LoGerfo *et al*., 1984; Roubos *et al*., 1995). If ET does contribute substantially to spasm then these drugs may not be completely effective. Calcium channel antagonists such as nifedipine are only partially effective in blocking vasoconstrictor effects of ET-1 (Stork & Cocks, 1994) as this agonist mobilizes intracellular calcium stores in addition to stimulating extracellular calcium influx (Ushio-Fukai *et al*., 1995). It has also been suggested that, *in vitro*, contractions to ET-1 are not fully reversed by sodium nitroprusside in vein grafts, whereas they are in arterial graft vessels such as mammary artery and gastroepiploic artery (Uydes-Dogan *et al*., 1996). ET_A antagonism might, therefore, prove more effective for the prevention of perioperative graft vasospasm than currently available therapies. In the long term, the vein grafts are particularly vulnerable to the increased local production of ET-1 in coronary artery disease. This may lead to constriction of the graft that, if superimposed on a thickened intima or atherosclerotic plaque, will reduce the already narrowed lumen, further compromising blood flow to the myocardium. If in addition to blocking the unwanted vasoconstrictor effect of ET-1, the efficacy of ET_A antagonists to prevent intimal hyperplasia of human blood vessels can also be demonstrated, then this class of compounds may also become invaluable in increasing the long term patency of the saphenous vein graft.

We would like to thank Rhoda Kuc for her excellent technical assistance. We are grateful to Jean Chadderton and the theatre and consultant staff of Papworth Hospital, Cambridgeshire, U.K. Supported by grants from the British Heart Foundation, Isaac Newton Trust and Royal Society.

References

AKAR, F., UYDES, B.S., AYRANCIOGLU, K., YENER, A., ASLAMACI, S., ARSAN, M., TÖRÜNER, A. & KANZIK, I. (1994). Endothelial function of human gastroepiploic artery in comparison with saphenous vein. *Cardiovasc. Res.,* **28,** 500–504.

ALBERTS, G.F., PEIFLEY, K.A., JOHNS, A., KLEHA, J.F. & WINKLES, J.A. (1994). Constitutive endothelin-1 overexpression promotes smooth muscle cell proliferation via an external autocrine loop. *J. Biol. Chem.,* **269,** 10112–10118.

ATKINSON, J.B., FORMAN, M.B., VAUGHN, W.K., ROBINOWITZ, M., MCALLISTER, H.A. & VIRMANI, R. (1985). Morphologic changes in long term saphenous vein bypass grafts. *Chest,* **88,** 341–348.

BACON, C.R., CARY, N.R.B. & DAVENPORT, A.P. (1996). Endothelin peptide and receptors in human atherosclerotic coronary artery and aorta. *Circ. Res.,* **79,** 794–801.

BATTISTINI, B., CHAILLER, P., D'ORLÉANS-JUSTE, P., BRIÈRE, N. & SIROIS, P. (1993). Growth regulatory properties of endothelins. *Peptides,* **14,** 385–399.

BAX, W.A., BOS, E. & SAXENA, P.R. (1993). Heterogeneity of endothelin/sarafotoxin receptors mediating contraction of the human isolated saphenous vein. *Eur. J. Pharmacol.,* **239,** 267–268.

BOURASSA, M.G., CAMPEAU, L., LESPÉRANCE, J. & GRONDIN, C.M. (1982). Changes in grafts and coronary arteries after saphenous vein aortocoronary bypass surgery: results at repeat angiography. *Circulation,* **65,** (Suppl II): 90–97.

BRODY, J.I, CAPUZZI, D.M. & FINK, G.B. (1996). In situ endothelin in coronary artery disease. *Angiology,* **47,** 1027–1032.

BULKLEY, B.H. & HUTCHINS, G.M. (1977). Accelerated 'atherosclerosis': A morphologic study of 97 saphenous vein coronary artery bypass grafts. *Circulation,* **55,** 163–169.

CAMPBELL, G.R., CAMPBELL, J.H., MANDERSON, J.A., HORRIGAN, S. & RENNICK, R.E. (1988). Arterial smooth muscle. A multifunctional mesenchymal cell. *Arch. Pathol. Lab. Med.,* **112,** 977–986.

CAMPEAU, L., ENJALBERT, M., LESPÉRANCE, J., VAISLIC, C., GRONDIN, C.M. & BOURASSA, M.G. (1983). Atherosclerosis and late closure of aortocoronary saphenous vein grafts: sequential angiographic studies at 2 weeks, 1 year, 5 to 7 years, and 10 to 12 years after surgery. *Circulation,* **68,** 1–7.

CHEN, S.J., CHEN, Y.F., OPGENORTH, T.J., WESSALE, J.L., MENG, Q.C., DURAND, J., DICARLO, V.S. & OPARIL, S. (1997). The orally active nonpeptide endothelin-A receptor antagonist A-127722 prevents and reverses hypoxia-induced pulmonary hypertension and pulmonary vascular remodelling in Sprague-Dawley rats. *J. Cardiovasc.,* **29,** 713–725.

CHESEBRO, J.H., CLEMENTS, I.P., FUSTER, V., ELVEBACK, L.R., SMITH, H.C., BARDSLEY, W.T., FRYE, R.L., HOLMES, D.R., VLIETSTRA, R.E., PLUTH, J.R., WALLACE, R.B., PUGA, F.J., ORSZULAK, T.A., PIEHLER, J.M., SCHAFF, H.V. & DANIELSON, G.K. (1982). A platelet-inhibitor-drug trial in coronary-artery bypass operations: Benefit of perioperative dipyridamole and aspirin therapy on early postoperative vein-graft patency. *N. Engl. J. Med.,* **307,** 73–78.

CHESTER, A.H., O'NEIL, G.S., ALLEN, S.P., LUU, T.N., TADJKARIMI, S. & YACOUB, M.H. (1992). Effect of endothelin on normal and diseased human coronary arteries. *Eur. J. Clin. Invest.,* **22,** 210–213.

COSTELLO, K.B., STEWART, D.J. & BAFFOUR, R. (1990). Endothelin is a potent constrictor of human vessels used in coronary revascularization surgery. *Eur. J. Pharmacol.,* **186,** 311–314.

DAVENPORT, A.P., BERESFORD, I.J.M., HALL, M.D., HILL, R.G. & HUGHES, J. (1988). Quantitative autoradiography. In *Molecular Neuroanatomy*, vol III, ed. van Leeuwen, F.W., Buijs, R.M., Pool, C.W., Pach, O. pp. 121–145. Amsterdam: Elsevier.

DAVENPORT, A.P., KUC, R.E., FITZGERALD, F., MAGUIRE, J.J., BERRYMAN, K. & DOHERTY, A.M. (1994). [^{125}I]PD151242: a selective radioligand for human ET_A receptors. *Br. J. Pharmacol.,* **111,** 4–6.

DAVENPORT, A.P., O'REILLY, G. & KUC, R.E. (1995). Endothelin ET_A and ET_B mRNA and receptors expressed by smooth muscle in the human vasculature: majority of the ET_A sub-type. *Br. J. Pharmacol.,* **114,** 1110–1116

DOHERTY, A.M., PATT, W.C., EDMUNDS, J.J., BERRYMAN, K.A., REISDORPH, B.R., PLUMMER, M.S., SHAHRIPOUR, A., LEE, C., CHENG, X.-M., WALKER, D.M., HALEEN, S.J., KEISER, J.A., FLYNN, M.A., WELCH, K.M., HALLAK, H., TAYLOR, D.G. & REYNOLDS, E.E. (1995). Discovery of a novel series of orally active non-peptide endothelin-A (ET_A) receptor-selective antagonists. *J. Med. Chem.,* **38,** 1259–1263.

EGUCHI, D., NISHIMURA, J., KOBAYASHI, S., KOMORI, K., SUGIMACHI, K. & KANAIDE, H. (1997). Down-regulation of endothelin B receptors in autogenous saphenous veins grafted into the arterial circulation. *Cardiovasc. Res.,* **35,** 360–367.

FERRER, P., VALENTINE, M., JENKINSWEST, T., WEBER, H., GOLLER, N.L., DURHAM, S.K., MOLLOY, C.J. & MORELAND, S. (1995). Orally-active endothelin antagonist BMS-182874 suppresses neointimal development in balloon-injured rat carotid arteries. *J. Cardiovasc. Pharmacol.,* **26,** 908–915.

FUSTER, V. & CHESEBRO, J.H. (1986). Role of platelets and platelet inhibitors in aortocoronary vein-graft disease. *Circulation,* **73,** 227–232.

GOLDMAN, S., COPELAND, J., MORITZ, T., HENDERSON, W., ZADINA, K., OVITT, T., DOHERTY, J., READ, R., CHESLER E., SAKO, Y., LANCASTER, L., EMERY, R., SHARMA, G.V.R.K., JOSA, M., PACOLD, I., MONTOYA, A., PARIKH, D., SETHI, G., HOLT, J., KIRKLIN, J., SHABETAI, R., MOORES, W., ALDRIDGE, J., MASUD, Z., DEMOTS, H., FLOTEN, S., HAAKENSON, C. & HARKER, L.A. (1988). Improvement in early saphenous vein graft patency after coronary artery bypass surgery with antiplatelet therapy: Results of a Veterans Administration Cooperative Study. *Circulation,* **77,** 1324–1332.

HASEGAWA, K., FUJIWARA, H., DOYAMA, K., INADA, T., OHTANI, S., FUJIWARA, T., HOSODA, K., NAKAO, K. & SASAYAMA, S. (1994). Endothelin-1-selective receptor in the arterial intima of patients with hypertension. *Hypertension,* **23,** 288–293.

HAUG, C., VOISARD, R., LENICH, A., BAUR, R., HÖHER, M., OSTERHUES, H., HANNEKUM, A., VOGEL, U., MATTFELDT, T., HOMBACH, V. & GRÜNERT, A. (1996). Increased endothelin release by cultured human smooth muscle cells from atherosclerotic coronary arteries. *Cardiovasc. Res.,* **31,** 807–813.

HYNYNEN, M., SAIJONMAA, O., TIKKANEN, I., HEINONEN, J. & FYHRQUIST, F. (1992). Increased plasma endothelin immunoreactivity during cardiopulmonary bypass: A preliminary observation. *J. Thoracic Cardiovasc. Surg.,* **103,** 1024–1025.

IVERT, T., HUTTUNEN, K., LANDOU, C. & BJÖRK, V.O. (1988). Angiographic studies of internal mammary artery grafts 11 years after coronary artery bypass grafting. *J. Thoracic Cardiovasc. Surg.,* **96,** 1–12.

KANSE, S.M., WIJELATH, E., KANTHOU, C., NEWMAN, P. & KAKKAR, V.V. (1995). The proliferative responsiveness of human vascular smooth-muscle cells to endothelin correlates with endothelin receptor density. *Lab. Invest.,* **72,** 376–382.

LERMAN, A., EDWARDS, B.S., HALLETT, J.W., HEUBLEIN, D.M., SANDBERG, S.M. & BURNETT, JR J.C. (1991). Circulating and tissue endothelin immunoreactivity in advanced atherosclerosis. *New. Engl. J. Med.,* **325,** 997–1001.

LIE, J.T., LAWRIE, G.M. & MORRIS, G.C. (1977). Aortocoronary bypass saphenous vein graft atherosclerosis. *Am. J. Cardiology,* **40,** 907–914.

LOGERFO, F.W., HAUDENSCHILD, C.D. & QUIST, W.C. (1984). A clinical technique for prevention of spasm and preservation of endothelium in saphenous vein grafts. *Arch. Surg.,* **119,** 1212–1214.

LÜSCHER, T.F., YANG, Z., TSCHUDI, M., VON SEGESSER, L., STULZ, P., BOULANGER, C., SIBENMANN, R., TURINA, M. & BÜHLER, F.R. (1990). Interaction between endothelin-1 and endothelium-derived relaxing factor in human arteries and veins. *Circ. Res.,* **66,** 1088–1094.

MAGUIRE, J.J. & DAVENPORT, A.P. (1995). ET_A receptor-mediated constrictor responses to endothelin peptides in human blood vessels *in vitro*. *Br. J. Pharmacol.,* **115,** 191–197.

MAGUIRE, J.J. & DAVENPORT, A.P. (1997). Endothelin (ET) receptor pharmacology in human saphenous vein grafts. *The Pharmacologist,* **39,** 78.

.

MAGUIRE, J.J. & DAVENPORT, A.P. (1998). PD156707: A potent antagonist of endothelin-1 in human diseased coronary arteries and vein grafts. *J. Cardiovasc. Pharmacol.,* **31,** (Suppl 1): S239–S240.

MAGUIRE, J.J., KUC, R.E. & DAVENPORT, A.P. (1997). Affinity and selectivity of PD156707, a novel nonpeptide endothelin antagonist, for human ET_A and ET_B receptors. *J. Pharmacol. Exp. Therap.,* **280,** 1102–1108.

MASOOD, I., PORTER, K.E., LONDON, N.M.J. & PRINGLE, J.H. (1996). Endothelin-1 expression in vein graft stenosis. *J. Vasc. Surg.,* **24,** 901–902.

MOLENAAR, P., KUC, R.E, & DAVENPORT, A.P. (1992). Characterization of two new ET_B selective radioligands, [^{125}I]-BQ3020 and [^{125}I]-[Ala^{1,3,11,15}]ET-1 in human heart. *Br. J. Pharmacol.,* **107,** 637–639.

O'NEIL, G.S., CHESTER, A.D., SCHYNS, C.J., TADJKARIMI, S., BORLAND, J.A.A. & YACOUB, M.H. (1994). Effect of surgical preparation and arterialization on vasomotion of human saphenous vein. *J. Thoracic Cardiovasc. Surg.,* **107,** 699–706.

RAMMOS, K.ST., KOULLIAS, G.J., HATZIBOUGIAS, J.D., ARGYRAKIS, N.P. & PANAGOPOULOS, P.G. (1996). Plasma endothelin-1 levels in adult patients undergoing coronary revascularization. *Cardiovasc. Surg.,* **4,** 808–812.

REYNOLDS, E.E., KEISER, J.A., HALEEN, S.J., WALKER, D.M., OLSZEWSKI, B., SCHROEDER, R.L., TAYLOR, D.G., HWANG, O., WELCH, K.M., FLYNN, M.A., THOMPSON, D.M., EDMUNDS, J.J., BERRYMAN, K.A., PLUMMER, M., CHENG, X.-M., PATT, W.C. & DOHERTY, A.M. (1995). Pharmacological characterization of PD156707, an orally active ET_A receptor antagonist. *J. Pharmacol. Exp. Ther.,* **273,** 1410–1417.

ROSSITER, S.J., BRODY, W.R., KOSEK, J.C., LIPTON, M.J. & ANGELL, W.W. (1974). Internal mammary artery versus autogenous vein for coronary bypass graft. *Circulation,* **50,** 1236–1243.

ROUBOS, N., ROSENFELDT, F.L., RICHARDS, S.M., CONYERS, R.A.J. & DAVIS, B.B. (1995). Improved preservation of saphenous vein grafts by the use of glyceryl trinitrate-verapamil solution during harvesting. *Circulation,* **92,** (Suppl II): 31–36.

RUSSELL, F.D., SKEPPER, J.N. & DAVENPORT, A.P. (1997). Detection of endothelin receptors in human coronary artery vascular smooth muscle cells but not endothelial cells by using electron microscope autoradiography. *J. Cardiovasc. Pharmacol.,* **29,** 820–826.

SERRADEIL-LE GAL, C., HERBERT, J.M., GARCIA, C., BOUTIN, M. & MAFFRAND, J.P. (1991). Importance of the phenotypic state of vascular smooth muscle cells on the binding and the mitogenic activity of endothelin. *Peptides,* **12,** 575–579.

STORK, A.P. & COCKS, T.M. (1994). Pharmacological reactivity of human epicardial coronary arteries: phasic and tonic responses to vasoconstrictor agents differentiated by nifedipine. *Br. J. Pharmacol.,* **113,** 1093–1098.

USHIO-FUKAI, M., NISHIMURA, J., KOBAYASHI, S. & KANAIDE, H. (1995). Endothelin-1 and endothelin-3 regulate differently vasoconstrictor responses of smooth muscle of the porcine coronary artery. *Br. J. Pharmacol.,* **114,** 171–179.

UYDES-DOGAN, B.S., NEBIGIL, M., S-ALSAMACI, M.D., ONUK, E., KANZIK, L. & AKBAR, F. (1996). The comparison of vascular reactivities of arterial and venous grafts to vasodilators: management of graft spasm. *Int. J. Cardiol.,* **53,** 137–145.

VICTOR, M.F., KIMBIRIS, D., ISKANDRIAN, A.S., MINTZ, G.S., BEMIS, C.E., PROCACCI, P.M. & SEGAL, B.L. (1981). Spasm of a saphenous vein bypass graft. *Chest,* **80,** 413–415.

VISWANATHAN, M., DE OLIVEIRA, A.M., JOHREN, O & SAAVEDRA, J.M. (1997). Increased endothelin ET(A) receptor expression in rat carotid arteries after balloon injury. *Peptides,* **18,** 247–255.

WANG, X., DOUGLAS, S.A., LOUDEN, C., VICKERY-CLARK, L.M., FEUERSTEIN, G.Z. & OLSTEIN, E.H. (1996). Expression of endothelin-1, endothelin-3, endothelin-converting enzyme, and endothelin-A and endothelin-B receptor mRNA after angioplasty-induced neointimal formation in the rat. *Circ. Res.,* **78,** 322–328.

WHITE, D.G., GARRATT, H., MUNDIN, J.W., SUMNER, M.J., VALLANCE, P.J. & WATTS, I.S. (1994). Human saphenous vein contains both endothelin ET_A and ET_B contractile receptors. *Eur. J. Pharmacol.,* **257,** 307–310.

YASUDA, M., KOHNO, M., TAHARA, A., ITIGANE, H., TODA, I., AKIOKA, K., TERAGAKI, M., OKU, H., TAKEUCHI, K. & TAKEDA, T. (1990). Circulating immunoreactive endothelin in ischaemic heart disease. *Am. Heart J.,* **119,** 801–806.

ZAMORA, M.R., STELZNER, T.J., WEBB, S., PANOS, R.J., RUFF, L.J. & DEMPSEY, E.C. (1996). Overexpression of endothelin-1 and enhanced growth of pulmonary artery smooth muscle cells from fawn-hooded rats. *Am. J. Physiol.,* **14,** L101–L109.

ZEIHER, A.M., GOEBEL, H., SCHÄCHINGER, V. & IHLING, C. (1995). Tissue endothelin-1 immunoreactivity in the active coronary atherosclerotic plaque. *Circulation,* **91,** 941–947.

(Received June 4, 1998
Revised September 24, 1998
Accepted November 3, 1998)

British Journal of Pharmacology (1999) 126, 451–456
http://www.stockton-press.co.uk/bjp

Absence of G-protein activation by μ-opioid receptor agonists in the spinal cord of μ-opioid receptor knockout mice

[1]Minoru Narita, [1]Hirokazu Mizoguchi, [1]Michiko Narita, [2]Ichiro Sora, [2,3]George R. Uhl & *,[1]Leon F. Tseng

[1]Department of Anesthesiology, Medical College of Wisconsin, Milwaukee, Wisconsin 53226, U.S.A.; [2]Molecular Neurobiology Branch, Intramural Research Program, National Institute on Drug Abuse, National Institutes of Health, Baltimore, Maryland 21224, U.S.A.; and [3]Department of Neurology and Neuroscience, Johns Hopkins University School of Medicine, Maryland 21224, U.S.A.

1 The ability of μ-opioid receptor agonists to activate G-proteins in the spinal cord of μ-opioid receptor knockout mice was examined by monitoring the binding to membranes of the non-hydrolyzable analogue of GTP, guanosine-5′-*O*-(3-[^{35}S]thio)triphosphate ([^{35}S]GTPγS).

2 In the receptor binding study, Scatchard analysis of [^{3}H][D-Ala^{2},NHPhe^{4},Gly-ol]enkephalin ([^{3}H]DAMGO; μ-opioid receptor ligand) binding revealed that the heterozygous μ-knockout mice displayed approximately 40% reduction in the number of μ-receptors as compared to the wild-type mice. The homozygous μ-knockout mice showed no detectable μ-binding sites.

3 The newly isolated μ-opioid peptides endomorphin-1 and -2, the synthetic selective μ-opioid receptor agonist DAMGO and the prototype of μ-opioid receptor agonist morphine each produced concentration-dependent increases in [^{35}S]GTPγS binding in wild-type mice. This stimulation was reduced by 55–70% of the wild-type level in heterozygous, and virtually eliminated in homozygous knockout mice.

4 No differences in the [^{35}S]GTPγS binding stimulated by specific δ_1- ([D-Pen^{2,5}]enkephalin), δ_2- ([D-Ala^{2}]deltorphin II) or κ_1- (U50,488H) opioid receptor agonists were noted in mice of any of the three genotypes.

5 The data clearly indicate that μ-opioid receptor gene products play a key role in G-protein activation by endomorphins, DAMGO and morphine in the mouse spinal cord. They support the idea that μ-opioid receptor densities could be rate-limiting steps in the G-protein activation by μ-opioid receptor agonists in the spinal cord. These thus indicate a limited physiological μ-receptor reserve. Furthermore, little change in δ_1-, δ_2- or κ_1-opioid receptor-G-protein complex appears to accompany μ-opioid receptor gene deletions in this region.

Keywords: knockout mice; endomorphins; G-proteins; homologous recombination; opioid peptides; μ-opioid receptors; signal transduction; spinal cord

Abbreviations: DAMGO, [D-Ala^{2},NHPhe^{4},Gly-ol]enkephalin; DPDPE, [D-Pen^{2,5}]enkephalin; GDP, guanosine-5′-*O*-(2-thio)-diphosphate; GTPγS, guanylyl-5′-*O*-(γ-thio)-triphosphate; U50,488H, trans(±)-3,4-dichloro-*N*-methyl-*N*-[2-(1-pyrrolidinyl)-cyclohexyl]; benzeneacetamide

Introduction

The μ-opioid receptor is expressed by neurons in several central nervous system regions, including the spinal cord dorsal horn. Its occupancy with agonist drugs such as morphine and agonist peptides produces many of the effects of opiate drugs, including much of the profound analgesic response attributed to the receptors localized in the spinal cord. Many synthetic opioids and derivatives of opium have reasonably-good affinities and selectivities for this receptor. Morphine and [D-Ala^{2},NHPhe^{4},Gly-ol]enkephalin (DAMGO) are useful ligands for probing μ-opioid receptor function. However, selective endogenous ligands for this receptor had not been clearly defined until recent successes of Zadina and colleagues (1997) who isolated two high-affinity μ-opioid receptor selective peptides ligands, endomorphin-1 (Tyr-Pro-Trp-Phe-NH_2) and -2 (Tyr-Pro-Phe-Phe-NH_2), from mammalian brain.

Recent cloning and expression studies have revealed that the μ-opioid receptor, and the related δ- and κ-opioid receptors are seven-transmembrane domain receptors whose actions are mediated through activation of heterotrimeric guanine nucleotide binding proteins (G-proteins) of several classes, including Gi- and Go-proteins (Chen *et al*., 1993; Law, 1995). The activation of G-proteins by the μ-opioid receptor can be measured by assessing agonist stimulation of membrane binding of the non-hydrolyzable analogue of GTP, guanosine-5′-*O*-(3-[^{35}S]thio)triphosphate ([^{35}S]GTPγS) (Traynor & Nahorski, 1995; Sim *et al*., 1995, 1996; Selley *et al*., 1997; Shimohira *et al*., 1997; Narita & Tseng, 1998). [^{35}S]GTPγS addition results in accumulation of a stable Gα-[^{35}S]GTPγS complex in brain membranes. It has been recently reported that endomorphins increased [^{35}S]GTPγS binding in rat brain (Sim *et al*., 1998), mouse spinal cord (Narita *et al*., 1998), SH-SY5Y human neuroblastoma cells (Harrison *et al*., 1998) and C_6 rat glioma cells stably expressing a cloned rat μ receptor (Alt *et al*., 1998). μ-Opioid agonist-stimulated [^{35}S]GTPγS binding in isolated membranes thus provide a functional measurement of agonist occupation of μ-opioid receptors and its efficacy in leading to activation of G-proteins.

Knockout mice with μ-opioid receptor gene deletions have been successfully developed by homologous recombination

*Author for correspondence at: Medical College of Wisconsin, Department of Anesthesiology, Medical Education Building – Room 462c, 8701 Watertown Plank Road, Milwaukee, WI 53226, U.S.A.

(Matthes *et al*., 1996; Sora *et al*., 1997b). These mice display profound gene-dose-dependent reductions in morphine analgesia in tests including tests of 'spinal' analgesia. The availability of transgenic μ-opioid receptor knockout mice allows us to determine the extent to which the μ-opioid receptor gene products are necessary for the expression of physiological actions by these newly discovered opioid peptides and alkaloids, including G-protein activation. The present study was thus designed to investigate the effects of μ-opioid receptor agonists including newly isolated opioid peptides endomorphin-1 and -2 on [^{35}S]GTPγS binding to spinal cord membranes obtained from mice expressing normal (wild-type), half-normal (heterozygous), and absent (homozygous) μ-opioid receptor complements. We discuss the data in light of the concepts of receptor reserve for μ-opioid receptors and the possible compensatory changes in the functions of other opioid receptor types in the presence of μ-opioid receptor gene deletions in this region.

Methods

Animals

μ-Opioid receptor knockout transgenic mice were maintained on C57BL/6 and 129Sv mixed genetic backgrounds as described (Sora *et al*., 1997a,b). Animals were housed five per cage in a room maintained at 22±0.5°C with an alternating 12 h light-dark cycle. Food and water were available *ad libitum*.

Membrane preparation

The spinal cord was removed from wild-type, and heterozygous and homozygous μ-opioid receptor knockout mice after decapitation. The spinal cord was homogenized in 20 volumes of ice-cold Tris buffer containing Tris-HCl (pH 7.4) (50 mM) for the μ-opioid receptor binding assay or ice-cold Tris-Mg^{2+} buffer containing Tris-HCl (pH 7.4) 50 mM, $MgCl_2$ 5 mM, and EGTA 1 mM for the [^{35}S]GTPγS binding assay. The homogenate was centrifuged at 48,000×*g* at 4°C for 10 min. The pellets were resuspended in Tris buffer or [^{35}S]GTPγS binding assay buffer containing Tris-HCl (pH 7.4) 50 mM, $MgCl_2$ 5 mM, EGTA 1 mM, and NaCl 100 mM and recentrifuged at 48,000×*g* at 4°C for 10 min. The final pellets were resuspended in each assay buffer and stored at −70°C until experiments.

μ-Opioid receptor binding assay

The μ-opioid receptor binding assays were carried out in duplicate with [tyrosyl-3,5-^{3}H(N)]-DAMGO ([^{3}H]DAMGO; 55.3 Ci mmol^{-1}; NEN, Boston, MA, U.S.A.) at 0.2–20 nM in a final volume of 1.0 ml which contained Tris-HCl (pH 7.4) buffer (50 mM) and 0.1 ml of the homogenated membrane fraction. The amount of membrane protein used in each assay was in the range of 120–170 μg, as determined by the method of Lowry *et al*. (1951). The test tubes were incubated for 120 min at 25°C. The specific binding was defined as the difference in binding observed in the absence and presence of 10^{-5} M unlabelled naloxone. The incubations were terminated by collecting the membranes on Whatman GF/B filters using a Brandel cell harvester (Model M-24, Brandel, MD, U.S.A.). The filters were then washed three times with 5 ml Tris-HCl buffer (pH 7.4) at 4°C and transferred to scintillation vials. Then, 0.5 ml of Soluene-350 (Packard Instrument Company, Inc., Meriden, CT, U.S.A.) and 4 ml of Hionic Fluor Cocktail (Packard Instrument Company) were added to the vials. After a 12 h equilibration period, the radioactivity in the samples was determined in liquid scintillation analyzer (Model 1600 CA, Packard Instrument Company). Values for Scatchard analysis represent the means±s.e.mean of three independent determinations.

[^{35}S]GTPγS binding assay

The reaction was initiated by the addition of membrane suspension (30–80 μg ml^{-1} of membrane proteins) into the

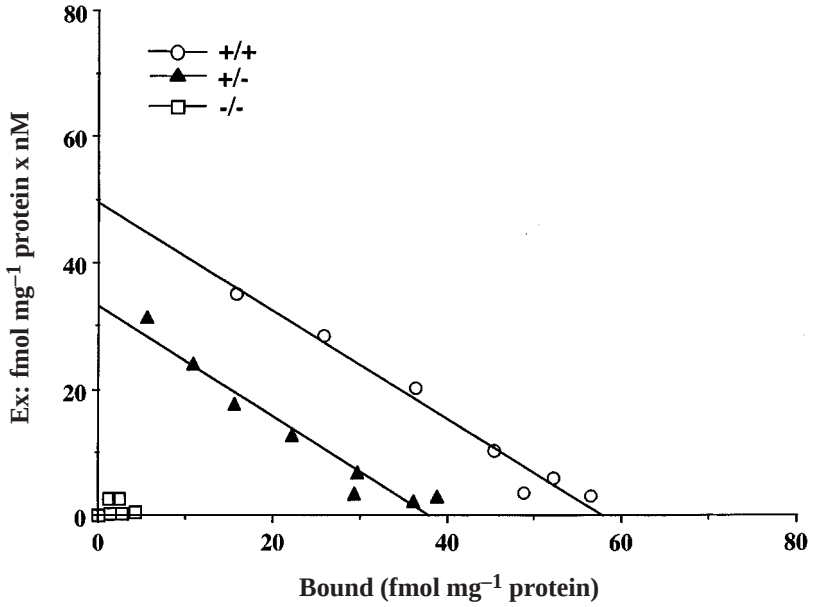

Figure 1 Scatchard analysis of [^{3}H]DAMGO binding to spinal cord membranes obtained from wild-type (+/+), heterozygous (+/−) and homozygous (−/−) μ-opioid receptor knockout mice. Membranes were incubated with [^{3}H]DAMGO at 0.2–20 nM in a final volume of 1.0 ml which contained Tris-HCl (pH 7.4) 50 mM buffer and 0.1 ml of the homogenated membrane fraction (120–170 μg) for 120 min at 25°C. The specific binding was defined as the difference in binding observed in the absence and presence of 10^{-5} M unlabelled naloxone. A representative experiment that was replicated three times is shown.

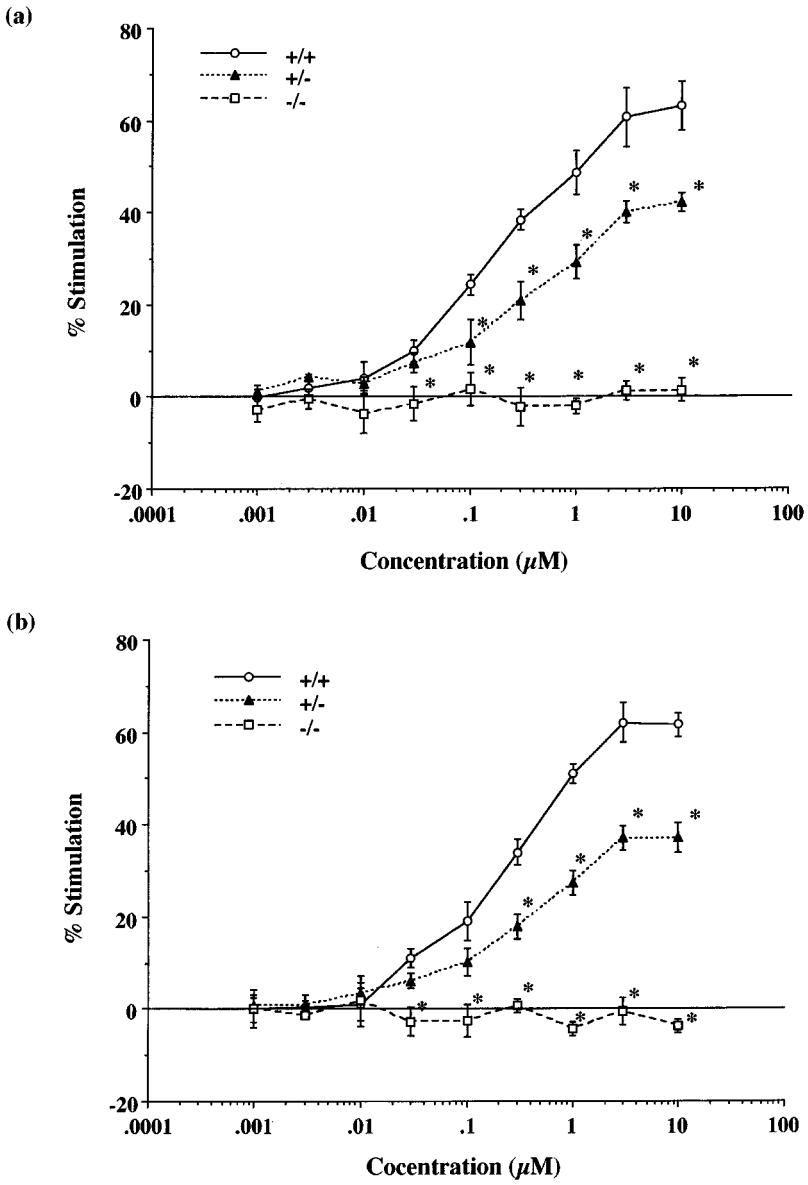

Figure 2 Comparison of the stimulation of [^{35}S]GTPγS binding to spinal cord membranes of wild-type (+/+), and heterozygous (+/−) and homozygous (−/−) μ-opioid receptor knockout mice by endomorphin-1 (a) and -2 (b). Membranes were incubated with [^{35}S]GTPγS (50 pM) and GDP (30 μM) with and without various concentrations of endomorphin-1 or -2 for 120 min at 25°C. The data are expressed as the percentage of basal [^{35}S]GTPγS (50 pM) binding measured in the presence of GDP and absence of agonist, and represent the means ± s.e.mean from at least three separate experiments. *$P<0.05$ vs wild-type mice.

assay buffer with the opioid receptor agonists, GDP 30 μM and [^{35}S]GTPγS (50 pM) (1000 Ci mmol^{-1}; Amersham, Arlington Heights, IL, U.S.A.). The suspensions were incubated at 25°C for 120 min and the reaction was terminated by filtering through Whatman GF/B glass filters using a Brandel cell harvester. The filters were then washed three times with 5 ml of Tris-HCl buffer (pH 7.4) and transferred to scintillation counting vials containing scintillation cocktail (0.5 ml of Soluene-350 and 4 ml of Hionic Fluor Cocktail). The radioactivity in the samples was determined with a liquid scintillation analyzer. Non-specific binding was measured in the presence of 10 μM unlabelled GTPγS.

Drugs

The drugs used in the present studies were: Tyr-Pro-Trp-Phe-NH_2 (endomorphin-1, Tocris Cookson Inc., Ballwin, MO, U.S.A.); Tyr-Pro-Phe-Phe-NH_2 (endomorphin-2, Tocris Cookson Inc.); [D-Ala^2,NHPhe^4,Gly-ol]enkephalin (DAMGO, Bachem California, Torrance, CA, U.S.A.); morphine (Mallinckrodt Chemical Works, St. Louis, MO, U.S.A.), [D-Pen^{2,5}]enkephalin (Bachem California), Tyr-D-Ala-Phe-Glu-Val-Val-Gly-NH_2 ([D-Ala^2] deltorphin II, Molecular Research Laboratories, Durham, NC); trans(±)-3,4-dichloro-*N*-methyl-*N*-[2-(1-pyrrolidinyl)-cyclohexyl] benzeneacetamide (U50, 488H, Research Biochemicals International, Natick, MA, U.S.A.); naloxone (Research Biochemicals International); guanylyl-5′-*O*-(γ-thio)-triphosphate (GTPγS, Research Biochemicals International); and guanosine-5′-*O*-(2-thio)-diphosphate (GDP, Sigma Chemical Company, St. Louis, MO, U.S.A.).

Statistical analysis

The data were expressed as means ± s.e.mean. The binding data for the determination of the density (B_{max}) and affinity (K_d) of binding sites were evaluated by a computer-assisted analysis, EDBA and LIGAND (Biosoft, Cambridge, U.K.).

Student's *t*-test was used for the statistical analysis of B_{max} and K_d values. Comparisons of all other data were performed *via* ANOVA followed by Newman-Keuls' test (Tallarida & Murray, 1987).

Results

The spinal cord membranes obtained from wild-type, heterozygous and homozygous μ-opioid receptor knockout mice were incubated with a range of [^{3}H]DAMGO concentrations (0.2–20 nM) for 2 h at 25°C. Figure 1 illustrates Scatchard plots for three genotypes. A mean B_{max} value of 61.6±4.9 fmol mg^{-1} protein with a K_d of 1.1±0.1 nM was found in the wild-type mice. The membranes obtained from heterozygous μ-opioid receptor knockout mice displayed a 41.3% reduction in the number of [^{3}H]DAMGO binding sites (36.1±3.6 fmol mg^{-1} protein; $P<0.01$, as compared to the wild-type mice) with no change in affinity (1.1±0.1 nM). The membranes obtained from homozygous μ-opioid receptor knockout mice showed no detectable [^{3}H]DAMGO binding sites.

Both endomorphins-1 and -2 (0.001–10 μM) produced concentration-dependent increases in [^{35}S]GTPγS binding to spinal cord membranes obtained from wild-type mice (Figure 2a and b). Maximal stimulation was 63.1±5.3 and 61.6±2.5%, respectively, using 10 μM peptide concentrations. As shown in Figure 3, the synthetic selective μ-opioid receptor agonist DAMGO and the prototype of μ-opioid receptor agonist morphine also stimulated [^{35}S]GTPγS binding in a concentration-dependent manner and produced a maximal stimulation of 94.4±9.6 and 65.1±1.3%, respectively, at 10 μM.

In heterozygous μ-opioid receptor knockout mice, [^{35}S]GTPγS binding stimulated by either endomorphin-1, -2, DAMGO or morphine was markedly decreased to 67, 60, 70 or 55% of the stimulation observed in wild-type mice, respectively. In homozygous mice, no stimulation of [^{35}S]GTPγS binding stimulated by either endomorphin-1, -2, DAMGO or morphine could be detected (Figures 2A, B and 3).

No significant changes in δ_1-, δ_2- or κ_1-opioid receptor functions were noted in μ-opioid receptor knockout mice. The δ_1-opioid receptor agonist [D-Pen^{2,5}]enkephalin (DPDPE), the δ_2-opioid receptor agonist [D-Ala^2]deltorphin II and the κ_1-opioid receptor agonist U-50,488H both produced robust stimulation of [^{35}S]GTPγS binding. As shown in Figure 4, DPDPE, [D-Ala^2]deltorphin II and U50,488H (10 μM) produced 17.6±2.5, 31.6±8.6 and 7.3±5.9% stimulation, respectively, in wild-type mice. The levels of [^{35}S]GTPγS binding stimulated by DPDPE, [D-Ala^2]deltorphin II or U50,488H in both heterozygous and homozygous μ-opioid receptor knockout mice were similar to those found in wild-type mice.

Discussion

The knockout mice used in the present study display gene dose-dependent reductions in the levels of μ-opioid receptor expression in the spinal cord. Heterozygous knockout animals manifest 40–50% reductions in μ-opioid receptor densities, whereas homozygous knockout mice display no detectable μ-opioid receptor binding or immunoreactivity (this study; Sora *et al.*, 1997b). Analyses of these animals provides direct evidence for μ-opioid receptor involvement in the expression of physiological actions by μ-opioid receptor agonists. The data from these studies documents that disruption of the mouse μ-opioid receptor gene ablates the G-protein activation in the mouse spinal cord by endomorphin-1 and -2 found in wild-type mice. Elimination of μ-opioid receptor expression in mutant mice virtually abolished both DAMGO- and morphine-stimulated [^{35}S]GTPγS binding. This agrees with our previous findings that μ-opioid receptor agonist-stimulated [^{35}S]GTPγS binding was completely blocked by μ-opioid receptor antagonists (Narita & Tseng, 1998). These findings clearly indicate that μ-opioid receptor gene products are the molecular target of endomorphins, DAMGO and morphine relevant to activation of G-proteins in the mouse spinal cord.

Regional differences in the relationships between μ-opioid receptor densities and pharmacological efficacies produced by

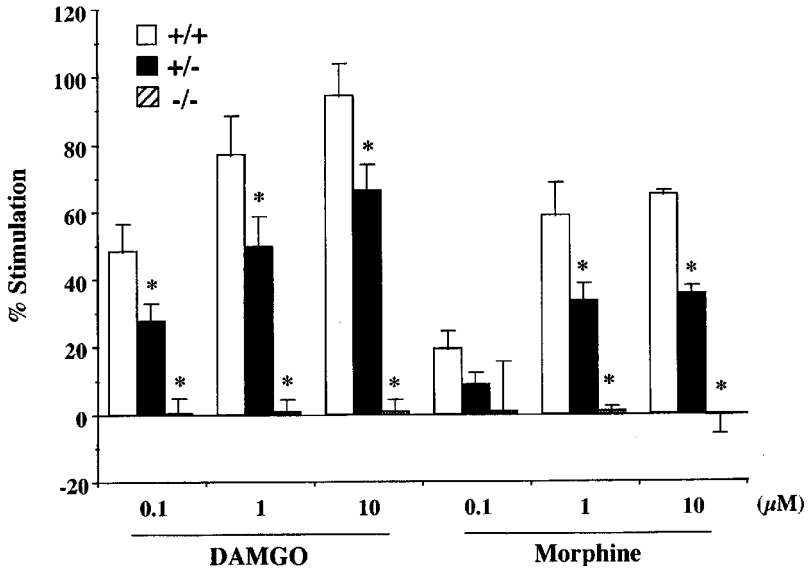

Figure 3 Effect of DAMGO and morphine on [^{35}S]GTPγS binding to spinal cord membranes of wild-type (+/+), and heterozygous (+/−) and homozygous (−/−) μ-opioid receptor knockout mice. Membranes were incubated with [^{35}S]GTPγS (50 pM) and GDP (30 μM) with and without different concentrations of DAMGO or morphine. The data are expressed as the percentage of basal [^{35}S]GTPγS (50 pM) binding measured in the presence of GDP and absence of agonist, and represent the means±s.e.mean from at least three separate experiments. *$P<0.05$ vs wild-type mice.

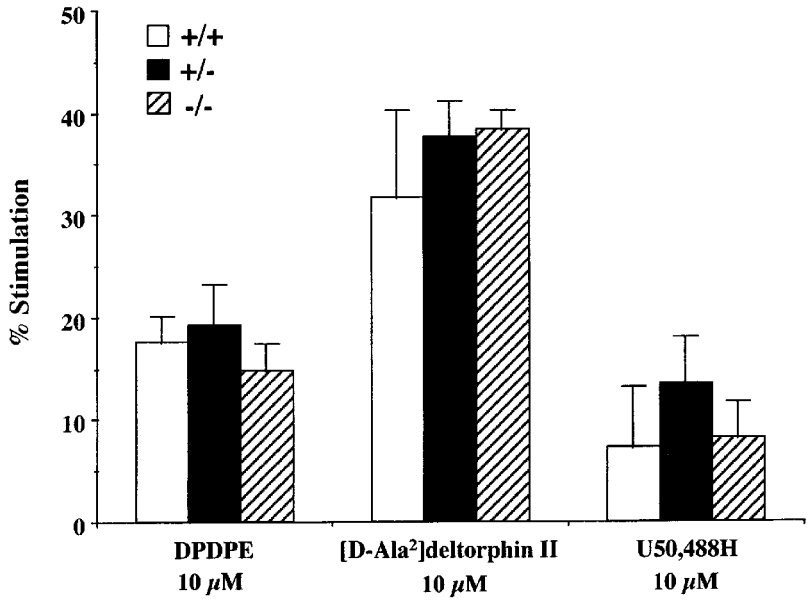

Figure 4 No differences in the [^{35}S]GTPγS binding stimulated by specific δ_1- (DPDPE), δ_2- ([D-Ala^2]deltorphin II) or κ_1- (U50,488H) opioid receptor agonists in the μ-opioid receptor knockout mice. The spinal cord membranes obtained from wild-type (+/+), and heterozygous (+/−) and homozygous (−/−) μ-opioid receptor knockout mice were incubated with [^{35}S]GTPγS (50 pM) and GDP (30 μM) with and without opioid agonists. The data are expressed as the percentage of basal [^{35}S]GTPγS (50 pM) binding measured in the presence of GDP and absence of agonist, and represent the means ± s.e.mean from at least three separate experiments.

μ-opioid receptor agonists could result from different patterns of the μ-opioid receptor reserve (Chavkin & Goldstein, 1984). Studies using heterozygous mice with half of the normal, wild-type μ-opioid receptor densities can provide information about physiologic μ-opioid receptor reserves. Previous analgesic tests in knockout mice suggest that even 50% reductions in spinal μ-opioid receptor densities alter baseline nociception and agonist-induced changes in nociceptive responses in the tail-flick assay, which largely reflects spinal antinociceptive influences (Sora *et al*., 1997b). In the present study, μ-opioid receptor agonist-stimulated [^{35}S]GTPγS binding was reduced by 55–70% in heterozygous mice, and virtually eliminated in homozygous knockout mice. Both this behavioural result and the current biochemical data thus support the idea that μ-opioid receptors are rate-limiting steps in the biochemical and physiological spinal cord pathways stimulated by endogenous and exogenous μ-opioid receptor agonists. Both lines of evidence indicate a limited physiological 'μ-opioid receptor reserve' in these spinal cord mechanisms.

It is possible that gene deletion strategies would produce compensatory changes in other receptor types associated with the deleted receptor. Quantitative autoradiography has revealed trends toward changes (10–15%) for δ- and κ-opioid receptor binding in some brain regions of μ-opioid receptor knockout mice (Kitchen *et al*., 1997). In the present study, however, we did not find any significant changes in δ_1-, δ_2- or κ_1-opioid receptor agonist-stimulated [^{35}S]GTPγS binding to spinal cord membranes in μ-opioid receptor knockout mice compared to wild-type mice. Matthes *et al*. (1998) have recently reported that mice lacking μ-opioid receptors do not display significant changes in either δ_1-, δ_2- or κ_1-opioid receptor agonist-activated G-proteins in the brain. These findings suggest that functional coupling of δ_1-, δ_2- and κ_1-opioid receptors to G-protein appears to be preserved in the process of μ-opioid receptor deletions. However, it should be also noted that some of antinociceptive actions of δ_1- and δ_2 - agonists when given intracerebroventricularly are less effective in μ-opioid receptor knockout mice than in wild-type mice (Sora *et al*., 1997a; Matthes *et al*., 1998). It is therefore worthwhile to examine more closely whether there could be physiological μ-receptor dependence of δ-receptor actions at the spinal cord level.

In conclusion, we have demonstrated profound gene-dose-dependent reductions in G-protein activation by μ-opioid receptor agonists including newly isolated peptides endomorphins in the mouse spinal cord. Furthermore, the preservation of δ_1-, δ_2- and κ_1-opioid receptor signalling properties in the process of μ-opioid receptor deletions provides no evidence for cross-talk among opioid receptors at the cellular level.

This work was supported by U.S. Public Health Service Grant DA 03811 from the National Institute on Drug Abuse (NIDA), National Institutes of Health and the Intramural Research Program, NIDA.

References

ALT, A., MANSOUR, A., AKIL, H., MEDZIHRADSKY, F., TRAYNOR, J.R. & WOODS, J.H. (1998). Stimulation of guanosine-5′-*O*-(3-[^{35}S]thio)triphosphate binding by endogenous opioids acting at a cloned mu receptor. *J. Pharmacol. Exp. Ther.*, **286,** 282–288.

CHAVKIN, C. & GOLDSTEIN, A. (1984). Opioid receptor reserve in normal and morphine-tolerant guinea pig ileum myenteric plexus. *Proc. Natl. Acad. Sci. U.S.A.*, **81,** 7253–7257.

CHEN, Y., MESTEK, A., LIU, J., HURLEY, J.A. & YU, L. (1993). Molecular cloning and functional expression of a μ-opioid receptor from the rat brain. *Mol. Pharmacol.*, **44,** 8–12.

HARRISON, L.M., KASTIN, A.J. & ZADINA, J.E. (1998). Differential effects of endomorphin-1, endomorphin-2, and Tyr-W-MIF-1 on activation of G-proteins in SH-SY5Y human neuroblastoma membranes. *Peptides,* **19,** 749–753.

KITCHEN, I., SLOWE, S.J., MATTHES, H.W.-D. & KIEFFER, B. (1997). Quantitative autoradiographic mapping of μ-, δ- and κ-opioid receptors in knockout mice lacking the μ-opioid receptor gene. *Brain Res.,* **778,** 73–88.

LAW, P.-Y. (1995). G-proteins and opioid receptors' function. In *The Pharmacology of Opioid Peptides,* ed. Tseng, L.F. Amsterdam: Harwood Academic Publishers, pp.109–130.

LOWRY, O.H., ROSEBROUGH, N.J., FARR, A.L. & RANDALL, R.J. (1951). Protein measurement with the Folin phenol reagent. *J. Biol. Chem.,* **193,** 265–275.

MATTHES, H.W.D., MALDONADO, R., SIMONIN, F., VALVERDE, O., SLOWE, S., KITCHEN, I., BEFORT, K., DIERICH, A., LE, M.M., DOLLE, P., TZAVARA, E., HANOUNE, J., ROQUES, B.P. & KIEFFER, B.L. (1996). Loss of morphine-induced analgesia, reward effect and withdrawal symptoms in mice lacking the mu-opioid-receptor gene. *Nature,* **383,** 819–823.

MATTHES, H.W.D., SMADJA, C., VALVERDE, O., VONESCH, J.-L., FOUTZ, A.S., BOUDINOT, E., DENAVIT-SAUBIÉ, M., SEVERINI, C., NEGRI, L., ROQUES, B.P., MALDONADO, R. & KIEFFER, B.L. (1998). Activity of the δ-opioid receptor is partially reduced, whereas activity of the κ-receptor is maintained in mice lacking the μ-receptor. *J. Neuroscience,* **18,** 7285–7295.

NARITA, M., MIZOGUCHI, H., OJI, G.S., TSENG, E.L., SUGANUMA, C., NAGASE, H. & TSENG, L.F. (1998). Characterization of endomorphin-1 and -2 on [^{35}S]GTPγS binding in the mouse spinal cord. *Eur. J. Pharmacol.,* **351,** 383–387.

NARITA, M. & TSENG, L.F. (1998). Evidence for the existence of the β-endorphin-sensitive 'ε-opioid receptor' in the brain: the mechanisms of ε-mediated antinociception. *Jpn. J. Pharmacol.,* **76,** 233–253.

SELLY, D.E., SIM, L.J., XIAO, R., LIU, QIXU & CHILDERS, S.R. (1997). μ-Opioid receptor-stimulated guanosin-5-*O*-(γ-thio)-triphosphate binding in rat thalamua and cultured cell lines: Signal transduction mechanisms underlying agonist efficacy. *Mol. Pharmacol.,* **51,** 87–96.

SIM, L.J., LIU, Q., CHILDERS, S.R. & SELLEY, D.E. (1998). Endomorphin-stimulated [^{35}S]GTPγS binding in rat brain: Evidence for partial agonist activity at μ-opioid receptors. *J. Neurochem.,* **70,** 1567–1576.

SIM, L.J., SELLY, D.E. & CHILDERS, S.R. (1995). In vitro autoradiography of receptor-activated G-proteins in rat brain by agonist-stimulated guanylyl 5′-[γ-[^{35}S]thio]-triphosphate binding. *Proc. Natl. Acad. Sci. USA,* **92,** 7242–7246.

SIM, J.S., SELLY, D.E., XIAO, R. & CHILDERS, S.R. (1996). Differences in G-protein activation by μ- and δ-opioid, and cannabinoid, receptors in rat striatum. *Eur. J. Pharmacol.,* **307,** 97–105.

SHIMOHIRA, I., TOKUYAMA, S., HIMENO, A., NIWA, M. & UEDA, H. (1997). Characterization of nociceptin-stimulated in site [^{35}S]GTPγS binding in comparison with opioid agonist-stimulated ones in brain regions of the mice. *Neurosci. Lett.,* **237,** 113–116.

SORA, I., FUNADA, M. & UHL, G.R. (1997a). The μ-opioid receptor is necessary for [D-Pen^{2},D-Pen^{5}]enkephalin-induced analgesia. *Eur. J. Pharmacol.,* **324,** R1–R2.

SORA, I., TAKAHASHI, N., FUNADA, M., UJIKE, H., REVAY, R.S., DONOVAN, D.M., MINER, L.L. & UHL, G.R. (1997b). Opiate receptor knockout mice define μ receptor roles in endogenous nociceptive responses and morphine-induced analgesia. *Proc. Natl. Acad. Sci. U.S.A.,* **94,** 1544–1549.

TALLARIDA, R.J. & MURRAY, R.B. (1987). *Manual of Pharmacological Calculation with Computer Programs.* New York: Springer.

TRAYNOR, J.R. & NAHORSKI, S.R. (1995). Modulation by μ-opioid agonists of guanosine-5′-*O*-(3-[^{35}S]thio)triphosphate binding to membranes from human neuroblastoma SH-SY5Y cells. *Mol. Pharmacol.,* **47,** 848–854.

ZADINA, J., HACKLER, L., GE, L.-J. & KASTIN, A.J. (1997). A potent and selective endogenous agonist for the μ-opiate receptor. *Nature,* **386,** 499–502.

(Received September 28, 1998
Revised October 27, 1998
Accepted November 3, 1998)

British Journal of Pharmacology (1999) 126, 457–466
http://www.stockton-press.co.uk/bjp

Effect of the cannabinoid receptor agonist WIN55212-2 on sympathetic cardiovascular regulation

[1]Nathalie Niederhoffer & *,[1]Bela Szabo

[1]Pharmakologisches Institut der Albert-Ludwigs-Universität, Hermann-Herder-Strasse 5, D-79104 Freiburg i. Br., Germany

1 The aim of the present study was to analyse the cardiovascular actions of the synthetic CB_1/CB_2 cannabinoid receptor agonist WIN55212-2, and specifically to determine its sites of action on sympathetic cardiovascular regulation.

2 Pithed rabbits in which the sympathetic outflow was continuously stimulated electrically or which received a pressor infusion of noradrenaline were used to study peripheral prejunctional and direct vascular effects, respectively. For studying effects on brain stem cardiovascular regulatory centres, drugs were administered into the cisterna cerebellomedullaris in conscious rabbits. Overall cardiovascular effects of the cannabinoid were studied in conscious rabbits with intravenous drug administration.

3 In pithed rabbits in which the sympathetic outflow was continuously electrically stimulated, intravenous injection of WIN55212-2 (5, 50 and 500 $\mu g\ kg^{-1}$) markedly reduced blood pressure, the spillover of noradrenaline into plasma and the plasma noradrenaline concentration, and these effects were antagonized by the CB_1 cannabinoid receptor-selective antagonist SR141716A. The hypotensive and the sympathoinhibitory effect of WIN55212-2 was shared by CP55940, another mixed CB_1/CB_2 cannabinoid receptor agonist, but not by WIN55212-3, the enantiomer of WIN55212-2, which lacks affinity for cannabinoid binding sites. WIN55212-2 had no effect on vascular tone established by infusion of noradrenaline in pithed rabbits.

4 Intracisternal application of WIN55212-2 (0.1, 1 and 10 $\mu g\ kg^{-1}$) in conscious rabbits increased blood pressure and the plasma noradrenaline concentration and elicited bradycardia; this latter effect was antagonized by atropine.

5 In conscious animals, intravenous injection of WIN55212-2 (5 and 50 $\mu g\ kg^{-1}$) caused bradycardia, slight hypotension, no change in the plasma noradrenaline concentration, and an increase in renal sympathetic nerve firing. The highest dose of WIN55212-2 (500 $\mu g\ kg^{-1}$) elicited hypotension and tachycardia, and sympathetic nerve activity and the plasma noradrenaline concentration declined.

6 The results obtained in pithed rabbits indicate that activation of CB_1 cannabinoid receptors leads to marked peripheral prejunctional inhibition of noradrenaline release from postganglionic sympathetic axons. Intracisternal application of WIN55212-2 uncovered two effects on brain stem cardiovascular centres: sympathoexcitation and activation of cardiac vagal fibres. The highest dose of systemically administered WIN55212-2 produced central sympathoinhibition; the primary site of this action is not known.

Keywords: Baroreflex; blood pressure; cannabinoid receptor; cardiovascular regulation; conscious rabbit; heart rate; plasma noradrenaline; pithed rabbit; presynaptic receptor; sympathetic nerve activity

Abbreviations: CB, cannabinoid; CP55940, (−)-cis-3-[2-hydroxy-4-(1,1-dimethylheptyl)phenyl]-trans-4-(3-hydroxypropyl)cyclohexanol; i.c., intracisternal; PRE, average of initial values (before drug application); SR141716A, N-piperidino-5-(4-chlorophenyl)-1-(2,4-dichlorophenyl)-4-methyl-3-pyrazole-carboxamide; WIN55212-2, R(+)-[2,3-dihydro-5-methyl-3-[(morpholinyl)methyl]pyrrolo[1,2,3-de]-1,4-benzoxazinyl]-(1-naphthalenyl)methanone mesylate

Introduction

Cannabinoids produce their typical effects by activation of specific G-protein-coupled receptors. Two cannabinoid receptors have been identified, CB_1 and CB_2 (Matsuda *et al*., 1990; Munro *et al*., 1993; for review see Howlett, 1995; Compton *et al*., 1996; Pertwee, 1997). The CB_1 receptor is preferentially located on neurons, whereas the CB_2 receptor occurs mainly on peripheral non-neuronal cells.

Pharmacological effects of cannabinoids in animals include hypokinesia, analgesia, catalepsy and hypothermia (for review see Howlett, 1995; Compton *et al*., 1996; Pertwee, 1997). Cannabinoids also elicit cardiovascular changes (for review see Dewey, 1986; Compton *et al*., 1996). In most experiments in anaesthetized animals, cannabinoids lowered blood pressure and heart rate, and this was generally attributed to depression of sympathetic tone and enhancement of cardiac vagal activity (rat: Graham & Li, 1973; Adams *et al*., 1976; Estrada *et al*., 1987; Varga *et al*., 1995, 1996; Vidrio *et al*., 1996; Lake *et al*., 1997a,b; dog: Cavero *et al*., 1973a,b, 1974; Jandhyala & Hamed, 1978; cat: Vollmer *et al*., 1974). In conscious animals, cannabinoids either caused moderate cardiovascular depression (rat: Birmingham, 1973; Vidrio *et al*., 1996; rabbit: Stark & Dews, 1980; monkey: Fredericks *et al*., 1981), or they had no effect or elicited hypertension or tachycardia (rat: Osgood & Howes, 1977; Kawasaki *et al*., 1980; Stein *et al*., 1996; Lake *et al*., 1997b; dog: Jandhyala & Hamed, 1978). In conscious humans, acute administration of cannabinoids elicited marked tachycardia accompanied by a small increase in blood pressure (Benowitz *et al*., 1979; Huestis *et al*., 1992), whereas long-term cannabinoid application produced hypotension and bradycar-

* Author for correspondence.

dia (Benowitz & Jones, 1975). In the majority of cardiovascular studies, Δ^9-tetrahydrocannabinol (the main active component from *Cannabis sativa*) or anandamide (a putative endogenous cannabinoid) was used as the agonist. Both compounds are agonists at CB_1 and CB_2 receptors (Felder *et al*., 1995; Showalter *et al*., 1996; see Pertwee, 1997) but also elicit effects independent of cannabinoid receptors (see Martin, 1986; Lake *et al*., 1997a,b).

In the majority of the above mentioned cardiovascular studies only blood pressure and heart rate were measured, and only few experiments were carried out which permitted determination of the site of interaction of cannabinoids with the cardiovascular system. To our knowledge, effects on sympathetic nerve activity have been determined only by Vollmer *et al*. (1974) and effects on the plasma concentration of catecholamines have not been examined. The information on cardiovascular effects of centrally administered cannabinoids is also limited (Cavero *et al*., 1973a,b; Vollmer *et al*., 1974). The aim of the present study was to determine the sites of interaction of cannabinoids with the sympathetic nervous system. To reach this goal, four kinds of experiment were carried out. (i) Peripheral prejunctional effects on noradrenaline release from sympathetic neurons were studied in pithed rabbits with electrically stimulated sympathetic outflow. (ii) Peripheral postjunctional vascular effects were studied in pithed rabbits which received a pressor infusion of noradrenaline. (iii) Effects on cardiovascular centres in the brain stem were examined by administration of cannabinoids into the cisterna cerebellomedullaris of conscious rabbits. (iv) Finally, the overall effect of systemically administered cannabinoids on cardiovascular regulation was studied in conscious rabbits; in these experiments, the electrical activity of renal postganglionic sympathetic axons was recorded by means of a chronically implanted electrode.

In most experiments, we used the synthetic aminoalkylindole compound WIN55212-2 as a cannabinoid agonist. This compound possesses affinity for both CB_1 and CB_2 cannabinoid receptors (in this respect it is similar to Δ^9-tetrahydrocannabinol and anandamide), its affinity for these receptors is high, and more importantly, its lack of affinity for a great number of neurotransmitter receptors and ion channels has been documented (Felder *et al*., 1995; Showalter *et al*., 1996; Kuster *et al*., 1993; for review see Pertwee, 1997). In a few experiments, the effects of WIN55212-2 were compared with the effects of WIN55212-3, the enantiomer of WIN55212-2, which in binding studies has very low affinity for cannabinoid receptors, and with the effects of CP55940, a mixed CB_1/CB_2 cannabinoid receptor agonist with a chemical structure markedly different from WIN55212-2.

Methods

Experiments were carried out on 40 rabbits of a local breed (derived from 'Deutscher Riesenscheck', obtained from Ketterer, Reute, Germany); rabbits were of either sex and weighed 1.4–2.9 kg. Four different experimental preparations were used.

Pithed rabbits with electrically stimulated sympathetic outflow

The method was basically as in Szabo *et al*. (1987). Briefly, rabbits were deeply anaesthetized with pentobarbitone (75 mg kg^{-1}) and artificially ventilated. The left carotid artery was cannulated for recording arterial pressure with a Statham P23Db transducer coupled to a bridge amplifier (Hugo Sachs Elektronik, Hugstetten, Germany). The heart rate was calculated from the pulsating blood pressure signal by an integrator (Hugo Sachs Elektronik, Hugstetten, Germany). The right carotid artery was also cannulated and served for blood sampling. Both jugular veins were cannulated and they served for administration of drugs. After relaxation of skeletal muscles by gallamine triethiodide (5 mg kg^{-1}), animals were pithed using a 3-mm-thick and 30-cm-long uninsulated stainless steel rod. The entire sympathetic outflow was continuously stimulated through the pithing rod (2 Hz, 100–140 mA, 0.5 ms square-waves pulses). This stimulation markedly increased blood pressure (from 57 ± 3 mmHg [$n = 14$] to 83 ± 4 mmHg [$n = 14$]) and the plasma noradrenaline concentration (from values lower than 10 pg ml^{-1} (see Urban *et al*., 1995, for plasma noradrenaline values in unstimulated pithed rabbits) to 310 ± 56 pg ml^{-1} [$n = 14$]); heart rate increased only moderately (from 233 ± 10 min^{-1} [$n = 14$] to 259 ± 9 min^{-1} [$n = 14$]). Thirty minutes after the beginning of electrical stimulation, an infusion of [^{3}H]noradrenaline was started (80 nCi kg^{-1} min^{-1}; 0.23 ng kg^{-1} min^{-1}); this tracer infusion did not change blood pressure and heart rate. Parameters were first determined 30–45 min (t = 0 min in subsequent text) after the beginning of the [^{3}H]noradrenaline infusion.

Pithed rabbits receiving a pressor infusion of noradrenaline

Rabbits were pithed as described above. Instead of electrical stimulation, vascular tone was raised by i.v. infusion of noradrenaline (2 μg kg^{-1} min^{-1}). This infusion markedly increased blood pressure (from 53 ± 4 mmHg [$n = 8$] to 79 ± 6 mmHg [$n = 8$]) but did not change heart rate (258 ± 11 min^{-1} [$n = 8$] before infusion and 261 ± 14 min^{-1} [$n = 8$] during infusion). Blood was not sampled. Parameters were first determined 30 min (t = 0 min) after the beginning of noradrenaline infusion.

Conscious rabbits with intracisternal drug administration

The method was basically as in Szabo *et al*. (1995). Briefly, under halothane anaesthesia (1.5–4%) in spontaneously breathing rabbits, a polyethylene catheter (0.28 mm i.d., 0.61 mm o.d., 25 cm length) was inserted 8 mm into the cisterna cerebellomedullaris through a hole in the atlanto-occipital membrane. The free end of the catheter was tunnelled to an incision in the neck. The wounds were sutured and at least 2 weeks were allowed for recovery before the first experiment was carried out in the conscious animal. Three experiments were carried out on one rabbit at intervals of 7 days. The order of treatments was randomized and no animal received a given kind of treatment twice. After the last experiment, the animals were killed by an overdose of pentobarbitone.

Before the experiments in conscious animals, the central ear artery (for recording arterial pressure and heart rate and for blood sampling) and a marginal ear vein (for administration of drugs) were cannulated under local anaesthesia. Also under local anaesthesia, the intracisternal catheter was recovered from under the skin. Parameters were first determined 45 min (t = 0 min) after recovery of the catheter.

Conscious rabbits receiving drugs intravenously

The method was basically as in Szabo *et al*. (1993). Briefly, an electrode was implanted under halothane anaesthesia (1.5–4%) in spontaneously breathing rabbits. The left kidney was

approached retroperitoneally and two sympathetic nerve trunks accompanying the renal artery were dissected free and slipped into the spirals of a stainless steel bipolar electrode. The nerves and electrode were then embedded in silicone gel. The free end of the electrode was tunnelled to an incision in the neck. The wounds were sutured and 3–4 days were allowed for recovery before the first experiment was carried out in the conscious animal. Two to three experiments were carried out on one rabbit at intervals of 3–4 days. The order of treatments was randomized and no animal received a given kind of treatment twice. After the last experiment, the animals were killed by an overdose of pentobarbitone.

Before the experiments in conscious animals, the central ear artery (for recording arterial pressure and heart rate and for blood sampling) and a marginal ear vein (for administration of drugs) were cannulated under local anaesthesia. Also under local anaesthesia, the electrode leads were recovered from under the skin. Parameters were first determined 45 min (t = 0 min) after recovery of the electrode leads.

Determination of noradrenaline plasma concentration and kinetic parameters

The method was basically as in Szabo & Schultheiss (1990). Briefly, the plasma concentrations of endogenous noradrenaline and [^{3}H]noradrenaline were determined in the plasma from 2-ml blood samples by alumina chromatography followed by high pressure liquid chromatography, electrochemical detection and liquid scintillation counting. The values were used to calculate the [^{3}H]noradrenaline plasma clearance and the rate of total body noradrenaline spillover into plasma (see also Esler *et al*., 1990). Since none of the treatments changed the [^{3}H]noradrenaline plasma clearance, values of this parameter are not given.

Protocol and evaluation of experiments

In pithed rabbits, either solvent (0.5 ml kg^{-1}) or increasing doses of WIN55212-2 (5, 50 and 500 μg kg^{-1}), WIN55212-3 (5, 50 and 500 μg kg^{-1}) or CP55940 (5, 50 and 500 μg kg^{-1}) were injected i.v. at t = 19, 37 and 55 min. One group of rabbits was pretreated at t = −10 min with the cannabinoid antagonist SR141716A (500 μg kg^{-1}; i.v.).

In conscious rabbits with an intracisternal catheter, either solvent (25 μl kg^{-1}) or increasing doses of WIN55212-2 (0.1, 1 and 10 μg kg^{-1}) were injected intracisternally (i.c.) at t = 19, 37 and 55 min. One group of rabbits was pretreated i.v. at t = −10 min with atropine (1 mg kg^{-1}).

In conscious rabbits with renal nerve recording, either solvent (0.5 ml kg^{-1}) or increasing doses of WIN55212-2 (5, 50 and 500 μg kg^{-1}) was injected i.v. at t = 19, 37 and 55 min. One group of rabbits was pretreated at t = −10 min with SR141716A (500 μg kg^{-1}; i.v.).

In all experimental groups, blood pressure and heart rate (and in some groups also renal sympathetic nerve activity) were read every 2 min from t = 0 to 68 min. Blood was sampled at t = 0, 14, 32, 50 and 68 min for the determination of the plasma noradrenaline concentration (and in some groups also for the determination of the [^{3}H]noradrenaline plasma concentration). In each experiment, values measured at t = 0 and 14 min were averaged (PRE), and all values were expressed as percentages of PRE.

Statistics

Means ± s.e.mean of n experiments are given throughout. Differences between groups were evaluated with the non-parametric two-tailed Mann-Whitney test; in the case of multiple comparisons the Bonferroni correction was employed. $P < 0.05$ was taken as the limit of statistical significance and only this level is indicated even if P was < 0.01 or < 0.001.

Drugs

Drugs were obtained from the following sources: atropine sulphate and (−)-noradrenaline (+)-bitartrate from Sigma (Deisenhofen, Germany); (−)-cis-3-[2-hydroxy-4-(1,1-dimethylheptyl)phenyl]-trans-4-(3-hydroxypropyl)cyclohexanol (CP55940) from Pfizer (Groton, CT, U.S.A.); 2-hydroxypropyl-β-cyclodextrin from Fluka (Neu-Ulm, Germany); N-piperidino-5-(4-chlorophenyl)-1-(2,4-dichlorophenyl)-4-methyl-3-pyrazole-carboxamide (SR141716A) from Sanofi (Montpellier, France); R(+)-[2,3-dihydro-5-methyl-3-[(morpholinyl)methyl] pyrrolo [1, 2, 3-de]-1,4-benzoxazinyl]-(1-naphthalenyl) methanone mesylate (WIN55212-2) and S(−)-[2,3-dihydro-5-methyl-3-[(morpholinyl)methyl]pyrrolo[1,2,3-de]-1,4-benzoxazinyl]-(1-naphthalenyl)methanone mesylate (WIN55212-3) from RBI (Köln, Germany); (−)-[ring-2,5,6-^{3}H]noradrenaline (specific activity, 59 Ci mmol^{-1}) from DuPont NEN (Bad Homburg, Germany).

WIN55212-2, WIN55212-3 and CP55940 were dissolved in 19% (i.v. injection) or 7.5% (i.c. injection) w/v solutions of 2-hydroxypropyl-β-cyclodextrin; further dilutions were made with the same solvent. SR141716A was dissolved in 66% DMSO. Atropine and (−)-noradrenaline were dissolved in 0.9% saline. [^{3}H]Noradrenaline was diluted with 0.02 M acetic acid to final concentration. I.v. and i.c. injections had a volume of 0.5 ml kg^{-1} and 25 μl kg^{-1}, respectively. [^{3}H]Noradrenaline and (−)-noradrenaline were infused at a rate of 1.92 ml h^{-1}. Doses refer to the salts.

Results

After an initial stabilization period, parameters were determined twice (at t = 0 and 14 min), and the values were averaged to obtain the PRE values. Values recorded later in any given experiment were expressed as percentages of PRE. The PRE values in the four experimental models are given in Table 1. Values recorded from unpretreated rabbits are similar to those obtained in the corresponding preparations in previous studies (compare with Szabo *et al*., 1987; 1993; 1995). Pretreatment with the cannabinoid antagonist SR141716A (500 μg kg^{-1}; i.v.) had no significant effect on the recorded parameters. Pretreatment with atropine (1 mg kg^{-1}; i.v.) produced the expected cardioacceleration.

Pithed rabbits with electrically stimulated sympathetic outflow (Figure 1)

An experimental sympathetic tone was maintained in these rabbits by electrical stimulation of preganglionic sympathetic neurons with an electrode in the spinal canal. Intravenous injection (0.5 ml kg^{-1}) of the solvent for WIN55212-2 caused short-lasting blood pressure increases without influencing heart rate. The plasma noradrenaline concentration and the spillover of noradrenaline into plasma decreased slightly in the solvent group. Intravenous injection of three increasing doses of the cannabinoid agonist WIN55212-2 (5, 50 and 500 μg kg^{-1}) dose-dependently and greatly reduced blood pressure, the plasma noradrenaline concentration and the spillover of noradrenaline into plasma; heart rate was not changed.

Pretreatment with SR141716A (500 μg kg^{-1}; i.v.) nearly abolished the hypotension produced by the two lower doses of WIN55212-2 and attenuated the hypotensive effect of the highest dose. SR141716A also attenuated the reduction of the plasma noradrenaline concentration and the noradrenaline spillover into plasma caused by WIN55212-2.

Intravenous injection of the inactive enantiomer WIN55212-3 (5, 50 and 500 μg kg^{-1}; same doses as of WIN55212-2) transiently increased blood pressure (Figure 2), an effect resembling the one occurring after injection of solvent (see Figure 1) and did not change the plasma noradrenaline concentration (Figure 2). Intravenous injection of another cannabinoid agonist, CP55940 (5, 50 and 500 μg kg^{-1}), produced effects (Figure 2) very similar to those of WIN55212-2: dose-dependent hypotension and a dose-dependent decrease of the plasma noradrenaline concentration.

Table 1 Absolute values of parameters before injection of solvent or WIN 55212-2 (PRE values[a])

Pretreatment	n	*Mean arterial pressure* (mmHg)	*Heart rate* (min^{-1})	*Renal sympathetic nerve activity* (impulses s^{-1})	*Plasma noradrenaline concentration* (pg ml^{-1})	*Noradrenaline spillover rate* (ng kg^{-1} min^{-1})
Pithed rabbits with electrically stimulated sympathetic outflow						
—	10	81±6	245±9		250±44	19±0.4
SR141716A i.v.[b]	4	87±5	269±20		372±160	34±17
Pithed rabbits receiving a pressor infusion of noradrenaline						
—	8	79±6	261±14			
Conscious rabbits with intracisternal drug administration						
—	16	75±2	196±8		149±19	
Atropine i.v.[c]	9	71±3	244±17*		170±40	
Conscious rabbits receiving drugs intravenously						
—	13	83±3	207±7	29±4	153±26	
SR141716A i.v.[b]	7	90±4	192±8	27±4	199±70	

[a]PRE values are averages of values measured at t=0 and 14 min. [b]SR141716A (500 μg kg^{-1}) was injected i.v. at t=−10 min. [c]Atropine (1 mg kg^{-1}) was injected i.v. at t=−10 min. *Significant difference ($P<0.05$) from unpretreated rabbits.

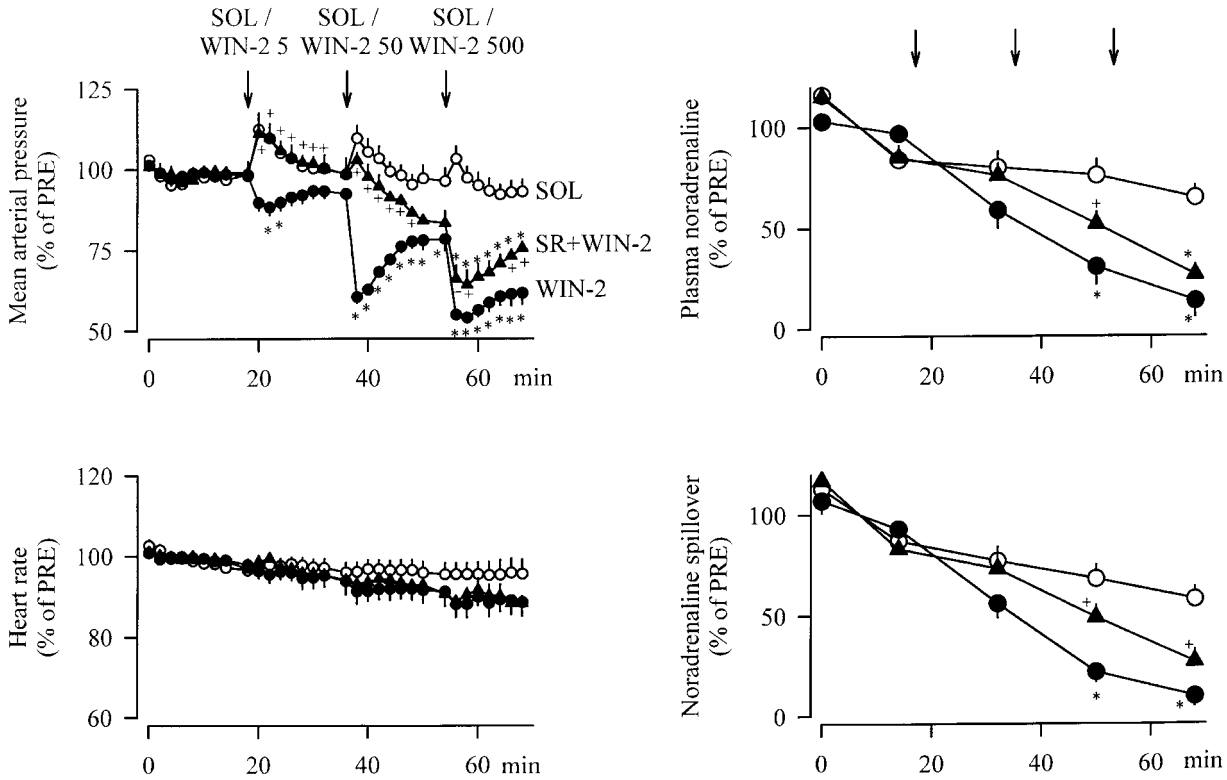

Figure 1 Effects of i.v. injections of solvent (SOL) and WIN 55212-2 (WIN-2) on mean arterial pressure, heart rate, plasma noradrenaline concentration and noradrenaline spillover rate in pithed rabbits with electrically stimulated sympathetic outflow. SOL (0.5 ml kg^{-1}) and WIN-2 (5, 50 and 500 μg kg^{-1}) were injected as indicated by arrows. One of the two WIN-2-groups was pretreated at t=−10 min with SR141716A (SR; 500 μg kg^{-1}; i.v.). Values are given as percentages of PRE values (Table 1). Means±s.e.mean from six (SOL), four (WIN-2) and four (SR+WIN-2) experiments. Differences from SOL: *$P<0.05$; differences from WIN-2: +$P<0.05$.

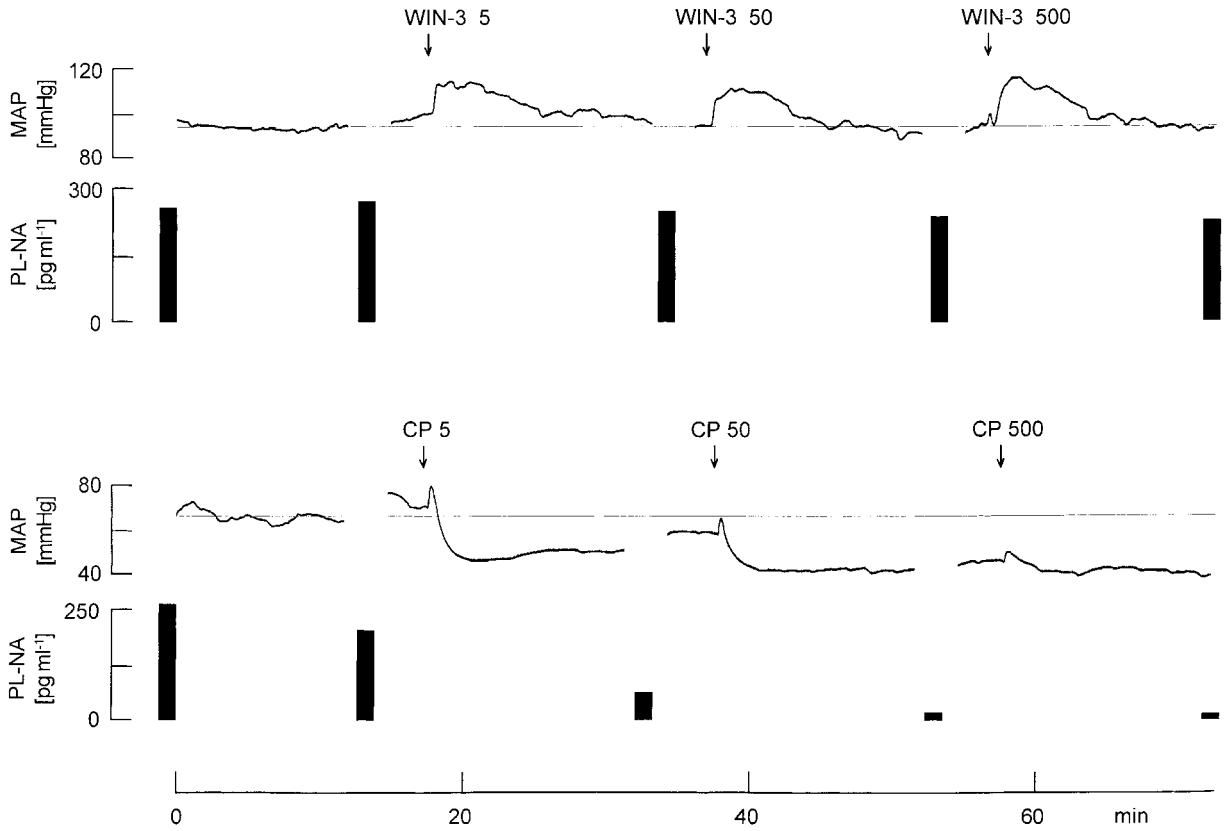

Figure 2 Effects of i.v. injections of either WIN55212-3 (WIN-3) or CP55940 (CP) on mean arterial pressure (MAP) and plasma noradrenaline concentration (PL-NA) in pithed rabbits with electrically stimulated sympathetic outflow. WIN-3 (5, 50 and 500 μg kg^{-1}) and CP (5, 50 and 500 μg kg^{-1}) were injected as indicated by arrows. Representative curves from three (WIN-3) and three (CP) experiments with similar results.

Pithed rabbits receiving a pressor infusion of noradrenaline (Figure 3)

An artificial vascular tone was maintained in these rabbits by intravenous infusion of noradrenaline. Intravenous injection of solvent caused short-lasting blood pressure increases and no change in heart rate. The effects of WIN55212-2 (5, 50 and 500 μg kg^{-1}) were similar: short-lasting blood pressure increases and no change in heart rate were observed. The effects of WIN55212-2 differed remarkably in the two pithed rabbit models: blood pressure decreased in animals with electrically stimulated sympathetic outflow (Figure 1), whereas only blood pressure increases (effect of the solvent) were observed in animals with a pressor infusion of noradrenaline (Figure 3).

Conscious rabbits with intracisternal drug administration (Figure 4)

Injection of the solvent (25 μl kg^{-1}) into the cisterna cerebellomedullaris caused no change in blood pressure, heart rate and the plasma noradrenaline concentration. When three increasing doses of WIN55212-2 (0.1, 1 and 10 μg kg^{-1}) were injected intracisternally, blood pressure was not changed by the two lower doses but was elevated after the highest dose. Central application of WIN55212-2 elicited pronounced and dose-dependent bradycardia and a dose-dependent increase in the plasma noradrenaline concentration.

When rabbits were pretreated with atropine (1 mg kg^{-1}; i.v.), the hypertension elicited by the highest dose of WIN55212-2 (10 μg kg^{-1}) was unchanged; in these animals,

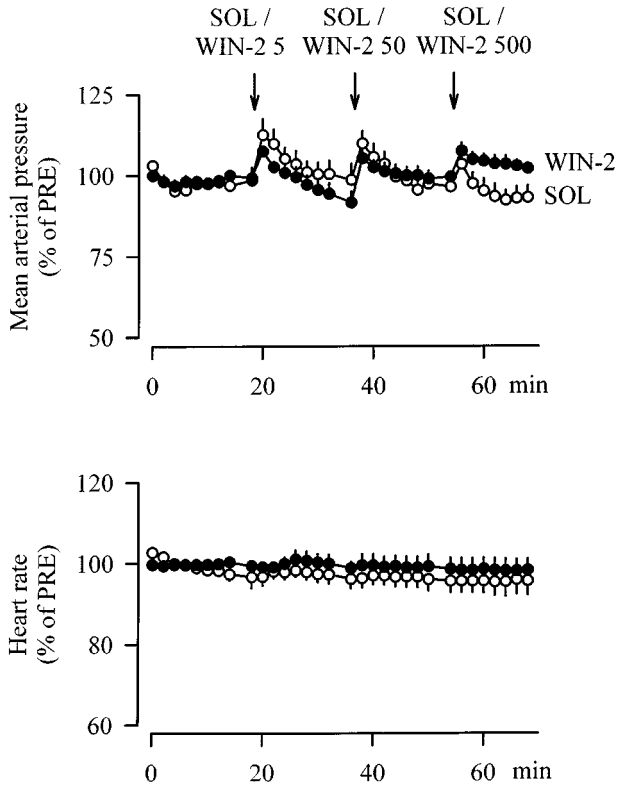

Figure 3 Effects of i.v. injections of solvent (SOL) and WIN 55212-2 (WIN-2) on mean arterial pressure and heart rate in pithed rabbits receiving a pressor infusion of noradrenaline. SOL (0.5 ml kg^{-1}) and WIN-2 (5, 50 and 500 μg kg^{-1}) were injected as indicated by arrows. Values are given as percentages of PRE values (Table 1). Means $\pm$s.e.mean from four (SOL) and four (WIN-2) experiments.

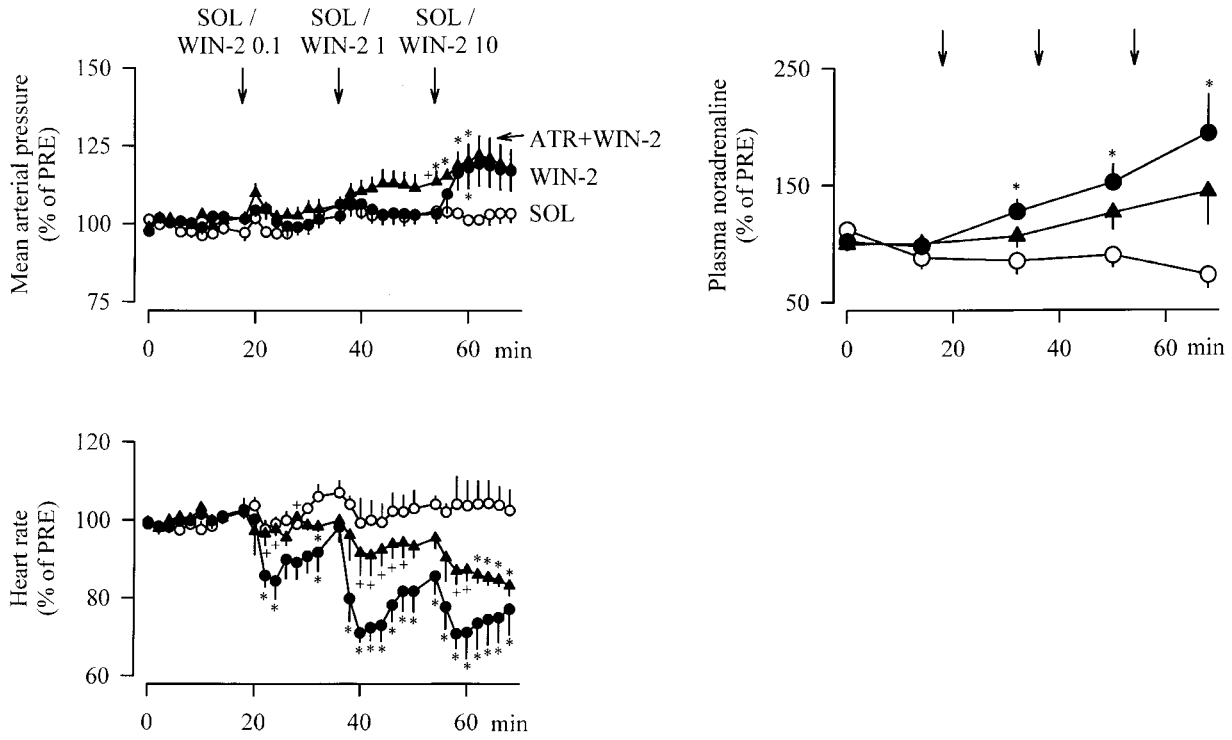

Figure 4 Effects of i.c. injections of solvent (SOL) and WIN 55212-2 (WIN-2) on mean arterial pressure, heart rate and plasma noradrenaline concentration in conscious rabbits. SOL (25 μl kg^{-1}) and WIN-2 (0.1, 1 and 10 μg kg^{-1}) were injected as indicated by arrows. One of the two WIN-2-groups was pretreated at t = −10 min with atropine (ATR; 1 mg kg^{-1}; i.v.). Values are given as percentages of PRE values (Table 1). Means ± s.e.mean from seven (SOL), nine (WIN-2) and nine (ATR + WIN-2) experiments. Differences from SOL: *$P<0.05$; differences from WIN-2: +$P<0.05$.

even a lower dose of WIN55212-2 (1 μg kg^{-1}) tended to increase blood pressure. Pretreatment with atropine abolished the bradycardia elicited by the lower doses of WIN55212-2 (0.1 and 1 μg kg^{-1}) and attenuated the bradycardia elicited by the highest dose (10 μg kg^{-1}). Atropine also attenuated the increase in the plasma noradrenaline concentration produced by WIN55212-2.

Conscious rabbits receiving drugs intravenously (Figure 5)

Intravenous injection of solvent (0.5 ml kg^{-1}) did not change blood pressure, heart rate, renal sympathetic nerve activity and the plasma noradrenaline concentration. Three increasing doses of WIN55212-2 (5, 50 and 500 μg kg^{-1}) were injected intravenously. The two lower doses caused a slight hypotension, bradycardia and an increase in the firing rate of the renal sympathetic nerves. The increase in the plasma noradrenaline concentration observed after these doses of WIN55212-2 was not significant. The pattern of effects changed after the highest dose of WIN55212-2 (500 μg kg^{-1}): blood pressure decreased on average (see below), a tachycardia appeared, and sympathetic nerve activity and plasma noradrenaline returned to the baseline. The response to the highest dose of WIN55212-2 was not uniform in all the rabbits. One rabbit (from $n=7$) was behaviourally excited and tried to jump in the cage; in this rabbit, blood pressure increased after the highest dose of WIN55212-2.

Pretreatment with SR141716A (500 μg kg^{-1}; i.v.) changed the effects of intravenously administered WIN55212-2 as follows. The bradycardia elicited by the two lower doses of WIN55212-2 (5 and 50 μg kg^{-1}) was markedly reduced. The enhancement of sympathetic nerve activity by these doses of WIN55212-2 was not changed by the antagonist. The effects produced by the highest WIN55212-2 dose (500 μg kg^{-1}) were modified by SR141716A to a greater extent. The hypotension produced by WIN55212-2 was slightly, but not significantly, attenuated. Instead of a tachycardia, the highest dose of WIN55212-2 produced a slight (non-significant) bradycardia. In the pretreated animals WIN55212-2 greatly increased renal sympathetic nerve firing and tended to increase the plasma noradrenaline concentration.

Discussion

The present results show that the mixed CB_1/CB_2 cannabinoid receptor agonist WIN55212-2 interferes with cardiovascular regulation by at least four mechanisms: prejunctional inhibition of transmitter release from postganglionic sympathetic neurons, central sympathoexcitation at the level of the brain stem, activation of cardiac vagal efferents at the level of the brain stem, and (at high systemic doses) central sympathoinhibition.

Peripheral prejunctional inhibition

In pithed rabbits with electrically stimulated sympathetic outflow, WIN55212-2 greatly reduced the spillover of noradrenaline into plasma, the plasma noradrenaline concentration and the blood pressure. The effects were mediated by specific cannabinoid receptors, because they were also elicited by another cannabinoid agonist from a different chemical class, CP55940, but not by WIN55212-3, the enantiomer of WIN55212-2 possessing very low affinity for cannabinoid binding sites. Antagonism of the effect of

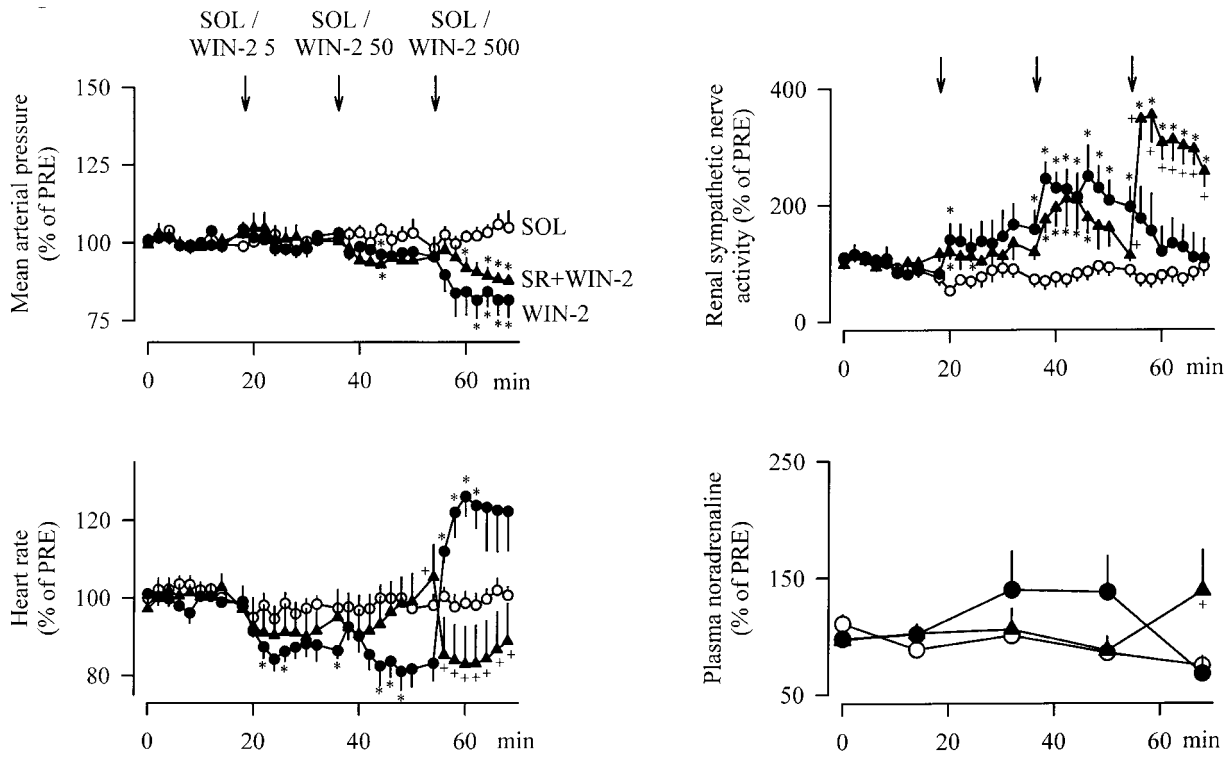

Figure 5 Effects of i.v. injections of solvent (SOL) and WIN 55212-2 (WIN-2) on mean arterial pressure, heart rate, renal sympathetic nerve activity and plasma noradrenaline concentration in conscious rabbits. SOL (0.5 ml kg^{-1}) and WIN-2 (5, 50 and 500 $\mu g\ kg^{-1}$) were injected as indicated by arrows. One of the two WIN-2-groups was pretreated at $t=-10$ min with SR141716A (SR; 500 $\mu g\ kg^{-1}$; i.v.). Values are given as percentages of PRE values (Table 1). Means ± s.e.mean from six (SOL), seven (WIN-2) and seven (SR + WIN-2) experiments. Differences from SOL: $^*P<0.05$; differences from WIN-2: $+P<0.05$.

WIN55212-2 by the CB_1-selective antagonist SR141716A (Rinaldi-Carmona *et al.*, 1994; Pertwee, 1997) verifies involvement of CB_1 cannabinoid receptors. Lack of full antagonism of the effects of the higher WIN55212-2 doses is probably due to insufficient tissue concentration of the antagonist during this late phase of the experiments. However, involvement of CB_2 cannabinoid receptors in the effects of the higher WIN55212-2 doses cannot be ruled out (see Griffin *et al.*, 1997, for peripheral neuronal CB_2 receptors). The blood pressure decrease seen after administration of WIN55212-2 was solely due to diminished release of transmitter, since WIN55212-2 did not influence vascular tone raised by an infusion of noradrenaline.

The diminished release of the sympathetic transmitter was probably not due to ganglionic inhibition, since it was mediated by cannabinoid receptors (see above) and since agonists of CB_1 and CB_2 cannabinoid receptors (Δ^9-tetrahydrocannabinol and anandamide) have no effect on ganglionic transmission (Cavero *et al.*, 1973a,b; Vollmer *et al.*, 1974; Varga *et al.*, 1996). The likely mechanism of the inhibition of transmitter release is activation of inhibitory prejunctional receptors on axon terminals of postganglionic sympathetic neurons. Such a mechanism is supported by *in vitro* observations: in mouse and rat vas deferens and rat heart, cannabinoids cause prejunctional inhibition (Pertwee *et al.*, 1992; Ishac *et al.*, 1996). Peripheral prejunctional inhibition of the release of sympathetic transmitter by cannabinoids in intact animals has been recently suggested by two groups. The suggestion by Varga *et al.* (1996) was based on their finding that cannabinoids reduced the increase in blood pressure, but not the increase in the sympathetic nerve firing rate, produced by electrical stimulation of presympathetic neurons in the rostral ventrolateral medulla oblongata. In the experiments of Malinowska *et al.* (1997) on pithed rats, cannabinoids reduced the electrical stimulation-evoked increase in blood pressure, but not the noradrenaline-evoked increase in blood pressure. It is interesting to note that results fully compatible with peripheral prejunctional inhibition of noradrenaline release by Δ^9-tetrahydrocannabinol were obtained by Cavero *et al.* already in 1973 (Cavero *et al.*, 1973b): in an anaesthetized dog preparation, in which the effect of Δ^9-tetrahydrocannabinol was restricted to peripheral tissues, Δ^9-tetrahydrocannabinol produced hypotension, and intact sympathetic innervation of the tissues was necessary for this effect. The authors did not conclude to peripheral prejunctional inhibition of noradrenaline release, probably because this type of neuromodulation was little known in 1973. Our results are the first demonstration of prejunctional inhibition of transmitter release from sympathetic neurons in a whole animal preparation by direct measurement of the transmitter. The inhibition of noradrenaline release and the hypotension was not accompanied by bradycardia in the present experiments. Bradycardia would be expected if noradrenaline release from cardiac sympathetic neurons were inhibited by a prejunctional mechanism. The explanation for the lack of a bradycardic response probably is the fact that cardiac sympathetic neurons are only weakly stimulated in our pithed rabbit preparation (see Szabo *et al.*, 1987).

The results obtained in pithed rabbits receiving a pressor infusion of noradrenaline permit two additional conclusions. Firstly, that WIN55212-2 has no direct effect on the heart. Secondly, and more importantly, that it does not cause direct vasoconstriction or vasodilatation. It was recently suggested that an endogenous cannabinoid may be involved in

endothelium-dependent vasorelaxation (Randall *et al*., 1996; Randall & Kendall, 1997). Lack of vasodilatation by an exogenous mixed CB_1/CB_2 cannabinoid receptor agonist makes it unlikely (at least in the rabbit) that an endogenous cannabinoid can serve as a vasodilator.

Central sympathoexcitation

Injection of WIN55212-2 into the cisterna cerebellomedullaris, i.e. into the vicinity of medullary and pontine cardiovascular regulatory centres, increased sympathetic tone as indicated by the elevated plasma concentration of noradrenaline. This sympathoactivation led to hypertension even despite marked bradycardia (see below). Experiments with antagonists were not carried out in this part of the study. Yet, involvement of cannabinoid receptors in the sympathoexcitation is likely, since very low doses of the selective (see Introduction) cannabinoid agonist WIN55212-2 elicited the response. Moreover, intracisternally applied CP55940 also increases blood pressure and the firing rate of renal sympathetic nerves (Niederhoffer & Szabo, unpublished observation). Cardiovascular effects of cannabinoids applied directly into the central nervous system have been studied, to our knowledge, three times. In cats, injection of Δ^9-tetrahydrocannabinol into the lateral cerebral ventricle elicited bradycardia without any change in blood pressure (Vollmer *et al*., 1974). In dogs with isolated and perfused cerebral circulation, cerebral administration of Δ^9-tetrahydrocannabinol caused bradycardia and hypotension (Cavero *et al*., 1973a,b). Thus, direct excitation of centres regulating sympathetic tone by cannabinoids was first observed in the present study, and it was demonstrated by measurement of the sympathetic transmitter in the blood. Increases in blood pressure, heart rate or vascular resistance after systemic administration of Δ^9-tetrahydrocannabinol have been repeatedly observed (Osgood & Howes, 1977; Jandhyala & Hamed, 1978; Benowitz *et al*., 1979; Kawasaki *et al*., 1980; Huestis *et al*., 1992); the sympathoexcitation shown in our study may be the basis of these changes.

Central activation of cardiac vagal efferents

Injection of low doses of WIN55212-2 into the cisterna cerebellomedullaris led to dose-dependent and strong bradycardia. Enhancement of cardiac vagal tone is the likely mechanism, since atropine antagonized the effect. Preliminary results show that intracisternally injected CP55940 also produces bradycardia (Niederhoffer & Szabo, unpublished observation). The bradycardia was also observed after systemic administration of WIN55212-2 (5 and 50 $\mu g\ kg^{-1}$), and this latter effect was attenuated by SR141716A. The results, thus, indicate that activation of CB_1 cannabinoid receptors in the brain stem enhances cardiac vagal activity. The nucleus tractus solitarii and the nucleus dorsalis nervi vagi possess cannabinoid binding sites (Mailleux & Vanderhaeghen, 1992) and, hence, are likely primary sites of action of cannabinoids for eliciting bradycardia. As mentioned above, bradycardia after central nervous application of cannabinoids was also observed by Vollmer *et al*. (1974) and Cavero *et al*. (1973a), and it was attributed to a decrease in cardiac sympathetic tone (Vollmer *et al*., 1974) and to enhanced cardiac vagal tone and to a decrease in cardiac sympathetic tone (Cavero *et al*., 1973a). Bradycardia has also been observed after systemic administration of cannabinoids and was thought to be partly due to an increase in cardiac vagal tone, since atropine, methylatropine or vagotomy attenuated the effect (Graham & Li, 1973; Varga *et al*., 1995; Vidrio *et al*., 1996).

Cooperation of primary actions after the two lower doses of WIN55212-2

Three primary effects of the cannabinoid agonist WIN55212-2 on cardiovascular function have been discussed separately above. Here we try to explain how the three effects combine to produce the overall cardiovascular response to this drug after systemic administration in conscious rabbits. The two lower doses of WIN55212-2 (5 and 50 $\mu g\ kg^{-1}$) are considered at first. Peripheral prejunctional inhibition of noradrenaline release by WIN55212-2 certainly operated in this model, yet blood pressure decreased only minimally, and the plasma noradrenaline concentration did not decrease. The explanation is the simultaneously occurring central sympathoexcitation, evident from the increase in firing of the renal sympathetic nerves; the primary site of action is probably the brain stem. The baroreceptor reflex probably also operates and counteracts the depressive effect of the peripheral prejunctional inhibition on blood pressure. The bradycardia observed after systemic administration is most probably due to enhancement of efferent cardiac vagal activity with a primary action in the brain stem.

Cooperation of primary actions after the highest dose of WIN55212-2: indication for central sympathoinhibition

The effects of the highest i.v. dose of WIN55212-2 (500 $\mu g\ kg^{-1}$) in conscious rabbits are more complex and not completely understood. Though blood pressure decreased markedly after this dose, sympathetic activity did not increase further (which would be expected from the central sympathoexcitation and from the function of the baroreflex), but declined toward the baseline which it reached at the end of the 14-min observation period; plasma noradrenaline decreased simultaneously. We interpret this decline in sympathetic activity as central sympathoinhibition. It is probably mediated by CB_1 receptors, because in animals pretreated with SR141716A, sympathetic nerve activity and the plasma noradrenaline concentration increased after the highest dose of WIN55212-2. The origin of the sympathoinhibition produced by WIN55212-2 is not known: sites of action rostrally or caudally from the brain stem, including the spinal cord, are all possible. Ganglionic inhibition cannot be excluded but seems unlikely, as discussed above. Not only sympathetic nerve activity and plasma noradrenaline changed their response pattern after the highest dose of WIN55212-2. The heart rate response changed as well: heart rate decreased after the two lower doses but increased after the highest dose. The mechanism of this tachycardia is not known, but baroreflex-mediated withdrawal of vagal tone in response to the hypotension is one possibility. As mentioned in the Introduction, Δ^9-tetrahydrocannabinol decreased blood pressure and heart rate in many experimental models (mostly anaesthetized animals) and this was often attributed to a central sympathoinhibition. The sympathoinhibition has been demonstrated directly only by Vollmer *et al*. (1974) by measurement of cardiac sympathetic nerve activity.

The present study reveals complex effects of a mixed CB_1/CB_2 cannabinoid receptor agonist on the cardiovascular system, including excitatory and inhibitory components. Enhancement and depression of cardiovascular function are both observed in humans consuming *Cannabis* products or receiving the main active component of *Cannabis*, Δ^9-tetrahydrocannabinol. For example, recrea-

tional doses of cannabinoids usually produce tachycardia with a slight increase in blood pressure (Benowitz *et al*., 1979; Huestis *et al*., 1992). In contrast, high doses or long-term application of cannabinoids can elicit orthostatic hypotension, hypotension and bradycardia (Benowitz & Jones, 1975).

The authors gratefully acknowledge the advice and support of Klaus Starke. The help of Claudia Schurr at determining plasma catecholamines was essential. We thank Pfizer (Groton, CT, U.S.A.) and Sanofi (Montpellier, France) for generous supply of CP55940 and SR141716A, respectively. The study was supported by the Deutsche Forschungsgemeinschaft (Sz 72/2-2). Dr Nathalie Niederhoffer is recipient of an Alexander von Humboldt fellowship.

References

ADAMS, M.D., CHAIT, L.D. & EARNHARDT, J.T. (1976). Tolerance to the cardiovascular effects of Δ^9-tetrahydrocannabinol in the rat. *Br. J. Pharmacol.,* **56,** 43 – 48.

BENOWITZ, N.L. & JONES, R.T. (1975). Cardiovascular effects of prolonged delta-9-tetrahydrocannabinol ingestion. *Clin. Pharmacol. Ther.,* **18,** 287 – 297.

BENOWITZ, N.L., ROSENBERG, J., ROGERS, W., BACHMAN, J. & JONES, R.T. (1979). Cardiovascular effects of intravenous delta-9-tetrahydrocannabinol: Autonomic nervous mechanisms. *Clin. Pharmacol. Ther.,* **25,** 440 – 446.

BIRMINGHAM, M.K. (1973). Reduction by Δ^9-tetrahydrocannabinol in the blood pressure of hypertensive rats bearing regenerated adrenal glands. *Br. J. Pharmacol.,* **48,** 169 – 171.

CAVERO, I., LOKHANDWALA, M.F., BUCKLEY, J.P. & JANDHYALA, B.S. (1974). The effect of (−)-Δ^9-trans-tetrahydrocannabinol on myocardial contractility and venous return in anesthetized dogs. *Eur. J. Pharmacol.,* **29,** 74 – 82.

CAVERO, I., SOLOMON, T., BUCKLEY J.P. & JANDHYALA, B.S. (1973a). Studies on the bradycardia induced by (−)-Δ^9-trans-tetrahydrocannabinol in anesthetized dogs. *Eur. J. Pharmacol.,* **22,** 263 – 269.

CAVERO, I., SOLOMON, T., BUCKLEY J.P. & JANDHYALA, B.S. (1973b). Studies on the hypotensive activity of (−)-Δ^9-trans-tetrahydrocannabinol in anesthetized dogs. *Res. Comm. Chem. Pathol. Pharmacol.,* **6,** 527 – 540.

COMPTON, D.R., HARRIS, L.S., LICHTMAN, A.H. & MARTIN, B.R. (1996). Marihuana. In *Pharmacological Aspects of Drug Dependence. Handbook of Experimental Pharmacology*. eds. Schuster, C.R. & Kuhar, M.J. pp. 83 – 158. Springer: Heidelberg.

DEWEY, W.L. (1986). Cannabinoid pharmacology. *Pharmacol. Rev.,* **38,** 151 – 178.

ESLER, M., JENNINGS, G., LAMBERT, G., MEREDITH, I., HORNE, M. & EISENHOFER, G. (1990). Overflow of catecholamine neurotransmitters to the circulation: source, fate, and functions. *Physiol. Rev.,* **70,** 963 – 985.

ESTRADA, U., BRASE, D.A., MARTIN, B.R. & DEWEY, W.L. (1987). Cardiovascular effects of Δ^9- and $\Delta^{9(11)}$-tetrahydrocannabinol and their interaction with epinephrine. *Life Sci.,* **41,** 79 – 87.

FELDER, C.C., JOYCE, K.E., BRILEY, E.M., MANSOURI, J., MACKIE, K., BLOND, O., LAI, Y., MA, A.L. & MITCHELL, R.L. (1995). Comparison of the pharmacology and signal transduction of the human cannabinoid CB_1 and CB_2 receptors. *Molec. Pharmacol.,* **48,** 443 – 450.

FREDERICKS, A.B., BENOWITZ, N.L. & SAVANAPRIDI, C.Y. (1981). The cardiovascular and autonomic effects of repeated administration of Δ-9-tetrahydrocannabinol to rhesus monkeys. *J. Pharmacol. Exp. Ther.,* **216,** 247 – 253.

GRAHAM, J.D.P. & LI, D.M.F. (1973). Cardiovascular and respiratory effects of cannabis in cat and rat. *Br. J. Pharmacol.,* **49,** 1 – 10.

GRIFFIN, G., FERNANDO, S.R., ROSS, R.A., McKAY, N.G., ASHFORD, M.L.J., SHIRE, D., HUFFMAN, J.W., YU, S., LAINTON, J.A.H. & PERTWEE, R.G. (1997). Evidence for the presence of CB_2-like cannabinoid receptors on peripheral nerve terminals. *Eur. J. Pharmacol.,* **339,** 53 – 61.

HOWLETT, A.C. (1995). Pharmacology of cannabinoid receptors. *Ann. Rev. Pharmacol. Toxicol.,* **35,** 607 – 634.

HUESTIS, M.A., SAMPSON, A.H., HOLICKY, B.J., HENNINGFIELD, J.E. & CONE, E.J. (1992). Characterization of the absorption phase of marijuana smoking. *Clin. Pharmacol. Ther.,* **52,** 31 – 41.

ISHAC, E.J.N., JIANG, L., LAKE, K.D., VARGA, K., ABOOD, M.E. & KUNOS, G. (1996). Inhibition of exocytotic noradrenaline release by presynaptic cannabinoid CB_1 receptors on peripheral sympathetic nerves. *Br. J. Pharmacol.,* **118,** 2023 – 2028.

JANDHYALA, B.S. & HAMED, A.T. (1978). Pulmonary and systemic hemodynamic effects of Δ^9-tetrahydrocannabinol in conscious and morphine-chloralose-anesthetized dogs: anesthetic influence on drug action. *Eur. J. Pharmacol.,* **53,** 63 – 68.

KAWASAKI, H., WATANABE, S. & UEKI S. (1980). Effects of chronic administration of Δ^9-tetrahydrocannabinol on the cardiovascular system, and pressor and behavioral responses to brain stimulation in freely moving rats. *Eur. J. Pharmacol.,* **65,** 63 – 69.

KUSTER, J.E., STEVENSON, J.I., WARD, S.J., D'AMBRA, T.E. & HAYCOCK, D.A. (1993). Aminoalkylindole binding in rat cerebellum: selective displacement by natural and synthetic cannabinoids. *J. Pharmacol. Exp. Ther.,* **264,** 1352 – 1363.

LAKE, K.D., COMPTON, D.R., VARGA, K., MARTIN, B.R. & KUNOS, G. (1997a). Cannabinoid-induced hypotension and bradycardia in rats is mediated by CB_1-like cannabinoid receptors. *J. Pharmacol. Exp. Ther.,* **281,** 1030 – 1037.

LAKE, K.D., MARTIN, B.R., KUNOS, G. & VARGA, K. (1997b). Cardiovascular effects of anandamide in anesthetized and conscious normotensive and hypertensive rats. *Hypertension,* **29,** 1204 – 1210.

MAILLEUX, P. & VANDERHAEGHEN, J.J. (1992). Distribution of neuronal cannabinoid receptor in the adult rat brain: a comparative receptor binding radioautography and *in situ* hybridization histochemistry. *Neuroscience,* **48,** 655 – 668.

MALINOWSKA, B., GODLEWSKI, G., BUCHER, B. & SCHLICKER, E. (1997). Cannabinoid CB_1 receptor-mediated inhibition of the neurogenic vasopressor response in the pithed rat. *Naunyn-Schmiedeberg's Arch. Pharmacol.,* **356,** 197 – 202.

MARTIN, B.R. (1986). Cellular effects of cannabinoids. *Pharmacol. Rev.,* **38,** 45 – 74.

MATSUDA, L.A., LOLAIT, S.J., BROWNSTEIN, B.J., YOUNG, A.C. & BONNER, T.I. (1990). Structure of a cannabinoid receptor and functional expression of the cloned cDNA. *Nature,* **346,** 561 – 564.

MUNRO, S., THOMAS, K.L. & ABU-SHAAR, M. (1993). Molecular characterization of a peripheral receptor for cannabinoids. *Nature,* **365,** 61 – 65.

OSGOOD, P.F. & HOWES, J.F. (1977). Δ^9-tetrahydrocannabinol and dimethyl-heptylpyran induced tachycardia in the conscious rat. *Life Sci.,* **21,** 1329 – 1336.

PERTWEE, R.G. (1997). Pharmacology of cannabinoid CB_1 and CB_2 receptors. *Pharmacol. Ther.,* **74,** 129 – 180.

PERTWEE, R.G., STEVENSON, L.A., ELRICK, D.B., MECHOULAM, R. & CORBETT, A.D. (1992). Inhibitory effects of certain enantiomeric cannabinoids in the mouse vas deferens and the myenteric plexus preparation of guinea-pig small intestine. *Br. J. Pharmacol.,* **105,** 980 – 984.

RANDALL, M.D., ALEXANDER, S.P.H., BENNETT, T., BOYD, E.A., FRY, J.R., GARDINER, S.M., KEMP, P.A., McCULLOCH, A.I. & KENDALL, D.A. (1996). An endogenous cannabinoid as an endothelium-derived vasorelaxant. *Biochem. Biophys. Res. Comm.,* **229,** 114 – 120.

RANDALL, M.D. & KENDALL, D. A. (1997). Involvement of a cannabinoid in endothelium-derived hyperpolarizing factor-mediated coronary vasorelaxation. *Eur. J. Pharmacol.,* **335,** 205 – 209.

RINALDI-CARMONA, M., BARTH, F., HEAULME, M., SHIRE, D., CALANDRA, B., CONGY, C., MARTINEZ, S., MARUANI, J., NELIAT, G., CAPUT, D., FERRARA, P., SOUBRIE, P., BRELIERE, J.C. & LE FUR, G. (1994). SR141716A, a potent and selective antagonist of the brain cannabinoid receptor. *FEBS Lett.* **350,** 240 – 244.

SHOWALTER, V.M., COMPTON, D.R., MARTIN, B.R. & ABOOD, M.A. (1996). Evaluation of binding in a transfected cell line expressing a peripheral cannabinoid receptor (CB2): identification of cannabinoid receptor subtype selective ligands. *J. Pharmacol. Exp. Ther.,* **278,** 989 – 999.

STARK, P. & DEWS, P.B. (1980). Cannabinoids. II. Cardiovascular effects. *J. Pharmacol. Exp. Ther.,* **214,** 131 – 138.

STEIN, E.A., FULLER, S.A., EDGEMOND, W.S. & CAMPBELL, W.B. (1996). Physiological and behavioural effects of the endogenous cannabinoid, arachidonylethanolamide (anandamide), in the rat. *Br. J. Pharmacol.,* **119,** 107 – 114.

SZABO, B., HEDLER, L., LICHTWALD, K. & STARKE, K. (1987). ACTH increases noradrenaline release in pithed rabbits with electrically stimulated sympathetic outflow. *Eur. J. Pharmacol.,* **136,** 391 – 399.

SZABO, B. & SCHULTHEISS, A. (1990). Desipramine inhibits sympathetic nerve activity in the rabbit. *Naunyn-Schmiedeberg's Arch. Pharmacol.,* **342,** 469 – 476.

SZABO, B., URBAN, R., LIMBERGER, N. & STARKE, K. (1995). Cardiovascular effects of agmatine, a 'clonidine-displacing substance', in conscious rabbits. *Naunyn-Schmiedeberg's Arch. Pharmacol.,* **351,** 268 – 273.

SZABO, B., URBAN, R. & STARKE, K. (1993). Sympathoinhibition by rilmenidine in conscious rabbits: involvement of α_2-adrenoceptors. *Naunyn-Schmiedeberg's Arch. Pharmacol.,* **348,** 593 – 600.

URBAN, R., SZABO, B. & STARKE, K. (1995). Involvement of peripheral presynaptic inhibition in the reduction of sympathetic tone by moxonidine, rilmenidine and UK 14304. *Eur. J. Pharmacol.,* **282,** 29 – 37.

VARGA, K., LAKE, K.D., HUANGFU, D., GUYENET, P.G. & KUNOS, G. (1996). Mechanism of the hypotensive action of anandamide in anesthetized rats. *Hypertension,* **28,** 682 – 686.

VARGA, K., LAKE, K., MARTIN, B.R. & KUNOS, G. (1995). Novel antagonist implicates the CB_1 cannabinoid receptor in the hypotensive action of anandamide. *Eur. J. Pharmacol.,* **278,** 279 – 283.

VIDRIO, H., SANCHEZ-SALVATORI, M.A. & MEDINA, M. (1996). Cardiovascular effects of (−)-11-OH-Δ^8-tetrahydrocannabinol-dimethylheptyl in rats. *J. Cardiovasc. Pharmacol.,* **28,** 332 – 336.

VOLLMER, R.R., CAVERO, I., ERTEL, R.J., SOLOMON, T.A. & BUCKLEY, J.P. (1974). Role of the central autonomic nervous system in the hypotension and bradycardia induced by (−)-Δ^9-trans-tetrahydrocannabinol. *J. Pharm. Pharmacol.,* **26,** 186 – 192.

(Received June 4, 1998
Revised October 24, 1998
Accepted November 4, 1998)

British Journal of Pharmacology (1999) 126, 467–477
http://www.stockton-press.co.uk/bjp

Effects of vanadium complexes with organic ligands on glucose metabolism: a comparison study in diabetic rats

[1]Bénédicte A. Reul, [3]Sean S. Amin, [2]Jean-Pierre Buchet, [1]Lumbe N. Ongemba, [3]Debbie C. Crans & *,[1]Sonia M. Brichard

[1]Endocrinology and Metabolism Unit, UCL 5530 AV Hippocrate 55, B-1200 Brussels, Belgium; [2]Industrial Toxicology Unit, University of Louvain, Faculty of Medicine, B-1200 Brussels, Belgium and [3]Department of Chemistry, Colarado State University, Fort Collins, Colorado, U.S.A.

1 Vanadium compounds can mimic actions of insulin through alternative signalling pathways. The effects of three organic vanadium compounds were studied in non-ketotic, streptozotocin-diabetic rats: vanadyl acetylacetonate (VAc), vanadyl 3-ethylacetylacetonate (VEt), and bis(maltolato)oxovanadium (VM). A simple inorganic vanadium salt, vanadyl sulphate (VS) was also studied.

2 Oral administration of the three organic vanadium compounds (125 mg vanadium element l^{-1} in drinking fluids) for up to 3 months induced a faster and larger fall in glycemia (VAc being the most potent) than VS. Glucosuria and tolerance to a glucose load were improved accordingly.

3 Activities and mRNA levels of key glycolytic enzymes (glucokinase and L-type pyruvate kinase) which are suppressed in the diabetic liver, were restored by vanadium treatment. The organic forms showed greater efficacy than VS, especially VAc.

4 VAc rats exhibited the highest levels of plasma or tissue vanadium, most likely due to a greater intestinal absorption. However, VAc retained its potency when given as a single i.p. injection to diabetic rats. Moreover, there was no relationship between plasma or tissue vanadium levels and any parameters of glucose homeostasis and hepatic glucose metabolism. Thus, these data suggest that differences in potency between compounds are due to differences in their insulin-like properties.

5 There was no marked toxicity observed on hepatic or renal function. However, diarrhoea occurred in 50% of rats chronically treated with VS, but not in those receiving the organic compounds.

6 In conclusion, organic vanadium compounds, in particular VAc, correct the hyperglycemia and impaired hepatic glycolysis of diabetic rats more safely and potently than VS. This is not simply due to improved intestinal absorption, indicating more potent insulin-like properties.

Keywords: Vanadium; organic ligands; glycolytic enzymes; gluconeogenic enzymes; gene expression; antidiabetic agents; streptozotocin-diabetic rats; toxicity

Abbreviations: C, non-diabetic control rats; D, untreated diabetic rats; GK, Glucokinase; L-PK, L-type pyruvate kinase; OGTT, oral glucose tolerance test; PEPCK, phosphoenolpyruvate carboxykinase; STZ, streptozotocin; VAc, vanadyl acetylacetonate; VEt, vanadyl ethylacetylacetonate; VM, bis(maltolato)oxovanadium; VS, vanadyl sulphate; WM, weight-matched diabetic rats

Introduction

Vanadium compounds mimic actions of insulin through alternative signalling pathways which involve the inhibition of phosphotyrosine phosphatases and the interplay between two non-insulin receptor tyrosine kinases (Elberg *et al*., 1997; Tsiani & Fantus, 1997). The insulin-like potential of vanadium has been demonstrated *in vitro*, and *in vivo* in rodents (where the oxidation states IV and V were found to be equipotent (Becker *et al*., 1994)), and more recently in human diabetic subjects (see Brichard & Henquin, 1995; Tsiani & Fantus, 1997). The clinical studies performed so far have used the simple naturally occurring inorganic vanadium salts (metavanadate (V) or vanadyl sulphate (VS, IV)) (Cohen *et al*., 1995; Goldfine *et al*., 1995; Boden *et al*., 1996).

Vanadium compounds have been synthesized (Posner *et al*., 1994; Caravan *et al*., 1995; Sakurai *et al*., 1995; Crans *et al*., 1997), among which organic vanadium (IV) complexes (vanadyl cation coordinated to an organic ligand) merit further attention. This study will focus on three of these complexes: vanadyl acetylacetonate (VAc), vanadyl 3-ethylacetylacetonate (VEt) and bis(maltolato)oxovanadium (VM). VM is the first and most studied vanadium complex in diabetic rodents. When administered acutely, VM is two to three times more effective than its inorganic analogue VS in lowering blood glucose. However, no direct comparison of the long-term effects of VM with VS has been reported (Yuen *et al*., 1993a,b; Yuen *et al*., 1995). VM has been licensed and is targeted to enter clinical trials in the near future (Orvig, personal communication). Recently, VAc was found to be a more potent stimulator of lipogenesis than VS in isolated rat adipocytes (Li *et al*., 1996). However, the potential efficiency of this compound has not yet been determined *in vivo*. VEt is a newly synthesized compound chemically related to VAc, the insulin-like properties of which have not been characterized.

In the present study, we compared the long-term effects of VAc, VEt and VM on glucose homeostasis and hepatic glucose metabolism in low-dose streptozotocin-treated rats which developed a non-ketotic, insulin-deficient condition of diabetes. The inorganic salt, VS, was also studied.

* Author for correspondence.

Methods

Animals

Male Wistar/CPB rats (7-week-old; 220 ± 1 g) were purchased from IFFA Credo (Brussels, Belgium) and used in two distinct experiments based on different routes and durations of vanadium administration. The animals were housed in individual cages at a constant temperature (22°C) with a fixed 12-h-light-dark cycle (lights on 07.00 – 19.00 h). In experiment 1, they were also housed for 1 week (week 8 of treatment) in metabolic cages permitting daily recording of food consumption and urine volume as well as daily fluid intake. All rats received a standard pellet diet (A04, Usine d'Alimentation Rationnelle, Villemoisson-sur-Orge, France) composed of (% of wet weight): 59 carbohydrate, 3 fat, 17 protein, 21 water-minerals-cellulose. Non-ketotic diabetes was induced by an i.v. injection of streptozotocin (STZ; 38 mg per kg body weight) into a tail vein. STZ was dissolved in cold 0.1 mol l^{-1} citrate buffer (pH 4.5) immediately before use. Control animals received buffer only.

All procedures have been approved by the University Animal Care Committee.

Experimental design

Experiment 1: Long-term administration of oral vanadium compounds Two separate populations of rats were used in this experiment; although, as the results obtained in both series were similar, they were pooled for presentation. In total, 64 rats were divided into seven experimental groups: non-diabetic control rats (C; $n=6$), untreated diabetic rats (D; $n=8$), and diabetic rats treated with one of the following four vanadium compounds [bis(maltolato)oxovanadium (VM; $n=10$), vanadyl ethylacetylacetonate (VEt; $n=11$), vanadyl acetylacetonate (VAc; $n=11$) and vanadyl sulphate (VS; $n=10$)], and calorie-restricted diabetic rats which were matched for body weight with the treated rats (weight-matched, WM; $n=8$). Seven days after injection of citrate buffer, body weight, plasma glucose and insulin levels of C rats were 258 ± 3 g, 6.4 ± 0.1 mmol l^{-1} and 3.5 ± 0.5 ng ml^{-1}, respectively. Seven days after injection of STZ, diabetic rats were assigned to untreated, weight-matched or treated groups as mentioned above. The six groups of diabetic rats had similar pre-treatment body weight (D, 238 ± 4 g; WM: 240 ± 4 g; VM, 238 ± 3 g; VEt, 240 ± 4 g; VAc, 240 ± 5 g; VS, 239 ± 3 g) and fed plasma glucose levels (D, 25.2 ± 0.7 mmol l^{-1}; WM, 25.3 ± 0.6 mmol l^{-1}; VM, 25.4 ± 0.8 mmol l^{-1}; VEt, 24.1 ± 1 mmol l^{-1}; VAc, 24.2 ± 1 mmol l^{-1}; VS, 25.1 ± 0.9 mmol l^{-1}). They were also matched, as seen *a posteriori*, for pre-treatment fed plasma insulin concentrations (D, 1.5 ± 0.6 ng ml^{-1}; WM, 1.8 ± 0.2 ng ml^{-1}; VM, 1.7 ± 0.2 ng mg^{-1}; VAc, 1.8 ± 0.2 ng ml^{-1}; VEt, 1.8 ± 0.2 ng ml^{-1}; VS, 1.6 ± 0.3 ng ml^{-1}).

The four treated groups received the appropriate vanadium compound dissolved in drinking solutions (distilled water empirically supplemented with 85 mmol l^{-1} NaCl; Heyliger *et al*., 1985), and solutions were freshly prepared every second day. Vanadyl acetylacetonate ($C_{10}H_{14}O_5V$) and vanadyl sulphate ($VOSO_4.3H_2O$) are commercially available, bis(maltolato)oxovanadium ($C_{12}H_{14}O_8V$) was prepared as previously described (Caravan *et al*., 1995) and vanadyl 3-ethylacetylacetonate ($C_{14}H_{22}O_5V$) was synthesized specifically for this experiment (Figure 1). Briefly, vanadyl 3-ethylacetylacetonate was obtained by adding 3-ethyl-2,4-pentanedione (5.00 g, 39.0 mmol) to vanadyl sulphate trihydrate (3.80 g, 17.5 mmol) in an acidic solution (10% H_2SO_4). In order for complexation to occur, the pH was raised to 6 with 10% sodium bicarbonate solution. Purification of the compound was achieved by dissolving the compound in chloroform, removing the impurities by filtration, and evaporating the solvent to dryness (Amin *et al*., manuscript submitted). As VEt was only moderately soluble in aqueous solution, it was necessary to sonicate it in order to obtain a complete dissolution. The colours of the administration solutions were as follows: VS, blue; VAc, turquoise; VEt, green and VM, yellowish-green.

The quantity required of each compound was calculated to yield the *same concentration of vanadium element* in the drinking solutions in all four groups. To partially overcome an initial aversion to the taste of vanadium and to ensure long-term fluid intake, this concentration was progressively increased during the first 4 weeks (from 40 to 125 mg l^{-1}), then remained unchanged until the end of the study (11 – 12 weeks). Vanadium intake per rat (expressed per kg body weight) was calculated on the basis of body weight, fluid intake, molecular mass and concentration. Because vanadium treatment was accompanied by a reduced weight gain, which may possibly influence glucose homeostasis (see Brichard & Henquin, 1995), a last group of untreated diabetic rats (WM) received a restricted amount of food to ensure a body weight gain similar to that of vanadium-treated rats. This amount was empirically adjusted daily and administered in two rations (one-third at 09.30 h and two-thirds at 18.00 h).

Experiment 2: Acute administration of intraperitoneal vanadium compounds Seven days after STZ injection, 32 diabetic rats were divided into four experimental groups treated with one of the four vanadium compounds (VM, $n=8$; VEt, $n=8$; VAc, $n=8$; VS, $n=8$). Rats received food *ad libitum* throughout the experiment. As in experiment 1, the four groups of rats were matched for pre-treatment body weight (VM, 231 ± 2 g; VEt, 230 ± 3 g; VAc, 231 ± 5 g; VS, 229 ± 4 g). They were also matched for pre-treatment fed plasma glucose levels. We had

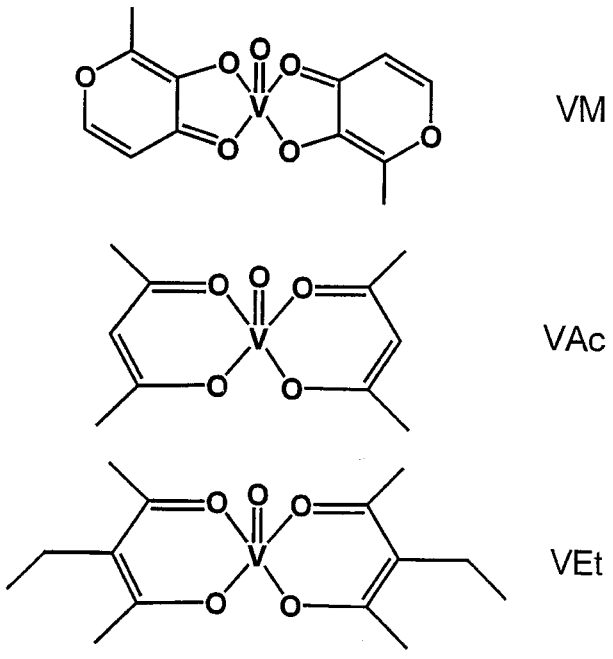

Figure 1 Chemical structures of the vanadium complexes with organic ligands: bis(maltolato)oxovanadium (VM), vanadyl acetylacetonate (VAc) and vanadyl ethylacetylacetonate (VEt).

also checked that i.p. injection of saline the day before the treatment (day −1) did not modify the glycemia (day 0). Thus, fed (08.30–09.00 h) plasma glucose levels (mmol l^{-1}) on days −1 and 0 were, respectively, 24.8±0.9 and 25.6±0.8 in VM, 25.1±0.8 and 25.7±0.5 in VEt, 25.0±1.1 and 26.1±1.3 in VAc, and 25.0±0.7 and 25.5±0.7 in VS rats. On day 0 (i.e. 7 days after STZ), rats received at 09.30 h a single i.p. injection of the appropriate compound dissolved in 9 g l^{-1} NaCl at a dose of 1.275 mg (or 0.025 mmol) vanadium element per kg body weight. This dose, much lower than that administered orally, was estimated from the knowledge that intestinal absorption of vanadium is low (Llobet & Domingo, 1984), and based on doses used in previous work (Yuen *et al*., 1993a). Subsequently, body weight was monitored on a daily basis and plasma glucose levels were measured on days 1, 4 and 5 after i.p. injection.

Sampling and tests

On several occasions, tail vein blood (100 μl) was collected from fed rats (between 08.30–09.00 h) for the determination of plasma glucose levels.

In experiment 1, at some time points, larger blood samples (250 μl) were also collected for plasma insulin or vanadium measurements. Additionally, all rats from this experiment underwent an oral glucose tolerance test (OGTT) after 6 weeks of treatment. On the day before the test, food was removed at 18.00 h (thus, WM rats did not receive their evening ration). The test started at 08.30 h. Glucose (30% w/v in water) was introduced directly into the stomach through a fine gastric catheter at a dose of 2 g kg body wt^{-1}. Rats were gently wrapped in a towel to restrain them during blood sampling. Between 11 and 12 weeks of treatment, the rats were killed by decapitation between 01.30 and 04.30 h (i.e. in the absorptive state). Pancreas, liver and muscle (tibialis anterior) were immediately removed, frozen in liquid nitrogen and stored at −70°C for subsequent insulin or RNA extraction, and for enzyme or vanadium measurements. Blood samples were also collected for determination of toxicological parameters.

RNA extraction and Northern blot analysis

Total RNA was isolated with an acid guanidinium-thiocyanate-phenol-chloroform mixture after removal of liver glycogen as previously described (Ozcelikay *et al*., 1996). The concentration of RNA was determined by absorbance at 260 nm. At 260–280 nm, all samples had an absorbance ratio of about 1.8. For Northern blot analysis, RNA (30 μg) was denaturated in a solution containing 2.2 mM formaldehyde and 50% formamide (v/v) by heating at 95°C for 2 min. RNA was then size-fractionated by 1% agarose gel electrophoresis, transferred to a Hybond-N membrane (Amersham Int., Amersham, Bucks, U.K.) and cross-linked by ultraviolet irradiation. The integrity and relative amounts of RNA were assessed by methylene blue staining of the blot.

The cDNA probes were kindly supplied by Drs P. Iynedjian for glucokinase (GK) (Iynedjian *et al*., 1987). A Kahn for pyruvate kinase (L-PK) (Simon *et al*., 1983) and R.W. Hanson for phosphoenolpyruvate carboxykinase (PEPCK) (Yoo-Warren *et al*., 1983). Probes were labelled with ^{32}P using the Multiprime labelling system kit (Amersham). Hybridizations with GK, L-PK, PEPCK probes and subsequent washings of the membranes were performed as reported earlier (Ozcelikay *et al*., 1996; Reul *et al*., 1997). The filters were thereafter exposed to Kodak X-OMAT AR films for 2–72 h at −70°C with intensifying screens. The same filters were successively hybridized with the different radiolabelled cDNA probes. The intensity of the mRNA bands on the blots was quantified by scanning densitometry (Sharp Scanner JX 325 combined with Image Master Software, Pharmacia, Uppsala, Sweden). To verify that each lane was loaded with equivalent amounts of total RNA, blots were hybridized with a synthetic oligonucleotide specific for ribosomal 18S RNA (Chan *et al*., 1984), and then levels of specific mRNAs were expressed relative to those of ribosomal 18S RNA.

Measurement of enzyme activities

The activities of GK (EC 2.7.1.1), L-PK (EC 2.7.1.40) and PEPCK (EC 4.1.1.32) were measured at 37°C, as previously described (Ozcelikay *et al*., 1996). L-PK activity was measured at 6.6 mM phosphoenolpyruvate (PEP) which corresponds to the maximal activity of the enzyme. Results were expressed as milliunits (mU) of enzyme per mg protein of liver cytosolic fraction, 1 mU of enzyme being defined as that amount which catalyzes the conversion of 1 nmol substrate per min under the assay conditions.

Analytical procedures

Plasma glucose was measured by a glucose oxidase method (Glucose Analyzer, Beckman, Fullerton, CA, U.S.A.) Plasma insulin was determined by a double-antibody radioimmunoassay, using rat insulin as standard (Novo Research Institute, Bagsvaerd, Denmark). Pancreatic insulin was extracted by homogenization and sonication of the tissue in acidified ethanol. Liver glycogen was measured after extraction with KOH, precipitation in ethanol, and hydrolysis with α-amyloglucosidase. Plasma urea, creatinine, glutamic-oxaloacetic transaminase, and glutamic-pyruvic transaminase were measured with a Hitachi 717 Automatic Analyzer (Tokyo, Japan). Proteins in liver cytosolic fractions or in urine were determined by the method of Bradford (Bio-Rad, Munich, Germany), using bovine serum albumin as standard. Plasma and tissue vanadium levels were measured by atomic absorption spectrometry, as described previously (Buchet *et al*., 1982).

Materials

STZ was obtained from Upjohn Co. (Kalamazoo, MI, U.S.A.), VAc and VS from Aldrich Chemie (Steinheim, Germany), molecular biology reagents from Sigma Chemical Co. (St. Louis, MO, U.S.A.) and substrates for measurement of enzyme activities from Boehringer-Mannheim (Mannheim, Germany).

Statistical analysis

Results are presented as means±s.e.mean for the indicated numbers of rats. Comparisons between the different groups of rats were carried out by analysis of variance followed by the Newman-Keuls test for multiple comparisons. When indicated, comparisons were performed between only two groups of rats by the unpaired Student's *t*-test. In experiment 2, the acute decrease in glycemia produced by the treatment was analysed within a same group by repeated measures of analysis of variance followed by the Newman-Keuls test. The correlation analysis was performed using Pearson's test. Differences were considered statistically significant when $P<0.05$.

Results

Experiment 1: Long-term administration of oral vanadium compounds

As expected, untreated diabetic (D) rats gained weight at a much lower rate than control (C) rats (Figure 2). The body weight of vanadium-treated rats (VM, VEt, VAc, VS) was slightly but similarly decreased in comparison to D rats (this phenomenon could partly be explained by an aversion to the element, Brichard *et al*., 1988). Diabetic rats submitted to moderate calorie restriction (WM) exhibited a body weight gain similar to that of treated rats (Figure 2). Average fed plasma glucose levels were around 25 mmol l^{-1} in D rats. Hyperglycemia was unmodified by calorie restriction, but was decreased by vanadium treatment. Among these compounds, VAc induced the fastest (from the fifth day onward) and largest decrease in glycemia [$P<0.05$ or less *vs* VS throughout the study (except at week 6) and *vs* VM or VEt at most time points]. Average fed plasma insulin levels were not

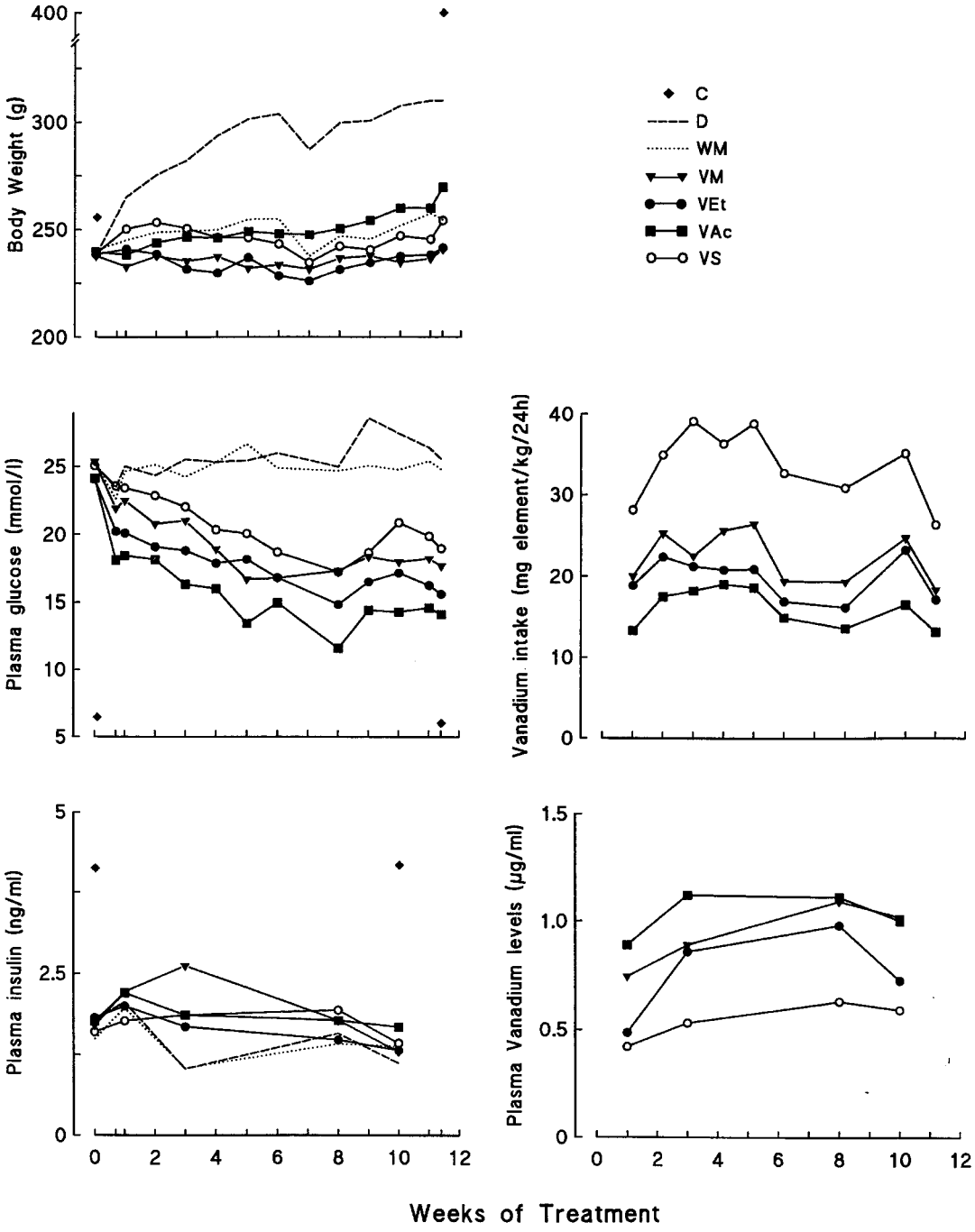

Figure 2 Influence of treatment with vanadium compounds on body weight, plasma glucose and insulin levels, and plasma concentrations and intake of vanadium in diabetic rats. Vanadium-treated diabetic rats receiving either VM, VEt, VAc or vanadyl sulphate (VS) compounds were compared to non-diabetic control (C), untreated diabetic (D) and body weight-matched diabetic (WM) rats. Each treated group received the same concentration of vanadium element in drinking solutions. This concentration was progressively increased during the first 4 weeks of the experiment (from 40 mg l^{-1} to 125 mg l^{-1}), and then remained unchanged until the end of the study (i.e. between 11 and 12 weeks). Values are means for 6–11 rats in each group. s.e.mean which were always <10% of the mean (except for insulin, 20% at week 3) were omitted for sake of clarity.

significantly different between vanadium-treated and untreated (D and WM) diabetic rats, and were reduced by ~50% compared to C rats ($P<0.01$ or less at each sampling).

The metabolic balance of the seven groups of rats was measured during week 8 of the treatment (Figure 3). Diabetic polydypsia, polyuria and glucosuria were partly attenuated by mere calorie restriction in WM rats, whereas larger reductions were produced by vanadium treatment. These reductions were more pronounced in rats treated with VM, VEt or VAc than in those treated with VS (Figure 3). Accordingly, daily consumption of vanadium element (provided in drinking solutions) was lower ($P<0.05$ or less) in rats receiving the organic compounds than in those receiving VS (Figure 2). In spite of higher levels of vanadium intake, VS rats exhibited the lowest ($P<0.05$ or less) levels of plasma vanadium throughout the study (Figure 2). Thus, there was no correlation between daily vanadium intake and the corresponding plasma vanadium levels at any time point studied ($r\leqslant 0.02$; data not shown). VS rats also presented the greatest urinary excretion rate of vanadium, possibly due to their higher urine output (Figure 3). Daily food intake was increased ~2.4 fold in D rats. It proved necessary to reduce by ~45% food consumption of WM rats to ensure a body weight evolution similar to that of treated rats. The energy consumption of rats receiving VM, VEt or VAc was slightly depressed when compared to those receiving VS. However, when food intake was corrected for urinary losses of glucose, energy consumption (cal/rat d^{-1}) was similar in all four groups of treated rats (VM: 43 ± 1; VEt: 43 ± 3; VAc: 45 ± 2; VS: 50 ± 3) (as well as in WM rats: 48 ± 2).

After an overnight fast, plasma glucose concentrations (time 0 of the OGTT) were lower ($P<0.01$ or less) in the four groups of treated rats than in D or WM rats, but were not different from those in C rats (Figure 4). Fasting plasma insulin levels were similar in diabetic rats whether they were treated or not, and were reduced by ~60% compared to those in C rats ($P<0.05$ or less, scarcely visible in Figure 4).

During the OGTT, plasma glucose levels remained less than 10 mmol l^{-1} in C rats, but rose to more than 30 mmol l^{-1} in D and WM rats and did not thereafter return to basal levels (Figure 4). In the four groups of vanadium-treated rats, glucose concentrations were consistently lower ($P<0.01$ or less) than in D or WM rats and were normalized at 180 min. Importantly, among the four treated groups, VAc rats had significantly lower plasma glucose levels than VS rats during the surge of glycemia ($P\leqslant 0.05$ or less at 15, 30 and 60 min by *t*-test). Accordingly, the integrated glucose responses (areas under the curves and above basal values) were reduced by ~35–60% in vanadium-treated rats as compared to D and WM rats, and by 25% in VAc rats compared to VS rats. In contrast to the rise of plasma insulin levels in C rats, the insulinemia and associated integrated insulin responses did not change and were similarly blunted in all six groups of diabetic rats (Figure 4).

Pancreatic insulin reserves (in μg pancreas^{-1}) were also markedly reduced (by ~95%, $P<0.001$) in diabetic rats whether they were treated (VM: 5 ± 0.8; VEt: 8 ± 3.2; VAc: 7 ± 1.6; VS: 3 ± 0.3) or not (D: 3 ± 0.6; WM: 3 ± 0.9), as compared to those in C rats (163 ± 13).

Hepatic glycogen stores (in mg g liver^{-1}), which were decreased by 55% in D rats (18 ± 2 *vs* 40 ± 3 in C rats;

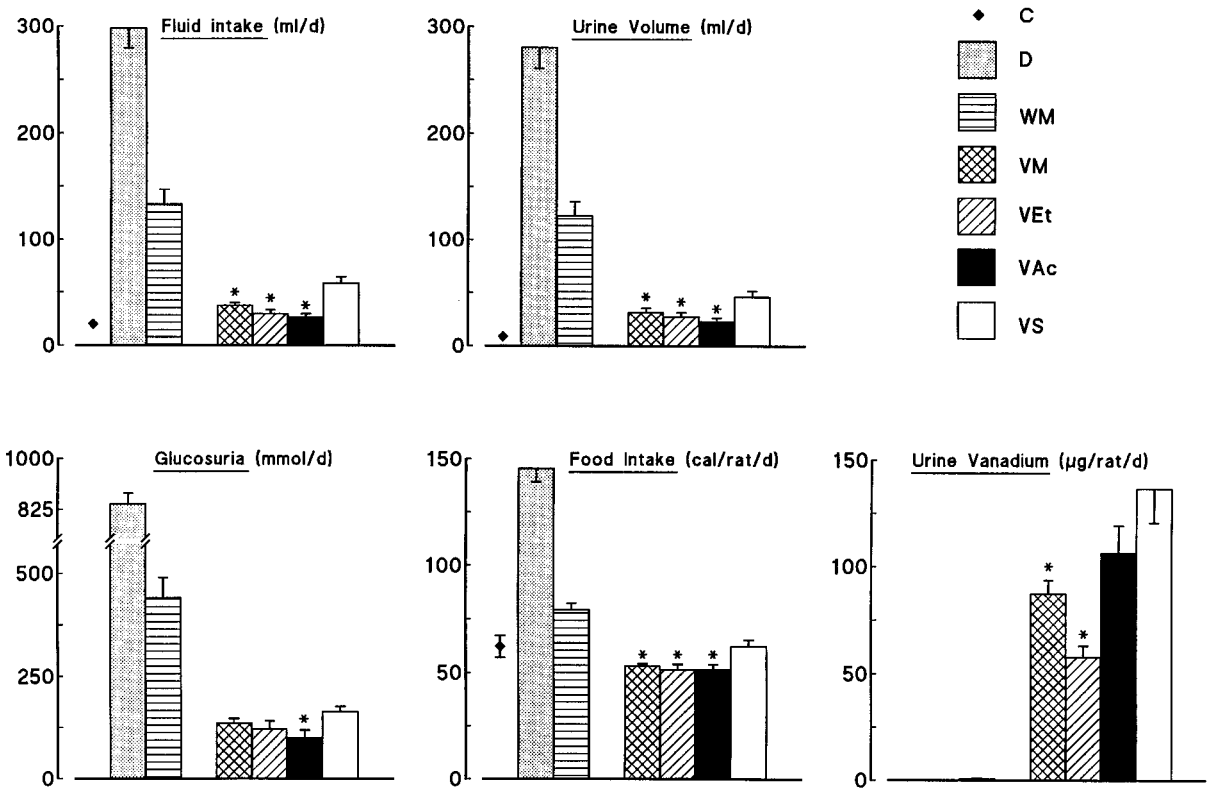

Figure 3 Metabolic balance of control (C), untreated diabetic (D), body weight-matched diabetic (WM) and vanadium-treated diabetic rats receiving one of the following compounds: bis(maltolato)oxovanadium (VM), vanadyl ethylacetylacetonate (VEt), vanadyl acetylacetonate (VAc) or (VS). Measurements were made daily during week 8 of the treatment, while the animals were housed in metabolic cages. Values are means$\pm$s.e.mean for 6–11 rats in each group. *$P<0.05$ or less for the indicated group of rats treated with organic (VM, VEt or VAc) *vs* inorganic (VS) vanadium compounds [ANOVA or *t*-test for glucosuria].

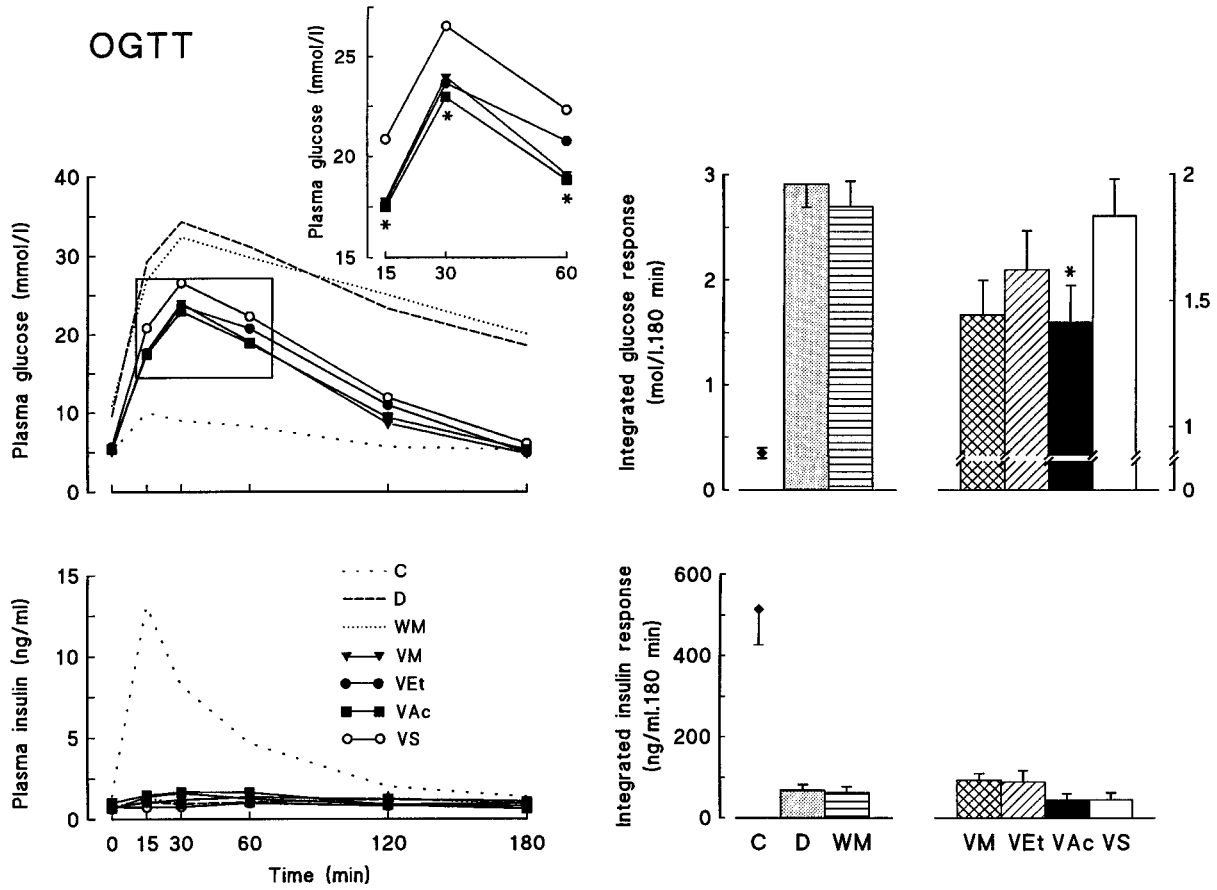

Figure 4 (Left panels) Plasma glucose and insulin levels during an oral glucose tolerance test (OGTT) in control (C), untreated diabetic (D), body weight-matched diabetic (WM) and vanadium-treated diabetic rats receiving either VM, VEt, VAc or VS compounds. (Insert) Early time points of glycemia in vanadium-treated rats. (Right panels) Integrated glucose and insulin responses during the OGTT. The test was performed after 6 weeks of treatment. Values are means $\pm$ s.e.mean for 6–11 rats in each group. In the left panels, s.e.mean which were always $<10\%$ of the mean were omitted for sake of clarity. $^*P \leqslant 0.05$ for the indicated group of rats treated with organic (VM, VEt or VAc) *vs* inorganic (VS) vanadium compounds (*t*-test).

$P<0.001$), were unmodified by calorie restriction (26 ± 3), but were fully and similarly replenished by vanadium treatment (VM: 42 ± 1; VEt: 43 ± 2; VAc: 44 ± 2; VS: 46 ± 2). Vanadium administration to diabetic rats also corrected the abnormal activity and expression of certain key enzymes involved in hepatic glucose metabolism, although the extent to which levels of activity and expression were corrected varied with the compounds used. GK activity and mRNA levels, which were markedly reduced in D and WM rats ($<15\%$ of C rats), were partly corrected by vanadium treatment. Among the four compounds used, VAc resulted in a greater restoration of both GK parameters than VS (Figure 5). L-PK activity and mRNA levels were also reduced in D and WM liver ($\sim30\%$ of C rats), and were corrected by vanadium administration (Figure 5). Again, the most complete restoration of L-PK parameters was achieved by VAc. Activity and mRNA levels of the gluconeogenic enzyme, PEPCK, were increased in diabetic liver (250–300% of C levels). These parameters remained unchanged by food restriction but were similarly normalized by all four vanadium compounds (no significant differences between them) (Figure 5).

Potential relationships between vanadium concentrations and the improvement of glucose homeostasis or hepatic glucose metabolism were examined. Besides plasma vanadium measurements, vanadium concentrations were also measured in two of the main target tissues for insulin action (liver and muscle) (Figure 6A). In liver, vanadium concentrations were the highest in VM and VAc rats and lowest in VS rats. Yet, the concentration reached in the later treated group remained larger ($P<0.001$) than those observed in C (0.02 ± 0.001 ng mg^{-1}, $n=3$) and D animals (0.01 ± 0.003 ng mg^{-1}, $n=4$). In muscle, the rats treated with the three organic compounds (VM, VEt, VAc) had significantly higher vanadium concentrations than those treated with VS, with the greatest value being produced by VAc. Vanadium concentrations in VS rats still remained ~15 fold higher than those in C (0.02 ± 0.01 ng mg^{-1}, $n=4$) or D (0.04 ± 0.01 ng mg^{-1}, $n=3$) rats. There were strong positive correlations between vanadium concentrations in liver ($r=0.73$, $P<0.0001$) or muscle ($r=0.63$, $P<0.0001$) and those observed in plasma (Figure 6B, end of the study; the former correlation being in agreement with that of Mongold *et al*., 1990). However, there was no correlation between plasma vanadium levels and plasma glucose levels at any time point studied (week 10 is shown on Figure 6B as an example; $r=0.18$, $P=0.25$). Likewise, there was neither a correlation between vanadium concentrations in muscle and final period of glycemia (not shown), nor between vanadium concentrations in liver and L-PK activity (Figure 6B) or mRNA (not shown). Similarly, there was no correlation between liver vanadium concentrations and GK parameters (not shown).

Twelve weeks of vanadium treatment had no obvious toxic side effects on renal or hepatic function (Table 1). The rise in urea observed in the four treated groups may reflect a

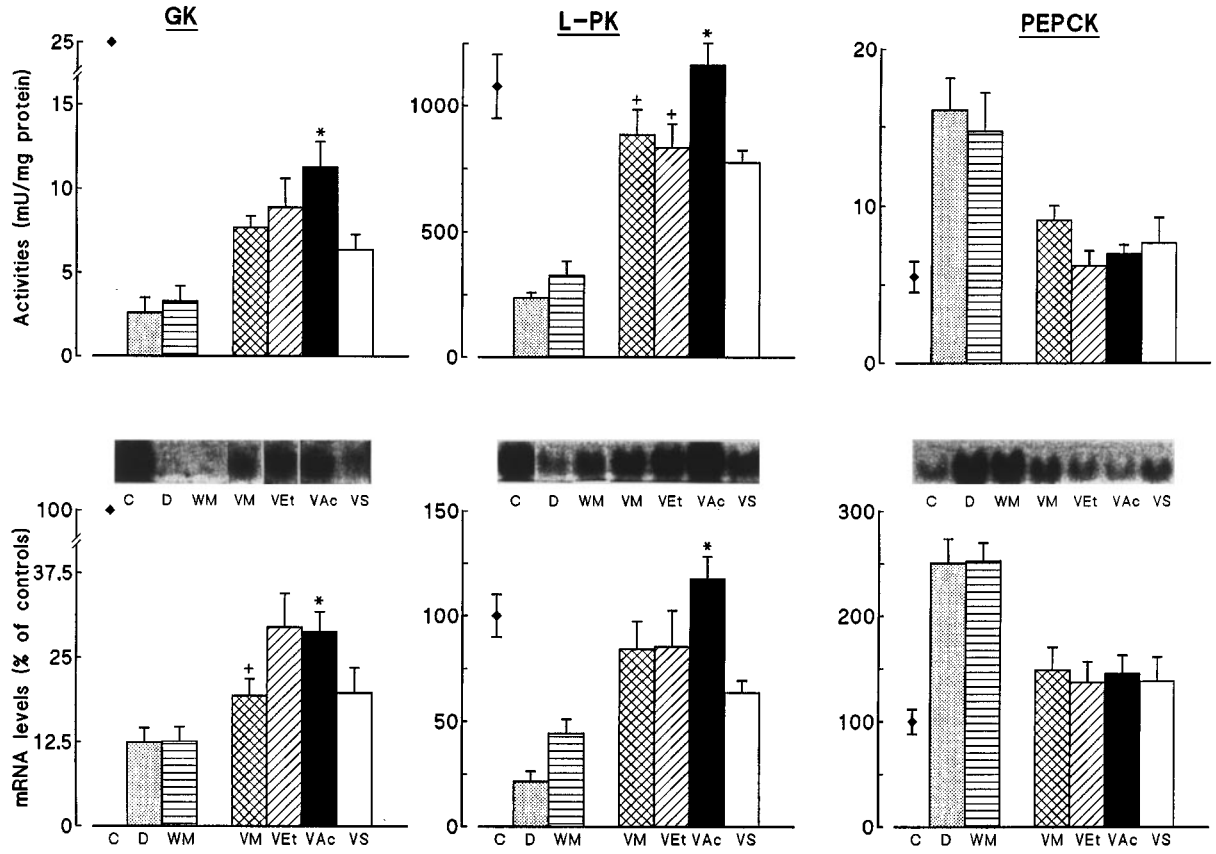

Figure 5 Influence of treatment with vanadium compounds on glucokinase (GK), L-type pyruvate kinase (L-PK) and phosphoenolpyruvate carboxykinase (PEPCK) activities and mRNA levels in the liver of diabetic rats. Values are means ± s.e.mean for 6–11 control (C), untreated diabetic (D), body weight-matched diabetic (WM) and vanadium-treated diabetic rats receiving either VM, VEt, VAc or VS compounds. mRNA levels obtained from Northern-blots, like those in the inserts, are expressed as percentages of values in C rats. $^*P<0.05$ or less for the indicated group of rats treated with organic (VM, VEt, or VAc) *vs* inorganic (VS) vanadium compounds. $+P<0.05$ for indicated group of rats treated with VM or VEt *vs* VAc treated rats (ANOVA or *t*-test (GK mRNA)).

marginal dehydration due to a decreased fluid consumption resulting from an aversion to the taste of vanadium (Brichard *et al*., 1988). Plasma creatinine levels were not different in untreated (D and WM) or vanadium-treated diabetic rats, and indeed were lower than those seen in C rats, which may result from a decrease in lean body mass. The creatinine clearance, which is augmented by diabetes due to a glomerular hyperfiltration rate (Jensen *et al*., 1981), was normalized in vanadium-treated rats, but this correction was not specific as it was achieved by mere calorie restriction (and decreased glucosuria) in WM rats. Accordingly, diabetic proteinuria was corrected in both WM and vanadium-treated diabetic rats. Levels of the liver cytosolic enzyme, GPT, which were elevated in diabetes due to hepatic steatosis (Ozcelikay *et al*., 1996), were unchanged by food restriction, but were specifically corrected by vanadium compounds. However, among these agents, VS resulted in diarrhoea in 50% of the rats from the sixth week of treatment onwards. In some animals, the diarrhoea was severe, leading to dehydration and weight loss. Two of ten VS rats subsequently died. Usually, the diarrhoea spontaneously ceases after treatment withdrawal or a reduction in the dose (Brichard & Henquin, 1995). In the present study, the treatment was maintained unchanged as the aim was to compare similar concentrations of vanadium element provided by the different compounds. No gastrointestinal disturbances were caused by any of the three organic compounds tested, which were likely better resorbed by the intestinal tract.

Experiment 2: Acute administration of intraperitoneal vanadium compounds

We next examined whether the blood glucose-lowering effect of the different vanadium compounds was affected when the gastrointestinal tract was bypassed (i.e. when the compounds were administered parenterally).

To this end, four groups of diabetic rats matched for initial body weight and glycemia, received a single i.p. injection of the appropriate vanadium compound (1.275 mg vanadium element per kg body weight). Under these conditions, only VAc induced a significant reduction in glycemia from day 1, an effect which persisted for up to 5 days. VM, VEt and VS were unable to induce such changes in glycemia (Figure 7). When blood samples were collected earlier (2, 4, 6 and 8 h after i.p. injection in day 0), we found no hypoglycaemic action for any of the compounds tested (not shown). Body weight (g) in the four groups was not significantly affected by the treatment (day 1: VM, 232 ± 3; VEt, 230 ± 2; VAc, 231 ± 4; VS, 230 ± 4 and day 5: VM, 239 ± 3; VEt, 238 ± 3; VAc, 238 ± 6; VS, 237 ± 5).

Discussion

This study shows that organic vanadium compounds, in particular VAc, ameliorate more efficaciously and with fewer apparent side-effects than VS the hyperglycemia and impaired

hepatic glucose metabolism seen in diabetic rats. This superiority is not simply due to an improved intestinal absorption, but may also be ascribed to more potent insulin-like properties.

The greater efficacy of VAc in lowering blood glucose may be explained partly by its greater efficiency of action on the diabetic liver. VAc reverses more potently than other compounds the impaired hepatic glycolysis (GK and L-PK activities), a correction which occurs at the pre-translational level. As this effect may partly be reproduced by treatment of rats with phlorizin (Brichard *et al.*, 1993), the superiority of VAc on liver could result from more profound alleviation of

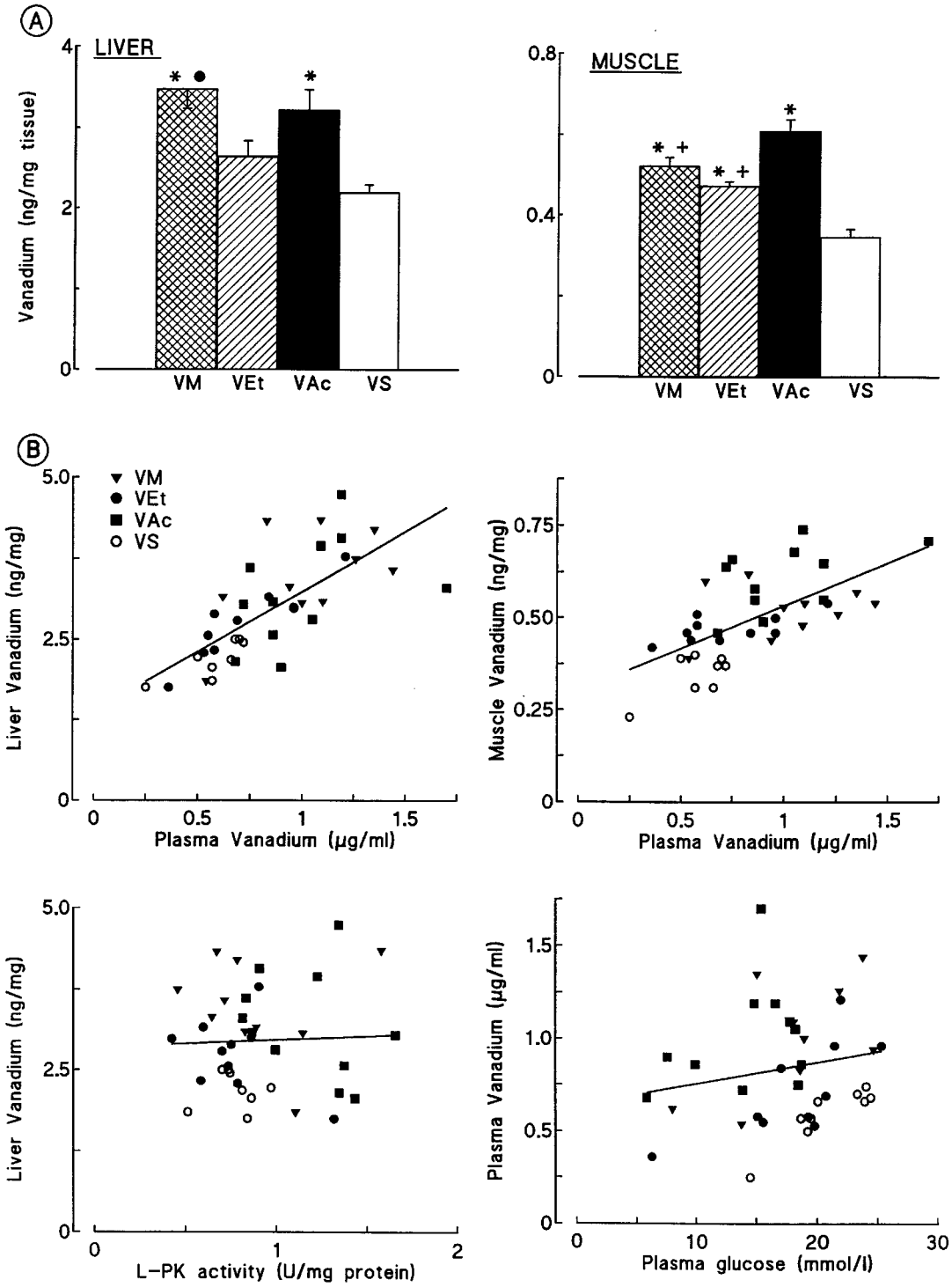

Figure 6 (A) Influence of treatment with vanadium compounds on vanadium concentrations in liver and muscle of diabetic rats. Values are means ± s.e.mean for 8–11 vanadium-treated diabetic rats receiving either VM, VEt, VAc or VS compounds. $*P<0.01$ or less *vs* VS rats; $\bullet P<0.05$ *vs* VEt rats; $+P<0.01$ or less *vs* VAc rats (ANOVA). (B) Upper panels: Relationships between tissue vanadium concentrations in liver and muscle *versus* plasma in treated rats. The whole population of treated (VM, VEt, VAc and VS together) rats was studied at the end of the experiment, the measurements being made after death (tissue) or after 10 weeks (plasma). Correlation coefficients were, respectively, $r=0.73$ for liver ($P<0.0001$) and $r=0.63$ for muscle ($P<0.0001$). Lower panels: Relationships between vanadium concentrations in liver and L-PK activity, and vanadium concentrations in plasma and glycemia in treated rats. Correlation coefficients were, respectively, $r=0.043$ ($P=0.8$) and $r=0.18$ ($P=0.25$).

Table 1 Influence of treatment with vanadium compounds on renal and hepatic function of diabetic rats

	C	*D*	*WM*	*VM*	*VEt*	*VAc*	*VS*
Plasma							
Urea (mg/dl)	41±1	35±1	39±2	50±5*	55±3*	51±3*	52±5*
Creatinine (mg/dl)	0.52±0.01	0.47±0.03†	0.45±0.01†	0.41±0.01†	0.45±0.01†	0.46±0.01†	0.42±0.01†
GOT (IU/l)	131±13	116±15	109±11	97±9	106±9	91±9	93±7
GPT (IU/l)	45±3	86±4†	76±6†	60±6*#	54±4*#	45±3*#	55±6*#
Creatinine clearance (ml/min)	2.4±0.1	3.2±0.1†	2.2±0.1*	1.9±0.1*	1.9±0.1*	1.8±0.1*	2.0±0.2*
Proteinuria (mg/24 h)	17±2	95±19†	13±1*	12±3*	8±1*	9±2*	13±4*

Values are means±s.e.mean for 6–11 control (C), untreated diabetic (D), body weight-matched diabetic (WM) and vanadium-treated rats receiving either VM, VEt, VAc or VS compound. Measurements were made after 12 weeks of treatment, except those of urinary determinations (week 8, during housing in metabolic cages). Three samples were taken for daily proteinuria and the obtained values were averaged for each rat. GOT, glutamic-oxaloacetic transaminase; GPT, glutamic-pyruvic transaminase. *$P<0.05$ or less *vs* D rats; †$P<0.05$ or less *vs* C rats; #$P<0.05$ or less *vs* WM rats (ANOVA).

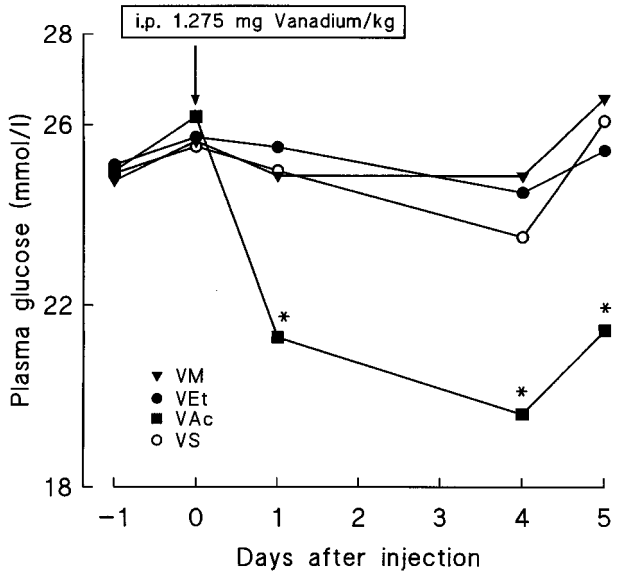

Figure 7 Influence of a single intraperitoneal injection of vanadium compounds on plasma glucose levels in diabetic rats. On day 0 (09.30 h), either VM, VEt, VAc or VS were injected into diabetic rats at a dose of 1.275 mg vanadium element per kg body weight. Values are means for eight rats in each group (s.e.mean which were always <10% of the mean were omitted for sake of clarity). *$P<0.05$ or less *vs* respective glycemia on day 0 (repeated measures of ANOVA).

glucose toxicity on this tissue. However, phlorizin treatment did not modify the low mRNA levels and activity of L-PK (Brichard *et al*., 1993). This suggests that VAc is more efficacious at eliciting insulin-like actions upon liver gene expression and metabolism.

Despite of the lowest levels of vanadium consumption, VAc rats had the highest levels of plasma or tissue vanadium. This may be due to a greater intestinal rate of absorption of the element, as urinary excretion of vanadium was low in all treated groups (1.5–2% of the ingested dose; compare Figures 2 and 3). Inorganic vanadium is usually poorly (1–10%) absorbed by the gastrointestinal tract (Llobet Domingo, 1984; Yuen *et al*., 1993b), and the organic ligand is expected to increase the lipophilicity of the vanadium complex and consequently its absorption (Yuen *et al*., 1993a).

Could the superiority of VAc be explained solely by these observations (i.e. higher intestinal absorption and subsequent higher plasma or tissue vanadium)? This is unlikely for several reasons. Firstly, VAc retained its potency when the gastrointestinal tract was bypassed. Thus, after a single i.p. injection of the element (1.275 mg vanadium kg^{-1}), only VAc significantly decreased the hyperglycemia in diabetic rats for up to 5 days. VS, VEt or VM were ineffective. This does not contradict a previous report where VM was effective by the i.p. route, but at substantially higher doses (3.21 mg vanadium kg^{-1}) (Yuen *et al*., 1995). Secondly, at week 7, VAc rats had strikingly lower glycemia as compared to VEt or VM rats in spite of similar levels of vanadium intake and plasma vanadium (Figure 2). Indeed, there was no apparent relationship between plasma vanadium and glucose levels throughout the study (i.e. at any time point examined). There was also no relationship between liver vanadium and hepatic glucose metabolism, [glycolytic parameters (GK or L-PK mRNA or activity) specifically improved by VAc in particular] or muscle vanadium and glycemia. Taken together, these data suggest that either circulating or tissue vanadium concentrations may not reflect true intracellular vanadium levels or that another confounding factor – as yet unidentified – may interfere with the situation *in vivo*. Alternatively, differences in potency between vanadium compounds are rather explained by differences in their insulin-like properties. Recent *in vitro* studies support the latter hypothesis. VAc was more effective than VS in stimulating lipogenesis in isolated adipocytes under conditions where both compounds permeated cells similarly (Li *et al*., 1996). These differences in insulin-like properties were accounted for by a higher redox stability of VAc as compared to VS (i.e. prolonged intracellular stability of vanadium (IV) against oxidation; Li *et al*., 1996). Higher hydrophilic stability could also be involved (Li *et al*., 1996; Crans, unpublished data).

In spite of their higher potency, organic vanadium compounds were not more toxic than VS. Firstly, like VS, they did not alter hepatic or renal function as shown by the lack of increase in liver cytolytic enzymes or in creatinine and proteinuria. Secondly, the slowing of body weight gain, a common feature of vanadium treatment (Brichard & Henquin, 1995) was similar for all compounds tested. It turned out that energy-restricted rats matched for body weight with vanadium rats, were also matched for net (i.e. corrected for glucosuria) energy consumption. This indicates that the decrease in body weight in vanadium-treated rats can largely be ascribed to the lower food intake rather than to an additional toxic effect. Vanadium-induced anorexia is currently an adverse reaction in insulin-deficient diabetic rats in a catabolic state, but might be regarded as an advantage in non-insulin-dependent diabetes which is often associated with obesity. Thirdly, diarrhoea

occurred in 50% of rats chronically treated with VS (thereby leading to increased mortality), but not in those rats receiving the organic compounds. In clinical studies with diabetic patients, VS and Na metavanadate, two inorganic vanadium salts, though given at much lower (~100 fold) doses than in animal studies, resulted in mild gastrointestinal symptoms (nausea, mild diarrhoea, abdominal cramps and flatulence) which were either transient or responded to a decrease in dose (Cohen *et al*., 1995; Goldfine *et al*., 1995; Boden *et al*., 1996). In agreement with previous work (Yuen *et al*., 1993a; McNeill *et al*., 1995), our study showed that modification of the vanadium species with organic ligands may decrease the gastrointestinal side-effects of the element, possibly by enhancing its rate of absorption.

The presence of an organic ligand within a vanadium complex may thus influence the potency and the toxicity of the compound. Increasing the mass of the ligand by introducing ethyl groups does not seem to improve the parent compound (*c.f.* VEt *vs* VAc). The chemical rules determining which ligands will generate the most suitable complexes are still unclear, but relevant in view of their potential therapeutic value. Ideally, the use of one ligand should even direct the complex into one insulin-target tissue in preference to another, as has been shown for peroxovanadium compounds (Bevan *et al*., 1995). Clearly, the development of new analogues of vanadium is of importance for the management of diabetes. Since vanadium can utilize non-insulin-dependent pathways to exert its insulin-like activities, these novel derivatives will be potentially interesting for the treatment of the insulin-resistant state associated with non-insulin-dependent diabetes.

We are grateful to Professor J.C. Henquin for critical comments, Dr R. Walters for revising the English version, and Mrs A.M. Pottier for skilled assistance. This work was supported by grants from the Foundation of Scientific and Medical Research (3.4513.93), the Fund for Scientific Development (University of Louvain), the Fonds S and J Pirart (ABD) (to S.M.B.), and the Institute for General Medical Sciences, National Institutes of Health (to D.C.C.). S.M.B. is Chercheur Qualifié of the Fonds National de la Recherche Scientifique.

References

BECKER, D.J., ONGEMBA, L.N. & HENQUIN, J.C. (1994). Comparison of the effects of various vanadium salts on glucose homeostasis in streptozotocin-diabetic rats. *Eur. J. Pharmacol.,* **260,** 169–175.

BEVAN, A.P., BURGESS, J.W., YALE, J.F., DRAKE, P.G., LACHANCE, D., BAQUIRAN, G., SHAVER, A. & POSNER, B.I. (1995). In vivo insulin mimetic effects of pV compounds: role for tissue targeting in determining potency. *Am. J. Physiol.,* **268,** E60–E66.

BODEN, G., CHEN, X., RUIZ, J., VAN ROSSUM, G.D.V. & TURCO, S. (1996). Effects of vanadyl sulfate on carbohydrate and lipid metabolism in patients with non-insulin-dependent diabetes mellitus. *Metabolism,* **45,** 1130–1135.

BRICHARD, S.M. & HENQUIN, J.C. (1995). The role of vanadium in the management of diabetes. *Trends Pharmacol. Sci.,* **16,** 265–270.

BRICHARD, S.M., HENQUIN, J.C. & GIRARD, J. (1993). Phlorizin treatment of diabetic rats partially reverses the abnormal expression of genes involved in hepatic glucose metabolism. *Diabetologia,* **36,** 292–298.

BRICHARD, S.M., OKITOLONDA, W. & HENQUIN, J.C. (1988). Long term improvement of glucose homeostasis by vanadate treatment in diabetic rats. *Endocrinology,* **123,** 2048–2053.

BUCHET, J.P., KNEPPER, E. & LAUWERYS, R. (1982). Determination of vanadium in urine by electrothermal atomic absorption spectrometry. *Anal. Chim. Acta.,* **136,** 243.

CARAVAN, P., GELMINI, L., GLOVER, N., HERRING, F.G., LI, H., MCNEILL, J.H., RETTIG, S.J., SETYAWATI, I.A., SHUTER, E., SUN, Y., TRACEY, A.S., YUEN, V.G. & ORVIG, C. (1995). Reaction chemistry of BMOV, Bis(maltolato)oxovanadium(IV)- a potent insulin mimetic agent. *J. Am. Chem. Soc.,* **117,** 12759–12770.

CHAN, Y.L., GUTELL, R., NOLLER, H.F. & WOOL, I.G. (1984). The nucleotide sequence of a rat 18S ribosomal ribonucleic acid gene and a proposal for the secondary structure of 18S ribosomal ribonucleic acid. *J. Biol. Chem.,* **259,** 224–230.

COHEN, N., HALBERTHAM, M., SHLIMOVICH, P., CHANG, C.J., SHAMSON, H. & ROSSETTI, L. (1995). Oral vanadyl sulfate improves hepatic and peripheral insulin sensitivity in patients with non-insulin dependent diabetes mellitus. *J. Clin. Invest.,* **95,** 2501–2509.

CRANS, D.C., KERAMIDAS, A.D., HOOVER-LITTY, H., ANDERSON, O.P., MILLER, M.M., LEMOINE, L.M., PLEASIC-WILLIAMS, S., VANDENBERG, M., ROSSOMANDO, A.J. & SWEET, L.J. (1997). Synthesis, structure, and biological activity of a new insulinomimetic peroxovanadium compound: Bisperoxovanadium imidazole monoanion. *J. Am. Chem. Soc.,* **119,** 5447–5448.

ELBERG, G., HE, Z., LI, J., SEKAR, N. & SHECHTER, Y. (1997). Vanadate activates membranous nonreceptor protein tyrosine kinase in rat adipocytes. *Diabetes,* **46,** 1684–1690.

GOLDFINE, A.B., SIMONSON, D.C., FOLLI, F., PATTI, M.E. & KAHN, C.R. (1995). Metabolic effects of sodium metavanadate in humans with insulin-dependent and noninsulin-dependent diabetes mellitus in vivo and in vitro studies. *J. Clin. Endocrinol. Metab.,* **80,** 3311–3320.

HEYLIGER, C.E., TAHILIANI, A.G. & MCNEILL, J.H. (1985). Effect of vanadate on elevated blood glucose and depressed cardiac performance of diabetic rats. *Science,* **227,** 1474–1477.

IYNEDJIAN, P.B., UCLA, C. & MACH, B. (1987). Molecular cloning of glucokinase cDNA. Development and dietary regulation of glucokinase mRNA in rat liver. *J. Biol. Chem.,* **262,** 6032–6038.

JENSEN, P.K., CHRISTIANSEN, J.S., STEVEN, K. & PARVING, H.H. (1981). Renal function in streptozotocin-diabetic rats. *Diabetologia,* **21,** 409–414.

LI, J., ELBERG, G., CRANS, D.C. & SHECHTER, Y. (1996). Evidence for the distinct vanadyl(+4)-dependent activating system for manifesting insulin-like effects. *Biochemistry,* **35,** 8314–8318.

LLOBET, J.M. & DOMINGO, J.L. (1984). Acute toxicity of vanadium compounds in rats and mice. *Toxicology Letters,* **23,** 227–231.

MCNEILL, J.H., YUEN, V.G., DAI, S. & ORVIG, C. (1995). Increased potency of vanadium using organic ligands. *Mol. Cell. Biochem.,* **153,** 175–180.

MONGOLD, J.J., CROS, G.H., VIAN, L., TEP, A., RAMANADHAM, S., SIOU, G., DIAZ, J., MCNEILL, J.H. & SERRANO, J.J. (1990). Toxicological aspects of vanadyl sulphate on diabetic rats: effects on vanadium levels and pancreatic B-cell morphology. *Pharmacol. Toxicol.,* **67,** 192–198.

OZCELIKAY, A.T., BECKER, D.J., ONGEMBA, L.N., POTTIER, A.M., HENQUIN, J.C. & BRICHARD, S.M. (1996). Improvement of glucose and lipid metabolism in diabetic rats treated with molybdate. *Am. J. Physiol.,* **270,** E344–E352.

POSNER, B.I., FAURE, R., BURGESS, J.W., BEVAN, A.P., LACHANCE, D., ZHANG-SUN, G., FANTUS, I.G., NGG, J.B., HALL, D.A., SOO LUM, B. & SHAVER, A. (1994). Peroxovanadium compounds: a new class of potent phosphotyrosine phosphatase inhibitors which are insulin mimetics. *J. Biol. Chem.,* **269,** 4596–4604.

REUL, B.A., BECKER, D.J., ONGEMBA, L.N., BAILEY, C.J., HENQUIN, J.C. & BRICHARD, S.M. (1997). Improvement of glucose homeostasis and hepatic insulin resistance in ob/ob mice given oral molybdate. *J. Endocrinol.,* **155,** 55–64.

SAKURAI, H., FUJII, K., WATANABE, H. & TAMURA, H. (1995). Orally active and long-term acting insulin-mimetic vanadyl complex: bis(picolinato)oxovanadium(IV). *Biochem. Biophys. Res. Com.,* **214,** 1095–1101.

SIMON, M.P., BESMOND, C., COTTREAU, D., WEBER, A., CHAUMET-RIFFAUD, P., DREYFUS, J.C., SALA TREPAT, J., MARIE, J. & KAHN, A. (1983). Molecular cloning for L-type pyruvate kinase and aldolase B. *J. Biol. Chem.,* **258,** 14576–14584.

TSIANI, E. & FANTUS, I.G. (1997). Vanadium Compounds: Biological Actions and Potential as Pharmacological Agents. *Trends Endocrinol. Metab.,* **8,** 51–58.

YOO-WARREN, H., MONAHAN, J.E., SHORT, J., SHORT, H., BRUZEL, A., WYNSHAW-BORIS, A., MEISNER, H.M., SAMOLS, D. & HANSON, R.W. (1983). Isolation and characterization of the gene coding for cytosolic phophoenolpyruvate carboxykinase (GTP) from the rat. *Proc. Natl. Acad. Sci. U.S.A.,* **80,** 3656–3660.

YUEN, V.G., ORVIG, C. & MCNEILL, J.H. (1993a). Glucose-lowering effects of a new organic vanadium complex, bis(maltolato)oxovanadium(IV). *Can. J. Physiol. Pharmacol.,* **71,** 263–269.

YUEN, V.G., ORVIG, C., THOMPSON, K.H. & MCNEILL, J.H. (1993b). Improvement in cardiac dysfunction in streptozotocin-induced diabetic rats following chronic oral administration of bis(maltolato)oxovanadium (IV). *Can. J. Physiol. Pharmacol.,* **71,** 270–276.

YUEN, V.G., ORVIG, C. & MCNEILL, J.H. (1995). Comparison of the glucose-lowering properties of vanadyl sulfate and bis(maltolato)oxovanadium(IV) following acute and chronic administration. *Can. J. Physiol. Pharmacol.,* **73,** 55–64.

(Received July 15, 1998
Revised October 14, 1998
Accepted October 21, 1998)

British Journal of Pharmacology (1999) 126, 478–484
http://www.stockton-press.co.uk/bjp

Bronchoconstrictor effect of thrombin and thrombin receptor activating peptide in guinea-pigs *in vivo*

*,[1]Carla Cicala, [1]Mariarosaria Bucci, [2]Gianfranco De Dominicis, [3]Pat Harriot, [1]Ludovico Sorrentino & [1]Giuseppe Cirino

[1]Dipartimento di Farmacologia Sperimentale, Universitá degli Studi di Napoli "Federico II", Via Domenico Montesano 49, 80131 Napoli, Italy; [2]Servizio di Anatomia Patologica, Ospedale Cardarelli 80131 Napoli, Italy; [3]Centre for Peptide and Protein Engineering, Queen's University of Belfast, Ireland, U.K.

1 Several thrombin cellular effects are dependent upon stimulation of proteinase activated receptor-1 (PAR-1) localized over the cellular surface. Following activation by thrombin, a new N-terminus peptide is unmasked on PAR-1 receptor, which functions as a tethered ligand for the receptor itself. Synthetic peptides called thrombin receptor activating peptides (TRAPs), corresponding to the N-terminus residue unmasked, reproduce several thrombin cellular effects, but are devoid of catalytic activity. We have evaluated the bronchial response to intravenous administration of human α-thrombin or a thrombin receptor activating peptide (TRAP-9) in anaesthetized, artificially ventilated guinea-pigs.

2 Intravenous injection of thrombin (100 u kg^{-1}) caused bronchoconstriction that was recapitulated by injection of TRAP-9 (1 mg kg^{-1}). Animal pretreatment with the thrombin inhibitor Hirulog™ (10 mg kg^{-1} i.v.) prevented thrombin-induced bronchoconstriction, but did not affect bronchoconstriction induced by TRAP-9. Both agents did not induce bronchoconstriction when injected intravenously to rats.

3 The bronchoconstrictor effect of thrombin and TRAP-9 was subjected to tolerance; however, in animals desensitized to thrombin effect, TRAP-9 was still capable of inducing bronchoconstriction, but not *vice versa*.

4 Depleting animals of circulating platelets prevented bronchoconstriction induced by both thrombin and TRAP-9.

5 Bronchoconstriction was paralleled by a biphasic change in arterial blood pressure, characterized by a hypotensive phase followed by a hypertensive phase. Thrombin-induced hypotension was not subject to tolerance and was inhibited by Hirulog™; conversely, hypertension was subject to tolerance and was not inhibited by Hirulog™. Hypotension and hypertension induced by TRAP-9 were neither subject to tolerance nor inhibited by Hirulog™.

6 Our results indicate that thrombin causes bronchoconstriction in guinea-pigs through a mechanism that requires proteolytic activation of its receptor and the exposure of the tethered ligand peptide. Platelet activation might be triggered by the thrombin effect.

Keywords: Thrombin; thrombin receptor activating peptide; proteinase activated receptor; Hirulog™; bronchoconstriction; lung

Abbreviations: BALF, bronchoalveolar lavage fluid; PAR-1, proteinase activated receptor 1; TRAP, thrombin receptor activating peptide

Introduction

It is known that following tissue damage, extrinsic coagulation pathway becomes activated and thrombin is formed by its precursor, prothrombin (Schiffrin, 1994; Cicala & Cirino, 1998). Much attention has recently been focused on the cellular responses triggered by thrombin, highlighting a role for this enzyme in cell activation and inflammation. Both *in vitro* and *in vivo* studies have demonstrated that thrombin is chemotactic for monocytes (Bar Shavit *et al*., 1983) and neutrophils (Bizios *et al*., 1986; Drake & Issekutz, 1992); this activity might be mediated by high affinity receptors demonstrated to be present on both macrophages and neutrophils (Kudhal *et al*., 1991; Sonne, 1988). Thrombin increases IL-1- and TNFα-induced neutrophil chemotaxis (Drake *et al*., 1992), it causes fibroblast and smooth muscle cell proliferation (Panettieri *et al*., 1995), stimulates endothelial cells to produce PGI_2 (Weksler *et al*., 1978); all these effects contribute to inflammation and tissue repair processes independently of haemostatic mechanisms.

Thrombin-like proteinases have been found in bronchoalveolar lavage fluids obtained from active immunized experimental animals (Linssen *et al*., 1991). The role of coagulation cascade activation and fibrin deposition during lung inflammation has been investigated; it has been shown that asthmatic subjects present alterations in coagulation parameters and an increase of platelet reactivity (Idell *et al*., 1989; Gresele *et al*., 1993; Fuchs-Buder *et al*., 1996). However, due to the lack of appropriate tools, such as specific inhibitors, the role of thrombin in bronchial asthma has never been addressed.

It is now clear that thrombin produces many of its biological activities through stimulation of proteinase activated receptor-1 (PAR-1) that is localized over the surface of several cells. PAR-1 is a seven transmembrane-domain

*Author for correspondence at: Department of Experimental Pharmacology, via D. Montesano 49, 80131 Naples, Italy; E-mail: carla.cicala@mailexcite.com

receptor, demonstrated to be cleaved by thrombin between Arginine[41] and Serine[42] residues, unmasking a new N-terminus peptide (14 aminoacids) which functions as a tethered ligand for the receptor itself (Vu *et al*., 1991; Coughlin *et al*., 1992). It has been shown that synthetic peptides, ranging between 5 and 14 aminoacids, called thrombin receptor activating peptides (TRAPs), corresponding to the N-terminus residue unmasked, are capable of reproducing several cellular effects of thrombin, but are devoid of the thrombin catalytic activity (Chao *et al*., 1992; Garcia *et al*., 1993; Hoffman & Church, 1993; Glusa & Paintz, 1994; Glusa *et al*., 1996). This finding has led to expand the knowledge of the role of thrombin in inflammation, indicating that some cellular events mediated by thrombin are independent of fibrin formation, since they can be reproduced by TRAPs.

Here, we have analysed comparatively the bronchial response to thrombin and TRAP-9 (a PAR-1 agonist peptide) in anaesthetized, artificially ventilated guinea-pigs, to investigate whether thrombin had any effect on *in vivo* bronchial smooth muscle contractility through activation of its receptor PAR-1 and the exposition of the tethered ligand peptide.

Preliminary results have been presented to the British Pharmacological Society Meeting in Bristol, in July 1997.

Methods

Measurement of bronchoconstriction and blood pressure

Guinea-pigs (Charles River, 400–500 g) were anaesthetized with sodium pentobarbitone (40 mg kg^{-1} i.p.) and Hypnorm^{TM} (0.5 ml kg^{-1} i.m.), placed supine on an operating table, a cannula was inserted into the trachea and were artificially ventilated with a constant volume, by a respiration pump (Ugo Basile, Varese, Italy; rate 60 breaths min^{-1}, 1 ml air per 100 g body weight), connected to a bronchospasm transducer (Ugo Basile, Varese, Italy). Spontaneous breathing was abolished by administration of pancuronium (2 mg kg^{-1} i.v.). Both cervical vagi nerves were transected at the level of the neck. The right jugular vein was cannulated for drug administration; the left carotid artery was cannulated with a cannula containing heparinized saline (5 u ml^{-1}) and connected to a pressure transducer for a continuous monitoring of arterial blood pressure. After surgery, a single dose of histamine (10 μg kg^{-1} i.v.) was administered to evaluate animal responsiveness to a bronchoconstrictor agent. Thrombin (50 and 100 u kg^{-1}, corresponding to 0.034 and 0.07 mg kg^{-1} respectively), TRAP-9 (0.1, 0.3 or 1 mg kg^{-1}) or the control peptide (1 mg kg^{-1}) were then administered intravenously each 20 min for three consecutive times.

Different groups of animals were administered the thrombin inhibitor Hirulog^{TM} (10 mg kg^{-1}) i.v., 30 min before giving thrombin (100 u kg^{-1} i.v.) or TRAP-9 (1 mg kg^{-1} i.v.). Experiments were also performed on rats using the above protocol described for guinea-pigs, thrombin (10, 30 or 50 u kg^{-1}) or TRAP-9 (1 mg kg^{-1}) were intravenously administered and the bronchial response was evaluated.

Cross-desensitization study

To evaluate if there was cross-desensitization to the effects of thrombin and TRAP-9, different groups of animals were treated with TRAP-9 (1 mg kg^{-1} i.v.) after three administrations of thrombin (100 u kg^{-1} i.v.) or, conversely, they were treated with thrombin (100 u kg^{-1} i.v.) after three administrations of TRAP-9 (1 mg kg^{-1} i.v.).

Bronchoalveolar lavage

At the end of the experiment, three bronchoalveolar lavages, with 5 ml of saline each, through a cannula inserted into the trachea, were performed. The saline was left in contact for 1 min and then aspirated with a syringe, placed in a graduated tube and then centrifuged at $200 \times g$ for 15 min. The supernatant was discarded and the pellet was suspended in 1 ml of saline.

Leucocyte count

Total leucocyte count was performed by diluting cells with Turk's solution (0.01% w/v crystal violet and 3% v/v acetic acid) and counted by an optical microscope. Differential cell analysis was performed on air-dried smears of cell suspension and counted by optical microscopy, under oil immersion.

Platelet depletion

Thrombocytopenia was induced by treating guinea-pigs with a polyclonal rabbit antiplatelet serum intravenously, prior to administration of either thrombin (100 u kg^{-1} i.v.) or TRAP-9 (1 mg kg^{-1} i.v.). The dose and the lag-time chosen were previously determined by dosing animals with 0.1, 0.3, 0.5 and 1 ml (i.v.) of the polyclonal antiplatelet serum, at time interval ranging between 1 and 20 h. A volume of 250 μl gave 3 h later a reduction in platelet count from $500.4 \pm 113.5 \times 10^3$ μl^{-1} to $49.5 \pm 9.30 \times 10^3$ μl^{-1} ($n=5$, $P<0.01$). Platelet count was performed on 100 μl of blood samples, withdrawn from the carotid artery, by using a hemocytometer, Cell Dyn 610 (Sequoia Turner).

Histology

In another set of experiments, after receiving three administrations of thrombin (100 u kg^{-1} i.v.) or TRAP-9 (1 mg kg^{-1} i.v.) guinea-pigs were killed and the lungs removed and placed in formalin (sol. 10% v/v). Section of lungs (10 μm) were embedded in paraffin and stained with ematoxylin eosin and the lung damage evaluated by optical microscopy.

Statistical analysis

Data are expressed as means $\pm$ s.e.mean and analysed with a computerized statistical package (Tallarida & Murray, 1987). Bronchoconstriction is expressed as percentage of bronchoconstriction relative to the maximum percentage (100%). Maximum bronchoconstriction was simulated by clamping the air piping upstream the tracheal cannula thereby diverting all pumped air to the transducer. Results are analysed with one way analysis of variance (ANOVA), followed by Bonferroni's test for multiple comparisons, or by one sample or unpaired two tailed Student's *t*-test when appropriate. A value of $P<0.05$ was taken as significant.

Drugs

TRAP-9 (SFLL**R**NPND), the control TRAP peptide (SFLL**A**NPND) and Hirulog^{TM} (Biogen, Cambridge, MA, U.S.A.) were prepared as previously described (Chao *et al*., 1992; Maraganore *et al*., 1990). Human α-thrombin and heparin were purchased from Sigma Chemical Co. (St. Louis,

MO, U.S.A.). Polyclonal rabbit antiplatelet serum was a kind gift of Prof C.P. Page (King's College, London, U.K.).

Results

Thrombin- and TRAP-9-induced bronchoconstriction

Intravenous administration to guinea-pigs of human α-thrombin at the dose of 50 u kg^{-1} caused a small, not significant, bronchoconstriction ($9.70 \pm 4.0\%$; $P > 0.05$ $n = 4$, one sample t-test), while at the dose of 100 u kg^{-1} (Figures 1a and 2a) caused a bronchoconstriction of $33.14 \pm 8.61\%$ ($P < 0.01$, one sample t-test; $n = 7$) that was reduced to $12.41 \pm 6.11\%$ ($P < 0.01$, Bonferroni's test versus first administration; $n = 7$) at the second administration and to $4.3 \pm 1.70\%$ ($P < 0.01$, Bonferroni's test versus first administration; $n = 7$) at the third administration. Intravenous administration of TRAP-9 at the dose of 0.1 mg kg^{-1} did not cause bronchoconstriction, at the dose of 0.3 mg kg^{-1} there was a trend towards bronchoconstriction ($2.67 \pm 1.76\%$; $P > 0.05$ $n = 3$, one sample t-test). Injection of TRAP-9 at the dose of 1 mg kg^{-1} (Figures 1b and 2c) induced a bronchoconstriction of $30.8 \pm 11.42\%$ ($P < 0.05$, one sample t-test; $n = 7$) which was reduced to $18.43 \pm 8.18\%$ (N.S. versus first administration; $n = 7$) at the second and to $4.76 \pm 1.61\%$ ($P < 0.01$ versus first administration; $n = 7$) at the third administration clearly mimicking thrombin profile. Doses of 1 mg kg^{-1} for TRAP-9 and 100 u kg^{-1} for thrombin were selected for all successive experiments. The control peptide did not show any bronchoconstrictor effect up to 1 mg kg^{-1}.

In a cross-desensitization study we found that animals no more responsive to thrombin exhibited bronchoconstriction following TRAP-9 administration; in contrast, animals no more responsive to TRAP-9 were also insensitive to thrombin administration (data not shown).

Pretreatment of animals with Hirulog™ (10 mg kg^{-1} i.v., 30 min before) abolished thrombin-induced bronchoconstriction, but did not change TRAP-9-induced bronchoconstriction (Table 1).

Neither thrombin (10, 30 or 50 u kg^{-1}) nor TRAP-9 (1 mg kg^{-1}) caused bronchoconstriction when administered intravenously to rats (data not shown).

Arterial blood pressure

Intravenous administration of thrombin to guinea-pigs at the dose of 50 and 100 u kg^{-1} caused a fast fall in blood pressure of 9.25 ± 1.75 mmHg ($n = 4$) and of 8.5 ± 1.9 mmHg ($n = 7$) respectively that was not subjected to desensitization. This decrease in blood pressure was followed by an increase in blood pressure that was of 10.50 ± 0.87 mmHg ($n = 4$) and of 11.86 ± 1.86 mmHg ($n = 7$) for 50 and 100 u kg^{-1} of thrombin, respectively. TRAP-9 given i.v., at the dose of 0.1, 0.3 or 1 mg kg^{-1} caused a similar pattern with a fast fall in blood pressure, followed by an increase. The hypotension for the doses of 0.1, 0.3 and 1 mg kg^{-1} was of 2.7 ± 1.60 mmHg ($n = 4$), 5.7 ± 1.45 mmHg ($n = 3$) and 6.57 ± 0.7 mmHg ($n = 7$) respectively and was not subjected to desensitization. The hypertension that followed was of 10.25 ± 1.44 mmHg ($n = 4$), 14.33 ± 4.05 mmHg ($n = 3$) and 23.00 ± 4.8 mmHg ($n = 7$) respectively, and was repeated unchanged at the second and at the third administration, for all three doses used, while, for thrombin, it was subjected to desensitization. The control peptide was completely inactive. Hirulog™, a stoichiometric inhibitor of thrombin, abolished thrombin-induced hypotension, without affecting the following increase in blood pressure. Conversely, Hirulog™ did not affect TRAP-9-induced changes in arterial blood pressure (Table 1).

Bronchoalveolar lavage

Total leucocyte count in bronchoalveolar lavage fluids (BALFs) obtained from animals injected either with thrombin (100 u kg^{-1} i.v.) or TRAP-9 (1 mg kg^{-1} i.v) was not significantly different from that obtained from control animals (control, $6.03 \pm 0.63 \times 10^6$, $n = 9$; thrombin, $8.19 \pm 0.78 \times 10^6$, $n = 6$; TRAP-9, $7.45 \pm 0.99 \times 10^6$, $n = 6$; $P > 0.05$).

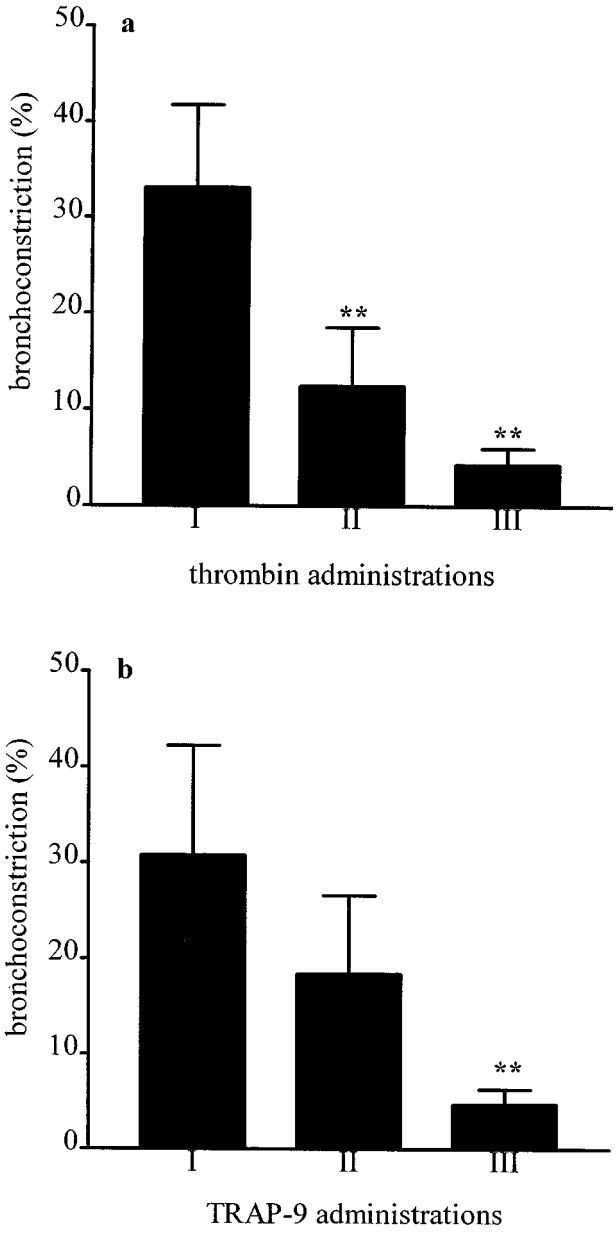

Figure 1 Bronchoconstriction induced by thrombin (a) and TRAP-9 (b). Thrombin (100 u kg^{-1} i.v.) or TRAP-9 (1 mg kg^{-1} i.v.) were injected for three consecutive times each 20 min. I, first administration; II, second administration; III, third administration. Each bar represents the mean of the response obtained from seven different animals. $^{**}P < 0.01$ versus first administration (Bonferroni's test).

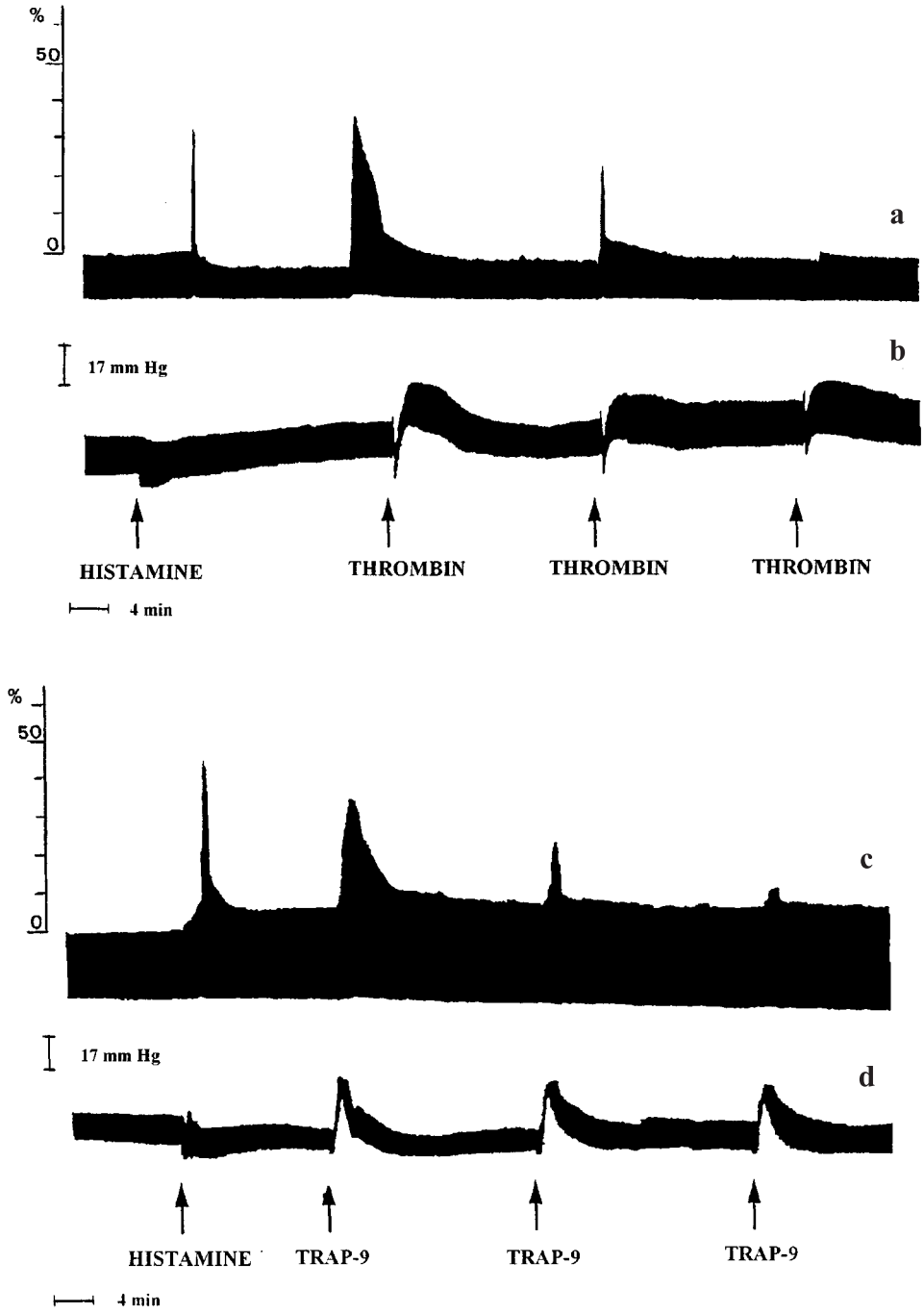

Figure 2 Typical traces representing thrombin- and TRAP-9-induced bronchoconstriction (a and c) and changes in arterial blood pressure (b and d). Thrombin (100 u kg^{-1}) and TRAP-9 (1 mg kg^{-1}) were administered for three consecutive times each 20 min, bronchoconstriction and arterial blood pressure were evaluated. Histamine (10 μg kg^{-1} i.v.) was previously administered to check animal responsiveness to a bronchoconstrictory agent.

Platelet depletion

Platelet depletion of guinea-pigs by a polyclonal rabbit antiplatelet serum prevented thrombin (100 u kg^{-1} i.v.) and TRAP-9 (1 mg kg^{-1} i.v) induced bronchoconstriction.

Histological analysis

Histological analysis of lung sections showed an extensive lung damage in animals injected with either α-thrombin (100 u kg^{-1} i.v.) or TRAP-9 (1 mg kg^{-1} i.v.); both bronchoconstriction and vasoconstriction were also evident (Figure 3).

Discussion

Intravenous administration of thrombin to guinea-pigs caused bronchoconstriction and this effect was reproduced by intravenous injection of TRAP-9. When animals were pretreated with Hirulog™, a stoichiometric thrombin inhibitor that binds the catalytic site of thrombin, thrombin-induced bronchoconstriction was abolished, while TRAP-9-induced bronchoconstriction was unchanged. This finding indicates that thrombin-induced bronchoconstriction requires thrombin catalytic activity and is likely mediated by the tethered ligand peptide exposed on the PAR-1 receptor following proteolytic

Table 1 Effect of Hirulog™ (Hir, 10 mg kg^{-1} i.v.) on thrombin (100 u kg^{-1}) and TRAP-9 (1 mg kg^{-1}) induced bronchoconstriction and changes in blood pressure.

Treatment		*Bronchoconstriction* (%)	*hypotension* (mmHg)	*Hypertension* (mmHg)	n
Thrombin	I	33.14±8.61*	8.50±1.90*	11.86±1.86*	7
	II	12.41±6.11*†	9.14±1.26*	3.43±1.90†	7
	III	4.30±1.70*†	7.70±1.43*	6.14±2.60†	7
Hir+ thrombin	I	0.00±0.00	0.00±0.00	9.00±2.98*	5
	II	0.00±0.00	0.00±0.00	4.62±2.13†	5
	III	0.00±0.00	0.00±0.00	2.80±1.96†	5
TRAP-9	I	30.80±11.42*	6.57±0.70*	23.00±4.80*	7
	II	18.43±8.18*	5.57±0.75*	21.86±2.80*	7
	III	6.60±0.92*†	6.14±1.40*	20.80±5.32*	7
Hir+ TRAP-9	I	23.80±9.41*	7.33±1.31*	23.17±1.94*	5
	II	6.60±0.92*	6.50±0.76*	23.50±2.67*	5
	III	5.20±1.46*	6.33±1.12*	23.00±2.48*	5

*$P<0.05$ versus hypothetical mean zero (one sample Student's *t*-test) and †$P<0.05$ versus first administration (Bonferroni's test).

activation. However, this mechanism cannot explain the tolerance to the bronchoconstrictor effect of both thrombin and TRAP-9, implying that the bronchoconstrictor effect is not dependent upon receptor activation only. Indeed, if bronchoconstriction had been dependent exclusively upon a receptor mechanism, desensitization should have occurred only to thrombin effect, due to receptor consumption, leaving unaffected TRAP-9 response due to its ability to stimulate the receptor directly.

Involvement of inflammatory cells was ruled out by the finding that in bronchial lavage there was no difference in leucocyte count between control and thrombin or TRAP-9-treated guinea-pigs. Similarly, mast cell degranulation, that we have previously shown to be involved in thrombin and TRAP-induced edema (Cirino *et al*., 1996), appeared not to be implicated since by histological analysis there was no evidence of degranulated mast cells in the tissue. Following this experimental evidence, we sought to investigate platelet involvement. It is widely documented that platelets behave as inflammatory cells, being able, under stimulation, to synthesize and secrete several mediators, among which are powerful bronchoconstrictor agents, such as histamine, serotonin, platelet activating factor (PAF) and arachidonic acid metabolites (Page, 1989). *In vitro*, both thrombin and TRAP-9 promote platelet activation and degranulation, the latter being able to stimulate platelets from primates and guinea-pigs, but not from other animal species (Kinlough-Rathbone *et al*., 1993; Connolly *et al*., 1994). *In vivo*, both agents cause ^{111}In-labelled platelet accumulation in the pulmonary vasculature of guinea-pigs (Chiu *et al*., 1997). In thrombocytopenic animals both thrombin and TRAP-9 did not cause bronchoconstriction, implying that platelet activation might be the trigger of the bronchoconstrictor effect observed in our experimental conditions. This hypothesis is further supported by the inability of both agents to cause bronchoconstriction when injected intravenously to rats, whose platelets lack the PAR-1 receptor.

Platelet degranulation by thrombin and TRAP-9 could also account for tolerance to bronchoconstrictor effect observed. Indeed, a similar effect has been observed for intravenous administration to guinea-pigs of PAF, which induces a platelet-dependent bronchoconstriction (Vargaftig *et al*., 1980). However, the finding that TRAP-9 was still able to

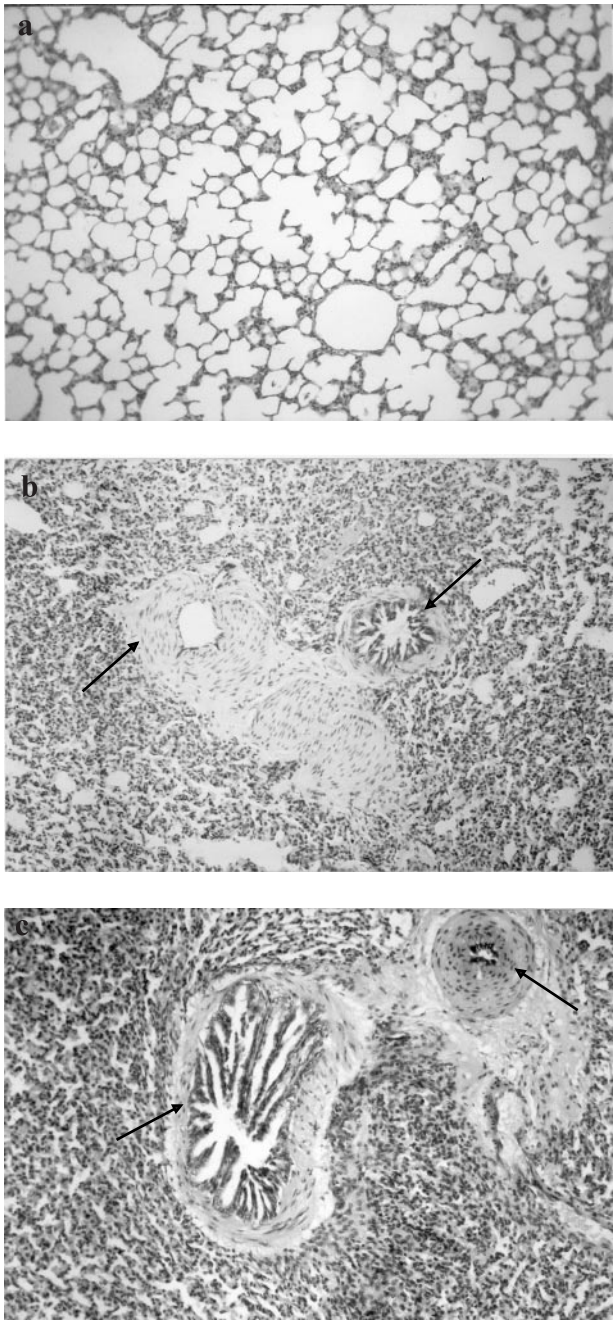

Figure 3 Histological analysis of lungs obtained from control animals (a; ×250), and thrombin (b; ×125) or TRAP-9 (c; ×250) injected animals. In b and c it is evident a strong bronchoconstriction (arrows) and vasoconstriction (arrows).

cause bronchoconstriction in guinea-pigs desensitized to thrombin effect strongly suggests that an additional mechanism, besides platelet degranulation, occurs. Interestingly, similar results have been obtained *in vitro*, on guinea-pig aortic preparations, where a thrombin receptor agonist peptide (TRAP 42-55) was able to cause relaxation of the tissue desensitized to thrombin action (Muramutsu *et al*., 1992; Yang *et al*., 1992). These differences have been attributed to differences of receptor dynamics depending on whether the receptor is activated by a free ligand or a tethered ligand. Furthermore, it is also possible that in addition to platelet stimulation the effect of thrombin and TRAP-9 is due to a direct action on bronchial smooth muscle, as has been observed, *in vitro*, using lung parenchymal smooth muscle (Mandhane *et al*., 1995).

The biphasic change in arterial blood pressure characterized by a rapid drop, followed by an equally rapid increase in blood pressure resembles the *in vitro* effect.

Thrombin effect on vascular tissues *in vitro* has been widely studied and it has been shown that thrombin induces in dog isolated coronary arteries, as well as in other vascular tissues, a slowly developing contraction characterized by an initial relaxation (Glusa & Paintz, 1994; Tesfamariam, 1994). Thrombin-induced hypotension was prevented by Hirulog™ pretreatment indicating that proteolytically active thrombin is essential for this effect. However, there was no tolerance to the effect observed, implying that even though receptor activation is necessary for the action, no receptor consumption occurs, or other mechanisms are involved in the hypotensive effect. Conversely, thrombin-induced hypertension was not affected by Hirulog™ pretreatment, but it was subject to tolerance suggesting that proteolytically active thrombin is not a requisite.

Lung histological analysis clearly showed for both thrombin and TRAP-9 not only an extensive lung damage characterized by alveolar atelectasia, but bronchial obstruction and also a pronounced vessel constriction. However, it is now clear that more than one PAR receptor is present in cells (Nystedt *et al*., 1994; Ishihara *et al*., 1997). *In vitro* studies have shown that thrombin and TRAPs causes smooth muscle contraction or relaxation depending on the vascular tissue considered (Muramutsu *et al*., 1992; Simonet *et al*., 1992; Yang *et al*., 1992; Tesfamariam, 1994), these variabilities of thrombin effects among tissues are probably linked to a different tissue distribution of PAR receptors. Thus, the different tolerance to the effects of thrombin and TRAP-9 observed might be dependent upon a different affinity of the two agents for different receptors. In addition, it could be that another region of the receptor is stimulated by thrombin or another receptor not proteolytically activated is involved. Thus, in the interpretation of the *in vivo* effects of thrombin and TRAPs, there could be a possible interaction of circulating thrombin with at least three different receptors, even if they have a different affinity.

In conclusion, our results show that thrombin causes bronchoconstriction in guinea-pig through a mechanism that involves the proteolytic activation of PAR-1 receptor. Thrombin effect is triggered by platelet activation but, besides this, other mechanisms might be involved, such as the stimulation of PAR-1 receptor on smooth muscle. This is to our knowledge the first study showing an effect of thrombin on the lung functionality *in vivo*, implying activation of, at least, PAR-1 receptor. Molecules able to antagonize the effects of TRAP on PAR-1 receptor could be useful in controlling bronchial asthma without interfering with haemostatic mechanisms.

This paper is dedicated to the memory of Prof Stuart Stone, a brilliant scientist and a good friend.

References

BAR-SHAVIT, R., KAHN, A. & WILNER, G.D. (1983). Monocyte chemiotaxis: Stimulation by specific exosite region in thrombin. *Science,* **220,** 728 – 731.

BIZIOS, R., LAI, L., FENTON II, J.W. & MALIK, A.B. (1986). Thrombin-induced chemiotaxis and aggregation of neutrophils. *J. Cell. Physiol.,* **128,** 485 – 490.

CHAO, B.H., KALKUNTE, S., MARAGANORE, J.M. & STONE, S.R. (1992). Essential groups in synthetic agonist peptides for activation of the platelet thrombin receptor. *Biochemistry,* **31,** 6175 – 6178.

CHIU, P.J.S., TETZLOFF, G.G., FOSTER, C., CHINTALA, M. & SYBERTZ, E.J. (1997). Characterization of in vitro and in vivo platelet response to thrombin and thrombin receptor-activating peptides in guinea pigs. *Eur. J. Pharmacol.,* **321,** 129 – 135.

CICALA, C. & CIRINO, G. (1998). Linkage between inflammation and coagulation: an update on the molecular basis of the crosstalk. *Life Sci.,* **62,** 1817 – 1824.

CIRINO, G., CICALA, C., BUCCI, M., SORRENTINO, L., MARAGANORE, J. & STONE, S.R. (1996). Thrombin functions as an inflammatory mediator through activation of its receptor. *J. Exp. Med.,* **183,** 821 – 827.

CONNOLLY, T.M., CONDRA, C., FENG, D., COOK, J., STRANIERI, M.T., REILLY, C.F., NUTT, R.F. & GOULD, R.J. (1994). Species variability in platelet and other cellular responsiveness to thrombin receptor-derived peptides. *Thromb. Haemost.,* **72,** 627 – 633.

COUGHLIN, S.R., VU, T.H., HUNG, D.T. & WHEATON, V. (1992). Characterization of a functional thrombin receptor. *J. Clin. Invest.,* **89,** 351 – 355.

DRAKE, W.T. & ISSEKUTZ, A.C. (1992). A role for α-thrombin in polymorphonuclear leukocyte recruitment during inflammation. *Sem. Thromb. Hemost.,* **18,** 333 – 340.

DRAKE, W.T., LOPES, N.N., FENTON II, J.W. & ISSEKUTZ, A.C. (1992). Thrombin enhancement of interleukin-1 and tumor necrosis factor-α induced polymorphonuclear leukocyte migration. *Lab. Invest.,* **67,** 617 – 627.

FUCHS-BUDER, T., DE MOERLOOSE, P., RICOU, B., REBER, G., VIFIAN, C., NICOD, L., ROMAND, J.A. & SUTER, P.M. (1996). Time course of procoagulant activity and D dimer in bronchoalveolar fluid of patients at risk for or with acute respiratory distress syndrome. *Am. J. Respir. Crit. Care Med.,* **153,** 163 – 167.

GARCIA, J.G.N., PATTERSON, C., BAHLER, C., ASCHNER, J., HART, C.M. & ENGLISH, D. (1993). Thrombin receptor activating peptides induce Ca^{2+} mobilization, barrier dysfunction, prostaglandin synthesis and platelet-derived growth factor mRNA expression in cultured endothelium. *J. Cell. Physiol.,* **156,** 541 – 549.

GLUSA, E. & PAINTZ, M. (1994). Relaxant and contractile responses of porcine pulmonary arteries to a thrombin receptor activating peptide (TRAP). *Arch. Pharmacol.,* **349,** 431 – 436.

GLUSA, E., PAINTZ, M. & BRETSCHNEIDER, E. (1996). Relaxant and contractile responses of porcine pulmonary arteries to thrombin and thrombin receptor activating peptides. *Sem. Thromb. Hemost.,* **22,** 261 – 265.

GRESELE, P., DOTTORINI, M., SELLI, M.L., IANNACCI, L., CANINO, S., TODISCO, T., ROMANO, S., CROOK, P., PAGE, C.P. & NENCI, G.G. (1993). Altered platelet function associated with the bronchial hyperresponsiveness accompanying nocturnal asthma. *J. Allergy Clin. Immunol.,* **91,** 894 – 902.

HOFFMAN, M. & CHURCH, F.C. (1993). Response of blood leukocytes to thrombin receptor peptides. *J. Leu. Biol.,* **54,** 145 – 151.

IDELL, S., JAMES, K.K., GILLIES, C., FAIR, D.S. & THRALL, R.S. (1989). Abnormalities of pathways of fibrin turnover in lung lavage of rats with oleic acid and bleomycin-induced lung injury support alveolar fibrin deposition. *Am. J. Pathol.,* **135,** 387 – 399.

ISHIHARA, H., CONNOLLY, A.J., ZENG, D., KAHN, M.L., ZHENG, Y.W., TIMMONS, C., TRAM, T. & COUGHLIN, S.R. (1997). Protease-activated receptor 3 is a second thrombin receptor in humans. *Nature,* **386,** 502 – 506.

KINLOUGH-RATHBONE, R.L., PERRY, D.W., GUCCIONE, A., RAND, M.L. & PACKMAN, M.A. (1993). Degranulation of human platelets by the thrombin receptor peptide SFLLRN: comparison with degranulation by thrombin. *Thromb. Haemost.,* **70,** 1019 – 1023.

KUDHAL, K., FISKER, S. & SONNE, O. (1991). A thrombin receptor in resident rat peritoneal macrophages. *Exp. Cell. Res.,* **193,** 45 – 53.

LINSSEN, M., LEMMERMANN, C.H., LIPPONER, L. & WILHELMS, O.H. (1991). Late phase increase of thrombin-like proteinase, protein, leukocytes in bronchoalveolar lavage (BAL) fluid and chemiluminescenze of BAL after ovalbumin aerosol inhalation by actively immunized rats. *Int. Arch. Allergy Appl. Immunol.,* **94,** 284–287.

MANDHANE, P., SAIFEDDINE, M., GREEN, F.H.I. & HOLLENBERG, M.D. (1995). Contractile actions of thrombin receptor-derived polypeptides in rat and guinea pig lung parenchymal smooth muscle. *Proc. West. Pharmacol.,* **38,** 93–96.

MARAGANORE, J.M., BOURDON, P., JABLONSKI, J., RAMACHANDRAN, K.L. & FENTON II, J.W. (1990). Design and characterization of hirulogs: a novel class of bivalent peptide inhibitors of thrombin. *Biochemistry,* **29,** 7095–7101.

MURAMUTSU, I., LANIYONU, A., MOORE, J.G. & HOLLENBERG, M.D. (1992). Vascular actions of thrombin receptor peptide. *Can. J. Physiol. Pharmacol.,* **70,** 996–1003.

NYSTEDT, S., EMILSSON, K., WAHLESTEDT, C. & SUNDELIN, J. (1994). Molecular cloning of a potential novel proteinase activated receptor 2. *Proc. Natl. Acad. Sci.,* **91,** 9208–9212.

PAGE, C.P. (1989). Platelets as inflammatory cells. *Immunopharmacology,* **17,** 51–59.

PANETTIERI JR, R.A., HALL, I.P., MAKI, C.S. & MURRAY, R.K. (1995). Alpha-Thrombin increases cytosolic calcium and induces human airway smooth muscle cell proliferation. *Am. J. Respir. Cell. Mol. Biol.,* **13,** 205–216.

SCHIFFRIN, E.L. (1994). The endothelium and control of blood vessel function in health and disease. *Clin. Invest. Med.,* **17,** 602–620.

SIMONET, S., BONHOMME, E., LAUBIE, M., THURIEAU, C., FAUCHERE, J.L. & VERBEUREN, T.J. (1992). Venous and arterial endothelial cells respond differently to thrombin and its endogenous receptor agonist. *Eur. J. Pharmacol.,* **216,** 135–137.

SONNE, O. (1988). The specific binding of thrombin to human polymorphonuclear leucocytes. *Scand. J. Clin. Lab. Invest.,* **48,** 831–838.

TALLARIDA, R.J. & MURRAY, R.B. (1987). Manual of pharmacologic calculations with computer programs. pp. 297. Springer Verlag: New York.

TESFAMARIAM, B. (1994). Distinct receptors and signaling pathways in α-thrombin- and thrombin receptor peptide-induced vascular contractions. *Circ. Res.,* **74,** 930–936.

VARGAFTIG, B.B., LEFORT, J., CHIGNARD, M. & BENVENISTE, J. (1980). Platelet activating factor induces a platelet-dependent bronchoconstriction unrelated to the formation of prostaglandin derivatives. *Eur. J. Pharmacol.,* **65,** 185–192.

VU, T.K., HUNG, D.T., WHEATON, V.I. & COUGHLIN, S.R. (1991). Molecular cloning of a functional thrombin receptor reveals a novel proteolytic mechanism of receptor activation. *Cell,* **64,** 1057–1068.

WEKSLER, B.B., LEY, C.W. & JAFFE, E.F. (1978). Stimulation of endothelial cell PGI_2 production by thrombin, trypsin and ionophore A23187. *J. Clin. Invest.,* **62,** 923–938.

YANG, S.G., LANIYONU, A., SAIFFEDINE, M., MOORE, G.J. & HOLLENBERG, M.D. (1992). Actions of thrombin and thrombin receptor peptide analogues in gastric and aortic smooth muscle: development of bioassays for structure-activity studies. *Life Sci.,* **51,** 1325–1332.

(Received June 19, 1998
Revised September 17, 1998
Accepted October 20, 1998)

British Journal of Pharmacology (1999) 126, 485–493
http://www.stockton-press.co.uk/bjp

Trigeminal nerve ganglion stimulation-induced neurovascular reflexes in the anaesthetized cat: Role of endothelin$_B$ receptors in carotid vasodilatation

[1]Pravin Raval, [1]Sharon Bingham, [2]Nambi Aiyar, [3]John D. Elliott, [1]A. Jackie Hunter, [2]Eliot H. Ohlstein & *,[1]Andrew A. Parsons

[1]Neurosciences Research, SmithKline Beecham Pharmaceuticals, New Frontiers Science Park, Harlow, Essex CM19 5AW, England, U.K.; [2]Cardiovascular Pharmacology, SmithKline Beecham Pharmaceuticals, Swedeland Road, King of Prussia, U.S.A.; [3]Medicinal Chemistry, SmithKline Beecham Pharmaceuticals, Swedeland Road, King of Prussia, U.S.A.

1 The effects of intravenous administration of endothelin (ET) receptor antagonists SB-209670 (0.001–10.0 mg kg^{-1}), SB-217242, SB-234551 (0.01–10.0 mg kg^{-1}) and BQ-788 (0.001–1.0 mg kg^{-1}) were investigated on trigeminal nerve ganglion stimulation-induced neurovascular reflexes in the carotid vasculature of the anaesthetized cat. Comparisons were made with sumatriptan (0.003–3.0 mg kg^{-1}) and α-CGRP$_{8-37}$ (0.001–0.1 mg kg^{-1}).

2 Trigeminal nerve ganglion stimulation produced frequency related increases in carotid blood flow, reductions in carotid vascular resistance and non-frequency related increases in blood pressure. Guanethidine (3 mg kg^{-1}, i.v.) blocked trigeminal nerve ganglion-induced increases in blood pressure but had no effect on changes in carotid flow or resistance. Maximal reductions in carotid vascular resistance was observed at 10 Hz, and this frequency was selected to investigate the effects of drugs on trigeminal nerve ganglion stimulation-induced responses in guanethidine treated cats.

3 Saline, α-CGRP$_{8-37}$ SB-209670 and BQ-788 had little or no effect on resting haemodynamic parameters. SB-217242 (10 mg kg^{-1}, $n=3$) produced a 56% reduction in arterial blood pressure whereas SB-233451 (10 mg kg^{-1}, $n=3$) produced a 30% reduction in carotid vascular resistance. Sumatriptan produced dose-related reductions in resting carotid flow and increases (max. 104% at 0.3 mg kg^{-1}, $n=5$) in vascular resistance.

4 SB-209670 ($n=6-7$), SB-217242 ($n=3$) and BQ-788 ($n=3$) produced inhibition of trigeminal nerve ganglion stimulation-induced reductions in carotid vascular resistance. Saline, SB-234551, α-CGRP$_{8-37}$ and sumatriptan had no effect.

5 These data demonstrate ET$_B$ receptor blockade attenuates the vasodilator effects of trigeminal nerve ganglion stimulation in the carotid vascular bed of guanethidine pretreated anaesthetized cats.

Keywords: SB-209670; SB-234551; SB-217242; trigeminal nerve ganglion; ET$_B$ receptor; sumatriptan; neurovascular reflex

Abbreviations: CdVR, carotid vascular resistance; CGRP, calcitonin gene-related peptide; TGN, trigeminal nerve ganglion stimulation; VIP, vasoactive intestinal polypeptide

Introduction

Electrical stimulation of the trigeminal nerve ganglion produces increases in blood flow (Goadsby & Duckworth, 1987; Goadsby & Edvinsson, 1993; 1994; Lambert *et al*., 1984), protein extravasation (Markowitz *et al*., 1987; Saito *et al*., 1988) and increases in brain stem cFos, but not c-jun and jun-D (Uhl *et al*, 1991; Shepheard *et al*., 1995). These experimental models have supported the concept of neurogenic inflammation as a mechanism for the development of migraine headache (Moskowitz & MacFarlane, 1993). Stimulation of sensory fibres appears to account for all the extravasation response (Markowitz *et al*., 1987) and detailed investigation has shown that sumatriptan and other 5-HT$_{1B/1D}$ agonists inhibit these effects (Buzzi & Moskowitz, 1990; Connor *et al*., 1997; Martin *et al*., 1997; Williamson *et al*., 1997).

A variety of NK-1 receptor antagonists also inhibit trigeminal nerve ganglion stimulation-induced extravasation in rats (Lee *et al*., 1994; O'Shaughnessy & Connor, 1994; Phebus *et al*., 1997; Shepheard *et al*., 1993, 1995). Some species differences do exist as the NK-1 antagonist, GR82334 blocks neurogenic inflammation in rats and guinea-pigs, whereas the calcitonin gene-related peptide (CGRP) receptor antagonist αCGRP$_{8-37}$ is effective in guinea-pigs, but not rats (O'Shaughnessy & Connor, 1994). Other agents that inhibit neurogenic extravasation include endothelin receptor antagonists (Brandli *et al*., 1995), sumatriptan analogues (Lee & Moskowitz, 1993) and a variety of other receptor agonists (Matsubara *et al*., 1992). However, a number of agents which show activity in this model, such as bosentan (May *et al*., 1996), CP-122288 (Roon *et al*., 1997) and LY-303870 (Goldstein *et al*., 1997) have not shown efficacy as acute migraine therapies in the clinic.

Trigeminal nerve ganglion stimulation also produces a reflex activation of autonomic ganglia which are involved in a reflex vasodilatation of the carotid vascular bed in the cat (Lambert *et al*., 1984). Stimulation of the trigeminal nerve ganglion produces release of both sensory (CGRP) and parasympathetic (vasoactive intestinal polypeptide, VIP) neurotransmitters (Buzzi *et al.,* 1991; Goadsby & Edvinsson, 1994), but does not appear to involve the sympathetic nervous system (Lambert *et al*., 1984). This interaction between afferent and efferent nervous systems is well documented in trigeminal nerve ganglion stimulation-induced reductions in common carotid vascular resistance in the cat (Lambert *et al*., 1984). Section of the VII nerve (parasympathetic) or pre-treatment

* Author for correspondence;
E-mail: andrew_a_parsons@sbphrd.com

with hexamethonium inhibited these reflex pathways (Lambert *et al*., 1984) which utilize VIP as the final mediator (Goadsby & MacDonald, 1985). A similar neurovascular reflex also operates in the intracranial circulation of the cat (Goadsby & Duckworth, 1987). In the rat, trigeminal fibres containing substance P and CGRP are present in parasympathetic ganglia forming basket-like arrangements with neurons (Suzuki *et al*., 1989a) and provide an anatomical basis for this neurovascular reflex. This pathway may also have clinical implications as inhibition of parasympathetic nerve has been suggested to mediate the antimigraine actions of intranasal lidocaine (Maizels *et al*., 1996).

It is known that sumatriptan produces complete inhibition of trigeminal nerve ganglion-induced extravasation in rats (Buzzi & Moskowitz, 1990), inhibits trigeminal nerve-ganglion-induced increases pial blood flow in cats (Goadsby & Edvinsson, 1993) and increases resting carotid vascular resistance (Perren *et al*., 1989) in cats. In contrast, sumatriptan has little effect on trigeminal nerve ganglion-induced neurovascular reflexes involving the parasympathetic nerve in cats (Lambert & Michalicek, 1996).

As endothelin-1 has been found in sensory nerves (Franco-Cereceda *et al*., 1991; Giaid *et al*., 1989) and ET receptor antagonists inhibit trigeminal nerve ganglion stimulation-induced extravasation (Brandli *et al*., 1995) and block cranial arterial vasodilatation (Maurice *et al*., 1997; Nilsson *et al*., 1997), the aims of the present studies were to explore the effects of endothelin receptor blockade on trigeminal nerve ganglion-induced neurovascular reflexes in comparison to the effects of sumatriptan and α-CGRP$_{8-37}$ on these responses.

Some of these results have been published in abstract form (Raval *et al*., 1996; 1997).

Methods

Experimental procedures

Animals This work was conducted in compliance with the Home Office Guidance on the operation of the Animals (Scientific Procedures) Act 1986, and was reviewed and approved by the SmithKline Beecham Procedures Review Panel.

Male cats (Hillgrove family farm), weight range 2.6–4.2 kg were housed in groups and allowed free access to food and water.

Surgical procedures

Cats were fasted overnight then anaesthetized with halothane (4%) in oxygen and maintained with intravenous administration of α-chloralose (120 mg kg^{-1} in a volume of 3 ml kg^{-1}). The trachea was cannulated and cats were artificially ventilated with room air at a rate of 30–35 strokes min^{-1} and tidal volume of 8 ml kg^{-1} which maintained blood oxygen and carbon dioxide tensions within normal limits. The right femoral artery was cannulated for measurement of blood pressure and derived heart rate and the left femoral vein for the administration of drugs.

Animals were placed in the prone position in a stereotaxic frame (David Kopf, California, U.S.A.) and bipolar electrodes (Rhodes NEX-100, Clark Electromedical, Reading, U.K.) were placed through a burr hole craniotomy on the right trigeminal nerve ganglion, calculated relative to Bregma at -9.5 mm in the arterior posterior direction and $+6.0$ mm in the lateral direction. An electromagnetic flow probe (Statham Gould diameter 1.5–2.0 mm) was placed around the right carotid artery and calibrated to a standard flow and recorded on a Gould flowmeter. Using the above co-ordinates, a bipolar electrode was advanced into the right trigeminal nerve ganglion which was stimulated briefly (10 Hz, 2 mA) using opposite polarity square wave pulses from 2 Grass constant current units (CCU, 1 A) driven by Grass stimulator isolation units (SIU, 5 A) and a Grass stimulator (S11). Correct placement of the electrode was indicated by strong lower jaw movements, salivation and an increase in carotid blood flow. This provides a useful marker of trigeminal nerve ganglion stimulation and was verified by direct current lesion of the trigeminal nerve in some animals.

In preliminary experiments, a frequency-response relationship was determined for changes in carotid blood flow and vascular resistance. The trigeminal nerve ganglion was stimulated (2 mA for 2 min) at 0.2, 0.5, 2, 5, 10 and 20 Hz and changes in blood pressure, heart rate, carotid blood flow and vascular resistance recorded following intravenous pretreatment with vehicle (saline) or guanethidine sulphate 3 mg kg^{-1}.

All subsequent experiments were conducted following administration of intravenous guanethidine sulphate 3 mg kg^{-1}. Two consecutive, reproducible control responses to trigeminal nerve stimulation were obtained at 30 min intervals before experiments were performed.

Physiological recordings

Physiological recordings were obtained using standard techniques as previously described by other groups in cats (Lambert *et al*., 1984; Lambert & Michalicek, 1996) and our Laboratory in dogs (Parsons *et al*., 1997). Systolic and diastolic blood pressures were recorded *via* the arterial cannulae connected to a pressure transducer (Bell & Howell). Pulsatile arterial blood pressure recordings were used to derive heart rate. Carotid blood flow was measured by electromagnetic flow probes. Which were calibrated to a range of standard flows through a glass capillary in accordance with the manufacturer's specifications. Blood flow was displayed on a Gould Flowmeter and all parameters were recorded on an 8 channel Lectromed chart recorder.

Pharmacological characterization

In separate experiments, the trigeminal nerve ganglion was stimulated at 30 min intervals for up to 2.5 h following intravenous administration of saline (0.1 ml kg^{-1}) 5 min prior to stimulation. Increasing doses of either SB-209670 (0.001–1 or 0.001–10.0 mg kg^{-1}, see below), SB-217242 or SB-234551 (0.01–10.0 mg kg^{-1}), BQ 788 (0.001–1.0 mg kg^{-1}), α-CGRP$_{8-37}$ (0.001–0.1 mg kg^{-1}) or sumatriptan (0.0003–3.0 mg kg^{-1}) were administered as a bolus (0.1 ml kg^{-1}), 5 min before nerve ganglion stimulation (10 Hz, 2 mA, 2 min) at 30 min intervals.

To investigate the duration of action of SB-209670, it was administered as doses between 0.001–1.0 mg kg^{-1} ($n=3$) and 0.001–10.0 mg kg^{-1} ($n=3$) and its effect on trigeminal nerve ganglion stimulation-evoked responses investigated 30 min following the last administration of compound.

Confirmation of αCGRP$_{8-37}$ activity in vivo

In a separate series of experiments, in guanethidine pretreated cats, we confirmed the blocking properties of α-CGRP$_{8-37}$ on CGRP-induced reductions in arterial blood pressure. In brief,

CGRP 100 ng kg^{-1} was administered intravenously prior to, and 30 min post intravenous administration of the CGRP receptor antagonist α-$CGRP_{8-37}$ (0.1 mg kg^{-1}).

Materials

SB-209670 (1RS-2SR,3RS)-3-(2-carboxymethoxy-4-methoxyphenyl)-5-(prop-1-yloxy) indane-2-carboxylic acid), SB-217242 ((+))-(1S,2R,3S)-3-[2-(2-hydroxeth-1-yloxy)-4-methoxphenyl]-1-(3,4,-methylenedioxyphenyl)-5-(prop-1-yloxy)indan-2-carboxylic acid), SB-234551 ((E)-α-[[1-butyl-5-[2-carboxyphenyl methoxy]-4-methoxyphenyl]-1H-pyrazol-4-yl]-methylene]-6-methoxy-1,3-benzodioxole-5-proanoic acid), α-$CGRP_{8-37}$ and guanethidine were synthesized at SmithKline Beecham Pharmaceuticals. α-Choralose was obtained from BDH (Germany). CGRP was obtained from Pennisula UK. Sumatriptan was extracted from commercially available sources by the Custom Synthesis Group, SmithKline Beecham. Imigran tablets were crushed and boiled with ethanol for 10 min, filtered whilst hot and allowed to cool and cystallize out of solution. The white solid was filtered off and dried *in vacuo*. The material was analysed and found to be >99% pure by h.p.l.c.. The structure of sumatriptan was confirmed by NMR. All drugs were dissolved in isotonic saline.

Data analysis

All data were entered into a PC and calculations performed using Excel. Carotid vascular resistance was calculated as mean arterial blood pressure divided by carotid blood flow. The following formula was used to calculate mean arterial blood pressure by ((systolic − diastolic blood pressure) × 1/3) + diastolic blood pressure.

Baseline mean arterial blood pressure, carotid flow and heart rate were measured before and after repeat administration of saline or each dose of compound under investigation and changes in carotid vascular resistance calculated. Trigeminal nerve ganglion stimulation-induced changes in mean arterial blood pressure, heart rate, carotid blood flow and calculated carotid vascular resistance were determined before and at the end of the 2 min stimulation period and the percentage change from control stimulation calculated. Control changes in mean arterial blood pressure, heart rate and carotid vascular resistance after nerve stimulation were derived from the mean values for the two responses obtained before administration of any drug. Effects of drugs on nerve stimulation were expressed as per cent inhibition of the control response.

The effects of pharmacological agents on resting carotid vascular resistance, heart rate and blood pressure were expressed as per cent change from initial resting values prior to drug administration.

To rule out the small effects of trigeminal nerve ganglion stimulation induced changes in arterial blood pressure on carotid blood flow, the effects of drugs were investigated on changes in carotid vascular resistance alone.

Data points were obtained from two groups of animals each receiving SB-209670 (0.001 mg kg^{-1} – 1.0 or 10 mg kg^{-1}), as no differences were observed between groups all data points were combined.

All data were subjected to ANOVA followed by Duncan's multiple range test with a significance level of $P<0.05$.

Results

Frequency response characteristics of trigeminal nerve ganglion stimulation

Trigeminal nerve ganglion stimulation (0.2 – 20 Hz) produced a frequency related increase in carotid blood flow and reduction in carotid vascular resistance both in the absence and in the presence of guanethidine (3 mg kg^{-1}, i.v.) pre-treatment (Figure 1). The maximal change in carotid blood flow was greater ($P<0.05$, Student's t-test) in control (75 ± 8.0%, $n=4$) than guanethidine pre-treated cats (59.0 ± 2.3%, $n=4$) and occurred at a stimulation frequency of 10 Hz in both groups. However, no significant differences in change in carotid vascular resistance were present between treatment groups with reduction of 34 ± 6.0 and 39 ± 5.5% in vehicle or guanethidine pre-treated animals respectively at this frequency. Trigeminal nerve ganglion stimulation produced marked but transient increases in mean arterial blood pressure which was abolished following guanethidine pre-treatment

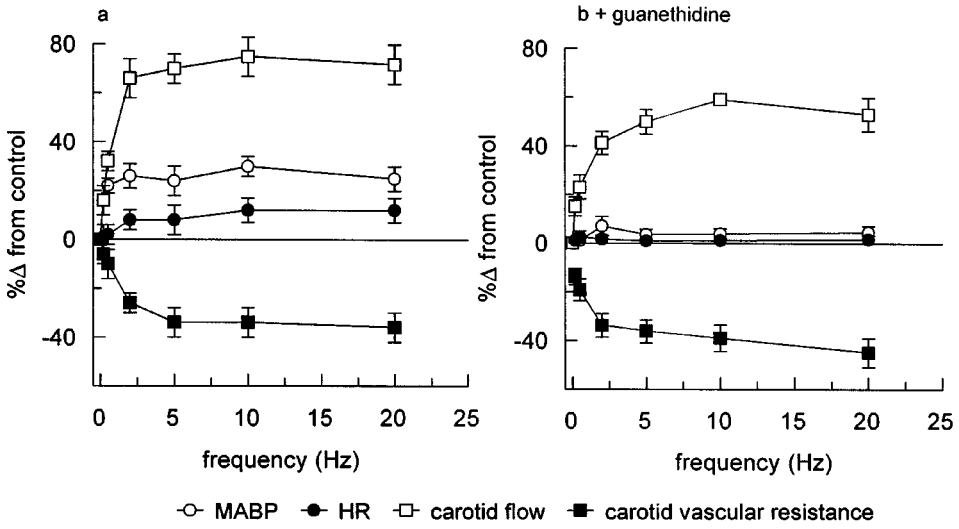

Figure 1 Effects of trigeminal nerve ganglion stimulation on changes in mean arterial blood pressure (MABP), heart rate (HR), carotid flow and carotid vascular resistance in (a) vehicle treated and (b) guanethidine (3 mg kg^{-1}, i.v.) treated animals ($n=4$ per group). Data points represent mean ± s.e.mean of per cent change from basal values in individual animals.

(Figure 1). Trigeminal nerve ganglion stimulation had little effect on heart rate in either group.

Therefore, the stimulation parameters of 2 mA at 10 Hz for 2 min were selected for further studies in the presence of guanethidine to remove effects of the sympathetic nervous system on mean arterial blood pressure.

Resting haemodynamic parameters

Resting haemodynamic variables in the presence of guanethidine are shown in Table 1. Mean arterial blood pressure, heart rate, carotid blood flow and calculated carotid vascular resistance were all in the expected range and not significantly different from animals treated with repeated saline (vehicle) administration (ANOVA) (not shown).

Effects of drugs on resting haemodynamic parameters

Saline (vehicle), α-CGRP$_{8-37}$ (0.001 – 0.1 mg kg^{-1}, i.v.) and BQ-788 (ET$_B$ selective antagonist; 0.001 – 1 mg kg^{-1}, i.v.) had no significant effect on mean arterial blood pressure (Figure 2), heart rate (not shown), carotid blood flow (not shown) or carotid vascular resistance (Figure 3). SB-209670 (ET$_{A/B}$ antagonist) produced a small, but statistically significant ($P<0.05$, $F=6.7$), dose related transient reduction in arterial blood pressure with a maximal decrease of $16\pm3.3\%$ following intravenous administration of 10 mg kg^{-1} (Figure 2). In contrast, SB-217242 produced dose related ($P<0.05$; $F=23.6$) transient (<5 min) decreases in mean arterial blood pressure (Figure 2). At the highest intravenous dose administered, SB-217242 produced a $56.8\pm5\%$ reduction in mean arterial blood pressure. This reduction in blood pressure precluded collection of carotid flow data in two animals as the flow signal was transiently lost, probably due to movement of the flow probe around the carotid artery. Restoration of the carotid blood flow signal occurred within 5 min which allowed inclusion of these animals for stimulation experiments. SB-234551 at 10 mg kg^{-1} also produced a lowering of mean arterial blood pressure ($27.0\pm4.4\%$, $n=3$, $P<0.05$; $F=10.7$, Figure 2) and a decrease in carotid vascular resistance of $30.6\pm4.4\%$ ($n=3$, $P<0.05$; $F=14.7$, Figure 3) with little effect on heart rate.

In contrast, sumatriptan had little effect on blood pressure (Figure 2) but produced marked dose-related increases ($P<0.05$; $F=3.1$) in carotid vascular resistance (Figure 3) with a maximal effect of $104.8\pm34.1\%$ observed at 0.3 mg kg^{-1} ($n=5$).

Effect of trigeminal nerve ganglion stimulation

Trigeminal nerve stimulation (10 Hz, 2 mA, 2 min) produced a small depressor response (<8%) with no effect on heart rate (Table 1). In contrast to the minor effects on the systemic circulation, trigeminal nerve ganglion stimulation produced an

Table 1 Mean$\pm$s.e.mean blood pressure, heart rate, carotid blood flow and calculated carotid vascular resistance in anaesthetized cats pre- and post-trigeminal nerve ganglion stimulation (10 Hz, 2 mA for 2 min) prior to drug administration

Status	*Arterial blood pressure* (mmHg)	*Heart rate* (beats min^{-1})	*Carotid blood flow* (ml min^{-1})	*Carotid vascular resistance* (mmHg min ml^{-1})
Before stimulation (basal)	76 ± 2	159 ± 3	16 ± 1	5.5 ± 0.4
After nerve ganglion stimulation	70 ± 2*	158 ± 3	27 ± 2*	3.0 ± 0.2*

Data is pooled from 30 animals pre-treated with guanethidine used in the present investigations. No differences were found in the resting haemodynamic variables from groups of animals receiving, saline (vehicle) α-CGRP$_{8-37}$ (0.001 – 0.1 mg kg^{-1}), sumatriptan (0.003 – 3.0 mg kg^{-1}), SB-209670 (0.001 – 10.0 mg kg^{-1}), BQ-788 (0.001 – 1.0 mg kg^{-1}), SB-217242 or SB-234551 (0.01 – 10.0 mg kg^{-1}). *Represents a significant difference from pre-stimulation baseline (paired t-test, $P<0.05$).

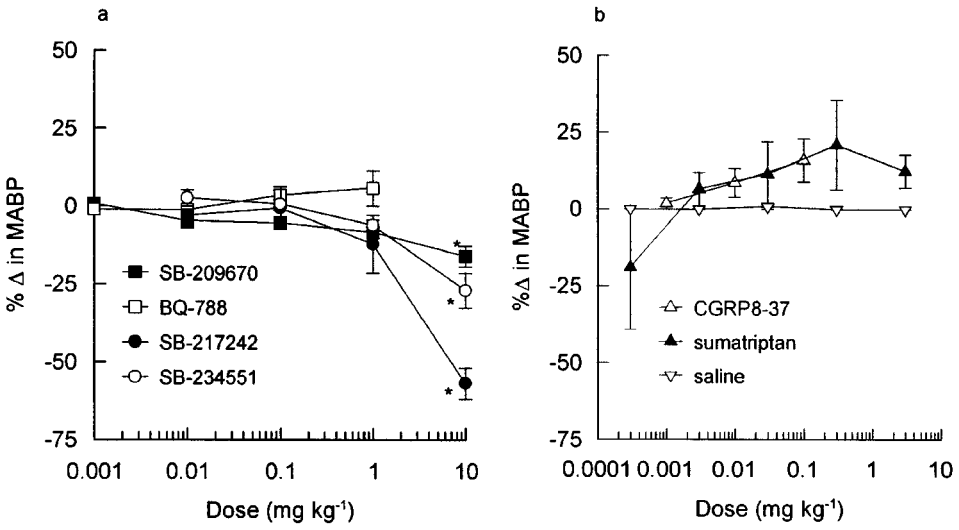

Figure 2 Effects of (a) SB-209670 ($n=3-7$), BQ-788 ($n=3$), SB-217242 ($n=3$), SB-234551 ($n=3$) or (b) CGRP$_{8-37}$ ($n=3$), sumatriptan ($n=4-5$) or saline (time matched controls, $n=2-3$) on resting mean arterial blood pressure (MABP). Data points represent means$\pm$s.e.mean of per cent change from basal values (*$P<0.05$, ANOVA with Duncan's multiple range test compared pre-drug values).

increase in mean ± s.e.mean carotid blood flow from 16 ± 1 to 27 ± 2 ml min^{-1}, which was associated with a concomitant reduction in mean ± s.e.mean vascular resistance from 5.5 ± 0.4 mmHg min^{-1} ml^{-1} to 3.0 ± 0.2 mmHg min^{-1} ml^{-1} (Table 1).

Pharmacological modulation of the trigeminal nerve ganglion stimulation-induced changes in carotid vascular resistance

Control responses to trigeminal nerve ganglion stimulation, before drug administration in each experimental group, produced reductions of carotid vascular resistance of 46.5 ± 2.7% in cats administered saline ($n = 3$), 45.6 ± 4.8% in SB-209670 ($n = 7$), 48.1 ± 2.1% in BQ-788 ($n = 6$), 44.5 ± 6.7% in SB-217242 ($n = 3$), 41.0 ± 3.3% in SB-234551 ($n = 3$), 40.9 ± 7.2% in sumatriptan ($n = 5$) and 54.0 ± 7.4% in α-$CGRP_{8-37}$ ($n = 3$) treated animals, respectively. Trigeminal nerve ganglion stimulation induced changes in carotid blood flow and carotid vascular resistance, but not arterial blood pressure were reproducible in saline (vehicle) treated animals over the experimental period. The effects of drug treatment on trigeminal nerve stimulation induced reductions in arterial blood pressure were not investigated further.

SB-209670 (0.001 – 10 mg kg^{-1}) dose-dependently inhibited trigeminal nerve ganglion stimulation-induced reductions ($P < 0.05$; $F = 4.2$) in carotid vascular resistance (Figure 4) with a maximum inhibition of 53.8 ± 6.4% ($P < 0.05$, $n = 3$) at 10 mg kg^{-1} (i.v.). SB-217242 (0.01 – 10 mg kg^{-1}) and BQ-788 (0.001 – 1 mg kg^{-1}) also inhibited trigeminal nerve ganglion stimulation-induced reduction in carotid vascular resistance at intravenous doses of 10 mg kg^{-1} (35 ± 16.1% inhibition, $n = 3$, $P < 0.05$; $F = 2.3$) and 1 mg kg^{-1} (39.3 ± 14.0% inhibition, $n = 3$, $P < 0.05$; $F = 1.9$) respectively (Figure 4). Comparison of the dose required to produce a 25% inhibition of the trigeminal ganglion stimulation-induced reduction of carotid vascular resistance shows the following rank order of antagonist potency (Figure 4). SB-209670 = BQ-788 > SB-217242. SB-234551 (0.01 – 1 mg kg^{-1}, i.v.), α-$CGRP_{8-37}$ (0.001 – 0.1 mg kg^{-1}) and sumatriptan (0.003 – 3 mg kg^{-1}, i.v.) had no

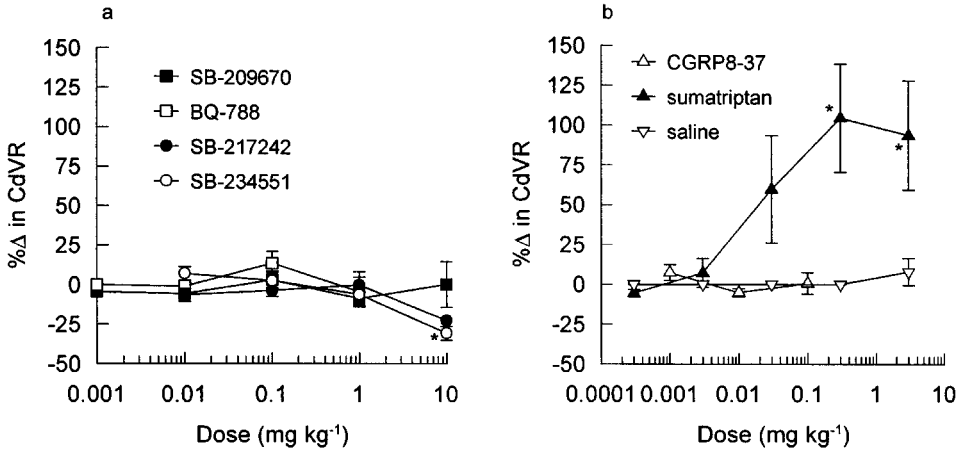

Figure 3 Effects of (a) SB-209670 ($n = 3 – 7$), BQ-788 ($n = 3$), SB-217242 ($n = 3$: at 10 mg kg^{-1}, $n = 1$), SB-234551 ($n = 3$) or (b) $CGRP_{8-37}$ ($n = 3$), sumatriptan ($n = 4 – 5$) or saline (time matched controls, $n = 2 – 3$) on resting carotid vascular resistance (CdVR). Data points represent means ± s.e.mean of per cent change from basal values (*$P < 0.05$). It should be noted that carotid flow values could not be recorded in two out of three animals following 10 mg kg^{-1} SB-217242 as marked reductions in blood pressure occurred.

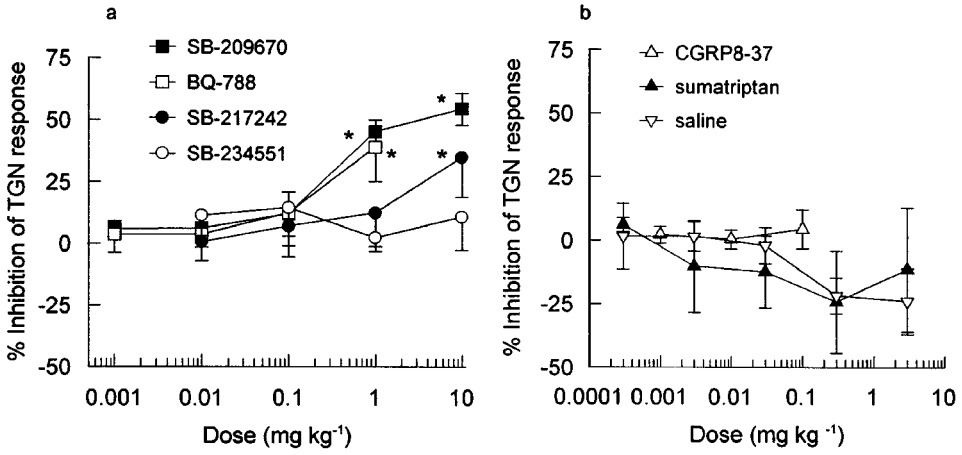

Figure 4 Effects of (a) SB-209670 ($n = 3 – 7$), BQ-788 ($n = 3$), SB-217242 ($n = 3$), SB-234551 ($n = 3$) or (b) $CGRP_{8-37}$ ($n = 3$), sumatriptan ($n = 4 – 5$) or saline (time matched controls, $n = 2 – 3$) on the trigeminal nerve (10 Hz, 2 mA, 2 min) mediated reduction in carotid vascular resistance in the anaesthetized cat. Data points represent means ± s.e.mean of the per cent inhibition of trigeminal nerve ganglion stimulation (TGN)-induced response from individual animals (*$P < 0.05$, ANOVA with Duncan's multiple range test compared to control neurogenic response).

significant effects on trigeminal nerve ganglion-induced reductions in carotid vascular resistance (Figure 4).

Duration of pharmacological effect of SB-209670

The inhibitory effects of SB-209670 ($0.001-1$ mg kg^{-1} or $0.001-10$ mg kg^{-1}) were also evaluated 30 min post administration. No significant effect on trigeminal nerve-mediated responses was observed (Figure 5) demonstrating a short duration of action of SB-209670 in this system.

Confirmation of $\alpha CGRP_{8-37}$ activity in vivo

In these experiments, resting arterial blood pressure was 66 ± 8 mmHg. CGRP (0.1 mg kg^{-1}) produced a mean reduction of 23 ± 3 mmHg ($n=3$) which was attenuated by approximately 50% by pre-treatment with α-CGRP$_{8-37}$ (0.1 mg kg^{-1}) to 10 ± 1 mmHg ($n=3$) (paired t-test $P<0.05$). Administration of CGRP had little effect on heart rate, indicating a lack of sympathetic reflexes due to guanethidine pretreatment.

Discussion

This study confirms previous observations of trigeminal nerve ganglion-mediated reductions in carotid vascular resistance in the cat (Lambert *et al*., 1984; Lambert & Michalicek, 1996). The degree of reduction in carotid vascular resistance was greater in the present study compared to the results of Lambert & Michalicek (1996), and may be a result of the different stimulation parameters used in each case. In the present study, high intensity stimulation (2 mA) was selected to provide compatibility with neurogenic extravasation experiments (1.2 mA) in rats (Brandli *et al*., 1995; Buzzi & Moskowitz, 1990; O'Shaughnessy & Connor, 1994) and guinea-pigs (1.5 mA) (O'Shaughnessy & Connor, 1994). To investigate the trigeminal nerve ganglion-induced neurovascular reflex between the sensory (trigeminal nerve) and parasympathetic systems, we pretreated animals with guanethidine to remove any confounding effects of stimulation of the sympathetic nerve, such as alteration of systemic arterial blood pressure. Other groups have used surgical lesion of the cervical sympathetic trunk as a routine procedure to achieve the same result in cats (Lambert *et al*., 1984).

In the absence of guanethidine, trigeminal nerve stimulation produced a pressor response in addition to increases in carotid flow and reductions in resistance. The changes in arterial blood pressure were abolished by pre-treatment with guanethidine indicating activation of the sympathetic nervous system in these effects. Such increases in blood pressure have been observed by other workers in rabbits (Kumada *et al*., 1977), rats (Spokes & Middlefell, 1995) and cats (Lambert *et al*., 1984; Lambert & Michalicek, 1996), the magnitude of which may be related to different stimulation parameters (Goadsby & Edvinsson, 1993). However, guanethidine had no effect on the change in carotid vascular resistance evoked by trigeminal nerve ganglion stimulation with a maximal increase in carotid flow obtained at a stimulation frequency of 10 Hz.

Trigeminal nerve ganglion stimulation has also been shown to enhance reductions in carotid vascular resistance in anaesthetized rats (Spokes & Middlefell, 1995). However, in anaesthetized guinea-pigs, trigeminal nerve ganglion stimulation only produced consistent reductions in carotid vascular resistance in guanethidine pretreated animals (Beattie & Connor, 1994) which may indicate a marked sympathetic involvement of this pathway in this species.

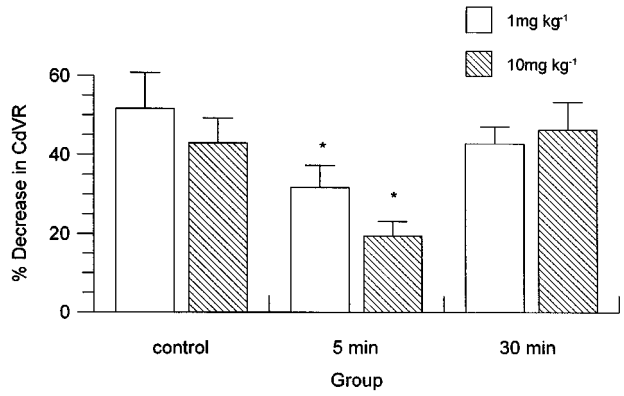

Figure 5 Effects of SB-209670 (1.0 or 10 mg kg^{-1}) 5 or 30 min post administration on the trigeminal nerve ganglion stimulation-induced reduction in carotid vascular resistance (CdVR). All animals received lower doses of SB-209670 as part of the ascending dose response investigation. Data points represent means$\pm$s.e.mean of change in carotid vascular resistance ($n=3$ per group) (*$P<0.05$, ANOVA followed by Duncan's multiple range test).

Effects of endothelin receptor antagonists on neurovascular reflexes

This study is the first to demonstrate that endothelin antagonists, which are effective inhibitors of trigeminal afferent fibre-induced extravasation (Brandli *et al*., 1995) also block trigeminal nerve ganglion-induced neurovascular reflex changes in carotid vascular resistance. SB-209670 is a non-peptide mixed ET$_{A/B}$ receptor antagonist (Ohlstein *et al*., 1994) with a binding affinity of 18 nM at human cloned ET$_B$ receptors. The peptide ET$_B$ receptor antagonist, BQ-788 shows selective binding to human ET$_B$ receptor (IC_{50} 1.2 nM in human heart) (Ishikawa *et al*., 1994), whereas SB-217242 has 100 fold (Ohlstein *et al*., 1996) and SB-234551 more than 500 fold selectivity (Ohlstein *et al*., 1998) for human cloned ET$_A$ receptors over human cloned ET$_B$ receptors. The rank order of antagonist potency in producing inhibition of the trigeminal nerve-induced reductions in carotid vascular resistance was SB-209670 = BQ-788 > SB-217242. SB-234551 had no effect. This rank order of potency is consistent with a role for ET$_B$ receptor activation mediating these effects in the anaesthetized cat.

Effects of endothelin receptor antagonists on resting haemodynamic parameters

It is important to note that SB-209670, BQ-788 and SB-217242 produced inhibition of trigeminal nerve-induced reductions in carotid vascular resistance with no effect on resting tone, indicating a direct effect on neuroeffector coupling with no local vascular effect. However, SB-217242 produced marked reductions in mean arterial blood pressure in the cat, whereas in the rat, SB-217242 (0.3–30 mg kg^{-1}, i.v.) had no significant haemodynamic effects (Ohlstein *et al*., 1996). SB-209670 and SB-234551 had a small effect on arterial blood pressure. This profile of activity does not parallel activity at the human cloned ET$_A$ receptor with pKi values of 12, 111 and 500 nM for SB-209670 (Ohlstein *et al*., 1994), SB-217242 (Ohlstein *et al*., 1996) and SB-234551 (Ohlstein *et al*., 1998) respectively. However, activity of these agents at feline endothelin ET$_A$ receptors is not known. SB-234551 also produced a small

decrease in baseline carotid vascular resistance which raises the possibility of a modulatory role for endothelin ET_A receptor activation in the maintenance of vascular tone in the guanethidine treated anaesthetized cat.

Potential inhibitory mechanisms of endothelin receptor antagonists on neurovascular reflexes

Despite inhibiting trigeminal evoked responses, SB-209670 ($0.001-1$ and $0.001-10$ mg kg^{-1}) produced only transient blockade and had little effect on trigeminal nerve ganglion stimulation-induced responses 30 min post administration. This may reflect a limited exposure of SB-209670 in the cat or tolerance to the effects of endothelin receptor blockade over time. Further experiment will be required to verify this observation.

Endothelin has been identified in both sensory neurones and glial cells (Giaid *et al*., 1989; Franco-Cereceda *et al*., 1991) and ET-3 release has been demonstrated from trigeminal sensory nerves (Brandli *et al*., 1995). ET_B receptor activation increases cholinergic nerve-mediated contraction in the bronchus (Fernandes *et al*., 1996). Possible explanations for the inhibitory effects of ET_B antagonists in this study therefore include inhibition of the vascular effects of released endothelins and/or inhibition of release of transmitters from parasympathetic or sensory nerves. Inhibition of ET_B receptor-mediated potentiation of parasympathetic nerve activity may produce a reduction in trigeminal nerve ganglion neurovascular reflexes.

Effects of calcitonin gene-related peptide receptor antagonist, $CGRP_{8-37}$

In the present study, we confirmed the pharmacological activity of $CGRP_{8-37}$ (0.1 mg kg^{-1}) which produced an approximate 50% inhibition of CGRP (100 ng kg^{-1})-induced reductions in mean arterial blood pressure. However, $CGRP_{8-37}$ had little effect on trigeminal nerve ganglion stimulation-induced neurovascular responses in the carotid vascular bed. In contrast the same dose of $CGRP_{8-37}$ completely inhibited sensory nerve-induced (neurogenic) protein extravasation in the meninges of the guinea-pig (O'Shaughnessy & Connor, 1994). Similar doses of $CGRP_{8-37}$ also inhibited trigeminal nerve ganglion-induced increases in facial skin blood flow (Escott *et al*., 1995) in rats. Lower doses of the antagonist (100 μg) also inhibited nasocilliary nerve-induced increases in cerebral blood flow (Goadsby, 1993) in cats.

Since the dose of CGRP receptor antagonist used in the present study was pharmacologically active, these data demonstrate that CGRP does not play a major role in trigeminal nerve induced neurovascular responses in the carotid circulation. Similar results were obtained in the guinea-pig (Beattie & Connor, 1994). In these studies, $CGRP_{8-37}$ (0.9 mg kg^{-1}) had no effect on trigeminal nerve ganglion-induced reductions in carotid vascular resistance, whereas a VIP receptor antagonist abolished this response (Beattie & Connor, 1994).

Collectively, these data show that stimulation of trigeminal nerve tracts may produce different responses dependent on whether the nerve (e.g. nasocillary) or nerve ganglion has been stimulated and the nature of the response investigated (e.g. dilatation or extravasation).

Effects of sumatriptan

Sumatriptan had no sustained effect on mean arterial blood pressure but produced marked increases in carotid vascular resistance as reported by Perren *et al*. (1989). It had no effect on trigeminal nerve-induced reductions in carotid vascular resistance. This observation is consistent with the results of Lambert & Michalicek (1996) who demonstrated that sumatriptan had no effect on changes in carotid vascular resistance or meningeal vascular resistance over a range of nerve stimulation frequencies. Similar results were obtained in rats where sumatriptan inhibited trigeminal nerve ganglion stimulation-induced extravasation but not reductions in carotid vascular resistance (Spokes & Middlefell, 1995).

However, sumatriptan has been shown to inhibit trigeminal nerve ganglion-induced increases in cortical blood flow in the cat (Goadsby & Edvinsson, 1993) when measured by laser doppler flowmetry. These observations again illustrate marked differences in pharmacological properties of agents modulating neuroeffector function. The overall response to an inhibitory agent may therefore depend on the local and neurovascular reflexes initiated by nerve stimulation.

Neurotransmitters and trigeminovascular reflexes

A number of neurotransmitter systems may be involved in sensory nerve induced neurogenic extravasation by antidromic release of neurotransmitters. For example, both NK-1 antagonists (GR 82334) and CGRP antagonists ($CGRP_{8-37}$) produce maximal inhibition of neurogenic extravasation in the guinea-pig (O'Shaughnessy & Connor, 1994). In the rat, administration of an ET_B receptor agonist, sarafotoxin S6c, produced marked protein extravasation which was inhibited by the neurokinin receptor antagonist, spantide, supporting an indirect effect of endothelin receptor agonists on inflammatory transmitter release from the trigeminal nerve (Brandli *et al*., 1995).

VIP mediates extracranial vasodilatation in the cat (Goadsby & MacDonald, 1985) *via* the parasympathetic nerve. In cats, trigeminal nerve ganglion stimulation-induced reductions in carotid vascular resistance and increases in cerebral blood flow were inhibited by lesion of the VIIth nerve and blocked by hexamethonium in most animals (Goadsby & Duckworth, 1987; Lambert *et al*., 1984). In guinea-pigs, VIP appears to mediate trigeminal nerve ganglion-induced reductions in carotid vascular resistance which are not blocked by hexamethonium (Beattie & Connor, 1994). The lack of effect of hexamethonium was taken to indicate a lack of ganglionic transmission in this response (Beattie & Connor, 1994). However, Substance P/CGRP containing cells forming basket-like structures around cell bodies of the sphenopalatine ganglion have been suggested to form a reflex arc which may not utilize acetylcholine as an excitatory transmitter (Suzuki *et al*., 1989b). Excitation of sensory nerve endings may therefore involve trigeminal nerve reflexes, which also involve parasympathetic pathways. The present study clearly demonstrates the capability of ET receptor antagonists to modulate this pathway.

It is apparent that ET receptor antagonists modulate both trigeminal nerve-induced extravasation (Brandli *et al*., 1995) and trigeminal nerve-induced neurovascular reflexes (this study). However, a degree of redundancy appears to be apparent in these pathways as a number of neurotransmitters have been shown to play a role in these responses. This suggestion may partly explain the failure of ET receptor antagonist (May *et al*., 1996) and NK-1 receptor antagonists (Goldstein *et al*., 1997) in the clinic and indicates that modulation of post-synaptic mechanisms may not provide adequate efficacy as an antimigraine agent. Future strategies

may be better directed to pre-synaptic inhibition of these pathways.

We conclude that ET_B receptor activation plays a significant role in modulation of trigeminal nerve ganglion induced-neurovascular responses in the carotid vascular bed of anaesthetized cats. Stimulation of 5-$HT_{1B/1D}$ receptors by sumatriptan or blockade of CGRP receptors has no effect. This model may be of use in determining the effects of novel agents on neurovascular reflexes.

The authors would like to thank Dr Neil Upton for helpful comments on the manuscript and Dr Brian Burpitt, Kirit Pancholi and Lynne Crawford from the Custom Synthesis Group, Medicinal Chemistry, Harlow for the supply of sumatriptan.

References

BEATTIE, D.T. & CONNOR, H.E. (1994). The influence of the trigeminal ganglion on carotid blood flow in anaesthetized guinea-pigs. *Br. J. Pharmacol.,* **112,** 262–266.

BUZZI, M.G., CARTER, W.B., SHIMIZU, T., HEATH, H. & MOSKOWITZ, M.A. (1991). Dihydroergotamine and sumatriptan attenuate levels of CGRP in plasma in rat superior sagittal sinus during electrical stimulation of the trigeminal nerve ganglion. *Neuropharmacology,* **30,** 1193–1200.

BUZZI, M.G. & MOSKOWITZ, M.A. (1990). The antimigraine drug (GR 43175), selectively blocks neurogenic plasma extravasation from blood vessels in dura mater. *Br. J. Pharmacol.,* **99,** 202–206.

BRANDLI, P., LOFFLER, B.-M., BREU, V., OSTERWALDER, R., MARIE, J.-P. & CLOZEL, M. (1995). Role of endothelin in mediating neurogenic plasma extravasation in rat dura mater. *Pain,* **64,** 315–322.

CONNOR, H.E., FENIUK, W., BEATTIE, D.T., NORTH, P.C., OXFORD, A.W., SAYNOR, D.A. & HUMPHREY, P.P.A. (1997). Naratriptan: Biological profile in animal models relevant to migraine. *Cephalalgia,* **17,** 145–152.

ESCOTT, K.J., BEATTIE, D.T., CONNOR, H.E. & BRAIN, S.D. (1995). Trigeminal ganglion stimulation increases facial skin blood flow in the rat: major role for calcitonin gene-related peptide. *Brain Res.,* **669,** 93–99.

FERNANDES, L.B., HENRY, P.J., RIGBY, P.J. & GOLDIE, R.G. (1996). $Endothelin_B$ (ET_B) receptor-activated potentiation of cholinergic nerve-mediated contraction in human bronchus. *Br. J. Pharmacol.,* **118,** 1873–1874.

FRANCO-CERECEDA, A., RYDH, M., LOU, Y.-P., DALSGAARD, C.-A. & LUNDBERG, J.M. (1991). Endothelin as a putative sensory neuropeptide in the guinea-pig: different properties in comparison with calcitonin gene-related peptide. *Reg. Peptides,* **32,** 253–265.

GIAID, A., GIBSON, S.J., IBRAHIM, N.B.N., LEGON, S., BLOOM, S.R., YANAGISAWA, M., MASAKI, T., VARNDELL, I.M. & POLAK, J.M. (1989). Endothelin-1, an endothelium-derived peptide, is expressed in neurons of the human spinal cord and dorsal root ganglia. *Proc. Natl. Acad. Sci. U.S.A.,* **86,** 7634–7638.

GOADSBY, P.J. (1993). Inhibition of calcitonin gene-related peptide by h-CGRP8–37 antagonizes the cerebral dilator response from nasociliary nerve stimulation in the cat. *Neurosci. Lett.,* **151,** 13–16.

GOADSBY, P.J. & DUCKWORTH, J.W. (1987). Effect of stimulation of trigeminal ganglion on regional cerebral blood flow in cats. *Am. J. Physiol.,* **253,** R270–R274.

GOADSBY, P.J. & EDVINSSON, L. (1993). The trigeminovascular system and migraine: Studies characterising cerebrovascular and neuropeptide changes seen in humans. *Ann. Neurol.,* **33,** 48–56.

GOADSBY, P.J. & EDVINSSON, L. (1994). Peripheral and central trigeminovascular activation in cat is blocked by the serotonin (5-HT)-1D receptor agonist 311C90. *Headache,* **34,** 394–399.

GOADSBY, P.J. & MACDONALD, G.J. (1985). Extracranial vasodilatation mediated by vasoactive intestinal polypeptide. *Brain Res.,* **329,** 285–288.

GOLDSTEIN, D.J., WANG, O., SAPER, J.R., STOLTZ, R., SILBERSTEIN, S.D.& MATHEW, N. (1997). Ineffectiveness of neurokinin-1 antagonist in acute migraine: a crossover study. *Cephalalgia,* **17,** 785–790.

ISHIKAWA, T., IHARA, M., NOGUCHI, K., MASE, T., MINO, N., SAEKI, T., FUKURODA, T., FUKAMI, T., OZAKI, S., NAGASE, T., NISHIKIBE, M. & YANO, M. (1994). Biochemical and pharmacological profile of a potent and selective endothelin-B receptor antagonist, BQ-788. *Proc. Natl. Acad. Sci. U.S.A.,* **91,** 4892–4896.

KUMADA, M., DAMPNEY, R.A.L. & REIS, D.J. (1977). The trigeminal depressor response: A novel vasodepressor response originating from the trigeminal system. *Brain Res.,* **119,** 305–326.

LAMBERT, G.A., BOGDUK, M., GOADSBY, P.J., DUCKWORTH, J.W. & LANCE, J.W. (1984). Decreased carotid arterial resistance in cats in response to trigeminal stimulation. *J. Neurosurg.,* **61,** 145–155.

LAMBERT, G.A. & MICHALICEK, J. (1996). Effect of antimigraine drugs on dural blood flows and resistances and the responses to trigeminal stimulation. *Eur. J. Pharmacol.,* **311,** 141–151.

LEE, W.S. & MOSKOWITZ, M.A. (1993). Conformationally restricted sumatriptan analogues, CP-122288 and CP-122,638 exhibit enhanced potency against neurogenic inflammation in the dura. *Brain Res.,* **626,** 303–305.

LEE, W.S., MOUSSAOUI, S.M. & MOSKOWITZ, M.A. (1994). Blockade by oral or parental RPR 100893 (a non-peptide NK1 receptor antagonist) of neurogenic plasma protein extravasation within guinea-pig dura mater and conjunctiva. *Br. J. Pharmacol.,* **112,** 920–924.

MAIZELS, M., SCOTT, B., COHEN, W. & CHEN, W. (1996). Intranasal lidocaine for treatment of migraine. A randomized, double-blind, controlled trial. *JAMA,* **276,** 319–321.

MARKOWITZ, S., SAITO, K. & MOSKOWITZ, M.A. (1987). Neurogenically mediated leakage of plasma protein occurs from blood vessels in dura mater but not brain. *J. Neurosci.,* **7,** 4129–4136.

MARTIN, G.W., ROBERTSON, A.D., MACLENNAN, S.J., PRENTICE, D.J., BARETT, V.J., BUCKINGHAM, J., HONEY, A.C., GILES, H. & MONCADA, S. (1997). Receptor specificity and trigeminovascular inhibitory actions of a novel 5-$HT_{1B/1D}$ receptor partial agonist, 311C90 (zolmitriptan). *Br. J. Pharmacol.,* **121,** 157–164.

MATSUBARA, T., MOSKOWITZ, M.A. & HUANG, Z. (1992). UK14,304, R(−)-alpha-methyl-histamine and SNS 201-995 block plasma protein leakage within dura mater by prejunctional mechanisms. *Eur. J. Pharmacol.,* **224,** 145–150.

MAURICE, M.C., GRATTON, J.P. & D'ORLEANS-JUSTE, P. (1997). Pharmacology of two novel mixed ETA/ETB receptor antagonists, BQ-928 and 238, in the carotid and pulmonary arteries of the perfused kidney of the rabbit. *Br. J. Pharmacol.,* **120,** 319–325.

MAY, A., GIJSMAN, H.J., WALLNOFER, A., JONES, R., DIENER, H.C. & FERRARI, M.D. (1996). Endothelin antagonist bosentan blocks neurogenic inflammation, but is not effective in aborting migraine attacks. *Pain,* **67,** 375–378.

MOSKOWITZ, M.A. & MACFARLANE, R. (1993). Neurovascular and molecular mechanisms in migraine headaches. *Cerebrovasc. Brain Metab. Rev.,* **5,** 159–177.

OHLSTEIN, E.H., NAMBI, P., DOUGLAS, S.A., EDWARDS, R.M., GELLAI, M., LAGO, A., LEBER, J.D., COUSINS, R.D., GAO, A., PEISHOFF, C.E., BEAN, J.W., EGGLESTON, D., ELSHOURBAGY, N., KUMAR, C., LEE, J.A., BROOKS, D.P., RUFFOLO, R.R., FEUERSTEIN, G., WEISTOCK, J., GLEASON, J.G. & ELLIOT, J.D. (1994). SB-209670, a rationally designed potent non-peptide endothelin receptor antagonist. *Proc. Natl. Acad. Sci. U.S.A.,* **91,** 8052–8056.

OHLSTEIN, E.H., NAMBI, P., HAY, W.P., GELLAI, BROOK, P., LUENGO, J., XIANG, J.N. & ELLIOTT, J.E. (1998). Nonpeptide endothelin receptor antagonists. XI: Pharmacological characterization of SB-234551, a high affinity and selective non-peptide ET_A receptor antagonist. *J. Pharmacol. Exp. Ther.,* **286,** 650–656.

OHLSTEIN, E.H., NAMBI, P., LAGO, A., HAY, D.W.P., BECK, G., FONG, K.-L., EDDY, E.P., SMITH, P., ELLENS, H. & ELLIOTT, J. (1996). Nonpeptide endothelin antagonists, VI: Pharmacological characterization of SB-217242, a potent and highly bioavailable endothelin receptor antagonist. *J. Pharmacol. Exp. Ther.,* **276,** 609–615.

O'SHAUGHNESSY, C.T. & CONNOR, H.E. (1994). Investigation of the role of tachykinin NK_1, NK_2 receptor and CGRP receptors in neurogenic plasma protein extravasation in dura mater. *Eur. J. Pharmacol.,* **263,** 193–198.

NILSSON, T., CANTERA, L., ADNER, M. & EDVINSSON, L. (1997). Presence of contractile endothelin-A and dilatory endothelin-B receptors in human cerebral arteries. *Neurosurgery,* **40,** 346–351.

PARSONS, A.A., PARKER, S.G., RAVAL, P., CAMPBELL, C.A., LEWIS, V.A., GRIFFITHS, R., HUNTER, A.J., HAMILTON, T.C. & KING, F.D. (1997). Comparison of the cardiovascular effects of the novel 5-HT1B/1D receptor agonist, SB 209509 (VML 251), and sumatriptan in dogs. *J. Cardiovasc. Pharmacol.,* **30,** 136–141.

PERREN, M.J., FWNIUK, W. & HUMPHREY, P.P.A. (1989). The selective closure of feline carotid arteriovenous anastomoses (AVAs) by GR 43175. *Cephalalgia,* **9,** 41–46.

PHEBUS, L.A., JOHNSON, K.W., STENGOL, P.W., LOBB, K.L., NIXON, J.A. & HIPSKIND, P.A. (1997). The non-peptide NK-1 receptor antagonist LY303870 inhibits neurogenic dural inflammation in guinea-pigs. *Life Science,* **60,** 1553–1561.

RAVAL, P., BINGHAM, S., OHLSTEIN, E.H. & PARSONS, A.A. (1996). Non-peptide $ET_{A/B}$ receptor antagonist, SB-209670, inhibits trigeminal nerve mediated events in the carotid vascular bed. *Cephalalgia,* **16,** 379.

RAVAL, P., PARSONS, A.A., BINGHAM, S., OHLSTEIN, E.H. & AIYAR, N. (1997). Comparison of the effects of BQ788, CGRP8–37 and sumatriptan on a trigemino-vascular reflex in the carotid vasculature. *Cephalalgia,* **17,** 396.

ROON, K., DIENER, H.C., ELLIS, P., HETTIARACHCHI, J., POOLE, P., CHRISTIANSEN, I., FERRARI, M.D. & OLESEN, J. (1997). CP-122288 blocks neurogenic inflammation, but is not effective in aborting migraine attacks: results of two controlled clinical trials. *Cephalalgia,* **17,** 245.

SAITO, K., MARKOWITZ, S. & MOSKOWITZ, M.A. (1988). Ergot alkaloids block neurogenic extravasation in dura mater: proposed action in vascular headaches. *Ann. Neurol.,* **24,** 732–737.

SHEPHEARD, S.L., WILLIAMSON, D.J., HILL, R.G. & HARGREAVES, R.J. (1993). The non-peptide neurokinin$_1$ receptor antagonist RP67580, blocks neurogenic plasma extravasation in the dura mater of rats. *Br. J. Pharmacol.,* **108,** 11–12.

SHEPHEARD, S.L., WILLIAMSON, D.J., HILL, R.G. & HARGREAVES, R.J. (1995). Comparison of the effects of sumatriptan and the NK_1 antagonist CP-99,994 on plasma extravasation in dura mater and c-fos mRNA expression in trigeminal nucleus caudalis of rats. *Neuropharmacology,* **34,** 255–261.

SPOKES, R.A. & MIDDLEFELL, V.C. (1995). Simultaneous measurement of plasma protein extravasation and carotid vascular resistance in the rat. *Eur. J. Pharmacol.,* **281,** 75–79.

SUZUKI, N., HARDEBO, J.E. & OWMAN, C. (1989a). Trigeminal fibre collaterals storing substance P and calcitonin gene-related peptide associate with ganglion cells containing choline acetyltransferase and vasoactive intestinal polypeptide in the sphenopalatine ganglion of the rat. An axon reflex modulating parasympathetic ganglionic activity? *Neuroscience,* **30,** 595–604.

SUZUKI, N., HARDEBO, J.E. & OWMAN, C. (1989b). Origins and pathways of cerebrovascular nerves storing substance P and calcitonin gene-related peptide in the rat. *Neuroscience,* **31,** 427–438.

UHL, G.R., WALTHER, D., NISHIMORI, T., BUZZI, M.G. & MOSKOWITZ, M.A. (1991). Jun B, jun D and c-fos mRNA's in nucleus caudalis neurones: Rapid selective enhancement by afferent stimulation. *Mol. Brain Res.,* **11,** 133–141.

WILLIAMSON, D.J., SHEPHEARD, S.L., HILL, R.G. & HARGREAVES, R.J. (1997). The novel anti-migraine agent rizatriptan inhibits neurogenic dural vasodilatation and extravasation. *Eur. J. Pharmacol.,* **328,** 61–64.

(Received August 12, 1998
Revised October 16, 1998
Accepted October 20, 1998)

British Journal of Pharmacology (1999) 126, 494–500
http://www.stockton-press.co.uk/bjp

Role of K^+ channels in A_{2A} adenosine receptor-mediated dilation of the pressurized renal arcuate artery

[1]H.M. Prior, *,[1]M.S. Yates & [1]D.J. Beech

[1]School of Biomedical Sciences, Worsley Building, University of Leeds, Leeds, LS2 9JT, England, U.K.

1 Adenosine A_{2A} receptor-mediated renal vasodilation was investigated by measuring the lumenal diameter of pressurized renal arcuate arteries isolated from the rabbit.

2 The selective A_{2A} receptor agonist CGS21680 dilated the arteries with an EC_{50} of 130 nM. The CGS21680-induced vasodilation was, on average, 34% less in endothelium-denuded arteries.

3 The maximum response and the EC_{50} for CGS21680-induced vasodilation in endothelium-intact arteries were not significantly affected by incubation with the K^+ channel blockers apamin (100 nM), iberiotoxin (100 nM), 3,4-diaminopyridine (1 mM), glibenclamide (1 μM) or Ba^{2+} (10 μM). However, a cocktail mixture of these blockers did significantly inhibit the maximum response by almost 40%, and 1 mM Ba^{2+} alone or 1 mM Ba^{2+} in addition to the cocktail inhibited the maximum CGS21680-response by 58% and about 75% respectively.

4 CGS21680-induced vasodilation was strongly inhibited when the extracellular K^+ level was raised to 20 mM even though the dilator response to 1 μM levcromakalim, a K_{ATP} channel opener drug, was unaffected.

5 CGS21680-induced vasodilation was inhibited by 10 μM ouabain, an inhibitor of Na^+/K^+-ATPase, but ouabain had a similar inhibitory effect on vasodilation induced by 30 nM nicardipine (a dihydropyridine Ca^{2+} antagonist) or 1 μM levcromakalim.

6 The data suggest that K^+ channel activation does play a role in A_{2A} receptor-mediated renal vasodilation. The inhibitory effect of raised extracellular K^+ levels on the A_{2A} response may be due to K^+-induced stimulation of Na^+/K^+-ATPase.

Keywords: Adenosine A_{2A} receptor; artery; kidney; potassium channel; potassium; Na^+/K^+-ATPase

Abbreviations: Ba^{2+}, barium chloride; BK_{Ca} channels, large conductance Ca^{2+}-activated K^+ channels; CGS21680, 2-(p-(carboxylethyl)-phenylethlamino)-5′-N-ethylcarboxamido adenosine; CPA, cyclopentyladenosine; 3,4-DAP, 3,4-diaminopyridine; EDHF, endothelium-derived hyperpolarizing factor; E_K, the K^+-equilibrium potential; K_{ATP} channels, ATP-sensitive K^+ channels; K_V channels, delayed rectifier K^+ channels; SK_{Ca} channels, small conductance Ca^{2+}-activated K^+ channels; TEA, tetraethylammonium chloride

Introduction

Adenosine is a paracrine regulator of cardiovascular function. In most vascular beds it is exclusively a vasodilator but in the kidney it can evoke vasoconstriction and vasodilation *via* A_1 receptor and A_2 receptors respectively (Holz & Steinhausen, 1987; Churchill & Bidani, 1990). As a consequence of its ability to induce both effects, adenosine produces a redistribution of renal blood flow with vasoconstriction in the outer cortex accompanied by vasodilation in the deep cortex and outer medulla (Miyamoto *et al*., 1988; Spielman & Arend, 1991). Thus, adenosine induces a corticomedullary redistribution of blood flow which is an early response to hypoperfusion (Brezis *et al*., 1991). The redistribution may prevent ischaemia of the S_3 segment of the proximal tubule and the thick ascending limb of the loop of Henle, sections of the nephron most vulnerable to hypoxia (Brezis *et al*., 1991).

Vasodilation in response to adenosine can occur *via* activation of A_{2A} or A_{2B} receptors which are known to be positively coupled to adenylyl cyclase (Collis & Hourani, 1993). It, therefore, seems reasonable to postulate the involvement of K^+ channel activation in the signal transduction mechanisms coupling A_2 receptors to vasodilation because large conductance Ca^{2+}-activated K^+ channels (BK_{Ca} channels), ATP-sensitive K^+ channels (K_{ATP} channels) and delayed rectifier K^+ channels (K_v channels) have all been shown to be stimulated by cyclic AMP during patch-clamp experiments on isolated smooth muscle cells (reviewed by Beech, 1997). Furthermore, notably in the coronary circulation, K^+ channel inhibitors have been shown to attenuate vasodilator effects of adenosine. Adenosine-induced dilation of coronary vessels in rat, rabbit, guinea-pig and pig is sensitive to inhibition by glibenclamide, an inhibitor of K_{ATP} channels (Von Beckerath *et al*., 1991; Jiang & Collins, 1994; Randall, 1995; Kuo & Chancellor, 1995). The study of Merkel *et al*. (1992) suggests, however, that this may not be an A_2-receptor mediated effect but rather one mediated by an atypical adenosine receptor. Furthermore, there seems to be variability between vascular beds because adenosine-induced relaxation is sensitive to glibenclamide in hamster cheek pouch arterioles and yet resistant to glibenclamide in rabbit cerebral arterioles (Taguchi *et al*., 1994). In addition, other types of K^+ channel may be involved because, in coronary vessels from the dog and rat, adenosine-induced dilation is sensitive to inhibition by tetraethylammonium ions (TEA) and iberiotoxin, indicating a role for BK_{Ca} channels (Cabell *et al*., 1994; Price *et al*., 1996).

A_{2A} receptor-mediated dilation and its underlying transduction mechanisms have not been investigated previously in arteries of the kidney and thus we have focused on a characterization of the response in one of the small arteries from within the kidney – the arcuate artery. The arcuate artery is the second branch from the renal artery and arches between the medulla and cortex, feeding into the interlobular artery and

* Author for correspondence; E-mail m.s.yates@leeds.ac.uk

afferent arteriole; thus, it plays a key functional role in the distribution of blood within the kidney. A primary aim of this study was to reveal the importance of K^+ channel activation to the A_{2A} effect of the intact renal arcuate artery studied under physiological pressurized conditions.

Methods

Male Dutch rabbits (1–2.5 kg) were killed by i.v. administration of heparinized (1000 u ml^{-1}) sodium pentobarbitone (70 mg kg^{-1}). Kidneys were removed and placed in cold Ca^{2+}-containing bath solution. The kidneys were decapsulated and divided longitudinally into four slices from which sections of arcuate artery were dissected, isolated and cleared of adhering tubules and connective tissue.

Segments of renal arcuate artery were mounted in an 8 ml chamber (Living Systems Instrumentation, Burlington, VT, U.S.A.), cannulated at both ends with glass cannulae and secured using monofilament nylon. The glass cannulae were filled with Krebs solution, which was maintained in the cannulae throughout all experiments. The distal cannula was closed and the proximal cannula was connected to a pressure-servo unit (Living Systems Instrumentation). The myograph was placed on the stage of an inverted trinocular microscope (Nikon) with attached video camera (Sony). The lumen diameter was continuously measured with a video dimension analyser (Living Systems Instrumentation) and presented using Origin 4.1 (Microcal Inc., U.S.A.) after on-line digital capturing at 0.1 Hz (Picolog, Pico Technology, Cambridge, U.K.).

Arteries were pressurized to 60 mmHg and continuously perfused with Krebs solution at a rate of 25 ml min^{-1}. The superfusate was at 37°C and gassed with 95% O_2, 5% CO_2. Viability of arteries was evaluated by their ability to constrict in response to 10 μM phenylephrine and presence of endothelium was confirmed by a dilator response to 10 μM acetylcholine. Endothelium was present in all experiments except when indicated. If endothelium was removed this was performed prior to pressurization of the artery by injecting air through the lumen. Confirmation that the smooth muscle was undamaged was obtained by demonstration of a dilation to 10 μM sodium nitroprusside. All vessels were equilibrated in Krebs solution for 2 h during which time most arteries developed myogenic tone. In all experiments, phenylephrine was added to the superfusate and adjusted to a concentration between 0.1 and 3 μM which ensured constriction at a level roughly half-way between fully-dilated and fully-constricted diameters. The concentration of phenylephrine was adjusted if a substance dilated or constricted the artery, thus maintaining a constant level of tone. Exposure of arteries to substances was done by their inclusion in the superfusate. The exception was when iberiotoxin was used on its own, and in these experiments the perfusion rate was reduced from 25 ml min^{-1} to 2 ml min^{-1} and substances were added directly to the perfusion chamber. At the end of each experiment, vessels were superfused with a Ca^{2+}-free solution containing EGTA (0.5 mM) to determine vessel diameter during maximal relaxation. In the figures, the lowest values on the diameter axes are the diameter observed in Ca^{2+}-free solution. Arterial diameter observed in Ca^{2+}-free solution is referred to as 100% dilation, and loss of the lumen as 100% constriction.

Krebs solution contained (mM): NaCl 119, KCl 4.7, $MgSO_4.7H_2O$ 1.17, $NaHCO_3$ 24, $CaCl_2$ 1.6, KH_2PO_4 1.18, EDTA 0.023, D-glucose 5. The Ca^{2+}-containing bath solution included (mM): NaCl 130, KCl 5, $CaCl_2$ 1.5, $MgCl_2$ 1.2, HEPES (N-[2-hydroxyethl]piperazine-N′-[2-ethanesulphonic acid]) 10, glucose 8 (pH 7.4). Generous gifts of CGS21680 and levcromakalim were from Ciba Geigy and SmithKline Beecham. CGS21680 is 2-(p-(carboxylethyl)-phenylethylami-

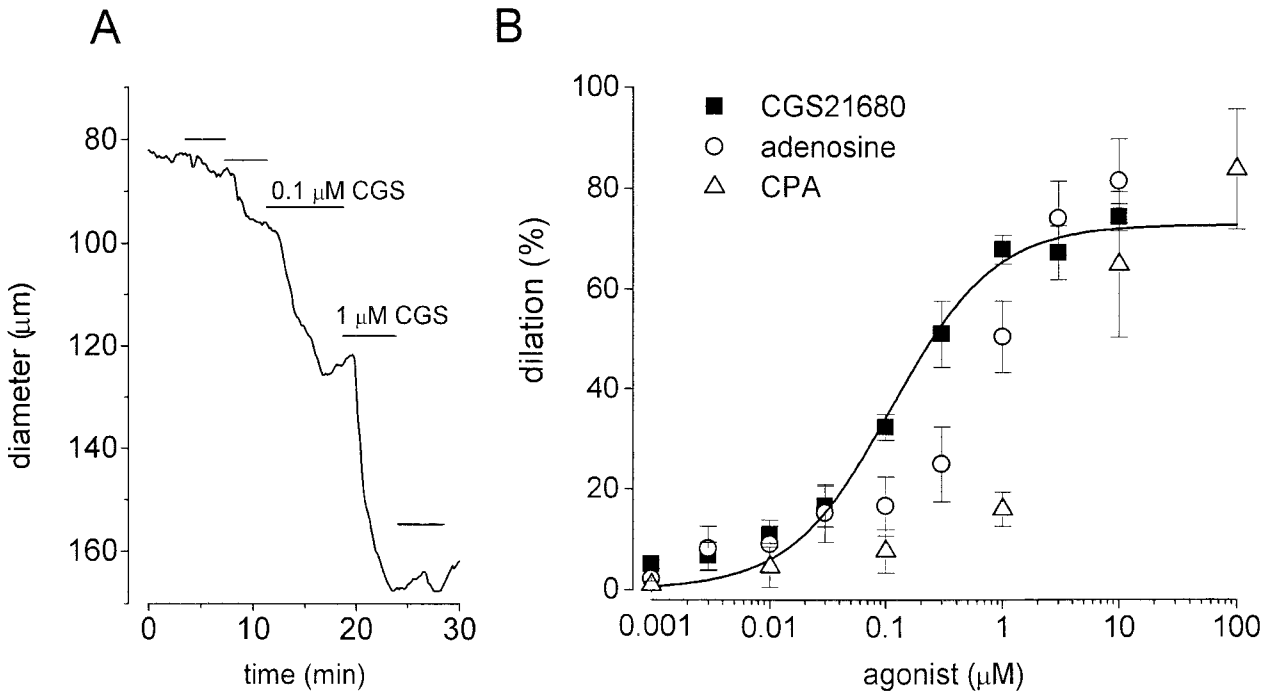

Figure 1 Vasodilation mediated by A_{2A} adenosine receptors in pressurized rabbit arcuate artery. (A) Plot of lumenal diameter for a typical experiment, showing concentration-dependent dilation in response to CGS21680. Horizontal bars indicate application of increasing concentrations of CGS21680 (1, 10, 100 nM, and 1 and 10 μM). The bottom of the ordinate is the diameter of the artery in Ca^{2+}-free Krebs solution in this Figure and Figures 2A, 3 and 4. (B) Mean ± s.e.mean percentage dilations in response to CGS21680 ($n=49$), adenosine ($n=6$) and CPA ($n=4$). The smooth curve is the Hill equation fitted to the mean data points for CGS21680 with a mid-point at 130 nM and a slope of 0.8.

no)-5′-N-ethylcarboxamido adenosine, and CPA is cyclopentyladenosine. Acetylcholine iodide, adenosine, CPA, apamin, glibenclamide, iberiotoxin, nicardipine, ouabain octahydrate, phenylephrine, sodium nitroprusside and tetraethylammonium chloride (TEA) were from Sigma (Poole, Dorset, U.K.). 3,4 DAP was from Fluka Chemika. Barium chloride (Ba^{2+}) was from Aldrich Chemical Co. (Dorset, U.K.). Glibenclamide and levcromakalim were prepared as a 10 mM stock solution in dimethylsulphoxide. All dilutions of stock solutions and other drugs were dissolved in distilled water or Krebs solution.

All results are given as means ± s.e.mean and statistical comparison were made by means of a Student's *t*-test, either paired or non-paired where appropriate. A $P<0.05$ indicated statistical significance. The value of *n* indicates number of arteries. Data presentation and mathematical fitting of functions to data using a least-squares method were performed by the program Origin 4.1.

Results

Adenosine, the selective A_{2A} agonist CGS21680, and the A_1 agonist CPA induced dilation of pressurized arcuate arteries (Figure 1). The rank order of potency of agonists was CGS21680 > adenosine > CPA with $-\log_{10}$ EC_{50} values of 6.9 ± 0.1 ($n=49$), 6.4 ± 0.2 ($n=6$) and 5.4 ± 0.2 ($n=4$) respectively. CGS21680 was used as the selective activator of A_{2A} receptors in subsequent experiments. There was no significant change in the maximum response or the EC_{50} for CGS21680-induced vasodilation when concentration-response curves were repeated four times under control conditions over a 3 h period in three separate experiments (data not shown). The magnitude of the response to CGS21680 in 174 arteries from different rabbits was not correlated with the level of basal constriction prior to adenosine receptor agonist application or with the concentration of phenylephrine (correlation coefficient 0.09; data not shown). Endothelium-denuded arteries were unresponsive to acetylcholine but responsive to CGS21680. In 19 endothelium-denuded arteries there was a 45.2 ± 5.0% dilation in response to 1 μM CGS21680 which compares with 69 ± 2% dilation in 73 endothelium-intact arteries. The difference is statistically significant ($P<0.001$). The dilator response to CGS21680 was absent in some arterial segments (29% of control experiments) and the mean values for intact and endothelium-denuded arteries both exclude experiments where there was no response to CGS21680.

The maximum response and the EC_{50} for CGS21680-induced vasodilation in endothelium-intact arteries were not significantly affected by several compounds which, at the correct concentration, are believed to be selective inhibitors of certain subtypes of K^+ channel. The CGS21680 response was not affected by: 100 nM apamin which blocks some small conductance Ca^{2+}-activated K^+ channels (SK_{Ca} channels); 1 mM 3,4-diaminopyridine which blocks many K_V channels; 1 μM glibenclamide which blocks K_{ATP} channels; or 10 μM Ba^{2+} which blocks current through strong inward rectifiers such as Kir2.1 (Table 1). Iberiotoxin blocks BK_{Ca} channels, but at neither 100 nM nor the high concentration of 1 μM, iberiotoxin had no significant inhibitory effect on the CGS21680-response (Table 1). TEA at 1 mM, which blocks BK_{Ca} channels but also other types of K^+ channel, significantly reduced the CGS21680-response (Table 1).

The most striking effect of a single K^+ channel blocker occurred with Ba^{2+} which largely prevented the CGS21680 response in some experiments (Figure 2A). On average, 0.1 and 1 mM inhibited the maximum CGS21680 effect by 45 and 58% respectively without any significant change in the EC_{50} (Figure 2B and Table 1).

Although apamin, iberiotoxin, 3,4-diaminopyridine, glibenclamide, and 10 μM Ba^{2+} had no effect on the CGS21680-response when applied on their own, they did significantly inhibit the CGS21680-response when applied as a cocktail mixture, on average reducing the maximum response by about 38% (Figure 2C and Table 1). In two experiments, 1 mM Ba^{2+} was included with the cocktail and there was strong inhibition of the CGS21680 effect (Table 1).

A common method used to indicate if K^+ channels are involved in a whole tissue response is to investigate the sensitivity of the response to increases in the extracellular K^+ concentration. When the concentration of K^+ in the superfusate was raised to 20 mM this essentially abolished the response to 1 μM CGS21680, reducing it to 9 ± 3% of the control value ($n=4$). The inhibitory effect of K^+ occurred at a critical level below 20 mM (Figure 3). In seven arteries, CGS21680-induced dilations were 82 ± 5 and 66 ± 11% in 5 and 10 mM K^+ respectively. In five of these arteries, 11 mM K^+ then abolished the CGS21680 effect, reducing it to 2 ± 1% of the control value, and in the other two arteries the response

Table 1 Effect of K^+ channel blockers on CGS21680-induced dilation in the pressurized arcuate artery

K^+ channel blocker		$^+$Maximal dilation % to CGS21680 Control	Plus blocker	$-log_{10}$ EC_{50} value Control	Plus blocker
Ba^{2+} 10 μM	(6)	81 ± 7	71 ± 11	6.9 ± 0.2	6.8 ± 0.2
Ba^{2+} 100 μM	(4)	82 ± 6	45 ± 18*	7.0 ± 0.3	6.4 ± 0.3
Ba^{2+} 1 mM	(4)	83 ± 6	35 ± 6**	7.3 ± 0.1	7.1 ± 0.4
TEA 1 mM	(5)	78 ± 8	51 ± 12**	7.1 ± 0.2	7.1 ± 0.3
Iberiotoxin 100 nM	(3)	84 ± 10	72 ± 10	n.d.	n.d.
Iberiotoxin 1 μM	(4)	40 ± 9	33 ± 11	n.d.	n.d.
Apamin 100 nM	(5)	84 ± 6	74 ± 7	6.9 ± 0.1	6.9 ± 0.1
3,4 DAP 1 mM	(6)	71 ± 7	54 ± 9	6.6 ± 0.1	6.7 ± 0.1
Glibenclamide 1 μM	(7)	76 ± 7	60 ± 14	6.9 ± 0.3	6.6 ± 0.2
Cocktail/10 μM Ba^{2+}	(5)	71 ± 5	44 ± 6**	7.1 ± 0.1	6.7 ± 0.2
Cocktail/1 mM Ba^{2+}	(2)	61 and 68	17 and 16	7.0 and 7.3	5.9 and 6.1

Maximal dilation ($^+$) was determined from CGS21680 concentration-response curves (0.001 – 10 μM), except iberiotoxin alone when only a single (1 μM) concentration of CGS21680 was used. Results are given as means ± s.e.mean with the number of experiments in parentheses. Hill equations were fitted to data points from individual experiments for the measurements of EC_{50} values. Significant difference with respect to control responses ($P<0.05$) using a one- (*) or (**) two-tailed paired Student's *t*-test. The cocktail contained 1 μM glibenclamide, 1 mM 3,4 diaminopyridine (3,4 DAP), 100 nM apamin, 100 nM iberiotoxin and Ba^{2+} (10 μM or 1 mM). Glibenclamide (1 μM) abolished 1 μM levcromakalim-induced vasodilation ($n=4$). n.d. indicates 'not done' because only 1 μM CGS21680 was used.

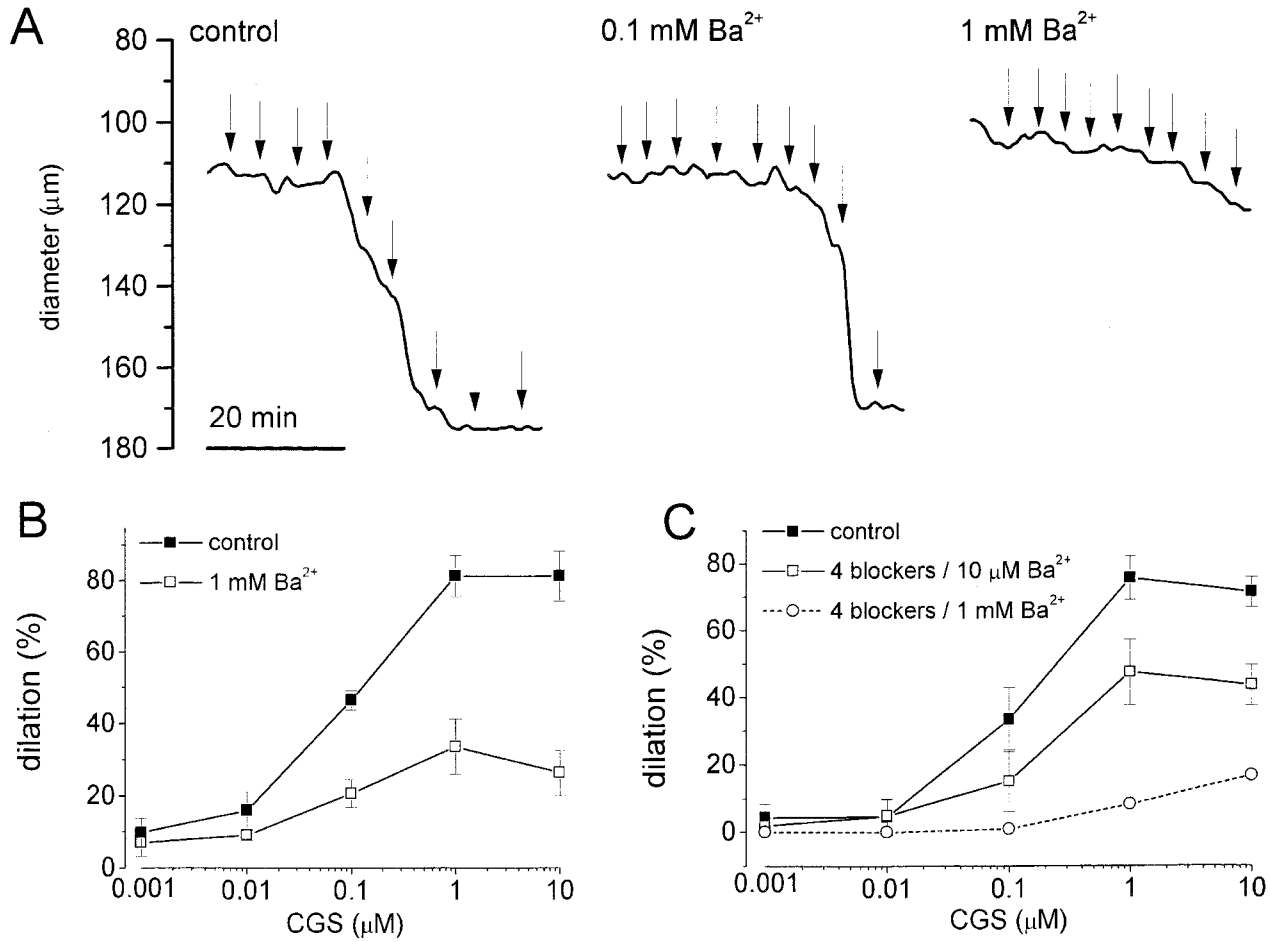

Figure 2 Effects of K^+ channel inhibitors on A_{2A}-mediated vasodilation. (A) Luminal diameter plotted against time for a single experiment where concentration-dilation relationships were constructed for increasing concentrations of CGS21680 (1, 3, 10, 30, 100, 300 nM and 1, 3 and 10 μM; indicated by nine vertical arrows for each section of trace, with 1 nM being the left-most arrow) in the presence of 0, 0.01, 0.1 and 1 mM Ba^{2+} in the superfusate (0.01 mM Ba^{2+} data are not shown). (B) Mean$\pm$s.e.mean dilations in response to CGS21680 in the absence ($n=4$) and presence of 1 mM Ba^{2+} ($n=4$). (C) Mean$\pm$s.e.mean dilations in response to CGS21680 in the absence ($n=5$) and presence of a cocktail of 1 μM glibenclamide, 1 mM 3,4 diaminopyridine, 100 nM apamin, 100 nM iberiotoxin, and either 10 μM Ba^{2+} ($n=5$) or 1 mM Ba^{2+} ($n=2$; error bars not included).

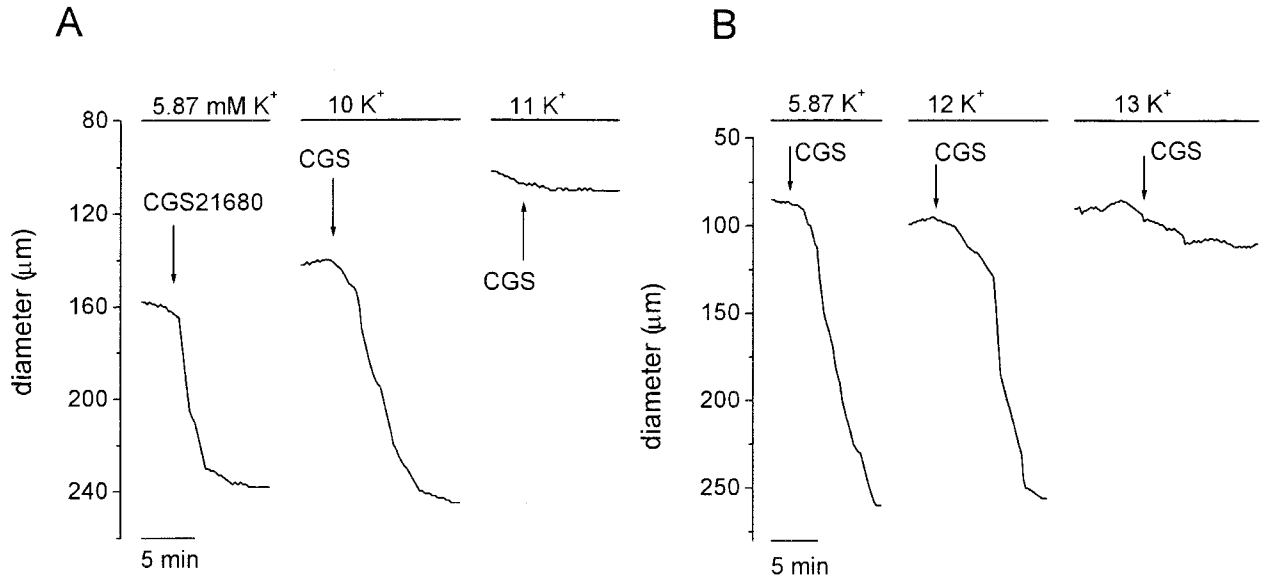

Figure 3 K^+-sensitivity of A_{2A}-mediated vasodilation. Lumenal diameter plotted against time, showing dilation induced by 1 μM CGS21680 in the presence of different levels of extracellular K^+ for two separate arcuate arteries. (A) In the presence of 5.87, 10 and 11 mM K^+, phenylephrine concentrations were 0.4, 0.5 and 0.7 μM respectively in order to maintain a constant level of tone as K^+ elicited vasodilation. (B) In the presence of 5.87, 12 and 13 mM K^+; phenylephrine concentrations were 0.2, 0.7 and 0.9 μM respectively.

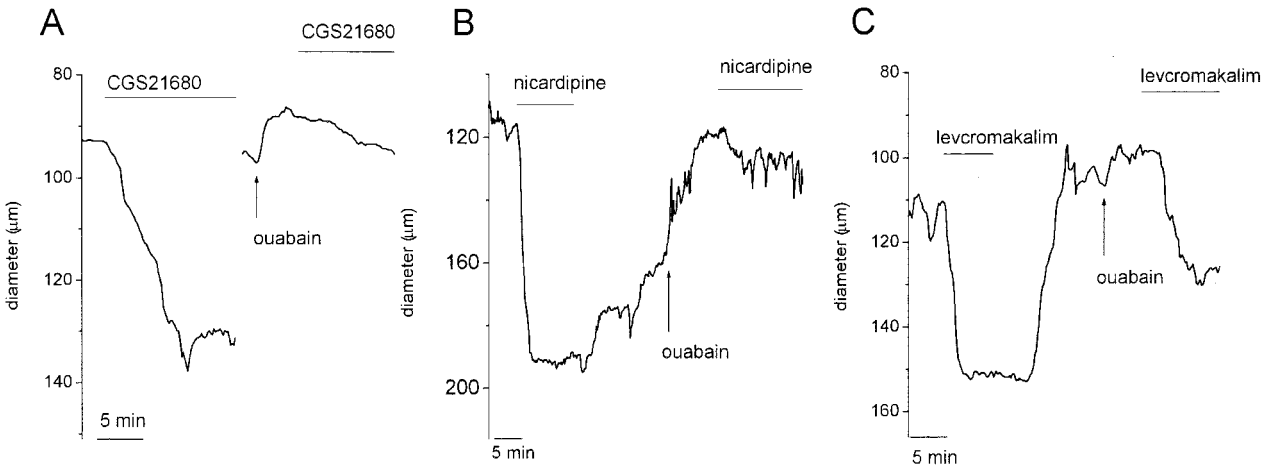

Figure 4 Inhibition of vasodilator responses following Na^+-pump inhibition. (A–C) Original traces of lumenal diameter against time for three separate arcuate arteries showing responses to 1 μM CGS21680 (A), 30 nM nicardipine (B) and 1 μM levcromakalim (C) before and in the presence of 10 μM ouabain.

was intact in 12 mM K^+ (46 and 91% dilations) and yet strongly inhibited by 13 mM K^+ (3 and 9% dilations). These raised levels of K^+ induced vasodilation by themselves and the loss of tone was compensated for by raising the phenylephrine concentration. Vasodilation induced by levcromakalim, an activator of K_{ATP} channels, was inhibited by high levels of K^+ but not by lower levels. Dilation induced by 1 μM levcromakalim was $91\pm8\%$ in 5.87 mM K^+ ($n=4$), $82\pm10\%$ in 20 mM K^+ ($n=4$) and absent in 80 mM K^+ ($n=2$).

Raised K^+ levels up to about 10 mM appear to induce vasodilation in the arcuate artery by stimulating the Na^+/K^+-ATPase (Prior *et al*., 1998a). Therefore, the effect of raised K^+ levels on the CGS21680-response could be explained by an involvement of Na^+/K^+-ATPase rather than K^+ channels in the A_{2A} receptor effect. On this basis, the effect of 10 μM ouabain was investigated because this compound inhibits Na^+/K^+-ATPase. Ouabain inhibited the 1 μM CGS21680 effect, reducing the dilation from 62.1 ± 4.4 to $21.2\pm5.8\%$ ($n=7$, $P<0.05$) (Figure 4). From concentration-response curves constructed in separate experiments the $\log_{10}$ IC_{50} value for the ouabain effect against the CGS21680-effect was -6.6 ± 0.3 ($n=8$). Ouabain (10 μM) also significantly inhibited dilator responses to 1 μM levcromakalim, reducing the dilation from 75.8 ± 7.8 to $26.7\pm11.2\%$ ($n=7$, $P<0.05$), and to 30 nM nicardipine, reducing the dilation from 58.3 ± 7.0 to $5.4\pm4.6\%$ ($n=7$, $P<0.05$) (Figure 4). Therefore, block of Na^+/K^+-ATPase inhibited A_{2A}-mediated vasodilation as well as inhibiting vasodilation induced by drugs which activate K_{ATP} channels (levcromakalim) and inhibit voltage-gated Ca^{2+} channels (nicardipine).

Discussion

A_{2A} adenosine receptor-mediated dilation has been characterized in pressurized intact arcuate artery segments. The data do not support an independent role for cyclic AMP-stimulated channels such as the K_{ATP} channel or the BK_{Ca} channel. However, the combined block of several of these K^+ channels, or the application of the general K^+ channel blockers tetraethylammonium and Ba^{2+}, produced data which point to the conclusion that K^+ channel activation has a role to play in the overall response to A_{2A} receptor activation. Sensitivity of the A_{2A} response to raised extracellular K^+ levels is often considered to be indicative of the involvement of K^+ channels. However, our experiments on the arcuate artery show that interpretation of the effect of the rather low concentrations of K^+ used in this study is difficult; the phenomenon may instead be explained by the stimulatory effect of K^+ on Na^+/K^+-ATPase.

The potency of CGS21680 on the arcuate artery is in the range expected for an A_{2A} receptor; an EC_{50} of 34 nM has been reported for porcine coronary artery (Zocchi *et al*., 1996) and an EC_{30} of 500 nM has been reported for rat aorta (Lewis *et al*., 1994). Moreover, CGS21680 has little or no efficacy at A_{2B} receptors. Studies of the guinea-pig pulmonary artery, where adenosine-induced dilation is considered to be mediated by A_{2B} receptors, have shown that 100 μM CGS21680 produced only a 4% dilation (Szentmiklosi *et al*., 1995) whilst no dilator response was seen at concentrations up to 30 μM (Broadley & Maddock, 1996). Therefore, we assume that the effects of CGS21680 observed in our study were mediated solely *via* A_{2A} adenosine receptors.

In the afferent arteriole, and in arteries such as the aorta and pulmonary artery of the guinea-pig, there is A_1 receptor-mediated vasoconstriction (Stoggall & Shaw, 1990; Szentmiklosi *et al*., 1995). However, in the arcuate artery we did not observe vasoconstriction in reponse to adenosine or the A_1 receptor agonist CPA. CPA did evoke vasodilation, although at concentrations similar to its binding affinity for A_2 receptors, IC_{50} 0.5 μM (Collis & Hourani, 1993) and therefore, CPA-induced dilation was probably mediated by A_{2A} receptors. The CPA response was not inhibited by 1 μM glibenclamide in the arcuate artery (data not shown), suggesting that it was not the same as that reported for porcine coronary artery (Merkel *et al*., 1992).

BK_{Ca} channels, K_{ATP} channels and K_V channels have been shown to be stimulated by cyclic AMP in isolated vascular smooth muscle cells (reviewed by Beech, 1997). Therefore, our data with selective blockers of these channels – when applied independently – are intriguing because they suggest either that the effects observed in isolated cells are not applicable to the intact blood vessel, or that the effect on one K^+ channel subtype is not, on its own, of any essential consequence for the response of the intact artery under physiological conditions. The latter explanation implies a parallel role of at least two K^+ channel subtypes, such that if one channel is blocked the other can take over the function and nothing appears to be changed. This hypothesis is supported by the observation that the cocktail mixture of K^+ channel blockers had a significant

inhibitory effect, whereas the individual blockers had no effect when applied in isolation.

Although we cannot be sure about the selectivity of 0.1 and 1 mM Ba^{2+} for K^+ channels it was striking that Ba^{2+} was very effective at blocking the CGS21680 effect in some experiments. Ba^{2+} is a general blocker of many types of K^+ channel and it was the only blocker of a background K^+-current recently identified in single arcuate artery smooth muscle cells (Prior *et al*., 1998b). Whether this background K^+ channel is coupled to A_{2A} receptors is unknown. We have not been able to test this hypothesis in isolated arcuate artery smooth muscle cells because of difficulty in obtaining reliable responses to CGS21680 in our isolated cell preparation. However, in five experiments we observed a hyperpolarization in response to CGS21680 (unpublished observations). This is, at least, supportive of studies on other blood vessels which suggest there can be K^+ channel activation in response to adenosine receptor activation and raised cyclic AMP levels in isolated vascular smooth muscle cells. The data also encourage the supposition that the K^+ channels mediating the A_{2A} effect are in part in the smooth muscle cells of the arcuate artery. Indeed, if one accepts the assumption that Ba^{2+} inhibited the CGS21680 effect solely because it was blocking K^+ channels, then it must be inferred that K^+ channel activity in the smooth muscle cells was important because the percentage inhibition caused by Ba^{2+}, with or without the cocktail of K^+ channel inhibitors, was larger than that which can be attributed to an endothelium-dependent component. Localization of some of the A_{2A}-coupled K^+ channels in endothelial cells is, nevertheless, by no means excluded.

The use of elevated levels of extracellular K^+ as a diagnostic tool for K^+ channel-mediated effects in blood vessels came into prominence with the advent of K_{ATP} channel opener drugs. A standard test came to be that 80 mM but not 20 mM extracellular K^+ 'blocks' K^+ channel opener effects (Edwards *et al*., 1992), and we confirmed this for the arcuate artery. The explanation for the 'block' is thought to be that in 80 mM K^+ the membrane potential becomes too close to E_K (the K^+-equilibrium potential) for K^+ channel opening to be of any functional consequence. From this argument we can infer that when the arcuate artery was in 20 mM K^+, the membrane potential was not 'too close to E_K' because activation of K_{ATP} channels produced normal vasodilation. A similar inference can be made about endothelium-derived hyperpolarizing factor (EDHF)-induced vasodilation which is also suggested to be mediated *via* K^+ channels and is inhibited by 15–25 mM K^+ (Parkington *et al*., 1995). A sharp cut-off effect of raising the extracellular K^+ level within the physiological range, similar to the A_{2A}-effect in arcuate artery, has also been observed for histamine and acetylcholine-induced hyperpolarizations in rat pulmonary arteries (Chen & Suzuki, 1989).

An explanation for the K^+-sensitivity of A_{2A}-mediated vasodilation, other than that it indicates an absolute K^+ channel-dependence of the A_{2A} effect, could be that raised K^+ levels and agonists at A_{2A} receptors both produce their effects by stimulating Na^+/K^+-ATPase. Indeed, the hypothesis that transduction of the A_{2A} response occurs *via* the Na^+/K^+-ATPase may seem attractive because A_{2A}-mediated vasodilation was inhibited by ouabain, and it seems that Na^+/K^+-ATPase may be stimulated by cyclic AMP (Morrison & Vanhoutte, 1996). However, we expanded our study of the action of ouabain to investigate its effects on other vasodilators (levcromakalim and nicardipine) which act *via* known mechanisms of action which differ from those of the A_2 receptor. These experiments showed that although ouabain was effective at concentrations which are consistent with an action on Na^+/K^+-ATPase, it was non-selective in its block of vasodilator mechanisms. A mechanism which could explain the non-selective block produced by ouabain is that Na^+/K^+-ATPase inhibition produced a rise in intracellular Ca^{2+} levels which inactivated L-type Ca^{2+} channels *via* the Ca^{2+}-induced inactivation mechanism, so leading to inhibition of any vasodilatory effect which depended on the function of voltage-gated Ca^{2+} channels (for example, one which involves hyperpolarization).

This study has provided evidence that K^+ channel activation is a necessary part of the transduction mechanism for A_{2A} adenosine receptor-mediated vasodilation in intact pressurized arteries from within the mammalian kidney. It seems the A_{2A} effect is not dependent on the activation of one particular K^+ channel subtype, as has been indicated by studies on single isolated cells, but that more than one K^+ channel subtype is involved in parallel, so that if one K^+ channel is blocked there is no deterioration in the overall vasodilatory response. The marked inhibitory effect of raised K^+ levels on the A_{2A} response is striking and it may serve to prevent an excessive drive towards vasodilation if the artery is exposed to adenosine and raised K^+ levels. The mechanism of the interaction is uncertain but we speculate that the ability of raised K^+ levels to cause hyperpolarization by stimulating of Na^+/K^+-ATPase may, in some way, inhibit the ability of A_{2A} receptor agonists to cause hyperpolarization due to activation of K^+ channels.

We are grateful to the Wellcome Trust for funding the research and thank Dr Guibert for comments on the manuscript.

References

BEECH, D.J. (1997). Actions of neurotransmitters and other messengers on Ca^{2+} channels and K^+ channels in smooth muscle cells. *Pharmac. Ther.,* **73,** 91–119.

BREZIS, M., ROSEN, S. & EPSTEIN, F.H. (1991). Acute renal failure. In: Brenner, B.M. & Rector, F.C. (eds). *The Kidney*. Vol 1, 4th Edn. pp. 993–1061. Philadelphia: W.B. Saunders Co.

BROADLEY, K.J. & MADDOCK, H.L. (1996). P_1-purinoceptor-mediated vasodilatation and vasoconstriction in hypoxia. *J. Aut. Pharmacol.,* **16,** 363–366.

CABELL, F., WEISS, D.S. & PRICE, J.M. (1994). Inhibition of adenosine-induced coronary vasodilation by block of large-conductance Ca^{2+} activated K^+ channels. *Am. J. Physiol.,* **267,** H1455–H1460.

CHEN, G. & SUZUKI, H. (1989). Some electrical properties of the endothelium-dependent hyperpolarisation recorded from rat arterial smooth muscle cells. *J. Physiol.,* **410,** 91–106.

CHURCHILL, P.C. & BIDANI, A.K. (1990). Adenosine and renal function. In: Williams, M. (ed). *Adenosine and Adenosine Receptors*. pp. 335–380. Clifton, New Jersey: The Humana Press.

COLLIS, M.G. & HOURANI, S.M.O. (1993). Adenosine receptor subtypes. *Trends Pharmacol. Sci.,* **14,** 360–366.

EDWARDS, G., DUTY, S., TREZISE, D.J. & WESTON, A.H. (1992). Effects of potassium channel modulators on the cardiovascular system. In: Weston, A.H. & Hamilton, T.C. (ed), *K Channel Modulators – Pharmacological, Molecular and Clinical Aspects,* Chapter 14, Oxford: Blackwell Scientific.

HOLZ, F.G. & STEINHAUSEN, M. (1987). Renovascular effects of adenosine receptor agonists. *Renal. Physiol.,* **10,** 272–282.

JIANG, C. & COLLINS, P. (1994). Inhibition of hypoxia-induced relaxation of rabbit isolated coronary arteries by N^G-monomethyl-L-arginine but not glibenclamide. *Br. J. Pharmacol.,* **111,** 711–716.

KUO, L. & CHANCELLOR, J.D. (1995). Adenosine potentiates flow-induced dilation of coronary arterioles by activating K_{ATP} channels in endothelium. *Am. J. Physiol.,* **269,** H541–H549.

LEWIS, C.D., HOURANI, S.M.O., LONG, C.J. & COLLIS, M.G. (1994). Characterization of adenosine receptors in the rat isolated aorta. *Gen. Pharmacol.,* **25,** 1381–1387.

MERKEL, L.A., LAPPE, R.W., RIVERA, L.M., COX, B.F. & PERRONE, M.H. (1992). Demonstration of vasorelaxant activity with an A1-selective adenosine agonist in porcine coronary artery: Involvement of potassium channels. *J. Pharmacol. Exp. Ther.,* **260,** 437–443.

MIYAMOTO, M., YAGIL, Y., LARSON, T., ROBERTSON, C. & JAMISON, R.L. (1988). Effects of intrarenal adenosine on renal function and medullary blood flow in the rat. *Am. J. Physiol.,* **255,** F1230–F1234.

MORRISON, K.J. & VANHOUTTE, P.M. (1996). Stimulation of the sodium pump by vasoactive intestinal peptide in guinea-pig isolated trachea: potential contribution to mechanisms underlying relaxation of smooth muscle. *Br. J. Pharmacol.,* **118,** 557–562.

PARKINGTON, H.C., TONTA, M.A., COLEMAN, H.A. & TARE, M. (1995). Role of membrane potential in endothelium-dependent relaxation of guinea-pig coronary arterial smooth muscle. *J. Physiol.,* **484,** 469–480.

PRICE, J.M., CABELL, J.F. & HELLERMAN, A. (1996). Inhibition of cAMP mediated relaxation in rat coronary vessels by block of Ca^{++} activated K^+ channels. *Life Sci.,* **58,** 2225–2232.

PRIOR, H.M., WEBSTER, N., QUINN, K.V., BEECH, D.J. & YATES, M.S. (1998a). K^+-induced dilation in a small renal artery: no role for inward rectifier K^+ channels. *Cardiovas. Res.,* **37,** 780–790.

PRIOR, H.M., YATES, M.S. & BEECH, D.J. (1998b). Functions of large conductance (BK_{Ca}), delayed rectifier (K_V) and background K^+ channels in the control of membrane potential in rabbit renal arcuate artery. *J. Physiol.,* **511,** 159–169.

RANDALL, M.D. (1995). The involvement of ATP-sensitive potassium channels and adenosine in the regulation of coronary flow in the isolated perfused rat heart. *Br. J. Pharmacol.,* **116,** 3068–3074.

SPIELMAN, W.S. & AREND, L.J. (1991). Adenosine receptors and signaling in the kidney. *Hypertension,* **17,** 117–130.

STOGGALL, S.M. & SHAW, J.S. (1990). The coexistence of adenosine A_1 and A_2 receptors in the guinea-pig aorta. *Eur. J. Pharmacol.,* **190,** 329–335.

SZENTMIKLOSI, A.J., UJFALUSI, A., CSEPPENTO, A., NOSZTRAY, K., KOVACS, P. & SZABO, J.Z. (1995). Adenosine receptors mediate both contractile and relaxant effects of adenosine in main pulmonary artery of guinea pigs. *Naunyn-Schmied. Arch. Pharmcol.,* **351,** 417–425.

TAGUCHI, H., HEISTAD, D.D., KITAZONO, T. & FARACI, F.M. (1994). ATP-sensitive K^+ channels mediate dilatation of cerebral arterioles during hypoxia. *Circ. Res.,* **74,** 1005–1008.

VON BECKERATH, N., CYRYS, S., DISCHNER, A. & DAUT, J. (1991). Hypoxic vasodilatation in isolated, perfused guinea-pig heart: an analysis of the underlying mechanisms. *J. Physiol.,* **442,** 297–319.

ZOCCHI, C., ONGINI, E., CONTI, A., MONOPOLI, A., NEGRETTI, A., BARALDI, P.G. & DIONISOTTI, S. (1996). The non-xanthine heterocyclic compound SCH 58261 is a new potent and selective A_{2a} adenosine receptor antagonist. *J. Pharmacol. Exp. Ther.,* **276,** 398–404.

(Received September 24, 1998
Revised October 15, 1998
Accepted October 21, 1998)

British Journal of Pharmacology (1999) 126, 501–507
http://www.stockton-press.co.uk/bjp

Modification of left ventricular hypertrophy by chronic etomoxir treatment

*,[1]Marian Turcani & [1,2]Heinz Rupp

[1]Institute of Physiology II, University of Tübingen, Tübingen, Germany

1 Etomoxir (2[6(4-chlorophenoxy)hexyl]oxirane-2-carboxylate), an irreversible carnitine palmitoyltransferase 1 inhibitor, reduces the expression of the myocardial foetal gene programme and the functional deterioration during heart adaption to a pressure-overload. Etomoxir may, however, also improve the depressed myocardial function of hypertrophied ventricles after a prolonged pressure overload.

2 To test this hypothesis, we administered racemic etomoxir (15 mg kg^{-1} day^{-1} for 6 weeks) to rats with ascending aortic constriction beginning 6 weeks after imposing the pressure overload.

3 The right ventricular/body weight ratio increased ($P<0.05$) by 20% in etomoxir treated rats ($n=10$) versus untreated rats with ascending aortic constriction ($n=10$). Left ventricular weight was increased ($P<0.05$) by 8%. Etomoxir blunted the increase in left ventricular chamber volume. Etomoxir raised the proportion of V_1 isomyosin ($35\pm4\%$ versus $24\pm2\%$; $P<0.05$) and decreased the percentage of V_3 isomyosin ($36\pm4\%$ versus $48\pm3\%$; $P<0.05$).

4 Maximum isovolumically developed pressure was higher in etomoxir treated rats than in untreated pressure overloaded rats (371 ± 22 versus 315 ± 23 mmHg; $P<0.05$). Maximum rates of ventricular pressure development ($14{,}800\pm1310$ versus $12{,}340\pm1030$ mmHg s^{-1}; $P<0.05$) and decline (6440 ± 750 versus 5040 ± 710 mmHg s^{-1}; $P<0.05$) were increased as well. Transformation of pressure values to ventricular wall stress data revealed an improved myocardial function which could partially account for the enhanced function of the whole left ventricle.

5 The co-ordinated action of etomoxir on ventricular mass, geometry and myocardial phenotype enhanced thus the pressure generating capacity of hypertrophied pressure-overloaded left ventricles and delayed the deleterious dilative remodelling.

Keywords: CPT-1 inhibitor; etomoxir; pressure overload; heart hypertrophy; heart failure; myosin isozymes; ventricular performance

Abbreviations: TDGA, 2-tetradecylglycidic acid; ACE, angiotensin converting enzyme; CPT-1, carnitine palmitoyltransferase I; POCA, clomoxir; P, left intraventricular pressure; V, left ventricular cavity volume; W, left ventricular wall volume; MHC, myosin heavy chains; $+dP/dt_{max}$, maximal rate of intraventricular pressure rise and decline; $-d\sigma/dt_{max}$, maximal rate of wall stress rise and decline; σ, mean wall stress; C_R, midwall circumference; $\pm dP/dt$, rate of intraventricular pressure rise and decline; $\pm d\sigma/dt$, rate of wall stress rise and decline

Introduction

Irreversible inhibitors of carnitine palmitoyltranferase I (CPT-1) such as 2-tetradecylglycidic acid (TDGA), L-hydroxyphenylglycine (oxfenicine), 2[5(4-chlorophenyl)pentyl]-oxirane-2-carboxylic acid (POCA, clomoxir) and 2[6(4-chlorophenoxy)hexyl]oxirane2-carboxylate (etomoxir) were originally developed as antidiabetic agents but proved to have significant effects on heart muscle. Although occasionally judged as cardiotoxic (Litwin *et al*., 1990) an increasing number of experimental and preliminary clinical studies indicate that these agents may be of potential value in the treatment and prevention of cardiac dysfunction of various etiologies.

Irreversible inhibitors of cardiac CPT-1 exhibited anti-ischaemic (Pearce *et al*., 1979; Higgins *et al*., 1980; Lopaschuk *et al*., 1988) and anti-arrhythmic (Corr *et al*., 1989; Yamada *et al*., 1994) effects in isolated hearts, improved cardiac performance in diabetic rats (Schmitz *et al*., 1995) retarded left ventricular dilatation and ameliorated pump function after large myocardial infarction in rats (Litwin *et al*., 1991).

In a clinical study, oxfenicine had beneficial effects in angina pectoris (Bergman *et al*., 1980). An open pilot clinical study showed that etomoxir administered on top of a standard therapy (ACE-inhibitors, diuretics, digitalis, beta-blockers), improved the clinical status and heart function at maximum exercise in patients with heart failure (Schmidt-Schweda & Holubarsch, 1997). Perhexiline, an anti-ischaemic agent and CPT-1 inhibitor (Kennedy *et al*., 1996), markedly ameliorated the symptomatic status in elderly patients with severe aortic stenosis (Unger *et al*., 1997). Although an oxygen-sparing metabolic effect of perhexiline was postulated as an underlying mechanism, other mechanisms should not be dismissed.

Etomoxir attenuates the expression of the foetal gene programme of the hypertrophied heart during cardiac adaptation to a pressure overload (Rupp *et al*., 1992a). This effect was associated with an improved ventricular and myocardial function (Turcani & Rupp, 1997). The effect of CPT-1 inhibition on cardiac gene expression appears to depend on a switch from fatty acid oxidation to predominantly glucose oxidation. Feeding a medium chain fatty acid diet prevented both cardiac hypertrophy and changes in myocardial phenotype (Lee *et al*., 1985; Rupp *et al*., 1995). In hypertrophied and failing heart, glucose is the preferred energy substrate (Taegtmeyer, 1994). However, a shift in fuel utilization due to

*Author for correspondence at: Institute of Pathophysiology, Medical School, Comenius University, Sasinkova 4, 811 08 Bratislava, Slovak Republic
[2]Current address: Molecular Cardiology Laboratory, Division of Cardiology, Philipps-University of Marburg, Marburg, Germany

a haemodynamic overload is associated with changes in the myocardial phenotype opposite to those arising from CPT-1 inhibition (Rupp *et al*., 1992a; Turcani & Rupp, 1997). It was, therefore, examined whether etomoxir can modify also a developed hypertrophy associated with an impaired myocardial function and thus provides the potential not only to restore the pump function of an overloaded ventricle but also to delay or prevent the transition to heart failure.

In the present study, we induced left ventricular hypertrophy by constricting the ascending aorta. A concentric hypertrophy with reactivation of the foetal gene programme (Feldman *et al*., 1993), compensated chamber performance but distinct signs of disturbed myocardial function is observed 6 weeks after pressure overload. Progressive left ventricular dilatation ensues associated with symptomatic left ventricular failure (Litwin *et al*., 1995).

Administration of etomoxir started 6 weeks after imposing the pressure overload. Six weeks after treatment, the haemodynamic performance of the isovolumically beating left ventricle, ventricular morphometry and myosin phenotype was assessed. Isovolumic contractions facilitate the evaluation of ventricular and myocardial performance independently of loading conditions, ventricular mass and geometry (Jacob *et al*., 1990). Changes in the myosin phenotype were examined because the progressively increased β-myosin heavy chain (MHC) expression is a persistent hallmark of the foetal gene programme (Imamura *et al*., 1991; Feldman *et al*., 1993; Schwartz *et al*., 1993).

Methods

Animal model

Male 3-week-old Wistar/WU rats were purchased from Charles-River (Kissleg, Germany) and housed at 21–23°C on 12 : 12-h light-dark cycle. The rats had free access to tap water and regular chow (Ssniff of Plange, Soest, Germany). Handling of animals and all experimental procedures were in accordance with the Institutional Guidelines of the University of Tübingen, Tübingen, Germany.

Pressure overload was induced by constriction of the ascending aorta (Turcani & Rupp, 1997) in 28 rats. Six weeks after surgery, eight rats with aortic constriction and eight sham operated rats were examined to assess the aorto-ventricular pressure gradient, left ventricular hypertrophy and myosin isozyme composition. The remaining 20 rats with ascending aortic constriction were divided into two groups. Racemic etomoxir (15 mg kg^{-1} day^{-1}) was administered to one group in the drinking water for 6 weeks. The dose was maintained by monitoring the daily water consumption and body weight. The selected dose has been shown not to induce hypertrophy while the effects on myocardial phenotype were preserved (Rupp *et al*., 1992b). Etomoxir was generously provided by Dr H.P.O. Wolf of Byk Gulden, Konstanz, Germany.

Measurement of left ventricular isovolumic contraction

The measurements were performed in open-chest rats under urethane anaesthesia (1.2 g kg^{-1} body weight, i.p.) as described previously (Hepp *et al*., 1974; Turcani & Rupp, 1997). A mediosternal thoracotomy was performed and the left ventricle was pierced at the apex with a steel cannula no. 1 connected to a Gould-Statham P23XL pressure transducer (Gould Electronics, Bilthoven, Netherlands). The right carotid artery was cannulated with polyethylene tubing (0.5 mm inner diameter) and forwarded to the aortic arch. The tubing was connected to a second Gould-Statham P23XL pressure transducer. Left ventricular pressure, left ventricular diastolic pressure (high amplification of left ventricular pressure), time derivative of ventricular pressure (dP/dt) and aortic pressure were recorded simultaneously on a Hellige Recomed recording system (Hellige, Freiburg, Germany).

For monitoring isovolumic contractions, the ascending aorta was clamped above the aortic valve for 6–8 s with forceps as verified by the absence of pulsatile pressure in the aortic arch. Small end-diastolic volumes, i.e. low preload values, were achieved by a short tightening of a string around the inferior vena cava. The preload increased gradually after relieving the inferior vena cava flow while clamping the aorta. This procedure was repeated 4–6 times. The functional analysis was based on the recording exhibiting the highest systolic pressure development.

Left ventricular passive pressure-volume relations were assessed after recording isovolumic contractions. The atrioventricular groove was ligated with a silk string and the right ventricle was emptied by incision. The left ventricle was filled with a defined volume of saline and emptied in 50 μl steps while recording the passive left ventricular pressure. Three reproducible pressure-volume curves were generated within 3–4 min after the ligation. No effects of anoxia on the pressure-volume relation could be detected within this period of time. Using the passive pressure-volume relation, end-diastolic cavity volumes required for further analysis were derived from the measured end-diastolic pressures.

Data analysis

The approach permitted the construction of complete left ventricular pressure-volume and stress-length diagrams. Left ventricular and myocardial function were thus assessed independently of left ventricular mass, geometry and loading conditions (Jacob *et al*., 1990). Systolic peak pressures that are equivalent to end-systolic pressures under the isovolumic conditions were plotted against end-diastolic volumes resulting in end-systolic pressure-volume curves. All auxotonic pressure-volume values had to reside within this isovolumically determined end-systolic pressure-volume relation. The area between end-systolic and end-diastolic pressure-volume curves up to maximum end-systolic pressure was used as an index of left ventricular working capacity. Transformation of the left ventricular pressure-volume diagram to the stress-length relation permitted the evaluation of myocardial performance when left ventricular mass and geometry are altered. Myocardial contractility was evaluated on the basis of normalized stress-length area, i.e. the area between the end-systolic and end-diastolic mean wall stress versus normalized midwall circumference (length) curves. In analogy with papillary muscle, the normalized midwall circumference was calculated as the ratio between a given midwall circumference and the midwall circumference associated with peak developed wall stress. Pressure-volume data were transformed into stress-length data using a thick-walled spherical shell. Since calculations assumed that the specific density of myocardium was 1 g cm^{-3}, left ventricular weight in grams equalled the ventricular wall volume in cm^3. Mean (systolic or diastolic) wall stress (σ) was derived from the following formula (Sandler & Dodge, 1963): $\sigma = P/\{[(V+W)/V]^{2/3}-1\}$, where P is left intraventricular pressure, V is left ventricular cavity volume, W is left ventricular wall volume. Since the contraction was isovolumic, end-diastolic volume derived from the passive pressure-volume curve was identical with the left ventricular

cavity volume (V) during the respective beat. Midwall circumference (C_R) was calculated according to: $C_R = \pi\{(3/4\pi)^{1/3}[(V^{1/3} + (V+W)^{1/3}]\}$ (Mirsky & Parmley, 1973). To evaluate the velocity of contraction and relaxation at the myocardial level, rate of mean wall stress rise ($+d\sigma/dt$) or decline ($-d\sigma/dt$) was calculated using the recorded $\pm dP/dt$ values by: $\pm d\sigma/dt = \pm(dP/dt)/\{[(V+W)/V]^{2/3} - 1\}$.

Myosin isozymes

For determination of myosin isozymes of the same cardiac region by non-dissociating polyacrylamide gel electrophoresis in the presence of pyrophosphate (Rupp *et al*., 1992b), a portion of the left ventricular free wall (about 100 mg) was cut from the apex to the base and stored in liquid nitrogen. The myosin isozymes were stained with Coomassie brilliant blue R250 and the gels were scanned using a Quick Scan densitometer (Helena Laboratories, Beaumont, TX, U.S.A.). The isozymes V_1, V_2, V_3 were quantitated by measuring peak heights. Isomyosin V_1 contains two α isoforms of heavy chain, isomyosin V_3 two β isoforms and V_2 is a hybrid myosin containing one α and one β heavy chain. Thus, the proportion of α-MHC could be calculated according to the equation: $\alpha\text{-MHC} = V_1 + V_2/2$.

Statistical analysis

Normality of distribution was checked by the Kolmogoroff-Smirnoff test, and equality of variances according to Cochran. Multiple comparisons were made by one-way analysis of variance and the *post hoc* Spjotvoll/Stoline test (Statistica/w, Statsoft, Tulsa, U.S.A.). Two-group comparisons were performed with two-tailed Student's *t*-test. Statistical significance was assumed at $P < 0.05$.

Results

The ascending aorta was constricted to 70% (Turcani & Rupp, 1997) of the original diameter in 28 five-week-old rats. Six weeks after surgery, the aorto-ventricular pressure gradient and the cardiac geometry was assessed in eight rats with ascending aortic constriction. During maturation of animals, a pressure gradient of 94 ± 8 mmHg developed between the left ventricle and ascending aorta. This gradual pressure overload gave rise to a concentric left ventricular hypertrophy while no signs of left ventricular failure were apparent (Table 1). At the myocardial level, an increased proportion of V_3 isomyosin was detected which is a characteristic feature of the foetal gene programme (Table 2). During the subsequent period, hypertrophy of the overloaded left ventricle continued which was associated with an increased left ventricular weight, cavity volume and further enhancement of V_3 isomyosin expression (Tables 1 and 2).

Administration of racemic etomoxir (15 mg kg^{-1} day^{-1}) for 6 weeks slightly stimulated growth of the right ventricle and to a lesser extent also of the overloaded and hypertrophied left ventricle (Table 1). No change in the volume of the left ventricular cavity accompanied, however, this additional ventricular mass gain. Etomoxir partially blunted the effect of pressure overload on the shift in isomyosin synthesis from predominantly V_1 to V_3 isoform (Table 2). The characteristic inverse relation between weight of the overloaded ventricle and α-MHC expression (Rupp & Jacob, 1986) was reversed. In etomoxir treated rats, left ventricular weight and α-MHC expression were thus positively correlated (Figure 1).

Isovolumic contraction of the hypertrophied left ventricle was improved after the etomoxir treatment. A higher developed systolic pressure and an augmented pressure-volume area reflected a greater overall ventricular working capacity (Table 3). To evaluate the velocity of ventricular contraction and relaxation, $+dP/dt_{max}$ and $-dP/dt_{max}$ were monitored. Increased peak values of these parameters demonstrate that the etomoxir treatment had accelerated the development and decline of the intraventricular pressure. Calculated parameters of myocardial function (normalized stress-length area, $\pm d\sigma/dt_{max}$) were increased as well (Table 3). Thus, at the myocardial level positive inotropic effect of the chronic etomoxir treatment could be postulated.

Discussion

Indexes of ventricular performance during auxotonic contraction are sensitive to changes in preload and afterload.

Table 2 Left ventricular myosin isozyme population

	Sham	*Aortic constriction*		
	6 weeks untreated (n = 8)	*6 weeks untreated* (n = 8)	*12 weeks untreated* (n = 10)	*12 weeks + etomoxir* (n = 10)
Myosin V_1 (%)	60 ± 6	45 ± 3*	24 ± 2†	35 ± 4‡
Myosin V_2 (%)	24 ± 3	28 ± 2*	28 ± 2	29 ± 1
Myosin V_3 (%)	16 ± 4	27 ± 2*	48 ± 3†	36 ± 4‡

Values are means ± s.d. *$P < 0.05$ compared with sham-operated untreated rats; †$P < 0.05$ compared with untreated rats with aortic constriction lasting 6 weeks; ‡$P < 0.05$ compared with untreated rats with aortic constriction lasting 12 weeks.

Table 1 Body weight, right and left ventricular weight and left ventricular cavity volume

	Sham	*Aortic constriction*		
	6 weeks untreated (n = 8)	*6 weeks untreated* (n = 8)	*12 weeks untreated* (n = 10)	*12 weeks + etomoxir* (n = 10)
Body weight (g)	303 ± 8	306 ± 12	371 ± 14†	378 ± 10
Right ventricular weight (mg)	177 ± 22	190 ± 13	197 ± 18	243 ± 12‡
Right ventricular weight/body weight (mg g^{-1})	0.59 ± 0.07	0.62 ± 0.06	0.53 ± 0.06†	0.64 ± 0.04‡
Left ventricular weight (mg)	637 ± 28	1027 ± 69*	1096 ± 33†	1184 ± 53‡
Left ventricular weight/body weight (mg g^{-1})	2.10 ± 0.07	3.35 ± 0.2*	2.96 ± 0.10†	3.14 ± 0.17‡
Left ventricular cavity volume (mm^3)	374 ± 28	334 ± 35	386 ± 37†	335 ± 31‡
Left ventricular cavity volume/wall volume	0.59 ± 0.05	0.33 ± 0.05*	0.35 ± 0.03	0.28 ± 0.03‡

Left ventricular cavity volume and left ventricular cavity volume/wall volume ratio are given for the common intraventricular pressure 6 mmHg. Values are means ± s.d. *$P < 0.05$ compared with sham-operated rats; †$P < 0.05$ compared with untreated rats with aortic constriction lasting 6 weeks; ‡$P < 0.05$ compared with untreated rats with aortic constriction lasting 12 weeks.

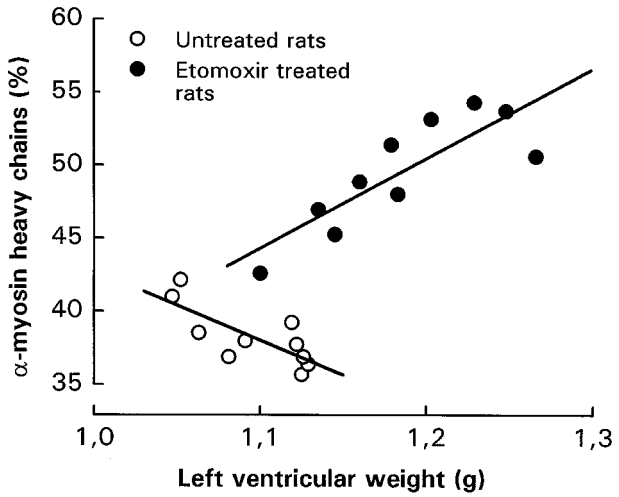

Figure 1 Correlation between left ventricular weight and proportion of α-MHC. Untreated rats (12 weeks after surgery) with aortic constriction (○), $y = 90.2 - 47.4\times$, $r = -0.760$, $P < 0.01$; etomoxir treated rats (12 weeks after surgery) with aortic constriction (●), $y = 23.3 + 61.5\times$, $r = 0.837$, $P < 0.003$.

Table 3 Functional parameters of isovolumically beating left ventricles of rats with ascending aortic constriction lasting 12 weeks

	Aortic constriction	
	Untreated (n = 10)	*+ Etomoxir* (n = 10)
Heart rate (beats min^{-1})	337 ± 47	319 ± 35
Peak developed pressure (mmHg)	315 ± 23	371 ± 22*
Peak developed mean wall stress (kPa)	31.6 ± 2.3	34.3 ± 2.0*
Left ventricular pressure-volume area (mJ)	8.79 ± 0.54	10.92 ± 0.63*
Left ventricular normalized stress-length area (kPa)	3.42 ± 0.45	4.03 ± 0.42*
Peak $+dP/dt_{max}$ (mmHg s^{-1})	12,340 ± 1030	14,800 ± 1310*
Peak $-dP/dt_{max}$ (mmHg s^{-1})	5040 ± 710	6440 ± 750*
Peak $+d\sigma/dt_{max}$ (kPa s^{-1})	1130 ± 90	1290 ± 130*
Peak $-d\sigma/dt_{max}$ (kPa s^{-1})	430 ± 30	520 ± 60*

Etomoxir treatment started 6 weeks after surgical constriction of the ascending aorta and lasted 6 weeks. Values are means ± s.d.; *$P < 0.05$; $+dP/dt_{max}$ and $+d\sigma/dt_{max}$, maximum rate of intraventricular pressure and ventricular wall stress rise; $-dP/dt_{max}$ and $-d\sigma/dt_{max}$, maximum rate of intraventricular pressure and ventricular wall stress decline. Peak observed values are given for $\pm dP/dt_{max}$ and $\pm d\sigma/dt_{max}$ independent on end-diastolic or end-systolic ventricular wall stress.

Moreover, ventricular loads depend not only on peripheral haemodynamic but also on ventricular mass, geometry and diastolic properties. To facilitate the comparison of different ventricles and to overcome problems arising from different loading conditions as well as to distinguish between ventricular and myocardial performance, isovolumic contractions were evaluated. Although some limitations related to non-simultaneous pressure and volume measurements, exclusion of right ventricular influences, assumptions on left ventricular geometry and physical properties of the myocardium remain, only absolute values of measured and calculated parameters might be influenced but not the relative difference detected after the etomoxir treatment. Acceleration of ventricular and myocardial contraction and relaxation also did not result from changes in heart rate since no differences in heart rates during isovolumic contractions were observed (Table 3).

Initial adaptation to a pressure overload in the rat model of ascending aortic stenosis is accomplished by an increased ventricular mass and changes in ventricular geometry which maintain ventricular wall stress in a normal range (Table 1; Litwin *et al*., 1995). In parallel, a foetal pattern of gene expression is reinduced (Table 2; Imamura *et al*., 1991). Although left ventricular chamber function is sufficiently enhanced to compensate for the haemodynamic overload, a subtle impairment of the myocardial function can be detected (Litwin *et al*., 1995). Foetal gene expression, deterioration of systolic and diastolic function and progressive enhancement of ventricular cavity volume characterize the further development (Tables 1 and 2; Feldman *et al*., 1993; Litwin *et al*., 1995).

The etomoxir treatment limited the foetal transformation of myosin molecules in the hypertrophied myocardium. Furthermore, the increased proportion of α-MHC was positively correlated ($P < 0.01$) with improved indices of myocardial function (Figure 2). An increased rate of cross-bridge cycling associated with higher proportion of α-MHC could account for acceleration of myocardial stress development (Winegrad, 1984) and decline (Brutsaert & Sys, 1989). However, the increased normalized ventricular stress-length area indicates a greater number of recruited cross-bridges. A raised availability of activator calcium may thus be postulated. In accordance with this contention is the finding that etomoxir treatment improved sarcoplasmic reticulum calcium pump activity (Vetter & Rupp, 1994) and mRNA abundance (Zarain-Herzberg *et al*., 1996).

Slightly but significantly increased left ventricular mass after etomoxir treatment suggests, that not only qualitative but also quantitative changes in cardiac genes expression are responsible for the enhanced maximal pressure-generating capability of the hypertrophied ventricles, i.e. for the increased peak values of developed ventricular pressure and maximum velocity of intraventricular pressure rise and decline (Table 3). Because the ventricular mass increment during the etomoxir treatment is dose dependent (Rupp *et al*., 1992b), the growth promoting effect of etomoxir could in principle be enhanced by increasing the dosage.

Administration of etomoxir prevented completely the enlargement of left ventricular chamber volume. This might be a consequence of the improved myocardial contractility induced by etomoxir. A direct etomoxir influence on ventricular remodelling should, however, not be dismissed. Cardiac growth induced by etomoxir and other irreversible CPT-1 inhibitors in non-overloaded ventricles is associated with concentric hypertrophy (Eistetter & Wolf, 1986; Litwin *et al*., 1990; Turcani & Rupp, 1997). Nevertheless, in contrast to pressure-overload hypertrophy, myosin V_1 proportion, sarcoplasmic reticulum calcium transport capacity and ventricular performance were increased (Rupp *et al*., 1992b; Vetter & Rupp, 1994; Turcani & Rupp, 1997).

Etomoxir and pressure-overload effects on ventricular hypertrophy appear to be additive. When etomoxir is administered in parallel with the induction of the pressure overload, additional hypertrophy of the overloaded ventricles occurs and the shift from α-MHC to β-MHC synthesis is attenuated in a dose dependent manner (Rupp *et al*., 1992a,b; Turcani & Rupp, 1997). The dose dependence of etomoxir effects is, however, different. The same etomoxir dose stimulates α-MHC expression to a greater extent when the proportion of isomyosin V_1 is low. Thus, the increase in the V_1 proportion was greater in the left versus right ventricle of normal rats (Vetter & Rupp, 1994) and in the overloaded

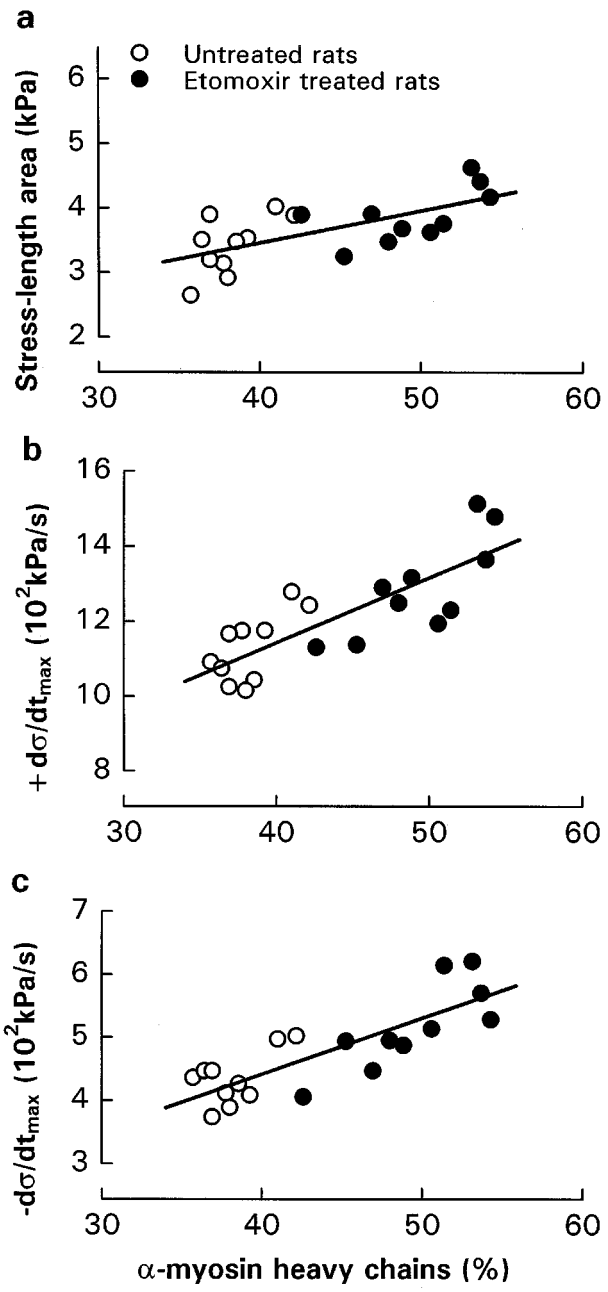

Figure 2 Correlation between the proportion of α-myosin heavy chain (MHC) and indices of myocardial function, normalized length-stress area (a), maximal rate of wall stress rise (b) and decline (c). Untreated rats (12 weeks after surgery) with aortic constriction (○), etomoxir treated rats (12 weeks after surgery) with aortic constriction (●). (a) $y=1.071+0.061\times$, $r=0.747$, $P<0.0002$; (b) $y=450.057+17.323\times$, $r=0.814$, $P<0.00001$; (c) $y=86.369+8.875\times$, $r=0.821$, $P<0.00001$.

hypertrophied left ventricle versus the left ventricle of sham-operated rats (Turcani & Rupp, 1997).

Induction of cardiac growth by irreversible CPT-1 inhibitors had been viewed as a cardiotoxic effect (Litwin *et al*., 1990). Nonetheless, despite the impaired calculated parameters of the passive diastolic properties, ventricular pump function was either not affected (Litwin *et al*., 1990) or even improved (Litwin *et al*., 1991; Turcani & Rupp, 1997). This may be related to the augmented and accelerated contraction and relaxation, increased ejection fraction and the shift in operating chamber stiffness (Litwin *et al*., 1990; 1991; Turcani & Rupp, 1997). Serious concerns originated also from an increased lipid accumulation in the heart and other organs in animals treated with CPT-1 inhibitors (Lullman *et al*., 1978; Litwin *et al*., 1990; Schmitz *et al*., 1995). This potentially toxic effect may not be necessarily related to the CPT-1 inhibition, and a 3-months chronic toxicological study in rats and dogs did not show any pathological changes apart from increased liver, heart and kidney weights in rats (Eistetter & Wolf, 1986).

The mechanisms underlying the etomoxir-induced hypertrophic growth with unique myocardial phenotype is unknown but appears to be related to CPT-1 inhibition. A diet with medium-chain fatty acids prevented the qualitative and quantitative changes in cardiomyocytes gene expression (Lee *et al*., 1985; Rupp *et al*., 1995). Hormonal activities which have qualitatively similar effects on myosin isozyme expression were not increased by etomoxir treatment (Rupp & Jacob, 1992). Particularly important may be the stimulating effect of etomoxir on glucose oxidation. However, the status of glucose oxidation is not clear in mechanically overloaded and hypertrophied hearts. There is increasing evidence that long-chain fatty acid oxidation is reduced and glucose utilization is enhanced in hypertrophied and failing hearts (Allard *et al*., 1994; Christe & Rodgers, 1994; El Alaoui-Talibi *et al*., 1997). It has also been speculated that this shift in fuel preference could lead to decreased ATP production and thus impaired pump function (Motterlini *et al*., 1992; Reibel *et al*., 1994; El Alaoui-Talibi *et al*., 1997). Carnitine deficiency (El Alaoui-Talibi *et al*., 1992; Motterlini *et al*., 1992; Reibel *et al*., 1994) and decreased expression of fatty acid oxidation enzymes (Sack *et al*., 1996) have been suggested as possible underlying mechanisms. A shift from fatty acid to glucose utilization may, however, also improve the energetic economy in hypertrophied and failing myocardium at reduced oxygen deliveries. Furthermore, the oxidative utilization of glucose seems to be decreased in hypertrophied hearts while only the glycolytic flux is enhanced (Bishop & Altschuld, 1970; Allard *et al*., 1994; Massie *et al*., 1995; El Alaoui-Talibi *et al*., 1997). Administration of propionyl-L-carnitine, an intervention that increases glucose oxidation, was shown to improve cardiac performance (Ferrari *et al*., 1992; Yang *et al*., 1992; Motterlini *et al*., 1992; Schönekess *et al*., 1995; El Alaoui-Talibi *et al*., 1997). Thus, positive consequences for the long-term cardiac adaptation to pressure overload may be expected also from stimulation of glucose oxidation by etomoxir, particularly when it restitutes myocardial phenotype and prevents dilatation of the left ventricle.

In summary, a 6 week treatment with the CPT-1 inhibitor etomoxir modifies ventricular mass, geometry and function as well as the foetal gene programme of pressure overloaded rat hypertrophied myocardium. Since etomoxir can apparently prevent myocardial and ventricular changes associated with the transition from compensated hypertrophied to failing hypertrophied heart, long term experimental and clinical studies on prevention of heart failure during chronic pressure overload appear to be warranted.

The study was supported by the Deutsche Forschungsgemeinschaft (Ru 245/7-1), the Alfred-Teufel-Stiftung and the Slovak Grant Agency No. 1/4114/97 and 1/4133/97. The experimental part of this study was performed at the Institute of Physiology II, University of Tübingen, Germany.

References

ALLARD, M.F., SCHÖNEKESS, B.O., HENNING, S.L., ENGLISH, D.R. & LOPASCHUK, G.D. (1994). The contribution of oxidative metabolism and glycolysis to ATP production in hypertrophied heart. *Am. J. Physiol.,* **267,** H742 – H750.

BERGMAN, G., ATKINSON, L., METCALFE, J., JACKSON, N. & JEWITT, D.E. (1980). Beneficial effect of enhanced myocardial carbohydrate utilisation after oxfenicine (L-hydroxyphenylglycine) in angina pectoris. *Eur. Heart J.,* **1,** 247 – 253.

BISHOP, S.P. & ALTSCHULD, R.A. (1970). Increased glycolytic metabolism in cardiac hypertrophy and congestive heart failure. *Am. J. Physiol.,* **218,** 153 – 159.

BRUTSAERT, D.L. & SYS, S.U. (1989). Relaxation and diastole of the heart. *Physiol. Rev.,* **69,** 1228 – 1315.

CHRISTE, M.E. & ROGERS, R.L. (1994). Altered glucose and fatty acid oxidation in hearts of the spontaneously hypertensive rat. *J. Mol. Cell. Cardiol.,* **26,** 1371 – 1375.

CORR, P.B., CREER, M.H., YAMADA, K.A., SAFFITZ, J.E. & SOBEL, B.E. (1989). Prophylaxis of early ventricular fibrillation by inhibition of acylcarnitine accumulation. *J. Clin. Invest.,* **83,** 927 – 936.

EISTETTER, K. & WOLF, H.P.O. (1986). Etomoxir. *Drugs of the Future,* **11,** 1034 – 1036.

EL ALAOUI-TALIBI, Z., GUENDOUZ, A., MORAVEC, M. & MORAVEC, J. (1997). Control of oxidative metabolism in volume-overloaded rat hearts: effects of propionyl-L-carnitine. *Am. J. Physiol.,* **272,** H1615 – H1624.

EL ALAOUI-TALIBI, Z., LANDORMY, S., LOIREAU, A., MORAVEC, J. (1992). Fatty acid oxidation and mechanical performance of volume-overloaded rat hearts. *Am. J. Physiol.,* **262,** H1068 – H1074.

FELDMAN, A.M., WEINBERG, E.O., RAY, P.E. & LORELL, B.H. (1993). Selective changes in cardiac gene expression during compensated hypertrophy and the transition to cardiac decompensation in rats with chronic aortic banding. *Circ. Res.,* **73,** 184 – 192.

FERRARI, R., DI LISA, F., DE JONG, J.W., CECONI, C., PASINI, E., BARBATO, R., MENABO, R., BARBIERI, M., CARBAI, E. & MUGELLI, A. (1992). Prolonged propionyl-L-carnitine pretreatment of rabbit: biochemical, hemodynamical and electrophysiological effects on the heart. *J. Mol. Cell. Cardiol.,* **24,** 219 – 232.

HEPP, A., HANSIS, M., GÜLCH, R. & JACOB, R. (1974). Left ventricular isovolumetric pressure-volume relations, 'diastolic tone', and contractility in the heart after physical training. *Basic Res. Cardiol.,* **69,** 517 – 531.

HIGGINS, A.J., MORVILE, M., BURGES, R.A., GARDINER, D.G., PAGE, M.G. & BLACKBURN, K.J. (1980). Oxfenicine diverts rat muscle metabolism from fatty acid to carbohydrate oxidation and protects the ischaemic heart. *Life Sci.,* **27,** 963 – 970.

IMAMURA, S.I., MATSUOKA, R. & HIRATSUKA, E. (1991). Adaptational changes of MHC expression and isozyme transition in cardiac overloading. *Am. J. Physiol.,* **260,** H73 – H79.

JACOB, R., BRÄNDLE, M., DIERBERGER, B. & ROSS, C.H. (1990). Conceptional and methodological basis for the evaluation of ventricular and myocardial mechanics. In: *Evaluation of cardiac contractility*. ed. Jacob R. pp. 75 – 100. Stuttgart/New York: Gustav Fischer.

KENNEDY, J.A., UNGER, S.A. & HOROWITZ, J.D. (1996). Inhibition of carnitine palmitoyltransferase-1 in rat heart and liver by perhexiline and amiodarone. *Biochem. Pharmacol.,* **52,** 273 – 280.

LEE, S.M., BAHL, J.J. & BRESSLER, R. (1985). Prevention of the metabolic effects of 2-tetradecylglycidate by octanoic acid in the genetically diabetic mouse (db/db). *Biochem. Med.,* **33,** 104 – 409.

LITWIN, S.E., KATZ, S.E., WEINBERG, E.O., LORELL, B.H., AURIGEMMA, G.P. & DOUGLAS, P.S. (1995). Serial echocardiographic-Doppler assessment of left ventricular geometry and function in rats with pressure-overload hypertrophy. Chronic angiotensin-converting enzyme inhibition attenuates the transition to heart failure. *Circulation,* **91,** 2642 – 2654.

LITWIN, S.E., RAYA, T.E., ANDERSON, P.G., LITWIN, C.M., BRESSLER, R. & GOLDMAN, S. (1991). Induction of myocard hypertrophy after coronary ligation in rats decreases ventricular dilatation and improves systolic function. *Circulation,* **84,** 1819 – 1827.

LITWIN, S.E., RAYA, T.E., GAY, R.G., BEDOTTO, J.B., BAHL, J.J., ANDERSON, P.G., GOLDMAN, S. & BRESSLER, R. (1990). Chronic inhibition of fatty acid oxidation: new model of diastolic dysfunction. *Am. J. Physiol.,* **258,** H51 – H56.

LOPASCHUK, G.D., WALL, S.R., OLLEY, P.M. & DAVIES, N.J. (1988). Etomoxir, a carnitine palmitoyltransferase I inhibitor, protects hearts from fatty acid-induced ischemic injury independent of changes in long chain acylcarnitine. *Circ. Res.,* **63,** 1036 – 1043.

LULLMAN, H., LULLMAN-RAUCH, R. & WASSERMANN, O. (1978). Lipidosis induced by amphiphilic cationic drugs. *Biochem. Pharmacol.,* **27,** 1103 – 1108.

MASSIE, B.M., SCHAEFER, S., GARCIA, J., MCKIRNAN, D., SCHWARTZ, G.G., WISNESKI, J.A., WEINER, M.W. & WHITE, F.C. (1995). Myocardial high-energy phosphate and substrate metabolism in swine with moderate left ventricular hypertrophy. *Circulation,* **91,** 1814 – 1823.

MIRSKY, I. & PARMLEY, W.W. (1973). Assessment of passive elastic stiffness for isolated heart muscle and the intact heart. *Circ. Res.,* **33,** 233 – 243.

MOTTERLINI, R., SAMAJA, M., TARANTOLA, M., MICHELETTI, R. & BIANCHI, G. (1992). Functional and metabolic effects of propionyl-L-carnitine in the isolated perfused hypertrophied rat heart. *Mol. Cell. Biochem.,* **116,** 139 – 145.

PEARCE, F.J., FORSTER, J., DELEEUW, G., WILLIAMSON, J.R. & TUTWILER, G.F. (1979). Inhibition of fatty acid oxidation in normal and hypoxic perfused rat hearts by 2-tetradecylglycidic acid. *J. Mol. Cell. Cardiol.,* **11,** 893 – 916.

REIBEL, D.K., UBOH, C.E. & KENT, R.L. (1994). Altered coenzyme A and carnitine metabolism in pressure-overloaded hypertrophied hearts. *Am. J. Physiol.,* **244,** H2090 – H2097.

RUPP, H., ELIMBAN, V. & DHALLA, N.S. (1992a). Modification of subcellular organelles in pressure-overloaded heart by etomoxir, a carnitine palmitoyltransferase I inhibitor. *FASEB J.,* **6,** 2349 – 2353.

RUPP, H. & JACOB, R. (1986). Correlation between total catecholamine content and redistribution of myosin isoenzymes in pressure loaded ventricular myocardium of the spontaneously hypertensive rat. *Basic Res. Cardiol.,* **81** (suppl. 1). 147 – 155.

RUPP, H. & JACOB, R. (1992). Metabolically-modulated growth and phenotype of the rat heart. *Eur. Heart J.,* **13** (suppl. D). 56 – 61.

RUPP, H., SCHULZE, W. & VETTER, R. (1995). Dietary medium-chain triglycerides can prevent changes in myosin and SR due to CPT-1 inhibition by etomoxir. *Am. J. Physiol.,* **269,** R630 – R640.

RUPP, H., WAHL, R. & HANSEN, M. (1992b). Influence of diet and carnitine palmitoyltransferase I inhibition on myosin and sarcoplasmic reticulum. *J. Appl. Physiol.,* **72,** 352 – 360.

SACK, M.N., RADER, T.A., PARK, S., BASTIN, J., MCCUNE, S.A. & KELLY, D.P. (1996). Fatty acid oxidation enzyme gene expression is downregulated in the failing heart. *Circulation,* **94,** 2837 – 2842.

SANDLER, H. & DODGE, H.T. (1963). Left ventricular tension and stress in man. *Circ. Res.,* **3,** 91 – 104.

SCHMIDT-SCHWEDA, S. & HOLUBARSCH, C. (1997). First clinical trial with etomoxir in patients with chronic heart failure II-III. *J. Mol. Cell. Cardiol.,* **29,** A55 (abstract).

SCHMITZ, F.J., RÖSEN, P. & REINAUER, H. (1995). Improvement of myocardial function and metabolism in diabetic rats by the carnitine palmitoyltransferase inhibitor etomoxir. *Horm. Metab. Res.,* **27,** 515 – 522.

SCHÖNEKESS, B.O., ALLARD, M.F. & LOPASCHUK, G.D. (1995). Propionyl-L-carnitine improvement of hypertrophied heart function is accompanied by an increase in carbohydrate oxidation. *Circ. Res.,* **77,** 726 – 734.

SCHWARTZ, K., CARRIER, L., MERCADIER, J.J., LOMPRE, A.M. & BOHELER, K.R. (1993). Molecular phenotype of the hypertrophied and failing myocardium. *Circulation,* **87,** VII-5 – VII-10.

TAEGTMEYER, H. (1994). Energy metabolism of the heart: from basic concepts to clinical applications. *Curr. Probl. Cardiol.,* **19,** 59 – 113.

TURCANI, M. & RUPP, H. (1997). Etomoxir improves left ventricular performance of pressure overloaded rat heart. *Circulation,* **96,** 3681 – 3686.

UNGER, S.A., ROBINSON, M.A. & HOROWITZ, J.D. (1997). Perhexiline improves symptomatic status in elderly patients with severe aortic stenosis. *Aust. N.Z.J. Med.,* **27,** 24 – 28.

VETTER, R. & RUPP, H. (1994). CPT-1 inhibition by etomoxir has a chamber-related action on cardiac sarcoplasmic reticulum and isomyosins. *Am. J. Physiol.,* **267,** H2091 – H2099.

WINEGRAD, S. (1984). Regulation of cardiac contractile proteins; correlations between physiology and biochemistry. *Circ. Res.,* **55,** 565 – 574.

YAMADA, K.A., MCHOWAT, J., YAN, G.-X., DONAHUE, K., PEIRICK, J., KLEBER, A.G. & CORR, P.B. (1994). Cellular uncoupling induced by accumulation of long-chain acylcarnitine during ischemia. *Circ. Res.,* **74,** 83–95.

YANG, X.P., SAMAJA, M., ENGLISH, E., BENATTI, P., TARANTOLA, M., CARDACE, G., MOTTERLINI, R., MICHELETTI, R. & BIANCHI, R. (1992). Hemodynamic and metabolic activities of propionyl-L-carnitine in rats with pressure-overload cardiac hypertrophy. *J. Cardiovasc. Pharmacol.,* **20,** 88–98.

ZARAIN-HERZBERG, A., RUPP, H., ELIMBAN, V. & DHALLA, N.S. (1996). Modification of sarcoplasmic reticulum gene expression in pressure overloaded cardiac hypertrophy by etomoxir. *FASEB J.,* **10,** 1303–1309.

(Received July 17, 1998
Revised September 15, 1998
Accepted October 22, 1998)

British Journal of Pharmacology (1999) 126, 508–514
http://www.stockton-press.co.uk/bjp

Block by fluoxetine of volume-regulated anion channels

[1]Chantal Maertens, [1]Lin Wei, [1]Thomas Voets, [1]Guy Droogmans & *,[1]Bernd Nilius

[1]KU Leuven, Laboratorium voor Fysiologie, Campus Gasthuisberg, B-3000 LEUVEN, Belgium

1 We have used the whole-cell patch clamp technique to study the effect of fluoxetine, a commonly used antidepressant drug, on the volume-regulated anion channel (VRAC) in calf pulmonary artery endothelial (CPAE) cells. We also examined its effects on other Cl^- channels, i.e. the Ca^{2+}-activated Cl^- current ($I_{Cl,Ca}$) and the cystic fibrosis transmembrane conductance regulator (CFTR) to assess the specificity of this compound for VRAC.

2 At pH 7.4 fluoxetine induced a fast and reversible block of the volume-sensitive chloride current ($I_{Cl,swell}$), with a K_i value of 6.0 ± 0.5 μM ($n = 6$-9). The blocking efficiency increased with increasing extracellular pH ($K_i = 0.32 \pm 0.01$ μM at pH 8.8, $n = 3$-9), indicating that the blockade is mediated by the uncharged form of fluoxetine.

3 Fluoxetine inhibited Ca^{2+}-activated Cl^- currents, $I_{Cl,Ca}$, activated by loading CPAE cells *via* the patch pipette with 1000 nM free Ca^{2+} ($K_i = 10.7 \pm 1.6$ μM at pH 7.4, $n = 3$-5). The CFTR channel, transiently transfected in CPAE cells, was also inhibited with a K_i value of 26.9 ± 9.4 μM at pH 7.4 ($n = 3$).

4 This study describes for the first time the effects of fluoxetine on anion channels. Our data reveal a potent block of VRAC at fluoxetine concentrations close to plasma concentrations. The results suggest a hydrophobic interaction with high affinity between uncharged fluoxetine and volume-activated chloride channels. Ca^{2+}-activated Cl^- currents and CFTR are also blocked by fluoxetine, revealing a novel characteristic of the drug as a chloride channel modulator.

Keywords: Patch-clamp; volume-regulated anion channels; fluoxetine; Ca^{2+}-activated Cl^- currents; cystic fibrosis transmembrane conductance regulator; endothelium

Abbreviations: CFTR, cystic fibrosis transmembrane conductance regulator; CPAE, calf pulmonary artery endothelial cells; EGTA, ethylene glycol-O,O'-bis(2-aminoethyl)-N,N,N′,N′-tetraacetic acid; FLX, fluoxetine; GFP; green fluorescent protein; HEPES, N-(hydroxyethyl)piperazine-N′-(2-ethanesulphonic acid); HTS, hypotonic solution; IBMX, 3-isobutyl-1-methylxanthine; $I_{Cl,Ca}$, Ca^{2+}-activated Cl^- current; $I_{Cl,Swell}$, swelling activated chloride current; ISO, isotonic solution; Kr, Krebs solution; TRIS, Tris(hydroxymethyl)aminomethane; VRAC, volume-regulated anion channel; WT, wild type

Introduction

Fluoxetine (FLX, Prozac), a substituted propylamine (Figure 1) prescribed for the treatment of depression, is assumed to derive its antidepressant activity from its ability to block the reuptake of 5-hydroxytryptamine, while it exerts minimal effects on other neurotransmitter reuptake systems (Wong *et al*., 1995). However, several studies have been published which show that, in addition to this selective action, many other effector systems are modulated. So far, inhibitory effects of Prozac have been demonstrated on cation channels, such as Ca^{2+} channels (Stauderman *et al*., 1992), K^+ channels (Farrugia, 1996; Rae *et al*., 1995; Tytgat *et al*., 1997) and Na^+ channels (Pancrazio *et al*., 1998). However, to our knowledge, effects of FLX on anion channels have never been studied.

In this study we have tested whether Prozac would also modulate volume regulated anion channels and the correspondent swelling-activated chloride current ($I_{Cl,swell}$). Many, if not all mammalian cells express volume-regulated anion channels (VRAC) which are important regulators of various cell functions such as cell volume, pH control, transport of osmolytes and the membrane potential (Nilius *et al*., 1996; 1997a; Okada, 1997; Strange *et al*., 1996; Kirk, 1997). Many inhibitors have been described, but most of them are also modulating other channels and a selective, high affinity VRAC blocker is still missing. Since FLX belongs to a family of propylamines with a $-CF_3$ group, supporting the idea that these compounds comprise in general promising candidates for high selectivity VRAC blockers (Roy *et al*., 1998), it was interesting to study its actions on VRAC.

Furthermore, we wanted to examine whether the Ca^{2+}-activated Cl^- current ($I_{Cl,Ca}$) and the cystic fibrosis transmembrane conductance regulator (CFTR) were also affected by FLX. CFTR is a non-rectifying, 8–10 pS, protein kinase A activated chloride channel (Cliff *et al*., 1992), belonging to the family of ATP-binding cassette proteins (Hyde *et al*., 1990). Mutations in the gene for this channel cause cystic fibrosis. $I_{Cl,Ca}$ is a strongly outwardly rectifying, 8 pS, calcium activated chloride current, described in various excitable and non excitable cells, including calf pulmonary artery endothelial (CPAE) cells (Nilius *et al*., 1997c).

We show here that FLX exerts a potent blocking effect on VRAC in endothelial cells at concentrations close to therapeutical concentrations. This finding may indicate that this channel is also a possible target of this drug. The Ca^{2+}-activated Cl^- current and CFTR are also affected by FLX.

Methods

Vector construction

We used the pCINeo/IRES-GFP plasmid (Trouet *et al*., 1997) for expressing wild type (WT) CFTR in CPAE. For insertion

*Author for correspondence;
E-mail: bernd.nilius@med.kuleuven.ac.be

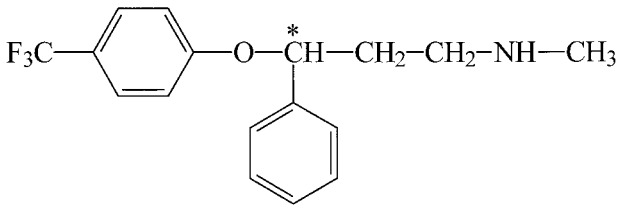

Figure 1 Chemical structure of fluoxetine.

of WT CFTR the green fluorescent protein (GFP)-vector was cut with *Eco*RI, dephosphorylated and thereupon blunt-ended with T4 DNA-polymerase. The WT CFTR cDNA was obtained from a pcDNA/CFTR plasmid through *Sac*I digestion. The obtained fragment was blunt-ended using T4 DNA-polymerase. Ligation was performed using standard procedures.

Cell culture and transfection

Cells from a cultured bovine pulmonary artery endothelial (CPAE) cell line (American Tissue Type Culture Collection, CCL 209) were used. The cells were grown in Dulbecco's modified Eagle's medium containing 20% foetal calf serum, 2 mM L-glutamine, 2 U ml^{-1} penicillin and 2 mg ml^{-1} streptomycin. Cultures were maintained at 37°C in a fully humidified atmosphere of 10% CO_2 in air.

Cells were detached by exposure to 0.05% trypsin in a Ca^{2+}- and Mg^{2+}-free solution, reseeded on gelatin coated cover slips, and kept in culture for 2 to 4 days before use. For electrophysiological experiments, only non-confluent single endothelial cells were used.

CPAE cells do not express CFTR (Nilius *et al*., 1997e). Therefore, cells were transiently transfected with WT CFTR in the pCINeo/IRES-GFP vector (Trouet *et al*., 1997) using the same method as described previously (Kamouchi *et al*., 1997). In short, 150,000 cells were incubated with a transfection cocktail containing 3 μg DNA and 12 μl polycationic Super-Fect Transfection Reagent (Qiagen, Hilden, Germany). Cells were then transferred to gelatin-coated cover slips 24 h after transfection and electrophysiological measurements were done during 2–4 days after transfection. Incorporation of WT CFTR in the bicistronic unit allows coupled expression of the channels and GFP. Transfected cells, positive for GFP, could be identified in the patch-clamp set up. GFP was excited at a wavelength between 450 and 490 nm and the emitted light was passed through a 520 nm long pass filter.

Solutions and drugs

The standard extracellular solution was a modified Krebs solution (Kr) containing (in mM): NaCl 150, KCl 6, $MgCl_2$ 1, $CaCl_2$ 1.5, glucose 10, N-(hydroxyethyl)piperazine-N′-(2-ethanesulphonic acid) (HEPES) 10, titrated with NaOH to pH 7.4. The osmolarity, as measured with a vapour pressure osmometer (Wescor 5500, Schlag, Gladbach, Germany), was 320 ± 5 mOsm.

$I_{Cl,swell}$: At the beginning of the patch-clamp recording, the Krebs solution was replaced by an isotonic-Cs^+ solution (ISO, 320 ± 5 mOsm) containing (in mM): NaCl 105, CsCl 6, $CaCl_2$ 1.5, $MgCl_2$ 1, D-mannitol 90, glucose 10, HEPES 10, adjusted to pH 7.4 with NaOH. Volume-sensitive Cl^- currents were activated by exposing the cells to a 25% hypotonic extracellular solution (HTS, 240 ± 5 mOsm), containing (in mM): NaCl 105, CsCl 6, $CaCl_2$ 1.5, $MgCl_2$ 1, glucose 10, HEPES 10 ($HTS_{7.4}$ and HTS_6) or Tris(hydroxymethyl)-aminomethane (TRIS) 10 ($HTS_{8.8}$), adjusted to pH 7.4 ($HTS_{7.4}$) or pH 6 (HTS_6) with NaOH or titrated to pH 8.8 ($HTS_{8.8}$) with HCl.

The standard pipette solution contained (in mM): CsCl 40, Cs-aspartate 100, $MgCl_2$ 1, $CaCl_2$ 1.93, ethylene glycol-O,O′-bis(2-aminoethyl)-N,N,N′,N′-tetraacetic acid (EGTA) 5, Na_2 ATP 4, HEPES 10, adjusted to pH 7.2 with CsOH (290 ± 5 mOsm).

The presence of Cs^+ instead of K^+ in the extra- and intracellular solutions blocked the inwardly rectifying K^+ currents, which are present in CPAE cells (Voets *et al*., 1996a). To suppress the Ca^{2+}-activated Cl^- current, the free Ca^{2+} concentration in the pipette solution was buffered at 100 nM, which is below the threshold for activation of this current (Nilius *et al*., 1997c), but which is sufficient for full activation of $I_{Cl,swell}$ during cell swelling in CPAE cells (Szücs *et al*., 1996).

$I_{Cl,Ca}$: Krebs solution was replaced by a slightly hypertonic Krebs-Cs^+ solution (345 ± 5 mOsm) containing (in mM): NaCl 150, CsCl 6, $MgCl_2$ 1, $CaCl_2$ 1.5, glucose 10, D-mannitol 25, HEPES 10, titrated with NaOH to pH 7.4. The slightly increased osmolarity prevented coactivation of VRAC. $I_{Cl,Ca}$ was activated by loading CPAE cells *via* the patch pipette with 1000 nM free Ca^{2+} as described previously (Nilius *et al*., 1997c,d). The standard pipette solution contained (in mM): CsCl 40, Cs-aspartate 100, $MgCl_2$ 1, $CaCl_2$ 4.33, EGTA 5, Na_2ATP 4, HEPES 10, adjusted to pH 7.2 with CsOH (290 ± 5 mOsm).

CFTR: To eliminate K^+ currents, Krebs solution was replaced by a Krebs-Cs^+ solution (320 ± 5 mOsm) containing (in mM): NaCl 150, CsCl 6, $MgCl_2$ 1, $CaCl_2$ 1.5, glucose 10, HEPES 10, titrated with NaOH to pH 7.4. The CFTR-channel was activated by a cocktail containing 100 μM 3-isobutyl-1-methylxanthine (IBMX) and 1 μM forskolin (both from Sigma-Aldrich Chemie) dissolved in the Krebs-Cs^+ solution. The standard pipette solution contained (in mM): CsCl 40, Cs-aspartate 100, $MgCl_2$ 1, $CaCl_2$ 1.93, EGTA 5, Na_2ATP 4, HEPES 10 adjusted to pH 7.2 with CsOH (290 ± 5 mOsm).

Fluoxetine hydrochloride was purchased from Sigma Aldrich.

Current measurements and data analysis

Whole-cell membrane currents were measured in ruptured patches. All experiments were performed at room temperature (20–23°C). Currents were monitored with an EPC-7 patch clamp amplifier (List Electronic, Germany) and sampled at 2 ms intervals (1024 points per record, filtered at 200 Hz), unless otherwise mentioned.

$I_{Cl,swell}$: In most experiments we applied a 'ramp' protocol, which consisted of: a step to −80 mV for 0.4 s, followed by a step to −150 mV for 0.1 s and a 1.3 s linear voltage ramp to +100 mV. This voltage protocol was repeated every 15 s from a holding potential of 0 mV. Current-voltage relations were constructed from the ramp current, and time courses were obtained by averaging the current in a small voltage window around +100 mV and −150 mV. In some experiments we used a 'step' protocol consisting of 1.5 s voltage steps, applied every 10 s from a holding potential of −50 mV to test potentials from −100 to +100 mV with increments of 40 mV. Currents were sampled at 1 ms intervals.

$I_{Cl,Ca}$ and CFTR: In all experiments we used a 'step' protocol consisting of 1.5 s voltage steps, applied every 10 s from a holding potential of −20 mV to test potentials from −100 to +100 mV with increments of 20 mV. Currents were sampled at 1 ms intervals.

Data were analysed in Winascd (G. Droogmans) and in Origin (MicroCal Software, Inc.). Pooled data are given as the means±s.e.mean.

Results

Fluoxetine inhibits various Cl^- channels

The CFTR-currents were activated by a cocktail containing 100 μM IBMX and 1 μM forskolin dissolved in the Krebs-Cs^+ solution, as described in detail elsewhere (Cuppens *et al.*, 1998). Figure 2a and b show CFTR-current traces in control conditions (a) and in the presence of 10 μM FLX (b), measured during the voltage step protocol, performed at pH 7.4. The corresponding current-voltage relations (Figure 2c) show that the CFTR currents are approximately equally inhibited at positive and negative potentials. The dose-inhibition curve at +100 mV was fitted to the equation

$$\%\ Inhibition = \frac{100}{1+\left(K_i / C\right)^p} \quad (1)$$

in which C is the drug concentration, p the Hill coefficient and K_i the drug concentration needed for half maximal block. The value of K_i was 26.9±9.4 μM ($n=3$).

Ca^{2+}-activated Cl^- currents were activated by loading CPAE cells *via* the patch pippete with 1 μM free Ca^{2+} as described previously (Nilius *et al.*, 1997d). Figure 2d and e show current traces in control conditions (d) and in the presence of 10 μM FLX (e), measured during the voltage step protocol, performed at pH 7.4. The corresponding current-voltage relations are shown in Figure 2f. The value of K_i (at +100 mV and pH 7.4) was 10.7±1.6 μM (n=3-5). Volume-activated chloride channels and the corresponding current, $I_{Cl,swell}$, were activated by replacing the isotonic solution (ISO) by the hypotonic solution (HTS), as described in detail

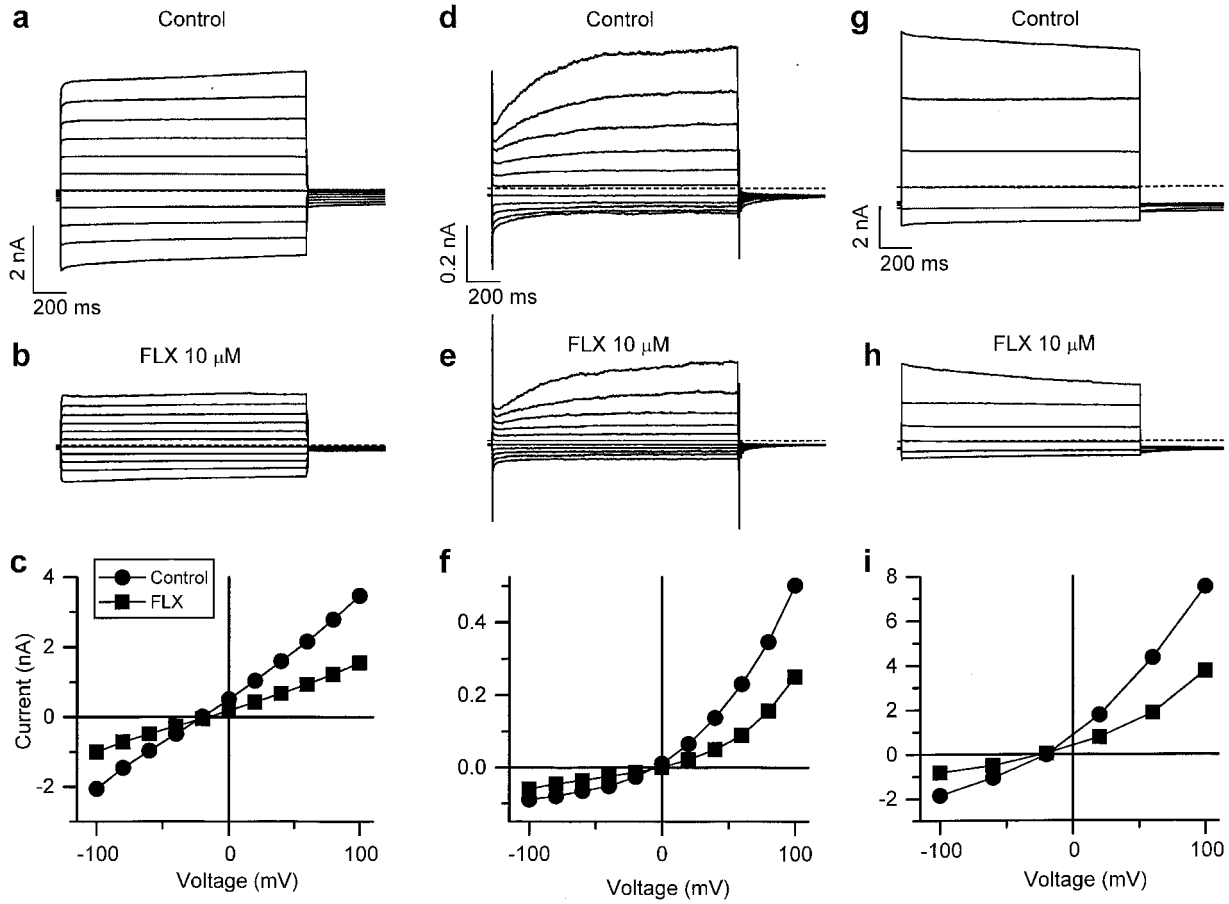

Figure 2 (a) CFTR-current traces in response to 1.5-s voltage steps to potentials from −100 to +100 mV (+20 mV increment), applied every 10 s from a holding potential of −20 mV. Sampling interval was 1 ms. The dashed line indicates zero current. Currents were measured in control conditions at pH 7.4. (b) Currents recorded in the presence of 10 μM FLX at pH 7.4 using the same protocol as in (a). (c) Current-voltage relations derived from the CFTR-current traces in (a) and in (b). Currents were measured at the end of the voltage steps. (d) $I_{Cl,Ca}$ current traces in control conditions using the same protocol as in (a). (e) Currents recorded in the presence of 10 μM FLX at pH 7.4 using the same protocol as in (a). (f) Current-voltage relations derived from the $I_{Cl,Ca}$ current traces in (d) and in (e). Currents were measured at the end of the voltage steps. (g) Current traces in response to 1.5-s voltage steps to potentials from −100 to +100 mV (+40 mV increment), applied every 10 s from a holding potential of −50 mV. Sampling interval was 1 ms. The dashed line indicates zero current. Currents were measured in control conditions at pH 7.4 ($HTS_{7.4}$). (h) Currents recorded in the presence of 10 μM FLX at pH 7.4 using the same protocol as in (g). (i) Current-voltage relations derived from the VRAC current traces in (g) and in (h). Currents were measured at the end of the voltage steps.

elsewhere (Nilius *et al*., 1994a). Figure 2g and h show current traces in control conditions (g) and in the presence of 10 μM FLX (h), measured during the voltage step protocol, performed at pH 7.4. The corresponding current-voltage relations (Figure 2i) show that the VRAC currents are approximately equally inhibited at positive and negative potentials. $I_{Cl,swell}$ and the Ca^{2+}-activated Cl^- current reverse at potentials more positive than the theoretical equilibrium potential for Cl^- because of permeation of organic anions such as aspartate in the pipette (for a detailed discussion see Nilius *et al*., 1997a, c). We will focus the following experiments on the interaction between FLX and VRAC.

Inhibition by fluoxetine of VRAC

Figure 3a shows a typical time course experiment in which two different concentrations of FLX (5 and 50 μM) were added to the external solution during a maintained superfusion with hypotonic solution ($HTS_{7.4}$). FLX induced a fast and concentration-dependent block of $I_{Cl,swell}$, which was almost complete at 50 μM. This block was fully reversible and recovery of the current upon washout was fast. Current-voltage relationships (Figure 3b) are obtained from voltage ramps before and after addition of the different drug concentrations. Very similar results were obtained in analogous experiments ($n \geqslant 7$).

At pH 7.4, FLX occurs mainly with one single positive charge, due to a secondary amine group with a pK_a value of 9.5. In order to investigate whether its inhibitory effect on $I_{Cl,swell}$ is mediated by the positively charged or by the neutral form, we performed experiments in which the pH of the HTS solution was increased to 8.8 ($HTS_{8.8}$) or decreased to 6.0 (HTS_6) during drug application. Short (1–2 min) changes in pH did not significantly affect the amplitude of currents measured in isotonic or hypotonic conditions, as described in detail elsewhere (Nilius *et al*., 1998). Figure 4a shows a typical time course experiment in which the pH of the external solution was changed during application of 5 μM FLX. Current-voltage relationships (Figure 4b) are obtained from voltage ramps before and after addition of 5 μM FLX at different pH values. Figure 4 shows that the inhibitory effect of 5 μM FLX on $I_{Cl,swell}$ is increased at higher pH and almost absent at lower pH values. Very similar results were obtained in analogous experiments ($n = 8$).

From the experimental protocols shown in Figures 3 and 4, we have evaluated the concentration dependence of the inhibition of $I_{Cl,swell}$ for FLX at two pH values (pH 7.4 and 8.8) and at +100 mV (Figure 5, filled squares for pH 7.4, filled circles for pH 8.8). The inhibition is expressed as the percentage reduction of the background corrected $I_{Cl,swell}$ at +100 mV. The background current (current under isotonic conditions) was not affected by FLX, except at the highest concentrations. At pH 7.4, the estimated value of K_i was 6.0 ± 0.5 μM, with a Hill coefficient of 1.04 ± 0.09. However, the estimated value of K_i for pH 8.8 was 0.32 ± 0.01 μM, with a Hill coefficient of 1.32 ± 0.05. This more potent block at higher pH could be explained by assuming that only the uncharged form of FLX exerts a blocking effect. The uncharged concentrations can be calculated by the following equation:

$$\log \frac{[base]}{[acid]} = pH - pk_a \qquad (2)$$

In the case of FLX, [*base*] corresponds to the concentration of the uncharged drug and [*acid*] to the concentration of the charged drug in the solution. It can be calculated that at pH 6 only 0.03% of FLX is in its uncharged form, while at pH 7.4 and 8.8 the uncharged form amounts to 0.8 and 19.9%

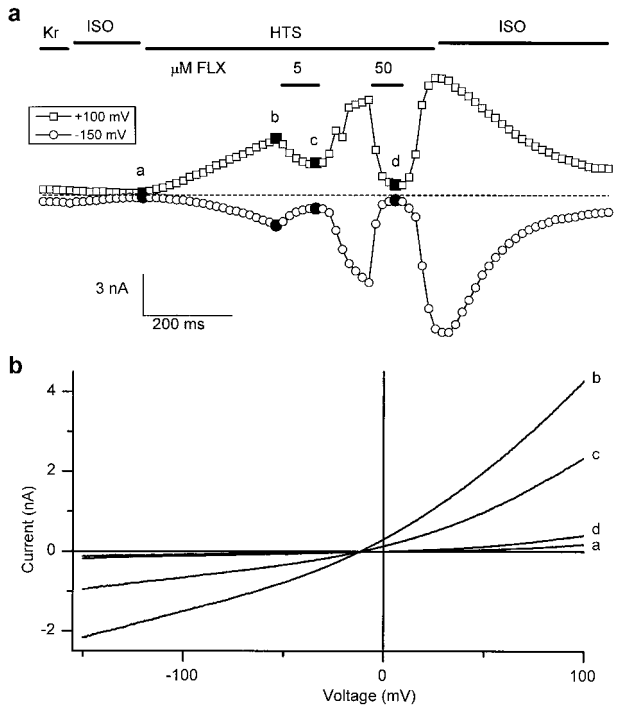

Figure 3 (a) Time course of activation of $I_{Cl,swell}$ during superfusion with hypotonic solution (HTS) (following superfusion with Krebs solution (Kr) and isotonic-Cs^+ solution (ISO)), reversible inhibition of the current with 5 and 50 μM of FLX and deactivation of the current after returning to isotonic-Cs^+ solution. The dashed line indicates zero current. Data were obtained from ramp protocols by averaging the current in a small voltage window around +100 mV and −150 mV. (b) Current-voltage relations obtained from voltage ramps at the times indicated in (a).

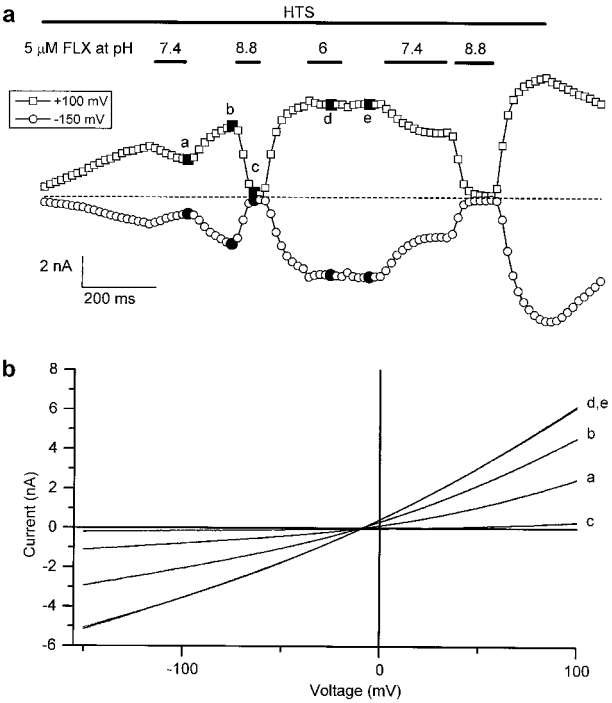

Figure 4 (a) Time course of the current at +100 mV and −150 mV showing the effect of different pH values on the block of $I_{Cl,swell}$ by 5 μM FLX. (b) Current-voltage relations were obtained from voltage ramps at the times indicated in (a).

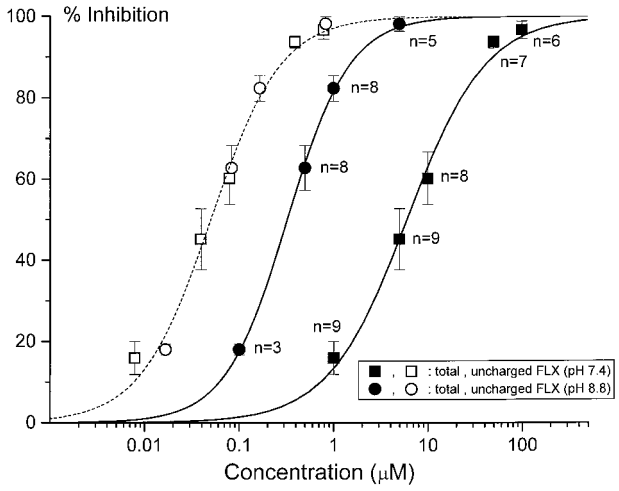

Figure 5 Dose-response curve for inhibition of VRAC by FLX at two different pH values: pH 7.4 and 8.8. Each data point represents the average ± s.e.mean of *n* cells as indicated. The filled line represents the best fit of the data to equation [1]. The open symbols represent the inhibition as a function of the effective concentration of the uncharged form as derived from the data points at pH 7.4 and 8.8 and calculated by equation [3]. The dashed line represents the best fit of the pooled data to equation (1).

respectively. Hence, a pH shift from pH 7.4 to 8.8 increases the concentration of the uncharged form approximately 20 fold. The same factor of increase is found when we compare the K_i values obtained at pH 7.4 and 8.8. This confirms the assumption that the blocking effect of FLX on $I_{Cl,swell}$ is exerted by the neutral form. The effective concentration of the uncharged form at each concentration of FLX ([FLX]) can be calculated by the following equation:

$$[base] = [FLX] \times \frac{10^{(pH-pK_a)}}{1 + 10^{(pH-pK_a)}} \qquad (3)$$

The open symbols in Figure 5 represent the inhibition as a function of the effective concentration of the uncharged form, as derived from the data points at pH 7.4 (open squares) and at pH 8.8 (open circles). It is obvious that the inhibition curves obtained at the two pH values are not significantly different if plotted as a function of the concentration of the uncharged form of FLX. The dashed line represents the best fit of the pooled data to equation [1]. The estimated K_i value for the non-ionised form of FLX was 50.1 ± 2.86 nM, with a Hill coefficient of 1.17 ± 0.08.

Discussion

The experimental results obtained in this study demonstrate a fast and concentration-dependent block of volume-regulated anion channels in endothelial cells by FLX. This blocking effect was not specific for VRAC, since Ca^{2+}-activated Cl^- channels and the cystic fibrosis transmembrane conductance regulator were also inhibited by the drug in a similar concentration range. These results could reveal a novel characteristic of the antidepressant drug FLX, *sc*. as a novel chloride channel modulator. In this context it is interesting to compare FLX with other chloride channel blockers. FLX is a voltage-independent chloride channel modulator. These differ in their sensitivity for blocking the channel (mM to μM range) and apparently there is no structural relationship. All compounds however seem to be relatively hydrophobic and contain aromatic parts, frequently phenolic structures. An amine function is often present and a $-CF_3$ group is likely to increase the blocking sensitivity (Roy *et al*., 1998). Relying on the structure of FLX it is also fair to catalogue the drug in the group of the voltage-independent chloride channel blockers such as tamoxifen, quinine and quinidine, mibefradil, (Nilius *et al*., 1994b, 1997b; Voets *et al*., 1996b), for a review see (Nilius *et al*., 1997a).

The inhibitory effect of FLX on VRAC is markedly potentiated at higher pH values. The pronounced pH-effect is not due to an effect on the channel itself, since short (1–2 min) changes in pH do not significantly affect the amplitude of currents measured in isotonic or hypotonic conditions (Nilius *et al*., 1998). Our results strongly suggest that inhibition of VRAC is mediated by the uncharged form of FLX. A possible explanation could be that the block is due to an intracellular action following permeation of the uncharged form through the cell membrane, as has been proposed for chromones (Heinke *et al*., 1995). However, if uncharged FLX enters the cell, it would be ionized immediately (the internal solution has a pH of 7.2) and subsequent wash-out would be rather slow. Since this is in contradiction to our results, it is more likely that the high affinity block by the neutral FLX is due to hydrophobic interactions with the channel protein(s) within the membrane bilayer. The voltage-independent nature of the block supports this hypothesis. A similar mechanism has been described for the inhibitory action of quinine and quinidine on $I_{Cl,swell}$ (Voets *et al*., 1996b). If we assume that only the non-ionized form of FLX is responsible for block of VRAC, the estimated K_i value is 50.1 ± 2.9 nM as derived from the measurements at pH 7.4 and 8.8.

In previous studies it has been shown that FLX inhibits cation channels. In most of these studies, however, the concentration at which FLX was found to affect these channels was much higher than the anticipated plasma concentrations in patients being treated for depression (Rae *et al*., 1995; Tytgat *et al*., 1997). Therapeutic blood levels range from 0.2 to 3.4 μM (Altamura *et al*., 1994; Baumann, 1996; Preskorn *et al*., 1991) and brain concentrations seem to be significantly higher than their corresponding plasma concentrations (Altamura *et al*., 1994). The apparent brain concentration of FLX relative to plasma is 20 : 1 (Karson *et al*., 1993). This concentration range fits with the blocking range for all Cl^- channels tested in this study. FLX might therefore affect Cl^- activity in the brain at the normally used therapeutic concentrations. In addition to the block of Ca^{2+}-activated Cl^- channels and CFTR, our data reveal for the first time a potent block of volume regulated anion channels, VRAC, by Prozac with K_i values close to plasma concentrations. It has been shown that VRAC is an ubiquitously expressed channel with very similar properties in many cell types (Nilius *et al*., 1994c). The functional importance of this channel has been discussed in detail and comprises among others, effects on volume regulation, osmolyte transport and electrogenesis (Nilius *et al*., 1997a; Okada, 1997; Strange *et al*., 1996). Because of these multiple effects, it is not unlikely that modulation of VRAC contributes to the numerous and complicated mechanisms of action of the psychotropic drug. This might be especially important, inasmuch as VRAC has been described in neuronal and glial cells and endothelial cells of the blood-brain barrier, and is critically involved in volume regulation and maintaining the osmotic composition of the fluid compartments in the central nervous system (Strange, 1992).

Interestingly, VRAC is also involved in glutamate release during cerebral ischemia (Bausch & Roy, 1996), and its

activation is tightly linked to the cellular energy metabolism, which may have significance for several human diseases such as stroke-like episodes (MELAS), encephalopathy, brain swelling and edema (Patel *et al*., 1998). Under all these circumstances, modulation of VRAC by Prozac may play a role in the overall action of this psychotropic drug. Therefore, brain Cl^- channels may provide multifunctional targets of FLX. In conclusion, volume-activated chloride currents are efficiently blocked by the uncharged form of fluoxetine. Given that the uncharged fluoxetine exerts its inhibitory effect in the nanomolar range, it might provide a lead compound for the development of novel modulatory, high affinity compounds of volume-activated chloride currents. Ca^{2+}-activated Cl^- currents and CFTR are also blocked by fluoxetine, revealing a novel characteristic of the drug as a chloride channel modulator.

We thank Drs J. Eggermont and J. Tytgat for many helpful discussions, Prof R. Casteels for critical reading of the manuscript and J. Prenen for excellent technical support. The technical help of D. Hermans, A. Florizone and M. Crabbé is greatly acknowledged. The work has been supported by grants from the Federal Belgian State (Interuniversity Poles of Attraction Programme, Prime Ministers Office IUAP Nr.3P4/23) and Flemish Government (F.W.O. G.0237.95, C.O.F./96/22-A0659), and by the European Commission (BMH4-CT96-0602). We thank Anne Vankeerberghen (Centre for Human Genetics) for providing WT CFTR. Ch. M. is a Research Assistant of the Flemish Fund for Scientific Research (F.W.O.-Vlaanderen).

References

ALTAMURA, A.C., MORO, A.R. & PERCUDANI, M. (1994). Clinical pharmacokinetics of fluoxetine. *Clin. Pharmacokinet.,* **26,** 201–214.

BAUMANN, P. (1996). Pharmacokinetic-pharmacodynamic relationship of the selective serotonin reuptake inhibitors. *Clin. Pharmacokinet.,* **31,** 444–469.

BAUSCH, A.R. & ROY, G. (1996). Volume-sensitive chloride channels blocked by neuroprotective drugs in human glial cells (U-138MG). *Glia,* **18,** 73–77.

CLIFF, W.H., SCHOUMACHER, R.A. & FRIZZELL, R.A. (1992). cAmp-activated Cl channels in Cftr-transfected cystic fibrosis pancreatic epithelial cells. *Am. J. Physiol.,* **262,** C1154–C1160.

CUPPENS, H., LIN, W., JASPERS, M., COSTES, B., TENG, H., VANKEERBERGHEN, A., JORISSEN, M., DROOGMANS, G., REYNAERT, I., GOOSSENS, M., NILIUS, B. & CASSIMAN, J.J. (1998). Polyvariant mutant cystic fibrosis transmembrane conductance regulator genes. The polymorphic (Tg)m locus explains the partial penetrance of the T5 polymorphism as a disease mutation. *J. Clin. Invest.,* **101,** 487–496.

FARRUGIA, G. (1996). Modulation of ionic currents in isolated canine and human jejunal circular smooth muscle cells by fluoxetine. *Gastroenterology,* **110,** 1438–1445.

HEINKE, S., SZÜCS, G., NORRIS, A., DROOGMANS, G. & NILIUS, B. (1995). Inhibition of volume-activated chloride currents in endothelial cells by chromones. *Br. J. Pharmacol.,* **115,** 1393–1398.

HYDE, S.C., EMSLEY, P., HARTSHORN, M.J., MIMMACK, M.M., GILEADI, U., PEARCE, S.R., GALLAGHER, M.P., GILL, D.R., HUBBARD, R.E. & HIGGINS, C.F. (1990). Structural model of ATP-binding proteins associated with cystic fibrosis, multidrug resistance and bacterial transport. *Nature,* **346,** 362–365.

KAMOUCHI, M., DROOGMANS, G. & NILIUS, B. (1997). G-protein modulated K^+ inward rectifier channels in macrovascular endothelial cells. *J. Physiol.,* **504,** 545–556.

KARSON, C.N., NEWTON, J.E., LIVINGSTON, R., JOLLY, J.B., COOPER, T.B., SPRIGG, J. & KOMOROSKI, R.A. (1993). Human brain fluoxetine concentrations. *J. Neuropsychiatry Clin. Neurosci.,* **5,** 322–329.

KIRK, K. (1997). Swelling-activated organic Osmolyte Channels. *J. Membr. Biol.,* **158,** 1–16.

NILIUS, B., EGERMONT, J., VOETS, T., BUYSE, G., MANOLOPOULOS, V. & DROOGMANS, G. (1997a). Properties of volume-regulated anion channels in mammalian cells. *Prog. Biophys. Mol. Biol.,* **68,** 69–119.

NILIUS, B., EGGERMONT, J., VOETS, T. & DROOGMANS, G. (1996). Volume-activated Cl^- channels. *Gen. Pharmacol.,* **27,** 1131–1140.

NILIUS, B., OIKE, M., ZAHRADNIK, I. & DROOGMANS, G. (1994a). Activation of a Cl^- current by hypotonic volume increase in human endothelial cells. *Journal of General Physiology,* **103,** 787–805.

NILIUS, B., PRENEN, J. & DROOGMANS, G. (1998). Modulation of volume-regulated anion channels by extra- and intracellular pH. *Pflügers Arch.,* **436,** 742–748.

NILIUS, B., PRENEN, J., KAMOUCHI, M., VIANA, F., VOETS, T. & DROOGMANS, G. (1997b). Inhibition by mibefradil, a novel calcium channel antagonist, of Ca^{2+}- and volume-activated Cl^- channels in macrovascular endothelial cells. *Br. J. Pharmacol.,* **121,** 547–555.

NILIUS, B., PRENEN, J., SZÜCS, G., WEI, L., TANZI, F., VOETS, T. & DROOGMANS, G. (1997c). Calcium-activated chloride channels in bovine pulmonary artery endothelial cells. *J. Physiol. (Lond.),* **497,** 95–107.

NILIUS, B., PRENEN, J., VOETS, T., VAN DEN BREMT, K., EGGERMONT, J. & DROOGMANS, G. (1997d). Kinetic and pharmacological properties of the calcium-activated chloride current in macrovascular endothelial cells. *Cell Calcium,* **22,** 53–63.

NILIUS, B., SEHRER, J. & DROOGMANS, G. (1994b). Permeation properties and modulation of volume-activated Cl^--currents in human endothelial cells. *Br. J. Pharmacol.,* **112,** 1049–1056.

NILIUS, B., SEHRER, J., VIANA, F., DE GREEF, C., RAEYMAEKERS, L., EGGERMONT, J. & DROOGMANS, G. (1994c). Volume-activated Cl- currents in different mammalian non-excitable cell types. *Pflügers Arch.,* **428,** 364–371.

NILIUS, B., SZÜCS, G., HEINKE, S., VOETS, T. & DROOGMANS, G. (1997e). Multiple types of chloride channels in bovine pulmonary artery endothelial cells. *Journal of Vascular Research,* **34,** 220–228.

OKADA, Y. (1997). Volume expansion-sensing outward-rectifier Cl-channel: fresh start to the molecular identity and volume sensor. *Am. J. Physiol.,* **273,** C755–C789.

PANCRAZIO, J.J., KAMATCHI, G.L., ROSCOE, A.K. & LYNCH, C. (1998). Inhibition of neuronal Na^+ channels by antidepressant drugs? *J. Pharmacol. Exp. Ther.,* **284,** 208–214.

PATEL, A.J., LAURITZEN, I., LAZDUNSKI, M. & HONORÉ, E. (1998). Disruption of mitochondrial respiration inhibits volume-regulated anion channels and provoke neuronal cell swelling. *J. NeuroSci.,* **18,** 3117–3123.

PRESKORN, S.H., SILKEY, B., BEBER, J. & DOREY, C. (1991). Antidepressant response and plasma concentrations of fluoxetine. *Ann. Clin. Psychiatry,* **3,** 147–151.

RAE, J.L., RICH, A., ZAMUDIO, A.C. & CANDIA, O.A. (1995). Effect of Prozac on whole cell ionic currents in lens and corneal epithelia. *Am. J. Physiol.,* **269,** C250–C256.

ROY, G., BERNATCHEZ, G. & SAUVÉ, R. (1998). Halide and alkyl phenols block volume-sensitive chloride channels in human glial cells (U-138MG). *J. Membr. Biol.,* **162,** 191–200.

STAUDERMAN, K.A., GANDHI, V.C. & JONES, D.J. (1992). Fluoxetine-induced inhibition of synaptosomal [3H]5-HT release: possible Ca^{2+}-channel inhibition. *Life Sci.,* **50,** 2125–2138.

STRANGE, K. (1992). Regulation of solute and water balance and cell volume in the central nervous system. *J. Am. Soc. Nephrol.,* **3,** 12–27.

STRANGE, K., EMMA, F. & JACKSON, P.S. (1996). Cellular and molecular physiology of volume-sensitive anion channels. *Am. J. Physiol.,* **270,** C711–C730.

SZÜCS, G., HEINKE, S., DROOGMANS, G. & NILIUS, B. (1996). Activation of the volume-sensitive chloride current in vascular endothelial cells requires a permissive intracellular Ca^{2+} concentration. *Pflügers Arch.,* **431,** 467–469.

TROUET, D., NILIUS, B., VOETS, T., DROOGMANS, G. & EGGERMONT, J. (1997). Use of a bicistronic GFP-expression vector to characterise ion channels after transfection in mammalian cells. *Pflügers Arch.,* **434,** 632–638.

TYTGAT, J., MAERTENS, C. & DAENENS, P. (1997). Effect of fluoxetine on a neuronal, voltage-dependent potassium channel (Kv1.1). *Br. J. Pharmacol.,* **122,** 1417–1424.

VOETS, T., DROOGMANS, G. & NILIUS, B. (1996a). Membrane currents and the resting membrane potential in cultured bovine pulmonary artery endothelial cells. *J. Physiol. (Lond.),* **497,** 95–107.

VOETS, T., DROOGMANS, G. & NILIUS, B. (1996b). Potent block of volume-activated chloride currents in endothelial cells by the uncharged form of quinine and quinidine. *Br. J. Pharmacol.,* **118,** 1869–1871.

WONG, D.T., BYMASTER, F.P. & ENGLEMAN, E.A. (1995). Prozac (fluoxetine, Lilly 110140), the first selective serotonin uptake inhibitor and an antidepressant drug: twenty years since its first publication. *Life Sci.,* **57,** 411–414.

(Received September 15, 1998
Revised October 19, 1998
Accepted October 22, 1998)

British Journal of Pharmacology (1999) 126, 515–521
http://www.stockton-press.co.uk/bjp

Endogenous nitric oxide in the maintenance of rat microvascular integrity against widespread plasma leakage following abdominal laparotomy

[1]Ferenc László & *,[2]Brendan J.R. Whittle

[1]Institute of Experimental Medicine, Hungarian Academy of Sciences, Budapest, Hungary; [2]The William Harvey Research Institute, St. Bartholomew's & The Royal London School of Medicine & Dentistry, London, England

1 The role of nitric oxide (NO) in the maintenance of microvascular integrity during minor surgical manipulation has been evaluated in the rat.

2 The NO synthase inhibitors, N^G-nitro-L-arginine methyl ester (L-NAME, 5 mg kg^{-1}, s.c.) and N^G-monomethyl-L-arginine (L-NMMA, 50 mg kg^{-1}, s.c.) had no effect on microvascular leakage of radiolabelled albumin over 1 h in the stomach, duodenum, jejunum, colon, lung and kidney in the un-operated conscious or pentobarbitone-anaesthetized rat.

3 In contrast, in anaesthetized rats with a midline abdominal laparotomy (5 cm), L-NAME (1–5 mg kg^{-1}, s.c.) or L-NMMA (12.5–50 mg kg^{-1}, s.c.) dose-dependently increased gastrointestinal, renal and pulmonary vascular leakage, effects reversed by L-arginine pretreatment (300 mg kg^{-1}, s.c., 15 min). These actions were not observed in anaesthetized rats that had only received a midline abdominal skin incision (5 cm).

4 Pretreatment with a rabbit anti-rat neutrophil serum (0.4 ml kg^{-1}, i.p.), 4 h before laparotomy, abolished the plasma leakage induced by L-NAME in all the organs investigated.

5 These results indicate that the following abdominal laparotomy, inhibition of constitutive NO synthase provokes vascular leakage in the general microcirculation, by a process that may involve neutrophils. Such effects could thus confound studies on the microvascular actions of NO synthase inhibitors using acute surgically prepared *in vivo* models. The findings thus suggest that constitutively-formed NO has a crucial role in the maintenance of acute microvascular integrity following abdominal surgical intervention.

Keywords: Constitutive nitric oxide synthase; eNOS; nitric oxide synthase inhibitors; vascular permeability; plasma loss; neutrophils; surgery; laparotomy

Abbreviations: eNOS, endothelial nitric oxide synthase; [^{125}I]HSA, [^{125}I]human serum albumin; iNOS, inducible nitrix oxide synthase; L-NAME, N^G-nitro-L-arginine methyl ester; L-NMMA, N^G-monomethyl-L-arginine; NO, nitric oxide; SNOG, S-nitroso-glutathione

Introduction

Nitric oxide (NO), synthesized in the vascular endothelium, by a calcium and calmodulin-dependent constitutive isoform of nitric oxide synthase (eNOS), plays a significant role in the regulation of vascular tone (Moncada & Higgs, 1995). Moreover, NO inhibits aggregation and adhesion of platelets to the vascular endothelium (Radomski *et al*., 1992; Moncada & Higgs, 1995) and may be involved in modulating the interaction of circulating leukocytes with the microvasculature (Kubes *et al*., 1991), thus further participating in the general homeostatic control of vascular beds.

NO, formed by eNOS has also been proposed to regulate resting microvascular permeability, since administration of the nitric oxide synthase inhibitor, N^G-nitro-L-arginine methyl ester (L-NAME) led to an increase in microvascular protein efflux in the cat mesentery, an effect reversed by the nitric oxide donor, nitroprusside (Kubes & Granger, 1992). Moreover, L-NAME elevated vascular protein extravasation in a number of organs of the rat (Filep & Földes-Filep, 1993; Filep *et al*., 1993). In contrast to these findings, in our previous studies we could not demonstrate that either L-NAME or the other nitric oxide synthase inhibitors including N^G-monomethyl-L-arginine (L-NMMA), aminoguanidine or N^G-iminoethyl-L-ornithine could cause increased plasma leakage in the rat intestine or other major organs (László & Whittle, 1997; László *et al*., 1994a,b, 1995a–c). Acute plasma leakage was, however, provoked by these NO synthase inhibitors, when administered at a time of low-dose endotoxin challenge, which itself did not increase microvascular leakage (László & Whittle, 1997; László *et al*., 1994a,b, 1995a–c). These latter findings imply that other factors, presumably acting on the microvasculature, in addition to eNOS inhibition, are required to provoke plasma leakage and accumulation in this model.

In the original studies where NO synthase inhibitors were shown to increase resting vascular permeability, the animals had been acutely surgically manipulated to prepare an exteriorized vascular bed (Kubes & Granger, 1992). In other studies where an increase in resting vascular permeability with L-NAME was observed, the rats had catheters implanted into the abdominal aorta and into the vena cava. 4 days before the study (Filep & Földes-Filep, 1993; Filep *et al*., 1993). Since it is known that wound healing takes some 10 days, in the latter studies a sterile wound-healing inflammatory process would likely to be in progress. In addition, vascular endothelial cells release a number of vasoactive mediators following irritation (Burnstock, 1990) a process which also could be activated during arterial or venous catheterization. However, in our

*Author for correspondence at: The William Harvey Research Institute, Charterhouse Square, London EC1M 6BQ, England, U.K.

studies where L-NAME failed to affect resting leakage of albumin, the animals had not undergone any surgical manipulation, although there were also differences between the actual measurements of permeability made in these studies.

In order to evaluate the possible effects of surgical intervention on plasma exudation using a standardized technique, in the present study, the acute effects of the NO synthase inhibitors, L-NAME and L-NMMA on microvascular leakage and accumulation of radiolabelled human serum albumin was evaluated in animals that had undergone various degrees of surgical manipulation. In addition, the involvement of neutrophils in any microvascular permeability changes following surgical intervention has also been investigated.

Methods

Surgical manipulation

Male Wistar rats (225–275 g) were fasted overnight, but allowed free access to water. The animals were separated into four groups. In the first group the animals were deemed to be conscious for the majority of the experimentation period, since the treatments were performed under transient halothane anaesthesia from which the animals had completely recovered within 2 min. Autopsy in this group, which was designated as the conscious surgically un-operated group, was performed under halothane anaesthesia within 1 min. In the second group, the animals received pentobarbitone (60 mg kg^{-1}, i.p.) to induce anaesthesia and were tracheotomized. In the third group, under pentobarbitone anaesthesia, a 5 cm long skin incision was performed on the abdominal region. The animals were tracheotomized and a gauze pad moistened with saline was placed on the skin incision. In the fourth group, in pentobarbitone-anaesthetized animals, a 5 cm long midline laparotomy in the abdominal wall was performed, without significant bleeding. Rats were tracheotomized and gauze moistened with saline was placed over the incision.

All groups were administered [^{125}I]human serum albumin ([^{125}I]HSA, 2 μCi kg^{-1}, i.v.) *via* a needle inserted into the tail vein for 3–4 s, and autopsy was performed 1 h later. The 1 h maximum time-point was chosen to exclude the involvement of inducible NO synthase (iNOS), that requires 2–3 h following challenge for expression, since this could modify vascular leakage and hence confound interpretation of the findings (Boughton-Smith *et al*., 1993). In one group, autopsy was performed 30 min after administration of radiolabelled albumin. In all of the anaesthetized groups, the body temperature was maintained on 36.5–37°C using a homeothermic control unit and underblanket (Harvard Instruments).

Plasma leakage

As a measure of vascular endothelial permeability, leakage of [^{125}I]HSA into tissue was determined in segments of the stomach, duodenum, jejunum, colon, lung and kidney. Blood was collected from the abdominal aorta into syringes containing trisodium citrate (final concentration 0.318%) and centrifuged (10,000 × *g*, 10 min, 4°C). The [^{125}I]HSA content of the plasma and segments of tissues was determined in a gamma-spectrometer (Nuclear Enterprises NE 1600) and the albumin content in tissues were calculated.

The control value for albumin accumulation was taken as the mean of the data of a group of control animals which received albumin only, which reflects basal albumin movement into tissues. In each experiment and for each procedure, this basal control mean value was calculated and subtracted from the value from each of the animals in each treatment group. The data were expressed as changes in albumin accumulation (Δ plasma leakage, μl plasma g^{-1} tissue), corrected for intravascular volume (László *et al*., 1994a, 1995c).

Intravascular volume

Changes in intravascular volume in gastric, duodenal, jejunal, colonic, pulmonary and renal tissues were determined in additional groups of rats by administering [^{125}I]HSA (2 μCi kg^{-1}) intravenously *via* the tail vein 2 min before tissue removal, in all groups investigated. The tissue and plasma content of radiolabel was determined and the intravascular volume was expressed as μl g^{-1} tissue (László *et al*., 1994a, 1995c).

Effect of L-NAME and L-NMMA on intestinal plasma leakage

In a set of rats from each of the groups, L-NAME (1–5 mg kg^{-1}, s.c.) or L-NMMA (1–50 mg kg^{-1}, s.c.) was injected concurrently with [^{125}I]HSA. Plasma leakage in the jejunum and colon was evaluated after 1 h. In separate groups, rats were pretreated with L-arginine (300 mg kg^{-1}, s.c.) 15 min before L-NAME (5 mg kg^{-1}, s.c.) administration, and jejunal and colonic plasma leakage was determined 1 h after L-NAME.

In a separate study, L-NAME (5 mg kg^{-1}, s.c.) was administered concurrently with laparotomy and [^{125}I]HSA, and plasma leakage in the jejunum and colon was measured 30 min later.

Plasma leakage in other organs

To evaluate the action of NO synthase inhibitors on plasma leakage in the stomach, duodenum, lung and kidney in conscious and laparotomized rats L-NAME (5 mg kg^{-1}, s.c.) was administered concurrently with [^{125}I]HSA, and plasma leakage in these tissues was measured 1 h later.

Effect of phenylephrine infusion on intestinal plasma leakage and blood pressure

In laparotomized rats, phenylephrine infusion (10 μg kg^{-1} min^{-1}, into the tail vein) was commenced immediately following administration of [^{125}I]HSA. Plasma leakage in the jejunum and colon was determined 1 h later.

In additional groups of anaesthetized rats, and rats with abdominal laparotomy, the effect of L-NAME (5 mg kg^{-1}, s.c.) or phenylephrine infusion (10 μg kg^{-1} min^{-1}, i.v.) on systemic arterial blood pressure was measured from a cannula inserted into the right carotid artery using a pressure transducer (Elcomatic) connected to a Grass Polygraph. The blood pressure was monitored over a 1 h period. The dose of phenylephrine was taken from previous studies in this model (László *et al*., 1994b).

Effect of S-nitroso-glutathione on intestinal plasma leakage and blood pressure

In laparotomized rats, infusion of the NO donor S-nitroso-glutathione (SNOG, 1 μg kg^{-1} min^{-1}) into the tail vein was commenced concurrently with the administration of L-NAME (5 mg kg^{-1}, s.c.). Plasma leakage in the jejunum and colon was measured 1 h later.

In another group of rats with abdominal laparotomy, the effect of infusion of SNOG (1 μg kg^{-1} min^{-1}) into the tail vein, on the actions of L-NAME (5 mg kg^{-1}, s.c.) on arterial blood pressure was monitored over a 1 h period. The dose of SNOG was taken from previous studies in this model (László *et al*., 1995c).

Effect of anti-neutrophil serum on plasma leakage

Rabbit anti-rat neutrophil serum (0.4 ml kg^{-1}, i.p.) Was administered 4 h before laparotomy. L-NAME (5 mg kg^{-1}, s.c.) was injected immediately after abdominal laparotomy, and plasma leakage was determined 1 h later, being thus 5 h after anti-neutrophil serum administration.

Chemicals

[^{125}I]human serum albumin was obtained from Amersham International (U.K.) and IZINTA, Budapest (Hungary). Rabbit anti-rat neutrophil serum was purchased from Accurate Chemical and Scientific Corporation (Westbury, New York, U.S.A.). All the other compounds were from Sigma Chemical Company (Poole, Dorset, U.K.).

Statistics

The data are expressed as means$\pm$s.e.mean from (n) rats per experimental group. For statistical comparisons, analysis of variance with the Bonferroni test was utilized, where $P<0.05$ was taken as significant.

Results

Effect of L-NAME or L-NMMA on intestinal plasma leakage following various surgical manipulations

In conscious un-operated rats, administration of L-NAME (5 mg kg^{-1}, s.c.) or L-NMMA (50 mg kg^{-1}, s.c.) did not affect intestinal plasma leakage over 1 h (Table 1).

In pentobarbitone-anaesthetized rats with or without incision of the abdominal skin, no significant change in plasma leakage was found in the jejunum ($\Delta19\pm14$ and $\Delta18\pm8$ μl g^{-1} tissue, respectively, $n=8-11$) or colon ($\Delta8\pm3$ and $\Delta0\pm3$ μl g^{-1} tissue, respectively, $n=8-11$). Furthermore, neither L-NAME (5 mg kg^{-1}, s.c.) nor L-NMMA (50 mg kg^{-1}, s.c.) affected jejunal or colonic plasma leakage in pentobarbitone-anaesthetized rats with or without skin incision (Table 1).

Abdominal laparotomy alone did not affect plasma leakage in the jejunum and colon, being $\Delta3\pm6$ and $\Delta2\pm3$ μl g^{-1} tissue over 1 h, respectively ($n=6$), as shown in Figures 1 and 2. However, in laparotomized animals, administration of L-NAME (1–5 mg kg^{-1}, s.c.) or L-NMMA (12.5–50 mg kg^{-1}, s.c.) provoked significant dose-dependent jejunal and colonic plasma leakage over 1 h. This effect was inhibited by pretreatment with L-arginine (300 mg kg^{-1}, s.c., 15 min before L-NAME), as shown in Figures 1 and 2.

In additional studies, plasma leakage in the jejunum and colon was observed 30 min after the administration of L-NAME (5 mg kg^{-1}, s.c.) with laparotomy ($\Delta35\pm8$ and $\Delta32\pm5$ μl g^{-1} tissue, respectively; $n=6$, $P<0.05$). This plasma leakage was significantly ($P<0.05$) smaller than that observed when L-NAME (5 mg kg^{-1}, s.c.) was administered concurrently with laparotomy and plasma leakage was investigated 1 h later ($\Delta88\pm12$ μl g^{-1} tissue in the jejunum and $\Delta55\pm9$ μl g^{-1} tissue in the colon, $n=8$).

Effect of L-NAME on plasma leakage in other organs

Administration of L-NAME (5 mg kg^{-1}, s.c.) had no action on resting plasma leakage in the stomach ($\Delta5\pm3$ μl g^{-1} tissue, $n=12$), duodenum ($\Delta0\pm11$ μl g^{-1} tissue, $n=11$), lung ($\Delta21\pm9$ μl g^{-1} tissue, $n=5$) and kidney ($\Delta3\pm3$ μl g^{-1} tissue, $n=5$) in conscious animals over 1 h (Figure 3).

Table 1 Jejunal and colonic plasma leakage (1 h) in conscious un-operated or barbiturate-anaesthetized rats or following incision of the abdominal skin in anaesthetized rats

Treatment	*Dose*	*Jejunum* ($\Delta\mu$l g^{-1})	*Colon* ($\Delta\mu$l g^{-1})
Conscious			
L-NAME	5 mg kg^{-1}	0$\pm$18	11$\pm$3
L-NMMA	50 mg kg^{-1}	3$\pm$9	3$\pm$5
Anaesthetized			
Control		19$\pm$14	8$\pm$3
L-NAME	5 mg kg^{-1}	25$\pm$12	9$\pm$5
L-NMMA	50 mg kg^{-1}	14$\pm$18	13$\pm$5
Skin incision			
Control		18$\pm$8	0$\pm$3
L-NAME	5 mg kg^{-1}	1$\pm$9	0$\pm$3
L-NMMA	50 mg kg^{-1}	3$\pm$6	1$\pm$4

Data are shown as plasma leakage in Δ μl plasma g^{-1} tissue, and expressed as means$\pm$s.e.mean, where $n=8-15$. The conscious rats received halothane anaesthesia briefly for drug administration; the anaesthetized group of rats received pentobarbitone (60 mg kg^{-1}, i.p.), while the skin incision group of rats had a 5 cm midline incision on the abdominal skin under pentobarbitone anaesthesia. N^{G}-nitro-L-arginine methyl ester (L-NAME) or N^{G}-monomethyl-L-arginine (L-NMMA) was injected s.c. 1 h prior to the assessment of plasma leakage. There are no significant changes from control plasma leakage in any of the groups.

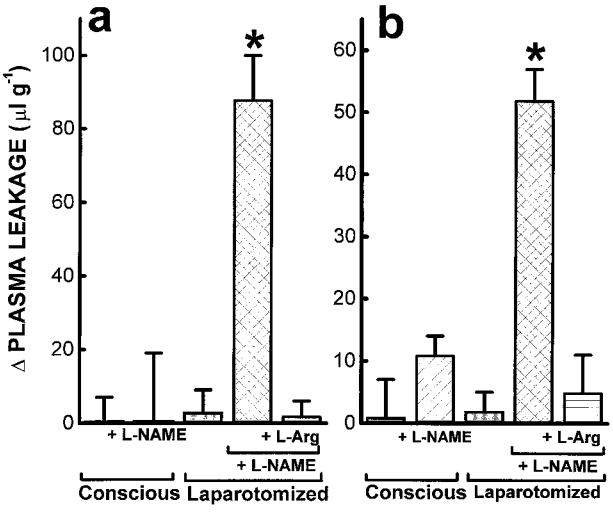

Figure 1 The vascular leakage, determined using radiolabelled albumin, following administration of N^{G}-nitro-L-arginine methyl ester (L-NAME, 5 mg kg^{-1}, s.c.) in the jejunum and colon of the conscious un-operated or anaesthetized rats with abdominal laparotomy over 1 h. The reversal by L-arginine (L-Arg, 300 mg kg^{-1}, s.c., 15 min before L-NAME) of the jejunal and colonic plasma leakage induced by L-NAME in the laparotomized rat is also shown. The columns indicate the leakage of plasma in Δ μl g^{-1} tissue. Data are given as the means$\pm$s.e.mean of five rats per group; statistical significance is shown as $*P<0.05$ compared to the control conscious untreated group.

Abdominal laparotomy alone did not provoke significant plasma leakage in the stomach, duodenum, lung and kidney over 1 h, being $\Delta 0 \pm 4$, $\Delta 0 \pm 8$, $\Delta 2 \pm 11$ and $\Delta 8 \pm 3$ μl g^{-1} tissue, respectively ($n=5$). However, administration of L-NAME (5 mg kg^{-1}, s.c.) following laparotomy caused significant plasma leakage in gastric, duodenal, pulmonary and renal tissues after 1 h (Figure 3).

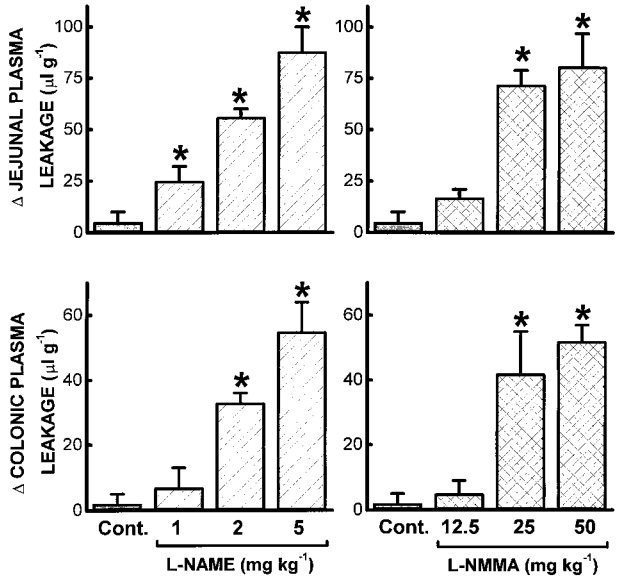

Figure 2 Induction of vascular leakage, determined using radiolabelled albumin, in the jejunum (upper panels) and colon (lower panels) by the administration of N^G-nitro-L-arginine methyl ester (L-NAME, 1–5 mg kg^{-1}, s.c.) or N^G-monomethyl-L-arginine (L-NMMA, 12.5–50 mg kg^{-1}, s.c.) in the anaesthetized rat with abdominal laparotomy over 1 h. Plasma leakage is expressed as Δ μl g^{-1} tissue. Data are given as the means$\pm$s.e.mean of 5–8 rats per group; statistical significance is shown as $^*P<0.05$ compared to the control (Cont.) untreated laparotomized group.

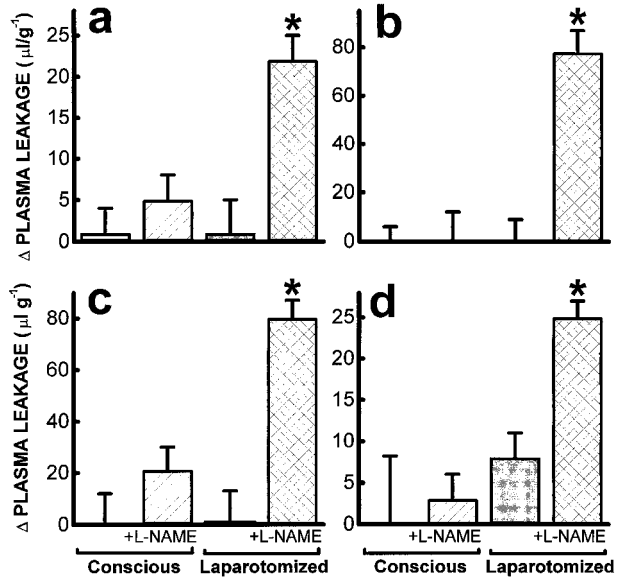

Figure 3 Vascular leakage, determined using radiolabelled albumin, induced by N^G-nitro-L-arginine methyl ester (L-NAME, 5 mg kg^{-1}, s.c.) in the stomach (a), duodenum (b), lung (c) and kidney (d) of the anaesthetized rat with abdominal laparotomy over 1 h. Plasma leakage is expressed as Δ μl g^{-1} tissue. Data are shown as the means$\pm$s.e.mean of five rats per group; statistical significance is shown as $^*P<0.05$ compared to the control untreated conscious group.

Effect of phenylephrine on blood pressure and intestinal plasma leakage

In laparotomized rats, infusion of phenylephrine (10 μg kg^{-1} min^{-1}, i.v.) elevated systemic arterial blood pressure over the 1 h period of administration (Figure 4). The increase in blood pressure by phenylephrine infusion was not significantly different from that caused by L-NAME (5 mg kg^{-1}, s.c.) as shown in Figure 4.

Infusion of phenylephrine (10 μg kg^{-1} min^{-1}, i.v.) did not provoke plasma leakage in the jejunum and colon over 1 h in laparotomized rats, being $\Delta 5 \pm 11$ and $\Delta 3 \pm 4$ μl g^{-1} tissue, respectively ($n=4$) as demonstrated in Figure 4.

Effect of S-nitroso-glutathione on intestinal plasma leakage and blood pressure

Intravenous infusion of the NO donor, S-nitroso-glutathione (SNOG, 1 μg kg^{-1} min^{-1} for 1 h) did not reduce blood pressure in laparotomized rats ($\Delta 2 \pm 4$, $\Delta 0 \pm 3$, Δ-3 ± 5 and $\Delta 4 \pm 5$ mmHg 15, 30, 45 and 60 min later, respectively; $n=4$). Furthermore, SNOG did not affect the elevation and blood pressure induced by L-NAME (5 mg kg^{-1}, s.c.) over 1 h (Figure 5).

Administration of this dose of SNOG abolished the increase in jejunal and colonic plasma leakage induced by L-NAME (5 mg kg^{-1}, s.c.) in laparotomized rats, as shown in Figure 5.

Effect of anti-neutrophil serum on plasma leakage

Pretreatment of rats with a rabbit anti-rat neutrophil serum (0.4 ml kg^{-1}, i.p.) 4 h before laparotomy, substantially

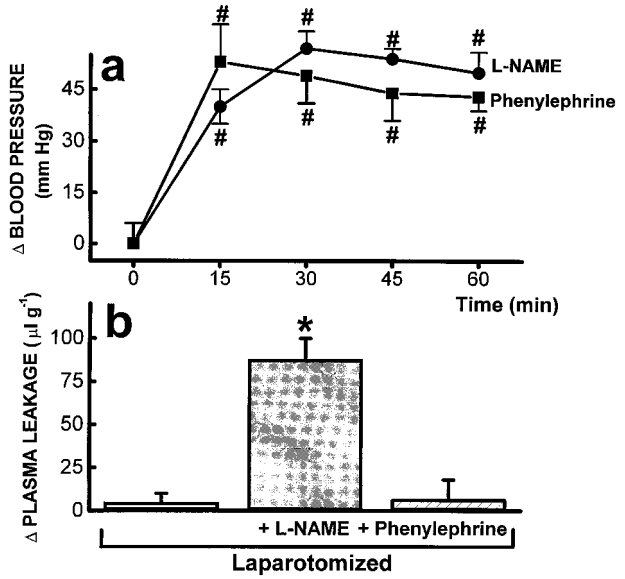

Figure 4 Increase of systemic arterial blood pressure following the administration of N^G-nitro-L-arginine methyl ester (L-NAME, 5 mg kg^{-1}, s.c.) or phenylephrine (10 μg kg^{-1} min^{-1}, i.v.) over 1 h in the anaesthetized rat with abdominal laparotomy (upper panel). Actions of L-NAME (5 mg kg^{-1}, s.c.) or phenylephrine (10 μg kg^{-1} min^{-1}, i.v.) on plasma leakage in the jejunum after 1 h in laparotomized rats are shown in the lower panel. Blood pressure changes are given as Δ mmHg compared to the untreated laparotomized group and plasma leakage is expressed as Δ μl g^{-1} tissue. Data are shown as the means$\pm$s.e.mean of four rats per group; statistical significance is shown as $\#P<0.05$ for difference in blood pressure difference compared to the control abdominal laparotomized group, and as $^*P<0.05$ for difference in plasma leakage compared to the control laparotomized group.

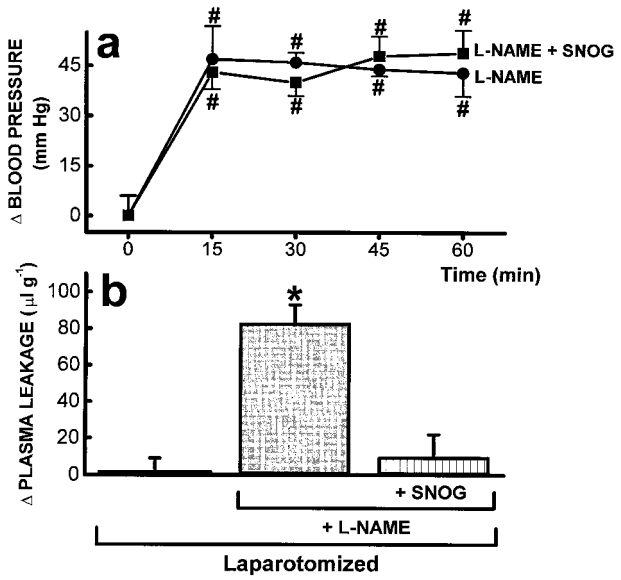

Figure 5 Changes in systemic arterial blood pressure over 1 h in the anaesthetized rat with abdominal laparotomy by the concurrent infusion of S-nitroso-glutathione (SNOG, 1 μg kg^{-1} min^{-1}, i.v.) with N^{G}-nitro-L-arginine methyl ester (L-NAME, 5 mg kg^{-1}, s.c.; upper panel). Actions of L-NAME (5 mg kg^{-1}, s.c.) with or without the concurrent intravenous infusion of SNOG (1 μg kg^{-1} min^{-1}) on plasma leakage in the jejunum after 1 h in laparotomized rats are shown in the lower panel. Blood pressure changes are shown as Δ mmHg compared to the untreated laparotomized group. Plasma leakage is expressed as Δ μl g^{-1} tissue. Data are shown as the means$\pm$s.e.mean of four rats per group; statistical significance is shown as $\#P<0.05$ for difference in blood pressure compared to the control laparotomized group, and as $*P<0.05$ for difference in plasma leakage compared to the control laparotomized group.

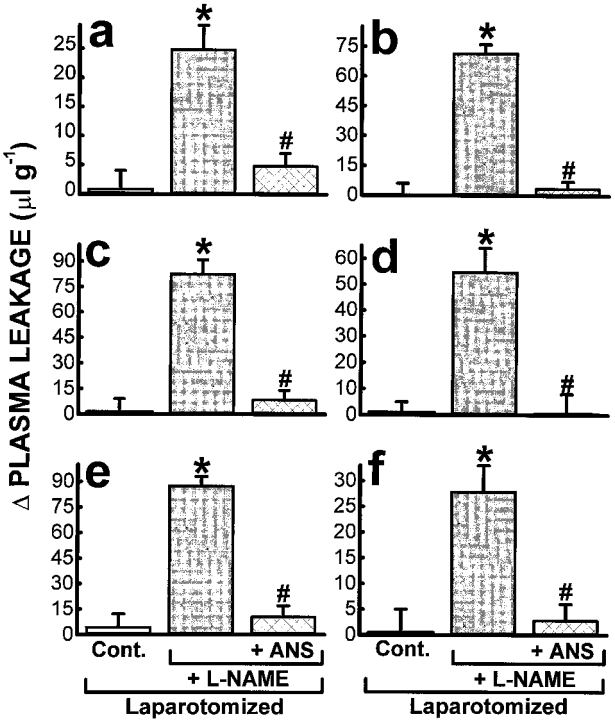

Figure 6 Inhibition of vascular leakage, determined using radiolabelled albumin, induced by N^{G}-nitro-L-arginine methyl ester (L-NAME, 5 mg kg^{-1}, s.c.) in the stomach (a), duodenum (b), jejunum (c), colon (d), lung (e) and kidney (f), of the anaesthetized rat with abdominal laparotomy over 1 h by the pretreatment with rabbit anti-rat neutrophil serum (ANS. 0.4 ml kg^{-1}, i.p., 4 h before laparotomy). Plasma leakage is expressed as Δ μl g^{-1} tissue. Data are shown as the means$\pm$s.e.mean of four rats per group; statistical significance is shown as $*P<0.05$ compared to the control (Cont.) laparotomized group and $\#P<0.05$ compared to the L-NAME-treated laparotomized group.

reduced L-NAME (5 mg kg^{-1}, s.c.)-provoked plasma leakage in the stomach, duodenum, jejunum, colon and lung (Figure 6). This dose of anti-neutrophil serum reduced the circulating neutrophil count by 85$\pm$5%, as determined on blood smears.

Intravascular volume

In control conscious un-operated rats, the intravascular volume was 71$\pm$8 μl g^{-1} tissue in the jejunum and 39$\pm$4 μl g^{-1} tissue on the colon ($n=6$). This intravascular volume did not change significantly in the jejunum and colon of anaesthetized rats, and in animals following skin incision or abdominal laparotomy. Neither L-NAME (5 mg kg^{-1}, s.c.) nor L-NMMA (50 mg kg^{-1}, s.c.) affected intravascular volume in any of the experimental groups and tissues investigated ($n=3-4$, data not shown). Infusion of phenylephrine (10 μg kg^{-1} min^{-1}, i.v.) did, however, significantly reduce intravascular volume, as measured in the jejunum and colon (by 44$\pm$1 and 46$\pm$4%, respectively, $n=4$, $P<0.01$).

Discussion

In the current study, no significant difference in albumin leakage and accumulation has been observed in tissues from un-operated conscious or anaesthetized rats, or in anaesthetized rats with a skin-incision or abdominal laparotomy under resting conditions, showing that these minor surgical interventions alone do not provoke changes in microvascular permeability to albumin. In contrast, abdominal laparotomy produced a time-dependent significant elevation in microvascular leakage in the jejunum and colon over 1 h following administration of the NO synthase inhibitors, L-NAME or L-NMMA. These NO synthase inhibitors had no such effect in conscious, anaesthetized or skin-incised rats. The increase in vascular leakage provoked by abdominal laparotomy following treatment with L-NAME was reversed by L-arginine, indicating that these effects involved the NO-L-arginine pathway. Involvement of constitutive NO synthase is more likely than the inducible isoform, since in previous studies it has been demonstrated that a minimum of 2 h is needed for the expression of iNOS (Salter *et al*., 1991; Boughton-Smith *et al*., 1993).

Inhibition of eNOS elevates blood pressure (Moncada *et al*., 1991; Moncada & Higgs, 1995). It is therefore possible that the increased vascular leakage by L-NAME and L-NMMA in the laparotomized rat in our study could in part reflect the enhanced perfusion pressure leading to increased blood flow (Granger *et al*., 1989). Administration of phenylephrine, which caused a similar elevation in blood pressure as L-NAME, did not provoke vascular leakage in the laparotomized rat, although any local actions on the microcirculation exerted by phenylephrine but not L-NAME, could obscure interpretation of these findings. In previous studies, L-NAME has been reported to enhance transcapillary protein flux without increasing capillary hydrostatic pressure in the surgically manipulated cat (Kubes & Granger, 1992). It is also unlikely that the accumulation of albumin provoked by L-NAME following laparotomy in our model could reflect an impairment of lymphatic drainage, since in previous studies, administration of L-NAME following surgical manipulation was shown to lead to 5 fold increase in lymphatic flow (Kubes

& Granger, 1992). Thus, since all of the experimental groups in the present study received the same low dose of radiolabelled albumin, and the tissues subsequently processed in an identical fashion, the most likely explanation for the current findings is that the enhanced tissue albumin accumulation is a consequence of endothelial dysfunction due to inhibition of eNOS by L-NAME or L-NMMA following laparotomy.

Infusion of the NO donor, SNOG in a dose that had no effect on the elevation in blood pressure caused by L-NAME substantially reduced the vascular leakage induced by L-NAME in the laparotomized rat. This observation is in agreement with previous findings by others that the NO donor nitroprusside reversed the elevation of vascular permeability provoked by L-NAME in a surgical preparation, an effect brought about without actions on capillary pressure (Kubes & Granger, 1992). NO donors also significantly attenuate intestinal microvascular injury following the administration of high doses of endotoxin (Boughton-Smith *et al*., 1990), infusion of platelet-activating factor (Boughton-Smith *et al*., 1992), or by the concurrent administration of L-NAME and low doses of endotoxin (László *et al*., 1995c).

NO donors decrease neutrophil function and adhesion both in *in vivo* and *in vitro* (Moilanen *et al*., 1993; Ma *et al*., 1993; Granger & Kubes, 1994). Administration of L-NAME enhances the adhesion of leukocytes to the vascular endothelium, assessed by *in vivo* microscopy in surgically prepared animals (Kubes *et al*., 1991; Arndt *et al*., 1993). Such events involve platelet-activating factor and leukotrienes (Arndt *et al*., 1993), as also found with the intestinal microvascular leakage provoked by L-NAME in endotoxin-challenged rats (László *et al*., 1994b; László & Whittle, 1995). Polymorphonuclear leukocytes are well-known to play a crucial role in the changes in microvascular permeability during inflammatory processes leading to tissue oedema (Wedmore & Williams, 1981). In the present study, the increase in plasma leakage by L-NAME in laparotomized rats was abolished by the pretreatment of a rabbit anti-rat neutrophil serum suggesting the involvement of neutrophils in these events. Thus, it is feasible that endogenous NO formed by eNOS could counteract the actions of neutrophil-derived mediators that are released subsequent to laparotomy.

On the basis of the present results, it is proposed that the relatively minor surgical intervention of opening the abdominal cavity during laparotomy causes wide-spread microvascular events throughout the body. These microvascular changes are modulated by NO, since following inhibition of constitutive NOS, laparotomy causes increased plasma loss from gastrointestinal organs, lung and kidney. The mechanisms underlying this apparent microvascular priming are unknown, but may reflect neuronal or humoral stimulation as a consequence of the surgical stress of laparotomy, as well as the activation or priming of the neutrophil. Although vascular endothelial dysfunction during and following surgical operations has been described earlier (Jarnum, 1961; Krakelund, 1971; Robarts, 1979; Akerström & Lisander, 1991), this was not observed with our acute abdominal laparotomy procedures, where no manipulation of the intestinal organs was performed. However, the current data suggests that should NO formation be compromized during surgical procedures, plasma and fluid loss would be augmented which could lead to hypovolaemia, as well as oedema formation and a decreased tissue oxygenization. It is possible therefore that administration of NO donors during major surgical interventions, in low doses which do not affect systemic arterial blood pressure, may be beneficial in preventing any vascular endothelial dysfunction.

The current studies thus may help to resolve the earlier apparent conflict that NO synthase inhibitors increase vascular permeability in studies with surgically prepared models (Kubes & Granger, 1992) whereas they have no effect in intact animals (László *et al*., 1994a,b, 1995a–c), although there are also differences between the experimental models utilized. However, such effects observed in the present study could therefore confound studies on the microvascular actions of NO synthase inhibitors using acute surgically manipulated *ex vivo* models. Moreover, since these vascular events appear to involve neutrophils, the action of NO synthase inhibitors on neutrophil activation and adhesion in surgically prepared vascular beds may require careful interpretation. The findings thus suggest that constitutively formed NO plays a more-crucial role in the maintenance of microvascular integrity during or following minor abdominal surgical intervention, than under more physiological conditions.

This work was supported in part by the Hungarian Ministry of Welfare (T-02 642/1996) and by the Hungarian Ministry of Higher Education (MKM FKFP 0045/1997 and PFP 2189/1998). We thank Professor Salvador Moncada for discussions during the conduct of this work.

References

AKERSTRÖM, G. & LISANDER, B. (1991). Tissue extravasation of albumin from intraabdominal trauma in rats. *Acta Anaesthesiol. Scand.,* **35,** 257–261.

ARNDT, H., RUSSEL, J.B., KUROSE, I., KUBES, P. & GRANGER, D.N. (1993). Mediators of leukocyte adhesion in rat mesenteric venules elicited by inhibition of nitric oxide synthesis. *Gastroenterology,* **105,** 675–680.

BOUGHTON-SMITH, N.K., DEAKIN, A.M. & WHITTLE, B.J.R. (1992). Actions of nitric oxide on the acute gastrointestinal damage induced by PAF in the rat. *Agents Actions,* **35,** C3–C9.

BOUGHTON-SMITH, N.K., EVANS, S.M., LÁSZLÓ, F., WHITTLE, B.J.R. & MONCADA, S. (1993). The induction of nitric oxide synthase and intestinal vascular permeability by endotoxin in the rat. *Br. J. Pharmacol.,* **110,** 1189–1195.

BOUGHTON-SMITH, N.K., HUTCHESON, I.R., DEAKIN, A.M., WHITTLE, B.J.R. & MONCADA, S. (1990). Protective effect of S-nitroso-N-penicillamine in endotoxin-induced acute intestinal damage in the rat. *Eur. J. Pharmacol.,* **191,** 485–488.

BURNSTOCK, G. (1990). Local mechanisms of blood flow control by perivascular nerves and endothelium. *J. Hypertension,* **8,** S95–S106.

FILEP, J.G. & FÖLDES-FILEP, É. (1993). Modulation by nitric oxide of platelet-activating factor-induced albumin extravasation in the conscious rat. *Br. J. Pharmacol.,* **110,** 1347–1352.

FILEP, J.G., FÖLDES-FILEP, É., ROSSEAU, A., SIROIS, P. & FURNIER, A. (1993). Vascular responses to endothelin-1 following inhibition of nitric oxide synthesis in the conscious rat. *Br. J. Pharmacol.,* **110,** 1213–1221.

GRANGER, D.N. & KUBES, P. (1994). The microcirculation and inflammation: modulation of leukocyte-endothelial cell adhesion. *J. Leukocyte Biol.,* **55,** 662–675.

GRANGER, D.N., KVIETYS, P.R., KORTHUIS, R.J. & PREMEN, A.J. (1989). The Gastrointestinal System. Motility and Circulation. In: *Handbook of Physiology*. Vol. 1, pp. 1405–1474. The Am. Physiol. Soc.: Bethesda, MD.

JARNUM, S. (1961). Plasma protein exudation in the peritoneal cavity during laparotomy. *Gastroenterology,* **41,** 107 – 118.

KRAKELUND, E. (1971). Loss fluid and blood to the peritoneal cavity during abdominal surgery. *Surgery,* **69,** 284 – 287.

KUBES, P. & GRANGER, D.N. (1992). Nitric oxide modulates microvascular permeability. *Am. J. Physiol.,* **262,** H611 – H615.

KUBES, P., SUZUKI, M. & GRANGER, D.N. (1991). Nitric oxide: an endogenous modulator of leukocyte adhesion. *Proc. Natl. Acad. Sci. U.S.A.,* **88,** 4651 – 4655.

LÁSZLÓ, F., EVANS, S.M. & WHITTLE, B.J.R. (1995a). Aminoguanidine inhibits both constitutive and inducible nitric oxide synthase isoforms in rat intestinal microvasculature in vivo. *Eur. J. Pharmacol.,* **272,** 169 – 175.

LÁSZLÓ, F. & WHITTLE, B.J.R. (1995). Colonic microvascular integrity in acute endotoxaemia: interactions between constitutive nitric oxide and 5-lipoxygenase products. *Eur. J. Pharmacol.,* **277,** R1 – R3.

LÁSZLÓ, F. & WHITTLE, B.J.R. (1997). Actions of isoform-selective and non-selective nitric oxide synthase inhibitors on endotoxin-induced vascular leakage in rat colon. *Eur. J. Pharmacol.,* **344,** 99 – 102.

LÁSZLÓ, F., WHITTLE, B.J.R., EVANS, S.M. & MONCADA, S. (1995b). Association of microvascular leakage with induction of nitric oxide synthase: effects of nitric oxide synthase inhibitors in various organs. *Eur. J. Pharmacol.,* **283,** 47 – 53.

LÁSZLÓ, F., WHITTLE, B.J.R. & MONCADA, S. (1994a). Time-dependent enhancement and inhibition of endotoxin-induced vascular injury in rat intestine by nitric oxide synthase inhibitors. *Br. J. Pharmacol.,* **111,** 1309 – 1315.

LÁSZLÓ, F., WHITTLE, B.J.R. & MONCADA, S. (1994b). Interactions of constitutive nitric oxide with PAF and thromboxane on rat intestinal vascular integrity in acute endotoxaemia. *Br. J. Pharmacol.,* **113,** 1131 – 1136.

LÁSZLÓ, F., WHITTLE, B.J.R. & MONCADA, S. (1995c). Attenuation by nitrosothiol NO donors of acute intestinal microvascular dysfunction in the rat. *Br. J. Pharmacol.,* **115,** 498 – 502.

MA, X.-L., LEFER, A.M. & ZIPKIN, R.E. (1993). S-nitroso-N-penicillamine is a potent inhibitor of neutrophil-endothelial interaction. *Endothelium,* **1,** 31 – 39.

MOILANEN, E., VUORINEN, P., KANKAANRANTA, H., METSÄ-KETELÄ, T. & VAAPATALO, H. (1993). Inhibition by nitric oxide-donors of human polymorphonuclear functions. *Br. J. Pharmacol.,* **109,** 852 – 858.

MONCADA, S. & HIGGS, E.A. (1995). Molecular mechanisms and therapeutic strategies related to nitric oxide. *FASEB J.,* **9,** 1319 – 1330.

MONCADA, S., PALMER, R.M.J. & HIGGS, E.A. (1991). Nitric oxide: physiology, pathophysiology, and pharmacology. *Pharmacol. Rev.,* **43,** 109 – 141.

RADOMSKI, M.W., REES, D.D., DUTRA, A. & MONCADA, S. (1992). S-nitroso-glutathione inhibits platelet activation *in vitro* and *in vivo*. *Br. J. Pharmacol.,* **107,** 745 – 749.

ROBARTS, W.M. (1979). Nature of the disturbance in the body fluid compartments during and after surgical operations. *Br. J. Surg.,* **66,** 691 – 695.

SALTER, M., KNOWLES, R.G. & MONCADA, S. (1991). Widespread tissue distribution, species distribution and changes in activity of Ca^{2+}-dependent and Ca^{2+}-independent nitric oxide synthases. *FEBS Lett.,* **291,** 145 – 149.

WEDMORE, C.V. & WILLIAMS, T.J. (1981). Control of vascular permeability by polymorphonuclear leukocytes in inflammation. *Nature,* **289,** 646 – 650.

(Received August 7, 1998
Revised October 23, 1998
Accepted October 26, 1998)

British Journal of Pharmacology (1999) 126, 522–528
http://www.stockton-press.co.uk/bjp

Neurogenic plasma leakage in mouse airways

*[1,2]Peter Baluk, [1,2]Gavin Thurston, [1,2]Thomas J. Murphy, [3,4]Nigel W. Bunnett & [1,2]Donald M. McDonald

[1]Cardiovascular Research Institute, University of California, San Francisco, California 94143-0130, U.S.A.; [2]Department of Anatomy, University of California, San Francisco, California 94143-0130, U.S.A.; and [3]Department of Surgery, University of California, San Francisco, California 94143-0130, U.S.A.; [4]Department of Physiology, University of California, San Francisco, California 94143-0130, U.S.A.

1 This study sought to determine whether neurogenic inflammation occurs in the airways by examining the effects of capsaicin or substance P on microvascular plasma leakage in the trachea and lungs of male pathogen-free C57BL/6 mice.

2 Single bolus intravenous injections of capsaicin (0.5 and 1 μmol kg^{-1}, i.v.) or substance P (1, 10 and 37 nmol kg^{-1}, i.v.) failed to induce significant leakage in the trachea, assessed as extravasation of Evans blue dye, but did induce leakage in the urinary bladder and skin.

3 Pretreatment with captopril (2.5 mg kg^{-1}, i.v.), a selective inhibitor of angiotensin converting enzyme (ACE), either alone or in combination with phosphoramidon (2.5 mg kg^{-1}, i.v.), a selective inhibitor of neutral endopeptidase (NEP), increased baseline leakage of Evans blue in the absence of any exogenous inflammatory mediator. The increase was reversed by the bradykinin B_2 receptor antagonist Hoe 140 (0.1 mg kg^{-1}, i.v.).

4 After pretreatment with phosphoramidon and captopril, capsaicin increased the Evans blue leakage above the baseline in the trachea, but not in the lung. This increase was reversed by the tachykinin (NK_1) receptor antagonist SR 140333 (0.7 mg kg^{-1}, i.v.), but not by the NK_2 receptor antagonist SR 48968 (1 mg kg^{-1}, i.v.).

5 Experiments using Monastral blue pigment as a tracer localized the leakage to postcapillary venules in the trachea and intrapulmonary bronchi, although the labelled vessels were less numerous in mice than in comparably treated rats. Blood vessels of the pulmonary circulation were not labelled.

6 We conclude that neurogenic inflammation can occur in airways of pathogen-free mice, but only after the inhibition of enzymes that normally degrade inflammatory peptides. Neurogenic inflammation does not involve the pulmonary microvasculature.

Keywords: Plasma leakage; endothelial cells; vascular permeability; substance P; capsaicin; Hoe 140; SR 140333; SR 48968; phosphoramidon; captopril

Abbreviations: ACE, angiotensin converting enzyme; NEP, neutral endopeptidase

Introduction

Capsaicin induces the release of substance P and other neurotransmitters from sensory nerves, causing plasma leakage *via* the activation of tachykinin NK_1 receptors on endothelial cells (Abelli *et al*., 1991a; Bowden *et al*., 1994; Jancsó *et al*., 1967). The neurogenic plasma leakage, part of the phenomenon known as neurogenic inflammation (Geppetti & Holzer, 1996; McDonald, 1997), has been well characterized in rat and guinea-pig airways, but it is not clear whether such leakage occurs in airways of mice, and if so, under what circumstances. Published studies of mouse airways report apparently contradictory results; some investigators have failed to observe substance P-induced plasma leakage in mouse airways (Buckley & Nijkamp, 1994), whereas others have reported it (Figini *et al*., 1997). In human airways, there is as yet no direct evidence for neurogenic inflammation (McDonald, 1997), and even high doses of capsaicin fail to induce plasma leakage (Greiff *et al*., 1995).

Recently, a capsaicin receptor has been cloned and localized in sensory neurons in dorsal root ganglia of rats and mice (Caterina *et al*., 1997), but it is not clear if it is present on the vagal sensory neurons that innervate the airways. In mouse organs such as urinary bladder, skin, and parts of the gastrointestinal tract innervated by capsaicin-sensitive nerves, plasma leakage can occur in response to substance P, either given directly or released by capsaicin, or in response to bradykinin (Figini *et al*., 1997; Inoue *et al*., 1993; Maggi *et al*., 1987a). Capsaicin-sensitive, substance P-containing nerves may have a role in mucosal exudation in mouse airways associated with a delayed hypersensitivity reaction (Buckley & Nijkamp, 1994) and in immune complex activation of the lung (Bozic *et al*., 1996). However, it is not clear which anatomical categories of vessels become leaky, and to our knowledge, there are no reports of the effect of capsaicin on plasma leakage in mouse airways. Furthermore, it has been suggested that in addition to the major role played by NK_1 tachykinin receptors in neurogenic plasma leakage in the airways of some species, NK_2 receptors can also have a minor role (Tousignant *et al*., 1993). However, there are no data on this point in mouse airways.

Our main goal was to determine whether neurogenic inflammation occurs in mouse airways. Another aim was to determine which airway blood vessels are involved, and whether there is any leakage in the lung. Lastly, we sought to examine the possible role of NK_1 and NK_2 receptors in neurogenic plasma leakage in the mouse trachea. Our strategy was to quantify the plasma leakage induced by substance P or

*Author for correspondence; E-mail: pbaluk@itsa.ucsf.edu

capsaicin using Evans blue dye as a tracer. Because tachykinins can be rapidly degraded by neutral endopeptidase (NEP) and angiotensin converting enzyme (ACE), we inhibited these enzymes, using phosphoramidon and captopril respectively. Because airway infections can change the activity of these enzymes (Borson *et al*., 1989), increase the expression of tachykinin receptors (Baluk *et al*., 1997), and potentiate plasma leakage (McDonald *et al*., 1991), all studies used specific pathogen-free male C57BL/6 mice, a strain in which airway responses have been studied in 'knockout' mice (Bozic *et al*., 1996; Figini *et al*., 1997). Leaky vessels were identified histologically using Monastral blue as a marker of plasma leakage, and the labelled vessels in mice were compared to corresponding vessels in rats. To examine the relative contribution of NK_1 and NK_2 tachykinin and B_2 bradykinin receptors in the leakage we used the selective receptor antagonists SR 140333 and SR 48968 and Hoe 140.

Methods

Animals

Pathogen-free male C57BL/6 mice (20–25 g in weight) from Charles River Laboratories (Hollister, CA, U.S.A.) were maintained in a barrier facility to prevent respiratory tract infections. The mice were anaesthetized with ketamine (100 mg kg^{-1}, i.m.) and xylazine (5 mg kg^{-1}, i.m.), and their body temperature was maintained by a heating pad. In experiments done for comparison, pathogen-free male F344 rats (200–250 g) from Simonsen Laboratories (Gilroy, CA, U.S.A.) were treated in an identical fashion to the mice.

Experimental protocol

Mice were pretreated with vehicle (0.9% NaCl) or with phosphoramidon (2.5 mg kg^{-1}, i.v.), captopril (2.5 mg kg^{-1}, i.v.), or both. Five min later Evans blue dye (30 mg kg^{-1}, i.v.) or Monastral blue pigment (30 mg kg^{-1}, i.v.) was injected and immediately thereafter substance P (1, 10 and 37 nmol kg^{-1}, i.v.) or capsaicin (0.5 or 1 μmol kg^{-1}, i.v.) was injected over 20 s (to minimize apnea). A stock solution of 5 μmol ml^{-1} capsaicin was prepared in a 1 : 1 : 8 mixture of ethanol, Tween-80 and 0.9% NaCl and diluted further for use with 0.9% NaCl; other drugs were dissolved in 0.9% NaCl. Baseline leakage of Evans blue was measured in mice injected with 0.9 NaCl (1 ml kg^{-1}, i.v.). Some groups of mice were pretreated with the antagonists Hoe 140 (D-Arg-[Hyp^3, Thi^5, D-Tic^7, Oic^8]-bradykinin; 0.1 mg kg^{-1}, i.v.) selective for bradykinin B_2 receptors (Wirth *et al*., 1991), or with SR 140333 ((S)1-{2-[3-(3,4-dichlorophenyl)-1-(3-isopropoxyphenylacetyl) piperidin-3-yl]ethyl}-4-phenyl-1-azoniabicyclo [2,2,2]octane chloride; 0.7 mg kg^{-1}, i.v.) selective for tachykinin NK_1 receptors (Emonds-Alt *et al*., 1993), or with SR 48968 ((S)-*N*-methyl-[4-(4-acetylamino-4-phenylpiperidino)-2-(3,4-dichlorophenyl)-butyl] benzamide; 1 mg kg^{-1}, i.v.) selective for NK_2 tachykinin receptors (Emonds-Alt *et al*., 1992; Maggi *et al*., 1993), administered 5 min before the phosphoramidon and/or captopril or before vehicle only. Five minutes after the inflammatory stimulus the chest was opened, both atria were cut, and the systemic circulation was perfused with a fixative containing paraformaldehyde (McDonald *et al*., 1991) for 2 min at a pressure of 120–140 mmHg *via* an 18 gauge needle inserted into the left ventricle. In addition, the pulmonary circulation was flushed for 1 min at a pressure of 20 mmHg. Tissues (trachea, 5 mm thick sections of left lung containing the hilum and main bronchus, dorsal skin of hind foot, and urinary bladder) were dissected, gently blotted, and weighed. Evans blue dye was extracted from the tissues using formamide, measured spectrophotometrically and expressed as ng dye mg^{-1} wet weight of tissue (Saria & Lundberg, 1983). Tracheas and urinary bladders used for identifying leaky vessels labelled by extravasated Monastral blue were prepared as whole mounts (McDonald *et al*., 1991), and 20 μm thick cryostat sections were cut of the lung.

Materials used

We used the following reagents: capsaicin, captopril, formamide, Monastral blue, phosphoramidon, phosphate buffered saline, Tween 80 (Sigma Chemical Company, St. Louis, MO, U.S.A.), Evans blue (EM Sciences, Cherry Hill, NJ, U.S.A.), ketamine (Parke-Davis, Morris Plains, NJ, U.S.A.), substance P (Peninsula Laboratories, Belmont, CA, U.S.A.), and xylazine (Butler, Colombus, OH, U.S.A.). The selective NK_1 and NK_2 receptor antagonists SR 140333 and SR 48968, respectively, were gifts from Dr Xavier Emonds-Alt, Sanofi Recherche, Montpellier, France, and Hoe 140, a selective bradykinin B_2 receptor antagonist, was a gift from Dr Klaus Wirth, Hoechst, Frankfurt, Germany.

Table 1 Microvascular leakage of Evans blue in urinary bladder and skin of C57BL/6 mice

Treatment	*Urinary bladder* (ng dye mg^{-1} tissue)	*Skin* (ng dye mg^{-1} tissue)
Baseline	2.43 ± 0.22	3.85 ± 0.68
Substance P 1 nmol kg^{-1}	5.88 ± 1.01	7.64 ± 4.03
Substance P 10 nmol kg^{-1}	33.01 ± 7.91*	11.71 ± 2.26*
Substance P 37 nmol kg^{-1}	21.66 ± 5.05*	10.40 ± 2.34*
Capsaicin 0.5 μmol kg^{-1}	5.98 ± 1.61	4.98 ± 0.34
Capsaicin 1.0 μmol kg^{-1}	20.28 ± 9.29*	4.50 ± 0.51
Phosphoramidon	13.30 ± 4.39*	5.30 ± 1.02
Captopril	20.68 ± 3.56*	7.02 ± 1.02
Phosphoramidon + captopril	31.55 ± 11.32*	7.98 ± 1.84
Hoe 140	2.19 ± 0.12	4.73 ± 0.83
SR 140333	2.66 ± 0.43	2.34 ± 0.53
Hoe 140 + phosphoramidon + captopril	3.70 ± 0.44*	7.03 ± 1.35*
Phosphoramidon + captopril + capsaicin 0.5 μmol kg^{-1}	45.98 ± 5.91*	9.70 ± 2.27*
SR 140333 + phosphoramidon + captopril + capsaicin 0.5 μmol kg^{-1}	18.98 ± 7.11*	7.00 ± 1.26

Microvascular leakage in urinary bladder and skin of anaesthetized pathogen-free C57BL/6 mice expressed as ng Evans blue dye mg^{-1} wet weight of tissue. Values are means ± s.e.mean; $n = 6–8$ for all groups, except for substance P 1 nmol kg^{-1} ($n = 5$). *Significantly different from baseline group ($P < 0.05$).

Statistics

Values are expressed as means ± s.e.mean. Differences between groups were determined by analysis of variance followed by the Dunn-Bonferroni *t*-test and were considered significant when $P<0.05$.

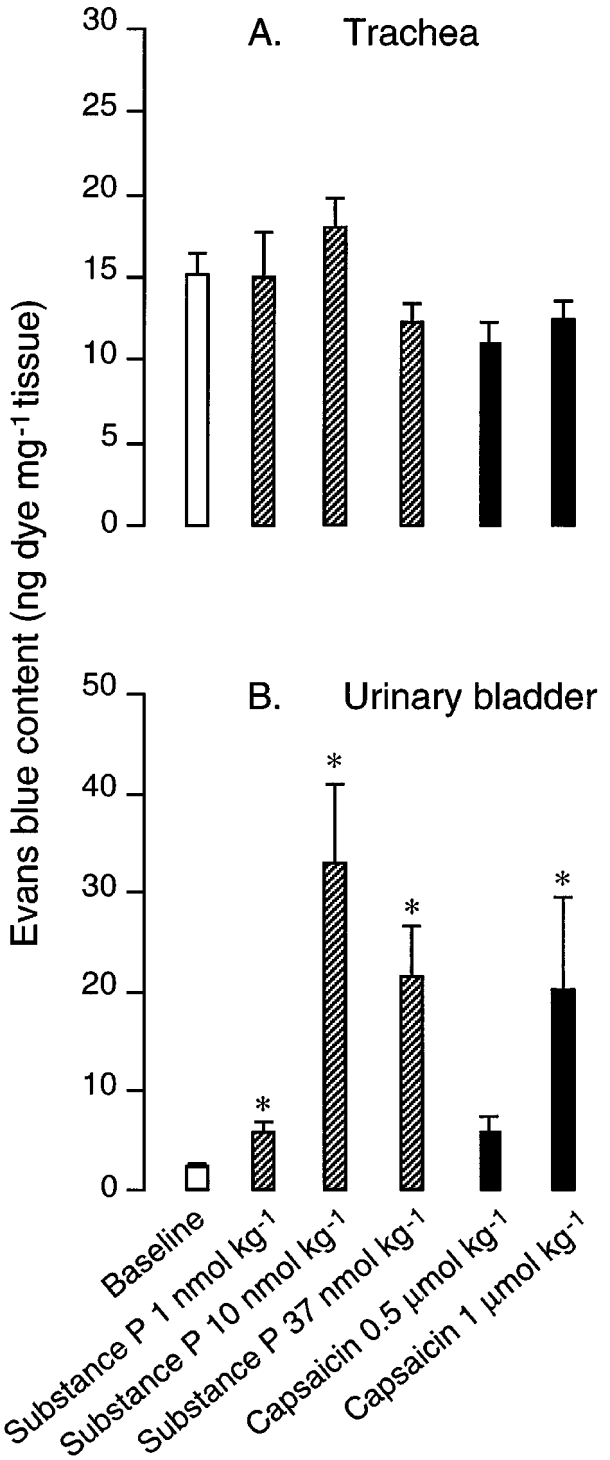

Figure 1 Comparison of plasma leakage in (A) trachea and (B) urinary bladder of pathogen-free C57BL/6 mice 5 min after intravenous injection of substance P or capsaicin. Baseline values measured in mice after vehicle alone. Values are means ± s.e.mean $n=5-8$ mice per group. $^*P<0.05$ compared to baseline group.

Results

In the absence of any stimulus, baseline leakage of Evans blue in the trachea, urinary bladder and other organs (Figure 1 and Table 1) was modest. In the absence of pretreatment, substance P (1, 10 and 37 nmol kg^{-1}, i.v.) or capsaicin (0.5 and 1 μmol kg^{-1}, i.v.) did not increase Evans blue leakage significantly above baseline in the trachea (Figure 1A). No blood vessels in the trachea were labelled with Monastral blue after substance P or capsaicin alone. Intravenous injection of capsaicin at doses up to 1 μmol kg^{-1} caused a transient (<1 min) apnea.

In the same mice, substance P (10 and 37 nmol kg^{-1}) significantly increased Evans blue leakage in the urinary bladder and skin, although the response to 37 nmol kg^{-1} was less than to 10 nmol kg^{-1} (Figure 1B and Table 1). On average, the leakage in the urinary bladder increased 2 and 8 fold after the 0.5 and 1 μmol kg^{-1} i.v. doses of capsaicin (Table 1).

Pretreatment with Hoe 140 significantly reduced baseline leakage in the trachea, but not in the urinary bladder or skin (Figure 2 & Table 1). Pretreatment with SR 140333 did not influence baseline in any organ (Figure 2 & Table 1). After pretreatment with captopril alone, but without capsaicin or substance P, there was a significant increase in the Evans blue leakage in the trachea (Figure 2). Captopril plus phosphoramidon had a slightly larger effect, but phosphoramidon alone had no effect (Figure 2). The leakage induced by captopril plus phosphoramidon was blocked by pretreatment with Hoe 140 (Figure 2). Similar results were found in the urinary bladder (Table 1).

Capsaicin produced a further dose-dependent increase in Evans blue leakage in the trachea of mice pretreated with captopril plus phosphoramidon (Figure 3). This increase was prevented by pretreatment with SR 140333, but not by SR

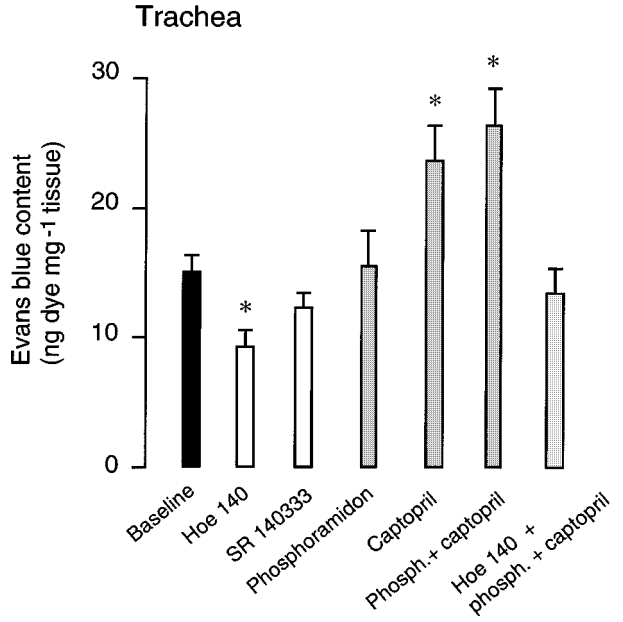

Figure 2 Increased plasma leakage in tracheas of pathogen-free C57BL/6 mice pretreated with phosphoramidon plus captopril 5 min before Evans blue and vehicle. Leakage is not increased when mice are pretreated with the bradykinin B_2 receptor antagonist Hoe 140 10 min before Evans blue. Pretreatment with Hoe 140 alone, but not SR 140333 alone, reduces baseline leakage. Values are means ± s.e.mean; $n=6-8$ mice per group. $^*P<0.05$ compared to baseline group.

48968 (Figure 3 and Table 1). However, neither SR 140333 nor SR 48968 blocked the component of the leakage produced by captopril plus phosphoramidon pretreatment. Similar results were found in the urinary bladder and skin (Table 1).

In the lung, baseline Evans blue values were higher than in the trachea and other tissues, but none of the treatments significantly increased the values above this baseline (Figure 4).

Monastral blue labelling showed that in the trachea the leaky vessels after captopril plus phosphoramidon pretreatment, followed by capsaicin were postcapillary venules and collecting venules (Figure 5A). The labelled venules in the mouse trachea were less branched and less abundant than in comparably treated rats (Figure 5B). After phosphoramidon and captopril pretreatment alone a few postcapillary venules were also labelled. The distribution pattern was similar to that observed after pretreatment and subsequent capsaicin injection, but the number of labelled vessels and intensity of labelling was much less. Monastral blue labelled venules extended to the extrapulmonary bronchi. Corresponding Monastral blue labelled venules were also found in the urinary bladder and skin. In cryostat sections of mouse lung, some postcapillary venules around the larger intrapulmonary bronchi with smooth muscle were labelled (Figure 5C), but smaller bronchioles and the pulmonary vasculature were not (Figure 5D). No labelled vessels were found in alveolar walls.

Discussion

The main finding of this study was that neurogenic plasma leakage could be induced in C57BL/6 mouse airways, but only after the inhibition of the enzymes that degrade tachykinins. The leaky vessels in the trachea and bronchi were postcapillary venules supplied by the systemic circulation. Neurogenic plasma leakage appeared to be mediated by NK_1 receptors. Blood vessels of the pulmonary circulation did not become leaky. In the trachea, leaky blood vessels were less abundant, and simpler in their branching pattern in mice than in rats.

Injection of even quite high doses of substance P and capsaicin failed to induce plasma leakage in airways of normal C57BL/6 mice. These inflammatory stimuli were sufficient to induce leakage in other organs supplied by sensory nerves, indicating that sufficient amounts of tachykinins were available to induce leakage in these organs. The highest dose of substance P used is more than that required to induce maximal leakage in the trachea of rats and guinea-pigs (Brokaw & White, 1994; Rogers *et al*., 1988), and this dose produces severe hypotension (Maggi *et al*., 1987b). We did not investigate higher doses of capsaicin because of the risk of fatal apnea.

According to the original description, the characteristics of neurogenic inflammation are plasma leakage and vasodilatation (Jancsó *et al*., 1967). In recent years, however, the term neurogenic inflammation has been used somewhat more broadly and vaguely, and has come to include other responses to activation of sensory nerves, including smooth muscle contraction, hypersecretion, mast cell degranulation, and activation of immune cells (Geppetti & Holzer, 1996). In the present report, we adhere to the original definition for clarity and for consistency with our earlier publications (McDonald, 1997).

Neurogenic inflammation apparently does not occur in species such as hamsters and rabbits that have a higher

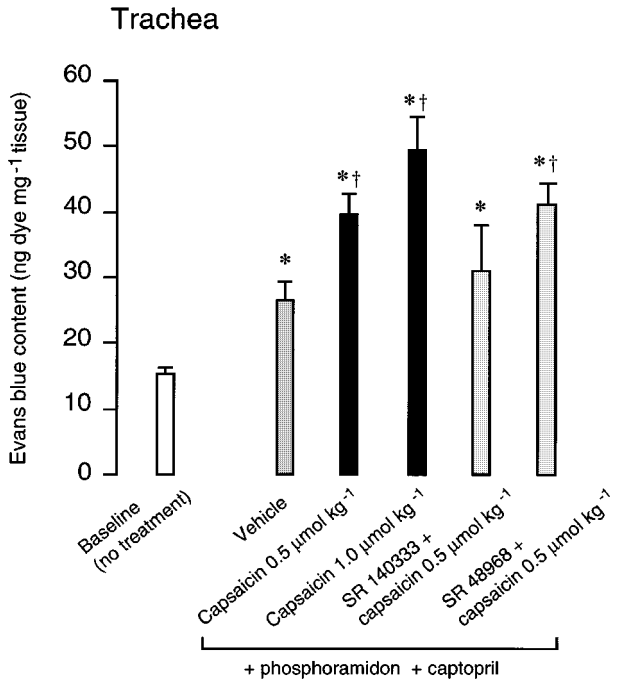

Figure 3 Capsaicin-induced leakage in tracheas of pathogen-free C57BL/6 mice pretreated with captopril alone or with phosphoramidon plus captopril given 5 min before Evans blue injection. The increase in leakage induced by capsaicin is prevented by pretreatment with the NK_1 receptor antagonist SR 140333 10 min in advance. Values are means ± s.e.mean; $n = 6-8$ mice per group. $^*P < 0.05$ compared to baseline group. $\dagger P < 0.05$ compared to phosphoramidon + captopril pretreated group.

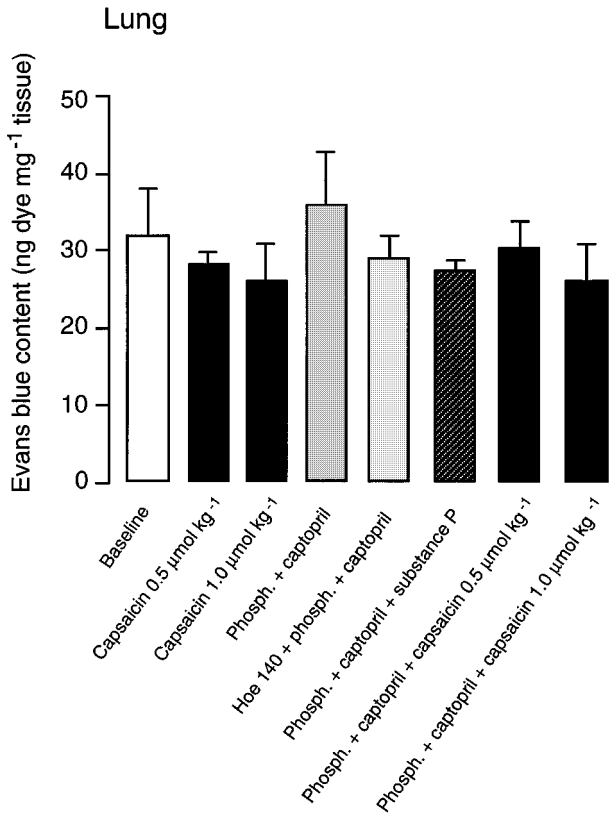

Figure 4 Plasma leakage in the middle portion of left lung containing the main bronchus of pathogen-free C57BL/6 mice. None of the treatments induced leakage significantly different from the baseline group. Values are means ± s.e.mean; $n = 5-8$ mice per group.

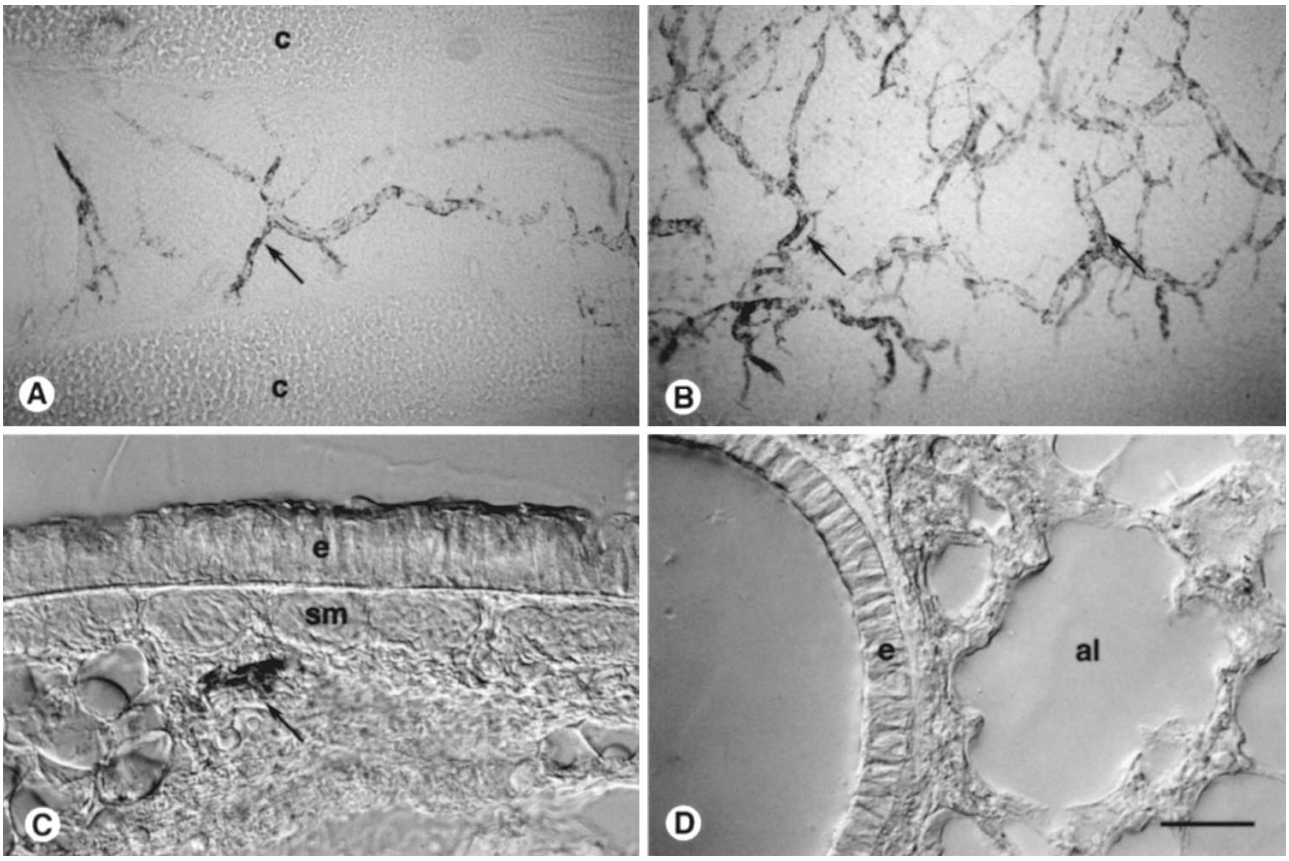

Figure 5 Photomicrographs of Monastral blue-labelled venules in whole mount preparations of tracheas from pathogen-free (A) C57BL/6 mice and (B) F344 rats, and in cryostat sections of mouse lung (C, D) after pretreatment with phosphoramidon plus captopril and challenge with capsaicin 0.5 μmol kg^{-1} (i.v.). (A) Labelled postcapillary venules (arrow) are sparse in mouse trachea (c, cartilage), but are more abundant (arrows) and more branched in rat trachea (B). (C) Mouse main stem intrapulmonary bronchus photographed by Nomarski differential interference microscopy (e, epithelium; sm, smooth muscle; arrow, Monastral blue-labelled postcapillary venule in bronchial adventitia). (D) Vessels around the epithelium (e) of a smaller bronchiole and vessels in the wall of an alveolus (al) are unlabelled. Scale bar: 200 μm for (A, B) and 50 μm for (C, D).

tolerance to capsaicin than mice, rats, and guinea-pigs (Glinsukon *et al*., 1980; McDonald, 1997). It is still not clear whether neurogenic inflammation really occurs in human airways (Baluk & McDonald, 1998; Barnes, 1996; McDonald, 1997). Although human airways undoubtedly contain sensory nerves, few of them contain substance P (Hislop *et al*., 1990; Luts *et al*., 1993). On the other hand, administration of substance P onto the nasal mucosa causes an increased amount of albumin in nasal secretions, and this can be interpreted as a manifestation of plasma leakage (Braunstein *et al*., 1991). However, there is no evidence that capsaicin can induce plasma leakage in human nasal mucosa (Greiff *et al*., 1995). In this respect, the situation in mouse airways, where it is rather difficult to induce neurogenic inflammation, is more similar to human airways than to rat or guinea-pig airways, where it is easy to induce leakage.

In agreement with previous studies in rats (Brokaw & White, 1994), we found that inhibition of neutral endopeptidase and angiotensin converting enzyme by phosphoramidon and captopril can elicit leakage even in the absence of capsaicin or substance P, suggesting that endogenous mediators are involved. Mice also resemble guinea-pigs and rats (Brokaw & White, 1994; Lötvall *et al*., 1991) in that inhibition of neutral endopeptidase alone by phosphoramidon is insufficient to increase leakage above baseline levels in the airways, although it can do so in the urinary bladder (Lu *et al*., 1997). A likely candidate for the endogenous inflammatory mediator that increases leakage in airways after captopril plus phosphoramidon is bradykinin. Evidence for this possibility is that bradykinin is efficiently degraded by angiotensin converting enzyme (Welches *et al*., 1993) and can induce dose-dependent leakage in the mouse trachea (Figini *et al*., 1997). The increased leakage was prevented by the bradykinin B_2 receptor antagonist Hoe 140, and pretreatment with Hoe 140 alone actually reduced baseline leakage.

It is unclear why different investigators have found different amounts of substance P-induced plasma leakage in mouse airways. Differences in routes of administration, measurement techniques, and the strains of mice used (Balb/c, Swiss-Morini, and C57BL/6) may contribute (Buckley & Nijkamp, 1994; Figini *et al*., 1997, present study). Another possibility is the presence of undetected respiratory tract infections. In rat airways, *Mycoplasma pulmonis* and Sendai virus infections can potentiate the effects of substance P (McDonald *et al*., 1991; Piedimonte *et al*., 1990). A reduction in neutral endopeptidase activity may be involved (Borson *et al*., 1989). *M. pulmonis* infections can also increase expression of NK_1 receptors on endothelial cells (Baluk *et al*., 1997). Mice with *M. pulmonis* infection appear to resemble rats in this respect and their airway blood vessels become more sensitive to substance P, so that substance P (3.7 nmol kg^{-1}, i.v.; lower than the doses used here) induced significant leakage in infected mice, but not in pathogen-free controls (Thurston *et al*., 1998). Therefore, only specific pathogen-free mice were used in the present study.

We examined whether NK_1 or NK_2 receptors mediate the leakage in mouse airways by blocking the capsaicin-induced

increase in leakage with the selective receptor antagonists SR 140333 and SR 48968. We found that the NK_1 receptor antagonist blocked the response but the NK_2 antagonist did not, and we conclude that neurogenic plasma leakage in the mouse trachea is mediated by NK_1 receptors, with no contribution from NK_2 receptors detectable by our technique. Similar findings have been reported for neurogenic inflammation in mouse skin (Inoue *et al*., 1997), and rat airways and urinary bladder (Abelli *et al*., 1991b; Ahluwalia *et al*., 1994).

Leaky vessels were less numerous in mice than in rats. In addition to the smaller sizes of airways and volumes of tissue, substance P-containing nerves may be sparser. The trachea of mice resembles bronchioles of larger species and sensory nerve fibres have been reported to be sparse in the mucosa and absent in the epithelium (Pack *et al*., 1984). In contrast, substance P-containing nerve fibres are abundant in the epithelium of guinea-pig and rat trachea (Baluk *et al*., 1992; Lundberg *et al*., 1984). In mouse lungs substance P-containing nerve fibres supply the airways, but not the intrapulmonary blood vessels (Verastegui *et al*., 1997). Finally, in mice, as in rats and guinea-pigs, only postcapillary venules of the tracheal and bronchial circulation become leaky, and vessels of the pulmonary circulation appear unresponsive to tachykinins or bradykinin.

We conclude that neurogenic inflammation can occur in mouse airways after the inhibition of enzymes that normally degrade inflammatory peptides, but does not involve the pulmonary microvasculature.

This work was supported in part by NIH Grants HL-24136 and DK-43207. We thank Dr Piero Geppetti of the University of Ferrara, Italy, for helpful discussions and sharing unpublished data. We are grateful to Dr Xavier Emonds-Alt of Sanofi Recherche, Montpellier, France and Dr Klaus Wirth of Hoechst, Frankfurt, Germany for kind gifts of SR 140333 and SR 48968, and Hoe 140 respectively.

References

ABELLI, L., MAGGI, C.A., ROVERO, P., DEL BIANCO, E., REGOLI, D., DRAPEAU, G. & GIACHETTI, A. (1991a). Effect of synthetic tachykinin analogues on airway microvascular leakage in rats and guinea-pigs: evidence for the involvement of NK-1 receptors. *J. Auton. Pharmacol.,* **11,** 267–275.

ABELLI, L., NAPPI, F., MAGGI, C.A., ROVERO, P., ASTOLFI, M., REGOLI, D., DRAPEAU, G. & GIACHETTI, A. (1991b). NK-1 receptors and vascular permeability in rat airways. *Ann. N.Y. Acad. Sci.,* **632,** 358–359.

AHLUWALIA, A., MAGGI, C.A., SANTICIOLI, P., LECCI, A. & GUILIANI, S. (1994). Characterization of the capsaicin-sensitive component of cyclophosphamide-induced inflammation in the rat urinary bladder. *Br. J. Pharmacol.,* **111,** 1017–1022.

BALUK, P., BOWDEN, J.J., LEFEVRE, P.M. & MCDONALD, D.M. (1997). Upregulation of substance P receptors in angiogenesis associated with chronic airway inflammation in rats. *Am. J. Physiol.,* **273,** L565–L571.

BALUK, P. & MCDONALD, D.M. (1998). Proinflammatory peptides in sensory nerves of the airways. In *Proinflammatory and Antiinflammatory Peptides*. ed. Said, S.I. pp. 45–87. New York: Marcel Dekker, Inc.

BALUK, P., NADEL, J.A. & MCDONALD, D.M. (1992). Substance P-immunoreactive sensory axons in the rat respiratory tract: a quantitative study of their distribution and role in neurogenic inflammation. *J. Comp. Neurol.,* **319,** 586–598.

BARNES, P.J. (1996). Sensory neuropeptides and airway disease. In *Neurogenic Inflammation*. eds. Geppetti, P. & Holzer, P. pp. 169–185. Boca Raton, FL: CRC Press, Inc.

BORSON, D.B., BROKAW, J.J., SEKIZAWA, K., MCDONALD, D.M. & NADEL, J.A. (1989). Neutral endopeptidase and neurogenic inflammation in rats with respiratory infections. *J. Appl. Physiol.,* **66,** 2653–2658.

BOWDEN, J.J., GARLAND, A.M., BALUK, P., LEFEVRE, P., GRADY, E.F., VIGNA, S.R., BUNNETT, N.W. & MCDONALD, D.M. (1994). Direct observation of substance P-induced internalization of neurokinin 1 (NK_1) receptors at sites of inflammation. *Proc. Natl. Acad. Sci. U.S.A.,* **91,** 8964–8968.

BOZIC, C.R., LU, B., HÖPKEN, U.E., GERARD, C. & GERARD, N.P. (1996). Neurogenic amplification of immune complex inflammation. *Science,* **273,** 1722–1725.

BRAUNSTEIN, G., FAJAC, I., LACRONIQUE, J. & FROSSARD, N. (1991). Clinical and inflammatory responses to exogenous tachykinins in allergic rhinitis [published erratum appears in Am Rev Respir Dis 1993 Dec; 148(6 Pt 1):following 1700]. *Am. Rev. Respir. Dis.,* **144,** 630–635.

BROKAW, J.J. & WHITE, G.W. (1994). Differential effects of phosphoramidon and captopril on NK1 receptor-mediated plasma extravasation in the rat trachea. *Agents Actions,* **42,** 34–39.

BUCKLEY, T.L. & NIJKAMP, F.P. (1994). Mucosal exudation associated with a pulmonary delayed-type hypersensitivity reaction in the mouse – role for the tachykinins. *J. Immunol.,* **153,** 4169–4178.

CATERINA, M.J., SCHUMACHER, M.A., TOMINAGA, M., ROSEN, T.A., LEVINE, J.D. & JULIUS, D. (1997). The capsaicin receptor: a heat-inactivated ion channel in the pain pathway. *Nature,* **389,** 816–824.

EMONDS-ALT, X., DOUTREMEPUICH, J.D., HEAULME, M., NELIAT, G., SANTUCCI, V., STEINBERG, R., VILAIN, P., BICHON, D., DUCOUX, J.P., PROIETTO, V., VANBROECK, D., SOUBRIE, P., LEFUR, G. & BRELIERE, J.C. (1993). In vitro and in vivo biological activities of SR 140333, a novel potent non-peptide tachykinin NK1, receptor antagonist. *Eur. J. Pharmacol.,* **250,** 403–413.

EMONDS-ALT, X., VILAIN, P., GOULAOUIC, P., PROIETTO, V., VAN BROECK, D., ADVENIER, C., NALINE, E., NELIAT, G., LE FUR, G. & BRELIERE, J.C. (1992). A potent and selective non-peptide antagonist of the neurokinin A (NK2) receptor. *Life Sci.,* **50,** L101–106.

FIGINI, M., EMANUELI, C., GRADY, E.F., KIRKWOOD, K., PAYAN, D.G., ANSEL, J., GEPPETTI, P. & BUNNETT, N. (1997). Substance P and bradykinin stimulate plasma extravasation in the mouse gastrointestinal tract and pancreas. *Am. J. Physiol.,* **272,** G786–G793.

GEPPETTI, P. & HOLZER, P. (1996). *Neurogenic Inflammation:* CRC Press.

GLINSUKON, T., STITMUNNAITHUM, V., TOSKULKAO, C., BURANAWUTI, T. & TANGKRISANAVINONT, V. (1980). Acute toxicity of capsaicin in several animal species. *Toxicon,* **18,** 215–220.

GREIFF, L., SVENSSON, C., ANDERSSON, M. & PERSSON, C.G.A. (1995). Effects of topical capsaicin in seasonal allergic rhinitis. *Thorax,* **50,** 225–229.

HISLOP, A.A., WHARTON, J., ALLEN, K.M., POLAK, J.M. & HAWORTH, S.G. (1990). Immunohistochemical localization of peptide-containing nerves in human airways: age-related changes. *Am. J. Respir. Cell Mol. Biol.,* **3,** 191–198.

INOUE, H., ASAKA, T., NAGATA, N. & KOSHIHARA, Y. (1997). Mechanism of mustard oil-induced skin inflammation in mice. *Eur. J. Pharmacol.,* **333,** 231–240.

INOUE, H., NAGATA, N. & KOSHIHARA, Y. (1993). Profile of capsaicin-induced mouse ear oedema as neurogenic inflammatory model – comparison with arachidonic acid-induced ear oedema. *Br. J. Pharmacol.,* **110,** 1614–1620.

JANCSÓ, N., JANCSÓ-GÁBOR, A. & SZOLCSÁNYI, J. (1967). Direct evidence for neurogenic inflammation and its prevention by denervation and by pretreatment with capsaicin. *Br. J. Pharmacol.,* **31,** 138–151.

LÖTVALL, J.O., ELWOOD, W., TOKUYAMA, K., BARNES, P.J. & CHUNG, K.F. (1991). Differential effects of phosphoramidon on neurokinin A- and substance P-induced airflow obstruction and airway microvascular leakage in guinea-pig. *Br. J. Pharmacol.,* **104,** 945–949.

LU, B., FIGINI, M., EMANUELLI, C., GEPPETTI, P., GRADY, E.F., GERARD, N.P., ANSEL, J., PAYAN, D.G., GERARD, C. & BUNNETT, N. (1997). The control of microvascular permeability and blood pressure by neutral endopeptidase. *Nature Med.,* **3,** 904 – 907.

LUNDBERG, J.M., HOKFELT, T., MARTLING, C.-R., SARIA, A. & CUELLO, C. (1984). Substance P-immunoreactive sensory nerves in the lower respiratory tract of various mammals including man. *Cell Tissue Res.,* **235,** 251 – 261.

LUTS, A., UDDMAN, R., ALM, P., BASTERRA, J. & SUNDLER, F. (1993). Peptide-containing nerve fibres in human airways – distribution and coexistence pattern. *Int. Arch. Aller. Immunol.,* **101,** 52 – 60.

MAGGI, C.A., GIULIANI, S., SANTICIOLI, P., ABELLI, L., GEPPETTI, P., SOMMA, V., RENZI, D. & MELI, A. (1987a). Species-related variations in the effects of capsaicin on urinary bladder functions: relation to bladder content of substance P-like immunoreactivity. *Naunyn-Schmied. Arch. Pharmacol.,* **336,** 546 – 555.

MAGGI, C.A., GIULIANI, S., SANTICIOLI, P., REGOLI, D. & MELI, A. (1987b). Peripheral effects of neurokinins: functional evidence for the existence of multiple receptors. *J. Auton. Pharmacol.,* **7,** 11 – 32.

MAGGI, C.A., PATACCHINI, R., GUILIANI, S. & GIACHETTI, A. (1993). In vivo and in vitro pharmacology of SR 48,968, a non-peptide tachykinin NK2 receptor antagonist. *Eur. J. Pharmacol.,* **234,** 83 – 90.

MCDONALD, D.M. (1997). Neurogenic Inflammation in the Airways. In *Autonomic Control of the Respiratory System.* ed. Barnes, P. pp. 249 – 290. Amsterdam: Harwood Academic Publishers.

MCDONALD, D.M., SCHOEB, T.R. & LINDSEY, J.R. (1991). *Mycoplasma pulmonis* infections cause long-lasting potentiation of neurogenic inflammation in the respiratory tract of the rat. *J. Clin. Invest.,* **87,** 787 – 799.

PACK, R.J., AL-UGAILY, L.H. & WIDDICOMBE, J.G. (1984). The innervation of the trachea and extrapulmonary bronchi of the mouse. *Cell Tissue Res.,* **238,** 61 – 68.

PIEDIMONTE, G., NADEL, J.A., UMENO, E. & MCDONALD, D.M. (1990). Sendai virus infection potentiates neurogenic inflammation in the rat trachea. *J. Appl. Physiol.,* **68,** 754 – 760.

ROGERS, D.F., BELVISI, M.G., AURSUDKIJ, B., EVANS, T.W. & BARNES, P.J. (1988). Effects and interactions of sensory neuropeptides on airway microvascular leakage in guinea-pigs. *Br. J. Pharmacol.,* **95,** 1109 – 1116.

SARIA, A. & LUNDBERG, J.M. (1983). Evans blue fluorescence: quantitative and morphological evaluation of vascular permeability in animal tissues. *J. Neurosci. Meth.,* **8,** 41 – 49.

THURSTON, G., MURPHY, T.J., BALUK, P., LINDSEY, J.R. & MCDONALD, D.M. (1998). Angiogenesis in mice with chronic airway inflammation: strain-dependent differences. *Am. J. Pathol.,* **153,** 1099 – 1112.

TOUSIGNANT, C., CHAN, C.C., GUEVREMONT, D., BRIDEAU, C., HALE, J.J., MACCROSS, M. & RODGER, I.W. (1993). NK2 receptors mediate plasma extravasation in guinea-pig lower airways. *Br. J. Pharmacol.,* **108,** 383 – 386.

VERASTEGUI, C., FERNANDEZ-VIVERO, J., PRADA, A., RODRIGUEZ, F., ROMERO, A., GONZALEZ-MORENO, M. & DE CASTRO, J.M. (1997). Presence and distribution of 5HT-, VIP-, NPY- and SP-immunoreactive structures in adult mouse lung. *Histol. Histopathol.,* **12,** 909 – 918.

WELCHES, W.R., BROSNIHAN, K.B. & FERRARIO, C.M. (1993). A comparison of the properties and enzymatic activities of 3 angiotensin processing enzymes – angiotensin converting enzyme, prolyl endopeptidase and neutral endopeptidase 24.11. *Life Sci.,* **52,** 1461 – 1480.

WIRTH, K., HOCK, F.J., ALBUS, U., LINZ, W., ALPERMANN, H.G., ANAGNASTOPOULOS, H., HENKE, S., BREIPOHL, G., KÖNIG, W., KNOLLE, J. & SCHÖLKENS, B.A. (1991). Hoe 140 a new potent and long acting bradykinin-antagonist: *in vivo* studies. *Br. J. Pharmacol.,* **102,** 774 – 777.

(Received August 28, 1998
Revised October 23, 1998
Accepted October 26, 1998)

British Journal of Pharmacology (1999) 126, 529–535
http://www.stockton-press.co.uk/bjp

Modulation of ET-1-induced contraction of human bronchi by airway epithelium-dependent nitric oxide release *via* ET_A receptor activation

*,[1]Emmanuel Naline, [2]Claude Bertrand, [1]Keltoum Biyah, [2]Yasushi Fujitani, [3]Toshikazu Okada, [4]Alain Bisson & [1]Charles Advenier

[1]Laboratoire de Pharmacologie, Faculté de Médecine Paris-Ouest, F-75270 Paris et Centre Hospitalier de Versailles, F-78150 Le Chesnay, France; [2]Respiratory Diseases & Allergy Department, Ciba-Geigy Ltd., CH-4002 Basel, Switzerland; [3]International Research Laboratories, Ciba-Geigy Japan Ltd, Takarazuka 665, Japan and [4]Centre Médico-Chirurgical du Val d'Or, F-92210 Saint Cloud, France.

1 The purpose of this work was to investigate whether endothelin-1 (ET-1) was able to induce the release of an inhibitory factor from the airway epithelium in isolated human bronchi and to identify this mediator as well as the endothelin receptor involved in this phenomenon.

2 In intact bronchi, ET-1 induced a concentration-dependent contraction ($-\log EC_{50} = 7.92 \pm 0.09$, $n = 18$) which was potentiated by epithelium removal ($-\log EC_{50} = 8.65 \pm 0.11$, $n = 17$). BQ-123 , an ET_A receptor antagonist, induced a significant leftward shift of the ET-1 concentration-response curve (CRC). This leftward shift was abolished after epithelium removal.

3 L-NAME (3×10^{-3} M), an inhibitor of nitric oxide (NO) synthase, induced a significant leftward shift of the ET-1 CRC, and abolished the potentiation by BQ-123 (10^{-8} M) of ET-1-induced contraction.

4 In intact preparations, the ET_B receptor antagonist BQ-788 induced only at 10^{-5} M a slight rightward shift of the ET-1 CRC. In contrast, in epithelium-denuded bronchi or in intact preparations in the presence of L-NAME, BQ-788 displayed a non-competitive antagonism toward ET-1-induced contraction.

5 IRL 1620, a selective ET_B receptor agonist, induced a contraction of the isolated bronchus ($-\log EC_{50} = 7.94 \pm 0.11$, $n = 19$). This effect was not modified by epithelium removal or by BQ-123. BQ-788 exerted a competitive antagonism against IRL 1620 which was similar in the presence or absence of epithelium.

6 These results show that ET-1 exerts two opposite effects on the human airway smooth muscle. One is contractile *via* ET_B-receptor activation, the other is inhibitory and responsible of NO release which counteracts *via* ET_A-receptor activation the contraction.

Keywords: Endothelin-1; human bronchus; ET_A receptors; ET_B receptors; IRL 1620; BQ-123; BQ-788; nitric oxide; airway epithelium

Abbreviations: ACh, acetylcholine; BAL, bronchoalveolar lavage fluid; CRC, concentration-response curve; ET-1, endothelin-1; NEP, neutral endopeptidase; NO, nitric oxide.

Introduction

Endothelin-1 (ET-1) was originally isolated as a potent vasoconstrictor peptide from a culture medium of endothelial cells (Yanagisawa *et al*., 1988). The biological actions of ET-1 are mediated through two distinct receptor subtypes, both of which belong to the G-protein coupled receptor superfamily, termed ET_A and ET_B receptors (Sakurai *et al*., 1992; Arai *et al*., 1993). Numerous studies have revealed the diverse biological action of this peptide in the lungs (Hay, 1995; Fernandes *et al*., 1996; Goldie *et al*., 1996). Furthermore, immunoreactive levels of ET were found to be elevated in bronchoalveolar lavage fluid (BAL) (Redington *et al*., 1995) and in airway epithelium of asthmatic patients (Springall *et al*., 1991) compared to healthy subjects, suggesting a pathophysiological role of ET-1 in bronchial asthma.

In guinea-pigs, endothelins are potent constrictors of airway smooth muscle both *in vitro* and *in vivo*. IRL 1620 (Suc-[Glu^9, $Ala^{11,15}$]ET-1(8,21)), a selective ET_B receptor agonist (Takai *et al*., 1992; James *et al*., 1993) induces contraction of the guinea-pig trachea with a comparable potency to the natural ligand ET-1 suggesting a major involvement of ET_B receptors in this response (Takai *et al*., 1992). In human bronchus, ET-1 is a potent constrictor agent (Advenier *et al*., 1990; Hay *et al*., 1993a; Nally *et al*., 1994; Goldie *et al*., 1995). Similarly, this effect seems to be mediated by non-ET_A receptors, presumably ET_B receptors (Hay *et al*., 1993c). In addition, prior investigations have demonstrated that removal of the epithelium from human bronchi or guinea-pig trachea augments contraction to ET-1. Firstly, it was postulated that epithelium ablation resulted in the suppression of the main source of neutral endopeptidase (NEP), the enzyme involved in part in ET-1 catabolism (Candenas *et al*., 1992). Secondly, ET-1 has also been reported to induce relaxation in precontracted rabbit and guinea-pig tracheal segments (Grunstein *et al*., 1991; Filep *et al*., 1993). These findings indicated that ET-1 was capable of releasing a relaxant factor from the airways under certain circumstances. Recently, nitric oxide (NO) has been suggested as an epithelial mediator following activation of epithelial receptor (Filep *et al*., 1993). Endothelin receptors

*Author for correspondence at: Laboratoire de Pharmacologie Respiratoire, 15, rue de L'Ecole de Medecine, 75006 Paris, France.

have been identified on human airway epithelial cells in culture (Takimoto *et al*., 1996). These findings led us to hypothesize that NO might modulate the contractile response of ET-1 in human bronchi.

The present experiments were designed to characterize further the contractile response of ET-1 in human bronchi using two endothelin antagonists, BQ-123 and BQ-788, known to be selective antagonists of ET_A and ET_B receptors, respectively (Ihara *et al*., 1992a,b; Ishikawa *et al*., 1994). Furthermore, we investigated the role of the epithelium on ET-1- as well as on IRL 1620-induced contraction.

This study provides evidence that ET-1 may have two opposite effects: one is contractile and linked to ET_B receptor stimulation; the other is inhibitory, dependent on ET_A receptors and linked to NO release.

Methods

Human bronchial tissue preparation

Bronchial tissues were removed from 59 patients (50 men and 9 women, mean age, 62.8 ± 1.3 years) with lung cancer at the time of the surgical operation. Just after resection, segments of bronchi were taken from an area as far as possible from the malignancy and were dissected free of parenchyma. They were placed in oxygenated Krebs-Henseleit solution (NaCl, 119; KCl, 5.4; $CaCl_2$, 2.5; KH_2PO_4, 1.2; $MgSO_4$, 1.2; $NaHCO_3$, 25; glucose, 11.7 mM) and stored overnight at 4°C. Previous experience in this laboratory and published data have demonstrated that overnight storage of tissue does not alter its reactivity. After removal of adhering fat and connective tissues, 4–8 rings (5–7 mm length × 1–2 mm internal diameter) of the same bronchus were prepared. The bronchial rings were suspended on tissue hooks in 5 ml organ baths containing Krebs-Henseleit solution, gassed with 95% O_2: 5% CO_2 and maintained at 37°C (pH 7.4). Each preparation was connected to a force displacement transducer (Statham UF-1) and isometric tension changes recorded on a polygraph. The preparations were equilibrated for 90 min with changes in fresh Krebs-Henseleit solution every 15 min before the start of each experiment. A load of 2–2.5 g was maintained throughout the equilibrium period. When required, the epithelium was removed by gently and repeated rubbing of the luminal surface with a cotton-tipped applicator, as described previously (Naline *et al*., 1989; Candenas *et al*., 1992). Experiments were conducted on parallel groups of 4–8 rings, one ring used as control. Only one concentration-response curve was recorded for each ring.

In all experiments, human bronchi were first contracted maximally with acetylcholine (3×10^{-3} M)(ACh) and then relaxed with theophylline (3×10^{-3} M). These concentrations did not alter subsequent responsiveness of the tissue. The tissue was then allowed to equilibrate for a further 60 min period.

Experimental procedures

Concentration-response curves to ET-1 or to the ET_B receptor selective agonist, IRL 1620 (10^{-11} to 3×10^{-7} M), were obtained by applying increasing concentrations at 10–15 min intervals. Contractile responses were expressed as a percentage of the maximal effect induced by acetylcholine (3×10^{-3} M). Following the equilibration period, tissues with or without epithelium were incubated (20 min) with L-NAME (10^{-4} to 3×10^{-3} M) (inhibitor of NO synthase) or L-Arg (3×10^{-3} M), with BQ-123 or BQ-788 (ET_A and ET_B receptor antagonists, respectively), or with vehicle before addition of cumulative concentrations of ET-1 or IRL 1620.

Analysis of data

$-\log EC_{50}$ values represent the negative logarithm of the concentration of ET-1 or IRL 1620 which induced a contraction equal to 50% of the maximal effect induced by acetylcholine (3×10^{-3} M). E_{max} values represent the maximal contraction induced by ET-1 or IRL 1620 and are expressed as percentage of acetylcholine (3×10^{-3} M). ACh 3×10^{-3} M induced maximal responses which were not modified by epithelium removal or L-NAME treatment (2.13 ± 0.30 g, $n = 12$; 1.81 ± 0.20 g, $n = 12$; 2.07 ± 0.23 g, $n = 15$ in control, after epithelium removal or after L-NAME treatment, respectively). pA_2 and pK_B values of antagonists were calculated according to Arunlakshana & Schild (1959) and Kenakin (1987), respectively. The competitive nature of the antagonism was evaluated by the Schild plot method (Arunlakshana & Schild, 1959) on data obtained with at least three concentrations of BQ-788 (10^{-7}–10^{-5} M and 10^{-9}–10^{-7} M) tested against ET-1 and IRL 1620, respectively. All values in the text and in the figures are expressed as means ± s.e.mean. Statistical analysis of the results was performed using Student's *t*-test (two-tailed, for paired samples), and *P* values lower than 0.05 were considered significant.

Drugs

Drugs used were ET-1 (Novabiochem, Läufelfingen, Switzerland), acetylcholine HCl (Pharmacie Centrale des Hôpitaux, Paris, France), N^G-nitro-L-arginine methyl ester (L-NAME) and L-Arginine (L-Arg) (Sigma, St Louis, MO, U.S.A.), BQ-123 and BQ-788 (Bachem, Bubendorf, Switzerland), IRL 1620 (International Research Laboratories, Ciba-Geigy Japan Ltd., Takarazuka, Japan).

ET-1 was dissolved in distilled water at concentration of 2.5×10^{-4} M and kept in small aliquots (200 μl) at −20°C until used. A fresh aliquot was used for each experiment. Dilutions were made in Krebs solution. BQ-123 and BQ-788 were dissolved with ethanol at concentration of 2.5×10^{-3} M and kept in small aliquots (200 μl) at −20°C until used. A fresh aliquot was used for each experiment. Dilutions were made first with ethanol/water (50/50) (concentration of 2.5×10^{-4} M) and then in Krebs solution. The maximal final concentration of ethanol was 0.02% and this concentration did not modify the maximal acetylcholine response. IRL 1620 was dissolved with ethanol at concentration of 2.5×10^{-3} M. Dilutions were made first with ethanol/water (50/50) (concentration of 2.5×10^{-4} M) and then in Krebs solution. L-NAME and L-Arg were dissolved in distilled water at concentration of 0.25 M and then in Krebs solution.

Results

Effect of epithelium removal on ET-1- and IRL 1620-induced contraction of human bronchi

Both ET-1 and IRL 1620 potently contracted isolated human bronchi ($-\log EC_{50}$ values of 7.92 ± 0.09, $n = 18$ and 7.94 ± 0.11, $n = 19$, respectively (Figure 1a and b). The contractile response induced by IRL 1620 was not affected by epithelium removal ($-\log EC_{50}$ values of 8.10 ± 0.09, $n = 12$; $P > 0.05$ compared to intact preparations) (Figure 1b). In contrast, the concentration-response curve for ET-1 was significantly shifted to the left after epithelium removal

($-\log EC_{50}$ values of 8.65 ± 0.11; shift of 0.73 ± 0.10 log unit, $n=17$, $P<0.001$) (Figure 1a).

Effect of BQ-123, L-NAME and BQ-788 on ET-1 induced contraction of human bronchi

Using intact human bronchi, BQ-123 ($10^{-8}-10^{-5}$ M) induced a significant potentiation of the ET-1 contractile response as shown by a leftward shift of the ET-1 concentration-response curves at all concentration tested (0.55–0.66 log unit) (Figure 2a; Table 2a). L-NAME (3×10^{-3} M) induced a significant leftward shift of the ET-1 concentration-response curve (0.44 ± 0.07 log unit, $n=15$, $P<0.001$) (Figure 2b; Table 2) and this potentiation was abolished by the presence of L-Arg (3×10^{-3} M; Table 2). However, after epithelium removal, BQ-123 ($10^{-8}-10^{-5}$ M) and L-NAME (3×10^{-3} M) had no significant effect on the ET-1 concentration-response curve (Table 2). In addition, the effects of L-NAME and BQ-123 were not additive in preparations with epithelium (Table 2).

The concentration-response curve for ET-1 was displaced significantly to the right by BQ-788 only with the highest concentration (10^{-5} M) in preparations with epithelium (shift to the right of 0.43 ± 0.10 log unit, $n=7$, $P<0.05$) (Figure 3a; Table 1). pK_B calculated according to Kenakin (1987) for a concentration of BQ-788 (10^{-5} M) was 5.08 ± 0.36 (Schild plot slope $= 0.68 \pm 0.08$, $n=7$, significantly different from unity, $P<0.05$). After epithelium removal, BQ-788 induced a concentration-dependent rightward shift of the ET-1 concentration-response curve (shift to the right of 0.56–1.21 log unit; Schild plot slope $= 0.70 \pm 0.10$, $n=6$, significantly different from unity, $P<0.05$ and $pK_B = 6.40 \pm 0.31$, $n=6$) (Figure 3b; Table 1). This improvement in the antagonistic activity of BQ-788 was also observed in intact preparations in the presence of L-NAME (3×10^{-3} M; shift to the right of 0.21–0.93 log unit; Schild plot slope $= 0.59 \pm 0.08$, $n=7$, significantly different from unity, $P<0.01$ and $pK_B = 5.86 \pm 0.28$, $n=7$) (Figure 3c).

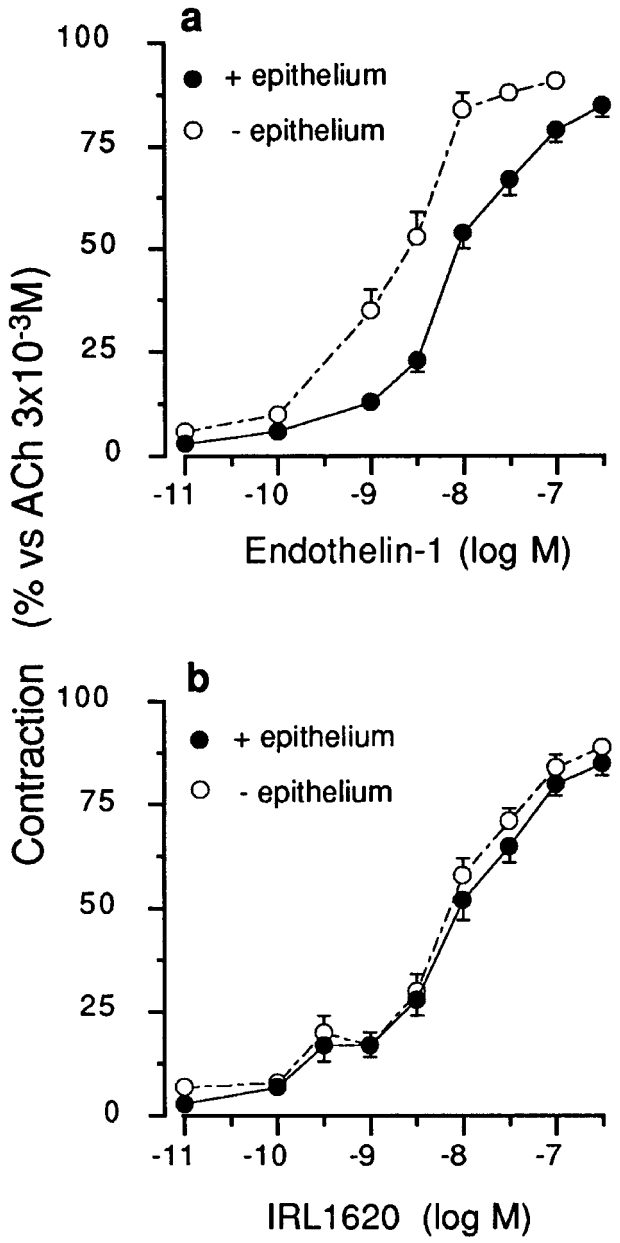

Figure 1 Effect of epithelium removal on (a) ET-1- and (b) IRL 1620-induced contraction of isolated human bronchi on intact preparations or after epithelium removal. Values are means ± s.e.mean ($n=12-19$).

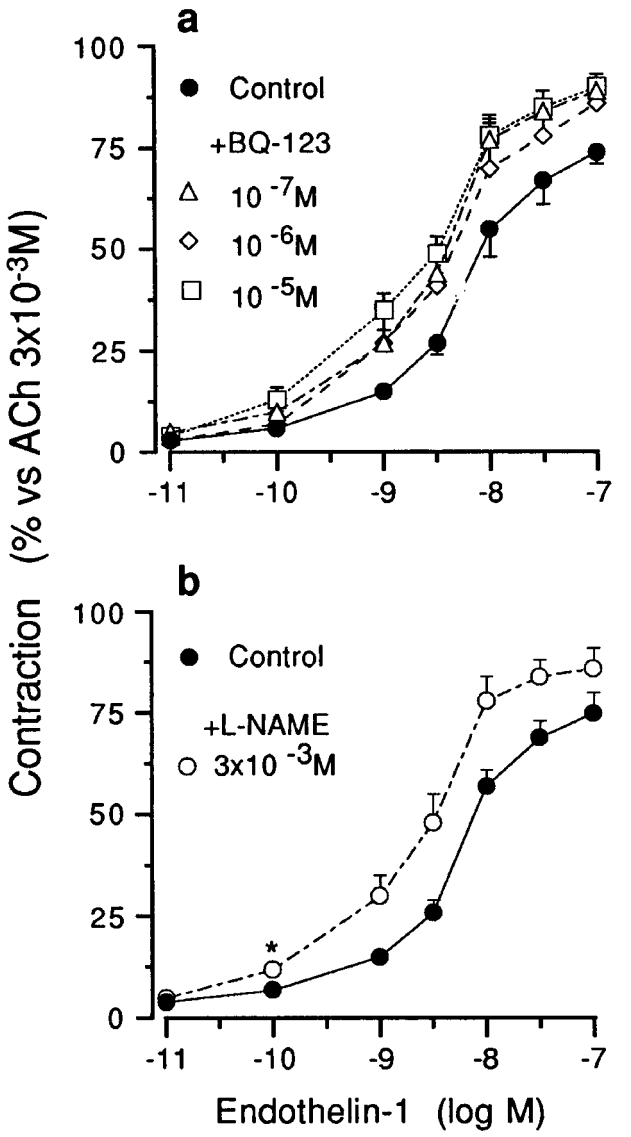

Figure 2 Comparative effect of BQ-123, an ET_A receptor antagonist (a), and L-NAME (3×10^{-3} M), a nitric oxide synthase inhibitor (b) on ET-1-induced contraction of intact isolated human bronchi. Values are means ± s.e.mean ($n=5-15$).

Effect of BQ-123 and BQ-788 on IRL 1620-induced contraction of human bronchi

The concentration-response curves for IRL 1620 were not modified by BQ-123 (10^{-8}–10^{-6} M; Table 1). Irrespective of the presence of the epithelium, BQ-788 (10^{-9}–10^{-7} M) induced a rightward shift of the IRL 1620 concentration-response curve (shift to the right of 0.18–2.06 log unit; Table 1). Antagonism by BQ-788 was competitive antagonism since maximal responses to IRL 1620 were not significantly reduced and the slope of Schild plot were not significantly different from unity in the presence ($pA_2 = 8.64 \pm 0.06$; slope $= 1.11 \pm 0.09$, $n = 7$) and in the absence ($pA_2 = 8.82 \pm 0.10$; slope $= 1.19 \pm 0.11$, $n = 5$) of the epithelium (Figure 4a and b; Table 1).

Discussion

The present results show that the airway epithelium plays a major role in the contractile response of the isolated human bronchi to ET-1. The results obtained with receptor-selective agonist and antagonists suggest that ET_A receptors are present on the airway epithelium mediating the release of nitric oxide which counteracts the contraction. In contrast, ET_B receptors seem to be located on airway smooth muscle cells mediating contraction.

The respiratory epithelium not only acts as a physical barrier but also contains enzymes to metabolize peptides or release mediators to modulate the responses of the underlying smooth muscle to a variety of bronchoconstrictors including ET-1 (Bertrand & Tschirhart, 1993). A potentiation of the contractile response to ET-1 after epithelium removal has already been reported in guinea-pig tracheae (Sarriá *et al*., 1990; Tschirhart *et al*., 1991) and human bronchi (Candenas *et al*., 1992) providing further confirmation of the regulatory role of airway epithelium in airway tone. In these studies, it was suggested that neutral endopeptidase EC 24.11 (NEP) was in part responsible for the potentiation of the ET-1 response after epithelium removal since inhibitors of this enzyme were able to partially mimic this effect (Tschirhart *et al*., 1991; Candenas *et*

Table 1 Shift of the concentration response curves of ET-1 and IRL 1620 in the presence of endothelin receptor antagonists

	+ *Epithelium*	− *Epithelium*
ET-1		
$-\log EC_{50}$	7.85 ± 0.13 (12)	8.78 ± 0.10 (9)
shifts after pretreatments with:		
BQ-123 10^{-8} M	0.51 ± 0.08 (12)***	0.00 ± 0.17 (5)
10^{-7} M	0.66 ± 0.20 (5)*	0.01 ± 0.08 (6)
10^{-6} M	0.62 ± 0.15 (6)**	0.23 ± 0.19 (8)
10^{-5} M	0.53 ± 0.10 (7)**	0.25 ± 0.13 (7)
$-\log EC_{50}$	8.10 ± 0.10 (9)	8.84 ± 0.19 (6)
shifts after pretreatments with:		
BQ-788 10^{-8} M	0.07 ± 0.04 (6)	0.06 ± 0.12 (5)
10^{-7} M	0.08 ± 0.06 (8)	0.06 ± 0.37 (6)
10^{-6} M	−0.15 ± 0.08 (8)	−0.56 ± 0.15 (6)*
10^{-5} M	−0.43 ± 0.11 (7)*	−1.21 ± 0.18 (6)**
IRL 1620		
$-\log EC_{50}$	7.74 ± 0.30 (5)	7.95 ± 0.17 (5)
shifts after pretreatments with:		
BQ-123 10^{-8} M	−0.03 ± 0.12 (5)	0.08 ± 0.29 (5)
10^{-7} M	0.02 ± 0.15 (5)	−0.16 ± 0.12 (5)
10^{-6} M	−0.11 ± 0.36 (4)	−0.35 ± 0.43 (5)
$-\log EC_{50}$	8.18 ± 0.12 (9)	8.12 ± 0.15 (7)
shifts after pretreatments with:		
BQ-788 10^{-9} M	−0.18 ± 0.02 (6)***	−0.26 ± 0.13 (3)
10^{-8} M	−0.68 ± 0.15 (7)**	−1.07 ± 0.08 (5)***
10^{-7} M	−1.98 ± 0.13 (8)***	−2.06 ± 0.24 (6)***

(n): number of experiments. Significant shift: *$P < 0.05$; **$P < 0.01$; ***$P < 0.001$.

Table 2 Shift of the concentration response curves of ET-1 in the presence of L-NAME (10^{-4} to 3×10^{-3} M) and/or BQ-123 10^{-8} M

	+ *Epithelium*	− *Epithelium*
$-\log EC_{50}$	7.85 ± 0.13 (12)	8.52 ± 0.04 (8)
shifts after pretreatments with:		
BQ-123 10^{-8} M	0.51 ± 0.08 (12)***	0.15 ± 0.11 (8)
L-NAME 10^{-4} M	0.18 ± 0.12 (5)	
L-NAME 10^{-3} M	0.23 ± 0.05 (5)*	
L-NAME 3×10^{-3} M	0.44 ± 0.07 (15)***	0.04 ± 0.14 (7)
BQ-123 10^{-8} M + L-NAME 3×10^{-3} M	0.41 ± 0.13 (9)*	0.09 ± 0.10 (7)
L-Arg 3×10^{-3} M + L-NAME 3×10^{-3} M	−0.02 ± 0.13 (7)	
$-\log EC_{50}$ (+ L-NAME 3×10^{-3} M)	8.28 ± 0.15 (7)	8.59 ± 0.11 (7)
shifts after pretreatments with:		
BQ-123 10^{-8} M	−0.01 ± 0.18 (7)	0.05 ± 0.12 (7)

(n): number of experiments. Significant shift: *$P < 0.05$; **$P < 0.01$; ***$P < 0.001$.

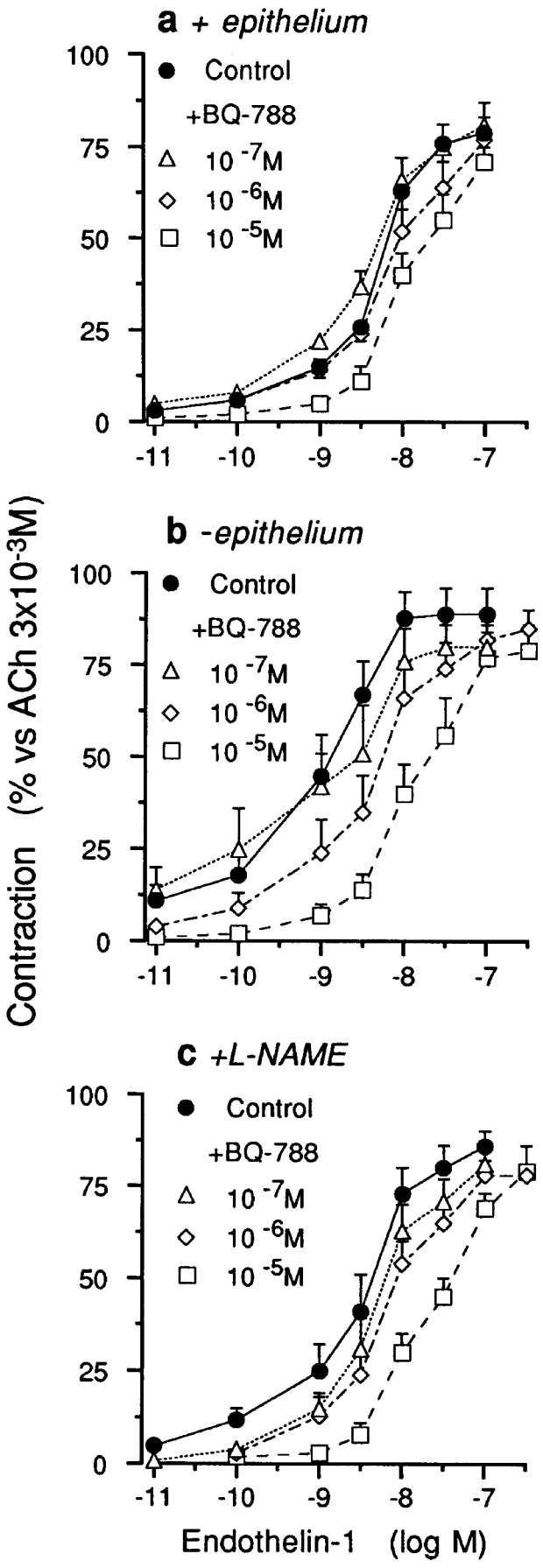

Figure 3 Effect of BQ-788, an ET_B receptor antagonist, on ET-1-induced contraction of isolated human bronchi with (a) or without (b) epithelium, or (c) in intact preparations in the presence of L-NAME (3×10^{-3} M). Values are means ± s.e.mean ($n = 5-9$).

al., 1992). However, the potentiation produced by the NEP inhibitor was smaller than the effect of epithelium removal (Candenas *et al*., 1992) suggesting the release of an epithelium-derived relaxant factor in response to ET-1. The presence of endothelin receptors on the airway epithelial cells in culture has been demonstrated in several species, including human (Wu *et al*., 1993; Ninomiya *et al*., 1995; Takimoto *et al*., 1996). In these systems, ET-1 was able to release a variety of arachidonic acid metabolites such as PGE_2 (Wu *et al*., 1993; Takimoto *et al*., 1996). Thus it may be speculated that ET-1 could induce the release of relaxant prostanoids in human bronchi. However, although ET-1 increased the release of several prostanoids in intact human bronchi, blockade of the cyclo-oxygenase pathway with indomethacin or sodium meclofenamate had no effect on the contraction induced by ET-1 (Advenier *et al*., 1990; Hay *et al*., 1993b). Recently, it has been shown that, under certain circumstances, human epithelial cells are able to produce NO (Robbins *et al*., 1994). Furthermore, in precontracted guinea-pig trachea, ET-1

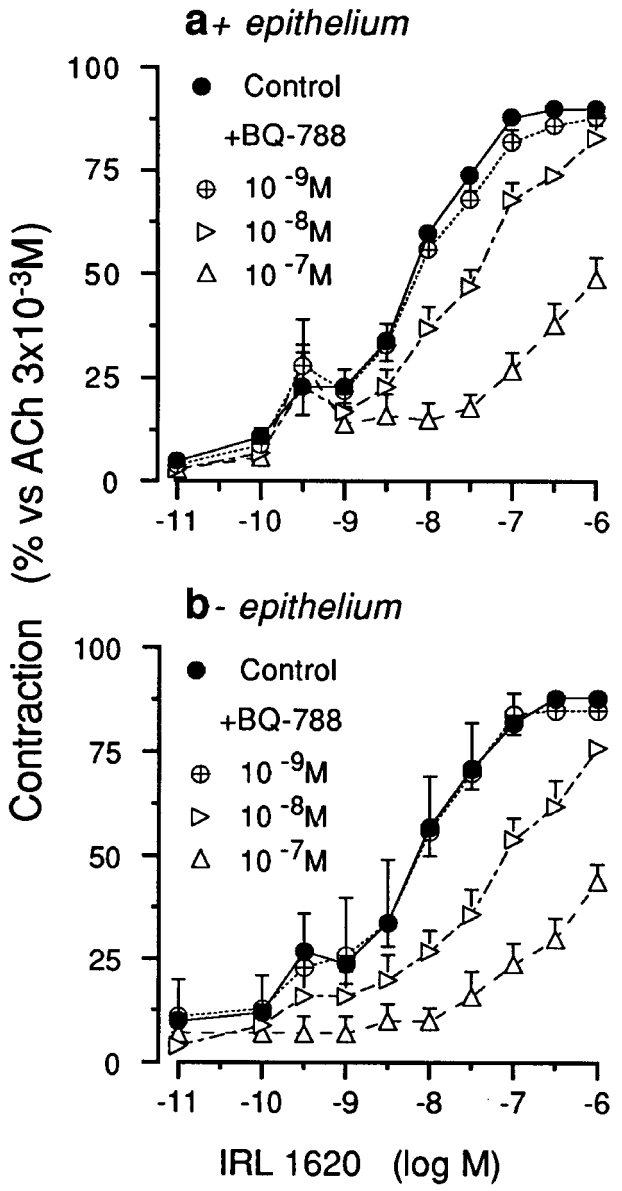

Figure 4 Effect of BQ-788 on IRL 1620-induced contraction of isolated human bronchi with (a) or without (b) epithelium. Values are means ± s.e.mean ($n = 5-9$).

is able to induce relaxation *via* epithelium-dependent NO release (Filep *et al*., 1993; Hadj-Kaddour *et al*., 1996). In this study, we have shown that L-NAME, an inhibitor of NO synthesis, potentiated ET-1-induced contraction only in the presence of the epithelium suggesting the release of NO from the epithelial layer. We also demonstrated the specificity of L-NAME action showing that L-Arg was able to reverse its effect.

To characterize the receptors involved in the NO release following ET-1, the effect of BQ-123 and BQ-788 were investigated. In intact human bronchi, BQ-123 induced a leftward shift of the concentration-response curve to ET-1 which was similar to the effect of L-NAME or epithelium removal. In contrast, BQ-788 did not potentiate ET-1-induced contraction in the same preparations and the concentration-response curve to IRL 1620, an ET_B selective agonist, was not affected by epithelium removal, BQ-123 or L-NAME. Collectively, these results would strongly suggest that ET-1-induced NO release is mediated *via* ET_A receptor activation on the airway epithelium. In addition, autoradiographic studies in human isolated airways revealed the presence of ET_A receptors at the epithelium level (Goldie *et al*., 1995). Moreover, studies with cultured epithelial cells indicated the predominant expression of ET_A receptors (Ninomiya *et al*., 1995; Takimoto *et al*., 1996). Finally, Gater *et al*. (1996) also reported a lack of effect of BQ-123 in human bronchi of which the epithelium had been removed. In contrast, it has been reported that BQ-123 (10 μM) had no effect on ET-1-induced contraction in intact human bronchi (Hay *et al*., 1993c). However, the method described in this study to clean the bronchi from parenchymal tissues, using a glass probe placed into the lumen, could damage the airway epithelium (Hay *et al*., 1993c). Furthermore, appreciable regional differences in the relative distribution of ET_A and ET_B receptors were described in the guinea-pig airways (Hay *et al*., 1993c). If such phenomena exits in the human airways, the fact that the bronchi used in the study by Hay and colleagues (1993c) had a bigger diameter (4–15 mm) than in the present study may explain a different modulation of the contraction by BQ-123. Although our results strongly suggest the involvement of ET_A receptor activation in NO release from the airway epithelium in human bronchi, the release, by these cells, of other mediators such as prostanoids following ET-1 application could not be excluded. However, the use of selective inhibitors or antagonists of these mediators did not modulate ET-1 induced contraction (Hay *et al*., 1993b) suggesting a major role of NO in the regulation of this response in intact human bronchi.

In intact human bronchi, IRL 1620, an ET_B selective agonist, was as potent as ET-1 to induce contraction of isolated human bronchi. Furthermore, contractions induced by IRL 1620 were competitively antagonized by BQ-788 suggesting a major role of ET_B receptors in the contraction of human bronchi. Surprisingly, BQ-788 (10 μM) was a very weak antagonist of ET-1 in intact human bronchi. Moreover, epithelium removal slightly improved the antagonistic activity of BQ-788, although the concentration-response curves to ET-1 were only rightward shifted for the highest concentrations of this antagonist ($\geqslant 1$ μM). The greater effectiveness of BQ-788 against IRL 1620 cannot be explained by lower binding affinity of this selective agonist compared to ET-1 since competitive binding experiments revealed almost identical displacement curves (Watakabe *et al*., 1992). However, IRL 1620 binds to endothelin receptors in a reversible manner, whereas ET-1 only dissociates very slowly from the binding sites (Watakabe *et al*., 1992) in several species including human (Nambi *et al*., 1994). This different sensitivity of agonists to antagonists would agree with previous observations that ET_A/ET_B non-selective receptor antagonists are more potent against responses to ET_B receptor agonists than ET-1 itself (Warner *et al*., 1993; Gater *et al*., 1996). These data suggest that the relative effectiveness of endothelin receptor antagonists varies with the agonist used. Recently, Fukuroda and colleagues (1996) have suggested a role for both ET_A and ET_B receptors in the contraction induced by ET-1 in human bronchi. In fact, they observed that ET-1-induced contraction was not antagonized by BQ-123 alone or BQ-788 alone but was blocked by combined treatment with both antagonists (Fukuroda *et al*., 1996). These data could explain the weak activity of BQ-788 used alone against ET-1 activity, although the antagonist activity of dual ET_A/ET_B antagonists was still weak in this preparation (Fukuroda *et al*., 1996) as well as in guinea-pig trachea (Battistini *et al*., 1994). Although these data would suggest the involvement of both ET_A and ET_B receptors in ET-1-induced contraction of the human bronchi, further studies with different ET_B selective antagonists are needed.

In conclusion, our results show that BQ-123 and L-NAME potentiated contractions to ET-1 in human bronchi suggesting the involvement of ET_A receptors in NO release. These ET_A receptors are most probably situated on the epithelial cells, since this potentiation was not seen in preparations without epithelium. Moreover, epithelial cells are likely to be the source of NO in human bronchi following ET_A receptor activation. The respective role of ET_A and ET_B receptors in the contraction induced by ET-1 in human bronchi will need further investigation using other selective ET_B receptor antagonists.

References

ADVENIER, C., SARRIÁ, B., NALINE, E., PUYBASSET, L. & LAGENTE, V. (1990). Contractile activity of three endothelins (ET-1, ET-2 and ET-3) on the isolated human bronchus. *Br. J. Pharmacol.,* **100,** 168–172.

ARAI, H., NAKAO, K., TAKAYA, K., HOSODA, K., OGAWA, Y., NAKANISHI, S. & IMURA, H. (1993). The human endothelin-B-receptor gene–structural organization and chromosomal assignment. *J. Biol. Chem.,* **268,** 3463–3470.

ARUNLAKSHANA, O. & SCHILD, H.O. (1959). Some quantitative uses of drug antagonists. *Br. J. Pharmacol. Chemother.,* **14,** 48–58.

BATTISTINI, B., WARNER, T.D., FOURNIER, A. & VANE, J.R. (1994). Characterization of ET_B receptors mediating contractions induced by endothelin-1 or IRL 1620 in guinea pig isolated airways: effects of BQ-123, FR 139317 or PD 145065. *Br. J. Pharmacol.,* **111,** 1009–1016.

BERTRAND, C. & TSCHIRHART, E.J. (1993). Epithelial factors: modulation of the airway smooth muscle tone. *Fundam. Clin. Pharmacol.,* **7,** 261–273.

CANDENAS, M.L., NALINE, E., SARRIÁ, B. & ADVENIER, C. (1992). Effect of epithelium removal and enkephalin inhibition on the bronchoconstrictor response to three endothelins of the human isolated bronchus. *Eur. J. Pharmacol.,* **210,** 291–297.

FERNANDES, L.B., HENRY, P.J., RIGBY, P.J. & GOLDIE, R.G. (1996). Endothelin-B (ET_B) receptor-activated potentiation of cholinergic nerve-mediated contraction in human bronchus. *Br. J. Pharmacol.,* **118,** 1873–1874.

FILEP, J.G., BATTISTINI, B. & SIROIS, P. (1993). Induction by endothelin-1 of epithelium-dependent relaxation of guinea pig trachea *in vitro*: role of nitric oxide. *Br. J. Pharmacol.,* **109,** 637–644.

FUKURODA, T., OZAKI, S., IHARA, M., ISHIKAWA, K., YANO, M., MIYAUCHI, T., ISHIKAWA, S., ONIZUKA, M., GOTO, K. & NISHIKIBE, M. (1996). Necessity of dual blockade of endothelin ET_A and ET_B receptor subtypes for antagonism of endothelin-1-induced contraction in human bronchi. *Br. J. Pharmacol.,* **117,** 995–999.

GATER, P., WASSERMAN, M. & RENZETTI, L. (1996). Effects of Ro 47-0203 on endothelin-1 and sarafotoxin S6c-induced contraction of human bronchus and guinea-pig trachea. *Eur. J. Pharmacol.,* **304,** 123–128.

GOLDIE, R.G., D'APRILE, A.C., CVETKOVSKI, R., RIGBY, P.J. & HENRY, P.J. (1996). Influence of regional differences in ET_A and ET_B receptor subtype proportions on endothelin-1-induced contractions in porcine isolated trachea and bronchus. *Br. J. Pharmacol.,* **117,** 736–742.

GOLDIE, R.G., HENRY, P.J., KNOTT, P.G., SELF, G.J., LUTTMANN, M.A. & HAY, D.W.P. (1995). Endothelin-1 receptor density, distribution, and function in human isolated asthmatic airways. *Am. J. Respir. Crit. Care Med.,* **152,** 1653–1658.

GRUNSTEIN, M.M., ROSENBERG, S.M., SHRAMM, C.M. & PAWLOWSKI, N.A. (1991). Mechanisms of action of endothelin-1 in maturing rabbit airway smooth muscle. *Am. J. Physiol.,* **260,** L434–L443.

HADJ-KADDOUR, K., MICHEL, A. & CHEVILLARD, C. (1996). Different mechanisms involved in relaxation of guinea-pig trachea by endothelin-1 and -3. *Eur. J. Pharmacol.,* **298,** 145–148.

HAY, D.W.P. (1995). Endothelins. In *Airways Smooth Muscle: Peptide Receptors. Ion Channels and Signal Transduction*. ed. Raeburn D. & Giembycz M.A. pp. 1–50. Basel: Birkhäuser Verlag.

HAY, D.W.P., HENRY, P.J. & GOLDIE, R. (1993a). Endothelin and the respiratory system. *Trends Pharmacol. Sci.,* **14,** 29–32.

HAY, D.W.P., HUBBARD, W.C. & UNDEM, B.J. (1993b). Endothelin-induced contraction and mediator release in human bronchus. *Br. J. Pharmacol.,* **110,** 392–398.

HAY, D.W.P., LUTTMANN, M.A., HUBBARD, W.C. & UNDEM, B.J. (1993c). Endothelin receptor subtypes in human and guinea-pig pulmonary tissues. *Br. J. Pharmacol.,* **110,** 1175–1183.

IHARA, M., ISHIKAWA, K., FUKURODA, T., SAEKI, T., FUNABASHI, K., FUKAMI, T., SUDA, H. & YANO, M. (1992a). *In vitro* biological profile of a highly potent novel endothelin (ET) antagonist BQ-123 selective for the ET_A receptor. *J. Cardiovasc. Pharmacol.,* **20,** S11–S14.

IHARA, M., NOGUCHI, K., SAEKI, T., FUKURODA, T., TSUCHIDA, S., KIMURA, S., FUKAMI, T., ISHIKAWA, K., NISHIKIBE, M. & YANO, M. (1992b). Biological profiles of highly potent novel endothelin antagonists selective for the ET_A receptor. *Life Sci.,* **50,** 247–255.

ISHIKAWA, K., IHARA, M., NOGUCHI, K., MASE, T., MINO, N., SAEKI, T., FUKURODA, T., FUKAMI, T., OSAKI, S., NAGASE, T., NISHIKIBE, M. & YANO, M. (1994). Biochemical and pharmacological profile of a potent and selective endothelin-B-receptor antagonist, BQ-788. *Proc. Natl. Acad. Sci. U.S.A.,* **91,** 4892–4896.

JAMES, A.F., URADE, Y., WEBB, R.L., KARAKI, H., UMEMURA, I., FUJITANI, Y., ODA, K., OKADA, T., LAPPE, R.W. & TAKAI, M. (1993). IRL 1620, Succinyl-[Glu9, Ala11,15]-endothelin-1(8–21), a specific agonist of the ET_B receptor. *Cardiovas. Drug Rev.,* **10,** 253–270.

KENAKIN, T.P. (1987). Pharmacologic analysis of drug receptor interaction. In *Drug Antagonism*. pp. 205–244. New York: Raven Press.

NALINE, E., DEVILLIER, P., DRAPEAU, G., TOTY, L., BACKDACH, H., REGOLI, D. & ADVENIER, C. (1989). Characterization of neurokinin effects and receptor selectivity in human isolated bronchi. *Am. Rev. Respir. Dis.,* **140,** 679–686.

NALLY, J.E., MCCALL, R., YOUNG, L.C., WAKELAM, M.J.O., THOMSON, N.C. & MCGRATH, J.C. (1994). Mechanical and biochemical responses to endothelin-1 and endothelin-3 in human bronchi. *Eur. J. Pharmacol.,* **288,** 53–60.

NAMBI, P., ELSHOURBAGY, N., WU, H.L., PULLEN, M., OHLSTEIN, E.H., BROOKS, D.P., LAGO, M.A., ELLIOTT, J.D., GLEASON, J.G. & RUFFOLO, R.R. (1994). Nonpeptide endothelin receptor antagonists .1. effects on binding and signal transduction on human endothelin-A and endothelin-B receptors. *J. Pharmacol. Exp. Ther.,* **271,** 755–761.

NINOMIYA, H., YU, X.Y., UCHIDA, Y., HASEGAWA, S. & SPANNHAKE, E.W. (1995). Specific binding of endothelin-1 to canine tracheal epithelial cells in culture. *Am. J. Physiol.,* **268,** L424.

REDINGTON, A.E., SPRINGALL, D.R., GHATEI, M.A., LAU, L.C.K., BLOOM, S.R., HOLGATE, S.T., POLAK, J.M. & HOWARTH, P.H. (1995). Endothelin in bronchoalveolar lavage fluid and its relation to airflow obstruction in asthma. *Am. J. Respir. Crit. Care Med.,* **151,** 1034–1039.

ROBBINS, R.A., BARNES, P.J., SPRINGALL, D.R., WARREN, J.B., KWON, O.J., BUTTERY, L.D.K., WILSON, A.J., GELLER, D.A. & POLAK, J.M. (1994). Expression of inducible nitric oxide in human lung epithelial cells. *Biochem. Biophys. Res. Commun.,* **203,** 209–218.

SAKURAI, T., YANAGISAWA, M. & MASAKI, M. (1992). Molecular characterization of endothelin receptors. *Trends Pharmacol. Sci.,* **13,** 103–108.

SARRIÁ, B., NALINE, E., MORCILLO, E., CORTIJO, J., ESPLUGUES, J. & ADVENIER, C. (1990). Calcium dependence of the contraction produced by endothelin (ET-1) in isolated guinea-pig trachea. *Eur. J. Pharmacol.,* **187,** 445–453.

SPRINGALL, D.R., HOWARTH, P.H. & COUNIHAN, H. (1991). Endothelin immunoreactivity of airway epithelium in asthmatic patients. *Lancet,* **337,** 697–701.

TAKAI, M., UMEMURA, I., YAMASAKI, K., WATAKABE, T., FUJITANI, Y., ODA, K., URADE, Y., INUI, T., YAMAMURA, T. & OKADA, T. (1992). A potent and specific agonist, Succinyl-[Glu9, Ala11,15]-endothelin-1(8–21), IRL 1620, for the ET_B receptor. *Biochem. Biophys. Res. Commun.,* **184,** 953–959.

TAKIMOTO, M., ODA, K., SASAKI, Y. & OKADA, T. (1996). Endothelin-A receptor-mediated prostanoid secretion via autocrine and deoxyribonucleic acid synthesis via paracrine signaling in human bronchial epithelial cells. *Endocrinology,* **137,** 4542–4550.

TSCHIRHART, E.J., DRIJFHOUT, J.W., PELTON, J.T., MILLER, R.C. & JONES, C.R. (1991). Endothelins: functional and autoradiographic studies in guinea-pig trachea. *J. Pharmacol. Exp. Ther.,* **258,** 381–387.

WARNER, T.D., ALLCOCK, G.H., CORDER, R. & VANE, J.R. (1993). Use of the endothelin antagonists BQ-123 and PD142893 to reveal three receptors mediating smooth muscle contraction and the release of EDRF. *Br. J. Pharmacol.,* **110,** 777–782.

WATAKABE, T., URADE, Y., TAKAI, M., UMEMURA, I. & OKADA, T. (1992). A reversible radioligand specific for the ET_B receptor-[^{125}I]Tyr13-Suc-[Glu9, Ala11,15]-Endothelin-1(8–21), [^{125}I]-IRL 1620. *Biochem. Biophys. Res. Commun.,* **185,** 867–873.

WU, T., RIEVES, D., LARYVÉE, P., LOGUN, C., LAWRENCE, M.G. & SHELHAMMER, J.H. (1993). Production of eicosanoids in response to endothelin-1 binding sites in airways epithelial cells. *J. Resp. Cell. Mol. Biol.,* **8,** 282–290.

YANAGISAWA, M., KURIHARA, H., KIMURA, S., TOMOBE, S., KOBAYASHI, M., YAZAKI, Y., GOTO, K. & MASAKI, T. (1988). A novel potent vasoconstrictor peptide produced by vascular endothelial cells. *Nature,* **332,** 411–415.

(Received August 12, 1998
Revised October 27, 1998
Accepted November 11, 1998)